The University Of Sheffield.

A genome-wide screen to identify novel *Staphylococcus aureus* factors associated with the subversion of macrophage phagosomal maturation

By:

Paul Edward Roberts Morris

A thesis submitted in partial fulfilment of the requirements for the degree of Doctor of Philosophy

The University of Sheffield
Faculty of Medicine
Department of Infection, Immunity and Cardiovascular Diseases

Submission Date: August 2021

Summary

Staphylococcus aureus is a major pathogen, causing significant morbidity, mortality, and healthcare-associated costs, complicated further by increasing antimicrobial resistance.

Macrophages, the resident tissue phagocyte are essential for bacterial clearance. *S. aureus* is rapidly internalised by macrophages, but phagosomal maturation is subverted to establish an intracellular population. Phagosomal maturation after bacterial ingestion normally involves sequential fusion with endosomes and lysosomes with reducing luminal pH, facilitating degradation of bacteria. In response to phagocytosis and phagosomal maturation, *S. aureus* gene expression adapts to the intracellular environment with up-regulation of multiple genes involved in resistance to oxidative stress and global regulation. A greater understanding of intracellular persistence is required to develop more effective treatment of *S. aureus.*

The first aim of this project was to confirm that *S. aureus* USA300 strain JE2 demonstrates this phenotype. Using an *in vitro* differentiated macrophage model, phagosomes containing the USA300 strain JE2 progress to a late phagosome state but fail mature to a phagolysosome state and to acidify appropriately.

The second aim was to develop a high-throughput microscopy protocol to screen intracellular bacterial acidification in macrophages. This enabled the final aim of assessing a USA300 strain JE2-derived library of transposon-mutated non-essential genes to identify genes associated with phagosomal acidification subversion. This novel screening tool can also be repurposed to investigate other pathogens to broaden knowledge of host:pathogen interaction.

A total of 15 genes were identified, including the regulators *agr* and *saeR*, and oxidative stress enzyme catalase. The protease ClpP, the terminal oxidase complex genes *qoxA* and *qoxC,* and the cytochrome assembly complexes *ctaB* and *ctaM* were novel findings in context of phagosomal acidification subversion. A greater understanding of these genes and their regulatory pathways will offer insight into the mechanisms utilised by *S. aureus* to subvert the host macrophage immune response and aid novel therapeutic target development.

Acknowledgements

Through the duration of this project, I have been fortunate to receive support, insight and encouragement from numerous people. Firstly, I would like to express my gratitude to Professor David Dockrell. From the very beginning of this project, David has been tireless in his support, a welcome critic, and a role model for combining clinical and academic pathways. I would not have made it to this point without his help. All my supervisors have been generous with their time and encouragement in taking a clinician from the wards and developing a basic scientist. It has been a privilege to be able to learn from Professor Steve Renshaw, Professor Simon Foster and Doctor Andrew Peden. I will endeavour to remain as enthusiastic and supportive during my career as they have been to me.

I would also extend my gratitude to the members of the respective laboratory groups for their teaching, support, and humour. From my first steps back into a basic science laboratory through to the completion of this project, I have had the pleasure of learning from numerous people, but I would particularly like to express my gratitude to Martin Bewley, Jamil Jubrail, Helen Marriott, Joby Cole, Paul Collini, Faith Tolliday, Emma Boldock, April Yang and Bartek Salamaga for their assistance. Also, Dr Steve Brown provided constant support at the Sheffield RNAi Screening Facility. It would also be remiss of me not to express my thanks to Katie Cooke and Jon Kilby for their support throughout this project.

I am very appreciative of the Medical Research Council for funding my clinical research training fellowship, without which this project would not have been possible. Additionally, the National Institute for Health Research academic clinical fellowship granted me the opportunity to initially develop this project. I would also like to thank the members of the department of Infectious Diseases within the Sheffield Teaching Hospitals NHS Trust for their support whilst I balanced clinical and academic commitments.

Finally, I must thank my amazing family. It has been a long road to get to this point, but Gayti has been unwavering in her kindness and understanding of my absences during countless evenings, nights, and weekends in the lab. Getting to this point would have been impossible without you. My parents, Ed and Betty, and parents-in-law, Goura and Badar, have come to our support throughout. Thank you too to Seren and Rohan. It’s been amazing the watch you grow up alongside this project, I have loved all the questions about “Daddy’s science” and thank you for forgiving me for missing bedtime stories. I love you all and thank you for your patience.

Abbreviations

ºC	Degree Celsius
ACME	Arginine catabolic mobile element
Agr	Accessory gene regulator
AhpC	Alkyl hydroperoxide
AIP	Autoinducing peptide
AirSR	Anaerobic iron-sulphur cluster-containing redox sensor/regulator
AMR	Antimicrobial resistance
APC	Antigen presenting cell
ArlRS	Autolysis-related locus regulator/sensor
ATCC	American type culture collection
ATP	Adenosine triphosphate
ATPase	Adenosine triphosphatase
BCV	Brucella containing vacuole
BHI	Brain heart infusion
BraRS	Bacitracin-resistance-associated regulator/sensor
BSA	Bovine serum albumin
C	Centigrade
CA	Community associated
CBA	Columbia blood agar
CC	Clonal complex
CCR1	C-C chemokine receptor type 1
CCR2	C-C chemokine receptor type 2
CD	Cluster of differentiation
CFU	Colony forming units
CHIPS	Chemotaxis inhibitory protein of *Staphylococcus aureus*
ClfA	Clumping factor A
Clp	Caseinolytic protease
ClpP	Caseinolytic protease proteolytic subunit
CO_2	Carbon dioxide
CoNS	Coagulase-negative Staphylococci
Csf-1	Colony stimulating factor 1
CR	Complement receptor
CR3A	Complement receptor 3A
CsoR	Copper-sensitive operon repressor
Cta	Chromosome assembly unit
CX3CR1	CX3C chemokine receptor 1
CXCR1	CXC chemokine receptor 1
CXCR2	CXC chemokine receptor 2
cyoE	Protoheme IX farnesyltransferase
DAPI	4',6-diamidine-2'-phenylindole dihydrochloride
DC	Dendritic cell
dH_2O	Distilled water
DMSO	Dimethyl sulphoxide
DNA	Deoxyribonucleic acid
dot/icm	Defect in organelle trafficking/intracellular multiplication
E. coli	Escherichia coli
e.g.	Exempli gratia (for example)
Eap	Extracellular adherence protein
ECACC	European Collection of Authenticate Cell Cultures
EEA1	Early endosome antigen-1
Efb	Extracellular fibrinogen-binding protein
EPCAM	Epithelial cell adhesion molecule
ER	Endoplasmic reticulum

Ery	Erythromycin
F_c	Fragment crystallisable region
F_cR	Fragment crystallisable region-domain receptor
FCS	Foetal calf serum
Fe^{2+}	Ferrous iron
Fe^{3+}	Ferric iron
FITC	Fluorescein isothiocyanate
FLIPr	Formyl peptide receptor (FPR)-like 1 inhibitory protein
FnBP	Fibronectin-binding protein
FPR	Formyl peptide receptor
Fur	Ferric uptake regulator
Gent	Gentamicin
GFP	Green fluorescent protein
GM-CSF	Granulocyte-macrophage colony-stimulating factor
GraRS	Glycopeptide-resistance-associated regulator/sensor
Gyr	Gyrase
H_2O_2	Hydrogen peroxide
h/i	Heat inactivated
HA	Hospital associated
Hla	α-haemolysin
Hlb	β-haemolysin
Hlg	γ-haemolysin
Hmp	Haemoglobin-like protein
HOPS	Homotypic fusion and protein sorting complex
HssRS	Haem-sensing regulator/sensor
ica	Intercellular adhesion operon
ICAM-1	Intercellular adhesion molecule 1 (CD54)
ICAM-2	Intercellular adhesion molecule 2 (CD102)
i.e.	Id est (that is)
IFN-γ	Interferon-γ
IL	Interleukin
ILCs	Innate lymphoid cells
iNOS	Inducible nitric oxide synthesis
ITAM	Immunoglobulin-gene family tyrosine activation motif
Kan	Kanamycin
kat	Catalase gene
LAMP	Lysosome-associated membrane protein
LAMP-1	Lysosome-associated membrane protein 1
LAMP-2	Lysosome-associated membrane protein 2
LCV	Legionella containing vacuole
LDH	Lactate dehydrogenase
LIMP	Lysosome integral membrane protein
Lin	Lincomycin
LDH	Lactate dehydrogenase
LPS	Lipopolysaccharide
Ly6C	Lymphocyte antigen 6C
Lys	Lysostaphin
M	Molar
M1	Classically activate macrophage
M2	Alternatively activated macrophages
M-CSF	Macrophage colony-stimulating factor
M-CSF-R	Macrophage colony-stimulating factor receptor
Mac-1	Macrophage-1 antigen
MARCO	Macrophage receptor with collagenous structure

Mcl-1	Myeloid cell leukaemic sequence 1 protein
MDM	Monocyte-derived macrophage
mecA	Methicillin encoded cassette A
Met	Methicillin
µg	Micrograms
MGE	Mobile genetic element
MHC	Major histocompatibility complex
MI	Mock infected
MLST	Multi-locus sequence typing
µM	Micromolar
mM	Millimolar
Mn	Manganese
MntR	Manganese transport repressor
MOI	Multiplicity of infection
MPO	Myeloperoxidase
MPS	Mononuclear phagocytic system
MRC1	Mannose receptor-1
MrgA	DNA protection during starvation homologue
MRSA	Methicillin-resistant *Staphylococcus aureus*
MSCRAMMs	Microbial surface components recognising adhesive matrix molecules
NK	Natural killer cell
nM	Nanomolar
NO	Nitric oxide
•NO	Nitric oxide radicals
NO_2	Nitrogen dioxide
NO_2^-	Nitrite
NOS	Nitric oxide synthase
NRAMP1	Natural resistance-associated macrophage protein 1
NTML	Nebraska transposon mutant library
O_2	Oxygen
O_2^-	Superoxide ion
OatA	O-acetyltransferase A
OCl^-	Hypochlorite
OD	Optical density
$ONOO^-$	Peroxynitrite
ORLP1	Oxysterol-binding protein-related protein 1
φ	Bacteriophage
PAMP	Pathogen-associated molecular pattern
PBMC	Peripheral blood mononuclear cell
PBS	Phosphate buffer solution
PCR	Polymerase chain reaction
PerR	Peroxide response regulator
PF	Paraformaldehyde
Pfu	Plaque-forming units
PHE	Public Health England
PI(3)P	Phosphatidylinositol-3-phosphate
PIA	Polysaccharide intercellular adhesion molecule
PMA	Phorbol 12-myristate acetate
PRR	Pattern recognition receptor
PSM	Phenol soluble modulin
PtpA	Tyrosine phosphatase
PVL	Panton-Valentine leucocidin
Qox	Quinol oxidase
Q-Q plot	Quantile-Quantile plot
^{R}	Resistant

Rab5	Ras associated protein 5
Rab7	Ras associated protein 7
RILP	Rab7-interacting lysosome protein
RNA	Ribonucleic acid
RNS	Reactive nitrogen species
ROS	Reactive oxygen species
RPMI 1640	Roswell Park Memorial Institute 1640
RT	Room temperature
S. aureus	*Staphylococcus aureus*
SAB	*Staphylococcus aureus* bacteraemia
SaeRS	*Staphylococcus aureus* exoprotein expression regulator/sensor
Sag	*Staphylococcus aureus* glucosaminidase
SaPI	*Staphylococcus aureus* pathogenicity island
SapM	Secreted acid phosphatase
Sar	Staphylococcal accessory regulator
SCC*mec*	Staphylococcal chromosomal cassette *mec*
SCIN	Staphylococcus complement inhibitor
SCV	Small colony variant
Sdh	Succinate dehydrogenase
SEM	Standard error of the mean
σ^B	Alternative sigma factor B
SigB	Alternative sigma factor B
SiglecH	Sialic acid-binding immunoglobulin-type lectin H
SNARE	Soluble N-ethylmaleimide-sensitive factor attachment protein receptor
Sod	Superoxide dismutase
SrrAB	Staphylococcus respirator response regulator/sensor
SrtA	Sortase A
SRSF	Sheffield RNAi Screening Facility
S. pneumoniae	*Streptococcus pneumoniae*
STRING	Search tool for the retrieval of interacting genes/proteins
STX	Syntaxin
T4SS	Type-4 secretor system
TAE	Tris-acetate EDTA buffer solution
TCS	Two-component (regulatory) system
Tet	Tetracycline
T_h1	T helper lymphocyte 1
T_h2	T helper lymphocyte 2
THP-1	THP-1 monocytic cell line
TIFF	Tagged image format
TLR	Toll-like receptor
Tn	Transposon
TNF	Tumour necrosis factor
TSB	Tryptone soya broth
TSST-1	Toxic shock syndrome toxin-1
TUoS	The University of Sheffield
UV	Ultraviolet
v/v	Volume for volume
VAMP	Vesicle associated membrane protein
VCAM-1	Vascular cell adhesion molecule 1
Vps	Vacuolar protein sorting
VraSR	Vancomycin-resistance associated sensor/regulator
Vti	Vps tail interactor
WT	Wild-type
w/v	Weight for volume
%	Percent

Table of Contents

Chapter 6: Discussion

Figures

Tables

Declaration

I, the author, confirm that the Thesis is my own work. I am aware of the University's Guidance on the Use of Unfair Means (www.sheffield.ac.uk/ssid/unfair-means). This work has not been previously been presented for an award at this, or any other, university.

Chapter 1
Introduction

1.1 The innate immune system

A function of the immune system is to protect the host from invading pathogens. The host must recognise, respond, contain and remove the threat to homeostasis (Janeway 1989). The innate immune system forms a highly effective first-line barrier to contend pathogen invasion in all species, ranging from primitive multicellular organisms to primates (Hoffmann & Akira 2013).

1.1.1 Comparison with the adaptive immune system

Immune mechanisms and responses present from birth, which were formerly viewed as not learned or adapted following exposure to pathogenic organisms, are termed innate. This system includes physical barriers, antimicrobial peptides and enzymes, dedicated phagocytic and effector cells and the alternative complement pathway (Medzhitov & Janeway 2000b). The major advantage of the innate system compared to the adaptive immune system is the rapid response time. Effective adaptive immune response requires clonal expansion of effector cells, necessitating several days in which the pathogen can inflict harm; the innate system is immediately activated by recognition of infection (Medzhitov & Janeway 2000b). Yet the innate immune system is more complicated than a simple holding strategy, it is integrally incorporated into the activation and co-ordination of the adaptive immune system (Janeway 1989). The recognition that organisms without an adaptive immune system demonstrate resistance to reinfection challenged the classical concept of the innate immune system lacking specificity and memory (Kurtz 2005). Contemporary understanding is that innate immune cells having experienced a priming event are modified to enhance host defence effector mechanisms, termed trained immunity (Netea et al. 2016). Exposure of monocytes or macrophages to a pathogen-associated molecular pattern, for example β-glucan, induces epigenetic modifications with enhanced cell activation, cytokine production and adjusted metabolic state (van der Meer et al. 2015). Trained immunity or innate immune memory subsequently enhances the immune response to reinfection (Netea et al. 2015).

The adaptive immune system requires specific activation via antigen recognition, presented by antigen-presenting cells, ultimately generating long-lasting memory to that specific antigen (Jenkins et al. 2001). Activation of the adaptive immune responses are integrally associated with the recognition and activation of innate immunity to microorganisms (Iwasaki & Medzhitov 2015). In parallel with the innate system, the adaptive system comprises humoral and cellular components. Lymphocytes are the cellular constituents, which originate from a common

lymphoid precursor cell distinct from the common myeloid progenitor (Kondo 2010). T lymphocytes, central to antigen-specific cell-mediated immunity, are subdivided by expression of CD4 or CD8 co-receptor expression. Divergent activation of $CD4^+$ T cells relates to the inflammatory context of the antigen presented (Zhu & Paul 2008). T helper 1 (T_h1) lymphocytes direct cell-mediate immunity, with T helper 2 (T_h2) lymphocytes directing a humoral response. Broadly, cell-mediated adaptive immunity is effected by $CD8^+$ lymphocytes (P. Wong & Pamer 2003) with B lymphocytes imparting humoral immunity via antibody production (Slifka & Ahmed 1998). Innate immune receptors are fixed in the genome which recognise conserved molecular patterns, whereas adaptive immune receptors specifically recognise infinite molecular structures (Medzhitov & Janeway 2000a).

1.1.2 Physical barriers

Physical anatomical barriers are an intrinsic defence mechanism versus microbial tissue penetrance via tight cellular junctions (Sperandio et al. 2015). Mucus, produced by mucosal and epithelial cells, forms a complementary physical and chemical membrane containing with antimicrobial proteins (Sperandio et al. 2015).

1.1.3 Recognition of microorganisms

The innate immune system recognises material from foreign microorganisms, or pathogen-associated molecular patterns (PAMPs), via non-clonal, germline-encoded receptors, termed pattern recognition receptors (PRRs) (Janeway 1989). PAMPs take the form of bacterial formylated peptides, lipopolysaccharides and lipoteichoic acids on bacterial cell surfaces or yeast cell wall mannans (Janeway 1989).

Broadly, PRRs are divided into humoral or cellular forms. A diverse range of humoral PRRs, which includes collectins, pentraxins and peptidoglycan recognition proteins, adhere to the specific molecular patterns of a bacterial surface in an antibody-independent manner. The professional phagocyte displays surface specific opsonin receptors, for example fragment Fc and complement receptors, which bind to their respective ligands that coat the bacteria and activate phagocytosis (Allen & Aderem 1996a). Diverse antimicrobial peptides are a form of secreted PRRs that achieve antimicrobial effect through pore insertion into cell membranes (Zasloff 2002). Other examples of secreted PRRs include collectins and lectins (e.g., mannose-binding lectin) that bind carbohydrates or lipid structures within microbial cell walls, with subsequent antimicrobial activity or stimulation of other innate immune responses, such as complement (Fujita et al. 2004; Epstein et al. 1996). The complement system has multiple roles within the immune system, which includes independent recognition and clearance of pathogens, and the opsonisation of phagocytic cell targets (Holers 2014).

Cell membrane and intracellular PRRs are sentinel regulatory receptors for the innate immune cells and anatomical barrier cells (Takeuchi & Akira 2010). Toll-like receptors (TLRs) are found in both plasma and endolysosome membranes (Beutler 2009). Lipopolysaccharide (LPS), a structural component of Gram-negative bacteria, causes shock and death within animal models (Beutler 2009). TLR-4 is a transmembrane LPS receptor, transducing a proinflammatory tumour necrosis factor (TNF) signal cascade (Beutler et al. 1985; Poltorak et al. 1998). 13 mammalian TLRs have been described (Dowling & Mansell 2016), each TLR has distinct ligands and proinflammatory signal transduction pattern, expressed across both immune and non-immune cells, in transmembrane or intracellular (endosomal) locations (Akira et al. 2006; Dowling & Mansell 2016). TLR activation and proinflammatory signalling have been associated with phagocytosis and phagosomal maturation (Blander & Medzhitov 2004) and adaptive immune system activation (Akira et al. 2006). Beyond TLRs, other families of cell surface and intracellular PRRs are now described, such as dectin-1 which is key to responses to fungal pathogens and intracellular nucleotide binding oligomerisation domain-like receptor (Takeuchi & Akira 2010). PRR also respond to host derived factors such as damage-associated molecular patterns like deoxyribonucleic acid released by nuclei and mitochondria, uric acid, and adenosine triphosphate released by damaged cells.

1.1.4 The innate cellular immune system

Metchnikoff first recognised that particular leucocytes are attracted to sites of infection or inflammation, and have the capacity to ingest and destroy pathogenic foreign material (Tauber 2003). The professional phagocytic cells, namely neutrophils, macrophages, and monocytes, as well as dendritic cells, constitute critical effector components of the innate immune system.

1.1.4.1 Neutrophils

Neutrophils are the most abundant of the circulating phagocytes (Hsieh et al. 2007), originating from the myeloblast cell lineage (Bainton et al. 1971). They belong to the polymorphonuclear granulocyte cell line to which the less populous eosinophils, basophils and mast cells also belong. During the initial stages of development distinct cytoplasmic secretory granules form that contain enzymes (Bainton et al. 1971; Borregaard & Cowland 1997). The respective granule subtypes contain heterogeneous populations of enzymes (Borregaard & Cowland 1997), but all contain lysozyme (Lollike et al. 1995).

The neutrophil is extremely short lived, with a reported half-life of 6-8 hours whilst in circulation, hypothetically attributed to the regulation of potential deleterious effects (Summers et al. 2010). The resting neutrophil population is divided equally in the blood between a circulating

pool and a marginating pool held within the microvasculature (Athens et al. 1961). With inflammatory stimuli, activated neutrophils are sequestered within the microvasculature via a selectin and integrin-dependent mechanism (Adams & S. Shaw 1994). Chemotactic factors induce neutrophil migration from endothelium towards the site of inflammation (Witko-Sarsat et al. 2000).

The other granulocytic cell types, namely basophils, eosinophils and mast cells share common features with neutrophils in addition to characteristic granule formation (Borregaard & Cowland 1997). These cells display PRRs and participate in an inflammatory response to stimulation, both microbial or host in the form of allergy (Stone et al. 2010). Eosinophils are multifaceted granulocytes similar to neutrophils, important to the control of parasitic defence (Y. Jung & Rothenberg 2014).

1.1.4.2 Innate lymphoid cells

A distinct component of the innate cellular immune system are the innate lymphoid cells (ILCs), that unlike other cellular components derive from lymphoid progenitors and populate most tissues (Klose & Artis 2016). Unlike T and B lymphocytes, ILCs are not dependent upon specific antigen stimulation (Walker et al. 2013). ILCs are subdivided by cytokine signature and are involved in immune regulation and tissue homeostasis. Group 1 ILCs, to which natural killer (NK) cells belong, generate a proinflammatory cytokine pattern (e.g., interferon-γ (IFN-γ) and TNF), akin to T_h1 cells (Spits et al. 2016). Group 2 ILCs, which characteristically produce interleukins (IL) IL-4, IL-5, IL-9 and IL-13, and group 3 ILCs, which produce IL-17A and IL-22, have profiles which reflect T_h2 and T helper-17 lymphocytes respectively (Klose & Artis 2016).

1.1.4.3 Mononuclear phagocytic cells

Monocytes and macrophages, or mononuclear phagocytes, arise from myelo-monocytic stems cells which differentiate via myeloblasts into monoblast and pro-monocyte precursor cells within bone marrow and the foetal liver (S. Gordon & P. R. Taylor 2005). Within the bone marrow, the promonocyte cell rapidly divides, but upon release the circulating monocytes are deemed end-stage (Van Furth & Cohn 1968). Circulating, non-dividing monocytes comprise 10% of peripheral circulating leucocytes. A non-circulating mature marginating monocyte population exists that reside within the microvasculature, which accounts for 50% of the total mature monocyte population (Van Furth & Sluiter 1986). Adding further complexity to the description of the monocyte population are the undifferentiated splenic monocytes that are recruited to inflamed tissues (Swirski et al. 2009).

Human monocytes are defined by the expression of the macrophage-colony stimulating factor (M-CSF) receptor, the CX3CR1 chemokine receptor CR3A (CD11b), CD11c and CD14 (Auffray et al. 2009; Geissmann et al. 2003). Monocytes have irregular cell shape, cytoplasmic vesicles and a high cytoplasm:nucleus ratio, yet distinct heterogeneous populations are evident, with variation in size and granularity (Auffray et al. 2009). Distinct populations of blood monocytes are apparent with differing functions suggested (Geissmann et al. 2003). Via a murine adoptive transfer system, inflamed tissue recruits short-lived $CX3CX1^{low}CCR2^{+}Gr1^{+}$ monocytes, whereas non-inflamed tissues recruit $CX3CX1^{hi}CCR2^{-}Gr1^{-}$ monocytes (Geissmann et al. 2003). The murine $CX3CX1^{low}CCR2^{+}Gr1^{+}$ ($Ly6C^{hi}CD62L^{+}$) monocytes resemble human $CD14^{+}$ classical monocytes, whereas the murine $CX3CX1^{hi}CCR2^{-}Gr1^{-}$ ($Ly6C^{low}CD43^{+}$) cells are comparable to human $CD14^{low}CD16^{hi}$ cells, termed CD16 monocytes, typically smaller and less granular than $CD14^{+}$ monocytes and absent of inflammatory chemokine receptors (e.g., CCR1, CCR2, CXCR1 & CXCR2) (Geissmann et al. 2003). The distribution within the mouse is approximately 50:50 between classical $Gr1(Ly6C)^{hi}$ and non-classical $Gr1(Ly\text{^}C)^{low}$, whereas classical $CD14^{+}$ monocytes constitute approximately 90% of blood monocytes within a healthy human (Strauss-Ayali et al. 2007). A third human monocyte population, termed intermediate ($CD14^{+}CD16^{+}$), is recognised as distinct from non-classical $CD14^{low}CD16^{hi}$ subset (Strauss-Ayali et al. 2007).

The divergence in monocyte characteristics may give rise to differing tissue mononuclear derivatives, with the $CD16^{+}$ monocytes repopulating resident tissue macrophages under steady state homeostasis versus $CD14^{+}$ supporting an inflammatory response (P. R. Taylor & S. Gordon 2003). Regulatory $CD16^{+}$ cells (half-life of 5 days) differ greatly from the short-lived inflammatory $CD14^{+}$ cells (half-life 20 hours) akin to neutrophils (Ginhoux & S. Jung 2014).

Monocyte PRRs are subject to chemokine stimulation, facilitating migration from circulation into tissues (Serbina et al. 2008). Approximately half of the circulating monocytes leave the bloodstream daily under steady state conditions (Geissmann et al. 2003). Circulating monocytes differentiate into tissue macrophages as well as other cells, e.g. dendritic cells that are specialised to present antigens to T lymphocytes and further regulate immune responses (Steinman et al. 1974; Geissmann et al. 2010).

Tissue macrophages are relatively abundant in all tissues, ranging from lymph nodes, the spleen, liver (Kupffer cells), the lung (alveolar macrophages), peritoneal (serosal) cavity and subcutaneous tissues, and are distinct from circulating monocytes (Van Furth & Cohn 1968). The mononuclear phagocytic system (MPS) model has circulating monocytes, having originated from the bone marrow, enter tissues and terminally differentiate into macrophages,

as observed in both in vitro and in vivo models (Ebert & Florey 1939; Bennett & Cohn 1966). Evolving evidence reveals a more complex system. Some tissue macrophages, and classical dendritic cells, originate and repopulate independent of monocytes (Yona et al. 2013; Hashimoto et al. 2013), supported by a plastic monocyte population recruited to inflamed tissues which differentiate to fulfil demand. Microglial cells and some Langerhans cells, macrophage equivalent cells of the CNS and skin respectively, derive from primitive embryonic (yolk sac-derived) macrophages, through a distinct differentiation pathway to that of monocyte-derived macrophages (MDMs) (Ginhoux & S. Jung 2014). The yolk sac-derived macrophages infiltrate all embryonic tissues, before foetal liver-derived macrophages, following the definitive haematopoiesis pathway, also colonise these tissues via the blood, and supplant the vast majority of the yolk sac-derived macrophages (Guilliams et al. 2013; Ginhoux & S. Jung 2014). The CNS is excepted from foetal liver-derived macrophage infiltration, with microglia derived entirely from the yolk-sac origin (Epelman, Lavine & Randolph 2014). Both yolk-sac derived and foetal liver-derived macrophages contribute to distinct cardiac macrophages populations (Epelman, Lavine, Beaudin, et al. 2014). Intestinal macrophages originate from monocyte-derived macrophages, which supplant the shorter lived embryological-origin macrophages (Guilliams & C. L. Scott 2017; Epelman, Lavine, Beaudin, et al. 2014).

Heterogeneity is apparent within macrophages of various tissues (alveolar, peritoneal, splenic macrophages & microglia), which display vast diversity in gene expression within a murine model (Gautier et al. 2012). Each tissue subset has a distinct molecular pattern, for example CD11a and epithelial cell adhesion molecule (EPCAM) (alveolar macrophages); CD93 and intercellular adhesion molecule 2 (ICAM-2) (peritoneal macrophages); vascular cell adhesion molecule (VCAM-1) and CD31 (splenic macrophages); CX3CR1 and sialic acid-binding immunoglobulin-type lectin H (SiglecH) (microglia) are specific to their tissue origins and function at these sites (Gautier et al. 2012).

Thought terminally differentiated with minimal proliferative capacity within the MPS model, when subjected to M-CSF stimulation macrophages can expand cell population to demand (L. C. Davies et al. 2013).

The long-lived tissue macrophages have vital homeostatic regulatory roles (L. C. Davies et al. 2013). Osteoclasts, derived from a shared macrophage predecessor, constantly repair and remodel bone, in their absence pathological changes manifest. The importance to tissue remodelling and homeostasis beyond bone are also demonstrated within the osteopetrotic mouse, devoid of M-CSF receptors, with atrophic mammary glands, hypogonadism (due to

both gonadal and hypothalamic-pituitary dysfunction) and small stature (failure of adipose tissue formation and muscles development) evident (Pollard 2009). Within glandular tissues, macrophages facilitate adaptations to nutrient and caloric homeostatic demands, and are associated with development of insulin resistance in chronic inflammatory conditions such as obesity (Wynn et al. 2013).

1.1.4.4 Macrophage activation and polarisation

The heterogeneous functions of macrophages are apparent within diverse activation profiles. Polarisation of macrophage activation has been proposed following exposure to cytokine or antimicrobial stimuli; classical and alternative activation states, and a comparable M1 and M2 grouping, reflect divergence of function subject to cytokine stimulation (Mills et al. 2000). The "classically" activated (or M1) macrophage refers to the state of activation often following challenge by a microorganism. Macrophages are capable of independent killing of internalised microorganisms, utilizing pathogen recognizing and microbicidal mechanisms shared with neutrophils.

The pro-inflammatory cytokine IFN-γ enhances macrophage microbicidal activity (Nathan et al. 1983) conferring a cell-mediated immune effector function to challenge intracellular pathogens (Mackaness 1962). The IFN-γ signal can originate from both innate and adaptive immune systems. Macrophage PRR stimulation by microorganisms stimulates expression of IL-12 and IL-18, demonstrated to recruit NK cells and T_h1 lymphocytes, and stimulate IFN-γ synthesis (Akira 2000). NK cells are capable of rapid, but transient, production of IFN-γ (Lieberman & Hunter 2002), whereas T_h1 cells provide a sustained pro-inflammatory signal, in an antigen-dependent manner (Nathan et al. 1983).

IFN-γ can independently activate macrophages, although some evidence indicates that a secondary synergistic signal may be required to prime the cell (Stout & Bottomly 1989). This signal may take the form of a microbial stimuli, e.g. LPS, or cytokine stimuli, e.g. TNF and granulocyte-macrophage colony-stimulating factor (GM-CSF) (Mantovani et al. 2004). The IFN-γ-activated M1 macrophage displays enhanced microbicidal behaviour, demonstrated with induction of the NADPH oxidase system, nitric oxide (NO) production and greater lysosomal enzyme production, plus enhanced antigen presentation via major histocompatibility complex (MHC) class II molecules (Schroder 2003). The classically activated macrophage expresses a pro-inflammatory cytokine signature of IL-1β, IL-6, IL-12, IL-23 and TNF-α (Mantovani et al. 2005). Phagocytosis of extracellular material can be converted from a receptor-mediated system to a macropinocytosis mechanism, enhancing the rate of intracellular microbicidal activity (BoseDasgupta & Pieters 2014).

The hypothesis of an “alternative” activation pathway originated from recognition of the T_h2 lymphocyte population with a distinct cytokine signature (Mosmann et al. 1986). This cytokine pattern promotes a humoral immune response, with expression of IL-4, IL-5, IL-10 and IL-13, with inhibition of macrophage cell-mediated immune behaviour (Mantovani et al. 2004). IL-4 and IL-13 specifically stimulate an alternative macrophage activation pattern with increased expression of the macrophage mannose receptor-1, a cell membrane PRR that detects constituent glycans of extracellular microorganisms (Stein et al. 1992; Doyle et al. 1994). Conversely, IFN-γ downregulates expression of MRC1 and the resultant macrophage endocytic behaviour (Mokoena & S. Gordon 1985). The alternative, or M2, activation state encompasses macrophages that do not meet the M1 phenotype, which comprises a diverse population, including those described above but also macrophages stimulated by alternative cytokines (e.g., IL-10), glucocorticoids, and immune complexes (Mantovani et al. 2004; Mosser & Edwards 2008). Exposure to various stimuli generates differing functional patterns under the M2 umbrella. Subset M2a derive from IL-4 and IL-13 stimulation and participate in T_h2 cell responses, which includes response to extracellular parasitic infection. Subset M2b derive from immune complex, antibody Fc-domain receptor (FcR) and TLR stimulation and participate in T_h2 cell activation and immunoregulation. The M2c subset are generated post IL-10 stimulation and participate in tissue remodelling and immunoregulation (Mantovani et al. 2004; Mosser & Edwards 2008). M-CSF and GM-CSF also participate in macrophage activation beyond haematopoiesis. Monocytes cultured in vitro with GM-CSF or M-CSF display characteristic polarised phenotypic patterns of pro-inflammatory (M1-type) or anti-inflammatory (M2-type) macrophages respectively (Verreck et al. 2004).

An alternative hypothetical perspective of classifying macrophage activation suggests a non-linear spectrum, encompassing proinflammatory/host defence, regulatory and wound-healing phenotype macrophage axes (Mosser & Edwards 2008). There is variation evident within the activated alternative macrophage phenotype following cytokine stimuli, with mixed ability to produce inflammatory cytokines evident (Mantovani et al. 2005). Plasticity of differentiated states is apparent. IL-4 stimulated macrophages, exhibiting M2a behaviour, convert to M2b phenotypic patterns if exposed to immune complexes (Edwards et al. 2006). However, translation of macrophage activation polarisation into in vivo functional disease models is complex, and difficult to replicate in vitro (L. C. Davies et al. 2013). It is also apparent that every activation stimulus produces a slightly different profile, and even for microorganisms, individual patterns of activation occur which although dominated by M1-associated modules can show varying degrees of activation of M2-associated transcriptional modules (Benoit et al. 2008).

1.2 Phagocytosis & phagosomal maturation

1.2.1 Phagocytosis

The transport of extracellular matter via progressive enclosure of the local extracellular membrane into the intracellular environment is termed endocytosis (Aderem & Underhill 1999). Endocytosis occurs constitutively in most cells, facilitating entry of nutrients or small molecules, including microorganisms, and modulates cell membrane protein expression (Swanson & Watts 1995). Pinocytosis, a form of endocytosis that internalises fluids and solutes, can be subdivided by the presence or absence of clathrin-coating of the vesicles, by receptor dependence and by size (Swanson & Watts 1995). Phagocytosis is a receptor-mediated, actin-dependent mechanism that facilitates ingestion of molecules >0.5μm (Aderem & Underhill 1999). Its purpose has evolved from nutritional maintenance to homeostasis and immunity through the uptake and degradation of infectious agents and senescent cells (Aderem & Underhill 1999).

Professional phagocytes display a diverse array of PRRs that recognise PAMPs and activate the phagocytosis pathway (Janeway 1989). A vast array of constitutive sentinel cellular PRRs target conserved components of the pathogen surface, including scavenger receptors (e.g., macrophage-receptor with collagenous structure (MARCO)) and C-type lectin receptors (e.g., mannose receptor c-type 1 (MRC1)) (Takeuchi & Akira 2010; Aderem & Underhill 1999). PRRs are essential to the phagocytosis of non-opsonised pathogens. Pathogen immune evasion can be achieved by restricting exposure of PAMPs to PRRs, the bacterial polysaccharide capsule prevents phagocytosis by this method (Karakawa et al. 1988). Specific antibodies directed against capsular antigens are required to opsonise encapsulated bacteria to overcome this virulence factor (Karakawa et al. 1988). Humoral PRRs, which include collectins, pentraxins and peptidoglycan recognition proteins function in concert with cellular mechanisms to opsonise pathogens prior to binding cell membrane opsonin receptors to stimulate phagocytosis (Aderem & Underhill 1999).

Upon ligand binding, the FcR group of transmembrane proteins associated with phagocytosis (FcγR I, IIA & III) must cross-link to stimulate src kinases (Ravetch 1997; Holowka et al. 2007). The immunoglobulin gene family tyrosine activation motifs (ITAM) that form part of the cytosolic FcR domain undergo tyrosine phosphorylation by the src kinases (Aderem & Underhill 1999). Phosphorylated ITAM domains recruit and activate the tyrosine kinase syk, which activates multiple pathways to stimulate proinflammatory cytokine expression and facilitates phagocytosis through cytoskeletal changes (Aderem & Underhill 1999). Actin polymerisation is fundamental to phagocytosis, and is dependent upon ITAM phosphorylation

and syk activation (Cox et al. 1996). Numerous adaptor proteins are recruited to the cytosolic FcγR complex following syk activation to enable downstream signalling (Flannagan et al. 2012). These adaptor proteins activate lipid-modification enzymes (e.g., phosphoinositide 3 kinase) and Rho family GTPases via recruitment of guanine nucleotide exchange factors (Flannagan et al. 2012). Conformational changes of the phagocyte enabling engulfment via actin polymerisation requires activation of the actin nucleation complex Arp2/3, which is dependent upon GTPases generating nucleation-promoting factors (e.g., Wiskott-Aldrich syndrome protein) (Flannagan et al. 2012).

Activation of macrophage transmembrane complement receptors (CR) and their downstream signalling cascade differs from that of FcR (Aderem & Underhill 1999). A co-stimulatory proinflammatory signal, such as TNF-α or GM-CSF, is necessary to internalise the bound opsonised pathogen. Actin polymerisation via Arp2/3 activation is conserved, in parallel with contingent actin nucleator mDia, both are activated by a CR-stimulated, tyrosine kinase-independent RhoA mechanism (Flannagan et al. 2012). Whereas FcR-mediated phagocytosis occurs by zipper process, where sequential Fc-FcR binding envelops the particle, complement-opsonised particles appear to passively sink into the phagocyte (Allen & Aderem 1996b). Phagocytosis mediation by CR does not elicit release of the pro-inflammatory effectors unlike phagocytosis mediated by FcR (Wright & Silverstein 1983; Aderem et al. 1985).

Upon activation the actin-myosin contractile system manipulates the cell architecture to extend pseudopods around the targeted particle until enveloped (Botelho & Grinstein 2011). A membrane-bound organelle, termed a phagosome, is formed by scission from the cell membrane, prompted by termination of the activation signal via ITAM domain dephosphorylation and phosphoinositide sequestration (Botelho & Grinstein 2011).

1.2.2 Phagosomal maturation

Maturation of the phagosome involves a highly coordinated sequence of membrane fusion and fission events with intracellular organelles, with the metamorphosis of an inert phagosome to an inhospitable, microbicidal phagolysosome (Desjardins et al. 1994). During maturation, the composition of the phagosomal membrane and luminal contents are actively altered by endosome fusion and fission (Desjardins et al. 1994).

1.2.2.1 The early phagosome

The early phagosome membrane is characterised by the presence of Rab5, a small GTPase, early endosome antigen 1 (EEA1) and an abundance of phosphatidylinositol-3-phosphate

(PI(3)P) (Figure 1.1) (Flannagan et al. 2012). Rab5 is the key regulatory component within the early phagosome, although the method of acquisition is not understood (Bucci et al. 1992). Rab 5 regulates early endosome attachment and motility along microtubules to target destinations (Nielsen et al. 1999). The numerous Rab proteins are distributed to distinct intracellular locations and regulate distribution of vesicular traffic between organelles (Zerial & McBride 2001). GTPase activity is regulated by a number of proteins that control GTP binding (Bucci et al. 1992). The activated GTP-bound Rab5 recruits and stimulates numerous effector proteins, an example being vacuole protein sorting (Vps) 34 which stimulates PI(3)P formation (Kinchen et al. 2008). This signalling lipid cascade is recognised by multiple effector proteins, including EEA1, and facilitates incorporation of stimulated proteins into the phagosome membrane. The tethering EEA1 protein, when associated with Rab5, serves to dock early endosomes to the phagosome membrane and then in union with soluble N-ethylmaleimide-sensitive factor attachment protein receptors (SNAREs) fuse the respective membranes (Christoforidis et al. 1999).

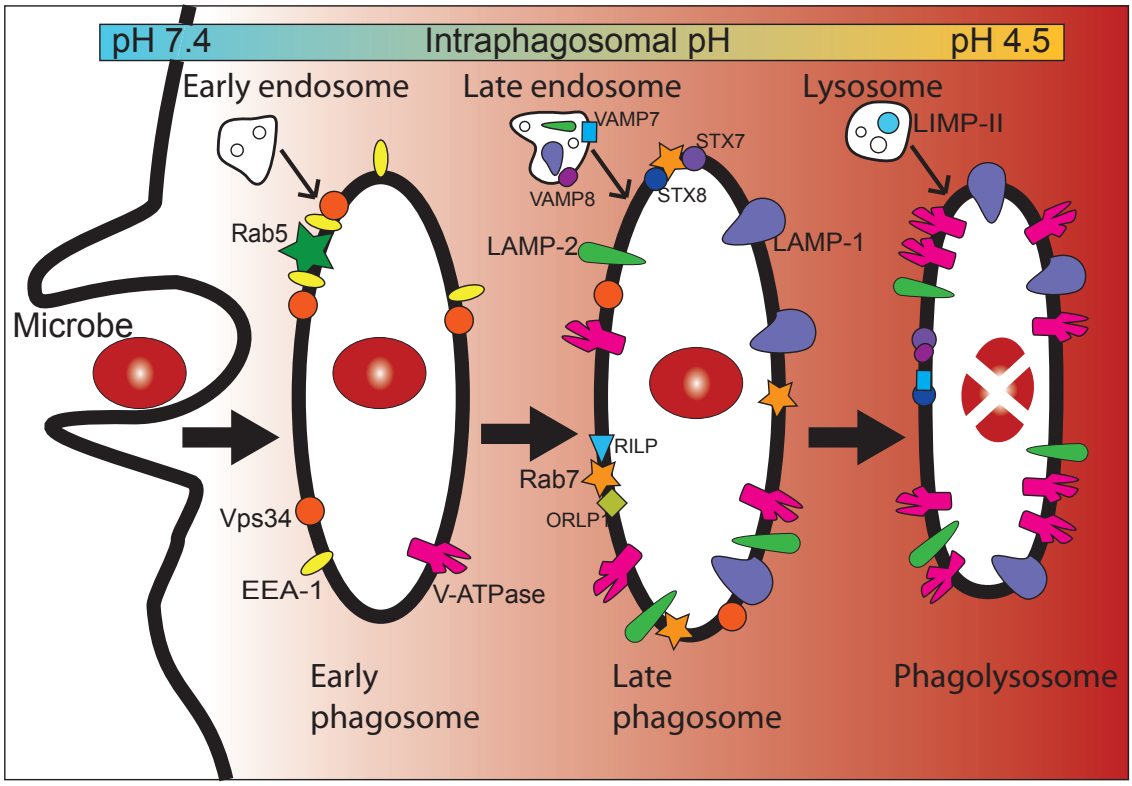

Figure 1.1 Phagosomal maturation.

Post-internalisation, the nascent phagosome acquires Rab5. The activated form of Rab5 acquires effector proteins EEA1 & Vps34, which facilitates docking and fusion of early endosomes and maturation towards the late phagosome. The late phagosome is characterised by substitution of Rab5 for Rab7 for which recruitment of LAMP1/2 is required.

The microbicidal phagolysosome forms following lysosome docking and fusion, mediated by target-SNAREs (STX7, STX8 & V-ti1-b) binding vesicular SNAREs (VAMP7/8). Progressive acquisition of phagosomal membrane vATPase enhances luminal acidification, required for microbial destruction.

1.2.2.2 The late phagosome

Progression from early to late maturation is defined by the substitution of Rab5 for Rab7 (Flannagan et al. 2012). Rab5 forms a complex with effector proteins Mon1a/b and Ccz-1 that serve to recruit and prime Rab7 for activation, whilst simultaneously inactivating Rab5 (Nordmann et al. 2010). The homotypic fusion and protein sorting (HOPS) complex is required to activate Rab7 (Rink et al. 2005). Active GTP-bound Rab7 is critical for phagosomal acidification and lysosome fusion (Harrison et al. 2003). Of the few Rab7 effector proteins identified, Rab7-interacting lysosomal protein (RILP) and oxysterol-binding protein-related protein 1 (ORLP1) coordinate traffic of the late phagosome centripetally into proximity with late endosomes and lysosomes. The late phagosome is also characterised by the presence of lysosome-associated membrane proteins (LAMP) 1 and 2, which are necessary for Rab7 recruitment and microbicidal activity (Huynh et al. 2007; Binker et al. 2007). Formation of the phagolysosome requires fusion of the mature phagosome to lysosomes, mediated by a SNARE complex of syntaxin 7 and 8, Vps10p tail interactor 1b (Vti1b) and vesicle-associated membrane proteins (VAMP) 7 and 8 (Wade et al. 2001).

1.2.2.3 The phagolysosome

The phagolysosome is defined by an acidic lumen (pH 4.5-5.0), active cathepsins, hydrolytic enzymes, oxidants and cationic peptides (Flannagan et al. 2012). The phagosome progressively accumulates vacuolar-ATPase (V-ATPase) from phagosome formation which drives increasing luminal acidification and progressive maturation (Desjardins et al. 1994; A. H. Gordon et al. 1980). The electrical potential generated via the V-ATPase is compensated for by additional ion channels that efflux cations and influx anions (Flannagan et al. 2012). Acidification serves to create an inhospitable environment for microbial growth, and also optimise activity of proteolytic enzymes (e.g., cathepsin D) (Huynh & Grinstein 2007).

1.2.3 Microbicidal activity of macrophages

The phagolysosome microbicidal strategy is multifaceted. Reactive oxygen species (ROS) and reactive nitrogen species (RNS) are well-characterised effectors. Phagocytic cells are capable of high-output production of ROS, with macrophages generating approximately half to one-third the amount of neutrophils (Nathan & Shiloh 2000).The NADPH oxidase NOX2 complex is a constitutive component on the phagosome membrane, which upon activation

transfers electrons from NADPH to oxygen (O_2) to generate superoxide anions (O_2^-) (Fang 2004). Bacterial products, for example LPS, or cytokines such as IFNγ or IL-8 trigger NADPH activation through translocation of multiple cytosolic proteins to the membrane-bound cytochrome c complex (Bogdan et al. 2000). Defective human NADPH oxidase activity is associated with recurrent bacterial infection, particularly *Staphylococcus aureus* infection (Babior 2004).

Dismutation of superoxide, either spontaneously or by superoxide dismutase (Sod) enzymes, forms hydrogen peroxide (H_2O_2), which in itself is deleterious to bacteria (Hyslop et al. 1995). Iron homeostasis is closely associated with the action of hydrogen peroxide (Fang 2011). Fenton chemistry generates the highly reactive hydroxyl free radicals OH^- and •OH from hydrogen peroxide, via oxidation of ferrous iron (Fe^{2+}) into ferric iron (Fe^{3+}) which is reduced back to ferrous iron in the presence of superoxide to allow the cycle to repeat (Bogdan et al. 2000). DNA bound to iron will be damaged subsequently. The deleterious effect is enhanced by increasing local iron concentration, accomplished by superoxide degrading iron storage proteins, for example ferritin, or from enzymatic [4Fe-4S] clusters (Keyer & Imlay 1996).

Hydrogen peroxide can be utilised by the myeloperoxidase (MPO) complex to produce microbicidal hypochlorite (OCl^-) by oxidation of chloride ions (J. E. Harrison & Schultz 1976). Although associated with microbial killing, and common to neutrophils azurophilic granules and macrophage lysosomes, individuals with defective MPO activity do not have increased incidence of bacterial disease (Lanza 1998). Within a murine MPO knock-out model of *S. aureus* infection, the gene was deemed dispensable (Nathan & Shiloh 2000).

In comparison, inducible nitric oxide synthase (iNOS), which generates nitric oxide radicals (•NO), is subject to transcriptional regulation via proinflammatory cytokine signal cascades, such as THFα and IFNγ, and hence slower to generate effector molecules (Fang 2004). Given potential deleterious effects to self, iNOS expression is tightly regulated at multiple levels (Bogdan et al. 2000). Reactions between the products of the MPO, iNOS and NOX2 pathways generate synergistic microbicidal products: within the MPO pathway, the addition of OCl^- and nitrite (NO_2^-) from iNOS pathway, generates nitryl chloride (NO_2Cl) and nitrogen dioxide (NO_2); the reaction between superoxide and •NO generates peroxynitrite ($ONOO^-$). Macrophages are adept at generating highly noxious synergistic products as they produce near equimolar levels of superoxide and nitric oxide (Nathan & Shiloh 2000). In the context of the acidified mature phagolysosome, recycling of nitrites (a product of NO oxidation) back to NO via dismutation of nitric oxide, will sustain inhospitable NO levels (MacMicking et al. 1997). Human

iNOS deficiency has not been recognised, but in a murine iNOS knock-out model of *S. aureus* infection, the iNOS was deemed contributory but not essential to host defence (Nathan & Shiloh 2000).

Independently, via ROS and NO, or in synergy via their joint reaction products RNS, these reactive species inflict injury and inhibit the capacity of pathogens to replicate (Flannagan et al. 2009). Each of these microbicidal products has different reactivity, stability, compartmentalisation and biological activity (Fang 2004) and often work synergistically (Nathan & Shiloh 2000). ROS-mediated, iron-associated damage of DNA damage manifests at low concentrations H_2O_2, whereas high H_2O_2 concentrations are linked to ROS-mediated damage to cellular targets, such as proteins, amino acids, lipids as well as Fe-S clusters and heme structures (Imlay 2003).

A plethora of antimicrobial proteins and peptides also act to either kill the organism or antagonise growth by restricting access to nutrients. Scavenger proteins, e.g. lactoferrin, or transmembrane ion channels, e.g. natural resistance-associated macrophage protein 1 (NRAMP1), limit availability of essential luminal nutrients Fe^{2+}, Zn^{2+} and Mn^{2+} (Cellier et al. 2007; Masson et al. 1969). Multiple groups of proteins act directly upon microbes and cause damage. The defensins and cathelicidins target the cell membrane, inserting pores that disrupt the integrity of the microbe (Lehrer et al. 1993; Zanetti 2005). The numerous hydrolases can be subdivided by target, with proteases divided further into endoprotease or exoprotease groups (Flannagan et al. 2009; Pillay et al. 2002):

- Carbohydrates: e.g., lysozyme.
- Lipids: e.g., phospholipase A2.
- Proteins:

  Endoproteases:
  - Cysteine proteases: e.g., cathepsins B, C, H, K, L, O, S & W.
  - Aspartate proteases: e.g., cathepsins D & E.
  - Serine proteases: e.g., cathepsin G.

  Exoproteases:
  - Carboxypeptidases: e.g., cathepsins A & X.
  - Aminopeptidases: e.g., cathepsins C & H.

Programmed cell death is an additional form of host defence against infection, particularly in disease caused by intracellular pathogens (Jorgensen et al. 2017). Apoptosis is a non-lytic form of programmed cell death with negligible inflammatory effect on local tissues (R. C. Taylor

et al. 2008). Induction of apoptosis is engaged when primary macrophage killing mechanisms have been exhausted, demonstrable in the context of *S. pneumoniae* infection when the macrophage canonical microbicidal controllable dose is exceeded (Dockrell et al. 2001). The apoptosis pathway is triggered by viable intraphagolysosomal bacteria and permeabilisation of the phagolysosome membrane which facilitates the release of activated cathepsin D (Bewley et al. 2011). Within differentiated macrophages, the expression of Bcl-2 antiapoptotic family members, predominantly the myeloid cell leukaemia sequence 1 protein (Mcl-1), regulates macrophage susceptibility to apoptosis (Marriott et al. 2005). Mcl-1 levels increase when the cell experiences homeostatic stress, for example when exposed to differentiation stimuli or certain cytotoxins (T. Yang et al. 1996). Mcl-1 expression increases following the initial stages of phagocytosis, attributed as compensatory to increased oxidative and nitrosative stress, and in the context of *S. aureus* infection remains elevated for an extended period compared to mock-infected cells, protecting the cell from apoptosis (Marriott et al. 2005; Koziel et al. 2009).

Downregulation of Bcl-2 antiapoptotic family members triggers dysregulation of mitochondrial homeostasis and mitochondrial outer membrane permeabilisation (Green & Reed 1998). The consequential release of mitochondrial contents, including cytochrome c, leads to the formation of the apoptosome and the activation of the caspase protease family, with the major effectors caspase-3, caspase-7 and caspase-7 undertaking extensive proteolysis during cell demolition (R. C. Taylor et al. 2008). The resultant apoptotic bodies are finally cleared by macrophages (Jorgensen et al. 2017).

Numerous lytic forms of programmed cell death can also occur, for example pyroptosis, but these are associated with greater degrees of inflammation and recruitment of additional phagocytic cells (Jorgensen & Miao 2015). Detection of some Gram-negative bacteria, e.g., Burkholderia spp., within the cytosolic environment initiates a signalling cascade incorporating caspase-1 and caspase-11. Intracellular bacteria are expelled by cell lysis, and with coordinated release of proinflammatory cytokines, secondary phagocytic cells can ingest and kill these pathogens (Jorgensen & Miao 2015).

1.3 Microbial immune evasion and intracellular persistence

1.3.1 Microbial evasion of phagocytosis

Numerous examples of microorganisms persisting within effector cells of the cell-mediated immune system have been described. Evasion of phagocytosis by restricting PRR detection is a common mechanism to many bacteria (Flannagan et al. 2012). The example of the bacterial capsule has been discussed earlier. In the context of *S. aureus*, multiple examples

of PRR antagonism have been described. Expression of the cell wall-associated protein A (SpA) enhances virulence through antagonism of opsonophagocytic mechanisms. Protein A features five immunoglobulin-binding domains that bind to the Fc region of humoral immunoglobulin-G and antagonises subsequent FcR binding and internalisation (Patel et al. 1987). Inhibition of opsonin deposition, or access to bound opsonin, by clumping factor A (ClfA) which binds and coats the bacterium with fibrinogen (Josefsson et al. 2001). Bacteria can also specifically subvert opsonisation by complement. The *Staphylococcus* complement inhibitor (SCIN) specifically binds and stabilises C3 convertases (C4b2a and C3bBb) on the bacterial surface, which antagonises C3b deposition central to all complement pathways (Rooijakkers et al. 2005). The extracellular fibrinogen-binding protein (Efb) binds C3d (part of the C3b complex), inhibiting complement activation and blocked phagocytosis (Lee et al. 2004). A further method to antagonise uptake is to subvert the PRR signalling cascades involving the Rho-GTPase family and PI3K, as utilised by *Yersinia* sp., *E. coli* and *Pseudomonas aeruginosa* (Dong et al. 2010; Cowell et al. 2000).

1.3.2 Microbial modulation of phagosomal maturation

Upon formation of the nascent phagosome and through the maturation process, specific pathogens can manipulate the host machinery to evade destruction (Table 1.1). Four broad strategies can be employed (C. C. Scott et al. 2003). Either the pathogen subverts the host endosomal trafficking machinery to establish a non-phagosomal organelle; arrests the maturation pathway; escapes from the phagosome into the cytoplasm; or resists antimicrobial effectors of a mature phagolysosome.

Mycobacteria tuberculosis employs multiple effector mechanisms to arrest phagosomal maturation, adapt host cell defences and escape the phagosome. Internalisation of *M. tuberculosis* is mediated by complement opsonisation and CR activation (Ernst 1998). Phagosome maturation is arrested at an early $Rab5^{+}$ stage, with failure to recruit the Rab5 effectors EEA1 and Vps34 in addition to reduced PI(3)P levels (Fratti et al. 2001). Two critical mycobacterial effectors are SapM and lipoarabinomannan. Both modulate PI(3)P levels, either directly via hydrolysis (SapM) or indirectly via reduced Vps34 recruitment, which is attributed to antagonism of cytosolic Ca^{2+} flux and probably the Vps34-recruiter protein, calmodulin (lipoarabinomannan) (Vergne et al. 2005). Pathogenic *Mycobacteria* spp. also possess the ability to escape the arrested phagosome, via the ESX-1 secretion system which expresses the CFP-10/ESAT-6 complex that contributes to pore formation (van der Wel et al. 2007).

Acidification of the phagosome, essential for phagosomal maturation, is inhibited by *M. tuberculosis* by interaction with V-ATPase (D. Wong et al. 2011). The secreted protein tyrosine

phosphatase (PtpA) binds to a subunit of V-ATPase and blocks its trafficking to the phagosome. Additionally, binding of PtpA to V-ATPase inhibits interaction with class C Vps complexes, for example the HOPS and core vacuole/endosome tethering (CORVET) complexes, which are essential for vesicle docking and phagosomal maturation (Sato et al. 2000; D. Wong et al. 2011). Disrupted V-ATPase activity, a hence phagosomal acidification, is achieved by other intracellular pathogens. *Legionella pneumophila* secretes a protein SidK which specifically binds to a subunit of V-ATPase and inhibits ATP hydrolysis, blocking proton influx (L. Xu et al. 2010).

Legionella pneumophila deviates normal phagosomal maturation to establish a distinct vacuole supportive for replication. The nascent phagosome is rapidly redirected away from the maturation pathway, as Rab5 fails to associate (Clemens et al. 2000). The niche "Legionella containing vacuole" (LCV) associates with endoplasmic reticulum (ER)-derived vesicles (Robinson & Roy 2006) and mitochondria (Tilney et al. 2001). Expression of the dot/icm ("Defect in Organelle Trafficking/Intracellular Multiplication") genes of *L. pneumophila* supports an effector protein type IV secretion system (T4SS), which ultimately subvert small GTPases Rab1 and Arf1 (Machner & Isberg 2006). These regulatory complexes direct the LCV to interact and harvest nutrients from the vesicular traffic between the ER and Golgi network (Isberg et al. 2009; Ingmundson et al. 2007). Thus, the pathogen avoids destruction via the phagolysosomal pathway and has hijacked the trafficking machinery of the host to attain nutrients essential for replication. *L. pneumophila* replicates with progressive volume expansion of the LCV and employs dot/icm effectors to inhibit host cell apoptosis (Isberg et al. 2009).

Other microorganisms co-opt the phagosomal cascade to establish pathogen-containing vacuoles. *Brucella* sp., e.g. *B. abortus*, employ similar evasion strategies to *L. pneumophila*, escaping from the phagosomal cascade and forming a vacuole in proximity to the ER (Celli et al. 2003). The Brucella-containing vacuole (BCV) transiently acquires Rab5 and EEA1 following interaction with early endosomes, with subsequent acquisition of LAMP1 but not Rab7 (Celli 2006). Expression of cyclic β-1,2-glucans and LPS, specifically smooth LPS O side chain, account for inhibition of late endosome and lysosome fusion, and this is hypothesised to occur through phagosome membrane lipid raft modification (Porte et al. 2003; Arellano-Reynoso et al. 2005). Progression to an intermediate state of phagosomal maturation results in luminal acidification, but this is necessary for survival (Porte et al. 1999). Acidic conditions stimulate expression of the VirB T4SS, required for redirection of the BCV into the ER vesicular trafficking system and replication (Celli 2006).

The environmental opportunistic bacteria *Burkholderia cepacia* complex arrest late phagosomal maturation at a $Rab7^+$, $LAMP1^+$ stage (Huynh et al. 2010). The mechanism is yet to be elucidated, but the bacteria impair Rab7 activation, inhibiting luminal acidification. A T4SS is also important to pathogenesis, with actin-modification via Rho-GTPase antagonism described, but the precise effector for the Rab7 antagonism remains elusive (Flannagan et al. 2011).

Coxiella burnetti shares pathogenic similarities with *Chlamydia* spp. with regard to intracellular persistence and biphasic life cycle (Heinzen et al. 1996). Within the extracellular environment, they exist as infectious, metabolically inactive small cell variants. Upon internalisation via endocytosis, the bacteria differentiate into active, replicative, large cell variants. Whereas *Chlamydia* spp. establish a vacuole distinct from the phagosome cascade, *C. burnetti* progresses through $Rab5^+$ and $Rab7^+$ compartments to a mature phagolysosome (Voth & Heinzen 2007). Maturation of the *Coxiella*-containing vacuole is delayed before lysosome fusion. Expression of the dot/icm T4SS, akin to *Legionella* sp., facilitates interaction with the autophagosome pathway, possibly to acquire nutrients essential for differentiation to the antimicrobial-resistant large cell variant (Voth & Heinzen 2007). Despite phagolysosome formation, *C. burnetti* can resist antimicrobial effectors, with an acidic environment required for replication (Heinzen et al. 1996).

Escaping from the phagosome into the cytosol accounts for the intracellular survival of a small number of bacteria that includes *Listeria monocytogenes*, *Francisella tularensis*, *Rickettsia* spp. and *Shigell*a spp.. Disruption of the phagosomal membrane is accomplished by insertion of a transmembrane pore (Gruenberg & van der Goot 2006). Following internalisation, *L. monocytogenes* progresses to a $Rab7^+$, PI(3)P abundant, $LAMP1^-$ late phagosome state with an acidified lumen (Henry et al. 2006). In response to luminal acidification, *L. monocytogenes* expresses listeriolysin O, a cholesterol-dependent toxin which forms a transmembrane pore (Beauregard et al. 1997). Rather than lyse the phagosome, insertion of the pore perturbs Ca^{2+} and H^+ transmembrane gradients, consequently halting late endosome and lysosome fusion (Shaughnessy et al. 2006). Escape by degradation of the phagosome membrane is associated with listeriolysin O plus two phospholipase C enzymes (Shaughnessy et al. 2006).

F. tularensis behaves in a similar pattern, progressing to an acidified phagosome, with transient association with Rab7, LAMP1 and LAMP2, but lysosomes fail to fuse, as demonstrated by absence of cathepsin D (Santic et al. 2008; Clemens et al. 2004). The membrane integrity of the *F. tularensis* containing phagosome becomes progressively

disrupted by an unknown mechanism, granting bacterial escape into the cytosol (Clemens & Horwitz 2007; Ozanic et al. 2015).

Genetic encoding of pore-forming proteins can be found in numerous pathogens, demonstrating a role in escaping from a vacuole in *L. monocytogenes* and *S. flexneri*, as well as the protozoa *Trypanosoma cruzi* and *Leishmania* spp. (Hybiske & Stephens 2008). *Rickettsia* spp. rapidly escape from nascent phagosomes utilizing an alternative mechanism, the vacuole is disrupted by phospholipases by an unrecognised mechanism (Renesto et al. 2003).

The mechanisms described so far require manipulation of the phagosomal trafficking machinery. If the pathogen containing vacuole cannot be disrupted, in the manner of *L. monocytogenes*, then the vacuole must be modified for pathogen survival. The lipid composition of the phagosome, to which PI(3)P contributes, and raft-formation, necessary for endosome fusion, are critical to maturation, and are manipulated by *Brucella* spp. and *M. tuberculosis*. Bacterial secretion systems of effector molecules, particularly T4SS, co-opt the trafficking machinery and deviates the pathogen-containing vacuole away from antimicrobial mediators. The last means of negating the antimicrobial phagolysosomal pathway is resistance to the numerous microbicidal effectors and will be discussed in specific regard to *S. aureus* below. This may entail resistance to acidic conditions, antimicrobial proteins, ROS, NO and sequestration of essential nutrients, but do not account for specific manipulation of phagosomal maturation (Flannagan et al. 2009).

Table 1.1 Pathogens and mechanisms used to arrest or escape the maturing phagosome

Microbe	Mechanism
M. tuberculosis	Early phagosomal arrest Hydrolysis of PI(3)P – SapM Antagonism of Vps34 recruitment via Ca^{2+} modulation – lipoarabinomannan Inhibition of V-ATPase – PtpA Phagosomal escape – ESX-1 secretion system
L. pneumophila	Subversion of early/nascent phagosomal dot/icm T4SS subverts Rab1 & Arf1 recruitment Inhibition of V-ATPase – SidK Forms ER-associated vacuole
Salmonella spp.	Early phagosome arrest

	Suspected antagonism of Rab5 to Rab7 conversion
Brucella sp.	Subversion of late phagosome Modulation of phagosome membrane lipid rafts Forms ER-associated vacuole
Burkholderia cepacia	Late phagosome arrest Suspected Rab7 activator antagonism via T4SS
Helicobacter pylori	Late phagosome arrest Inhibition of Rab7 activation
L. monocytogenes	Late phagosome arrest Disturbed Ca^{2+} and H^{+} flux – Listeriolysin O pore insertion
Francisella spp.	Late phagosome arrest Unknown mechanism, pore insertion suspected
S. aureus	Late phagosome arrest Unknown mechanism
Coxiella burnetti	Phagolysosome Progression to phagolysosome transiently delayed T4SS identified
Phagosomal Escape	Mechanism
M. tuberculosis	Early phagosome escape – ESX-1 secretion system
L. monocytogenes	Late phagosome escape Listeriolysin O pore insertion & phospholipase C action
Francisella spp.	Late phagosome escape Suspected pore insertion
Shigella spp.	Pore forming toxin – IpaB & IpaC (Hybiske *et al.* 2008)
Rickettsia spp.	Phospholipase A2 secretion (Hybiske *et al.* 2008)
S. aureus	Pore-forming toxins, e.g., phenol soluble modulins

1.4 *Staphylococcus aureus*

1.4.1 Epidemiology

Staphylococcus aureus is a major global medical pathogen, associated with both community and hospital-acquired infections. It has the potential to cause a wide range of disease, ranging from superficial skin infections to deep tissue pathologies such as infective endocarditis. The burden of *S. aureus* infection to society is substantial, with growing healthcare-associated costs and mortality (de Kraker et al. 2011).

S. aureus bloodstream infection, otherwise known as bacteraemia (SAB), is one of the most common forms of bloodstream infection, the incidence of which has grown considerably over recent decades (Frimodt-Møller et al. 1999). Within the UK, the incidence of SAB is 21 cases per 100,000 population (Santic et al. 2008). The incidence of SAB in the UK has remained

consistent since mandatory report was introduced in 2011, with 12,390 cases reported to Public Health England between April 2020 and March 2021 (Public Health England, 2021). The mandatory reporting has demonstrated a progressive decline in the incidence of methicillin-resistant *S. aureus* (MRSA) bacteraemia cases, with rates of 1.2 per 100,000 population (Public Health England 2021). Conversely, in the same period there has been a 33.4% increase in incidence of methicillin-sensitive *S. aureus* (MSSA) bacteraemia cases. This increase has been associated with increasing community-associated onset cases. Of the MSSA bacteraemia cases, 71.5% were of community onset between April 2020 and March 2021 (Public Health England, 2021).

Within the European Union, SABs account for almost 1000 excess hospital bed days at a cost of than €170 million annually, with over 12,000 excess deaths (de Kraker et al. 2011). The costs are related to the significant mortality and morbidity; the 30-day mortality rate is approximately 30% and 43% develop complications (Wyllie et al. 2006; Fowler et al. 2003).

1.4.2 Clinical management & antimicrobial resistance

With the advent of anti-staphylococcal treatments, resistant strains rapidly emerged associated with greater virulence. The prevalence of MRSA and vancomycin-resistant *S. aureus* strains in hospital and community settings poses a significant challenge to global healthcare (Boyce et al. 2005; Howe et al. 1998; Zetola et al. 2005). In the pre-penicillin era, SAB was associated with a mortality of over 80%, and almost universally fatal in the over 40 year old population (Skinner & Keefer 1941).

Optimal antimicrobial management of SAB remains ill-defined (Thwaites et al. 2011). Despite prompt therapy, persistent SAB (i.e. present for at least 3 days after starting effective treatment) occurs in 38% of cases, and is the strongest predictor for complications (Khatib et al. 2006; Fowler et al. 2003). The risk increases with antimicrobial resistance (Hawkins et al. 2007).

S. aureus has conventionally been considered an extracellular pathogen, yet intracellular persistence is demonstrable in both professional and non-professional phagocytic cells (Rogers & Tompsett 1952; Melly et al. 1960; Kapral & Shayegani 1959). *S. aureus* persisting in the intracellular environment adapt to host antimicrobial responses (Ellington et al. 2005; Eiff et al. 2001). Escape of the intracellular reservoir of latent bacteria formed within the host cell could facilitate relapsing metastatic infections (Ellington et al. 2005). A clinical trial utilising adjunctive rifampicin, an antibiotic able to achieve intracellular penetration, with standard of care antibiotic therapy for treatment of SAB failed to demonstrate any overall benefit compared

to standard antibiotic therapy (Thwaites et al. 2018). This trial did however demonstrate a statistically significant reduction in the rate of bacterial and clinically-defined disease recurrence with the use of rifampicin. A better understanding of intracellular persistence is required to develop more effective treatment for *S. aureus*.

Following recovery from *S. aureus* infection, the host remains vulnerable to future infection. Immunological memory fails to generate as a consequence of superantigen immunosuppressive effects during infection (T. J. Foster 2005; Fraser & Proft 2008). Attempts to develop a vaccine against *S. aureus* have, to date, failed when assessed within human trials (Proctor 2012; Fowler & Proctor 2014).

1.4.3 The microorganism

Members of the *Staphylococcus* genus are Gram-positive cocci, 0.5 – 1.5μm in diameter that occur singly, and in pairs, tetrads, short chains and irregular grapelike clusters (Götz et al. 2006). Staphylococci are non-motile, non-spore forming, usually catalase positive and typically unencapsulated or with a limited capsule (Götz et al. 2006). Most species are facultative anaerobic organisms, positive for catalase and benzidine tests, with most displaying rapid growth in aerobic conditions (Götz et al. 2006). The staphylococci cell wall consists of a thick (typically 60 – 80 nm) homogenous layer, consisting of peptidoglycan, teichoic acid, and protein (Götz et al. 2006). The physical properties of peptidoglycan confer a rigid cell shape and ameliorates the high internal osmotic pressure to maintain the integrity of the cell (Silhavy et al. 2010).

The genus *Staphylococcus* belongs to the Staphylococcaceae family, which also includes the lesser-known genera *Gemella, Jeotgalicoccus, Macrococcus, Nosocomiicoccus* and *Salinicoccus,* of the Bacillales order within the Firmicutes phylum (Public Health England, 2020). To date, there are 53 recognised species of staphylococci and 28 subspecies (Public Health England, 2020). Only a few are pathogenic in the absence of predisposing factors (Que & Moreillon 2010). The pathogenic *S. aureus* is distinct within the *Staphylococcus* genus given the significantly greater number of adhesin and toxin genes compared to coagulase-negative staphylococci (CoNS) (Que & Moreillon 2010). *S. aureus* is phenotypically defined by pigmented colonies, with demonstrative properties of catalase, staphylocoagulase, clumping factor, haemolysins and thermonuclease (Götz et al. 2006).

Morphological variants, in the form of small colony variants (SCV) are commonly isolated from recurrent protracted infections, for example chronic osteomyelitis and infected osteosynthetic prostheses (Que & Moreillon 2010). The development of SCVs is classically associated with

antimicrobial exposure, typically aminoglycosides, driving selective pressure for mutations within the respiratory chain (Kahl et al. 2016). Functional resistance to antimicrobial therapeutic agents, other than the selecting agent, is common (Kahl et al. 2016).

1.4.4 Ecology

Staphylococci are ubiquitous colonisers of skin and mucosa of primates, as well as domestic animals and birds, but infrequently upon non-primate wild animals (Kloos 1980). Staphylococci have greatest success of colonisation areas featuring pilosebaceous units, sweat glands and the mucous membranes surrounding opening of body cavities, including axilla and perineum (Götz et al. 2006). Specifically, *S. aureus* has a niche preference for anterior nares, either as a resident or transient member of the normal flora (Kluytmans et al. 1997). Human colonisation with *S. aureus* is common, approximately 30% of the population are colonised, which increases in populations with medial comorbidities, and is associated with development of disease (Wertheim et al. 2005).

1.4.5 The *Staphylococcus aureus* genome

Since the *S. aureus* genome was first sequenced in 2001 (Kuroda et al. 2001) over thirteen thousand genome assemblies have been detailed in public databases (ncbi.nlm.nih.gov/genome). The circular genome has a median size of 2.83 Mb, encoding a median 2747 sequences (https://www.ncbi.nlm.nih.gov/genome/genomes/154). The *S. aureus* genome can display approximately 22% variability between different strains (Lindsay & Holden 2004). The variation is found within the accessory genome of comprising approximately 25% of the whole genome, with the highly conserved core genome constituting the remaining 75% (Lindsay & Holden 2004). These variable regions frequently determine virulence and antibiotic resistance profiles which in turn enables successful dissemination into an environment (Holden et al. 2013).

Genome evolution can develop through several mechanisms, for example, random point mutations causing single nucleotide polymorphism or variations in core genes via duplications of repeat regions or deletions. But the greatest driver of variation of virulence factors (and antibiotic resistance) occurs within the *S. aureus* accessory genome, through horizontal transfer the of mobile genetic elements (MGE), comprising of bacteriophages (φ), pathogenicity islands, plasmids, transposons (Tn) and staphylococcal cassette chromosomes (Malachowa & DeLeo 2010). The MGE can even be acquired from different bacterial species; the transfer of the vancomycin-resistance determining operon *vanA*, encoded by Tn*1546*, between an *Enterococcus* to *S. aureus* serves as an example (Perichon & Courvalin 2009).

Variation is evident within isolates of the same genetic background, termed clonal complex (CC), with asymmetric distribution of MGE. The often-used example of variable clinical virulence is the superantigen toxic shock syndrome toxin-1 (TSST-1) which is expressed by approximately 20% of natural isolates (Lindsay et al. 1998). Across clinical isolates, the gene that encodes TSST-1 is located on the MGE *S. aureus* pathogenicity island 1 (SaPI1) and this MGE is able to spread horizontally within distinct clonal complexes (Lindsay et al. 1998). Phages (φ80α and φ11) mobilise SaPI1 from the donor strain and subsequently transferred the MGE into naïve recipients.

Progressive accumulation of genetic information concerning *S. aureus*, through multi-locus sequence typing (MLST), has resulted into subdivisions of CC lineages (Lindsay 2010a). The CC is defined as containing matched sequence types which share at least five of seven identical housekeeping genes with at least one other sequence type in the group (Day et al. 2001). If all seven alleles are identical, the isolates are termed clones. *S. aureus* populations consist of about ten dominant human lineages and many minor lineages (Lindsay 2010b). The MLST method unifies CCs to a shared ancestor, which then enables the evolution of *S. aureus* CCs to be traced. The largest of these are CC1, CC5, CC8 and CC15. Of note, CC5 and CC8 have generated the majority of the major pandemic MRSA clones; CC5 contains multiple community-associated (CA-) methicillin-resistant *S. aureus* (MRSA) strains CA-MRSA and hospital-acquired (HA) MRSA strains, including USA100 strains; CC8 contains the CA-MRSA epidemic clone USA300, and strains COL and Newman. CC1 contains multiple CA-MRSA strains including MW2/USA400 (Monecke et al. 2011). Molecular diagnostic methods has allowed for identification of dominant clones with linkage of pathogenic features, ecologies and dissemination (Lindsay 2010a).

The complete genome sequence of the CA-MRSA clone USA300, used for these studies, was reported in 2006 (Diep et al. 2006). Since initially isolated in 2000 (Pan et al. 2003), it has become established as one of the two dominant CA-MRSA strains in North America (along with MW2/USA400), associated with skin and soft tissue infections and invasive disease (Francis et al. 2005; Miller et al. 2005). The genome consists of 2.872 Mb chromosome and three plasmids, with the majority of the accessory genome spread across five MGEs (Diep et al. 2006). Known virulence factors and resistance determinants are encoded within these MGEs and two plasmids, these include: the type IV staphylococcal chromosomal cassette *mec* (SCC*mec* IV) conferring methicillin resistance; the arginine catabolic mobile element (ACME) type I facilitating the arginine deiminase pathway and oligopeptide permease system; staphylococcal pathogenicity island 5 (SaPI5) facilitating expression enterotoxins; prophage φSA2usa includes genes encoding the Panton-Valentine leucocidin; φSA3usa contains genes

that encode the chemotaxis inhibitory protein (CHIP) and staphylokinase; plasmid pUSA02 confers tetracycline resistance; pUSA03 confers macrolide, lincosamides, streptogramin B and mupirocin resistance (Diep et al. 2006).

Within a murine infection model and *in vitro* neutrophil assays, USA300 was significantly more virulent than clinical strains COL and MRSA252 (Voyich et al. 2005)

1.4.6 *Staphylococcus aureus* antimicrobial resistance

S. aureus has developed resistance to virtually all antibiotic classes in clinical use (Que & Moreillon 2010). Antimicrobial resistance (AMR) can take the form of acquired resistance through antimicrobial inactivation, for example penicillinase; antimicrobial target modification, for example enterococci attain glycopeptide resistance via expression of alternate peptidoglycan precursors that bind vancomycin less effectively (Gold 2001); or by decreasing antimicrobial access to the target, for example the multidrug efflux pumps that expel fluoroquinolones from the bacterial cell (J. Davies & D. Davies 2010)

Acquisition of AMR occurs promptly after widespread application of an antibiotic (J. Davies & D. Davies 2010). In the context of penicillin, its discovery by Fleming took place in 1928 (Fleming 1929), and clinical usage commenced from the 1940s (Abraham et al. 1941). Even before clinical application, a penicillin resistance mechanism had been identified within an *Escherichia coli* strain which secreted penicillinase (Abraham & Chain 1940), and within a few months of widespread application, clinical penicillin-resistant *S. aureus* was evident (Rammelkamp & Maxon 1942). The widespread application of penicillin ultimately limited its practicality; experimentally, antibiotic pressure was demonstrated to drive the development of AMR (Klimek et al. 1948).

S. aureus AMR is acquired predominantly by horizontal gene transfer (Lowy 2003). Within the USA300 accessory genome, multiple AMR mechanisms are encoded: β-lactams (SCC*mec* IV); fluoroquinolones (chromosomal mutation of drug target gyrase gene *gyrA*); tetracycline (plasmid pUSA02 *tetK* gene); macrolides, lincosamides and mupirocin (pUSA03 *ermC* and *ileS*) (Diep et al. 2006).

1.5 *Staphylococcus aureus* pathogenesis

Given the significance of *S. aureus* clinical disease, acquiring an understanding of host-pathogen interaction has been sought since the recognition that *S. aureus* causes disease (Ogston 1882). *S. aureus* possesses a multitude of virulence factors, which may be structural or secreted, with the purpose to gain an evolutionary survival advantage across various

environments (T. J. Foster 2005). In order to successfully infect the host, *S. aureus* must colonise a site, overcome host resistance mechanisms, obtain essential nutrients for growth and then spread to new foci (Lowy 1998).

1.5.1 Regulation

S. aureus pathogenicity is a consequence of responsive regulatory systems which sense and react to stimuli, from both the environment and bacterial population, subsequently modulating expression of a vast array of virulence factors (Haag & Bagnoli 2017). In the context of the stages of infection described above, the initial challenge is for a few bacteria to adherence to host tissue and begin to replicate whilst simultaneously negating host defensive strategies (T. J. Foster 2005). Adaptation is necessary, for once a *S. aureus* population has bloomed, the emphasis must change to obtaining adequate nutrients from the environment, redeploying resources to more suited virulence factors.

The two-component system (TCS) accessory gene regulator (Agr) is central to *S. aureus* adaptability, controlling expression of surface adhesion molecules and exoproteins in a growth-phase dependent manner (Novick 2003). The two operons of Agr are promoted by promotor 2 (P2) and promotor 3 (P3). Constitutive low-level P2 expression generates the autoinducing peptide (AIP), a correlate for bacterial density, via the AIP-precursor AgrD, which undergoes proteolysis by the transmembrane AgrB protein. Amplification of transmembrane AgrC activation, a histidine kinase sensor, by AIP concentration promotes the activity of the transcription response regulator AgrA. The P2 operon thus functions within a positive feedback loop. Control of transcription and translation of multiple virulence factors derives from the P3 operon-encoded effector molecule RNAIII that promotes exotoxin expression (including the cytotoxins haemolysins α, β, γ, and δ, PVL and superantigens) whilst downregulating surface bound proteins (Novick 2003).

The hypothesised Agr model at low bacterial concentration, thus low-level AIP, promotes surface protein expression (e.g., collagen binding protein and clumping factors A and B) supporting initial adherence to the tissue structures; population growth requires adaptation towards nutrient acquisition, sourced from local host tissue destruction by toxin production. In the context of intracellular persistence, hypothetically the lumen of an enclosed *S. aureus*-containing phagosome will serve to concentrate AIP levels, ultimately promoting exotoxin expression and phagosomal lysis (Wesson et al. 1998).

S. aureus possesses 16 TCS regulators, plus an additional TCS within the SCC*mec* (Kuroda et al. 2001), consisting of an archetypal membrane histidine kinase sensor and response

regular (Novick 1991). In addition to virulence gene expression, TCS regulators are associated with antibiotic resistance, cell wall metabolism, respiration, and nutrient sensing (Table 1.2) (Haag & Bagnoli 2017).

Table 1.2 Two-component system regulators of *S. aureus*

Adapted from (Haag & Bagnoli 2017). The Nebraska transposon mutant library (NTML) strain code is also detailed for later reference to findings within this study.

TCS	Alternate name(s)	Function	NTML code
WalRK	YycFG, VicRK, MicAB	Cell wall homeostasis (Dubrac et al. 2007); Upregulation of SaeRS function (Delauné et al. 2012)	n/a
TCS2[§]		Kdp-like potassium transport (Freeman et al. 2013)	n/a
TCS3		Unknown	n/a
LytRS		Autolysis, murein hydrolase activity (Brunskill & Bayles 1996) Biofilm formation (Sharma-Kuinkel et al. 2009)	LytR NE0958 LytS NE0147
GraRS	ApsRS	Cationic antimicrobial peptide resistance (S.-J. Yang et al. 2012) Antimicrobial resistance (Howden et al. 2008) Oxidative stress resistance (Falord et al. 2011)	GraR NE0481 GraS NE1756
SaeRS		Immune evasion (Olson et al. 2013) Host tissue adherence (Liang et al. 2016) Biofilm formation (Mrak et al. 2012)	SaeR NE1622 SaeS NE1296
TCS7		Unknown	n/a
ArlRS		Adhesion (Fournier & Hooper 2000); Autolysis downregulation(Fournier & Hooper 2000) Virulence factor expression downregulation (Fournier et al. 2001)	ArlR NE1684 ArlS NE1183
SrrAB	ShrSR, ResED	Aerobic and anaerobic respiration (Kinkel et al. 2013); Virulence (Richardson et al. 2006); Resistance to nitrosative stress & hypoxia (Kinkel et al. 2013; Wilde et al. 2015); QoxABCD/cytochrome biosynthesis (Kinkel et al. 2013) *S. aureus* Nitric oxide synthase regulator (James et al. 2019);	SrrA NE1309 SrrB NE0588
PhoPR		Phosphate homeostasis & cell wall maintenance (Botella et al. 2014)	PhoR NE0618 PhoP NE1486
AirSR	YhcRC	Oxygen sensing (Sun et al. 2011) Reactive oxygen species resistance, via staphyloxanthin production (J. W. Hall et al. 2017)	

VraSR		Cell wall biosynthesis (Kuroda et al. 2004) Antimicrobial susceptibility (Kuroda et al. 2004; Mehta et al. 2011)	VraS NE0823 VraR NE0554
AgrAC		Virulence (Gillaspy et al. 1995); Structural and secreted virulence factor expression. Quorum sensing (George et al. 2019) Phenol-soluble modulin expression (Queck et al. 2008)	AgrA NE1532 AgrC NE873
KdpED		Potassium homeostasis (Freeman et al. 2013) Virulence & intracellular survival (Freeman et al. 2013)	KdpD NE0423 KdpE NE1249
HssRS		Haem homeostasis (Wakeman et al. 2014)	
NreCBA		Nitrogen homeostasis, aerobic & anaerobic respiration (Fedtke et al. 2002);	NreC NE1669 NreB NE1157
BraRS	NsaRS, BceRS	Bacitracin susceptibility (Kawada-Matsuo et al. 2014).	BraR NE1643 BraS NE1116

[§]Contained within SCC*mec*, not present in all strains;

In addition to Agr, the *S. aureus* exoprotein (Sae) TCS participates in global regulation of virulence factor expression (Giraudo et al. 1994). Extrinsic agents with potential to cause membrane injury, for example H_2O_2 or H^+, serve to activate the Sae TCS (Geiger et al. 2008). Other regulators, notably Agr and the global regulator ferric iron uptake regulator (Fur), influence Sae function (Johnson et al. 2011). Activity of both Sae and Fur are required for induction of *S. aureus* oxidative stress response and exotoxin production, hypothesised to reflect reduced iron availability being an environmental marker for contact with host and thus immune evasion requirements. Sae TCS activation is integral to the expression of multiple virulence factors, notably haemolysin-α, -β and -δ (Giraudo et al. 1997), PVL (Geiger et al. 2008), SCIN and CHIPS (Rooijakkers et al. 2006), and host adhesion complexes (Harraghy 2005).

The alternative sigma factor B (σ^B) represent the second major mechanism for environmental stimuli response (Novick 2003). External challenges to homeostasis, for example temperature, energy source depletion and chemical stimuli , prompt σ^B expression which is subject to post-translational regulation (P. F. Chan & S. J. Foster 1998b). The global regulatory σ^B effect however is reciprocal to Agr, upregulating exoprotein expression at early growth phase and with a downregulatory effect upon secreted proteins towards stationary growth phase (Bischoff et al. 2004).

The staphylococcal accessory regulator (Sar) locus of DNA-binding proteins, that includes SarA, is capable of regulating numerous genes (Novick 2003). SarA binds to AT-rich

sequences, which includes at least one site within the Agr operon (Cheung et al. 1992). As a consequence to SarA binding, translation of the respective genes are affected, including increased expression of the Agr operons (Cheung et al. 1997) and downregulation of many other genes (P. F. Chan & S. J. Foster 1998a).

1.5.2 Subversion of chemotaxis

Van de Velde and colleagues demonstrated that leucocytes migrated to sites within the pleural cavity of a rabbit post *S. aureus* injection (Van de Velde 1894). This example is representative of the initial phase of host-pathogen interaction, namely the migration of host immune cells to the site of infection. *S. aureus* can subvert leucocyte migration, thus remaining remote to potential harm. The chemotaxis inhibitory protein of staphylococci (CHIPS) inhibits pro-chemotactic signalling through blockade of the C5a-receptor and formyl peptide receptor (FPR), which in combination with the blockade of the intracellular adhesion molecule-1 (ICAM-1) by the bacterial extracellular adherence protein (Eap), antagonises phagocyte migration to sites of infection (de Haas et al. 2004; Chavakis et al. 2002). Within the nascent period of infection, expression of CHIPS is beneficial for development of local infection (de Haas et al. 2004). Additional examples include the protease Staphopain A which blocks neutrophil recruitment via cleavage of CXCR2 and subsequent chemokine signalling (Laarman et al. 2012); the FRP-like 1 (FPRL1) inhibitory protein (FLIPr) blocks FPRL1, with effect akin to that of CHIPS (Prat et al. 2006);

1.5.3 Adhesion to host tissue

MSCRAMMs (microbial surface components recognising adhesive matrix molecules) which are anchored to the bacterial cell wall, bind to specific host tissue matrix constituents (T. J. Foster 2019). Although a number have an undetermined ligand, specific examples have been demonstrated to participate in pathogenesis. As previously described, clumping factors A and B (ClfA & ClfB) bind to platelet GPIIb/IIIa via fibrinogen cross-linking, thus in theory supporting wound colonisation, whilst also cloaking the bacteria from opsonin binding. In addition to ClfA, fibronectin-binding proteins A and B (FnBPA & FnBPB) have been associated with development of infective endocarditis in a rat model (Que et al. 2005). The experimental model demonstrates the adhesion factors contribute to tissue colonisation during the establishment of infection. Likewise, in a model of osteomyelitis, the collagen-binding protein (Cna) mediates attachment to collagenous tissues and establish infection in bone (Elasri et al. 2002).

1.5.4 Biofilm

The biofilm, a scaffold within which dormant bacterial communities gather is formed of an extracellular polysaccharide and protein-based network (Götz 2002). Formation of the biofilm

requires initial adherence of the bacterial cell to a material surface. Subsequently, the bacteria grow and generate the slime-like polysaccharide intercellular adhesin (PIA), under the control of the *ica* (intercellular adhesion) operon (Götz 2002). Within the PIA, bacteria are protected from host immune function and antimicrobial agents (R. Patel 2005).

1.5.5 Subversion of opsonisation

As discussed above, evasion of host immune interaction by restricting PRR detection is a common mechanism to many bacteria (Flannagan et al. 2012). *S. aureus* blocks immunoglobulin-G binding via protein A (A. H. Patel et al. 1987); opsonin deposition by ClfA (Josefsson et al. 2001); C3b deposition via SCIN binding C3 convertases (Rooijakkers et al. 2005); Efb binds to C3d inhibiting complement activation (Lee et al. 2004). Additionally, the presence of the extracellular polysaccharide capsule aids pathogenesis, with demonstratively reduced phagocyte internalisation (Nilsson et al. 1997).

1.5.6 Secreted factors

S. aureus is capable of leucocyte lysis by expression of numerous pore-forming cytolytic toxins that damage cell membranes and subsequent lysis (Prévost et al. 1995). The original description of leucocidins also came from the work of Van de Velde and colleagues also demonstrated that virulent *S. aureus* strains would cause leucocyte death (Van de Velde 1894). Distinction between leucocidins developed, particularly between α-haemolysin (Hla) and the specificity of Panton-Valentine leucocidin (PVL) towards granulocytes (Panton & Valentine 1932; Gladstone & van Heyningen 1957). The small pore-forming toxin Hla and PVL are recognised virulence factors in the pathogenesis of *S. aureus* pneumonia and sepsis (Powers & Wardenburg 2014). PVL belongs to a family of bi-component leucotoxins characterised by their leuco-cytolytic action, which includes leucocidin AB/GH, leucocidin ED and γ-haemolysin (Hlg) (Yoong & Torres 2013). The specificity of PVL leucotoxicity to innate immune cells has been demonstrated with the specific binding of the PVL complex to the complement receptors C5aR and C5L2, expressed by neutrophils, monocytes and macrophages, but not lymphocytes (A. S. N. Spaan et al. 2013).

In what initially seems a conflicting concept, Hla has been associated with a cytoprotective effect upon infected macrophages (Koziel et al. 2015). As noted previously, internalisation of *S. aureus* triggers sustained upregulated expression of the macrophage anti-apoptotic regulator Mcl-1 (Koziel et al. 2009). This observation was subsequently shown to be dependent upon intracellular expression of Hla, with increased Mcl-1 level, upregulated NFκB activation and IL-6 secretion. The effect was could be partially antagonised via inhibition of

the TLR2, leading to Koziel *et al*. concluding that the intracellular PRR participate in sensing intracellular *S. aureus*, having escaped from the phagosome via the effect of Hla (Koziel et al. 2015).

Whereas the leucotoxins described above are highly-specific towards leucocytes, phenol soluble modulins (PSMs) are indiscriminate in cell target (Peschel & Otto 2013). PSMs, common to the *Staphylococcus* species, have significant receptor-independent cytolytic activity and have been associated with increased virulence, particularly within MRSA strains (Wang et al. 2007; Peschel & Otto 2013). The pore-forming toxins have also been proposed to lyse phagosomes to facilitate intracellular escape, notably PSMs (Grosz et al. 2013; Surewaard et al. 2013). Although genetically conserved within the staphylococcal genome, variable expression of PSMs is evident between strains, regulated by the global regulator *agr* (Queck et al. 2008; Wang et al. 2007).

1.5.7 Resistance to host microbicidal effector mechanisms

S. aureus evasion of antimicrobial effector mechanisms once internalised into the phagosome are numerous (T. J. Foster 2005). In response to local environmental changes associated with phagocytosis and phagosomal maturation, *S. aureus* modulates gene expression of virulence factors to adapt to the intracellular environment via global regulatory elements discussed in greater detail previously (Voyich et al. 2005; Cheung et al. 2004). In the context of phagocytosis, expression of the regulatory elements Sae, Vra and SarA were up-regulated, with repression of Agr and σ^B operons (Voyich et al. 2005). In additional models, expression of Sar is associated with intracellular persistence (Gresham et al. 2000).

Resistance to oxidative stress via ROS is achieved through multiple mechanisms, broadly categorised as: enzymatic detoxification; scavenger molecules; iron sequestration; repair mechanisms; and regulator stress responses (Fang 2004). *S. aureus* express two superoxide dismutases, the dominant SodA and SodM, which convert superoxide to H_2O_2 and O_2 (Karavolos 2003). Catalase, found within the bacterial cytoplasm, converts H_2O_2 to O_2 and water (Mandell 1975). The *S. aureus* peroxiredoxins, for example alkylhydroperoxide reductase (AhpC), reduce alkyl hydroperoxides to their respective alcohols, are induced upon exposure to H_2O_2 (Poole 2005). Catalase and AhpC demonstrate compensatory regulation, both being under (negative) regulation by the peroxide response regulator (PerR) (Cosgrove et al. 2007). The flavohaemoglobin Hmp (haemoglobin-like protein) confers an additional oxidoreductase functions, including NO reduction and alkylhydroperoxide reduction (Bonamore & Boffi 2007). As opposed to enzymatic detoxification, scavenging molecules detoxify ROS non-enzymatically. Examples include the cell wall carotenoid staphyloxanthin

pigment, cytoplasmic thioredoxin and free manganese ions (Mn^{2+}) (G. Y. Liu et al. 2005; Horsburgh, Wharton, et al. 2002).

Homeostatic regulation of essential transition metals, which includes iron, copper, manganese, and zinc, is necessary to negate toxicity given their role in electron transfer and generation of ROS, as discussed previously. Given the importance of these elements to bacterial metabolic function, the host actively limits the opportunity for bacteria to obtain them, demonstrated by the NRAMP1 active transportation of Mn ions from the phagosome lumen (Jabado et al. 2000). In the example of iron homeostasis, *S. aureus* features specific transporters and storage proteins, for example ferritin and the Dps-homologue MrgA, to limit free cytoplasmic iron (Horsburgh, Ingham, et al. 2001). The intake and storage of iron is regulated by the ferric uptake regulator (Fur) (Horsburgh, Ingham, et al. 2001). Within a *Salmonella* model, unregulated free intracellular Fe^{2+} enhances susceptibility to H_2O_2 (Velayudhan et al. 2007). Fur binds a specific DNA sequence when complexed with Fe^{2+}. Acting as a repressor, it restricts transcription of Fe^{2+} acquisition and transport systems; Fur also promotes expression of catalase, hence antagonising the Fenton reaction (Horsburgh, Ingham, et al. 2001). PerR represses expression of several genes integral to ROS resistance, including catalase, AhpC and MrgA, when complexed with Fe^{2+} or Mn^{2+} (Horsburgh, Wharton, et al. 2002). Exposure to H_2O_2 dissociates the metal ions, consequently removing PerR repression. Within a murine *S. aureus* skin abscess model, a *perR* mutant was significantly attenuated, indicating its role in virulence (Horsburgh, Clements, et al. 2001).

Homeostatic regulatory mechanisms which detect fluctuations in fundamental metabolic pathway intermediates are sensitive to damage inflicted by ROS and RNS. As exemplified by Fur, fluctuations in Fe^{2+} concentrations, potentially secondary to enzyme complex Fe-S cluster damage by ROS, trigger a reactionary cascade. Similar regulatory pathways which are sensitive to damage inflicted by oxidative or nitrosative stress have been recognised. Akin to Fur, the manganese transport repressor (MntR) and copper-sensitive operon repressor (CsoR) instigate stress response following ROS exposure (Horsburgh, Wharton, et al. 2002; Baker et al. 2010). Multiple regulators have been demonstrated to be sensitive to oxidative stress, for example MsaB (also known as CspA) (Pandey et al. 2019), and nitrosative stress, for example SrrAB TCS (Kinkel et al. 2013). Voyich *et al*. demonstrated that in response to neutrophil phagocytosis, *S. aureus* upregulated expression of the stress response genes *katA, sodA-M, ahpC, dps,* thioredoxin and thioredoxin reductase as well as regulators Fur, SaeRS, SarA and VraRS, and numerous metabolism and haemolysin genes (Voyich et al. 2008).

An alternative means to negate ROS and RNS toxicity is for the sites of damage to be repaired. Although the majority of the experimental evidence derives from other bacterial species, homologues to repair effectors have been identified in *S. aureus* (Gaupp et al. 2012). Bacteria deficient in repair mechanisms have greater susceptibility to phagocytes and reduced virulence (Fang 2004). These mechanisms include DNA and protein repair systems, for example thioredoxin reductase, methionine sulfoxide reductase and Fe-S cluster repair systems (Gaupp et al. 2012).

Resistance to RNS injury is also suggested in strains of *S. aureus* by the presence of genes encoding an arginine deiminase system, a virulence factor utilised by *Streptococcus pyogenes* (Diep et al. 2006). Antimicrobial peptides can be resisted by a combination of anionic cell wall components, carotenoid pigments, inhibition by staphylokinase and direct cleavage by proteinases (A. N. Spaan et al. 2013). Amino acid substitutions of cell wall constituents repel defensin peptides by electron repulsion, for example the multiple peptide resistance factor (MprF) protein alters phosphatidylglycerol composition (Peschel et al. 2001). Lysozyme is countered by the acetylation of peptidoglycan, the cell wall target of lysozyme, by O-acetyltransferase A (OatA) (Bera et al. 2004).

1.5.8 The interaction between macrophages and *S. aureus*

Macrophages are the resident tissue phagocyte and critical to the removal of deleterious pathogens. The capacity for macrophages to independently eradicate *S. aureus* can be demonstrated in a neutropenic murine model (Rehm et al. 1980). Neutrophils are also important in the defence of the host against *S. aureus* challenge, but *S. aureus* is capable of resisting killing by these professional phagocytes (A. N. Spaan et al. 2013).

Despite multiple virulence factors to circumvent phagocytosis, *S. aureus* are rapidly internalised by macrophages, primarily through non-opsonic pathways (e.g., the scavenger receptor MARCO) and at low inocula intracellular bacteria are effectively killed by tissue macrophages (Jonsson et al. 1985; Palecanda et al. 1999; Jubrail et al. 2016). Tissue macrophage capacity to clear bacteria is easily overwhelmed at increased inocula, suggesting pathogen immune subversion (Jubrail et al. 2016).

An evolving intracellular persistence pattern has emerged in which *S. aureus* survive in phagosomes for extended periods (3-4 days), with upregulation of antiapoptotic factors, before induction of macrophage necrosis (Koziel et al. 2009; Kubica et al. 2008). Similar conclusions have been reached by the Dockrell group which demonstrated initial intracellular killing of *S. aureus* in macrophages is only partially effective and the delayed killing mechanism apoptosis-

associated killing is not engaged (Jubrail et al. 2016). Macrophages readily ingest *S. aureus* but the ability to kill declines over time. The *S. aureus*-containing vacuole progresses to a $LAMP1^+/LAMP2^+$ late phagosome state but fails to appropriately acidify or gain phagosome-lysosome fusion markers (e.g., lysosomal integral membrane protein, LIMP-II). Activation of the lysosomal protease cathepsin D, a critical stimulus for apoptosis-associated killing, which helps sensitise the macrophage for apoptosis upstream of engagement of a mitochondrial pathway of apoptosis, does not occur (Jubrail et al. 2016).

Recent publications also documented impaired phagosomal maturation within differing models of mononuclear differentiation. Within a less differentiated mononuclear cell that more akin to a monocyte, *S. aureus* was located within a $LAMP1^+$ acidified phagosome devoid of cathepsin D (Tranchemontagne et al. 2015). Similar findings were found within a macrophage model stimulated with M-CSF to an M2 activation phenotype, where intracellular *S. aureus* progressed to a $LAMP1^+$ acidified vacuole consistent with a phagolysosome, in which it was able to replicate before escaping into the cytoplasm (Flannagan et al. 2016). The discrepancies in luminal acidification could be attributed to differing phagosome pH regulation between human M1 and M2 macrophages. An M1 phagosome has reduced V-ATPase activity compared to an M2 phagosome, which is associated with delayed fusion with late endosome and lysosomes (Canton et al. 2014). Within the M1 phagosome, protons are consumed in reaction with ROS to form hydrogen peroxide, which in combination with proton efflux via voltage- and zinc ion-sensitive channels results in reduced phagosome acidification (Canton et al. 2014).

1.6 Summary

Professional phagocytes of the immune system are essential in the protection of the host against infection. But the corruption of their antimicrobial function by *S. aureus* challenges conventional medical management. Metastatic spread of *S. aureus* is a recognised complication of infection, for which professional phagocytes are hypothesised vehicles for pathogenic dissemination (Gresham et al. 2000; Thwaites & Gant 2011; Ellington et al. 2005). Transplantation of infected neutrophils from sites of infection into a naïve animal results in infection (Gresham et al. 2000). Only a few infected phagocytes may be required, with metastatic infection arising from just a few bacteria that have passed through the “bottleneck” of the phagocyte (Prajsnar et al. 2012). The macrophage would serve as an ideal phagocytic host to the parasitic *S. aureus* due to the longer life cycles and migratory capacity to lymphoid tissue (Bellingan et al. 1996). The purpose of this project is to obtain greater understanding of how the privileged niche of intracellular *S. aureus* develops within macrophages and will

facilitate the development of new therapeutic strategies through identification of microbial and host factors regulating this process.

Chapter Two
Materials & Methods

2.1 Cell line maintenance

2.1.1 Cell line maintenance media

2.1.1.1 Roswell Park Memorial Institute 1640 medium

Roswell Park Memorial Institute 1640 (RPMI 1640) medium with 2 mmol l^{-1} L-glutamine (Lonza). Stored at 4°C.

2.1.2 THP-1 cell line

The human leukaemic cell line THP-1 has a distinct monocyte phenotypic pattern (Tsuchiya et al. 1980). The THP-1 cell expresses surface Fc and C3b receptors and demonstrates phagocytic behaviour and lysozyme synthesis.

2.1.2.1 THP-1 cell maintenance

THP-1 cells (ATCC) were maintained in RPMI 1640 media supplemented with 10% (v/v) heat inactivated foetal calf serum (h/i FCS). The THP-1 cells were split twice per week at a dilution of 1:3 in sterile T75 flasks. The THP-1 cell culture was maintained at 37°C with 5% carbon dioxide (CO_2).

2.1.2.2 THP-1 cell differentiation

THP-1 cells were differentiated using 200 nM phorbol 12-myristate acetate (PMA) (Sigma) in RPMI 1640 media supplemented with 10% h/i FCS (Daigneault et al. 2010). The THP-1 cells were seeded at a concentration of 4 x 10^5 cells ml^{-1}, with 1 ml added to each well of a 24 well format or 100µl added to each well of a 96 well format. As treatment with the PMA stimulus results in some cell loss, the THP-1 cells were seeded at approximately double the target concentration of 2 x 10^5 cells ml^{-1}. Following 3 days incubation with PMA, the media was removed, the cells gently were washed with phosphate buffer solution (PBS) and replaced with fresh RPMI 1640 media supplemented with 10% h/i FCS. The THP-1 cells were then incubated at 37°C with 5% CO_2 for an additional 5 days to further differentiate THP-1 cells towards a tissue macrophage phenotype (Daigneault et al. 2010). The granularity of the THP-1 cell increases after 3 days in fresh media (day 6 in total) and continues to increase over time. Viability of the THP-1 cell however reduces with time. Therefore a 5-day rest period (8 days in total after initial stimulation) is optimal for differentiation versus viability (Daigneault et al. 2010).

2.1.3 Monocyte derived macrophages

2.1.3.1 Monocyte derived macrophage isolation and differentiation

Whole blood was collected from healthy human donors that have provided informed written consent to participate. The South Sheffield Research Ethics Committee provided ethical approval for the collection of blood for the study of monocyte derived macrophages.

Peripheral blood mononuclear cells (PBMC) were isolated using Ficoll Plaque (GE healthcare) density centrifugation from whole blood. Blood was decanted aseptically into T75 culture flasks. Within a sterile 50 ml conical centrifuge tube, 12.5 ml Ficoll Plaque was added to 25 ml of blood. Each tube was centrifuged at 1500 x *g* for 23 minutes. The serum was subsequently discarded, and the cell layers transferred to fresh conical centrifuge tubes and centrifuged at 1000 x *g* for 13 minutes. The resulting supernatants were discarded, and the pellets removed gently. The pellets were combined and re-suspended in sterile PBS and centrifuged at 1000 x *g* for 13 minutes. The supernatant was discarded and the PBMC pellet re-suspended in 10 ml RPMI 1640 media with 2 mmol l^{-1} L-glutamine supplemented with 10% h/i FCS.

PBMCs were diluted to a concentration of 2 x 10^6 cells ml^{-1}, with 1 ml added to each well of a 24 well format or 100μL added to each well of a 96 well format. After 24 hours, non-adherent cells were removed, and adherent monocyte derived macrophage (MDM) cells cultured in fresh RPMI 1640 media supplemented with 10% h/i FCS. Media was replaced twice weekly until the differentiated cells were used at day 14.

2.1.3.2 Monocyte derived macrophage polarisation

Protocol 2.1.3.1 results in the generation of an unpolarised MDM phenotype. A M1 polarised macrophage phenotype was obtained followed the above protocol supplemented with 20 ng ml^{-1} human granulocyte-macrophage-colony stimulating factor (GM-CSF) (Gibco) to the culture media. M2 polarised MDMs were obtained following protocol 2.1.3.1 supplemented with 10 ng ml^{-1} human macrophage-colony stimulating factor (M-CSF) (Gibco).

2.2 Bacterial preparation and maintenance

2.2.1 Bacteriological media

Media were prepared using distilled water (dH_2O) and were sterilised by autoclaving for 20 minutes at 121°C and 15 psi.

2.2.1.1 Brain heart infusion broth

Brain Heart Infusion (BHI)(Oxoid) 37g l^{-1}

1% (w/v) Bacteriological agar (VWR) was added to make BHI agar.

2.2.1.2. Tryptone soya broth

Tryptone Soya Broth (TSB)(Oxoid) 30 g l^{-1}

1% (w/v) Bacteriological agar was added to make TSB agar.

2.2.1.3. Columbia blood agar

Columbia agar (base)(VWR) 42 g l^{-1}

Heat-sensitive additives added when media cooled to 45 – 50°C.

2.2.1.4 LK broth

Tryptone (Oxoid) 10 g l^{-1}

Yeast extract (Oxoid) 5 g l^{-1}

KCl 7 g l^{-1}

1.5% (w/v) Bacteriological agar was added to make LK bottom agar.

0.5% (w/v) Bacteriological agar was added to make LK top agar.

2.2.2 Bacterial strains

2.2.2.1 *S. aureus* strains

The *S. aureus* strains used in this study are listed in Table 2.1.

Strains were grown from –80°C Microbank beads (Pro Lab Diagnostics) and cultured onto TSB agar plates and mixed with antibiotics where required to maintain resistance markers as detailed in Table 2.1. For long-term storage, a single colony was inoculated into Microbank bead stocks and stored at –80°C.

For liquid culture, ten colonies of the desired *S. aureus* strain were added to 25 ml BHI broth and grown aerobically at 37°C with 5% CO_2, shaken at 250 rpm. Exponential growth phase defined as an $OD_{600nm} \approx 1.0$. Upon attainment of logarithmic growth, cultures were divided into 1 ml aliquots in 1.5 ml micro-centrifuge tubes and stored at –80°C.

Table 2.1 *S. aureus* strains used in this study

Strain	Description	Growth Conditions
SH1000	Functional *rsbU*$^{+}$ derivative of 8325-4 (Horsburgh, Aish, et al. 2002)	TSB media
Newman	Constitutively active *sae* strain (Duthie & Lorenz 1952)	TSB media
USA300 JE2	Plasmid cured USA300_FPR3757, Met^{R} (Fey et al. 2012)	TSB media
SH1001 agr::tet	Constructed by A. Needham	TSB media plus 5 μg ml^{-1} Tetracycline
SH1000 saeR::Tn551	Constructed by T. Prajsnar	TSB media plus 5 μg ml^{-1} Erythromycin
SH1000 sarA::kan	Constructed by L. Wright	TSB media plus 50 μg ml^{-1} Kanamycin
SH1000 fur::tet	Constructed by L. Wright	TSB media plus 5 μg ml^{-1} Tetracycline
SH1000 perR::kan	Constructed by L. Wright	TSB media plus 50 μg ml^{-1} Kanamycin
SH1000 mntR::tet	Constructed by L. Wright	TSB media plus 5 μg ml^{-1} Tetracycline
SH1000 sodA::Tn917	Constructed by L. Wright	TSB media plus 5 μg ml^{-1} Erythromycin
SH1000 sodM::tet	Constructed by L. Wright	TSB media plus 5 μg ml^{-1} Tetracycline
SH1000 sagA::tet	Constructed by V. Fairclough	TSB media plus 5 μg ml^{-1} Tetracycline
SH1000 sagB::kan	Constructed by B. Turner	TSB media plus 50 μg ml^{-1} Kanamycin
NE92-JE2	USA300 *qoxA*::Tn *bursa aurealis* Ery^{R} Lin^{R} Constructed by J. Connolly	TSB media plus 5 μg ml^{-1} Erythromycin & 25 μg ml^{-1} Lincomycin
NE92-SH	SH1000 *qoxA*::Tn *bursa aurealis* Ery^{R} Lin^{R} Constructed by J. Connolly	TSB media plus 5 μg ml^{-1} Erythromycin & 25 μg ml^{-1} Lincomycin
NE95-JE2	USA300 *agrB*::Tn *bursa aurealis* Ery^{R} Lin^{R} Constructed by J. Connolly	TSB media plus 5 μg ml^{-1} Erythromycin & 25 μg ml^{-1} Lincomycin
NE95-SH	SH1000 *agrB*::Tn *bursa aurealis* Ery^{R} Lin^{R}	TSB media plus

	Constructed by J. Connolly	5 μg ml^{-1} Erythromycin & 25 μg ml^{-1} Lincomycin
NE224-JE2	USA300 hypothetical protein SAUSA300_0192 disrupted by Tn *bursa aurealis* Ery^R Lin^R Constructed for this study	TSB media plus 5 μg ml^{-1} Erythromycin & 25 μg ml^{-1} Lincomycin
NE224-SH	SH1000 hypothetical protein SAUSA300_0192 disrupted by Tn *bursa aurealis* Ery^R Lin^R Constructed for this study	TSB media plus 5 μg ml^{-1} Erythromycin & 25 μg ml^{-1} Lincomycin
NE229-JE2	USA300 hypothetical protein SAUSA300_1119 disrupted by Tn *bursa aurealis* Ery^R Lin^R Constructed by J. Connolly	TSB media plus 5 μg ml^{-1} Erythromycin & 25 μg ml^{-1} Lincomycin
NE229-SH	SH1000 hypothetical protein SAUSA300_1119 disrupted by Tn *bursa aurealis* Ery^R Lin^R Constructed by J. Connolly	TSB media plus 5 μg ml^{-1} Erythromycin & 25 μg ml^{-1} Lincomycin
NE714-JE2	USA300 *mtnN*::Tn *bursa aurealis* Ery^R Lin^R Constructed for this study	TSB media plus 5 μg ml^{-1} Erythromycin & 25 μg ml^{-1} Lincomycin
NE714-SH	SH1000 *mtnN*::Tn *bursa aurealis* Ery^R Lin^R Constructed for this study	TSB media plus 5 μg ml^{-1} Erythromycin & 25 μg ml^{-1} Lincomycin
NE732-JE2	USA300 *qoxB*::Tn *bursa aurealis* Ery^R Lin^R Constructed for this study	TSB media plus 5 μg ml^{-1} Erythromycin & 25 μg ml^{-1} Lincomycin
NE732-SH	SH1000 *qoxB*::Tn *bursa aurealis* Ery^R Lin^R Constructed for this study	TSB media plus 5 μg ml^{-1} Erythromycin & 25 μg ml^{-1} Lincomycin
NE873-JE2	USA399 *agrC*::Tn *bursa aurealis* Ery^R Lin^R Constructed by J. Connolly	TSB media plus 5 μg ml^{-1} Erythromycin & 25 μg ml^{-1} Lincomycin
NE873-SH	SH1000 *agrC*::Tn *bursa aurealis* Ery^R Lin^R Constructed by J. Connolly	TSB media plus 5 μg ml^{-1} Erythromycin & 25 μg ml^{-1} Lincomycin
NE912-JE2	USA300 *clpP*::Tn *bursa aurealis* Ery^R Lin^R Constructed by J. Connolly	TSB media plus 5 μg ml^{-1} Erythromycin & 25 μg ml^{-1} Lincomycin

NE912-SH	SH1000 *clpP*::Tn *bursa aurealis* Ery^R Lin^R Constructed by J. Connolly	TSB media plus 5 μg ml^{-1} Erythromycin & 25 μg ml^{-1} Lincomycin
NE945-JE2	USA300 *brnQ*::Tn *bursa aurealis* Ery^R Lin^R Constructed for this study	TSB media plus 5 μg ml^{-1} Erythromycin & 25 μg ml^{-1} Lincomycin
NE1048-JE2	USA300 *pyrP*::Tn *bursa aurealis* Ery^R Lin^R Constructed by J. Connolly	TSB media plus 5 μg ml^{-1} Erythromycin & 25 μg ml^{-1} Lincomycin
NE1048-SH	SH1000 *pyrP*::Tn *bursa aurealis* Ery^R Lin^R Constructed by J. Connolly	TSB media plus 5 μg ml^{-1} Erythromycin & 25 μg ml^{-1} Lincomycin
NE1084-JE2	USA300 hypothetical protein SAUSA300_1017 disrupted by Tn *bursa aurealis* Ery^R Lin^R Constructed for this study	TSB media plus 5 μg ml^{-1} Erythromycin & 25 μg ml^{-1} Lincomycin
NE1084-SH	SH1000 hypothetical protein SAUSA300_1017 disrupted by Tn *bursa aurealis* Ery^R Lin^R Constructed for this study	TSB media plus 5 μg ml^{-1} Erythromycin & 25 μg ml^{-1} Lincomycin
NE1366-JE2	USA300 *katA*::Tn *bursa aurealis* Ery^R Lin^R Constructed for this study	TSB media plus 5 μg ml^{-1} Erythromycin & 25 μg ml^{-1} Lincomycin
NE1366-SH	USA300 *katA*::Tn *bursa aurealis* Ery^R Lin^R Constructed for this study	TSB media plus 5 μg ml^{-1} Erythromycin & 25 μg ml^{-1} Lincomycin
NE1374-JE2	USA300 *tagB*::Tn *bursa aurealis* Ery^R Lin^R Constructed for this study	TSB media plus 5 μg ml^{-1} Erythromycin & 25 μg ml^{-1} Lincomycin
NE1374-SH	SH1000 *tagB*::Tn *bursa aurealis* Ery^R Lin^R Constructed for this study	TSB media plus 5 μg ml^{-1} Erythromycin & 25 μg ml^{-1} Lincomycin
NE1386-JE2	USA300 uncharacterized leucocidin-like protein 1 SAUSA300_1974 disrupted by Tn *bursa aurealis* Ery^R Lin^R Constructed by D. Yang	TSB media plus 5 μg ml^{-1} Erythromycin & 25 μg ml^{-1} Lincomycin
NE1434-JE2	USA300 *ctaB*::Tn *bursa aurealis* Ery^R Lin^R Constructed by J. Connolly	TSB media plus 5 μg ml^{-1} Erythromycin & 25 μg ml^{-1} Lincomycin

NE1434-SH	SH1000 *ctaB*::Tn *bursa aurealis* Ery^R Lin^R Constructed for this study	TSB media plus 5 μg ml^{-1} Erythromycin & 25 μg ml^{-1} Lincomycin
NE1509-JE2	USA300 ABC transporter ATP-binding protein SAUSA300_0630 disrupted by Tn *bursa aurealis* Ery^R Lin^R Constructed by J. Connolly	TSB media plus 5 μg ml^{-1} Erythromycin & 25 μg ml^{-1} Lincomycin
NE1509-SH	SH1000 ABC transporter ATP-binding protein SAUSA300_0630 disrupted by Tn *bursa aurealis* Ery^R Lin^R Constructed by J. Connolly	TSB media plus 5 μg ml^{-1} Erythromycin & 25 μg ml^{-1} Lincomycin
NE1532-JE2	USA300 *agrA*::Tn *bursa aurealis* Ery^R Lin^R Constructed by J. Connolly	TSB media plus 5 μg ml^{-1} Erythromycin & 25 μg ml^{-1} Lincomycin
NE1532-SH	SH1000 *agrA*::Tn *bursa aurealis* Ery^R Lin^R Constructed by J. Connolly	TSB media plus 5 μg ml^{-1} Erythromycin & 25 μg ml^{-1} Lincomycin
NE1543-JE2	USA300 *qoxC*::Tn *bursa aurealis* Ery^R Lin^R Constructed for this study	TSB media plus 5 μg ml^{-1} Erythromycin & 25 μg ml^{-1} Lincomycin
NE1543-SH	SH1000 *qoxC*::Tn *bursa aurealis* Ery^R Lin^R Constructed for this study	TSB media plus 5 μg ml^{-1} Erythromycin & 25 μg ml^{-1} Lincomycin
NE1555-JE2	USA300 *codY*::Tn *bursa aurealis* Ery^R Lin^R Constructed for this study	TSB media plus 5 μg ml^{-1} Erythromycin & 25 μg ml^{-1} Lincomycin
NE1555-SH	SH1000 *codY*::Tn *bursa aurealis* Ery^R Lin^R Constructed for this study	TSB media plus 5 μg ml^{-1} Erythromycin & 25 μg ml^{-1} Lincomycin
NE1622-JE2	USA300 *saeR*::Tn *bursa aurealis* Ery^R Lin^R Constructed by J. Connolly	TSB media plus 5 μg ml^{-1} Erythromycin & 25 μg ml^{-1} Lincomycin
NE1622-SH	SH1000 *saeR*::Tn *bursa aurealis* Ery^R Lin^R Constructed by J. Connolly	TSB media plus 5 μg ml^{-1} Erythromycin & 25 μg ml^{-1} Lincomycin
NE1662-JE2	USA300 *miaB*::Tn *bursa aurealis* Ery^R Lin^R Constructed for this study	TSB media plus 5 μg ml^{-1} Erythromycin & 25 μg ml^{-1} Lincomycin
NE1662-JE2	SH1000 *miaB*::Tn *bursa aurealis* Ery^R Lin^R	TSB media plus

	Constructed for this study	5 μg ml^{-1} Erythromycin & 25 μg ml^{-1} Lincomycin
NE1688-JE2	USA300 *sle1*::Tn *bursa aurealis* Ery^R Lin^R Constructed for this study	TSB media plus 5 μg ml^{-1} Erythromycin & 25 μg ml^{-1} Lincomycin
NE1688-SH	SH1000 *sle1*::Tn *bursa aurealis* Ery^R Lin^R Constructed for this study	TSB media plus 5 μg ml^{-1} Erythromycin & 25 μg ml^{-1} Lincomycin
NE1770-JE2	USA300 *sucD*::Tn *bursa aurealis* Ery^R Lin^R Constructed for this study	TSB media plus 5 μg ml^{-1} Erythromycin & 25 μg ml^{-1} Lincomycin
NE1770-SH	SH1000 *sucD*::Tn *bursa aurealis* Ery^R Lin^R Constructed for this study	TSB media plus 5 μg ml^{-1} Erythromycin & 25 μg ml^{-1} Lincomycin
NE1908-JE2	USA300 ABC transporter ATP-binding protein SAUSA300_1911 disrupted by Tn *bursa aurealis* Ery^R Lin^R	TSB media plus 5 μg ml^{-1} Erythromycin & 25 μg ml^{-1} Lincomycin
NE1908-SH	SH1000 ABC transporter ATP-binding protein SAUSA300_1911 disrupted by Tn *bursa aurealis* Ery^R Lin^R Constructed by J. Connolly	TSB media plus 5 μg ml^{-1} Erythromycin & 25 μg ml^{-1} Lincomycin

Met^R = methicillin resistant; Ery^R = erythromycin resistant; Lin^R = lincomycin resistant.

2.2.2.2 Nebraska transposon mutant library (NTML)

The NTML is an ordered collection of 1,952 sequence-defined *bursa aurealis* transposon (Tn) insertion mutant strains, each containing a single mutation within a nonessential gene within *S. aureus* USA300 strain JE2 (Fey et al. 2012). The JE2 parent strain is a plasmid-cured derivative of the community-associated MRSA isolate USA300 LAC strain. The library is detailed in appendix section 1.1.

The NTML was stored at –80°C in twenty 96-well microtitre plates, encompassing 1,920 mutant strains. Plates were thawed on ice and a sterilised 96-pin replicator (Beokel Industries) was used to inoculate sterile media in a microtitre plate. Plates were then incubated at 37°C for 24-48 hours, depending upon media used. Plates were stored at –80°C if not immediately used experimentally.

2.2.2.3 Other bacteria strains

Streptococcus pneumonia strains used in this study are listed in Table 2.2.

Table 2.2 Other bacterial strains used in this study

Strain	Description	Growth Conditions
S. pneumoniae strain D39	Virulent capsular type 2 clinical isolate D39	BHI media with 20% FCS
S. pneumoniae strain D39 ΔCPS	Non-encapsulated derivative of strain D39 (Provided by Dr A Fenton, TuoS)	BHI media with 20% FCS
S. pneumoniae strain R6	Non-encapsulated derivative of strain D39 (Provided by Dr T Mitchell, University of Birmingham)	BHI media with 20% FCS

2.2.3 Bacterial growth

2.2.3.1 Growth curves

A single *S. aureus* colony was used to inoculate 5ml of BHI broth and incubated overnight at 37°C with 5% CO_2 on an orbital shaker at 250 rpm. From the overnight culture, 1 ml was used to inoculate 25 ml of pre-warmed BHI broth and re-incubated at 37°C with 5% CO_2, shaking at 250 rpm. *S. pneumoniae* strains were grown from a single colony added to 25 ml of pre-warmed BHI supplements with 20% FCS without shaking. Bacterial growth was monitored by serial optical density measurements, recorded by spectrophotometry.

2.2.3.2 Bacterial culture for experiments

To prepare a live *S. aureus* culture for experiments, a single colony was used to inoculate 5 ml bacteriological media containing antibiotics as specified in Table 2.1 and incubated overnight at 37°C with 5% CO_2 on an orbital shaker at 250 rpm. From the overnight culture, 1 ml was used to inoculate 50ml sterile media, containing required antibiotic (Table 2.1), and re-incubated at 37°C and 250 rpm on an orbital shaker until exponential phase growth was reached. Exponential growth phase culture samples were also stored in 1ml aliquots and at -80°C. *S. pneumoniae* was cultured as above and grown to mid-exponential growth phase and then frozen at -80°C.

2.2.3.3 Determining bacterial density

2.2.3.3.1 Spectrophotometric measurement (OD_{600})

A Jenway 6100 spectrophotometer, using a wavelength of 600nm, was used to obtain serial optical density (OD_{600}) measurements until stationary phase was reached. Samples were diluted with fresh media when necessary to reduce concentration to a measurable level.

2.2.3.3.2 Direct cell counts (CFU ml^{-1})

Direct cell counts were performed to quantify viable bacterial numbers. Liquid bacterial suspensions were serially diluted 1:10 in PBS in duplicate and 10µl of each dilution spotted onto appropriate bacteriological media agar in triplicate, allowed to dry and incubated at 37°C overnight. The number of colony forming units (CFU) was counted directly the following day.

2.2.4 Phage transduction and confirmation

2.2.4.1 Preparation of phage lysate

The bacteriophage ϕ11 was used for the phage transduction of *S. aureus* during this study. The ϕ11, which is specific to *S. aureus*, is a temperate, transducing, 45Kb phage that requires Ca^{2+} ions to maintain infectivity (Novick 1991).

A single colony of the donor *S. aureus* strain was inoculated into 5 ml BHI media, containing appropriate antibiotics where required, and grown overnight at 37°C. Subsequently, 300µL of the overnight culture was added to 5ml BHU, 5 ml phage buffer and 100µL stock SH1000 ϕ11 phage lysate, and incubated stationary for 6-24h at 25°C. Once the mixture had become clear, the lysate was filter sterilized using a 0.22µm filter and stored at 4°C.

To determine the phage titre, *S. aureus* SH1000 was grown in 5ml BHI to an approximate OD_{600}=0.5. The SH1000 ϕ11 phage lysate was serially diluted with phage buffer, and 100µL of each dilution was added to 400µl of the SH1000 culture plus 50µL 1M $CaCl_2$. The mixtures were incubated stationary for 10min at 21°C**.** Subsequently, each mixture was combined with 5 ml warmed phage LK top agar solution, and then overlaid onto pre-heated phage LK bottom agar plate. The plates were incubated at 37°C for up to 48 hours, and the resulting plaque-forming units (pfu) were quantified. Optimal phage lysates had titres in the range of 10^7 – 10^{10} pfu ml^{-1}.

2.2.4.2 Phage transduction

The recipient *S. aureus* strain was inoculated into 50 ml LK broth and incubated overnight at 37°C, 250 rpm. The bacteria were then collected by centrifugation, 5000 rpm for 10 minutes at 21°C, and resuspended in 3 ml LK broth. The transduction mixture was created by adding 500µL recipient strain solution to 1ml LK broth, 10µL 1M $CaCl_2$ plus 500µL phage lysate. A negative control mixture was created in parallel, containing the same constituents without the phage lysate. These mixtures were incubated stationary for 25 minutes at 25°C, then 15 minutes at 25°C, 250rpm. Subsequently, 1ml of ice-cold 0.02 M sodium citrate added, and mixtures incubated on ice for 5 minutes. The transduction mixtures were centrifuged at 5000

rpm for 10 minutes at 4°C and supernatant removed. The resulting pellets were resuspended in 1ml ice-cold 0.02 M sodium citrate and incubated on ice for 45-60 minutes. Onto LK plus 0.05% (w/v) sodium citrate agar plates, supplemented with the selective antibiotics erythromycin and lincomycin, 100μL aliquots of the transduction mixture or control mixture was spread. The plates were incubated at 37°C for 24 – 72 hours. Resultant colonies were re-cultured onto BHI agar supplemented with selective antibiotics.

2.2.4.3 Polymerase chain reaction (PCR) techniques

2.2.4.3.1 Primer design

The primers designed for this study are detailed in Table 2.3

Table 2.3 Primers used in this study

Primer	Sequence (5' – 3')	Length (nucleotides)	Annealing Temperature (°C)	GC content (%)
NE0224F	GGTGAAGTATGCGTTTTCAATAC	23	57.1	39.1
NE0224R	ATACTTGCATTCAAACAGCAC	21	54.0	38.1
NE0714F	GCATCGAATTCACTGTTATGAGTTC	25	59.7	40.0
NE0714R	GTCTGAAACTGCACGAACTAC	21	57.9	47.6
NE0732F	CTTCATGGCAATGCCATTTATC	22	56.5	40.9
NE0732R	GCGAATGTCGGGATAATTTCTG	22	58.4	45.5
NE0945F	TCTTAACTTACGCCCCTACTAC	22	58.4	45.5
NE0945R	ACCATGCAATCACAAAGAAG	20	53.2	40.0
NE1084F	AAACGTACACGTGTCAGTATG	21	55.9	42.9
NE1084R	CGTTTCTCCACCTGGATATAATAC	24	59.3	41.7
NE1366F	CGAGGATTTGCGTTAAAGTTC	21	55.9	42.9
NE1366R	CCAACACCTTTAGGTTGGTTTAC	23	58.9	43.5
NE1374F	TCCTTTGTATTGATGGTGGTTC	22	56.5	40.9
NE1374R	TGAATTGTCGTGTGCGTTAC	20	55.3	45.0
NE1386F	GTACGTTAGCACTATCGACTAC	22	58.4	45.5
NE1386R	GGATTAAACCCTTCAGACACAG	22	58.4	45.5
NE1543F	GTTTCCAAATCGATCACGGATATC	24	59.3	41.7
NE1543R	AACAACATCTAAGAAGTGCCAG	22	56.5	40.9
NE1555F	GTATTCCCACCTGAAAACAGAG	22	58.4	45.5
NE1555R	CACCCTTTACACAATCACG	19	54.5	47.4
NE1662F	TCACAAGAAGAGTCAGTAGTG	21	55.9	42.9
NE1662R	CTGATTCATTTGGATACCCTAC	22	56.5	40.9
NE1688F	GTATCAGGTACTGCTAGCTC	20	57.3	50.0

NE1688R	TCCAACTTTTCAGCTTGTG	19	52.4	42.1
NE1758F	CACACCAGAATTACACGCAG	20	57.3	50.0
NE1758R	TTTGCCCTCCTAAGATTTCG	20	55.3	45.0
NE1770F	CGAAAATAGTAGCAGGTGTG	20	55.3	45.0
NE1770R	AATGATTGCACCAGCATG	18	51.4	44.4

The design of the primers was based upon the genome of *S. aureus* USA300 FPR3757 strain. Details of the precise transposon insertion site of each NTML mutant was attained from the NARSA/NTML database. The short oligonucleotides (18-25 nucleotides) were designed approximately 400 nucleotides upstream and downstream of the respective insertion sites. The primer sequence was designed in the 5' – 3' direction for forward and backward strands. All sequences were designed to contain 40-50% GC nucleotide content, terminating with a GC base pair, and with annealing temperatures 55-60°C. Sequences containing denucleated repeats and greater than three base repeats were avoided. The primers were assessed using the NCBI Primer-BLAST tool (http://www.ncbi.nlm.nih.gov/tools/primer-blast/) to prevent non-specific binding to other sites within the *S. aureus* genome. The primers were synthesised by Eurofins MWG operon (http://www.eurofinsdna.com) and prepared in nuclease-free water to a stock 100μM concentration and a 10μM working concentration, stored at -20°C.

2.2.4.4 DNA amplification

The high-fidelity Phusion polymerase Master Mix (Thermo Scientific) was used for 3'-5' proof-reading activity. A master mix was prepared on ice using the following combination:

Template DNA	25μL
Phusion high-fidelity Master Mix (2X)	50ng
Forward primer (10μM)	1μL
Reverse primer (10μM)	1μL
Nuclease free H_2O	make up to 50μL

A Veriti Thermal Cycler (Applied Biosystems) was used to conduct PCR. The following thermal cycling program employed:

Heat lid to 105°C

Initial denaturation	1 cycle	98°C	30s
Denaturation	30 cycles	98°C	15s
Annealing		48-60°C	15s
Extension		72°C	15-30 s/kb
Final extension	1 cycle	72°C	7 min

PCR products were stored at -20°C.

2.2.4.5 Agarose gel electrophoresis

DNA samples were separated by electrophoresis in 1% (w/v) agarose gels in 1 x Tris-acetate-EDTA buffer solution. To allow visualisation of DNA under UV light, 5-10 μL of Ethidium Bromide (10 mg ml^{-1}, BioRad) was added to the agarose gel when poured into the horizontal casting tray. The horizontal submerged gels were run using a HU15 standard horizontal tank (Life Technologies, Scie-Plas).

DNA samples were mixed at a ratio of 10:1 with 10X loading buffer (ThermoScientific) and pipetted into gel wells. GeneRuler™ 1 Kb DNA ladder (ThermoScientific) was loaded into a gel well to facilitate subsequent estimation of DNA fragment size. DNA was electrophoresed at 110V for 30-60 minutes, at room temperature, to achieve separation of bands. The DNA was visualised at 260 nm, using UVi Tec Digital transilluminator and camera system and UVi Doc Gel documentation system.

2.3 Antibiotics

All antibiotics used in this study are listed in Table 2.4.

Antibiotic stock solutions prepared by dissolving antibiotics in the appropriate solvent before filter sterilising (0.22 μm pore size) and storing at –20°C. For use in liquid media, antibiotic stock solutions were added prior to usage. For use in agar plates, molten agar was cooled to 55°C before addition of antibiotics.

Table 2.4 Antibiotic stock solutions and concentrations

Antibiotic	**Stock concentration (mg ml^{-1})**	**Solvent**	***S. aureus* working concentration (μg ml^{-1})**
Erythromycin (Ery)	5	100% v/v ethanol	5
Gentamicin (Gent)	40	dH_2O	100
Kanamycin (Kan)	50	dH_2O	50
Lincomycin (Lin)	25	50% v/v ethanol	25
Lysostaphin (Lys)	5	100% v/v DMSO	20
Tetracycline (Tet)	5	100% v/v ethanol	5

2.4 Chemicals, compounds, and enzymes

Concentrations, storage, and solvent stock solutions are details in Table 2.5.

Table 2.5 Stock solutions and concentrations

Stock solution	Stock concentration	Solvent	Storage	Working Concentration
Acrylamide (AccuGel) (National Diagnostics)	40 %	-	RT	-
Ammonium persulfate (APS) (Sigma)	-	dH_2O	4°C	20 % (w/v)
Anti-actin (Rabbit; polyclonal) (Sigma-Aldrich)	-	PBS	4°C	1:2000
Anti-cathepsin D (Goat; polyclonal) (R&D systems)	-	PBS	4°C	1:1000
Anti-procathepsin D/intermediates (Mouse; monoclonal) (Abcam)	-	PBS	4°C	1:1000
Anti-mouse IgG Alexa Fluor®488 (Goat) (ThermoFisher)	2 mg ml^{-1}	PBS	4°C, in dark	1-10 µg ml^{-1}
Anti-rabbit IgG Alexa Fluor® 568 (Goat) (ThermoFisher)	2 mg ml^{-1}	PBS	4°C, in dark	1-10 µg ml^{-1}
Bovine Serum Albumin (BSA) (Biowhitaker)	30% (w/v)	PBS	4°C	3% (w/v)
CellEvent™ Caspase-3/7 Green Flow Cytometry Assay Kit (Life Technologies)	-	-	–20°C, in dark	-
4'.6-diamidine-2'-phenylindole dihydrochloride (DAPI)	5 mg ml^{-1}	dH_2O	–20°C, in dark	300 ng ml^{-1}
Dimethyl Sulfoxide (DMSO) (Sigma)	≥99.7%	-	RT	-
EDTA	-	dH_2O	RT	0.5 M, pH 8
EGTA	-	dH_2O	RT	0.5 M, pH 8
Ficoll-Paque™ PLUS (GE Healthcare)	1.078 g ml^{-1}	EDTA	RT, in dark	-

Foetal Calf Serum (FCS) (Promocell)	-	-	–20°C	10% (w/v)
Formaldehyde (Polysciences)	10%, methanol free	dH_2O	RT	4%
Glycine	1 M	dH_2O	RT	0.1 M
Goat Serum	-	-	–20°C	1%
Human Granulocyte-Macrophage Colony Stimulating Factor (GM-CSF) (Gibco)	10 µg	dH_2O	–20°C	20 ng ml^{-1}
Human Macrophage Colony Stimulating Factor (M-CSF) (Gibco)	10 µg	dH_2O	–20°C	10 ng ml^{-1}
Paraformaldehyde (PF) (BDH Lab Supplies)	4% (w/v)	PBS	–20°C	2 – 4% (w/v)
Phorbol 12-myristate acetate (PMA) (Sigma)	100 µM	DMSO	–20°C, in dark	200 nM
pHrodo™ Red, succinimidyl ester (ThermoFisher)	2.55 mM	DMSO	–20°C, in dark	0.5 mM
Protease inhibitor (Roche, 1836170)	Tablet	dH_2O	–20°C	Dissolved in 2ml
Saponin (Sigma)	≥10% (w/v)	PBS	4°C, in dark	2% (w/v)
Sodium dodecyl sulphate (SDS) solution (Sigma, 05030)	20%	dH_2O	RT	-
TEMED (N,N,N',N'-Tetramethylethylenediamine) (Sigma)	~ 99 %	-	RT	-
Trichloroacetic acid (TCA) (Sigma)	100%	-	RT	-
To-Pro®-3 stain (ThermoFisher)	-	-	–20°C, in dark	1:10,000
Tris-HCl (Sigma)	1 M	-	RT	-
Tris (Sigma)	3 M	-	RT	-

Triton™ X-100 (Sigma)	-	-	RT	-
Vectashield™ Antifade Mounting Medium with DAPI (Vector Labs)	-	-	4°C, in dark	DAPI 1.5 µg l^{-1}

Table 2.6 Plastics used in study

Item	Source
50ml centrifuge tubes	Sarstedt
1.5ml microcentrifuge tubes	Sarstedt
T25 flasks	Corning
6-well flat bottom cell culture-treated plates	Corning
24-well flat bottom cell culture-treated plates	Corning
96-well flat bottom cell culture-treated, microplates	Corning
96-well flat-bottom µClear® white (opaque) sided microplates	Greiner

2.4.1. Histological fixation

Media was removed from the wells and replaced with 4% formaldehyde (Polysciences) and incubated for 15 minutes at room temperature. The formaldehyde was removed, the wells washed with sterile PBS, then fixative quenched by incubating cells with 0.1 M glycine in PBS for 5 minutes at room temperature. The glycine was removed, and wells washed with PBS.

2.4.2 Preparation of solutions

2.4.2.1 Tris Buffered Solution (TBS) – EDTA solution

1 M Tris-HCl, pH 7.4	5ml
1 M NaCl	37.5ml
0.5 M EDTA	2.5ml
0.5 M EGTA	2.5ml
dH_2O	180ml (total volume 250ml)

2.4.2.2 TBS-EDTA-SDS lysis buffer solution

1M Tris-HCl pH 7.4	2ml
1M NaCl	15ml
0.5M EDTA	1ml
0.5M EGTA	1ml
20% SDS	5ml
dH_2O	72ml (total volume 100ml)

2.4.3 Preparation of buffers and gels for Western blotting

2.4.3.1 Loading buffer

2 M Tris-HCl pH 6.8	10ml
20% glycerol	10ml
0.005%bromophenol blue	125µl
2% SDS	5ml
dH_2O	to make total volume 49ml
1 mM DTT (stored -20°C)	1ml (add immediately before use)

2.4.3.2 10X Running buffer

Glycine	190g
Tris base	30.3g
20% SDS	50ml
dH_2O	to make total volume 1000ml

2.4.3.3 10X Transfer buffer

Glycine	14.5g
Tris base	29g
20% SDS	9.25ml
dH_2O	to make total volume 400ml

2.4.3.3 1X Transfer buffer

10X Transfer buffer	10ml
Methanol	20ml
dH_2O	to make total volume 100ml

2.4.3.4 Resolving Gels

	15%	12%	10%	8%	6%
Water (ml)	5.3	6.4	7.2	7.9	8.7
40% Acrylamide (ml)	5.6	4.5	3.8	3.0	2.3
1.5M Tris pH 8.8 (ml)	3.8	3.8	3.8	3.8	3.8
20% SDS (µL)	75	75	75	75	75
20% APS (µL)	150	150	150	150	150
TEMED (µL)	6	6	6	6	6

Makes 2 x 1.5mm gels.

2.4.3.5 Stacking Gel

40% acrylamide	620µl
0.5 M Tris pH 6.8	1260µl
20% SDS	25µl
20% APS	50µl
TEMED	5µl

Makes 1 x 1.5 mm gel.

2.4.3.6 Blocking solution

Skim milk powder	5 g
Tween 20	200µl
PBS	to make total volume 100ml

2.5 Bacterial infection of cell cultures

THP-1 cells or MDM cells were differentiated at a final density of 2 x 10^5 cells ml^{-1} (as described in section 2.1). Prior to bacterial challenge, existing media was removed, cells washed with warmed PBS before warmed RPMI 1640 media supplemented with 10% h/i FCS was added.

If using bacterial stock stored at –80°C the aliquot was thawed to room temperature. Liquid *S. aureus* culture, either thawed or live culture, was centrifuged at 9400 x *g* for 1 minute. The supernatant was discarded, and the pellet re-suspended in 1ml sterile PBS. This wash cycle was repeated thrice.

The desired volume of the liquid bacterial culture was added to differentiated macrophages in media to achieve the required multiplicity of infection (MOI). Infected macrophage culture was placed on ice for 1 hour to permit bacteria adherence to macrophages, and subsequently incubated at 37°C with 5% CO_2 for the required period.

At the desired time point, the infected media was removed, and the well was washed thrice with ice-cold sterile PBS to halt internalisation. RPMI 1640 with 10% h/i FCS supplemented with 20 µg ml^{-1} lysostaphin was added and the macrophages were then incubated at 37°C for 30 minutes to eradicate extracellular bacteria. Alternatively, 100 µg ml^{-1} gentamicin was used in place of lysostaphin, due to stock limitations. For each condition, 10 µl samples were spotted onto appropriate bacteriological media agar in triplicate, allowed to dry and incubated at 37°C overnight, to confirm sterility achieved. Antibiotic-containing media was removed, and wells were washed with ice-cold sterile PBS thrice.

2.6 Determination of viable intracellular bacteria using an antibiotic protection assay

Lysostaphin can be used to lyse both extracellular and adherent *S. aureus* rapidly from macrophages *in vitro* (Easmon et al. 1978). Intracellular *S. aureus* are not affected by low concentration lysostaphin as it is not internalised by the phagocytic cell (Easmon et al. 1978).

Enumeration of intracellular bacterial number was achieved using an antibiotic protection assay, utilising an antibiotic that eradicates extracellular bacteria only (Baughn & Bonventre 1975).

Macrophages were challenged with bacteria as per section 2.5. Following the removal of antibiotic-containing media and subsequent washing, 250 µl of 2% (w/v) saponin (Sigma) was added to the wells and incubated at 37°C with 5% CO_2 for 12 minutes. The cholesterol-binding property of saponin causes the macrophage cell membrane to be permeabilised without affecting bacterial membranes. After incubation, 750 µl sterile PBS was added to the saponin and cells lysed by repeated vigorous pipetting. Direct bacterial cell counts were performed on the resultant mixture as per section 2.2.3.3.2.

2.7 Antibiotic pulse-chase killing assay

An antibiotic pulse-chase assay is used to quantify the rate of decay of intracellular bacteria numbers. As detailed in section 2.6., lysostaphin eradicates extracellular and adherent *S. aureus* without affecting intracellular bacteria.

Following a *S. aureus* challenge of macrophages and subsequent treatment with 20 µg ml^{-1} lysostaphin (section 2.2.4.), RPMI 1640 media with 10% h/i FCS containing 2 µg ml^{-1} lysostaphin was added to the wells to allow for the tracking of the killing of intracellular bacteria without phagocytosis of extracellular bacteria. At desired time periods, enumeration of intracellular *S. aureus* performed as per section 2.6.

2.8 Microscopy

2.8.1 Microscopes

2.8.1.1 Leica DMRB fluorescent microscope

Objective lenses 10x, 40x and 100x, with emission filters for DAPI, GFP and Texas Red. No capacity for digital image collection.

2.8.1.2 Olympus BX61 upright epifluorescence microscope

Objective lenses 10x, 20x, 60x and 100x, with emission filters for DAPI, CFP, YFP, GFP, RFP and Texas Red. Motorised microscope, images collected with Hamamatsu Orca monochrome camera through Velocity imaging software.

2.8.1.3 Zeiss LSM510 Meta Inverted confocal/multiphoton upright microscope

Objective lens 63x using Argon and Chameleon lasers, with emission filters for DAPI, CFP, GFP, RFP and Texas Red. Motorised microscope.

2.8.1.4 ImageXpress® Micro high-content fluorescent microscope

An ImageXpress® Micro high-content fluorescent microscope (Molecular Devices) was utilised for all high-throughput experiments. Objective lenses 20x and 40x, with emission filters for DAPI, GFP, Deep Red, Texas Red and Far Red were available. For the high-throughput screen, the 20x objective was used with emission filters for DAPI (1-6300-0442, Molecular Devices), GFP (1-6300-0450, Molecular Devices) and Texas Red (1-6300-0442, Molecular Devices). The metadata created was stored on an MDCstore database.

2.8.2 Imaging software

Tagged image file format (TIFF) images obtained to collect images without data compression.

2.8.2.1 FIJI

Fiji (Fiji Is Just ImageJ) is an open-source imaging software adapted from ImageJ (Schneider et al. 2012) for bioscience image analysis (Schindelin et al. 2012).

2.8.2.2 Velocity

Velocity software (PerkinElmer) used to collect and process images with Olympus BX61 epifluorescence system, permitting deconvolution and co-localisation functions.

2.8.2.3 MetaXpress®

MetaXpress® 3.1 software (Molecular Devices) designed to be used with ImageXpress Micro system. Images collected processed using custom algorithms (journal) to identify macrophage number, total bacterial number, and pHrodo™ positive or negative bacteria. AcuityXpress® software used to analyse segmented images to generate multiparametric data sets.

2.8.3. Immunofluorescent microscopy

2.8.3.1. 4',6-diamidine-2'-phenylindole dihydrochloride staining

4',6-diamidine-2'-phenylindole dihydrochloride (DAPI) fluoresces when bound to DNA with absorption maximum at 358 nm and emission maximum at 461 nm. When cells were seeded onto coverslips, 25 µl Vectashield™ antifade mounting medium containing 1.5 g l^{-1} DAPI (Vector Labs) was used. Cells retained within wells were counterstained with 300 nM DAPI in PBS and incubated for 5 minutes at room temperature, then washed thrice with sterile PBS.

2.8.3.2. Adherent bacteria labelling

Immunofluorescent histochemistry was used to define intracellular versus adherent bacteria. Extracellular and adherent *S. aureus* were identified using an anti-staphylococcal primary antibody (Zytomed Systems) and fluorescent secondary antibody. The intracellular *S. aureus* remained unstained as the antibody is unable to enter the macrophage.

Macrophages were differentiated and challenged with *S. aureus* and fixed as described previously (sections 2.2.4. and 2.5.1). Liquid was removed from the wells and replaced with 3% (v/v) bovine serum albumin (Biowhitaker) in PBS and incubated for 30 minutes at room temperature to saturate free binding sites on plastic or protein binding sites. This media was removed and the wells washed with PBS. The fixed material was incubated with anti-staphylococcal rabbit polyclonal IgG primary antibody (Zytomed Systems) at 1:1000 ratio with PBS for 10 minutes at room temperature. Subsequently, the cells were washed and incubated with an anti-rabbit goat-origin Alexa Fluor 568 secondary antibody (Invitrogen) diluted 1:250 in PBS containing Triton X-100 and 1% goat serum, for 10 minutes at room temperature.

Infected cells were counterstained with DAPI to identify unstained intracellular *S. aureus* (section 2.8.2.1.). 100 random macrophages were counted and the total number of DAPI positive bacteria determined, representative of all bacteria. Adherent bacteria counterstained with Alexa Fluor 568 counted and subtracted from DAPI positive total to calculate intracellular bacteria.

2.8.3.3. Phagosomal fusion/tethering machinery labelling

An immunohistochemical screen was used to obtain a mechanistic understanding of phagosomal maturation and the failure of *S. aureus*-containing phagosome maturation.

Following fixation, differentiated macrophages on coverslips were incubated with 1ml 3% BSA solution in PBS at room temperature for 30 minutes. BSA solution was removed, and the coverslips washed thrice with PBS. Delivery of the primary antibody to the intracellular target required the use of 0.01% saponin solution to permeabilise the macrophage cell membrane. The primary antibody was added to the saponin solution at the desired working dilution (Table 2.4) and incubated overnight at 4°C in the dark. The coverslips were washed and incubated in the presence of a fluorescent secondary antibody directed against the primary antibody origin, diluted 1:250 in PBS containing Triton X-100 and 1% goat serum, for 90 minutes at room temperature in the dark. Coverslips were washed and mounted onto glass slides with mounting media and counterstained with DAPI.

Table 2.7 Phagosomal trafficking machinery antibody targets

Antibody Target	Detail	Antibody Origin	Dilution
LAMP1	Lysosome-associated membrane protein 1	Mouse (Abcam)	1:200
LAMP2	Lysosome-associated membrane protein 2	Mouse (Abcam)	1:200
LIMP-II	Lysosome integral membrane protein-II	Rabbit (Abcam)	1:100

2.8.3.4. pH rhodamine (pHrodo™) labelling of bacteria

The pH sensitive dye pHrodo™ (ThermoFisher) increases in fluorescence as local environmental pH becomes more acidic, with absorption maximum at 566 nm and emission maximum at 590 nm. The pHrodo™ Red succinimidyl ester readily conjugates with primary amine groups of proteins, producing stable carboxamide bonds.

pHrodo™ was stored suspended in anhydrous dimethylsulfoxide (DMSO) at concentration of 2.55 mM at –20°C in the dark. 200 µl of a liquid bacteria culture was prepared with a concentration of approximately 1 x 10^9 CFU ml^{-1} in sterile PBS, to which 0.5 µl of 2.55 mM pHrodo™ Red was added and incubated at 37°C with 5% CO_2 for 30 minutes. Labelled *S. aureus* was centrifuged at 9400 x *g* for 60 seconds and the supernatant removed. Unreacted dye was removed by resuspending the bacterial pellet in 1ml of 25mM Tris solution, pH 8.5. Tris solution contains primary amines to bind free dye optimally at slightly basic pH. The bacterial solution was centrifuged, the supernatant removed, and the pellet resuspended in 1ml sterile PBS, centrifuged again and supernatant removed and resuspended in 1ml RPMI 1640 with 10% h/i FCS.

2.8.3.4.1 pH rhodamine (pHrodo™) labelling of bacteria within 96-well format

The NTML 96-well plate was thawed on ice and 5 µl from each well added to 195µl BHI within a sterile U-bottomed 96-well plate. The plate was then incubated at 37°C with 5% CO_2 overnight. A repeat subculture using the same method was established, incubated at 37°C with 5% CO_2 for 3 hours. The 96-well plate was centrifuged at using Rotanta 460 R centrifuge with swing-out rotor (no. 5624), with plate inside carrier (no. 5628) using cradle (no. 4626) and bio-containment lid (no. 5629); plate centrifuged at 2000 x *g* for 5 min at 4°C to facilitate removal of supernatant and resuspension in 100µl PBS supplemented with 0.25µl 2.55mM pHrodo™ and then incubated at 37°C with 5% CO_2 for 30 minutes with constant shaking, max. 5Hz. Labelled NTML mutants centrifuged at 2000 x *g* for 5 min at 4°C, supernatant removed,

and pellet resuspended in 100 µl PBS pH 9. Repeat centrifugation and pellet resuspended in 100 µl 25 mM Tris pH 8.4. Repeat centrifugation and pellet resuspended in 100 µl PBS pH 8. Repeat centrifugation and pellet resuspended in 200 µl PBS pH 7.4.

2.8.3.4.2 pH rhodamine (pHrodo™) labelled NTML challenge of macrophage cell culture

To achieve an estimated MOI = 5, 2 µl pHrodo™-labelled NTML mutant liquid culture added to MDMs with 100 µl warmed RPMI 1640 media supplemented with 10% h/i FCS. Plate incubated on ice, in dark, for 60 min, before incubation at 37°C with 5% CO_2 for 3 hours.

At the desired time point, the infected media was removed, and the well was washed twice with ice-cold sterile PBS to halt internalisation. RPMI 1640 with 10% h/i FCS supplemented with 20 µg ml^{-1} lysostaphin was added and then incubated at 37°C with 5% CO_2 for 30 minutes to eradicate extracellular bacteria. For each condition, samples were spotted onto appropriate bacteriological media agar, allowed to dry, and incubated at 37°C overnight, to confirm sterility achieved. Antibiotic-containing media was removed and 50 µl fresh media supplemented with CellMask™ deep red plasma stain in ratio 2:10000, then incubated at 37°C with 5% CO_2 for 10 minutes. This media was then removed and MDMs washed twice with 200 µl PBS, before fixation with 100 µl 4% formaldehyde, incubated at 37°C for 15 minutes. Formaldehyde removed and 50 µl PBS with 3 µM DAPI added to well, incubated at 37°C for 5 minutes. DAPI-containing PBS removed and well washed thrice with PBS, before final addition of 200 µl PBS and imaged as soon as possible, storing plates at 4°C in dark.

2.9 Measurement of active cathepsin D

2.9.1 Cell lysis and protein extraction

Differentiated THP-1 cells grown in T25 flasks (2 x 10^6 cells $flask^{-1}$) were challenged with *S. aureus* stains Newman or USA300 JE2 (MOI = 5) or *S. pneumoniae* strain D39 (MOI = 10) or mock infected. Following an 8-hour period of infection, the THP-1 cells were washed in TBS-EDTA buffer and lysed with TBS-EDTA-SDS lysis buffer with protease inhibitor (1:25 lysis buffer ratio). 100% TCA added to precipitate DNA. Lysate centrifuged, 13,000 rpm, 4 min, 4°C. Following removal of supernatant, pellet suspended in 3 M Tris and incubated for 60 min, before dilution with dH_2O to achieve 1.5 M Tris protein solution.

2.9.2 Gel electrophoresis

12% SDS-PAGE resolving and stacking gels prepared as above. Gel tank filled with 1X running buffer, prepared as above. To prepared protein ahead of electrophoresis, 15µL protein solution combined with 5µL loading buffer and boiled at 100 °C for 5 min, subsequently

centrifuged at max speed for 10 s, then loaded into well. Following separation samples were blotted onto nitrocellulose membranes (Bio-Rad Labs.) Transfer confirmed by Ponceau S staining. Blots blocked with blocking solution immunodetection performed. Primary antibody diluted in 5ml blocking buffer and incubated overnight on a rolling platform at 4°C; secondary antibody diluted in 5ml blocking buffer and incubated for 90 min on a rolling platform at 4°C. Enhanced chemiluminescence (ECL) blotting substrates (BioRad) applied and imaged.

2.10 Measurement of lactate dehydrogenase release

Differentiated THP-1 cells grown in 24-well plates, at density of 2 x 10^5 cells ml^{-1}, were challenged with *S. aureus* stains Newman or USA300 JE2 or heat-killed USA300 JE2 (MOI = 5) or mock infected. Following a 20-hour period of infection, the media was collected transferred to a 96-well plate. Measurement of lactate dehydrogenase (LDH) release from macrophages utilised the colourimetric Cytotox 96 cell viability kit (Promega) following manufacturers instructions. The absorbance signal was measured using a Flash Varioskan.

2.11 Measurement of macrophage apoptosis and necrosis

Differentiated THP-1 cells grown in 6 well plates, at density of 2 x 10^5 cells ml^{-1}, were challenged with *S. aureus* stains Newman or USA300 JE2 (MOI = 5) or mock infected. At the desired time point, adherent cells were scraped and media collected. The samples were centrifuged at 500 x *g* for 5 minutes and washed in cold PBS twice. Cells finally resuspended in 100μL of reaction buffer. Apoptosis and necrosis assessed using the CellEvent™ caspase 3/7 green flow cytometry assay kit (Life Technologies) and TO-PRO-3 stain (ThermoFisher) respectively following manufacturers instructions. Measurement of apoptosis and necrosis by flow cytometric measurement using a four-colour FACSCalibur flow cytometer. Forward- and side-scatter light used to identify cell populations by size and granularity. In all experiments, 10,000 events were captured and analysed with FlowJo software v9.3.2.

2.12 Statistical analysis

Statistical analysis was performed using Prism version 7.0 – 9.0 (GraphPad). The following p value cut offs were used: * $p<0.05$; ** $p<0.01$; *** $p<0.001$; **** $p<0.0001$; NS – non-significant.

Mathematical modelling undertaken using R software, version 3.6.3, with adapted open-source R/Bioconductor statistical analysis package for cell-based high-throughput screens (cellHTS2) (Boutros et al. 2006; Pelz et al. 2010; Boutros et al. 2019).

Chapter 3

The interaction between *Staphylococcus aureus* USA300 strain JE2 and macrophages

3.1 Executive summary

The aim of the following chapter was to characterise the internalisation of *S. aureus* USA300 strain JE2 by macrophages and subsequent subversion of phagosomal maturation and intracellular killing. The findings demonstrated that USA300 strain JE2 is internalised by macrophages and remain viable within the intracellular environment. Following phagocytosis, the USA300 strain JE2-containing phagosome subverts maturation and inhibits host microbicidal effector functions, facilitating intracellular persistence. The *S. aureus*-containing phagosome failed to acidify appropriately, failed to acquire the phagosome-lysosome fusion marker LIMP-II and failed to activate the lysosomal protease cathepsin D. These events indicate that maturation to the microbicidal phagolysosome state is antagonised by *S. aureus*. Bacterial factors are essential for phagosomal subversion as heat-killed *S. aureus* failed to subvert phagosomal acidification.

3.2 Introduction

The primary defence against *Staphylococcus aureus* infection is the innate immune system. Tissue resident macrophages fulfil a sentinel role in the recognition of pathogenic material and subsequent recruitment and activation of host defences (T. J. Foster 2005). As discussed previously (section 1.2), macrophages are adept at recognising and removing pathogenic material. Yet *S. aureus* is also capable of adaptation to evade the effector functions of the innate immune system, including inhibition of recruitment; cytotoxin production; resistance to phagocytosis; and resistance to antimicrobial effector mechanisms (T. J. Foster 2005).

The body of evidence for intracellular persistence, within both professional and non-professional phagocytic cell types, of *S. aureus* has expanded significantly since originally recognised (Rogers & Tompsett 1952; Garzoni & Kelley 2009). Within the intracellular environment, *S. aureus* is protected from further host immune effector functions as well as cell-impermeant antimicrobial therapeutic agents (Thwaites & Gant 2011). A mechanistic understanding for the persistence of intracellular *S. aureus*, or failure of the host macrophage to eradicate the pathogen is emerging (Jubrail et al. 2016; Gresham et al. 2000).

A tipping point between *S. aureus* clearance and persistence is evident, experimentally demonstrated by Dr Jubrail within the Dockrell group, whereby macrophages have a finite capacity for intracellular killing of *S. aureus* Newman strain (Jubrail et al. 2016). It would be expected that following macrophage internalisation, within the maturing phagosome, *S.*

aureus is exposed to acidic conditions, antimicrobial peptides, reactive oxygen species and reactive nitrogen species (Peschel 2002). However, it is evident that *S. aureus* subverts this process, is able to resist macrophage microbicidal effector function, has an extended intracellular persistence within macrophage phagosomes before delayed induction of necrosis (Kubica et al. 2008; Jubrail et al. 2016). How exactly persistence occurs remains unclear, but inhibition of phagosomal maturation is dependent upon bacterial factors, as it is reversed by heat-killed *S. aureus* Newman strain (Jubrail et al. 2016; Prajsnar et al. 2021).

The evidence generated from the work of Dr Jubrail concerning the interaction between macrophages and *S. aureus* was acquired using the strains Newman and SH1000, both common laboratory strains. Dr Jubrail demonstrated intracellular accumulation of *S. aureus*, with the failure of killing was related to period of exposure and the *S. aureus* challenge dose, within differentiated macrophages. Dr Jubail's later work began to explore the mechanisms of *S. aureus* persistence, detailing the failure of the *S. aureus*-containing phagosome to appropriately progress to the microbicidal phagolysosomal state.

The overall aim of this project is to identify bacterial factors which enable subversion of the phagosomal maturation pathway. An ordered mutant library of *S. aureus* provides the opportunity to perform a comprehensive evaluation of gene function. The Nebraska transposon (Tn) mutant library (NTML) contains 1,920 sequence-defined *bursa aurealis* Tn-insertion mutants derivative of *S. aureus* USA300 strain LAC, each with a single non-essential gene deletion (Fey et al. 2012). The CA-MRSA clone USA300 is the most prominent community-acquired MRSA strain in the USA, associated with invasive disease, including severe sepsis and necrotising pneumonia (Seybold et al. 2006; Francis et al. 2005; Klevens et al. 2007). The complete genome sequence of USA300 has been detailed (Diep et al. 2006), in addition to description of specific defining molecular markers (David et al. 2013). USA300 has been demonstrated to have greater virulence than other MRSA strains with greater resistance to killing by human neutrophils (Voyich et al. 2005). The NTML has been generated within USA300 strain JE2, a plasmid-cured derivative of USA300 strain LAC to ensure compatibility with Tn (Fey et al. 2012). Consequently, prior to investigation of the NTML, definition of the interaction between USA300 strain JE2 and human macrophages is necessary.

3.3 Aims and objectives

I. Assess internalisation of USA300 strain JE2 by macrophages.
II. Assess if challenge with USA300 strain JE2 demonstrates failure of phagosomal maturation and acidification within macrophages.

III. Assess if challenge with USA300 strain JE2 results in altered levels of macrophage necrosis or apoptosis.

3.4 Macrophage internalisation of *S. aureus* USA300 strain JE2

Previous work undertaken within the Dockrell laboratory group by Dr Jubrail demonstrated that macrophages challenged with the common laboratory *S. aureus* strains Newman and SH1000 exhaust intracellular killing and establish an intraphagosomal population (Jubrail et al. 2016). Most intracellular killing of Newman and SH1000 strains occurred within the initial 30 minutes after phagocytosis was prevented, with persistence of viable intracellular bacteria. To assess if intracellular persistence is unique to *S. aureus* strains Newman and SH1000, the USA300 strain JE2 was assessed.

The USA300 strain JE2 demonstrated a similar trend to Newman and SH1000 strains. The greatest rate of intracellular killing occurred within the 30-minute period following removal of extracellular bacteria which prevented further phagocytosis (Figure 3.1 A-C). Subsequently, the rate of killing decreased with time with persistence of viable intracellular bacteria. Following 16 hours bacterial exposure there was no significant change, consistent with the proposed exhaustion of intracellular killing mechanism. The results support the conclusion that intracellular persistence of *S. aureus* is not strain specific.

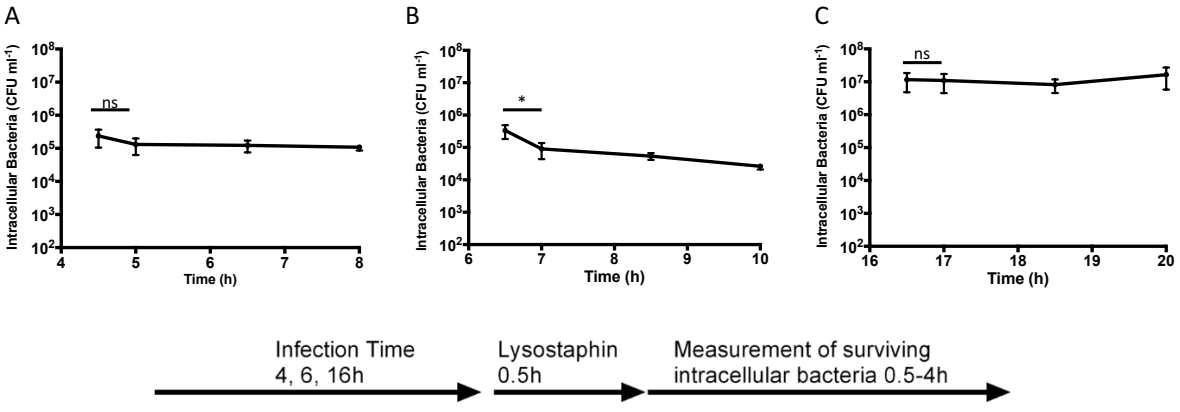

Figure 3.1 *S. aureus* USA300 strain JE2 persists intracellularly.

Differentiated THP-1 macrophages were challenged by *S. aureus* USA300 strain JE2 at a MOI of 5 bacteria per macrophage for 4, 6 and 16 hours, and after high-dose lysostaphin treatment for 0.5 hours were either lysed or maintained in low-dose lysostaphin for 0.5 – 3.5 hours and lysed at each time point for intracellular colony forming units estimation. **A**) 4-hour, **B**) 6-hour, **C**) 16-hour bacterial challenge. The data represent the mean with the standard error of the

mean performed as three individual experiments, each in duplicate, *p<0.05, paired t-test, comparing first two time points.

3.5 Lysostaphin does not account for initial killing of intracellular *S. aureus* following phagocytosis.

A potential explanation for the initial decay in the intracellular *S. aureus* population may be the internalisation of lysostaphin into the macrophage phagosome containing *S. aureus*. Easmon *et al*. have previously demonstrated that low-dose lysostaphin does not affect intracellular *S. aureus* populations and is not internalised by professional phagocytes (Easmon et al. 1978). To confirm that high-dose lysostaphin is not responsible for killing intracellular *S. aureus*, the experiments were designed to subject macrophages containing intracellular *S. aureus* to high-dose lysostaphin. Following a standard lysostaphin pulse-chase assay of intracellular *S. aureus* killing, repeat exposure to high-dose lysostaphin pulses caused no difference in intracellular bacterial number compared to standard procedure (Figure 3.2A). A second experiment was devised using wild-type Newman strain and a kanamycin-resistant mutant Newman strain, with both strains sensitive to lysostaphin (Figure 3.2B). A fourteen-hour infection was chosen to saturate the killing mechanisms of the macrophage, thus no change in intracellular bacterial number would be expected. The results demonstrate that the kanamycin-resistant (Kan^R) mutant strain was phagocytosed, but there was no decline in intracellular number post-lysostaphin exposure. The wild-type strain numbers were consistent between the subset free from lysostaphin exposure (WT), and the subset exposed (Kan^S). The experiments support the use of lysostaphin to eradicate extracellular *S. aureus* without affecting intracellular number.

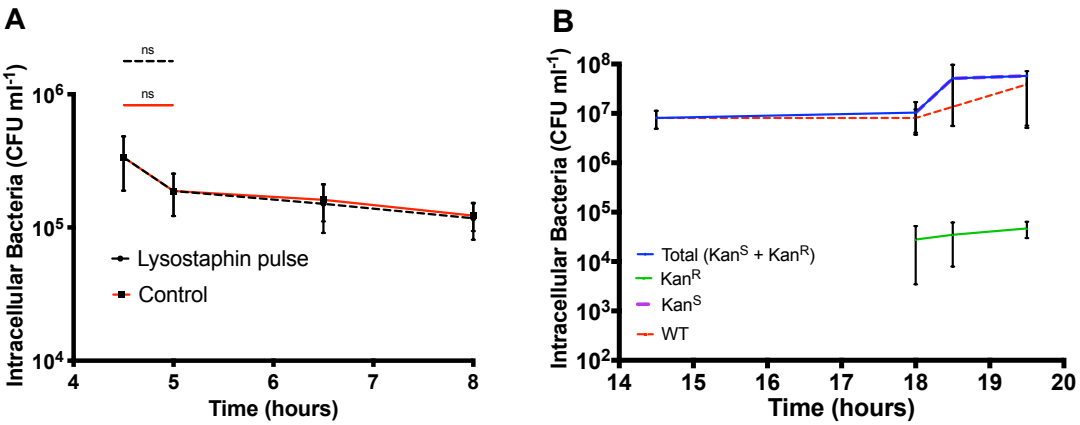

Figure 3.2 Lysostaphin does not account for initial killing of intracellular *S. aureus*

A) Differentiated THP-1 macrophages were challenged with *S. aureus* Newman strain for 4 hours. The kinetics of intracellular killing were estimated using a lysostaphin pulse-chase as

standard or with further 30-minute high-dose lysostaphin pulses at 6 h or 7.5 h followed by macrophage lysis for intracellular CFU estimation. Data represent the mean and standard error of the mean, two individual experiments performed in duplicate. Two-way ANOVA with Tukey's multiple comparison test comparing the first two time points in both conditions and comparing between conditions, no significant difference.

B) Differentiated THP-1 macrophages were challenged with wild-type *S. aureus* Newman strain for 14 hours and then incubated with high-dose kanamycin for 30 minutes to remove extracellular and adherent bacteria. Subsequently cultures were divided. The WT cultures were maintained in low-dose kanamycin until lysed at 18 and 19.5 hours provided a control population of intracellular bacterial. The second culture set were additionally challenged by kanamycin-resistant *S. aureus* Newman (referred to as Kan^S + Kan^R cultures) for 3 hours and then incubated with high-dose lysostaphin for 30 minutes. The cell cultures were either lysed or maintained in low-dose lysostaphin for 0.5 – 1.5 hours and lysed to estimate intracellular CFU. Lysates were cultured onto standard media agar or media agar supplemented with kanamycin to determine total (Kan^S + Kan^R) and Kan^R intracellular CFU. The Kan^S intracellular CFU was estimated by subtracting Kan^R CFU from the total (Kan^S + Kan^R) CFU. Data represent the mean and standard error of the mean, three individual experiments performed in duplicate. Two-way ANOVA with Tukey's multiple comparison test between time points in each condition and between conditions at each time point, no significant difference found.

3.6 The *S. aureus* USA300 strain JE2-containing phagosome matures to a late phagosome state

Generation of the microbicidal phagolysosome from the nascent phagosome requires sequential membrane fusion and fission events, as previously discussed (section 1.2.2) (Desjardins et al. 1994). The Dockrell group have previously demonstrated that the *S. aureus* Newman strain progresses to a LAMP-1 and LAMP-2 positive compartment, consistent with a late phagosome phenotype (Jubrail et al. 2016).

To prove that this is not a specific Newman strain observation, I assessed the acquisition of LAMP-1 and LAMP-2 by the *S. aureus* USA300 strain JE2-containing phagosome (Figures 3.3 – 3.5). The results demonstrate that the number of intracellular bacteria that associate with a LAMP-1 positive compartment progressively increases over time (Figure 3.4). This is consistent with the *S. aureus*-containing phagosome maturing to a late stage, as described previously. Following cessation of further phagocytosis by removing extracellular bacteria, the intracellular bacteria remained in a LAMP-1 and LAMP-2 positive compartment (Figures 3.4 and 3.5). These findings are consistent with previous assessment of *S. aureus* Newman strain by Dr Jubrail.

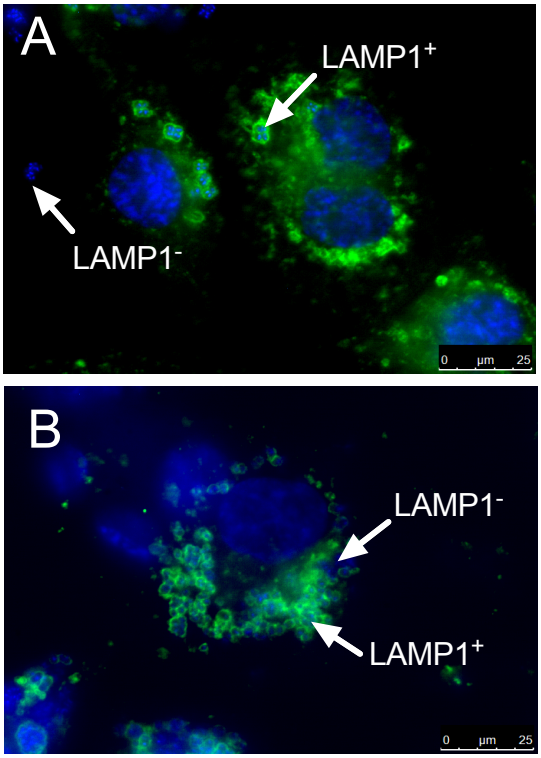

Figure 3.3 Phagosomes containing *S. aureus* USA300 strain JE2 acquire LAMP-1. Differentiated THP-1 macrophages were challenged with *S. aureus* USA300 strain JE2 at a MOI of 5 for 6 hours, then incubated with high-dose lysostaphin for 0.5 hours, macrophages were either fixed and stained or maintained in low-dose lysostaphin for up to a further 4 hours. Extracellular bacteria identified by labelling with primary rabbit anti-staphylococcal antibody and secondary anti-rabbit antibody (Alexa Fluor 568, red) (not shown). Having permeabilised the macrophage, intracellular immunofluorescent labelling performed utilising primary mouse anti-LAMP1 antibody and secondary anti-mouse antibody (Alexa Fluor 488, green). DAPI counterstain (blue) utilised to identify macrophage nuclei and bacteria. Representative microscopic images obtained using x63 oil immersion lens of the Zeiss LSM510 NLO Meta Inverted confocal upright microscope. Arrows indicate examples of DAPI-stained *S. aureus* co-localising with LAMP-1 ($LAMP1^+$) or not co-localising with LAMP-1 ($LAMP1^-$).

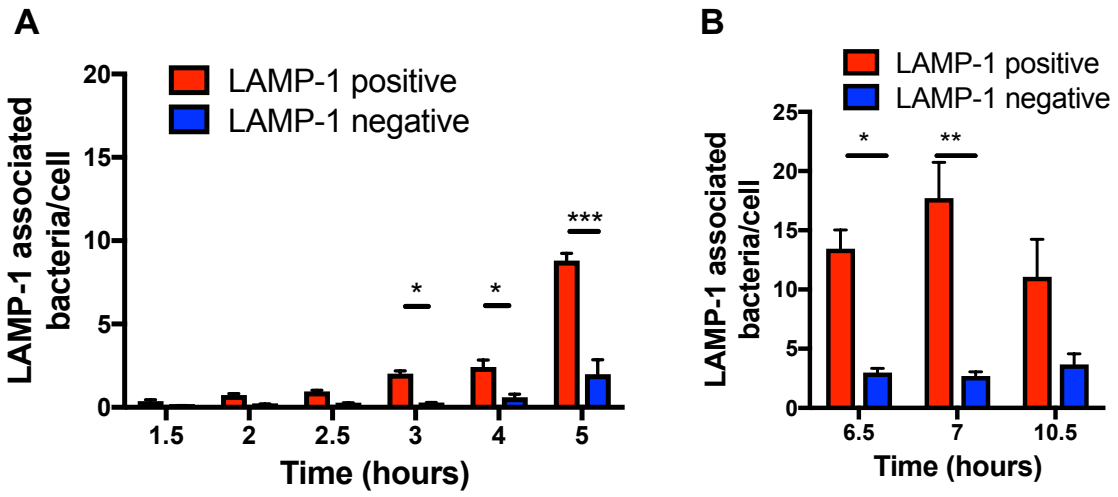

Figure 3.4 Phagosomes containing *S. aureus* USA300 strain JE2 acquire LAMP-1.

(**A**) Differentiated THP-1 macrophages were challenged with *S. aureus* USA300 strain JE2 at a MOI of 5 for 1.5 – 5 hours then fixed. Immunofluorescent labelling performed, utilising primary mouse anti-LAMP1 antibody and secondary anti-mouse antibody (Alexa Fluor 488). DAPI counterstain utilised to identify macrophage nuclei and bacteria. One hundred macrophages (DAPI-positive) were counted per sample and number of extracellular bacteria (DAPI-positive, Alexa Fluor 568-positive), intracellular bacteria (DAPI-positive, Alexa Fluor 568-negative) and intracellular bacteria co-localising with LAMP-1 (DAPI-positive, Alexa Fluor 568-negative, Alexa Fluor 488-positive) were estimated at respective time points.

(B) Differentiated THP-1 macrophages were challenged for 6 hours, then incubated with high-dose lysostaphin for 0.5 hours, macrophages were either fixed and stained or maintained in low-dose lysostaphin for up to a further 4 hours. One hundred macrophages (DAPI-positive) were counted per sample and number of extracellular bacteria (DAPI-positive, Alexa Fluor 568-positive), intracellular bacteria (DAPI-positive, Alexa Fluor 568-negative) and intracellular bacteria co-localising with LAMP-1 (DAPI-positive, Alexa Fluor 568-negative, Alexa Fluor 488-positive) were estimated at respective time points. The data represent 3 individual experiments performed in duplicate. *p<0.05, **p<0.01, ***p<0.001, Two Way ANOVA with Sidak's post-test.

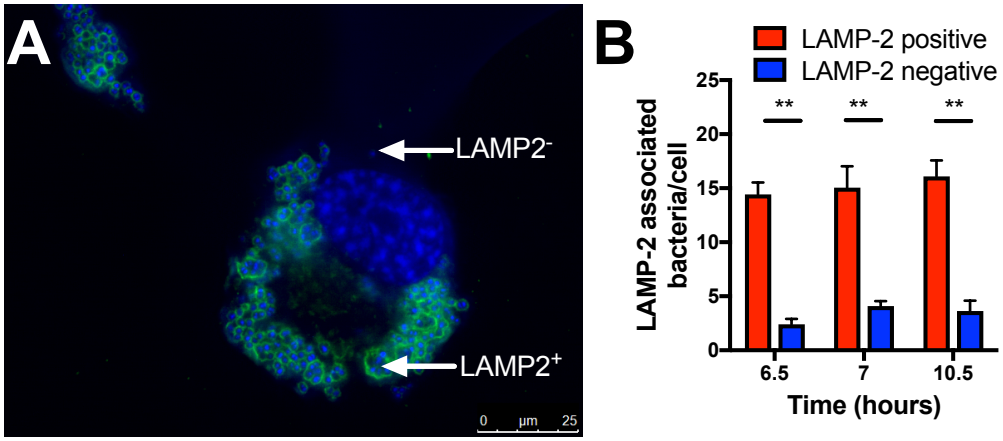

Figure 3.5 Phagosomes containing *S. aureus* USA300 strain JE2 acquire LAMP-2. Differentiated THP-1 macrophages were challenged with *S. aureus* USA300 strain JE2 at a MOI of 5 for 6 hours, then incubated with high-dose lysostaphin for 0.5 hours, macrophages were either fixed and stained or maintained in low-dose lysostaphin for up to a further 4 hours. Extracellular bacteria identified by labelling with primary rabbit anti-staphylococcal antibody and secondary anti-rabbit antibody (Alexa Fluor 568, red) (not shown). Having permeabilised the macrophage, intracellular immunofluorescent labelling performed utilising primary mouse anti-LAMP2 antibody and secondary anti-mouse antibody (Alexa Fluor 488, green). DAPI counterstain (blue) utilised to identify macrophage nuclei and bacteria. (**A**) Representative microscopic images obtained using x63 oil immersion lens of the Zeiss LSM510 NLO Meta Inverted confocal upright microscope. Arrows indicate examples of DAPI-stained *S. aureus* co-localising with LAMP-2 ($LAMP2^+$) or not co-localising with LAMP-2 ($LAMP2^-$). (**B**) One hundred macrophages (DAPI-positive) were counted per sample and number of extracellular bacteria (DAPI-positive, Alexa Fluor 568-positive), intracellular bacteria (DAPI-positive, Alexa Fluor 568-negative) and intracellular bacteria co-localising with LAMP-2 (DAPI-positive, Alexa Fluor 568-negative, Alexa Fluor 488-positive) were estimated at respective time points. The data represent 3 individual experiments performed in duplicate. **p<0.01, Two Way ANOVA with Sidak's post-test.

3.7 The *S. aureus* USA300 strain JE2-containing phagosome fails to mature to a phagolysosome state, defined by acquisition of LIMP-II

As defined above, the *S. aureus*-containing phagosome matures to a late phagosome state, defined by acquisition of LAMP-1 and LAMP-2. The *S. aureus* Newman-containing phagosome however does not acquire LIMP-II, a marker of phagosome-lysosome fusion, indicative of maturation failure (Jubrail et al. 2016).

I assessed the acquisition of LIMP-II by the *S. aureus* USA300 strain JE2-containing phagosome utilising a matched protocol to the assessment of LAMP acquisition (Figures 3.6). The majority of intracellular bacteria failed to co-localise with a LIMP-II positive compartment up to 10.5 hours post-bacterial challenge. This is indicative of the failure for the *S. aureus*-containing phagosome to fuse with lysosomes. These findings are again consistent with previous assessment of *S. aureus* Newman strain by Dr Jubrail. Therefore, the failure of maturation to a phagolysosomal state can be concluded to be a phenotype of all *S. aureus* strains.

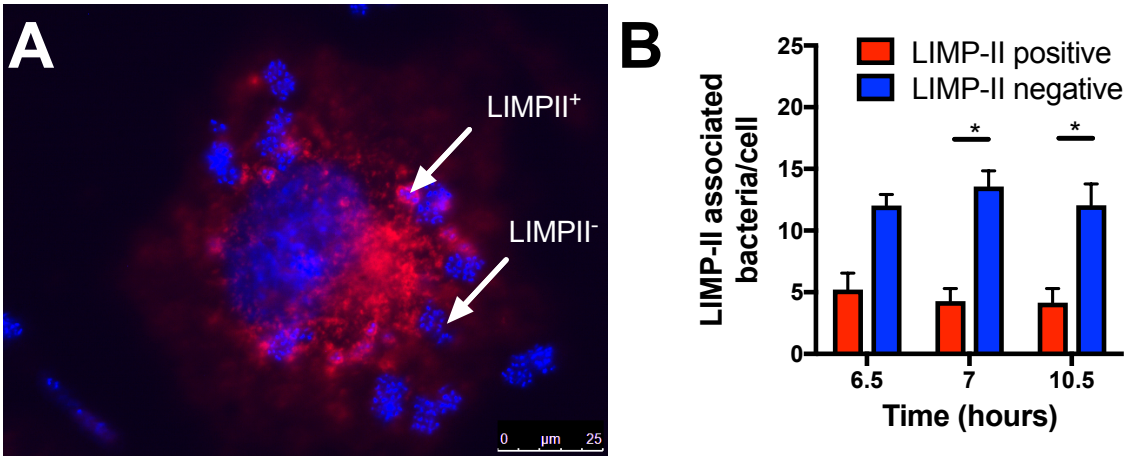

Figure 3.6 Phagosomes containing *S. aureus* USA300 strain JE2 fail to acquire LIMP-II
Differentiated THP-1 macrophages were challenged with *S. aureus* USA300 strain JE2 at a MOI of 5 for 6 hours, then incubated with high-dose lysostaphin for 0.5 hours, macrophages were either fixed and stained or maintained in low-dose lysostaphin for up to a further 4 hours. Immunofluorescence labelling performed, utilising primary rabbit anti-LIMP-II antibody and secondary anti-rabbit antibody (Alexa Fluor 568) (red). DAPI counterstain (blue) utilised to identify macrophage nuclei and bacteria. (**A**) Representative microscopic images obtained using x63 oil immersion lens of the Zeiss LSM510 NLO Meta Inverted confocal upright microscope. Arrows indicate examples of DAPI-stained *S. aureus* co-localising with LIMP-II ($LIMPII^+$) or not co-localising with LIMP-II ($LIMPII^-$). (**B**) One hundred macrophages (DAPI-positive) were counted per sample and number of intracellular bacteria (DAPI-positive) and intracellular bacteria co-localising with LIMP-II (DAPI-positive, Alexa Fluor 568-positive) were estimated at respective time points. The data represent 3 individual experiments performed in duplicate. *p<0.05, Two Way ANOVA with Sidak's post-test.

3.8 The *S. aureus*-containing phagosome fails to mature to a phagolysosome state, defined by activation of cathepsin D.

The microbicidal phagolysosome is further defined by an acidic lumen (pH < 5), active cathepsins, hydrolytic enzymes, oxidants and cationic peptides as previously described (section 1.3.2). Activation of cathepsin D, a lysosomal protease, has been demonstrated to be a critical stimulus for apoptosis-associated killing in the context of *S. pneumoniae* challenge (Bewley et al. 2011). Having demonstrated that the *S. aureus*-containing phagosome fails to acquire LIMP-II, a defining characteristic of the mature phagolysosome, I investigated the recruitment and activation of cathepsin D in the context of *S. aureus* challenge.

In an experiment performed with Dr Martin Bewley, we demonstrated that macrophages fail to activate cathepsin D when challenged with *S. aureus*. The experiment demonstrated that macrophages challenged with *S. pneumoniae* for 8 hours resulted in increased activated cathepsin D levels compared to mock infected macrophages, as previously demonstrated within the literature (Bewley et al. 2011). Macrophages challenged with either *S. aureus* Newman or USA300 JE2 during an equivalent period failed to activate cathepsin D, indicating that this observation is not strain specific.

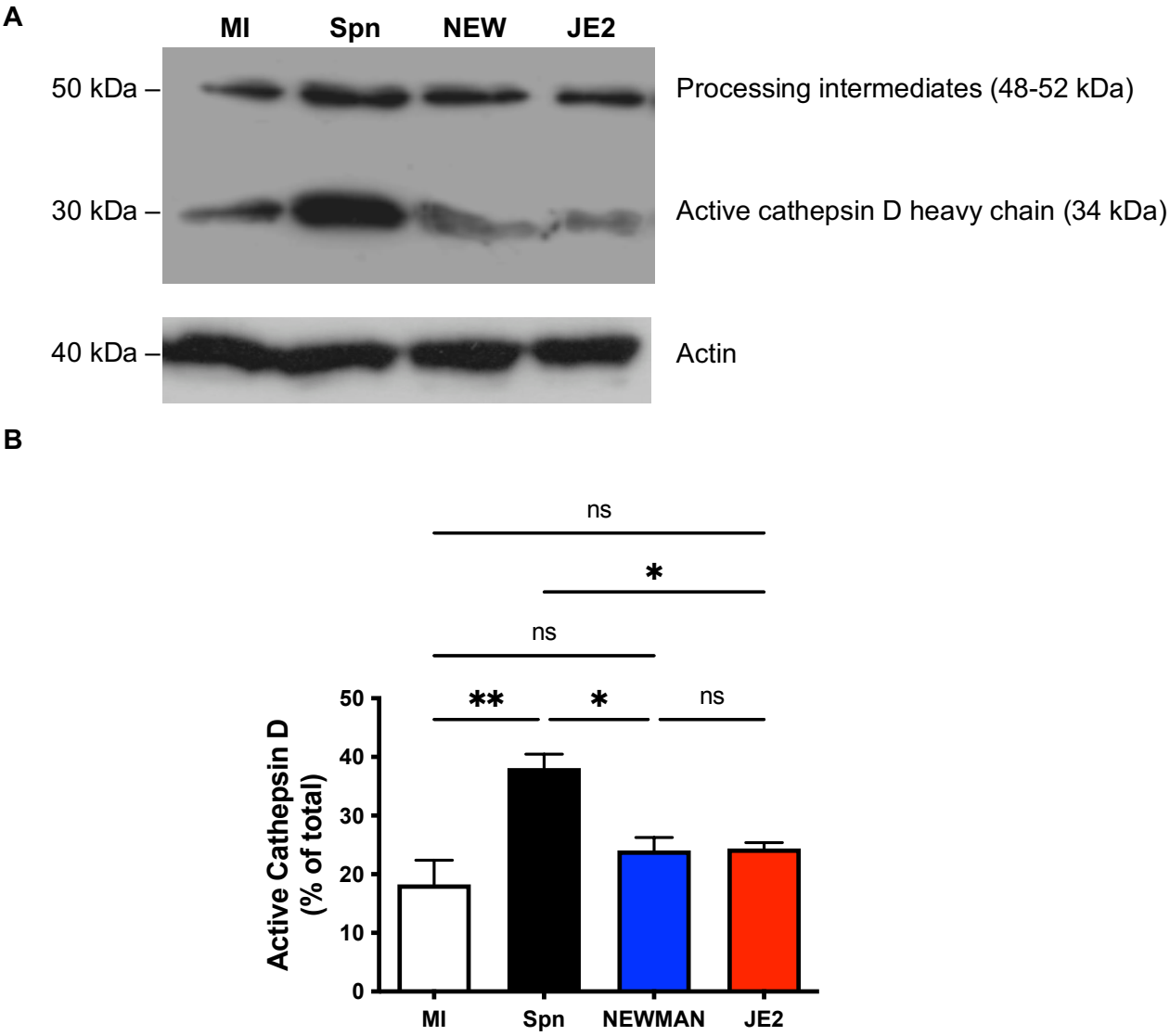

Figure 3.7 *S. aureus* infected macrophages fail to activate cathepsin D.

Differentiated THP-1 macrophages were challenged for 8 hours with *S. aureus* Newman (NEW) or USA300 JE2 (JE2) strains, *S. pneumoniae* (Spn) at a MOI of 5 or mock infected (MI). (**A**) Protein obtained from the THP-1 cells probed with anti-cathepsin D to identify processing intermediates of cathepsin D (inactive) and the active heavy chain of cathepsin D. Actin was used as a loading control. (**B**) The percentage expression of active cathepsin D by densitometry relative to total cathepsin D. The data represent three individual experiments. ns not significant, *p < 0.05, **p< 0.01; ordinary one-way ANOVA with Tukey's multiple comparison test.

3.9 Labelling *S. aureus* with the pH-sensitive dye pHrodo™

Phagosomal maturation is associated with the progressive acidification of the intra-phagosomal compartment by accumulation of membrane V-ATPases, as discussed

previously. The decrease in phagosomal pH is both a consequence of and a requirement for progressive maturation, including the activation of cathepsin D (Flannagan et al. 2012). Therefore, having demonstrated that the *S. aureus*-containing phagosome fails to mature appropriately, assessment of intraphagosomal pH is appropriate.

The fluorescence of the pH sensitive dye pHrodo™ increases as the pH decreases in its immediate environment, and can be used to label bacteria (Jubrail et al. 2016). The procedure for labelling bacteria has been described previously (section 2.8.3.4). To confirm that the pHrodo™ dye or the reagents used in the labelling procedure does not affect bacterial viability, liquid bacterial cultures were divided and either labelled or not with pHrodo™ (Figure 3.7). The results demonstrate that the labelling bacteria with pHrodo™ does not alter viability.

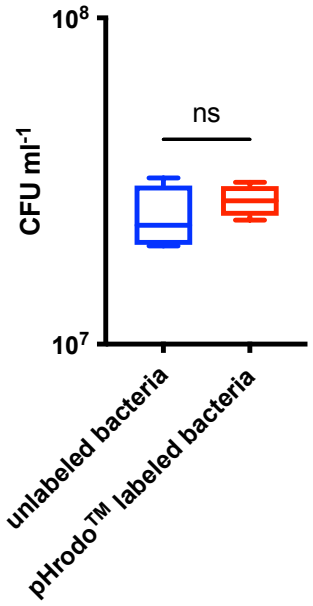

Figure 3.8 Viability of *S. aureus* not affected by pHrodo™ labelling
S. aureus USA300 strain JE2 liquid culture was divided into equal volumes and either labelled with pHrodo™ or left unlabelled. Number of colony forming units subsequently estimated of both conditions to compare viability.. Data represented as box and whisker plot, four individual experiments. Unpaired t test, ns non-significant.

Given the fluorescence of pHrodo™ was to be used as a surrogate for intraphagosomal pH, it was necessary to confirm the pH range at which optimal fluorescence emission occurs. Consequently pHrodo™-labelled *S. aureus* was assessed in a range of pH adjusted buffers (pH 4 – 7.4) and fluorescence assessed by microscopy (Figure 3.9).

The fluorescence of the pHrodo™-labelled *S. aureus* strain (Figure 3.9A) progressively increased with decreasing environmental pH. Unlabelled *S. aureus* emitted no fluorescence signal detectable within the red filter (Figure 3.9B). Therefore, the labelling of *S. aureus* with pHrodo™ to assess progression to an acidified compartment appears a valid approach with which to assess phagolysosomal pH.

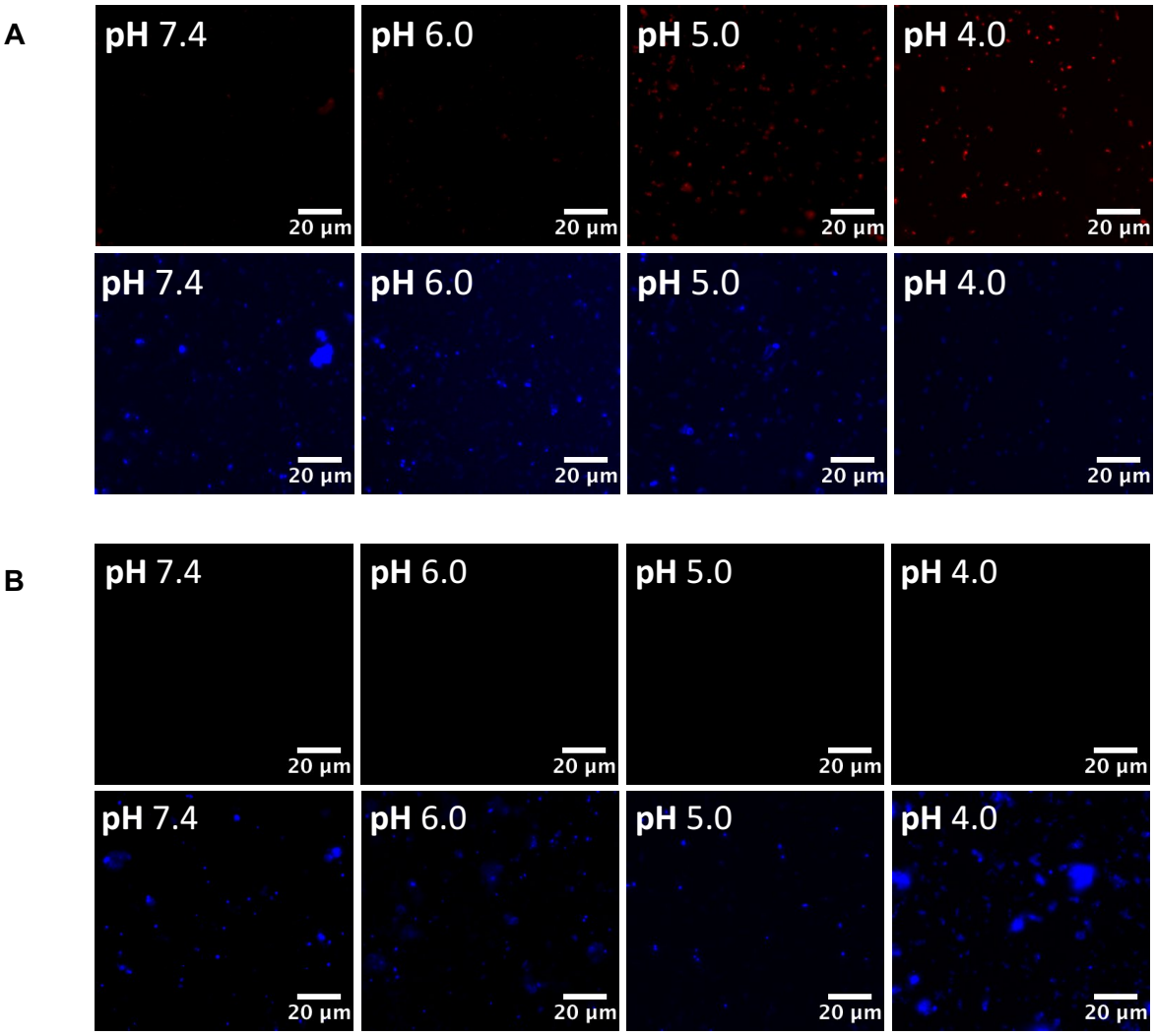

Figure 3.9 The fluorescence of pHrodo™-labelled *S. aureus* increases in acidic conditions.

S. aureus, (**A**) pHrodo™-labelled and (**B**) pHrodo™-unlabelled, counterstained with DAPI, suspended in pH-adjusted buffer solution. Images obtained with ImageXpress® Micro microscope with emission filters for Texas Red (top row) and DAPI (bottom row). For each condition, nine frames were obtained. Brightness and contrast normalised for all images.

3.10 The majority of intracellular *S. aureus* USA300 strain JE2 fail to traffic to acidified compartments

During phagosomal maturation, from nascent phagosome to phagolysosome, the intraphagosomal compartment becomes increasingly acidic. Phagocytosed bacteria would be expected to traffic to an acidic phagolysosome where they would be degraded by multiple microbicidal effector mechanisms. However, work by Dr Jubrail demonstrated that intracellular *S. aureus* strain Newman fails to progress to a mature phagolysosome and the majority remain in a non-acidified compartment (Jubrail et al. 2016).

To confirm that this observation was not limited to the Newman strain, *S. aureus* USA300 strain JE2 labelled with pHrodo^{TM} were used to challenge differentiated macrophages to assess for progression to an acidified intracellular location. Cultures were fixed and counterstained as described previously (section 2.8.3.5). The results were consistent with that of *S. aureus* Newman strain. The majority of intracellular *S. aureus* USA300 strain JE2 fail to localise to an acidified phagosome irrespective of the duration of infection, despite ongoing internalisation (Figures 3.10 and 3.11). This phenotype did not change with more prolonged incubation either (Figure 3.11), suggesting that acidification of the phagosome was inhibited. The pattern of phagosomal maturation inhibition was reversed if the *S. aureus* bacteria were heat-killed prior to macrophage challenge (Figures 3.12 and 3.13). This suggests that *S. aureus* actively express bacterial factors that antagonise phagosomal maturation.

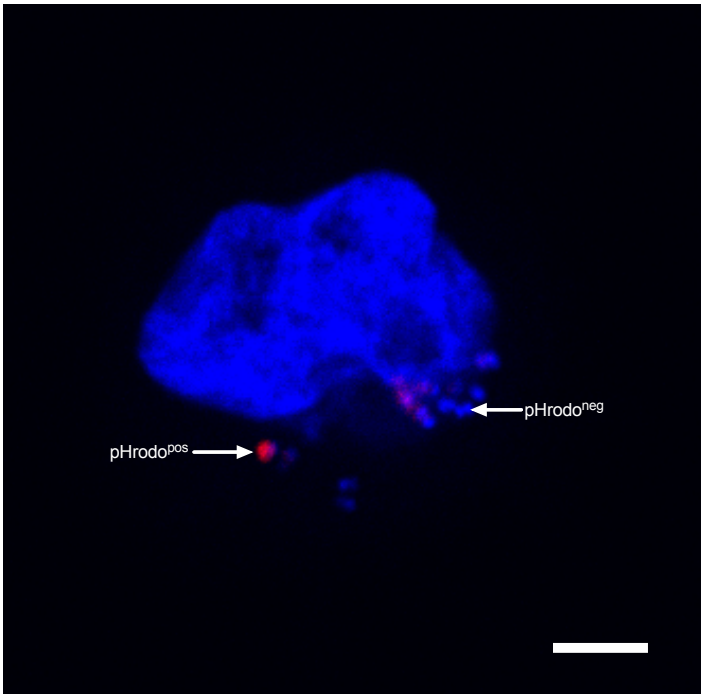

Figure 3.10 Macrophages traffic *S. aureus* USA300 strain JE2 to phagosomes that are not appropriately acidified.

Differentiated THP-1 macrophages were challenged with pHrodo™-labelled *S. aureus* USA300 strain JE2 at a MOI of 5 bacteria per macrophage for 4 hours then incubated with high-dose lysostaphin for 0.5 hours to eradicate extracellular bacteria, and then fixed. DAPI counterstain (blue) utilised to identify macrophage nuclei and bacteria. Representative microscopic images obtained using x63 oil immersion lens of the Zeiss LSM510 NLO Meta Inverted confocal upright microscope. Arrows indicate examples of intracellular acidified *S. aureus* (DAPI-positive, pHrodo-positive (red)) or intracellular non-acidified *S. aureus* (DAPI-positive, pHrodo-negative (blue)).

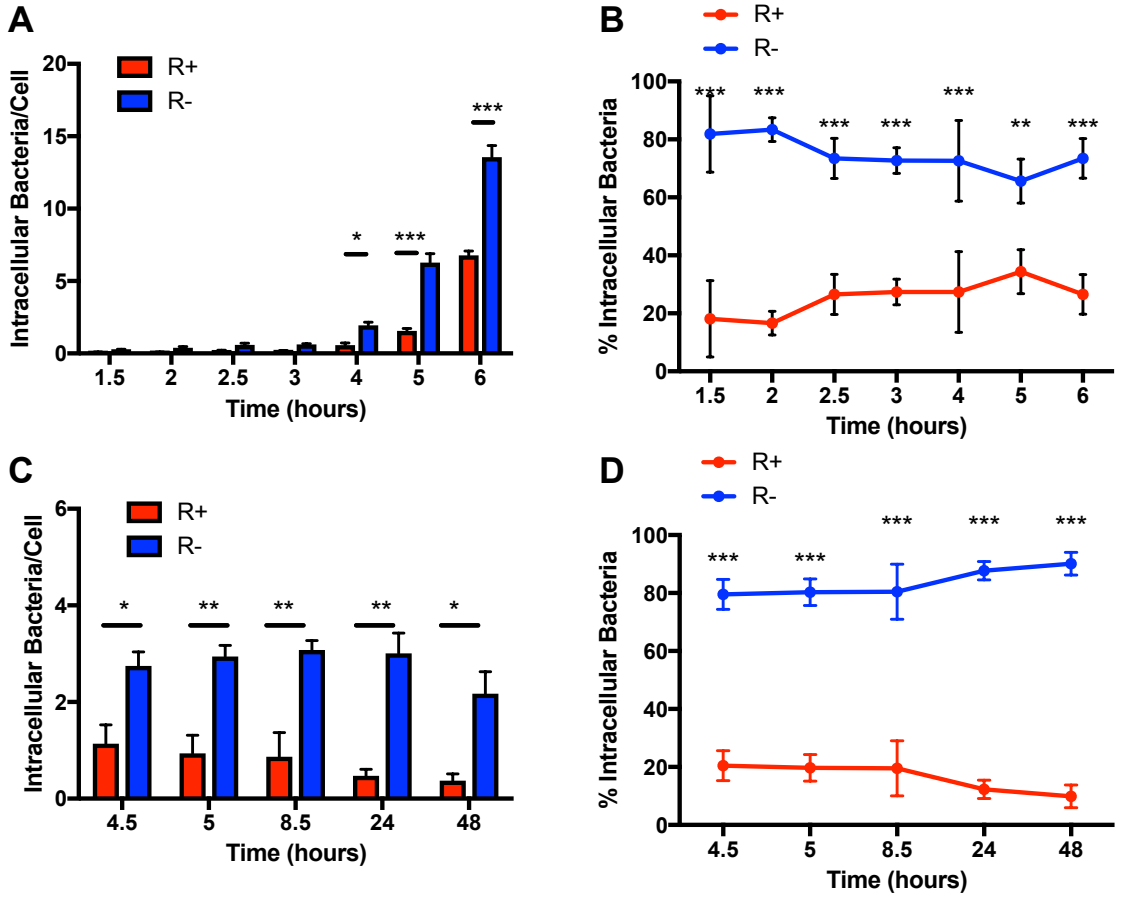

Figure 3.11 Macrophages traffic *S. aureus* USA300 strain JE2 to phagosomes that are not appropriately acidified.

Differentiated THP-1 macrophages were challenged with pHrodo™-labelled *S. aureus* USA300 strain JE2 at an MOI of 5 bacteria per macrophage for 1.5 – 6 hours (**A-B**) or for 4 hours then after high-dose lysostaphin treatment for 0.5 hours were maintained in low-dose lysostaphin up to 48 hours (**C-D**). One hundred macrophages were counted, and the number of intracellular pHrodo™ fluorescent (R+) or non-fluorescent (R-) bacteria per cell (**A** and **C**) and percentage of intracellular fluorescent or non-fluorescent bacteria (**B** and **D**) were estimated. Data represent three individual experiments performed in duplicate. *p<0.05, **p<0.01, ***p<0.001, Two Way ANOVA with Sidak's Post Test R+ vs. R-.

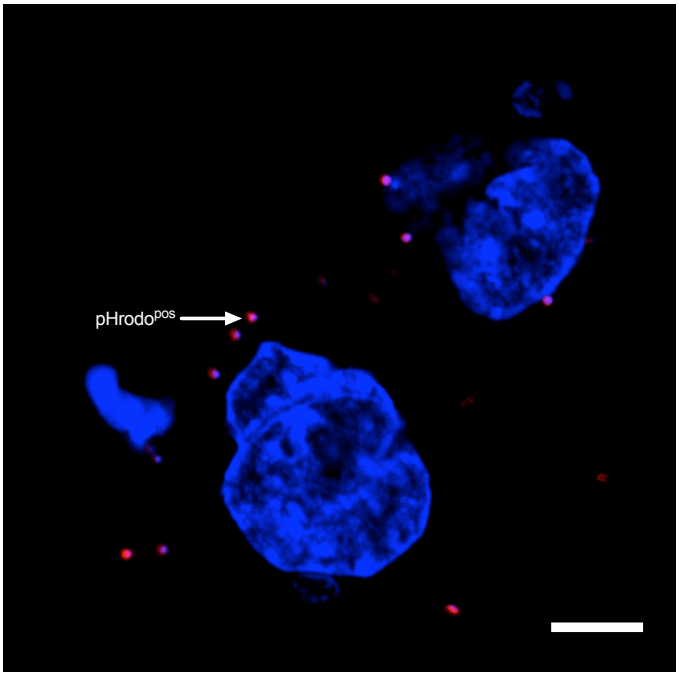

Figure 3.12 Macrophages traffic heat-killed *S. aureus* USA300 strain JE2 to acidified phagosomes.

Differentiated THP-1 macrophages were challenged with heat-killed pHrodo^{TM}-labelled *S. aureus* USA300 strain JE2 at a MOI of 5 bacteria per macrophage for 4 hours then incubated with high-dose lysostaphin for 0.5 hours to eradicate extracellular bacteria, and then fixed. DAPI counterstain (blue) utilised to identify macrophage nuclei and bacteria. Representative microscopic images obtained using x63 oil immersion lens of the Zeiss LSM510 NLO Meta Inverted confocal upright microscope. Arrows indicate examples of intracellular acidified *S. aureus* (DAPI-positive, pHrodo-positive (red)) or intracellular non-acidified *S. aureus* (DAPI-positive, pHrodo-negative (blue)).

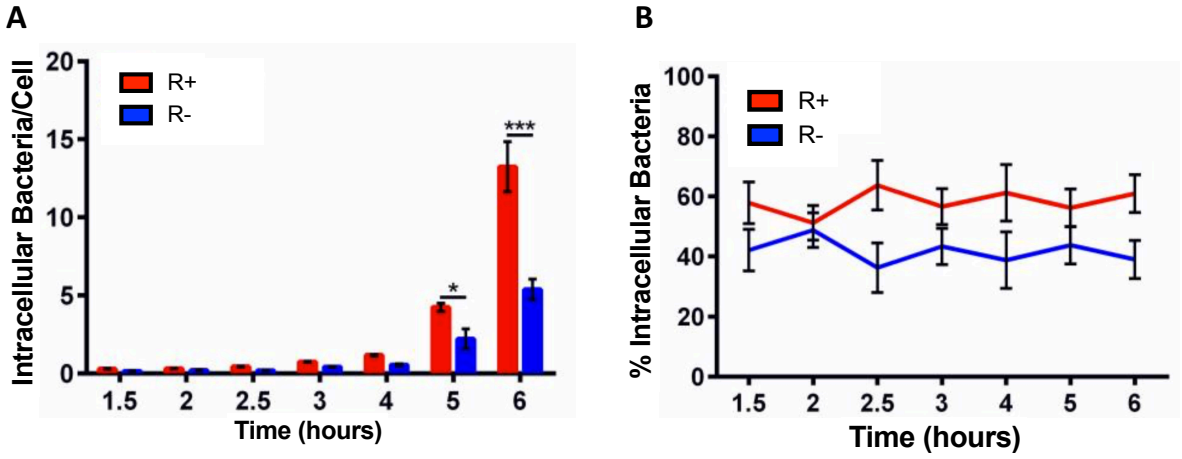

Figure 3.13 Macrophages traffic heat-killed *S. aureus* USA300 strain JE2 to acidified phagosomes.

Differentiated THP-1 macrophages were challenged with heat-killed pHrodo™-labelled *S. aureus* USA300 strain JE2 at a MOI of 5 bacteria per macrophage for 1.5 – 6 hours (**A-B**). One hundred macrophages were counted, and number of intracellular pHrodo™ fluorescent (R+) or non-fluorescent (R-) bacteria per cell (**A**) and percentage of intracellular fluorescent or non-fluorescent bacteria (**B**) were estimated. Data represent three individual experiments performed in duplicate. *p<0.05, **p<0.01, ***p<0.001, Two Way ANOVA with Sidak's Post Test R+ vs. R-.

3.11 *S. aureus* challenge causes macrophage plasma membrane disruption and cell lysis

Having demonstrated intracellular persistence of *S. aureus* within a phagosome that had failed to mature appropriately, the consequence of this observation to the host cell was investigated. As described previously (section 1.6), within many non-professional phagocyte cell types *S. aureus* escapes the phagosome (Bayles et al. 1998). This mechanism of escape has been attributed to expression of pore-forming toxins (Prévost et al. 1995).

Macrophages challenged by *S. aureus* Newman and USA300 JE2 respectively were assessed for evidence of cytotoxicity in the form of plasma membrane permeabilisation. The measurement of lactate dehydrogenase (LDH), an indicator of cytotoxicity, was achieved using a colourimetric assay (Bewley et al. 2014), performed with Dr Bewley. The results demonstrate statistically significant release of LDH from macrophages challenged with *S. aureus* USA300 strain JE2 compared to mock infected macrophages (Figure 3.14). The *S.*

aureus Newman strain demonstrated a small, but statistically significant rise in LDH compared to mock infected.

The disruption of the *S.* aureus-containing phagosome can be inferred from this evidence for permeabilisation of the host cell plasma membrane at 20 hours post initial exposure. Determining the juncture at which the integrity of the phagosome membrane is disrupted is not possible within this experiment, but loss of the phagosomal membrane integrity would be one possible explanation of failure of phagosomal luminal acidification.

A second assay of host cell viability was undertaken. Utilising the TO-PRO-3 stain, which is impermeant to live cells but penetrates disrupted plasma membranes, quantification of dead cells can be achieved. Macrophages either mock-infected or challenged with *S. aureus* Newman or USA300 strain JE2s for between 4 to 20 hours. At the respective time points, macrophages were stained with TO-PRO-3 and analysed by flow cytometry. This experiment was performed with Dr Bewley. Consistent with the LDH release assay, macrophage cell death is apparent at 16 hours following challenge with *S. aureus* (Figure 3.15). Assessment at the earlier time points of 4 and 6 hours respectively did not identify any significant macrophage death. Both *S. aureus* strains assessed, Newman and USA300 JE2 caused cell death following 16- and 20-hour challenge compared to mock-infected. As demonstrated within the LDH release assay, the USA300 strain JE2 causes greater cell lysis than that of Newman.

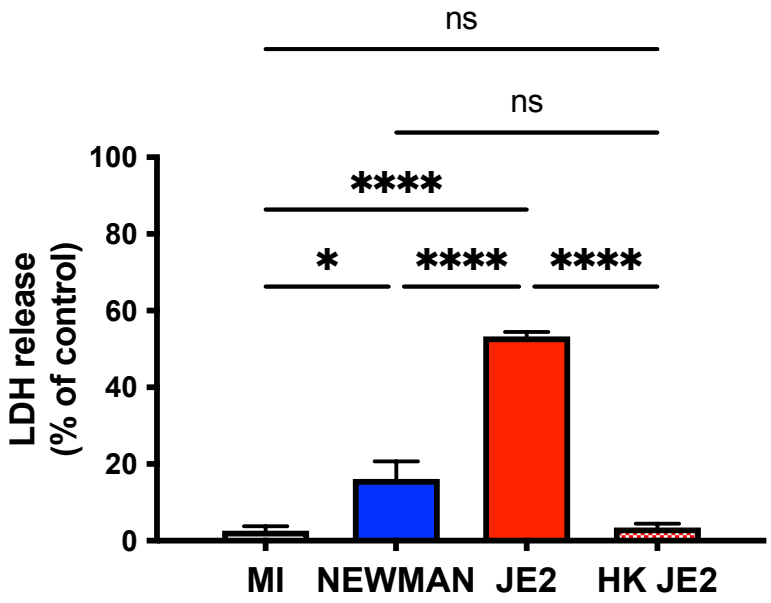

Figure 3.14 *S. aureus* infection causes host cell plasma membrane permeabilisation. Differentiated THP-1 macrophages were challenged for 20 hours with *S. aureus* Newman (NEW), *S. aureus* USA300 JE2 (JE2) or heat-killed *S. aureus* USA300 JE2 (HK JE2) strains at a MOI of 5 or mock infected (MI). Release of lactate dehydrogenase measured for each condition. The data represent three individual experiments, performed in duplicate. ns not significant, *p < 0.05, ****p < 0.0001, ordinary one-way ANOVA with Tukey's multiple comparison post-test.

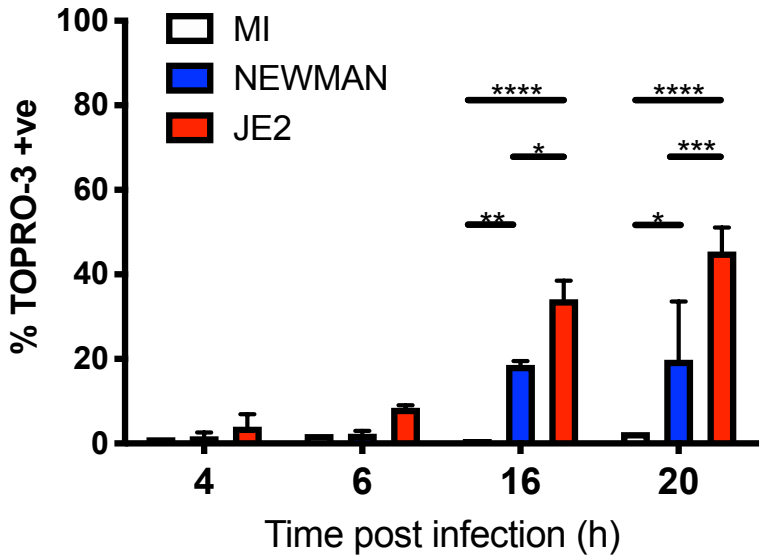

Figure 3.15 *S. aureus* infection causes host cell necrosis.
Differentiated THP-1 macrophages were challenged for up to 20 hours with either *S. aureus* Newman (NEWMAN), *S. aureus* USA300 JE2 (JE2) strains at a MOI of 5 or were mock infected (MI). A fluorescent marker of host cell necrosis, TOPRO-3, was quantified in live cells at specified time points by flow cytometry. The data represent three individual experiments, performed in duplicate. *p < 0.05, **p < 0.01, ***p < 0.001, ****p < 0.0001, two-way ANOVA with Sidak's post-test.

3.12 Macrophage apoptosis as defence against *S. aureus* is not observed.

As previously discussed, (section 1.4), apoptosis, or non-lytic programmed cell death, is an important form of host defence against infection, particularly against intracellular pathogens (Jorgensen et al. 2017). In the context of intracellular *S. pneumoniae* infection, following exhaustion of canonical microbicidal effector mechanisms, engagement of apoptosis is demonstrable (Dockrell et al. 2001). The apoptosis-mediated killing pathway requires translocation of activated cathepsin D from the phagolysosome into the cytoplasm via lysosomal membrane permeabilisation (Bewley et al. 2011). Cathepsin D induced downregulation of the anti-apoptotic Mcl-1 initiates a cascade involving sequential caspase activation and disintegration of the host cell (Jorgensen et al. 2017).

I have demonstrated that macrophages fail to recruit and activate cathepsin D following *S. aureus* challenge (Figure 3.7). It is therefore expected that apoptosis will not be engaged by macrophages infected with *S. aureus.*

To confirm that apoptosis mediated killing of intracellular *S. aureus* does not occur, macrophages either mock-infected or challenged with *S. aureus* Newman or USA300 strain JE2s for between 4 to 16 hours were probed for caspase activity. At the respective time points, caspase activity was measured using a CellEvent™ caspase 3/7 green flow cytometry assay kit. This experiment was performed with Dr Bewley. The activation of either caspase-3 or caspase-7 within macrophages, inferred as an indicator of apoptosis, was quantified. The cell permeant assay reagent is cleaved by active caspase-3 or caspase-7 proteins, resulting in DNA binding and fluorescence emittance. This experiment was performed in parallel with the TO-PRO-3 assay to simultaneously identify dead macrophage cells.

The experiment did not find evidence of macrophage caspase activation within the period of *S. aureus* exposure (Figure 3.16). This data corresponds with previously published work concerning the role of *S. aureus*-induced cytoprotection via upregulation of the anti-apoptotic regulator Mcl-1 and inhibition of apoptosis (Koziel et al. 2009).

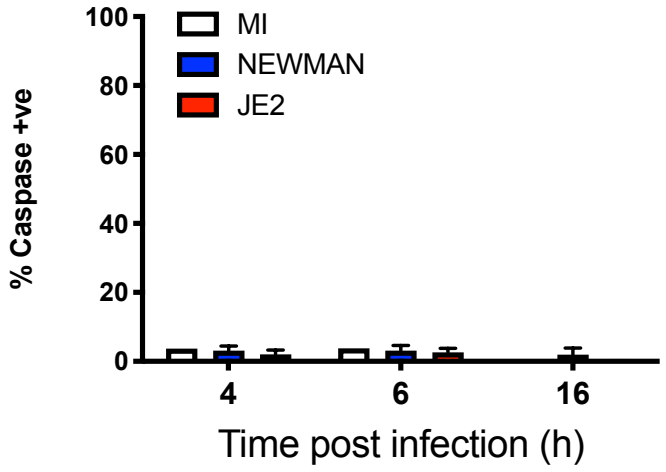

Figure 3.16 *S. aureus* infection causes minimal host cell apoptosis.
Differentiated THP-1 macrophages were challenged for up to 20 hours with either *S. aureus* Newman (NEWMAN), *S. aureus* USA300 JE2 (JE2) strains at a MOI of 5 or were mock infected (MI). Caspase 3 activity measured in live cells at specified time points by flow cytometry. The data represent three individual experiments, performed in duplicate. Two-way ANOVA with Sidak's post-test.

3.13 Challenge of polarised macrophages with pHrodo^{TM}-labelled *S. aureus* USA300 strain JE2

There is an increasing volume of evidence supporting the ability of *S. aureus* to resist killing within professional phagocytes (Flannagan et al. 2016; Tranchemontagne et al. 2015; Jubrail et al. 2016; Kubica et al. 2008). There is consensus that intracellular *S. aureus* traffics to a mature phagosome compartment and that cathepsin D activation is inhibited (Flannagan et al. 2016). However there are conflicting conclusions made regarding the environmental pH within the *S. aureus*-containing phagosome (Flannagan et al. 2015). These discrepancies could be attributable to differences in experimental protocol. A model utilising a less differentiated mononuclear cell line that models monocytes documented impaired phagosomal maturation with acidification (Tranchemontagne et al. 2015). The failure of phagosomal luminal acidification may be specific to differentiated macrophages which have a greater density of lysosomes (Daigneault et al. 2010). *S. aureus* challenge of MDM differentiated and polarised with macrophage-colony stimulating factor (M-CSF) stimulation towards an M2 phenotype failed to replicate the phagosomal maturation defect (Flannagan et al. 2016). This may indicate that the observed phagosomal defect selectively involves cells specialised to perform innate host defence by classical activation, an M1 phenotype (Mills et al. 2000).

In order to investigate maturation of the *S. aureus*-containing phagosome within differentiated macrophages polarised with either GM-CSF or M-CSF to produce phenotypes that although not identical share many characteristics of classically described M1 or M2 phenotypes (Mills et al. 2000; Canton et al. 2014). MDM were cultured as previously described plus additional polarizing stimuli. Supplemental GM-CSF (20 ng ml^{-1}) or M-CSF (10 ng ml^{-1}) polarised differentiation of MDM towards an M1 or M2 phenotype respectively. Unpolarised MDM were also cultured without additional stimulation to provide comparison to these stimuli. The respective MDM cell phenotypes were then challenged with pHrodo^{TM}-labelled *S. aureus* USA300 JE2 at MOI of 5 for 4 hours. The results demonstrate that differentiated macrophages which are unpolarised or polarised to a M1 phenotype fail to traffic *S. aureus* to an acidified compartment (Figure 3.17). This phagosomal maturation defect was not evident within M2 phenotype macrophages.

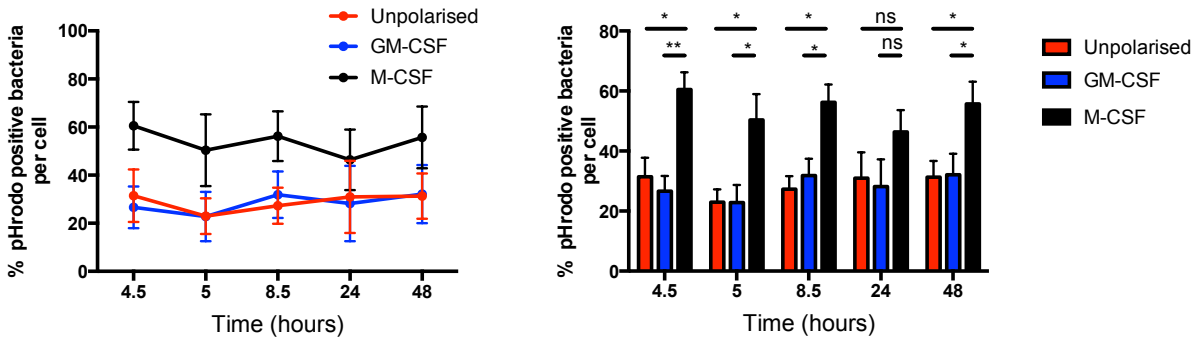

Figure 3.17 Trafficking of USA300 JE2 *S. aureus* to acidified phagosome varies by macrophage phenotype.

MDM were cultured for 14 days with 20 ng ml^{-1} GM-CSF (M1 phenotype), 10 ng ml^{-1} M-CSF (M2 phenotype) or medium alone (unpolarised). Differentiated MDM were challenged with pHrodoTM-labelled *S. aureus* USA300 strain JE2, MOI = 5, for 4 hours and subsequently incubated in the presence of lysostaphin and maintained for up to 48 hours post infection. For each condition, one hundred macrophages were counted and the number of intracellular fluorescent bacteria (DAPI-positive, pHrodo-positive) and intracellular non-fluorescent bacteria (DAPI-positive, pHrodo-negative) were estimated. The data represent the mean with standard error of the mean; n=3, statistics by Two-way ANOVA.

3.14 Conclusions

These findings are consistent with previous investigations of the interaction between *S. aureus* and macrophages differentiated *in vitro* to a tissue macrophage phenotype (Jubrail et al. 2016). Differentiated macrophages phagocytose all the *S. aureus* strains and mutants tested at this juncture; thus, it is concluded that the observation is not strain specific. Additionally, the USA300 strains JE2 following phagocytosis can be located within a late phagosome, that subverts appropriate phagosomal maturation to an acidified, LIMP-II positive phagolysosome. Bacterial factors are essential to subverting this pathway, as if the USA300 strain JE2 is heat-killed prior to macrophage challenge, the bacteria do progress to an acidified compartment, indicative of appropriate phagosomal maturation.

The fate of the USA300 strain JE2 infected macrophages is similar to that of those infected by strain Newman. The *S. aureus*-containing phagosomes fail to acquire activate cathepsin D, a further marker of phagolysosomal formation (as described in section 1.2.2.3) (Huynh & Grinstein 2007). The failure to activate cathepsin D is directly associated with the failure of the infected macrophage to engage apoptosis-mediated killing (Bewley et al. 2011). The results obtained are consistent with this description, with both strains Newman and JE2 failing to initiate the caspase pathway associated with apoptosis.

In comparison to strain Newman, the USA300 strain JE2 had a greater cytotoxic effect upon the macrophage. With sustained exposure, there is evidence of macrophage plasma membrane permeabilisation, as demonstrated with LDH release assay and the TOPRO-3 fluorometric assay. Both strains caused host cell permeabilisation in comparison to mock-infected macrophages. A statistically significant greater degree of host cell injury was associated with USA300 strain JE2 compared to Newman.

The Newman strain, isolated from a human infection in 1952 (Duthie & Lorenz 1952), has been extensively employed in experimental models of infection. Both strains belong to the CC8 lineage thus share a common progenitor, but whereas strain Newman has evolved from an epidemic archaic clone (CC8a) containing SCC*mec* I, the USA300 strain LAC has derived from the endemic USA500 clone (CC8e) containing SCCmec Iva (Bowers et al. 2018). Both strains are associated with cytotoxicity. Most virulence factors are shared, including Hla, Hlg, Hld, Hlb, PSMα and leucotoxin LukE (Li et al. 2009).

The major differences between the two sub-lineages is the presence of the PVL and ACME genes within the USA300 LAC genome. PVL has been demonstrated to cause pore formation within PMA-differentiated THP-1 macrophages with subsequent cell death (A. S. N. Spaan et al. 2013). Additionally, USA300 strains have a greater virulent phenotype compared to other strains assessed in animal infection models (Li et al. 2009). In a murine bacteraemia model where mice were infected with 10^8 cfu of specific MRSA strains from CC8, USA300 clones caused near complete fatalities, whereas COL, an archaic clone closely matched to strain Newman, caused no mortality. The USA300 clones were associated with a significantly greater systemic TNFα and IFNγ cytokine response when measured in blood at time of death compared to COL. Li *et al*. also demonstrated that USA300 clones caused significantly more neutrophil lysis (70-80%) compared to other strains (<10%), including COL, which reflects my findings and that of other groups (Voyich et al. 2005). However, in an assay of neutrophil lysis post-phagocytosis of either a wild-type USA300 clone or an isogenic PVL knock-down mutant there was no observable difference (Voyich et al. 2006).

An alternative explanation for the observed difference between the Newman strain and USA300 strain JE2 is the level of expression of virulence factors. Li *et al*. also demonstrated greatly increased Hla and PSMα1 production from USA300 clones compared to other CC8 lineage strains. PSMα have been identified to be critical to the escape of *S. aureus* from phagosomes and ultimately the lysis of neutrophils (Grosz et al. 2013; Surewaard et al. 2013).

As previously discussed in section 1.5.1, *S. aureus* virulence factors are subject to regulation. Thus, the finding that expression of RNAIII, taken as a correlate for Agr activity, was significantly increased in the USA300 clones compared to other strains (Li et al. 2009).

Although the data generated and evidence within the literature supports the concept of the USA300 strain JE2 having a hypervirulent phenotype, excessive virulence may curtail the ability of *S. aureus* to secure an intracellular immune privileged niche within a professional phagocyte (Thwaites & Gant 2011). Within a rabbit model, USA300 strain LAC was associated with causing lethal sepsis, but less frequently with infective endocarditis. Conversely, strain Newman caused significant IE but was less associated with lethal sepsis (Spaulding et al. 2012).

The evidence generated indicates that the USA300 strain JE2 is a valid strain to assess *S. aureus* genetic factors that account for subversion of phagosomal maturation within macrophages. Within the early phase (4-6h) of *S. aureus* infection of macrophages there is no demonstrably significant cell death, either in the form of necrosis, via cell lysis, or apoptosis. The USA300 strain JE2-containing phagosome fails to progress to an acidified phagolysosomal state.

As discussed, there is consensus that *S. aureus* traffics to a mature phagosomal compartment and is able to resist killing with no demonstrable cathepsin D activation (Flannagan et al. 2016; Tranchemontagne et al. 2015; Jubrail et al. 2016; Kubica et al. 2008). However, there are discrepancies within the *in vitro* differentiated macrophage models utilised between these groups; within a less differentiated mononuclear cell phenotype, phagosomal acidification was evident (Tranchemontagne et al. 2015); within differentiated macrophages with a M2 polarised phenotype, *S. aureus* was also associated with phagosomal acidification (Flannagan et al. 2016). Within a different differentiated macrophage model, specifically murine bone marrow derived macrophages, heat-killed *S. aureus* are associated with an acidified phagosome, whereas the pH of phagosomes containing live *S. aureus* was actively neutralised (Sokolovska et al. 2013).

I demonstrated that within differentiated macrophages, either unpolarised or with a GM-CSF induced M1 phenotype, the *S.* aureus-containing phagosome failed to acidify. Using a M-CSF induced M2 phenotype macrophage, the data obtained demonstrates phagosomal acidification consistent with results of Flannagan *et al*. This may indicate that the observed phagosomal defect selectively involves cells specialised to perform innate host defence by classical activation, a M1 phenotype (Mills et al. 2000).

Heterogeneity in phagosomal maturation between classically activated M1 and alternatively activated M2 polarised macrophages may account for the functional versatility of these populations (Canton et al. 2014). The homeostatic removal of apoptotic and necrotic cells by the M2 macrophage (Galli et al. 2011) would be supported by the rapid and profound acidification of the M2 phagosome enhancing the clearance of engulfed material (Canton et al. 2014). The classically activated M1 macrophage fulfils the function of clearing pathogens though delivery to the degradative phagolysosome and enhanced antigen presentation (Lawrence & Natoli 2011).

Sokolovska *et al*. demonstrated that upon internalisation of *S. aureus* (live or heat-killed), the phagosome is rapidly coated with activated caspase-1, which was subsequently associated with inhibitory regulation of NOX2 activity. This finding was dependent upon early generation of ROS, although ROS were not derived from NOX2, but independent of TLR signalling or V-ATPase activity. Phagosomes containing Gram-negative bacteria do not accumulate activated caspase-1, indicating the importance of the cargo within the phagosome. Within mutant macrophage cell lines with either the NLRP3-inflammasome component genes (*Nlrp3*$^{-/-}$ and *Asc*$^{-/-}$) or caspase-1 gene (*Ice*$^{-/-}$) knocked out, a greater and more sustained level of phagosome-associated ROS was evident post-*S. aureus* internalisation, compared to a small transient increase in wild-type macrophages. Utilising a phagosome pH dissipation assay following internalisation of either live or heat-killed *S. aureus*, application of the V-ATPase inhibitor Bafilomycin A resulted in reversal of phagosomal acidification to a neutral pH. Application of a caspase-1 inhibitor resulted in a partial reversal of acidification. Additionally, the *Nlrp3*$^{-/-}$, *Asc*$^{-/-}$ and *Ice*$^{-/-}$ mutant macrophages showed impaired phagosome acidification (Sokolovska et al. 2013).

Thus, a model was formed consisting of *S. aureus* internalisation triggering a transient NOX2-independent ROS burst leads to activation of the NLRP3-inflammasome, with activated caspase-1 coating the phagosome cytosolic surface. An electrogenic gradient is generated by the influx of protons into the phagosome by V-ATPase, which is counterbalanced by cation efflux via multiple channels and buffered by hydroxyl ions generated by NOX2. Hence, antagonism of V-ATPase or caspase-1 activation results in an imbalance towards NOX2 generation of ROS. Simply, the levels of ROS inversely correlate with phagosomal luminal pH (Sokolovska et al. 2013). These conclusions are analogous to that of Canton *et al*. who demonstrated that the M1 phagosome fails to acidify, attributed to relative equivalent activity of NOX2 and proton leak via voltage-gated proton channels, yet the M2 phagosome is rapidly acidified as the balance is weighted towards that of the proton pump (Canton et al. 2014).

My own findings, in addition to the evidence discussed above, indicate that the reduced phagosomal acidification is specific to the proinflammatory macrophage phenotype that respond to bacterial infection within host tissues. ROS-mediated killing of *S. aureus* has been demonstrated to be essential to clearance (Pizzolla et al. 2012) and may therefore be the primary method of killing within a M1 macrophage. Therefore, sustained high levels of phagosomal ROS may account for the failure of phagosome acidification. However, the hypothesis is confounded by demonstration of comparable ROS production with phagocytosis of *S. pneumoniae* where appropriate phagosomal acidification and maturation is evident (Jubrail et al. 2016). Another conflicting piece of evidence is that intraphagosomal live *S. aureus* is associated with sustained caspase-1 activation and IL-1β release when compared to heat-killed *S. aureus* (Sokolovska et al. 2013). This indicates that *S. aureus* actively sustains the inflammasome, with sustained ROS generation to buffer phagosomal acidification. The Dockrell group have demonstrated that ROS production is not deficient in response to *S. aureus* infection (Jubrail et al. 2016). Acidification is essential for the progressive phagosomal maturation and the activity of pH-sensitive antimicrobial enzymes, delivered via endosome and lysosome fusion, to enable microbial killing and immune signalling (Huynh & Grinstein 2007; Wolf et al. 2011). Therefore, *S. aureus* may tolerate ROS in order to prevent activating microbicidal proteases (Reeves et al. 2002).

Ahead of investigating possible bacterial factors that subvert phagosomal maturation, it is appropriate that this investigation is conducted within the monocyte-derived macrophage model of infection given the above findings.

Chapter 4

Development of a screen to identify *Staphylococcus aureus* genetic factors that subvert macrophage phagosomal maturation

4.1 Executive Summary

The aim of the following chapter was to develop a screen to identify *S. aureus* genes associated with the subversion of phagosomal maturation. Having established that the USA300 strain JE2-containing phagosome fails to acidify appropriately, a microscopy screen of single-gene mutants was developed. A candidate screen of *S. aureus* single-gene mutants demonstrated multiple genes were associated with subversion of phagosomal acidification. These included genes previously demonstrated as essential for intracellular survival, for example *agr* and *saeR*. Subsequently, a high-content microscopy screen was developed and optimised to enable a comprehensive assessment of a *S. aureus* transposon mutant library.

4.2 Introduction

Several *Staphylococcus aureus* virulence factors have been identified that facilitate immune evasion (T. J. Foster 2005). As previously discussed, subversion of phagosomal maturation by *S. aureus* is dependent upon bacterial factors since it is reversed by heat-killing (Sokolovska et al. 2013). My own data and that of the Dockrell group has demonstrated that *S. aureus* inhibits phagosomal acidification, which is required for progressive maturation and acquirement of antimicrobial peptides (Jubrail et al. 2016).

Upon internalisation into the professional phagocyte, *S. aureus* responds to local environmental stimuli to alter expression of multiple genes (Voyich et al. 2005). Assessment of *S. aureus* USA300 strain LAC gene expression was assessed between 30 – 180 minutes following phagocytosis by human neutrophils *in vitro*. Voyich *et al*. demonstrated that prompt global changes in gene expression were evident following phagocytosis, with altered expression of near 1000 genes detected in strain LAC. Most of these genes were either unknown or related to general metabolism, but also included genes associated with stress response (for example, catalase, thioredoxin, thioredoxin reductase, alkyl hydroperoxide reductases and superoxide dismutases); virulence and defence mechanisms (for example, ClfA, FnbB); toxins and haemolysins (for example, Hla, Hlb, Hlg); gene regulation (for example, SarA, SaeRS, Fur). This informative assessment also gave insight into temporal gene expression, for instance the oxidative stress response elements were maximally expressed within the initial 60 minutes, associated with maximal exposure of ROS. The virulence factors Hla, aureolysin, protein A and sortase A were also identified as important to intracellular survival in a macrophage model (Kubica et al. 2008). However, within this *in vitro*

S. aureus challenge of macrophages assay, the regulatory elements deemed essential for intracellular survival were, in part, contradictory to Voyich *et al*. Neutrophil phagocytosis was associated with upregulated expression of *saeRS*, *vraRS* and *sarA* and the repression of *agr* and *sigB* (Voyich et al. 2005). However, Kubica *et al*. demonstrated that *sigB* and *agr* expression was essential to survival in differentiated macrophages (Kubica et al. 2008).

The work completed by Voyich *et al*. provides clear evidence of the complex response *S. aureus* makes to the challenge of persisting within the inhospitable environment of the phagosome. The adapted gene expression pattern identified is in response to numerous stimuli, not only exposure to ROS and H^+ ions, but to changes in access nutrients and O_2. The bacterial mechanisms that facilitate extended intracellular persistence within macrophage phagosomes before delayed induction of necrosis remains unclear. (Kubica et al. 2008; Jubrail et al. 2016). I aim to identify the *S. aureus* genes that are associated with subverting acidification of the phagosome. The identification of the essential bacterial factors for intracellular persistence will be necessary to identify novel therapeutic targets for *S. aureus* and potentially against other facultative intracellular bacteria.

The resources and facilities available within the University of Sheffield have enabled me to develop the *in vitro* fluorescent microscopy assessment of the acidification of phagosomes containing *S. aureus* into a high-content microscopy screen of the *S. aureus* genome. The Nebraska transposon mutant library (NTML), generated within the laboratory of Professor Bayles of the University of Nebraska Medical Center, has been generously made available to the Foster laboratory. The mutant library will enable a comprehensive assessment of 1,920 *S. aureus* genes. Thus, the aim of this chapter is to develop and adapt the pHrodo™ assay previously utilised into a high-throughput microscopy screen. This has been made possible via the Sheffield RNAi screening facility (SRSF), both regarding technological equipment and the expertise of Dr. Stephen Brown, manager of the SRSF.

4.3 Aims and objectives

I. To screen candidate genes to prove concept that *S. aureus* genetic factors are required to subvert phagosomal acidification.
II. To establish a mechanism to label a single-gene mutant *S. aureus* library with the pH-sensitive marker pHrodo™.
III. To establish a high-content microscopy screen to identify bacterial mutants that fail to inhibit phagosomal maturation.

4.4 Assessment of phagosomal acidification using a candidate screen of *S. aureus* SH1000 single-gene mutant strains

Having established that acidification of the *S. aureus*-containing phagosome is not strain specific, and that heat-killed *S. aureus* is unable to subvert acidification, I hypothesised that this observation is dependent upon expression of bacterial factors. As discussed previously, several *S. aureus* virulence factors have been demonstrated to be essential for intracellular persistence. The data published by Voyich *et al*. indicated that expression of greater than one thousand genes are either upregulated or downregulated in response to phagocytosis (Voyich et al. 2005). With the expert guidance of Professor Foster, I identified candidate bacterial genes previously demonstrated to be important to *S. aureus* virulence. Within the Foster group bacterial library, numerous candidate gene deletion mutant strains derived from the parental *S. aureus* SH1000 strain have previously been created and validated (Table 2.1). Thus, it was possible to investigate the role of specific *S. aureus* genes in phagosomal acidification through their absence.

S. aureus wild-type SH1000, heat-killed SH1000 and SH1000 gene mutant strains were labelled with pHrodo™ and used to challenge differentiated macrophages to assess for progression to an acidified intracellular location. Wild-type and heat-killed SH1000 strain served as negative and positive control for phagosomal acidification respectively as previously demonstrated.

4.4.1 *S. aureus* global regulatory mechanisms

The two-component regulatory system genes *agr* and *saeR*, alternative sigma factor B and the DNA-binding protein gene *sarA*, having been previously demonstrated as essential to intracellular survival (Voyich et al. 2005; Voyich et al. 2008; Kubica et al. 2008) underwent assessment of phagosomal acidification.

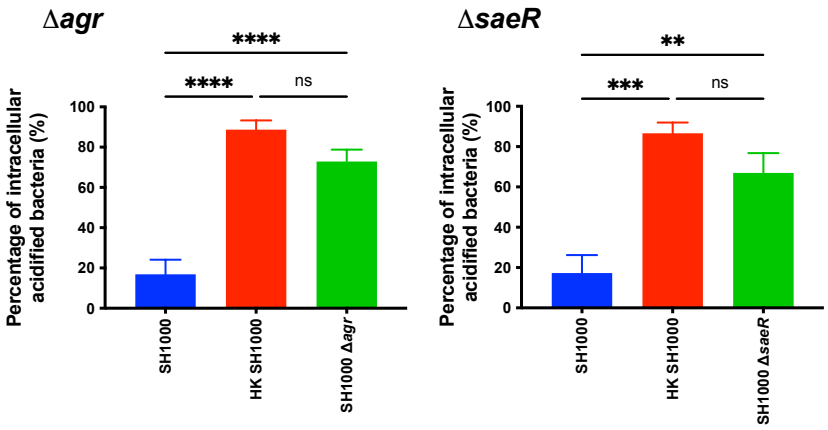

Figure 4.1 The two-component system accessory gene regulator (Agr) and *S. aureus* exoprotein expression regulator (SaeR) are associated with the subversion of phagosome acidification.

Monocyte-derived macrophages were challenged with pHrodo™-labelled *S. aureus* SH1000, heat-killed SH1000 (HK SH1000) and either (Δ***agr***) SH1000 *agr::tet* deletion mutant (SH1000 Δ*agr*) or (Δ***saeR***) SH1000 *saeR::Tn551* deletion mutant (SH1000 Δ*saeR*) strains at a MOI of 5 for 4 hours, then incubated with high-dose lysostaphin for 0.5 hours to eradicate extracellular bacteria, and then fixed. For each condition, one hundred macrophages were counted, and the number of intracellular fluorescent bacteria (DAPI-positive, pHrodo-positive) and intracellular non-fluorescent bacteria (DAPI-positive, pHrodo-negative) were estimated. Data displayed as mean percentage of total intracellular bacteria that were pHrodo™ fluorescent per cell. The data represent (Δ***agr***) n = 6 individual experiments; or (Δ***saeR***) n = 5 individual experiments, presented as mean with standard error of the mean (SEM); ns non-significant, **p<0.01, ***p<0.001, ****p<0.0001, ordinary one-way ANOVA with Tukey's multiple comparison post-test.

The *S. aureus agr* deletion mutant fails to inhibit phagosomal maturation (Figure 4.1). The agr two-component global regulator controls expression of *S. aureus* virulence factors as well as additional accessory gene functions (Novick 2003), and has been previously identified as an essential factor for intracellular survival in macrophages (Kubica et al. 2008). Both the *agr* and the *saeR* two-component regulatory systems are associated with upregulation of cytotoxins which could facilitate phagosomal escape. The *saeR* has also been associated with intracellular survival previously (Voyich et al. 2005; Gresham et al. 2000).

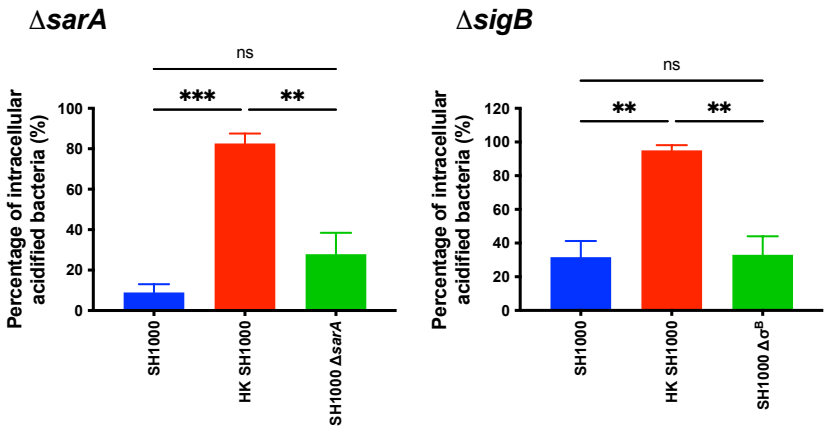

Figure 4.2 The global regulators staphylococcal accessory regulator A (SarA) and accessory sigma B (σ^B) are not associated with the subversion of phagosome acidification.

Monocyte-derived macrophages were challenged with pHrodo™-labelled *S. aureus* SH1000, heat-killed SH1000 (HK SH1000) and either (Δ***sarA***) SH1000 *sarA::kan* deletion mutant (SH1000 Δ*sarA*) or (Δ***sigB***) SH1000 ***σ^{B}::tet*** deletion mutant (SH1000 Δ***σ^{B}***) strains at a MOI of 5 for 4 hours, then incubated with high-dose lysostaphin for 0.5 hours to eradicate extracellular bacteria, and then fixed. For each condition, one hundred macrophages were counted, and the number of intracellular fluorescent bacteria (DAPI-positive, pHrodo-positive) and intracellular non-fluorescent bacteria (DAPI-positive, pHrodo-negative) were estimated. Data displayed as mean percentage of total intracellular bacteria that were pHrodo™ fluorescent per cell. The data represent (Δ***sarA***) n = 4 individual experiments; or (Δ***sigB***) n = 3 individual experiments, presented as mean with SEM. ns non-significant **p<0.01, ***p<0.001, ordinary one-way ANOVA with Tukey's multiple comparison post-test.

Figure 4.2 demonstrates that both SarA and alternative sigma factor B (**σ^{B}**) were not associated with subversion of phagosomal acidification. In the context of intracellular persistence within macrophages, SarA has previously been demonstrated to be non-essential (Kubica et al. 2008). However, within the same study **σ^{B}** was found to be essential to intracellular survival. The finding that **σ^{B}** is not associated with phagosomal acidification subversion following a 4-hour challenge of macrophages may be related to time of exposure. Environmental challenges to *S. aureus* homeostasis stimulates expression of **σ^{B}** and is then subject to post-translational regulation (P. F. Chan et al. 1998). The **σ^{B}** regulon includes multiple virulence-associated genes but operates in a reciprocal pattern to the *agr* locus with upregulation of cell wall proteins and downregulation of toxins and exoproteins in a growth-phase dependent manner (Bischoff et al. 2004). Expression of **σ^{B}** is greatest during the stationary phase of growth (P. F. Chan et al. 1998). It is therefore possible that within the time-period of this assay, the regulatory effect of **σ^{B}** will not be fully exerted.

4.4.2 Toxins and haemolysins

Both the Agr and SaeRS regulons are associated with lysis of human professional phagocytes following phagocytosis, with promotion of exotoxin expression (Novick 2003; Voyich et al. 2008; Voyich et al. 2009). Cytolytic toxins disrupt the host cell membrane are established as virulence factors (Powers & Wardenburg 2014). The pore-forming toxins have also been proposed as a mechanism of escape from the host phagosome, and potential dissipation of intra-phagosomal proton concentration (Grosz et al. 2013; Surewaard et al. 2013).

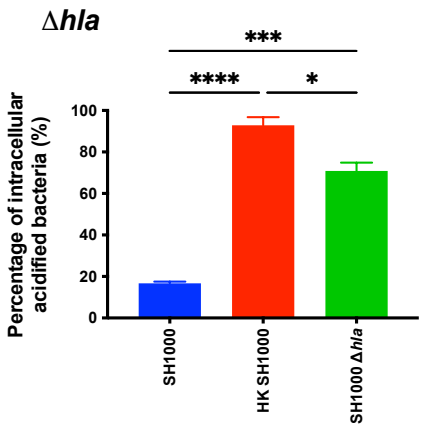

Figure 4.3 The haemolysin-α (Hla) toxin is associated with the subversion of phagosome acidification.

Monocyte-derived macrophages were challenged with pHrodo™-labelled *S. aureus* SH1000, heat-killed SH1000 (HK SH1000) and SH1000 *hla::ery* deletion mutant (SH1000 Δ*hla*) strain at a MOI of 5 for 4 hours, then incubated with high-dose lysostaphin for 0.5 hours to eradicate extracellular bacteria, and then fixed. For each condition, one hundred macrophages were counted, and the number of intracellular fluorescent bacteria (DAPI-positive, pHrodo-positive) and intracellular non-fluorescent bacteria (DAPI-positive, pHrodo-negative) were estimated.. Data displayed as mean percentage of total intracellular bacteria that were pHrodo™ fluorescent per cell. The data represent n = 3 individual experiments presented as mean with SEM. *p<0.05, ***p<0.001, ****p<0.0001, ordinary one-way ANOVA with Tukey's multiple comparison post-test.

The haemolysin-α mutant fails to subvert phagosomal acidification (Figure 4.3). This finding supports the hypothesis that pore-forming toxins disrupt the phagosome membrane, potentially antagonising the progressive acidification of intra-phagosomal environment.

4.4.3 Oxidative stress response regulators

Within the maturing macrophage phagosome, *S. aureus* will be subject to multiple microbicidal effectors, including reactive oxygen species (ROS). *S. aureus* resistance to oxidative stress is multifaceted, encompassing enzymatic detoxification, scavenger molecules, iron sequestration, and repair mechanisms (Fang 2004). These resistance mechanisms are mediated, in part, by transcriptional regulators. The peroxide response regulator (PerR) is a negative regulator of catalase and alkylhydroperoxide reductase (AhpC), which detoxify hydrogen peroxide (H_2O_2) and peroxides respectively (Cosgrove et al. 2007), and is required for *S. aureus* virulence (Horsburgh, Clements, et al. 2001)

The bacterial intracellular concentration of transition metals, for example iron and manganese, are finely regulated (Horsburgh, Ingham, et al. 2001; Horsburgh, Wharton, et al. 2002). The intake and storage of iron is regulated by the ferric uptake regulator (Fur) (Horsburgh, Ingham, et al. 2001). Iron, in the form of heme, is widely utilised within *S. aureus* as a prosthetic group in numerous proteins with diverse functions, including the respiratory chain and oxidative stress response proteins, for example catalase and myeloperoxidase (Wachenfeldt & Hederstedt 2002; Gaupp et al. 2012). But excessive iron is toxic. The Fenton reaction, where intracellular ferrous (Fe^{2+}) ions and endogenous H_2O_2 react to generate toxic hydroxyl radicals and enhances ROS-mediated killing on *S. aureus* (Imlay et al. 1988; Hoepelman et al. 1990). Fur, and it's analogue PerR, regulate expression of iron storage proteins and catalase which antagonise the Fenton reaction (Horsburgh, Ingham, et al. 2001). Fur has also been found to influence Sae function, hypothetically to promote iron-acquisition via exotoxin-mediated lysis of host cells (Johnson et al. 2011).

The manganese transport repressor (MntR) regulates intracellular concentrations of Mn^{2+} ions, through repression of Mn^{2+} uptake systems when Mn^{2+} levels are elevated (Horsburgh, Wharton, et al. 2002). Horsburgh *et al.* demonstrated that Mn^{2+} uptake is required for virulence, intracellular survival, and resistance to ROS. Akin to iron ions, Mn^{2+} ions are present as co-factors within multiple bacterial proteins, including superoxide dismutases enzymes (Karavolos 2003) and potentially within respiratory chain complexes (Bolshakov et al. 2010). The expression of PerR has also been demonstrated to be dependent upon Mn^{2+} levels, with repression of *perR* evident in the presence of high Mn^{2+} levels (Horsburgh, Clements, et al. 2001).

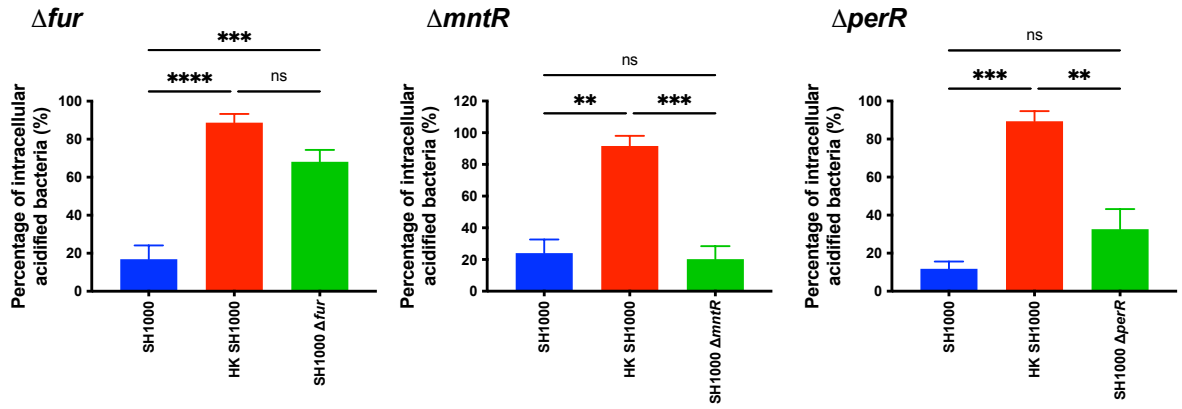

Figure 4.4 The stress regulator ferric uptake regulator (Fur) was associated with the subversion of phagosome acidification, but the manganese transport repressor (MntR) and the peroxide response regulator (PerR) were not.

Monocyte-derived macrophages were challenged with pHrodo™-labelled *S. aureus* SH1000, heat-killed SH1000 (HK SH1000) and either (Δ***fur***) SH1000 *fur::tet* deletion mutant (SH1000

Δ*fur*), (Δ***mntR***) SH1000 *mntR::tet* deletion mutant (SH1000 Δ*mntR*) or (Δ***perR***) SH1000 *perR::kan* deletion mutant (SH1000 Δ*perR*) strains at a MOI of 5 for 4 hours, then incubated with high-dose lysostaphin for 0.5 hours to eradicate extracellular bacteria, and then fixed. For each condition, one hundred macrophages were counted, and the number of intracellular fluorescent bacteria (DAPI-positive, pHrodo-positive) and intracellular non-fluorescent bacteria (DAPI-positive, pHrodo-negative) were estimated. Data displayed as mean percentage of total intracellular bacteria that were pHrodo^{TM} fluorescent per cell. The data represent (Δ***fur***) n = 6 individual experiments; (Δ***mntR***) n = 4 individual experiments; (Δ***perR***) n = 4 individual experiments presented as mean with SEM. ns non-significant, **p<0.01, ***p<0.001, ****p<0.0001, ordinary one-way ANOVA with Tukey's multiple comparison post-test.

The finding that the SH1000 *fur* deletion mutant failed to prevent phagosomal acidification is novel (Figure 4.4). The *fur* deletion mutant would be incapable of countering increasing intracellular Fe^{2+} concentrations, which will be deleterious to the bacteria in the presence of superoxide. Fur is also known to stimulate catalase activity (Horsburgh, Ingham, et al. 2001). A *fur* deletion mutant has previously been demonstrated to have reduced resistance to oxidative stress (Horsburgh, Ingham, et al. 2001).

The *mntR* and *perR* mutants failed to exhibit any significant difference in comparison to the wild-type control (Figure 4.4). As PerR is a negative regulator of catalase and AhpC, these enzymes would be de-repressed (Cosgrove et al. 2007). The role of MntR is not clear, but in the absence of *mntR,* intracellular Mn^{2+} levels would be disrelated.

4.4.4 Reactive oxygen species stress response effectors

As discussed above, *S. aureus* resistance to oxidative stress is multifaceted (Fang 2004). The two *S. aureus* superoxide dismutase (Sod) enzymes, encoded by *sodA* and *sodM* are responsible for the removal of superoxide radicals (Karavolos 2003). The role of the Sod enzymes in virulence is controversial, with conflicting evidence for their importance (Karavolos 2003; Clements et al. 1999). The antioxidant proteins catalase and AhpC are required for intracellular persistence (Cosgrove et al. 2007). Both are subject to regulation via PerR in a compensatory manner, as mutation within the *ahpC* gene results upregulation in *katA* expression and enhanced resistance to H_2O_2, and mutation in *katA* is compensated by *ahpC* expression (Cosgrove et al. 2007).

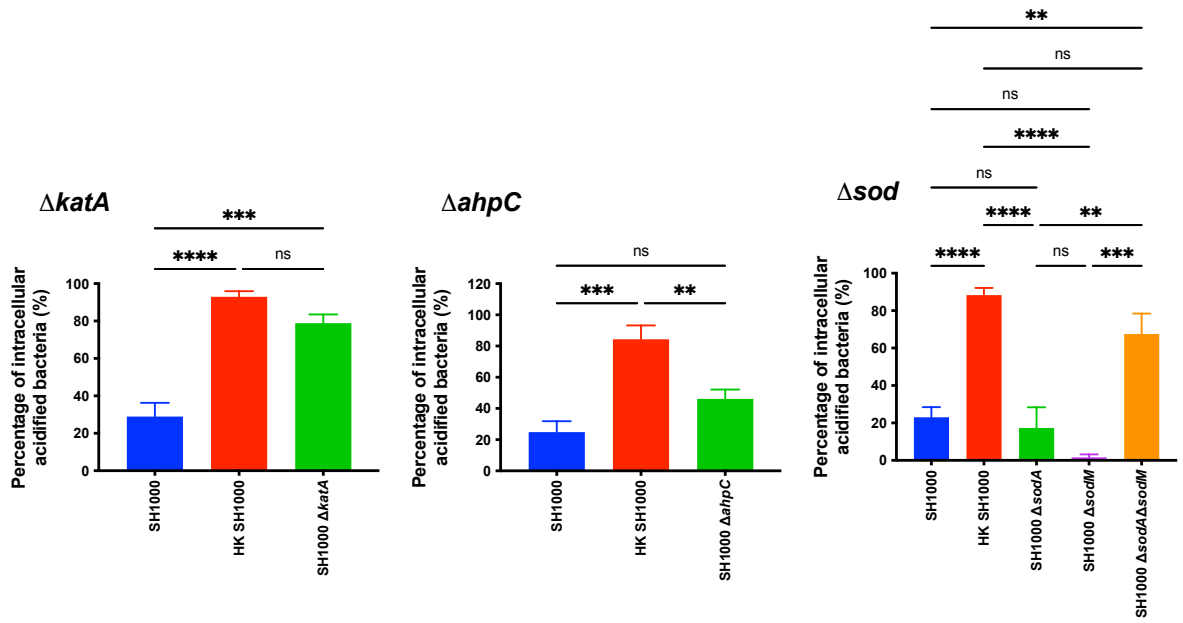

Figure 4.5 The oxidative stress resistance mechanism effectors catalase (KatA) and superoxide dismutases (Sod) were associated with the subversion of phagosome acidification, but alkyl hydroperoxide C (AhpC) was not.

Monocyte-derived macrophages were challenged with pHrodo™-labelled *S. aureus* SH1000, heat-killed SH1000 (HK SH1000) and either (Δ***katA***) SH1000 *katA::Tn917* deletion mutant (SH1000 Δ*katA*), (Δ***ahpC***) SH1000 *ahpC::tet* deletion mutant (SH1000 Δ*aphC*) or (Δ***sod***) SH1000 *sodA::Tn917* deletion mutant (SH1000 Δ*sodA*), SH1000 *sodM::tet* (SH1000 Δ*sodM*) or SH1000 *sodA::Tn917 sodM::tet* (SH1000 Δ*sodA*Δ*sodM*) strains at a MOI of 5 for 4 hours, then incubated with high-dose lysostaphin for 0.5 hours to eradicate extracellular bacteria, and then fixed. For each condition, one hundred macrophages were counted, and the number of intracellular fluorescent bacteria (DAPI-positive, pHrodo-positive) and intracellular non-fluorescent bacteria (DAPI-positive, pHrodo-negative) were estimated. Data displayed as mean percentage of total intracellular bacteria that were pHrodo™ fluorescent per cell. The data represent (Δ***katA***) n = 4 individual experiments; (Δ***ahpC***) n = 5 individual experiments; (Δ***sod***) n = 3 – 5 individual experiments presented as mean with SEM. ns non-significant, **p<0.01, ***p<0.001, ****p<0.0001, ordinary one-way ANOVA with Tukey's multiple comparison post-test.

Figure 4.5 demonstrates that *katA* is required for subversion of phagosomal acidification, but *ahpC* is not. As discussed above, these two antioxidant genes demonstrate redundancy. As noted by Cosgrove *et al.*, the absence of *ahpC* increased resistance to H_2O_2, additionally *katA* was identified as being more important in the response to external and higher levels of endogenous H_2O_2 (Cosgrove et al. 2007). A compensatory mechanism was also evident within

the single *sod* mutants, but in the double mutant (*sodA sodM*) failure to subvert phagosomal acidification was evident.

4.4.5 Iron storage proteins

Having identified that Fur is associated with subversion of phagosomal acidification, additional iron homeostasis factors were investigated. In the presence of free intracellular Fe^{2+} ions, *S. aureus* upregulates expression of the iron-storage proteins ferritin (Ftn) and the DNA protection during starvation (Dps)-homologue MrgA (Horsburgh, Clements, et al. 2001). Elevated intracellular Fe^{2+} concentrations were found to induce the PerR regulon, with subsequent increased expression of Ftn and MrgA in order to sequester free iron (Horsburgh, Clements, et al. 2001).

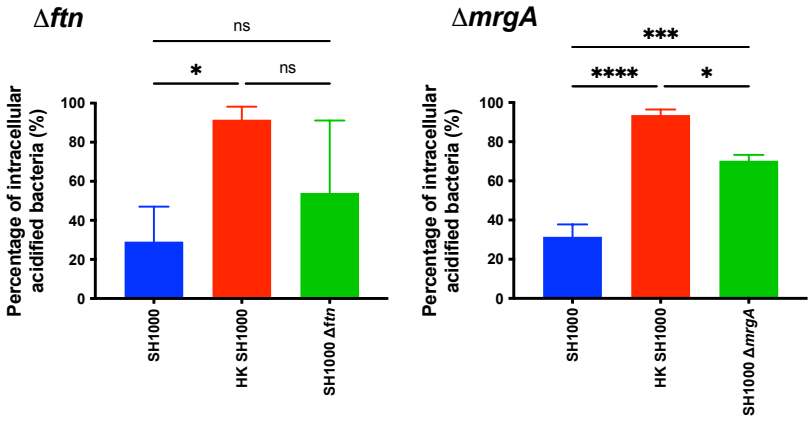

Figure 4.6 The iron storage protein Dps-homologue MrgA was associated with the subversion of phagosome acidification, but the iron storage protein ferritin (Ftn) was not

Monocyte-derived macrophages were challenged with pHrodo™-labelled *S. aureus* SH1000, heat-killed SH1000 (HK SH1000) and either (Δ***ftn***) SH1000 *ftn::tet* deletion mutant (SH1000 Δ*ftn*), or (Δ***mrgA***) SH1000 *mrgA::tet* deletion mutant (SH1000 Δ*mrgA*) strains at a MOI of 5 for 4 hours, then incubated with high-dose lysostaphin for 0.5 hours to eradicate extracellular bacteria, and then fixed. For each condition, one hundred macrophages were counted, and the number of intracellular fluorescent bacteria (DAPI-positive, pHrodo-positive) and intracellular non-fluorescent bacteria (DAPI-positive, pHrodo-negative) were estimated. Data displayed as mean percentage of total intracellular bacteria that were pHrodo™ fluorescent per cell. The data represent (Δ***ftn***) n = 3 individual experiments; (Δ***mrgA***) n = 4 individual experiments presented as mean with SEM. ns non-significant, *p<0.05, ***p<0.001, ****p<0.0001, ordinary one-way ANOVA with Tukey's multiple comparison post-test.

Figure 4.6 demonstrates that the *mrgA* mutant is associated with subversion of phagosomal acidification, but the *ftn* mutant did not meet statistical significance. The importance of iron homeostasis is supported by this observation. It is not apparent if in the absence of *mrgA* expression that alternative iron storage methods compensate for this deficit. Hypothetically, loss of an iron storage resource would increase the levels of free Fe^{2+} ions, which would promote the deleterious Fenton reaction.

4.4.6 Staphylococcal cell wall proteins

The sortase proteins are integral to the sorting and anchoring of surface proteins within the bacterial cell wall (Mazmanian et al. 1999). The expression of sortase A (SrtA), an extracellular transpeptidase, was demonstrated to be essential for survival and escape from within macrophages (Kubica et al. 2008). The SrtA enzyme has been found to be highly resistant to oxidative stress, attributed to catalytic cysteine residue (Melvin et al. 2011). It was also of interest to explore if modification of the bacterial cell wall would cause an impaction upon resistance to acidification. The peptidoglycan hydrolases, which includes the *S. aureus* glucosaminidase A (SagA) and B (SagB), are required for cell wall integrity (Y. G. Y. Chan et al. 2016). In the absence of *sagB,* the cell wall peptidoglycan chain length is increased, with a resultant increase in bacterial cell stiffness (Wheeler et al. 2015). Virulence of *S. aureus* is augmented by particulate peptidoglycan (Boldock et al. 2018). Within this work by Boldock *et al.,* I demonstrated that intracellular killing of bacteria within differentiated macrophages in the presence of particulate peptidoglycan was reduced in comparison to the absence of peptidoglycan (data not shown). Hence, it was relevant to investigate if these cell wall enzymes participated in the subversion of phagosomal acidification.

Neither *srtA, sagA* or *sagB* mutants were found to subvert phagosomal acidification (Figure 4.7). Kubica *et al.* associated that a mutant deficient in protein A shared the same phenotype as the *srtA* mutant regarding survival within the intracellular macrophage environment (Kubica et al. 2008). Kubica *et al.* also proposes that anchoring of microbial surface components recognising adhesive matrix molecules (MSCRAMMs) by sortase A as an alternative mechanism by which intracellular survival is achieved. Peptidoglycan chain length does not appear to directly affect phagosomal acidification. Boldock *et al.* proposed that *S. aureus* may respond to the detection of peptidoglycan with enhanced virulence to facilitate host immune subversion (Boldock et al. 2018).

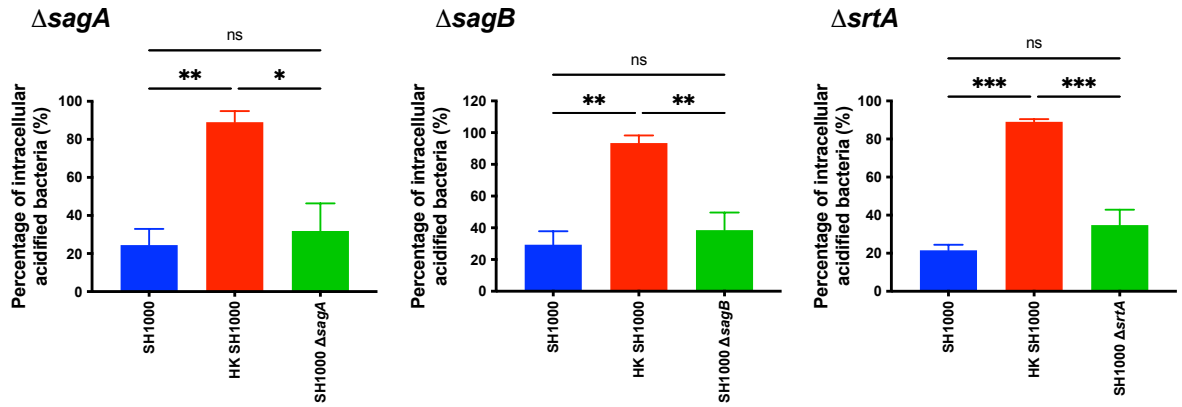

Figure 4.7 The cell wall protein regulators *S. aureus* glucosaminidase A (SagA) and B (SagB) and sortase transpeptidase (SrtA) were not associated with the subversion of phagosome acidification.

Monocyte-derived macrophages were challenged with pHrodo™-labelled *S. aureus* SH1000, heat-killed SH1000 (HK SH1000) and either (Δ***sagA***) SH1000 *sagA::tet* deletion mutant (SH1000 Δ*sagA*), (Δ***sagB***) SH1000 *sagB::kan* deletion mutant (SH1000 Δ*sagB*) or (Δ***srtA***) SH1000 Δ*srtA* deletion mutant strains at a MOI of 5 for 4 hours, then incubated with high-dose lysostaphin for 0.5 hours to eradicate extracellular bacteria, and then fixed. For each condition, one hundred macrophages were counted, and the number of intracellular fluorescent bacteria (DAPI-positive, pHrodo-positive) and intracellular non-fluorescent bacteria (DAPI-positive, pHrodo-negative) were estimated. Data displayed as mean percentage of total intracellular bacteria that were pHrodo™ fluorescent per cell. The data represent (Δ***sagA***) n = 4 individual experiments; (Δ***sagB***) n = 5 individual experiments; (Δ***srtA***) n = 3 individual experiments presented as mean with SEM. ns non-significant, *p<0.05, **p<0.01, ***p<0.001, ordinary one-way ANOVA with Tukey's multiple comparison post-test.

4.5 Development of a customised analysis algorithm to measure features within digital microscopy images.

Utilising the NTML required several adaptations to the prior method used in the challenge of macrophages with pHrodo^{TM}-labelled bacteria. The methods used above utilised fixed material mounted upon slides, imaged using the Leica DMRB fluorescent microscope, with the features of interest counted by the operator (described in methods section 2.8.3.4 and 2.5). Therefore, the initial objective was to convert from the format from mounted coverslips to performing the assay within a 96-well format to enable high-throughput screening.

The Molecular Devices ImageXpress^{MICRO} microscope, available within the Sheffield RNAi Screening Facility (SRSF), is capable of imaging biological material within a 96-well format and has been specifically designed to facilitate high-throughput high-content microscopy screening assays (Brown 2010). Following the advice of the SRSF, 96-well flat-bottom μClear® white (opaque) sided microplates by Greiner were used for the study, given compatibility with the high-throughput microscopy and cell culture requirements.

Prior to undertaking screening of the NTML, assay optimisation was necessary, with the aim to numerate, per macrophage, intracellular bacteria that had been acidified or not.

4.5.1 Optimisation of bacterial pHrodo^{TM} staining.

The 1,920 *S. aureus* mutant strains comprising the NTML are stored within the Foster laboratory at –80ºC, divided across twenty 96-well plates. Three copies of each NTML plate were created for this study and stored at –80ºC (methods section 2.2.2.2).

Previous investigation of the NTML within the Foster laboratory by Dr. Dingyi Yang, specifically in regard to bacterial factors contributing to neutrophil lysis, has led to the optimisation of NTML growth ahead of phagocyte challenge (D. Yang et al. 2019). Having created multiple replicates of the NTML, prior to labelling, each plate was thawed, and mutant strains inoculated into fresh media and cultured overnight, as described in methods section 2.8.3.4.1. As demonstrated by Dr Yang, within either BHI or RPMI (+10% v/v FBS), the parental USA300 strain JE2 entered an exponential growth phase after 2-hours of incubation, with stationary growth apparent at 4- or 6-hours when cultured in BHI or RPMI respectively (D. Yang 2018). Adhering to the operating procedure of Dr Yang, the overnight culture was followed by a 3-hour subculture (1:20) in fresh BHI media, yielding approximately 5 x 10^8 CFU ml^{-1} within 200μL of media. The subculture was conducted within a sterile round bottom 96-well plate to

facilitate centrifugation using a Rotanta 460 R centrifuge with a swing out rotor and featuring a bio-containment cradle and lid.

The methods for labelling bacteria with pHrodo^{TM} are described in methods section 2.8.3.4.1. Prior to staining, the bacterial culture was centrifuged and resuspended in sterile PBS pH 7.4. The pHrodo^{TM} Red, succinimidyl ester stain forms a stable carboxamide bond with free amine groups, hence removal of free protein was required to negate artefactual staining. Following a second cycle of washing, the bacteria suspended in 200μL PBS pH 7.4 was mixed with 0.5μl 2.55μM pHrodo^{TM} and incubated in darkness at 37ºC whilst shaken, as per standard procedure. Post-labelling the bacterial suspension was washed to remove unbound pHrodo^{TM}. As per the previously established protocol, the wash steps entailed centrifugation and resuspension. Given that reduced bacteria viability was observed using basic PBS during labelling (pH 8.5) and the initial wash (pH 9), the labelling procedure was adapted to neutral PBS as per manufacturer recommendations. However, the wash with the basic (pH 8.4) Tris buffer which contains primary amines, was maintained to quench residual unbound or remove weakly bound pHrodo^{TM}. The rationale for the basic conditions is that the ε-amine group of lysine has a pK_a of approximately 10.5, and for conjugation to occur, the amine group must remain non-protonated, hence the manufacturer recommends using slightly basic buffers for the conjugation reaction. However, the amine terminus of proteins has a lower pK_a, hence a neutral pH will favour labelling of this amine group.

4.5.2 Optimisation of macrophage challenge with pHrodo^{TM}-labelled bacteria.

Human primary blood mononuclear cells (PBMC) were seeded into sterile Greiner 96-well μclear® (190μm ± 20μm film thickness) flat-bottom plates which had been pre-treated at production with a physical surface treatment to aid cell adhesion. PBMCs were seeded at a density of 2 x 10^6 cells ml^{-1}, 100μl per well, as per the standard operating procedure. The resultant differentiated MDMs at a density of approximately 2 x 10^5 cells ml^{-1} and were used between days 14 and 21.

The differentiated MDMs were challenged by the pHrodo^{TM}-labelled NTML mutant strains at an approximate multiplication of infection (MOI) of 5 for a total of 4 hours. The justification for these MOI and period of infection values derives from prior data obtained using the parental USA300 strain JE2 (Figure 3.11) where statistical significance was initially demonstrated. As detailed above, the pHrodo^{TM}-labelled NTML mutant strains had been grown to an approximate density of 5 x 10^8 CFU ml^{-1}, thus 2μl of the bacterial suspension was added to MDMs cultured in 100μl RPMI 1640 supplemented with 10% (v/v) FCS.

Following the standard operating procedure, the cell culture plates containing the *S. aureus* challenged MDMs were incubated on ice for 60 minutes in darkness, before further incubation at 37ºC for 180 minutes. At the 4-hour juncture, the infected media was removed and the MDMs were carefully washed with ice-cold PBS to halt phagocytosis. The infected MDMs were then re-cultured in fresh media supplemented with 20μg ml^{-1} lysostaphin to remove residual extracellular *S. aureus*. Prior to fixation with 4% formaldehyde, the MDMs were stained with CellMask™ Deep Red plasma membrane stain. The plasma membrane stain demarcates the cell boundary, defining the intracellular environment during high-content microscopy screen segmentation. The plasma membrane binding properties of the CellMask™ stain are conferred by a lipophilic moiety and negatively charged hydrophilic dye, which are maintained following fixation with formaldehyde. Finally, the infected MDMs are counterstained with the nucleic acid stain DAPI to demarcate both MDM and bacterial nucleotides.

4.5.3 Optimisation of automated fluorescent microscopy and data extraction

Imaging of the 96-well microplates took place promptly after staining and fixation. Due to minor geometric differences between microplates, automated robotic loading of sequential plates was not feasible. The microplates were loaded manually into the Molecular Devices ImageXpress^{MICRO} imaging system, and the focal depth or Z-pattern was manually determined for each microplate. Due to inconsistencies between the microplates, as a minimum each plate would require Z-pattern amendment, often requiring adjustment between different columns or rows to negate differences between neighbouring wells. Consequently, the undertaking of microscopy required an operator presence throughout.

For each well, multiple discrete sites that were geometrically consistent across all wells could be imaged using the “fit sites to well” command. To image multiple plates promptly without foregoing adequate sampling of macrophage numbers, five sites per well were imaged. The resulting images of five sites consistently captured greater than 300 MDMs per well, a value utilised in previous *S. aureus*-macrophage interaction assays (Jubrail et al. 2016).

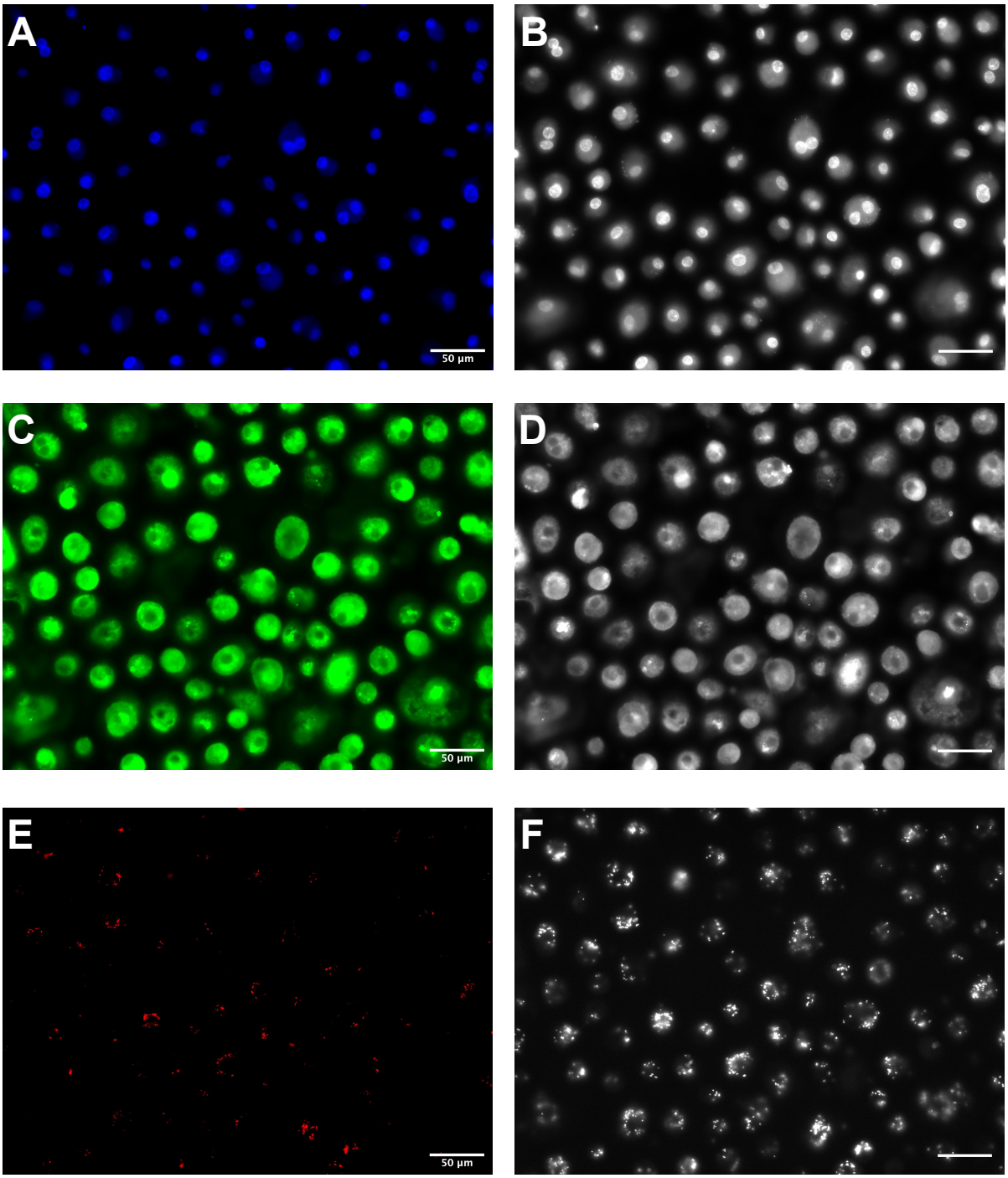
A
50 µm
B
C
50 µm
D
E
50 µm
F

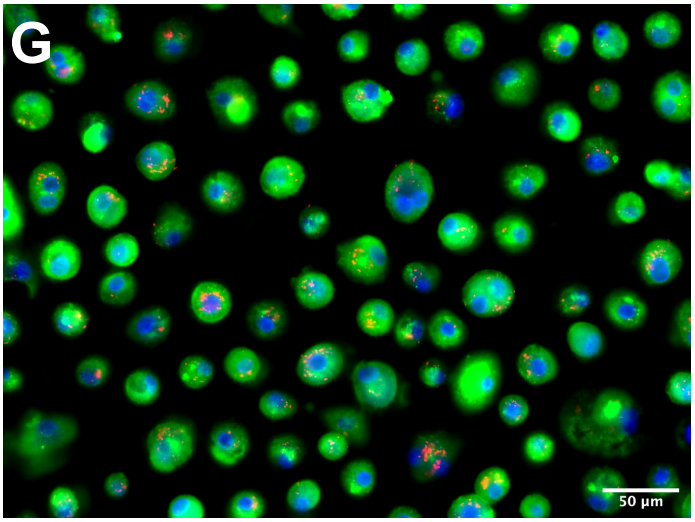

Figure 4.8 Representative microscopy images of human monocyte-derived macrophages challenged with heat-killed *S. aureus* USA300 strain JE2.

MDMs were challenged with heat-killed *S. aureus* USA300 strain JE2 labelled with pHrodo at an estimated MOI of 5 for 4 hours. Extracellular bacteria removed by washing and lysed with lysostaphin for 0.5 hours. Material stained with CellMask^{TM}, fixed, and counterstained with DAPI. Images acquired using high-throughput Molecular Devices ImageXpress^{MICRO} imaging system, using 20X objective with (A & B) DAPI filter, (C & D) CY5 filter, (E & F) Texas Red filter. Images A, C & E presented by wavelength. Images B, D, & F presented in greyscale. Image G represents merged image. Scale bar represents 50µm.

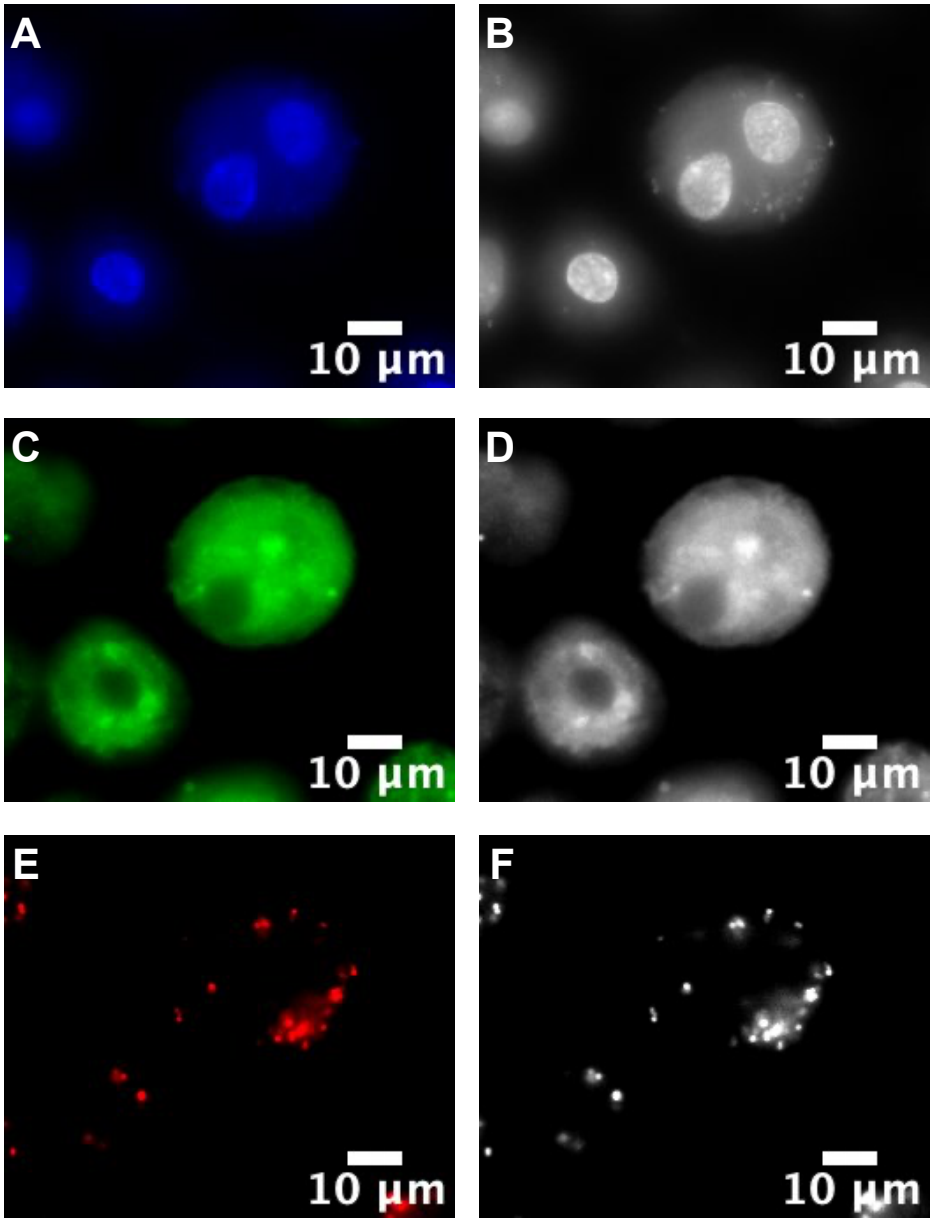

Figure 4.9 Representative microscopy images of human monocyte-derived macrophages challenged with heat-killed *S. aureus* USA300 strain JE2.

MDMs were challenged with heat-killed *S. aureus* USA300 strain JE2 labelled with pHrodo at an estimated MOI of 5 for 4 hours. Extracellular bacteria removed by washing and lysed with lysostaphin for 0.5 hours. Material stained with CellMask^{TM}, fixed, and counterstained with DAPI. Images acquired using high-throughput Molecular Devices ImageXpress^{MICRO} imaging system, using 20X objective with (A & B) DAPI filter, (C & D) CY5 filter, (E & F) Texas Red filter. Images A, C & E presented by wavelength. Images B, D, & F presented in greyscale. Scale bar represents 10μm.

For imaging, a 20X objective was selected to detect bacteria, and three acquisition wavelengths were required to image the respective fluoroprobes, using the filter sets DAPI, Texas Red and CY5/Far Red (Figure 4.8). The respective exposure times were adjusted following use of the "auto exposure" tool to obtain optimal signal to noise ratio. To detect the $DAPI^+$ pixels corresponding to bacteria, the sample would need to be overexposed as the brightest $DAPI^+$ pixels corresponded to the nuclei of macrophages.

To compensate for small Z-pattern differences between wells, a second image acquisition was undertaken with a 2μm offset from the original image acquired. This option was more advantageous with respect to throughput rather than collecting a Z-series and subsequent compression into one image termed a Z-series projection. The associated MetaXpress® analysis software package includes the mathematical operation "add" which combines the intensity values of the two acquired images (Figure 4.10.2). For each corresponding pixel position, the add operation sums the intensity values from the respective sources, then displays the pixel with the summative value in a new image. The images were acquired as 16-bit images, thus the mathematical operation resultant image intensity values from were restricted to the range 0 – 65,535. This action was performed for the purpose of imaging bacteria using the DAPI and Texas Red filter sets (Figure 4.10.3), as there was minimal difference in plasma membrane dimensions observed within this Z-series. The Z-offset was automatically adjusted for both respective wavelengths. Given the approximate physical diameters of the macrophage nucleus (>10μm) and *S. aureus* (<1μm), obtaining two images with a 2μm Z-offset served to capture discreet bacteria without a perceived difference in the macrophage nucleus.

All images collected were stored locally on the SRSF RNAi image server, with the metadata linked to the images stored separately on the MDCstore database. From these locations, the Molecular Devices MetaXpress® analysis software package is purposed to evaluate and measure objects within images. Basic measurement tools are inbuilt into the software, for example shape, area, and intensity of objects within an image. However, these tools were insufficient to extract meaningful information regarding bacteria within the intracellular environment of a macrophage. The software provides the user with the ability to create a custom algorithm, or "journal", for such a purpose.

The MetaXpress® "Custom Module Editor" facilitates repetitive, complex processing of images to obtained customised measurements. Using an iterative process, pilot data images were

utilised to construct a measurement tool to quantify macrophage number, total intracellular bacteria, and total intracellular acidified bacteria (Figures 4.10.1 to 4.10.15).

As described above, the initial processing step was the mathematical operation “add” to create single images acquired by the DAPI and Texas Red filter sets (Figures 4.10.2 and 4.10.3). The resulting image for respective wavelengths was in effect a Z-projection of pixels representative of discrete bacteria and multiple macrophage nuclei contiguous between Z-series. Segmentation tools were then used to define objects within the pre-processed 16-bit grayscale images from the background. Macrophage nuclei were defined by the “find round objects” tool, using the DAPI image within a set geometrical range and signal intensity greater than background (Figure 4.10.5). The macrophage cell outline was also defined but the same tool applied to the CY5/Far Red image (Figure 4.10.6 and 4.10.7). The resultant binary mask images included incomplete features at the edges of the image. Such objects were excluded using the “remove border objects” tool (not shown).

Identification of bacteria required additional pre-processing stages prior to optimise isolation during segmentation. The DAPI and Texas Red Z-projection images were both subjected to a “top hat” filter (Figures 4.10.9 and 4.10.12), adapted from an “open” filter, which detects small bright features of a known spatial size and shape. For both DAPI and Texas Red images, the “open” filter detects circular shaped objects and subtracts the original image from this filter image to create the “top hat” filter image. Subsequently, the “find round objects” filter was applied to this image to create a binary mask image of fluoroprobe positive bacteria (Figures 4.10.10 and 4.10.13). DAPI positive pixels that were isolated by this method that were also identified during creation of the macrophage nuclei mask were excluded using the logical operations tool. The two binary mask images derived from the DAPI images were subject to the Boolean operator “andnot” to generate a mask of DAPI positive pixels outside of the macrophage nuclei mask (Figures 4.10.11 and 4.10.14). Thus, a binary mask image of all bacteria was derived. Another logical operation was performed to remove the macrophage nuclei from the macrophage cell mask, generating a binary mask image of the macrophage intracellular space minus the nucleus (Figure 4.10.8).

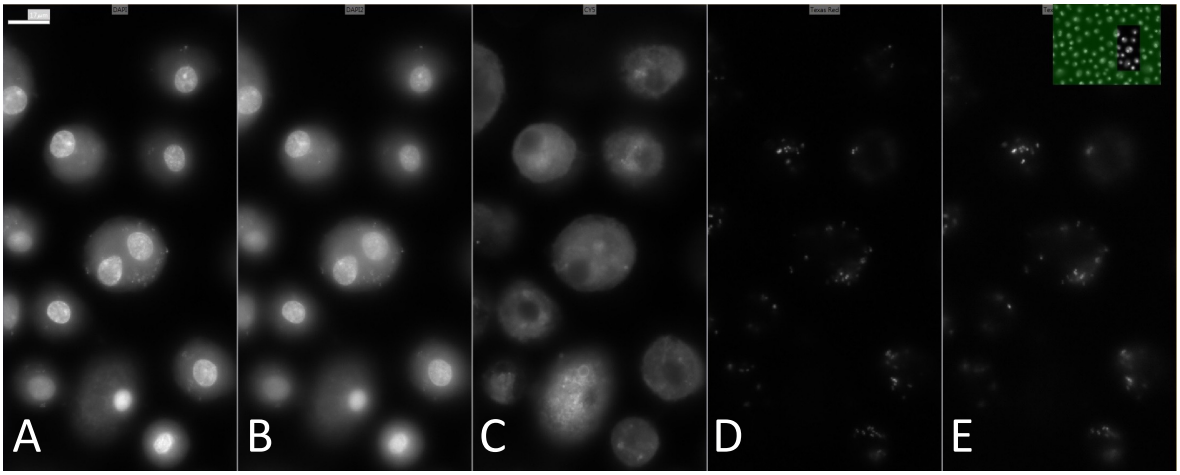

Figure 4.10.1 Representative image of raw image files imported into MetaXpress® Custom Module Editor.

Image magnified; scale bar represents 17μm. (**A**) DAPI raw image 1 (**B**) DAPI raw image 2. (**C**) CY5 raw image. (**D**) Texas Red raw image 1. (**E**)Texas Red raw image 2.

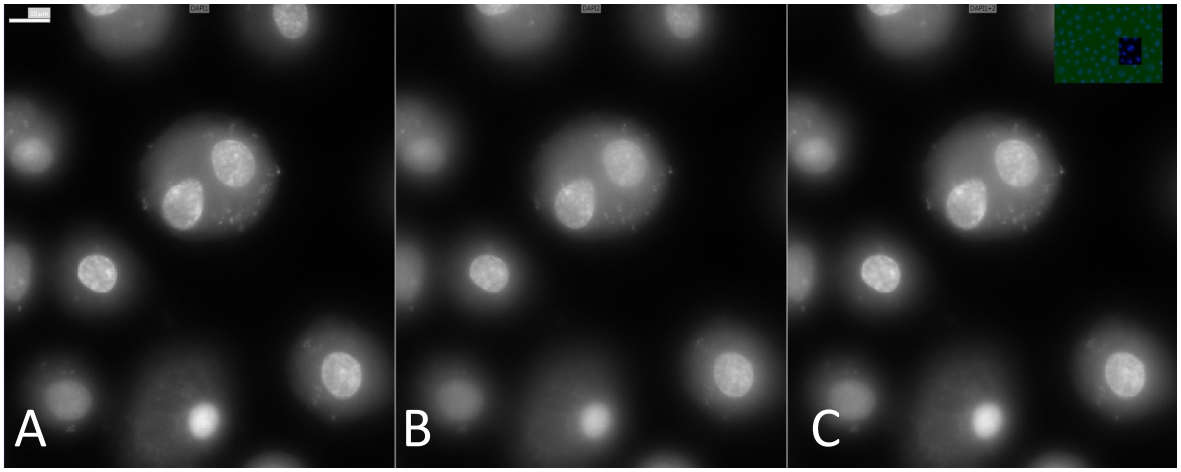

Figure 4.10.2 Representative image of MetaXpress® Custom Module Editor DAPI "Add" function.

Image magnified; scale bar represents 10μm. (**A**) DAPI raw image 1. (**B**) DAPI raw image 2. (**C**) DAPI "add" function composite image.

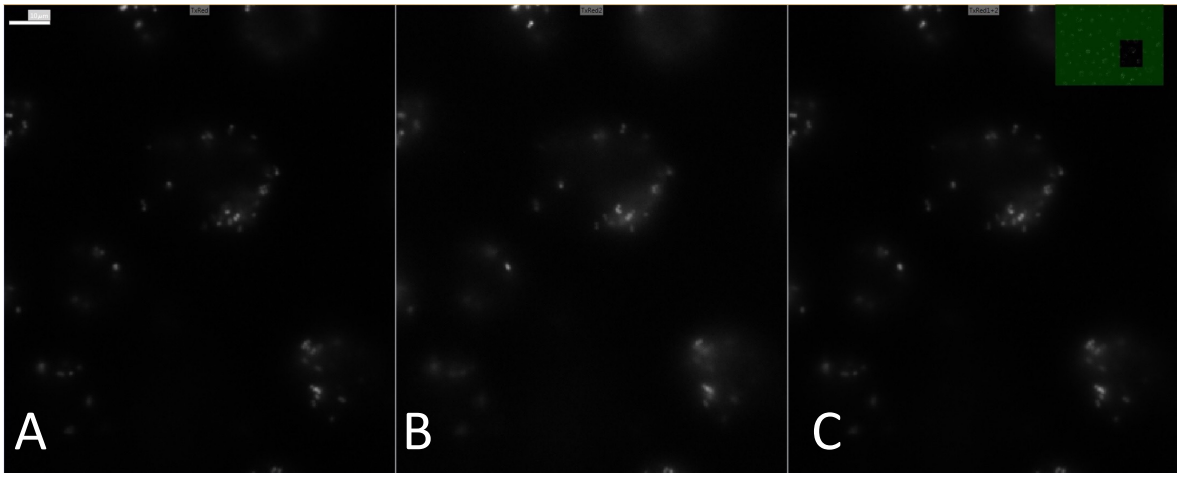

Figure 4.10.3 Representative image of MetaXpress® Custom Module Editor Texas Red "Add" function

Image magnified; scale bar represents 10μm. (**A**) Texas Red raw image 1. (**B**) Texas Red raw image 2. (**C**) Texas Red "add" function composite image.

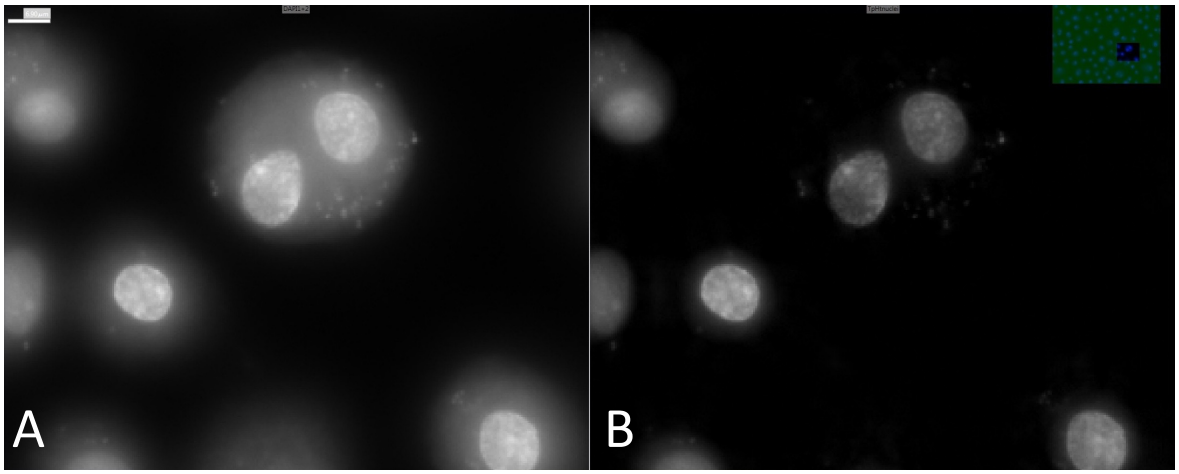

Figure 4.10.4 Representative image of MetaXpress® Custom Module Editor DAPI "Top Hat" filter.

Image magnified; scale bar represents 6.9μm. (**A**) DAPI "add" function composite image. (**B**) DAPI Top Hat post-filter image (filter criteria: shape "circle", size "50" pixels). Used to identify macrophage nuclei.

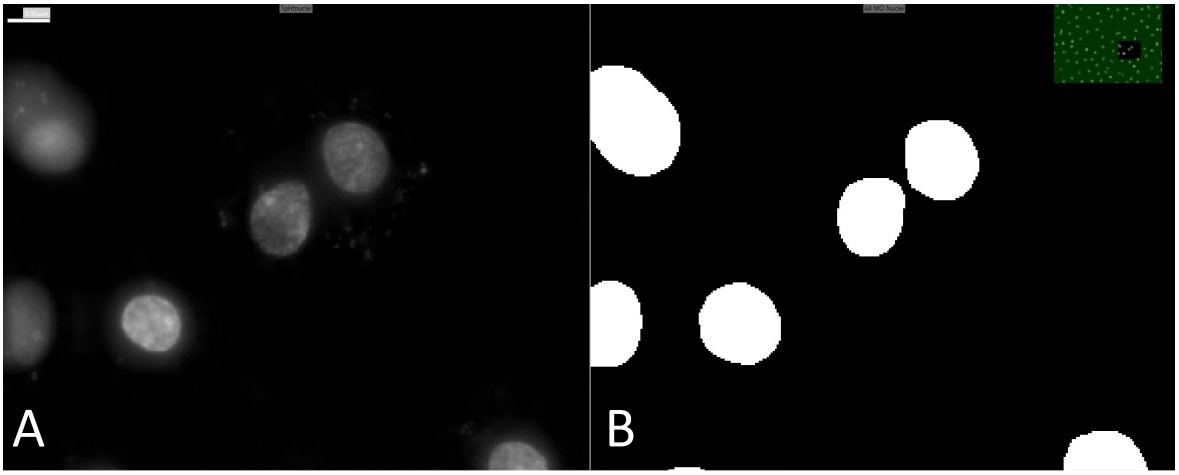

Figure 4.10.5 Representative image of MetaXpress® Custom Module Editor DAPI "Find Round Objects" filter.

Image magnified; scale bar represents 6.9μm. (**A**) DAPI Top Hat post-filter image, (filter criteria: shape "circle", size "50" pixels). Used to identify macrophage nuclei. (**B**) DAPI "Find Round Objects" post-filter image (size and intensity criteria: approximate width range 6 – 20μm, intensity above local background 300). Used to create macrophage nuclei mask.

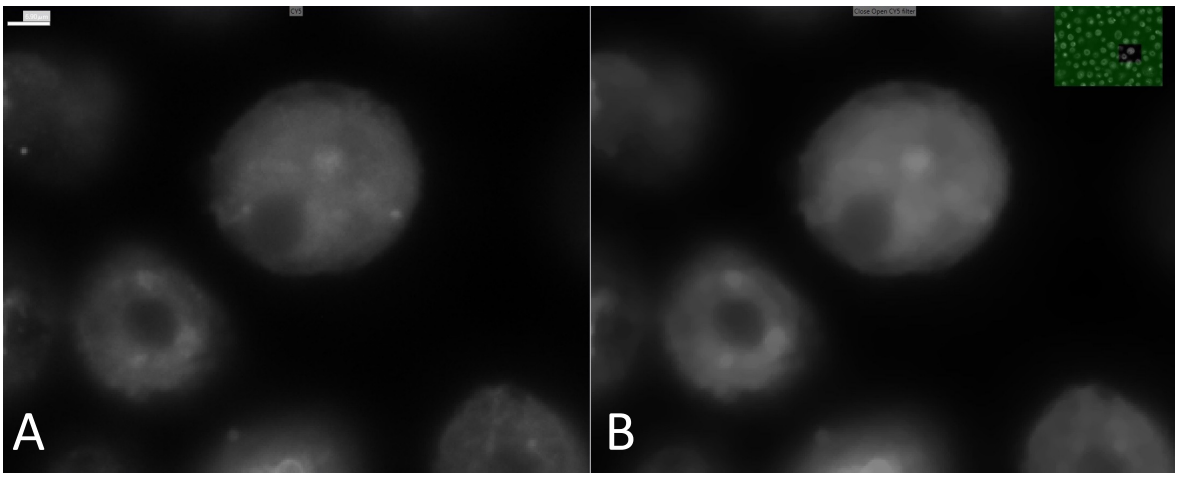

Figure 4.10.6 Representative image of MetaXpress® Custom Module Editor CY5 "Close Open" filter.

Image magnified; scale bar represents 6.9μm. (**A**) CY5 raw image. (**B**) CY5 "Close Open" post-filter image (filter criteria: shape "circle", size "5" pixels). Filter combines "Close" and "Open" filters to correct for both bright and dark noise spots. Used to identify macrophage cell membrane.

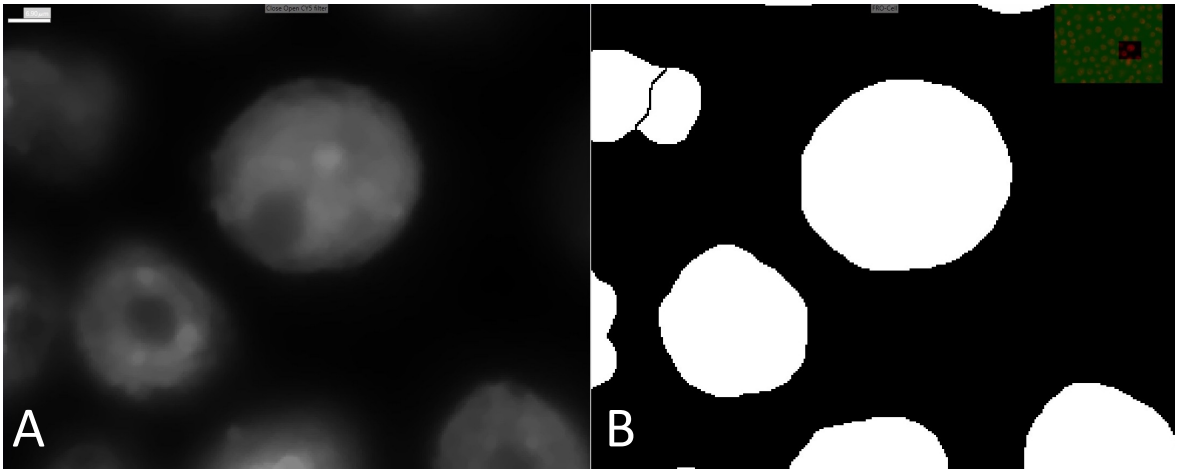

Figure 4.10.7 Representative image of MetaXpress® Custom Module Editor CY5 "Find Round Objects" filter.

Image magnified; scale bar represents 6.9μm. (**A**) CY5 "Close Open" post-filter image. Used to identify macrophage cell membrane. (**B**) CY5 "Find Round Objects" post-filter image (size and intensity criteria: approximate width range 8 – 48μm, intensity above local background 5). Used to create macrophage intracellular area mask.

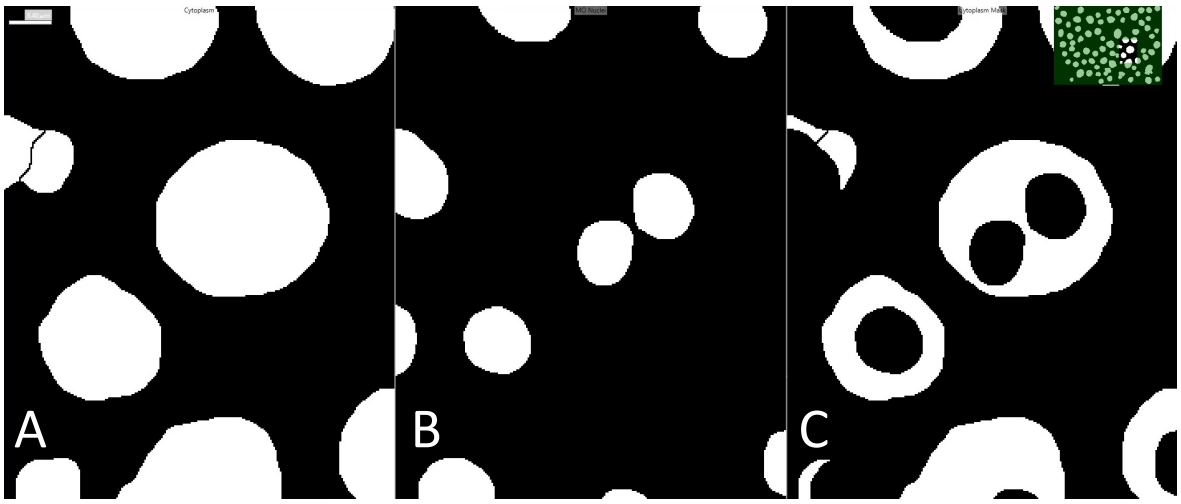

Figure 4.10.8 Representative image of MetaXpress® Custom Module Editor Logical Operation to define intracellular macrophage area excluding nuclei.

Image magnified; scale bar represents 8.4μm. (**A**) CY5 "Find Round Objects" post-filter image, mask representation of macrophage intracellular area. (**B**) DAPI "Find Round Objects" post-filter image, mask representation of macrophage nuclei. (**C**) Logical operation to create mask representation of macrophage intracellular area excluding nucleus. A Boolean operator applied to the two binary mask images to determine which pixels will be displayed in resulting binary mask image.

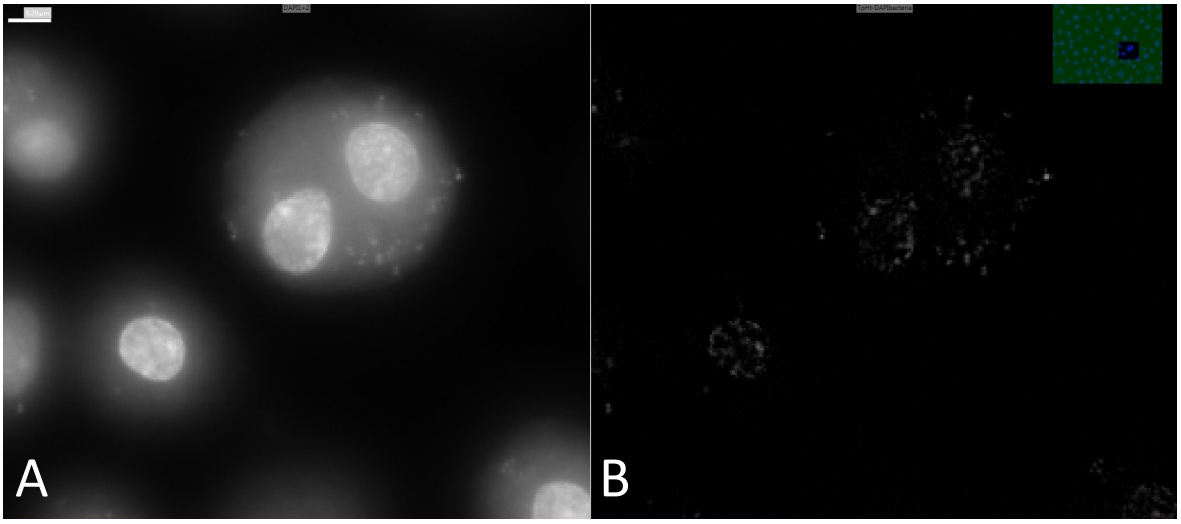

Figure 4.10.9 Representative image of MetaXpress® Custom Module Editor DAPI "Top Hat" filter.

Image magnified; scale bar represents 6.2μm. (**A**) DAPI "add" function composite image. (**B**) DAPI "Top Hat" post-filter image (filter criteria: shape "circle", size "5" pixels). Used to identify $DAPI^+$ bacteria.

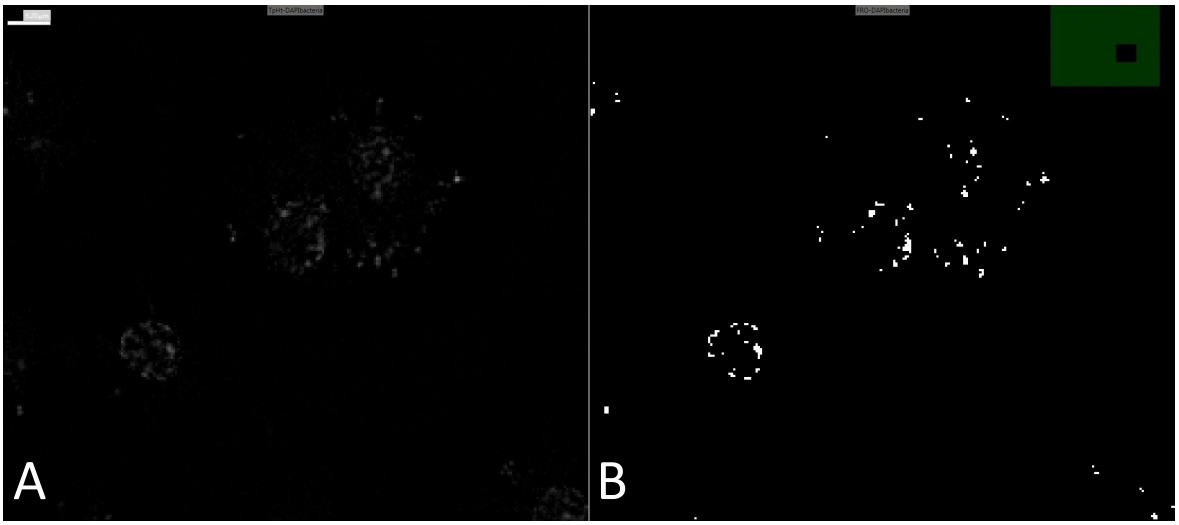

Figure 4.10.10 Representative image of MetaXpress® Custom Module Editor DAPI "Find Round Objects" filter to identify small $DAPI^+$ objects.

Image magnified; scale bar represents 6.2μm. (**A**) DAPI "Top Hat" post-filter image (filter criteria: shape "circle", size "5" pixels). (**B**) DAPI "Find Round Objects" post-filter image (size and intensity criteria: approximate width range 0.6 – 2.75μm, intensity above local background 400). Used to create $DAPI^+$ bacteria mask.

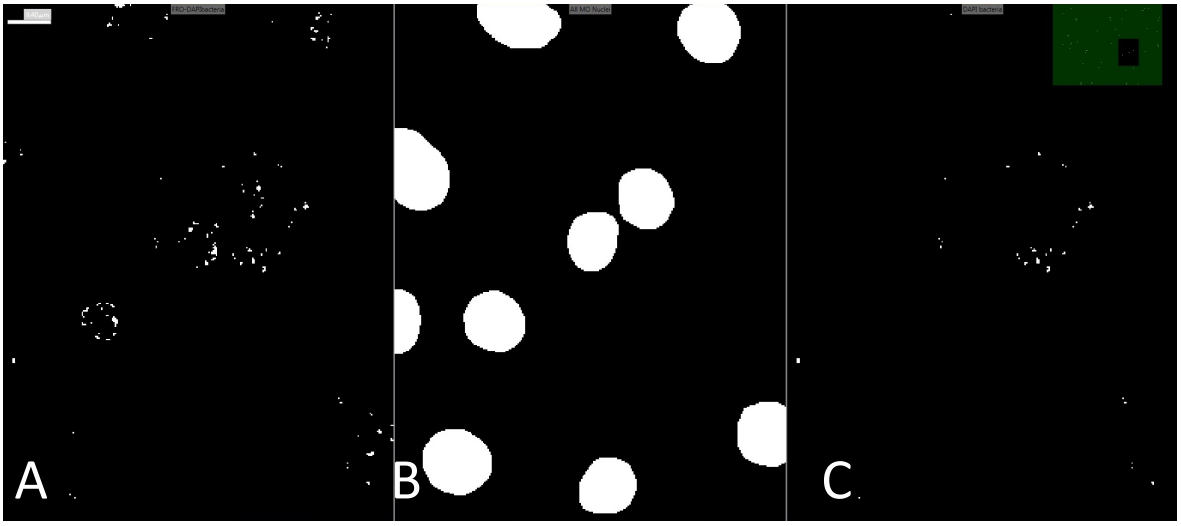

Figure 4.10.11 Representative image of MetaXpress® Custom Module Editor Logical Operation to define DAPI$^+$ bacteria having excluding macrophage nuclei DAPI$^+$ pixels.
Image magnified; scale bar represents 9.4μm. (**A**) DAPI "Find Round Objects" post-filter image. Representing DAPI$^+$ bacteria mask. (**B**) DAPI "Find Round Objects" post-filter image, mask representation of macrophage nuclei. (**C**) Logical operation to create mask representation of DAPI$^+$ bacteria excluding DAPI$^+$ pixels demarcated as macrophage nucleus. A Boolean operator applied to the two binary mask images to determine which pixels will be displayed in resulting binary mask image.

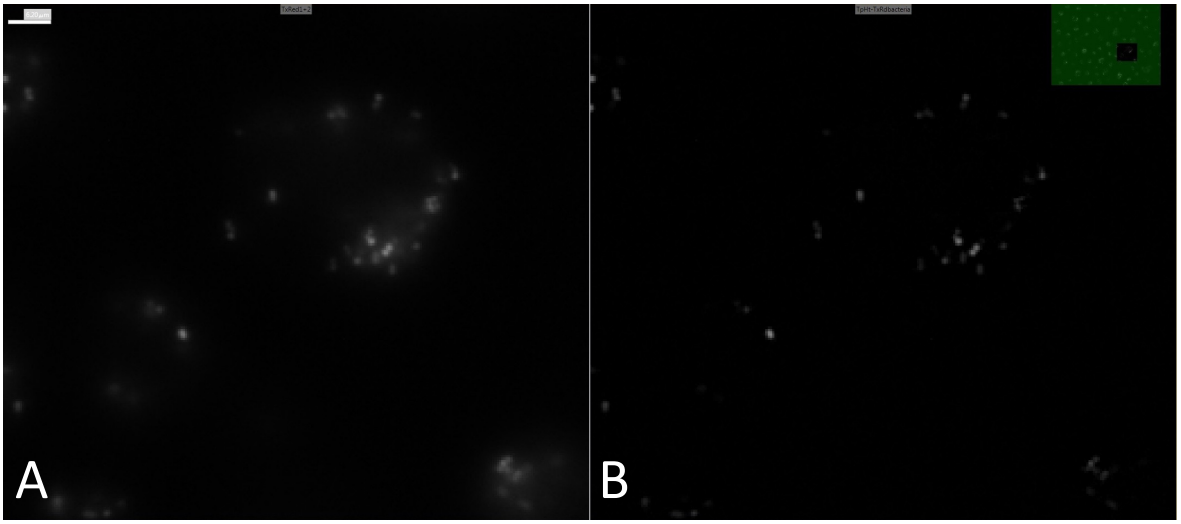

Figure 4.10.12 Representative image of MetaXpress® Custom Module Editor Texas Red "Top Hat" filter.
Image magnified; scale bar represents 6.2μm. (**A**) Texas Red "add" function composite image. (**B**) Texas Red Top Hat post-filter image (filter criteria: shape "circle", size "5" pixels). Used to identify pHrodo$^+$ bacteria.

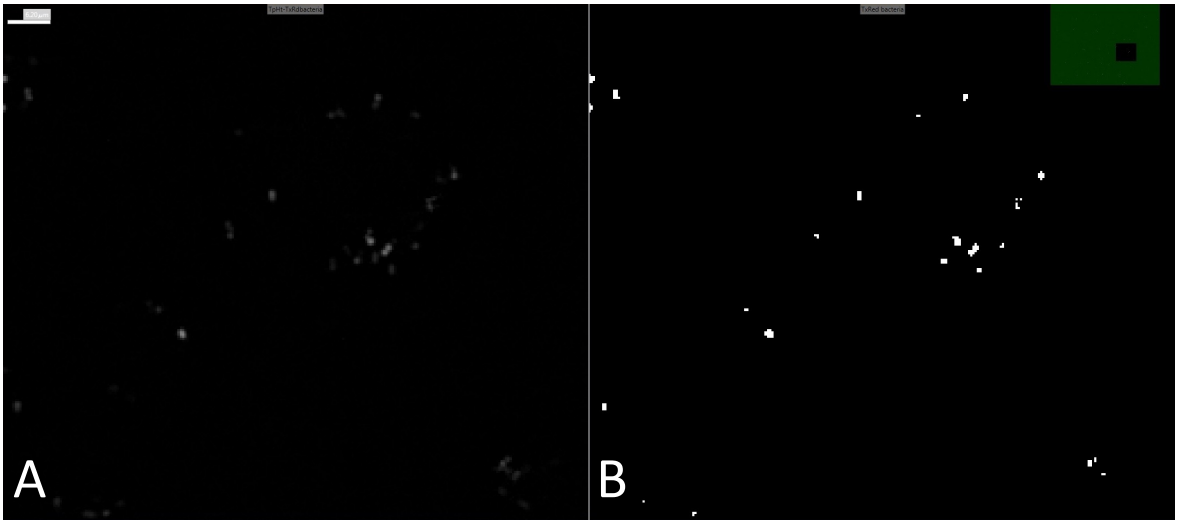

Figure 4.10.13 Representative image of MetaXpress® Custom Module Editor Texas Red "Find Round Objects" filter.

Image magnified; scale bar represents 6.2μm. (**A**) Texas Red Top Hat post-filter image (filter criteria: shape "circle", size "5" pixels). Used to identify pHrodo$^+$ bacteria. (**B**) Texas Red "Find Round Objects" post-filter image (size and intensity criteria: approximate width range 0.5 – 2.1μm, intensity above local background 250). Used to create pHrodo$^+$ bacteria mask.

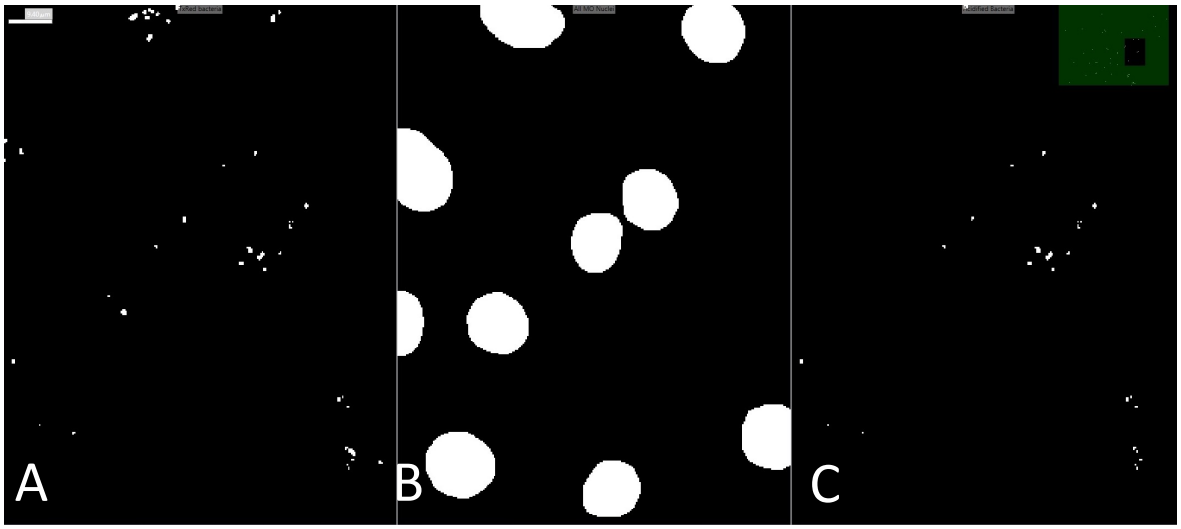

Figure 4.10.14 Representative image of MetaXpress® Custom Module Editor Logical Operation to define pHrodo$^+$ bacteria excluding any located within macrophage nuclei mask.

Image magnified; scale bar represents 9.4μm. (**A**) Texas Red "Find Round Objects" post-filter image. Representing pHrodo$^+$ bacteria mask. (**B**) DAPI "Find Round Objects" post-filter image, mask representation of macrophage nuclei. (**C**) Logical operation to create mask representation of pHrodo$^+$ bacteria excluding area demarcated as macrophage nucleus.

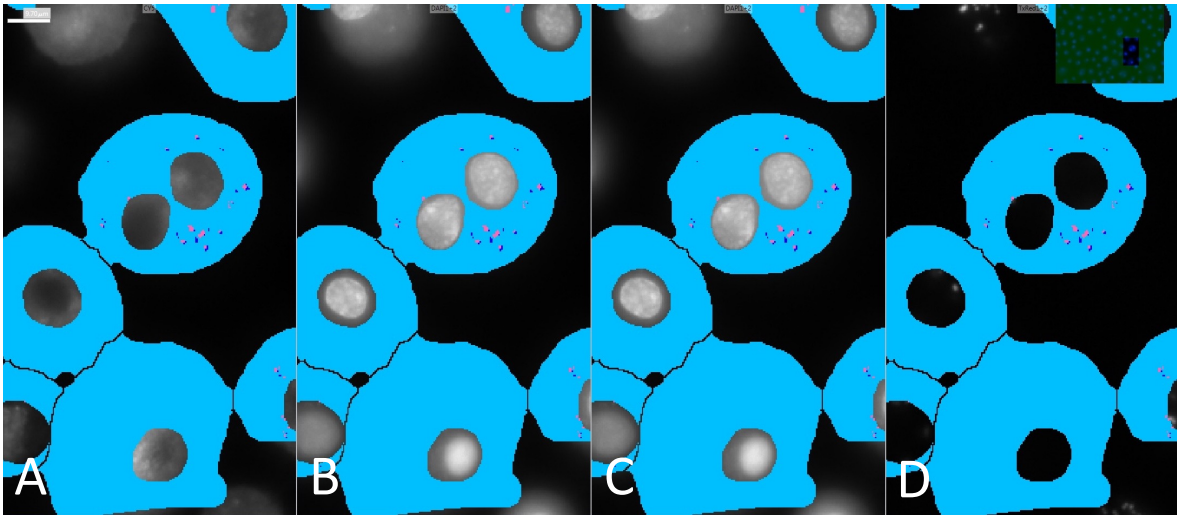

Figure 4.10.15 Representative image of MetaXpress® Custom Module Editor Measure Operation.

Image magnified, scale bar represents 9.7μm. (**A**) CY5 raw image. (**B**) DAPI "add" function composite image. (**C**) DAPI "add" function composite image. (**D**) Texas Red "add" function composite image. Each image overlayed with mask representation of macrophage intracellular area excluding nucleus (cyan), mask representation of $DAPI^+$ bacteria (blue) and mask representation of $pHrodo^+$ bacteria (pink). MetaXpress® Custom Module Editor Measure Operation commanded to measure number of respective masks identified within area imaged.

To quantify features of interest, the "measure mask" tool utilises the binary masks generated (Figure 4.10.15). Using the macrophage cell outline mask, derived from the CY5/Far Red filter image, the number of macrophage nuclei, derived from the DAPI filter image, was quantified. Likewise, the number of acidified bacteria, derived from the Texas Red filter image, and the total number of bacteria, derived from the DAPI filter image, that were within the macrophage intracellular space mask were quantified. The resulting measurement data was then exported from the MetaXpress® program as a text file (.txt), having defined the measurement groups required.

4.5.4 Data analysis.

The open-source R/Bioconductor statistical analysis package for cell-based high-throughput screens (cellHTS2) formed the basis for analysing the data obtained from the microscopy screen (Boutros et al. 2006; Pelz et al. 2010; Boutros et al. 2019). The package produced by Boutros *et al*. has been designed to be a reproducible tool for screeners to adapt for purpose (Boutros et al. 2019), facilitating normalisation, scoring and summarisation of large data sets.

The cellHTS2 package operates within the R software program (version 3.6 was used). For the R program to read the generated intensity data, creation of specific input files was necessary. These included the individual results file or raw intensity data files detailing the measurements from each replicate and each channel and the "plate list file" detailing the individual result files, including information regarding plate, replicate and channel. Within R, these files are read, and the data assembled into a single *cellHTS* R object that can then be subsequently analysed as commanded.

The *cellHTS* object was subsequently configured with files containing descriptive information about the screen to provide contextual information regarding the experiments. The primary descriptive file (description.txt) contains all information related to the entire screen, for example, the bacteria used, and assay undertaken. The plate configuration file (plateconf.txt) was used to annotate measured data with basic information, with the value labelled as either a control, an experimental sample or an empty well. The screen annotation file (annotation.txt) maps the specific location, i.e., the plate and well, of the specific variable, i.e., the NTML mutant under assessment. The final descriptive file is the screen log (screenlog.txt) that is used to detail any individual measurement that are invalid or excluded from analysis. The adapted cellHTS2 package command script is displayed in Figure 4.11.

The data structure of the *cellHTS* object is arranged in three-dimensional array. The first dimension corresponds to the NTML mutant used in the assay, which is organised by plate, well column and row. Thus, the first dimension has 1,920 values. The second-dimension concerns assay information obtained in relation to the first dimension, for example, number of acidified ($pHrodo^+$) bacteria. The third dimension corresponds to information obtained from a different channel but still in relation to the other dimensions, for example, total $DAPI^+$ bacteria. As three parameters were retrieved from the NTML screen, namely macrophage number, total bacterial and total acidified bacteria, a total of six analyses were undertaken. The cellHTS package allows dual channel analyses as described above. The dual channel analyses, termed experiment 1 (total bacteria versus macrophage number); experiment 2 (acidified bacteria versus macrophage number); experiment 3 (acidified bacteria versus total bacteria).

Additionally, these outputs can be analysed as single channels, creating a two-dimensional *cellHTS* R object, which comprised experiment 4 (macrophage number); experiment 5 (total bacteria); and experiment 6 (acidified bacteria).

Having formed a configured and annotated *cellHTS* object for each experimental analysis, the object undergoes data normalisation, followed by scoring of replicates and summarisation. Median normalisation was performed on an initial plate-by-plate basis thus adjusting for possible plate effects. The raw value underwent $\log_2$ transformation, thus converting the scale from multiplicative to additive, followed by median normalisation by subtracting the median value from the transformed data value. On the rare occasion that the data value was zero which resulted in an error during $\log_2$ transformation, this value was manually replaced with the value 0.01, and recorded within the screen log file. The variance of per-plate normalised values was then adjusted by dividing this value by the median absolute deviations across the whole experiment.

After normalisation, the values for each replicate underwent feature scaling, also termed standardisation in the cellHTS script, replacing the normalised values by their z-scores, and conferring the properties of a standard normal distribution. Simplistically, the z-score represents the number of standard deviations the specific data point is from the mean. The purpose is to make measurements comparable within and across plates and removing systemic variations. For this screen, the z-score is obtained by subtracting the overall median from the normalised intensity value for any given well and replicate, the result of which is then divided by the median absolute deviation. The z-score is estimated for each replicate by consideration of the distribution of intensities across all plates and wells deemed samples in the plate configuration file. The cellHTS script summarises the replicates post-standardisation, calculating a single score for each of the NTML mutant strains. For this screen, the mean replicate value is detailed. Finally, the cellHTS package exports the scored “hit list” as well as summary tables and plots for user interpretation.

```
source("http://bioconductor.org/biocLite.R")
biocLite(character(), ask=FALSE)
rm(biocLite)
source("http://bioconductor.org/biocLite.R")
biocLite("cellHTS2")
library(cellHTS2)
#Need to specify exact data path to locate raw data files, see example below, also required for configuration file,
screen log file, description file & annotation file.
dataPath = "/SRSF Analysis/Secondary Screen/Exp3"
#Specify novel experiment name
expName = "NTML2"
#Specify novel output file name for results
outPath = paste(dataPath, "outPEM_analysis/")
confFile = file.path(dataPath, "NTML2_plateconf.txt")
logFile = file.path(dataPath, "NTML2_screenlog.txt")
desFile = file.path(dataPath, "NTML2_Description.txt")
geneIDs = file.path(dataPath, "NTML2_annotation.txt")
posControls = ""
negControls = ""
#load the data and layouts, logs etc. into R
x <- readPlateList("NTML2_platelist.txt", name = expName, path = dataPath)
x <-configure(x,confFile = confFile, logFile = logFile, descripFile = desFile, path = dataPath)
xn <-summarizeChannels(x,fun = function (r1,r2) r1/r2)
#normalize plates to the median of the plate values
xnp <- normalizePlates(xn, scale = "multiplicative", log = FALSE, method = "median", varianceAdjust =
"byExperiment")
#score wells within each replicate by calculating a z-score for each well based on replicate median and MAD
xsc <- scoreReplicates(xnp, sign = "+", method = "zscore")
#summarize the replicates by taking the mean value for each (options include median, max, min)
xf <- summarizeReplicates(xsc, summary = "mean")
xfw <- annotate(xf, geneIDFile= "NTML_annotation.txt", path = dataPath)
#create boxplots of controls and sample scores
pdf(dataPath, "ctrls.pdf", paper="a4r", height=0, width=0)
scores<- Data(xsc)
boxplot(scores~wellAnno(x), col=rainbow(10))
#make a spreadsheet table for all the results - separate replicates:
table1<-Data(xsc)
write.table(table1, "NTML2_table3.xls", sep="\t", quote=F, col.names=F, row.names=F)
#write report
out <- writeReport(raw=x, normalized=xnp, scored=xf, force=TRUE, plotPlateArgs = TRUE, imageScreenArgs =
list(zrange=c(-4,8), ar=1),map=TRUE, outdir=outPath)
```

Figure 4.11 Adapted cellHTS2 R/Bioconductor script for analysis of *S. aureus* NTML strain intracellular acidification following macrophage challenge.

4.6 Challenge of monocyte-derived macrophages against pHrodo™-labelled *S. aureus* USA300 strain JE2 within a 96-well plate format.

Prior to screening of the NTML, pilot assessments were performed using the parenteral wild-type USA300 strain JE2 within the 96-well format.

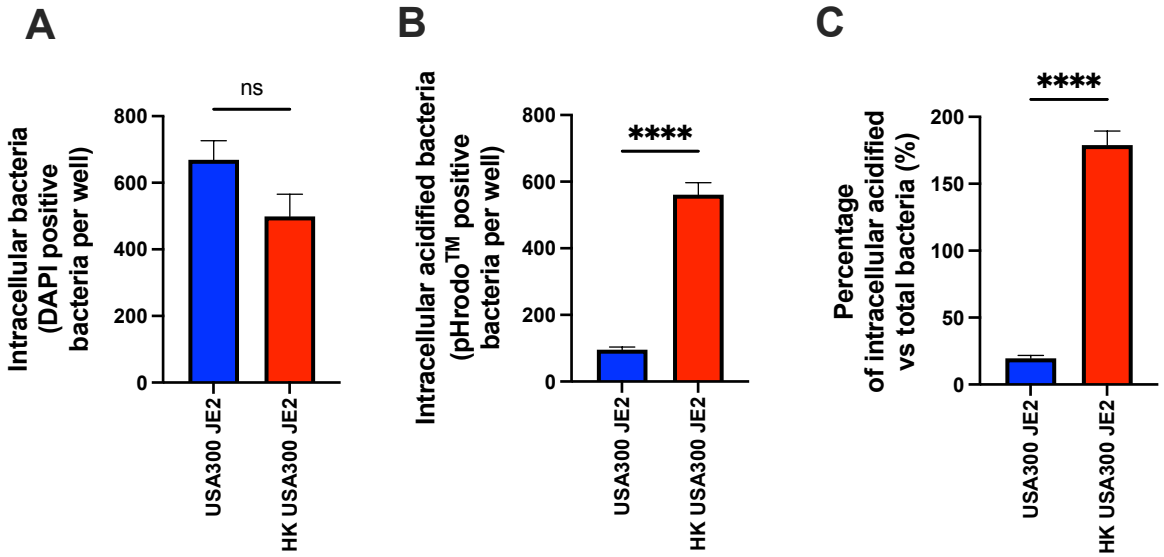

Figure 4.12 High-throughput microscopy assessment of intracellular *S. aureus* USA300 strain JE2 acidification following challenge of differentiated macrophages.

MDMs were challenged with either live or heat-killed *S. aureus* USA300 strain JE2 labelled with pHrodo at an estimated MOI of 5 for 4 hours within 96-well format. Extracellular bacteria removed by washing and lysed with lysostaphin for 0.5 hours. Images acquired using ImageXpress^{MICRO} high-throughput microscope and analysed using customised MetaXpress® algorithm. (**A**) Plot of intracellular DAPI^{+} bacteria per well by condition. Data represent 3 experiments, performed in 8 replicates. Ns (non-significant), unpaired t-test. (**B**) Plot of intracellular pHrodo^{+} bacteria per well by condition. Data represent 3 experiments, performed in 8 replicates. ****p<0.0001, unpaired t-test. (**C**) Plot of percentage of intracellular acidified bacteria versus total intracellular bacteria per well. Data represent 3 experiments, performed in 8 replicates. ****p<0.0001, unpaired t-test.

Using the protocols described within this chapter, a high-throughput microscopy assessment of differentiated MDMs challenged with either live or heat-killed *S. aureus* labelled with pHrodo™ can detect differential intracellular acidification of bacteria (Figure 4.12). This observation validates the adapted protocols, enabling screening of the NTML.

4.7 Conclusions

Utilising a candidate screen approach informed by Professor Foster and published evidence, several genes were associated with the subversion of phagosomal acidification. Kubica *et al.* demonstrated in an *in vitro* macrophage model of *S. aureus* infection that the global regulator *agr* was required for intracellular survival (Kubica et al. 2008). Within neutrophils, the two-component regulator *saeRS* has also been associated with intracellular survival (Gresham et al. 2000; Voyich et al. 2005). Both the SH1000 *agr* and *saeR* mutant strains failed to subvert phagosomal acidification which is a requirement for maturation to a microbicidal phagolysosome (Desjardins et al. 1994).

A mechanistic understanding for how *agr* and *saeR* subvert macrophage phagosomal maturation has yet to be established. Greater than 100 genes are differentially regulated by *agr* (Dunman et al. 2001). A common hypothesis is the association between *agr* and *saeR* regulation of cytotoxin expression (Surewaard et al. 2013; Nygaard et al. 2012; DuMont et al. 2013; Grosz et al. 2013). Phenol-soluble modulin-α (PSMα) is associated with phagosome escape, but the role of α-toxin is controversial but has been associated with neutrophil lysis post-phagocytosis (DuMont et al. 2013). Within the candidate screen, the SH1000 *hla* mutant subverted phagosomal acidification. The implication is that α-toxin dissipates an escalation phagosomal proton concentration and then facilitates escape from the phagosome by impairing phagosomal membrane integrity (Jarry et al. 2008).

Whereas most of these observations have been obtained within either a non-professional phagocyte or a neutrophil model of infection, within macrophages *S. aureus* can persist in the intracellular environment for up to 5 days (Kubica et al. 2008; Jubrail et al. 2016). This suggests differential expression of α-toxin, and other pore-forming toxins, to subvert and escape the phagosome, but not to lyse the host cell, in order to establish a latent infection.

Kubica *et al.* also demonstrated that *sarA* is not associated with intracellular survival within macrophages (Kubica et al. 2008). This validates the finding that the SH1000 *sarA* mutant fails to subvert phagosomal acidification. Within the same study (Kubica et al. 2008), the alternative sigma factor B ($\boldsymbol{\sigma}^{B}$) was associated with intracellular survival. However, I did not find an association between $\boldsymbol{\sigma}^{B}$ and subversion of phagosomal acidification. $\boldsymbol{\sigma}^{B}$ exerts a pleiotropic regulatory effect on numerous genes, operating in a reciprocal pattern to *agr* (L. N. Shaw et al. 2006; Bischoff et al. 2004). As a consequence of $\boldsymbol{\sigma}^{B}$ expression, there is marked reduction in *agr* and secreted exoprotein expression but enhanced pigmentation (L. N. Shaw et al. 2006). Expression of pigmentation is associated with resistance to ROS (G. Y. Liu et al.

2005). For the candidate screen, the SH1000 mutants had been grown to a mid-exponential growth phase and then frozen. Prior to a 4-hour macrophage challenge, the mutants were thawed on ice and labelled with pHrodo™. As noted previously, expression of σ^B is greatest during the stationary phase of growth (P. F. Chan et al. 1998). Hypothetically, the regulatory effect of σ^B will not have been apparent given the experimental design.

The candidate screen also identified genes associated with resistance to oxidative stress were associated with subversion of phagosomal acidification. The SH1000 *katA* and double *sodA sodM* mutants progressed to an acidified phagosome, the single *sodA* and *sodM* mutants however did not. The superoxide dismutase complexes, which detoxify superoxide radicals to H_2O_2, are required for virulence with murine infection models (Karavolos 2003; Das & Bishayi 2010). Within the candidate screen, it is possible that the functional superoxide dismutase enzyme compensated for the single gene mutant. The double *sodA sodM* mutant strain demonstrates a growth defect in the absence of environmental Mn^{2+} ions (Karavolos 2003) which may be true of the intra-phagosomal environment.

The antioxidant enzyme catalase is necessary for intracellular persistence via detoxification of H_2O_2 (Cosgrove et al. 2007). The *katA* gene is negatively regulated by the regulator *perR,* hence in the SH1000 *perR* mutant catalase activity is expected to be enhanced (Cosgrove et al. 2007). Within *S. aureus*, four iron-dependent global regulators (Fur, PerR, Zur and MntR) are associated with resistance to oxidative stress (Horsburgh, Ingham, et al. 2001; Horsburgh, Wharton, et al. 2002; Horsburgh, Clements, et al. 2001; Lindsay & S. J. Foster 2001). The SH1000 *fur* mutant was also associated with the failure to subvert phagosomal acidification. Fur is integral to the regulation of iron homeostasis (Horsburgh, Ingham, et al. 2001). Ferrous ions (Fe^{2+}) are integral to a diverse array of bacteria enzymes (Wachenfeldt & Hederstedt 2002) but tight regulation of Fe^{2+} concentration is essential as toxicity is associated with increased levels (Imlay et al. 1988).

Common to most prokaryotic organisms but with structural variation, Fur has a diverse regulatory effect beyond iron homeostasis (Fillat 2014). As concluded by Horsburgh *et al.,* within *S. aureus* Fur is integral to the interaction between metal ion homeostasis and stress resistance (Horsburgh, Ingham, et al. 2001). In a murine infection model, the *fur* mutant had reduced virulence (Horsburgh, Ingham, et al. 2001; Horsburgh, Clements, et al. 2001). This was attributed to mechanisms beyond the reduced expression of *katA,* which is positively regulated by Fur, as a *katA* mutant displayed no attenuation of virulence. Within *Salmonella typhimurium* and *Helicobacter pylori,* both intracellular pathogens, the Fur regulon is associated with acid tolerance and demonstrates an acid-sensing function (H. K. Hall & J. W.

Foster 1996; Gancz et al. 2006). Increased expression of *fur* has also been demonstrated within *Escherichia coli* in the presence of oxidative stress (Zheng et al. 1999). The finding that a *S. aureus fur* mutant is associated with subversion of phagosomal maturation is novel, and merits greater investigation.

The candidate screen has indicated that several genes and regulatory pathways are associated with the antagonism of macrophage phagosomal acidification. The additional aims of this chapter were to develop a procedure to complete a high-throughput screen of the *S. aureus* genome. The experience acquired by the Foster laboratory in handling the NTML, coupled with the experience that I have gained from the Dockrell group in maintaining macrophage cell cultures makes this possible. The added expertise of the Sheffield RNAi Screening Facility has supported my development of a high-throughput microscopy screening algorithm to process and analyse the data collected. This novel screening tool can also be repurposed to investigate other pathogens to broaden knowledge of host:pathogen interaction.

Chapter 5

A screen to identify *Staphylococcus aureus* genetic factors that subvert macrophage phagosomal maturation

5.1 Executive Summary

The aim of the following chapter was to screen the Nebraska Transposon Mutant Library (NTML) to identify *S. aureus* genes associated with the subversion of phagosomal maturation. Of the 1,920 mutants assessed within the primary screen, 180 mutants that progressed to secondary screening. A total of 24 mutants identified from the secondary screen were progressed to a final screen. A total of 15 genes were identified, including the regulators *agr* and *saeR*, and the oxidative stress enzyme catalase. The screen identified novel factors associated with subversion of phagosomal acidification, including the protease ClpP, the terminal oxidase complex genes *qoxA* and *qoxC*, and the cytochrome assembly complexes *ctaB* and *ctaM*.

5.2 Introduction

The work undertaken to this point has demonstrated the subversion of phagosomal maturation in a differentiated macrophage model following challenge with *S. aureus*. This has progressed from challenge with wild-type laboratory strains to using a limited number of candidate gene mutant strains. Evidence for the role of virulence gene regulators in intracellular survival, and cytolytic toxins in the escape from phagosomes have been published (Voyich et al. 2005; Kubica et al. 2008; Surewaard et al. 2013). The aim of this chapter is to complete a comprehensive assessment of the *S. aureus* genome to assess genetic factors associated with the subversion of phagosomal acidification, a fundamental aspect of phagocyte antimicrobial effector function. The identification of the essential bacterial factors for intracellular persistence will be necessary to identify novel therapeutic targets for *S. aureus* and potentially against other facultative intracellular bacteria.

5.3 Aims and Objectives

I. To screen the whole Nebraska Transposon Mutant Library (NTML) to identify a shortlist of *S. aureus* genes associated with subversion of phagosomal acidification.
II. To screen the generated shortlist of NTML strains associated with subversion of phagosomal acidification to generate a ranked list.
III. Validate the *S. aureus* genes found to have maximal subversive impact on phagosomal acidification.

5.4 The primary screen of the NTML strains to identify genes associated with subversion of phagosomal acidification.

The aim of the primary screen was to screen all strains within the NTML to obtain a short-list to progress to a secondary screen process based upon degree of intracellular acidification. The procedure for replicating and culturing the twenty stock NTML 96-well plates has been previously described. Differentiated human MDMs were used experimentally between 14 – 21 days, with an approximate density of 2 x 10^5 cells ml^{-1} within 96-well Greiner µClear flat bottomed tissue-culture treated plates. The sub-cultured 96-well NTML plate was grown to an exponential growth phase and subsequently labelled with the pH-sensitive label pHrodo™.

The MDMs were then challenged with the pHrodo™-labelled NTML strains at an approximate MOI of 5 and incubated for a period of 4 hours. As described in greater detail previously, the extracellular bacteria were removed through washing and antibiotic application. Application of the plasma membrane stain CellMask™ preceded fixation, followed by DAPI counterstaining. Fluorescent microscopy of the 96-well plates was undertaken within the ImageXpress^{MICRO} (Figure 5.1), and images processed using associated MetaXpress® software as previously described. Raw data values, appropriately formatted, were then subjected to the adapted-for-purpose cellHTS2 R/Bioconductor analysis package to generate normalised, summarised and scored outputs in respect to the three dual-channel and three single-channel assessments.

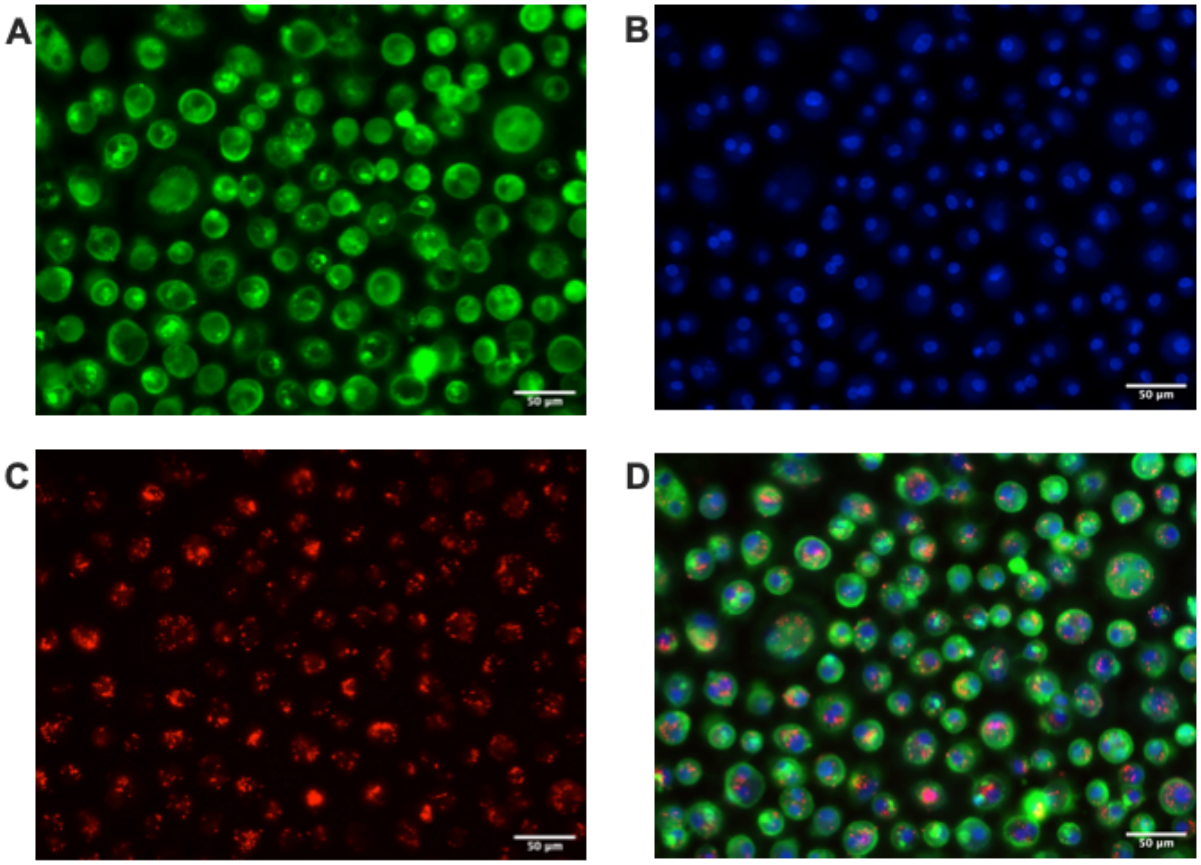

Figure 5.1 Representative high-content microscopy images of differentiated macrophages challenged with heat-killed *S. aureus* USA300 strain JE2.

Differentiated monocyte-derived macrophages were challenged with pHrodo^{TM}-labelled heat-killed *S. aureus* USA300 strain JE2 at a MOI of 5 bacteria per macrophage for a period of 4 hours within 96-well format. Images acquired using ImageXpress^{MICRO} high-throughput microscope. (**A**) CellMask^{TM} plasma membrane stain of MDMs visualised with GFP emission filter. (**B**) DAPI stain of MDMs and intracellular bacteria visualised with DAPI emission filter. (**C**) pHrodo^{TM} positive intracellular bacteria visualised with Texas Red emission filter. (**D**) Merged image.

5.4.1 Controls

As the NTML occupied all 96-wells within a plate, live and heat-killed wild-type USA300 strain JE2, established previously as negative and positive controls, were assessed against differentiated MDMs acquired from the same donor. In addition, mock-infected MDMs were used to assess for "noise" associated with the false detection of $DAPI^+$ or $pHrodo^+$ pixels equating to bacteria within the custom module editor algorithm of MetaXpress® software.

Across all the MDM plates (n=20) there was a mean 383 macrophages identified within each well assessed (Figure 5.2 A). It is observed that within the mock-infected wells no significant number of either $DAPI^+$ or $pHrodo^+$ bacteria were identified when compared to wells containing bacteria (Figure 5.2B-C). Therefore, the false positive identification of either bacteria probe is deemed insignificant.

A statistically significant difference was demonstrated in the comparison of $pHrodo^+$ bacteria between the live and heat-killed USA300 JE2 control strains. This is demonstrated in both raw number of $pHrodo^+$ bacteria per well (Figure 5.2C) and the ratio of $pHrodo^+$ bacteria by $DAPI^+$ bacteria (Figure 5.2D). There was no significant difference in the raw number of $DAPI^+$ bacteria in the respective control groups. The analysis of these control samples validates the subsequent use of the high-throughput fluorescent microscopy screen.

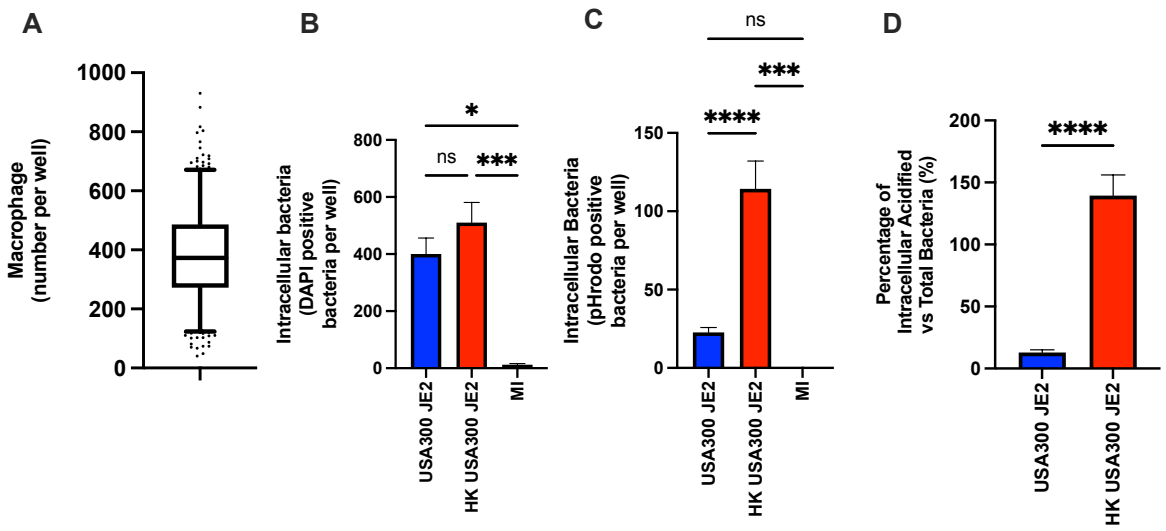

Figure 5.2 Primary NTML screen summary of controls.

Differentiated monocyte-derived macrophages were challenged with either pHrodo^{TM}-labelled live or heat-killed *S. aureus* USA300 strain JE2 at a MOI of 5 bacteria per macrophage, or mock infected (MI) for a period of 4 hours within 96-well format. Images acquired using ImageXpress^{MICRO} high-throughput microscope. (**A**) Box and whiskers plot of MDM number per well (n=20, total 388 wells assessed, mean 383, interquartile range 214). (**B**) Plot of intracellular DAPI^{+} bacteria per well by condition. Data represent 20 experiments, performed in 6-8 replicates. Ns (non-significant), *p<0.05, ***p<0.001, ordinary one-way ANOVA with Tukey's multiple comparison test. (**C**) Plot of intracellular pHrodo^{+} bacteria per well by condition. Data represent 20 experiments, performed in 6-8 replicates. Ns (non-significant) ***p<0.001, ****p<0.0001, ordinary one-way ANOVA with Tukey's multiple comparison test. (**D**) Plot of percentage of intracellular acidified bacteria versus total intracellular bacteria per well. Data represent 20 experiments, performed in 6-8 replicates. ****p<0.0001, unpaired t-test.

5.4.2 Primary Screen of NTML

The primary interest of the screen was to identify an association between a *S. aureus* gene and the subversion of phagosomal acidification. The scored values pertaining to the assessment of total bacterial number and total acidified bacterial number, and normalisation of the data are represented by heat maps (Figure 5.3) and box-plot analyses (Figure 5.4). The heat maps display a colour-encoded score for each respective NTML mutant, distributed across 1,920 wells. Thus, the spread of values can be visualised. Where either no bacteria or acidified bacteria were identified, the heat map portrays this outcome, for example plate 18, replicate 3, wells G11 and G12.

By representing the normalised data visually, identification of technical screening problems, such as edge effects, can be achieved. For example, all wells located within plate 18, replicate 1, column 12, returned with a high positive z-score indicative of minimal bacterial acidification. The box-plots also demonstrate that the spread of z-scores in plate 10 is greater in comparison with other NTML plates. The raw data values (Figure 5.5) of total bacteria number and total acidified bacteria for the replicates of plate 10 are of lower values compared to the other NTML plates. The cellHTS2 R/Bioconductor analysis package generates an analysis report for each respective NTML plate, including replicate intensity plots (Figure 5.6) and reproducibility plots (Figure 5.5). As demonstrated in these figures, a few wells across all three replicates have invalid intensity values, indicating the absence of bacteria from these wells. For example, well F2, containing the NTML mutant NE926 (putative lipoprotein mutant), resulted in invalid intensity values in replicates 2 and 3. Consequently, there is no value for well F2 in the plot of standard deviations (Figure 5.7).

The outcomes of the screen can also be reviewed as a whole, presented in the formats of a frequency distribution histogram and normal Q-Q (Quantile) plot (Figure 5.8). The P value acquired from the D'Agostino and Pearson normality test ($P<0.0001$) does not indicate if the population distribution is Gaussian or not, but that a randomly selected sample of data is highly probable to deviate from a Gaussian distribution. The distribution is skewed to the right (skewness 0.74) with more values present in the tails than a Gaussian distribution (kurtosis 4.47). The positive kurtosis reflects the number of outlying values beyond normal distribution. The difference between population mean (0.149) and median scores (0.013), standard deviation 1.328, reflects the skewed distribution to the right. The descriptive statistical values of the histogram indicate that most *S. aureus* mutant strains are not associated with phagosomal acidification. The normal Q-Q plot demonstrates that the population data is not normally distributed in its entirety, with outlier samples deviating from the reference line representative of expected normally distributed values.

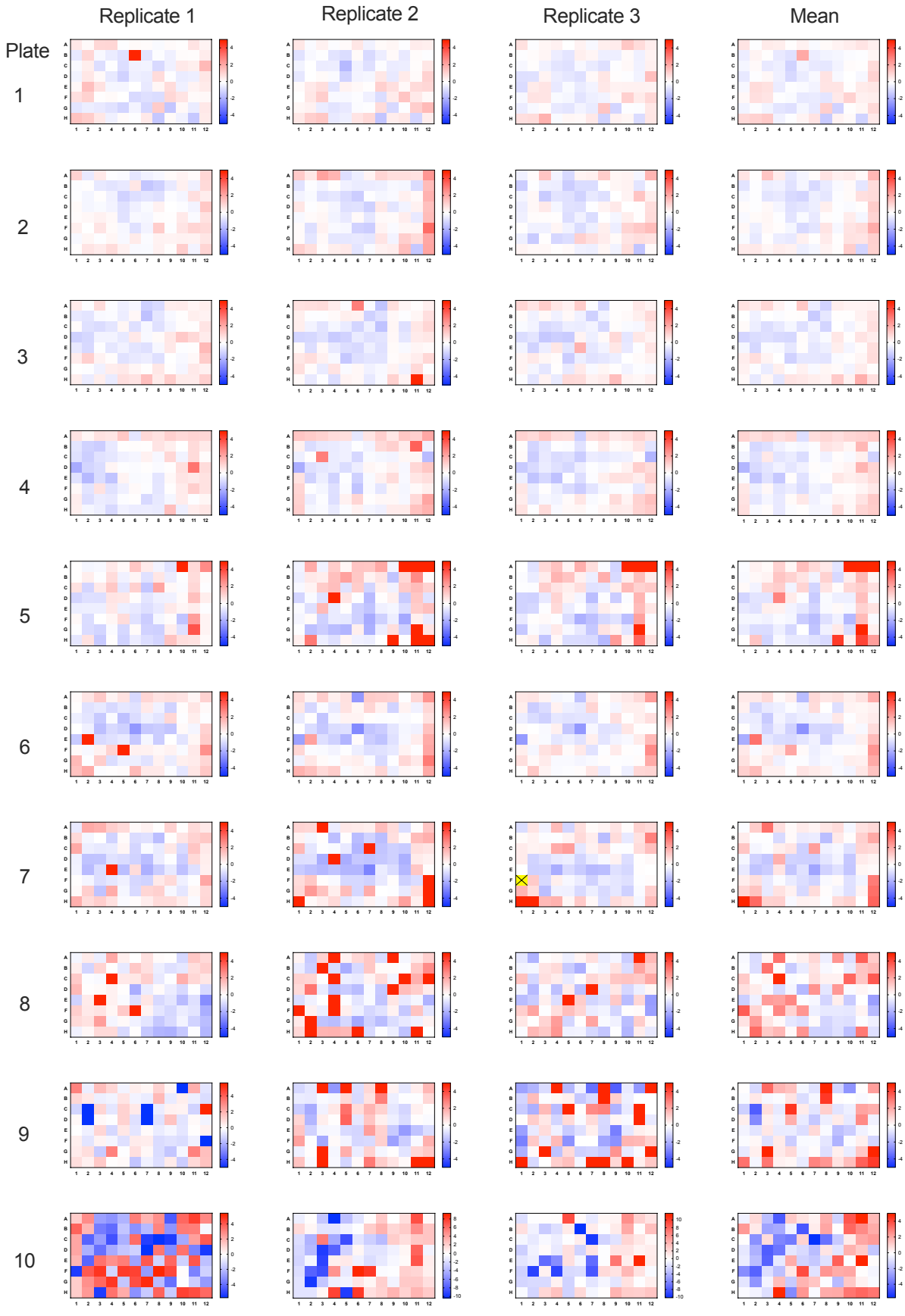
Plate
Replicate 1
Replicate 2
Replicate 3
Mean
1
2
3
4
5
6
7
8
9
10

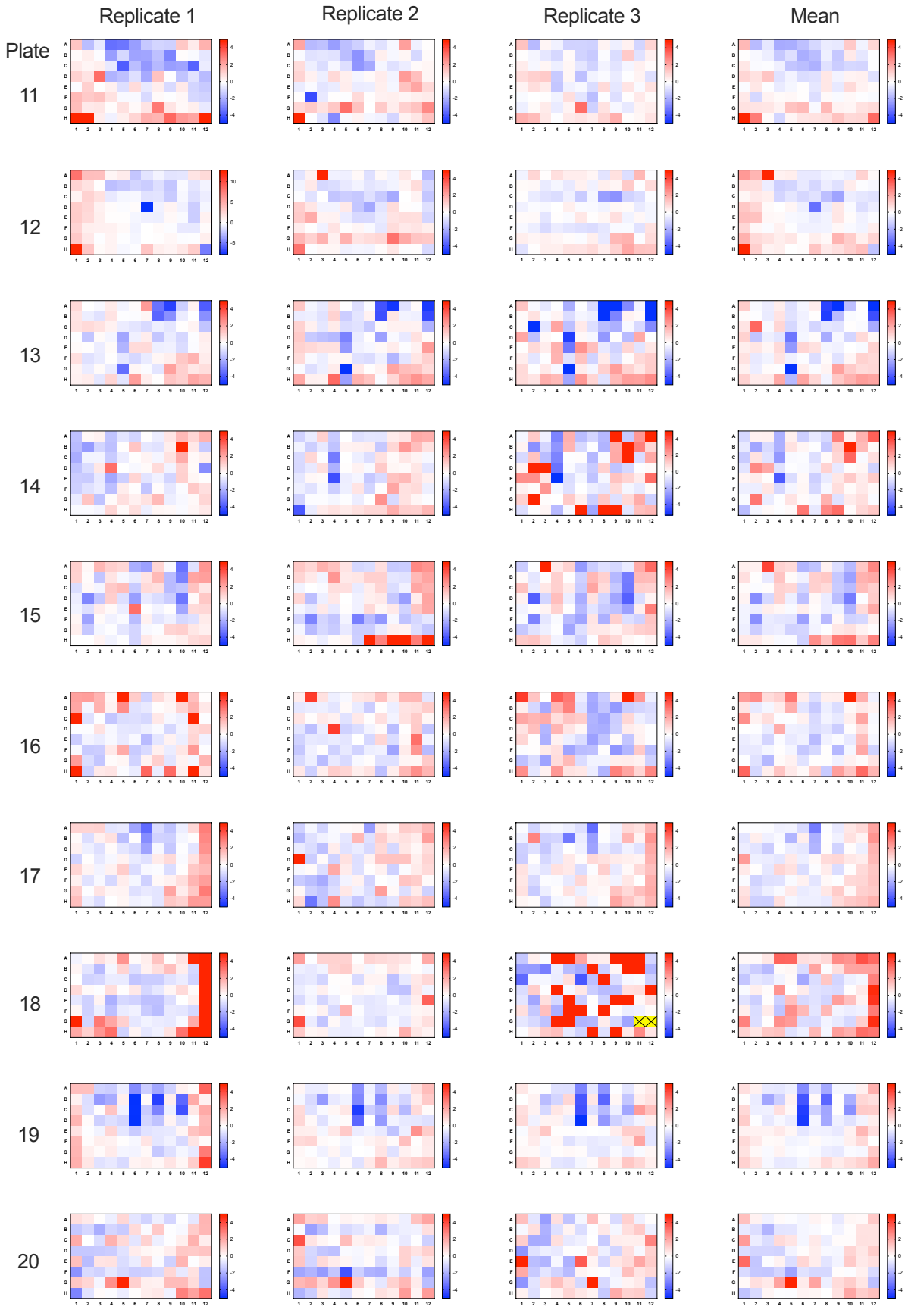
Replicate 1
Replicate 2
Replicate 3
Mean
Plate
11
12
13
14
15
16
17
18
19
20

Figure 5.3 Primary NTML screen heat map representation.

Assessment of acidified bacteria versus total bacteria. Data presented in 20 plates, examined in triplicate, representing normalised data (z-scores) with final column representative of mean value. The extremes of the scale represented as blue (lowest values, greater acidification) and red (highest values, less acidification), with white representative of 50th percentile. Invalid data (empty well) represented as yellow with a cross.

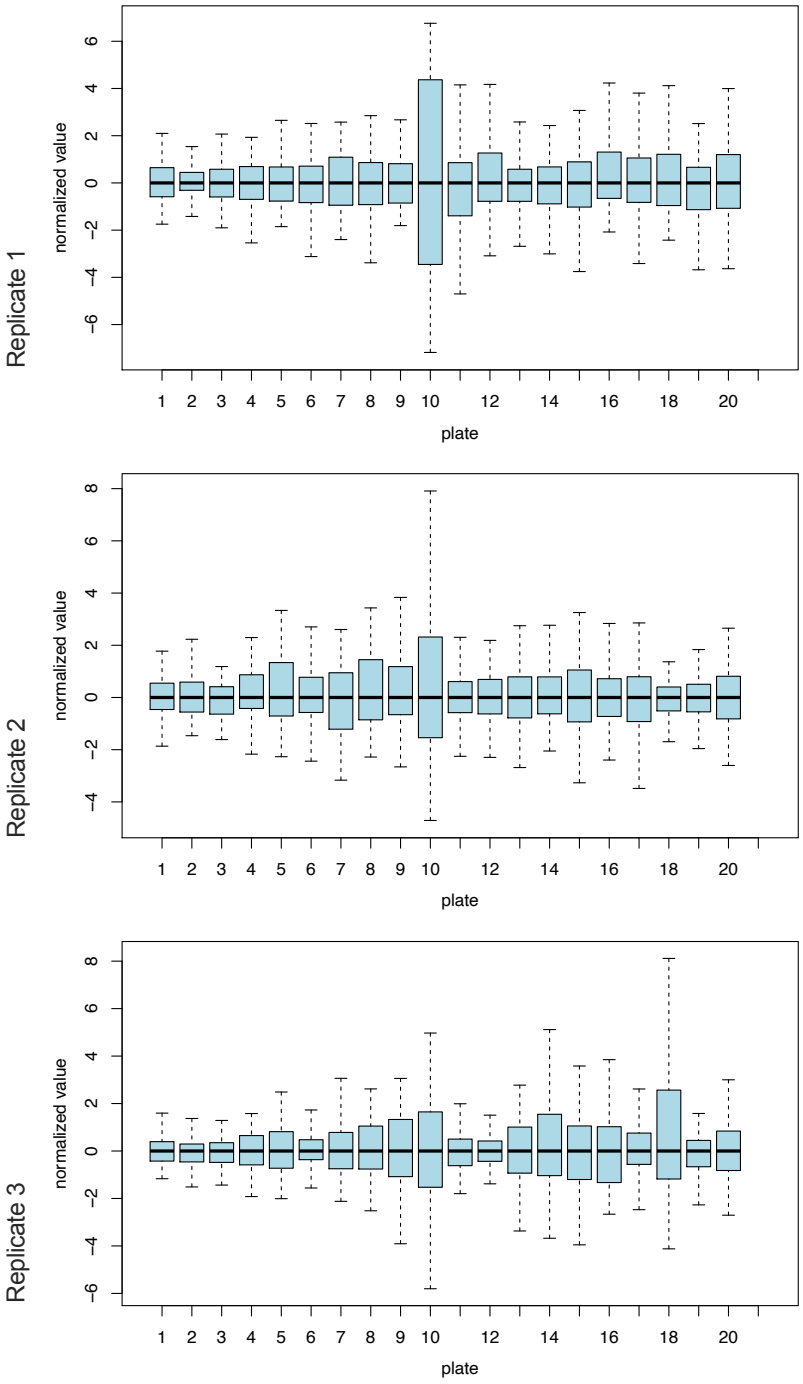

Figure 5.4 Primary NTML screen box and whisker plots of normalised data by plate. Acidified bacteria versus total bacteria box-plot representation of data normalised across NTML. Each plate summarised as box plot, where the box extends from the 25th and 75th percentiles, with the central line plotted at the plate median. The whiskers demarcate the 5th and 95th percentiles.

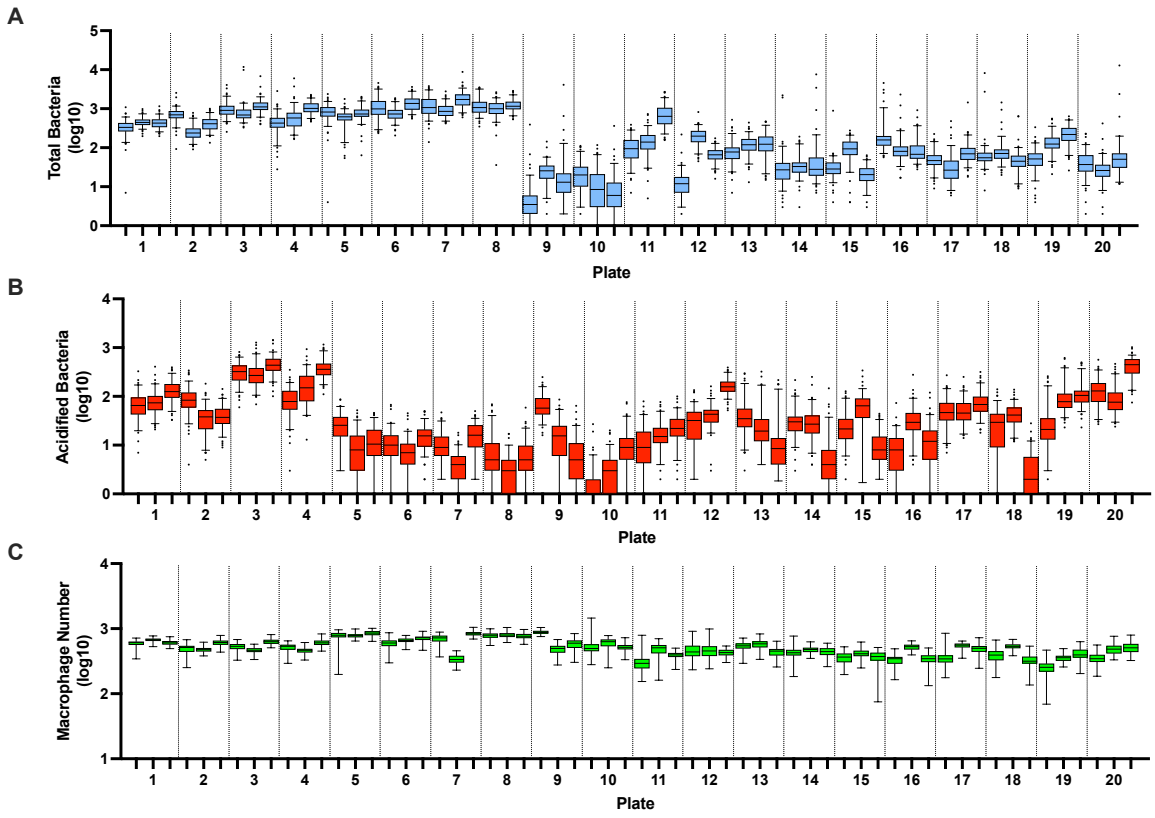

Figure 5.5 Primary NTML screen box and whisker plots of summarised raw data by plate and replicate.

(A) Raw values of total bacteria number; (**B**) Raw values of total acidified bacteria number; (**C**) Raw values of total macrophage cell number. Each NTML plate replicate (1-3) summarised as box plot, where the box extends from the 25th and 75th percentiles, with the central line plotted at the plate median. The whiskers demarcate the 5th and 95th percentiles.

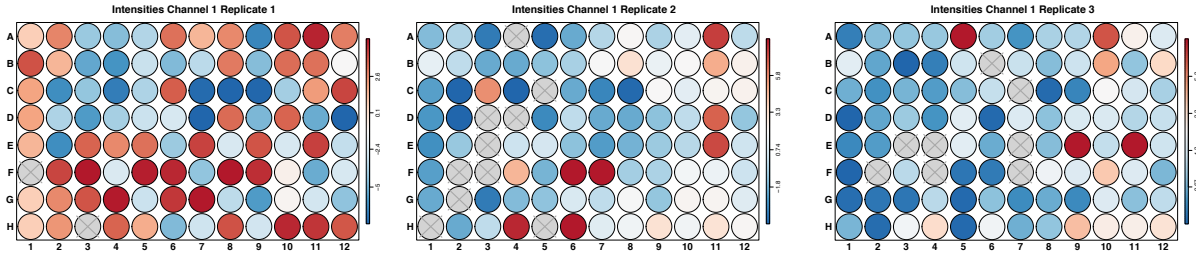

Figure 5.6 Primary NTML screen plate 10, normalised intensities of replicate assays. Heat map representation of normalised raw values obtained from assessment of NTML screen plate 10 across three replicates. Wells where no value obtained represented in grey with cross. Low values indicated by blue colour; higher values indicated by red colour.

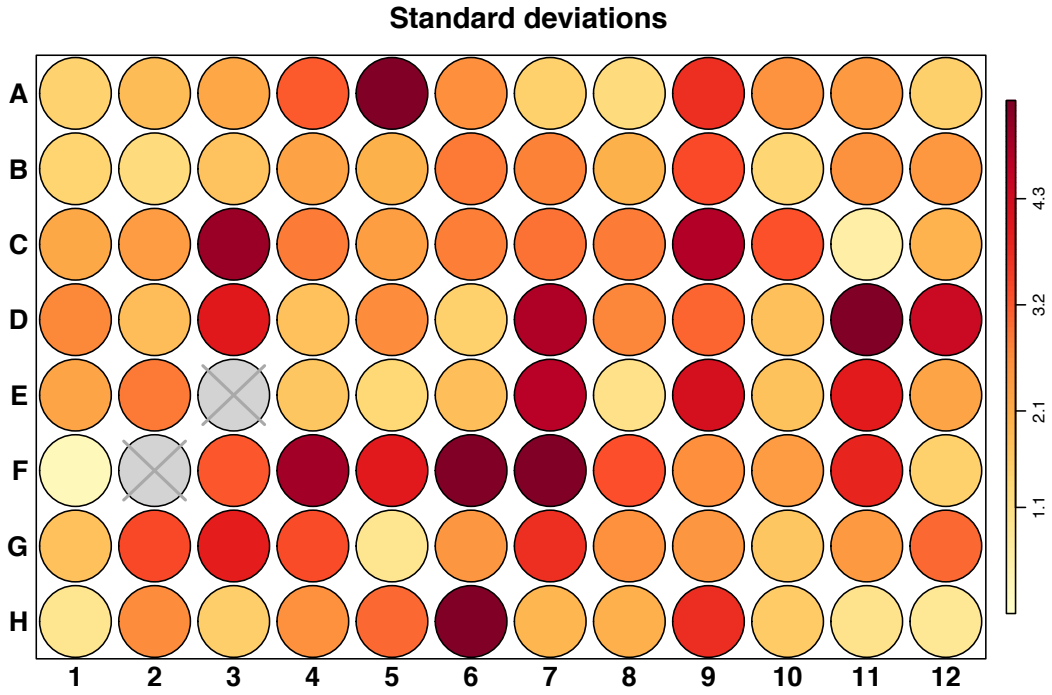

Figure 5.7 Primary NTML screen plate 10, standard deviation between replicates. Heat map representation of the standard deviation between replicates (n = 3) following assessment of NTML screen plate 10. Wells in which only one value obtained indicated in grey. Repeatability standard deviation 3.11 for entire plate.

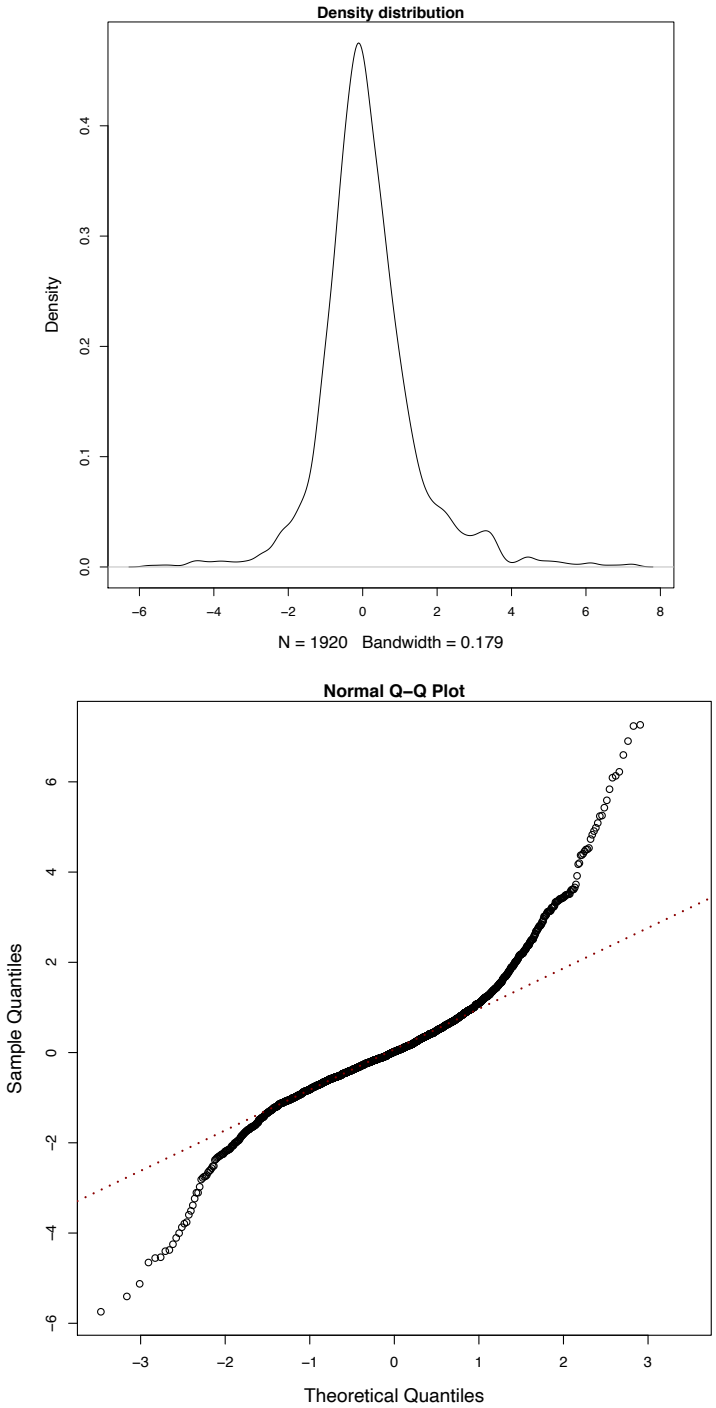

Figure 5.8 Primary NTML screen summary.

Density plot of the assay z-score distribution (D'Agostino & Pearson test: K2 340.3, P<0.0001). Normal Q-Q plot of the assay z-scores, deviations from the line indicate non-normally distributed values. The left-hand tail represents NTML mutants with greater intracellular acidification, and the right-hand tail represents NTML mutants with less intracellular acidification.

5.4.3 Defining true hits from the primary NTML screen

The aim of the primary screen was to identify 180 NTML mutant strains maximally associated with intracellular bacterial acidification for further investigation. These NTML mutants will have a negative Z-score from the above screening analysis, visually represented within the normal Q-Q plot (Figure 5.8) as the lower left corner. The Z-score is a measure of the probability that the ratio of bacterial acidification versus total bacterial number occurred by chance. Z-scores of -1, -2 and -3 correspond to the probabilities of 32%, 5% and 0.3% respectively. From the primary screen, 57 NTML mutants had a mean Z-score less than -2; 222 NTML mutants had a mean Z-score less than -1. As a precedent for defining "hits", a Z-score of ±2 (equivalent to a p-value of <0.05) has been accepted as being of statistical significance (Fisher et al. 2012). An additional factor for defining a cut off is the number of "hits" to be included in subsequent assessments. Within the present example, using the z-score as a cut-off of would result in either an excess of candidates (e.g., Z-score < -1) or too few to populate a 96-well plate (e.g., Z-score < -2). Therefore, the cut-off was defined at the 180 NTML mutants with the greatest Z-score, to populate two 96-well plates including experimental controls.

Additional appraisal of this group with a Z-score greater than -1 was required to exclude false positive NTML mutants. As previously described, visual representation of data aids identification of technical screening errors which may have resulted in unreliable data values for specific wells. Heat maps can be used to visually identify spatial abnormalities indicative of this. The first point of quality assessment is to ensure that a standard number of macrophages were sampled per well. The raw data summarised data for each screen plate replicate has been demonstrated above (Figure 5.5C). This data can also be visualised using a heat map demonstrating outlying values across individual wells (Figure 5.9A). Spatial abnormalities are evident through analysis of the heat-map, although there are no consistent patterns, for example edge effects, for outlying values across all plates. The majority of values are normally distributed as demonstrated with the normal Q-Q plot (Figure 5.9C). Four wells had a mean Z-score of less than -3, and 33 wells had a mean Z-score of less than -2. The NTML mutants deficient of the accessory regulator A (SarA NE1193; Z-score -3.02) and *Staphylococcus aureus* exoprotein regulator (saeR NE1622; Z-score -2.23) were found in this group. Within the SH1000 strain, the saeR mutant was found to be associated with intraphagosomal acidification with statistical significance (Figure 4.1) and occurs within the primary screen with a mean Z-score of -1.18. Conversely, SarA had not been found to be statistically associated with intraphagosomal acidification within the SH1000 strain mutant (Figure 4.2), but within the primary screen obtained a Z-score -3.22. Both these regulatory genes are associated with virulence factor expression. Therefore, the finding that the mean macrophage numbers in these respective wells are lower than expected may be due to

bacterial factors rather than mechanical error. Given the interest in these genes, and the potential for cytolytic function, the low macrophage number was not deemed sufficient to exclude these candidates from secondary screening.

The desired outcome of the primary screen was to identify NTML mutants that result in greatest intracellular acidification. When comparing the total number of acidified bacteria to total bacteria, the desired ratio would be close to 1. Therefore, false positive results may arise when an excess of acidified bacteria or minimal DAPI positive bacteria are identified. It is to be expected that the total acidified number of bacteria should always be less that the total bacteria number, given that the DAPI signal should not be lost by intraphagosomal acidification.

Within the single channel analysis of (DAPI-stained) total bacterial number (Figure 5.10), 32 wells had a mean Z-score of less than -3; 61 wells had a mean Z-score of less than -2. These wells were predominantly located within NTML plate 10, as visualised within the heat-map, where few bacteria were identified. Within the single channel analysis of acidified bacterial number (Figure 5.11) where a positive Z-score is reflective of higher numbers than expected, 20 wells had a mean Z-score of greater than 3; 72 wells had a mean Z-score of greater than 2; and 246 wells had a mean Z-score greater than 1. Of the 20 NTML mutants with a Z-score greater than 3, 7 were also identified as outliers within the single-channel analysis of total bacterial number in respect to fewer bacteria than expected. Given that the raw data values of these NTML mutants have a greater acidified bacteria number compared to total bacteria, these values were deemed to represent false positive results and excluded from further analysis.

The complete list of NTML scores are detailed in appendix table 7.2. The final “hit list” of 180 NTML mutant strains that are to progress to secondary confirmation screening are detailed in appendix table 7.3.

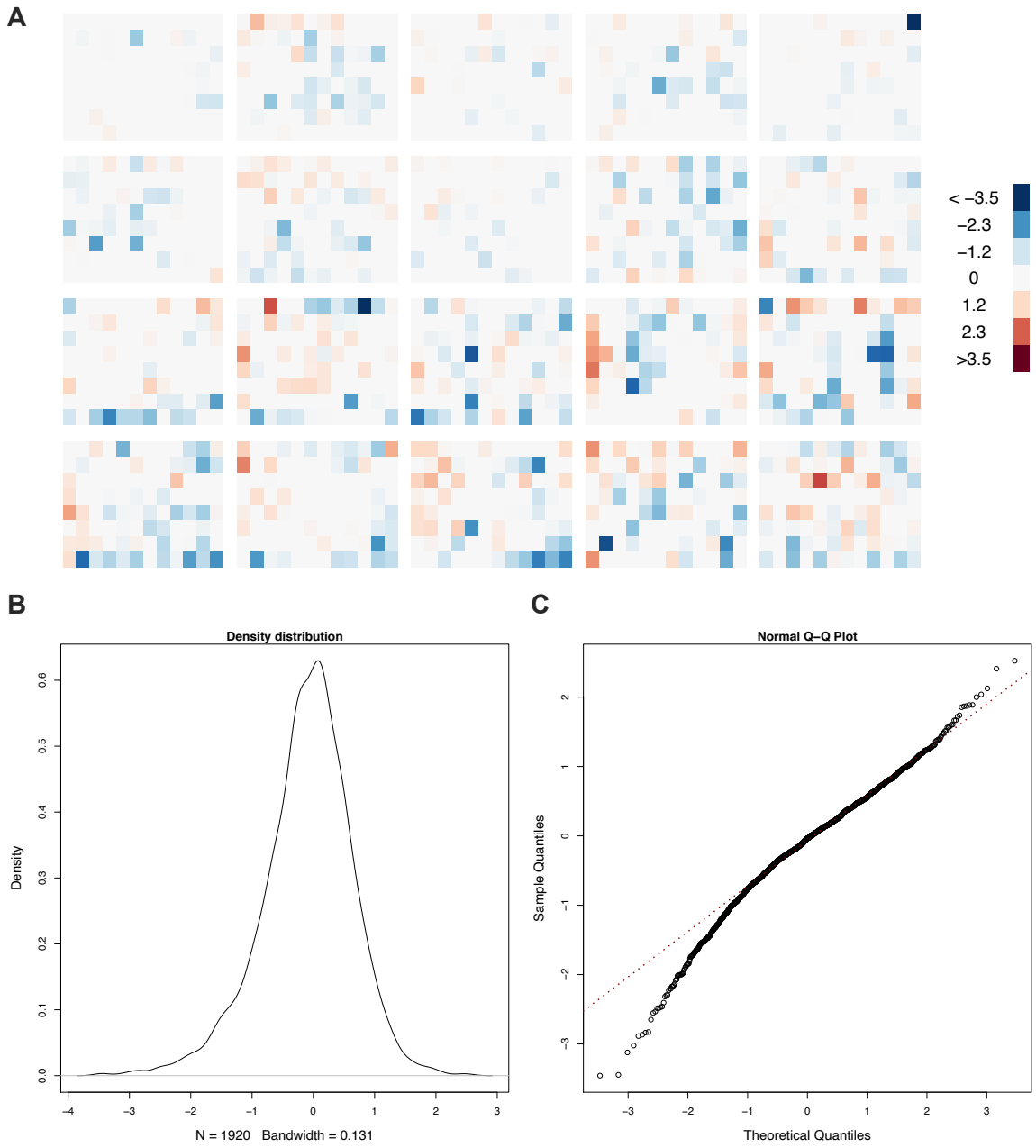

Figure 5.9 Summary representations of the mean scored values for total macrophage number per well.

Heat map representation. Data presented in 20 plates in sequential arrangement from right to left, representing normalised data (z-scores). The extremes of the scale represented as blue (lowest values, lesser number of macrophages) and red (highest values, greater number of macrophages), with white representative of 50th percentile. (**B**) Density plot of the assay z-score distribution (D'Agostino & Pearson test: K2 141.8, P<0.0001; skewness -0.55, kurtosis 1.33). (**C**) Normal Q-Q plot of the assay z-scores, deviations from the line indicate non-normally distributed values.

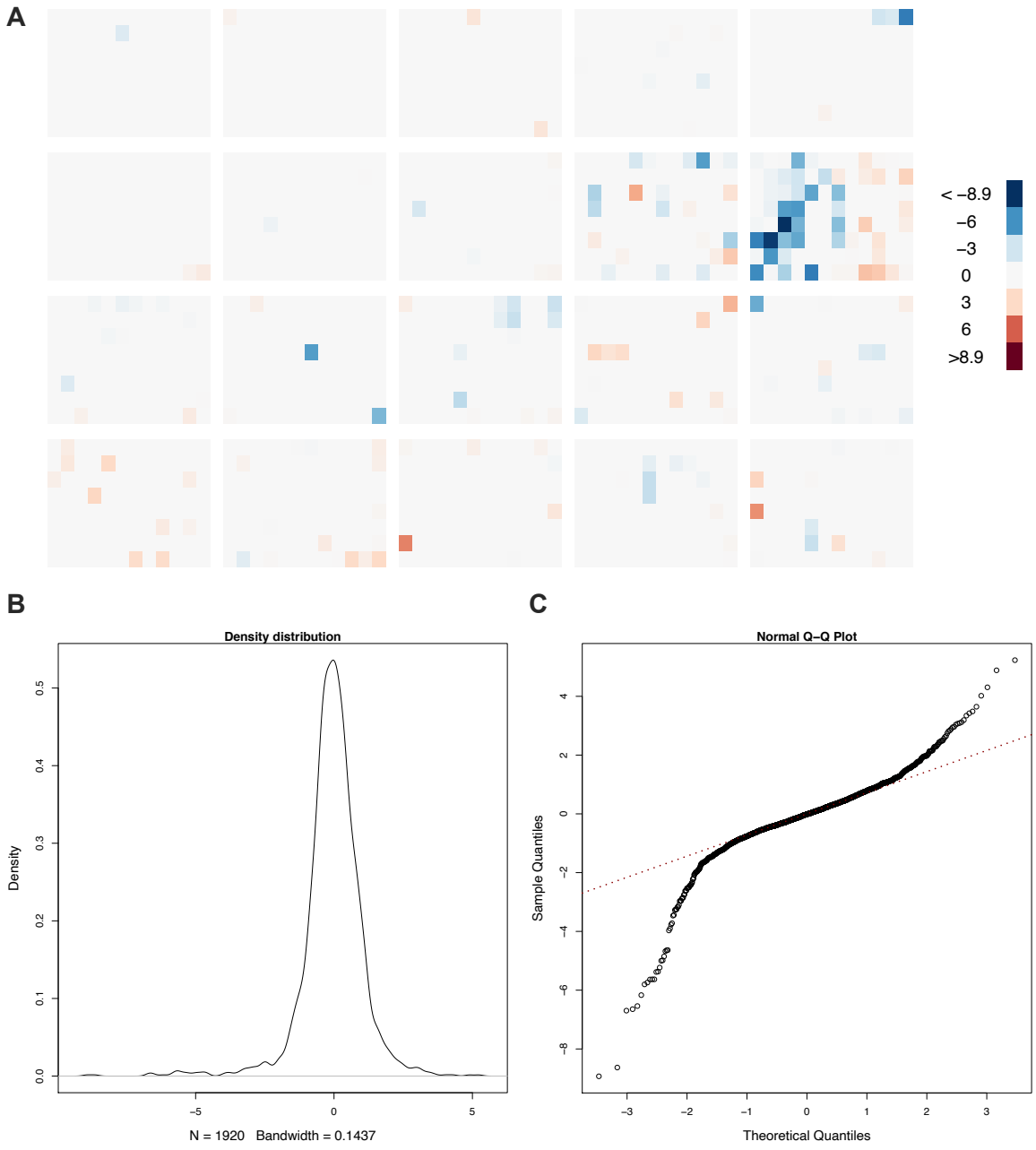

Figure 5.10 Summary representations of the mean scored values for total bacteria number per well.

Data presented in 20 plates in sequential arrangement from right to left, representing normalised data (z-scores). The extremes of the scale represented as blue (lowest values, lesser number of bacteria) and red (highest values, greater number of bacteria), with white representative of 50th percentile. (**B**) Density plot of the assay z-score distribution (D'Agostino & Pearson test: K2 762.3, P<0.0001; skewness -1.52, kurtosis 10.32). (**C**) Normal Q-Q plot of the assay z-scores, deviations from the line indicate non-normally distributed values.

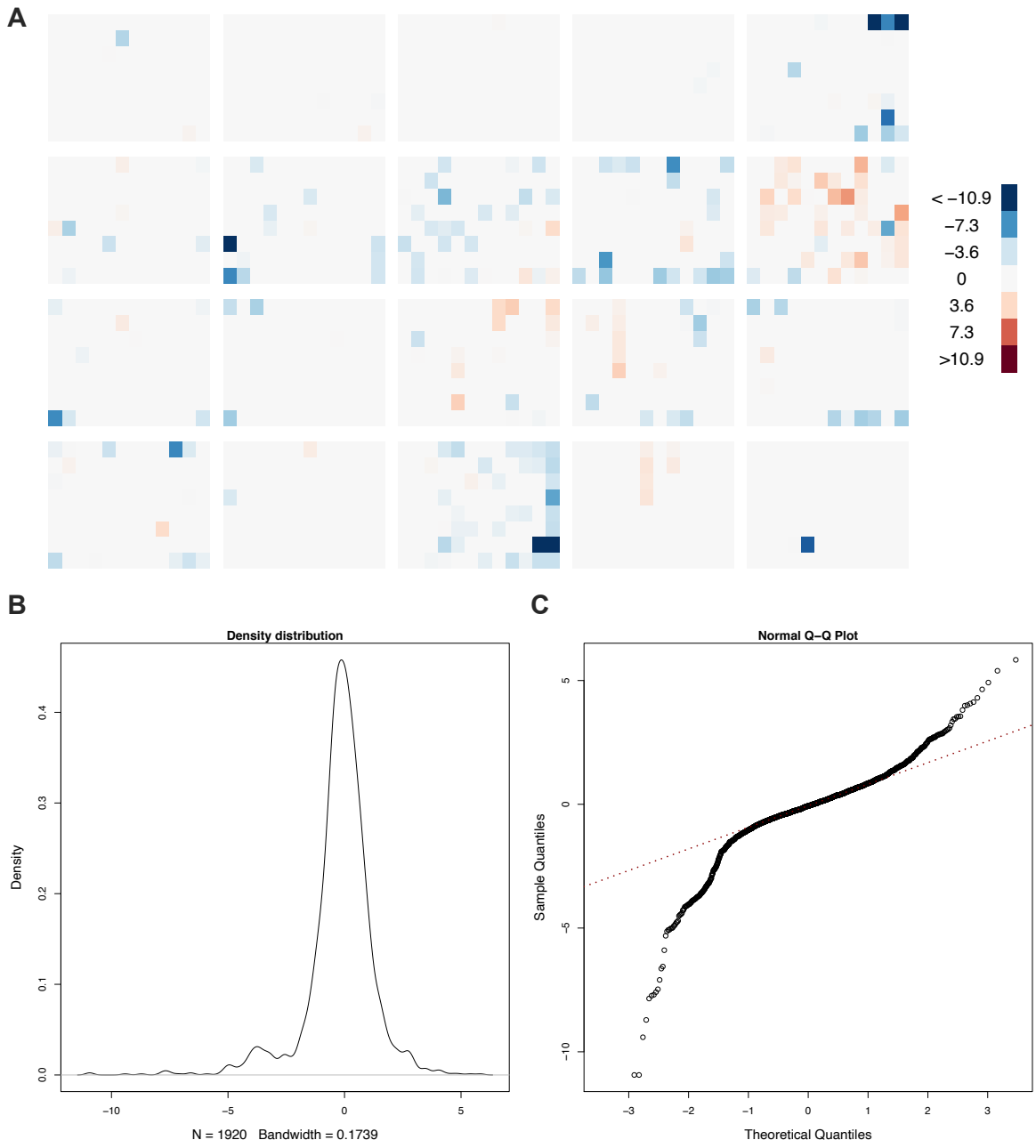

Figure 5.11 Summary representation of the mean scored values for total acidified bacteria number per well.

Data presented in 20 plates, representing normalised data (z-scores). The extremes of the scale represented as blue (lowest values, lesser number of acidified bacteria) and red (highest values, greater number of acidified bacteria), with white representative of 50th percentile. (**B**) Density plot of the assay z-score distribution (D'Agostino & Pearson test: K2 732.0, P<0.0001; skewness -1.57, kurtosis 8.05). (**C**) Normal Q-Q plot of the assay z-scores, deviations from the line indicate non-normally distributed values.

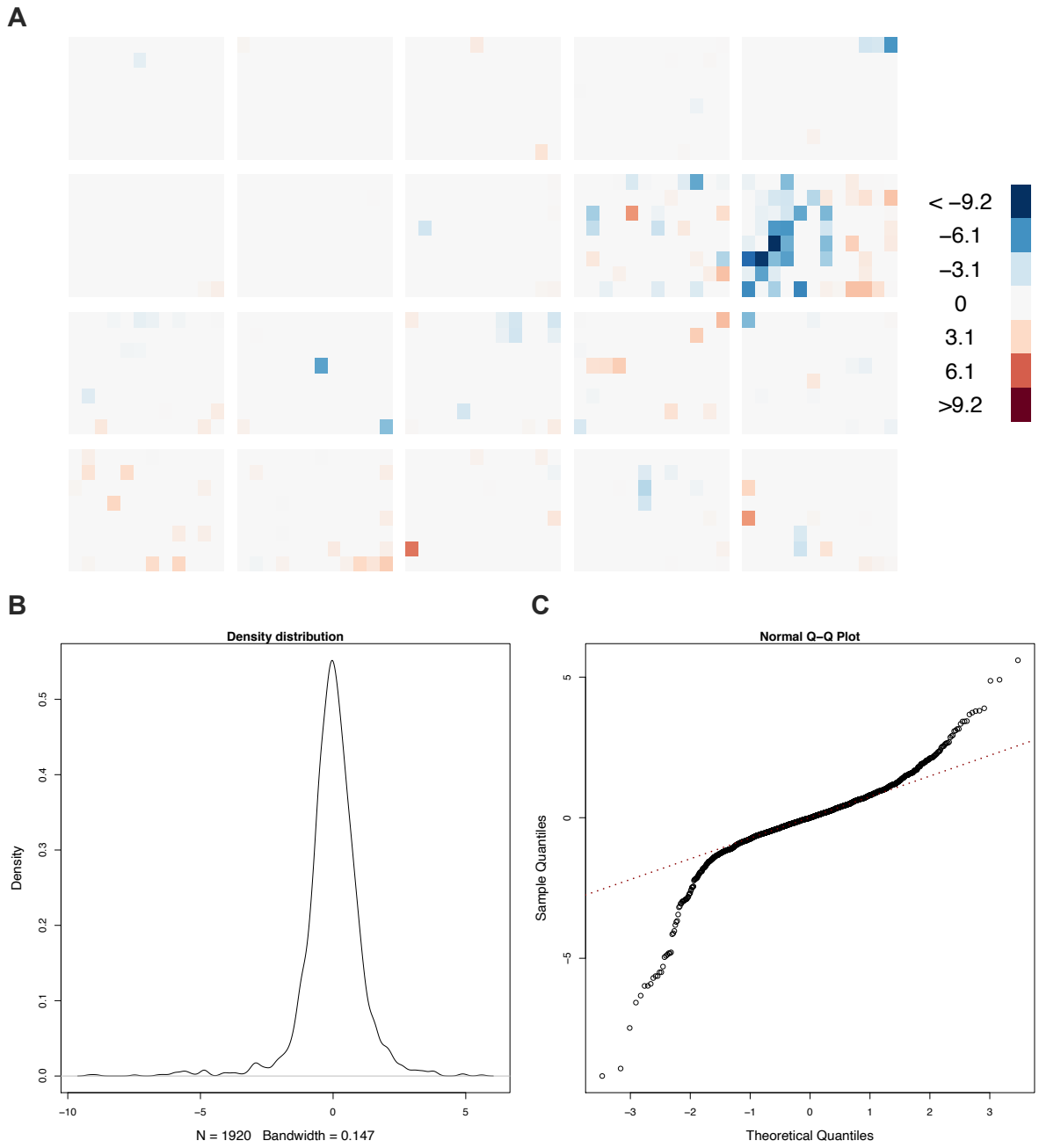

Figure 5.12 Summary representations of the mean scored values for total bacteria number per well versus total macrophage number.

Data presented in 20 plates in sequential arrangement from right to left, representing normalised data (z-scores). The extremes of the scale represented as blue (lowest values, lesser number of bacteria) and red (highest values, greater number of bacteria), with white representative of 50th percentile. (**B**) Density plot of the assay z-score distribution (D'Agostino & Pearson test: K2 759.4, P<0.0001; skewness -1.49, kurtosis 10.3). (**C**) Normal Q-Q plot of the assay z-scores, deviations from the line indicate non-normally distributed values.

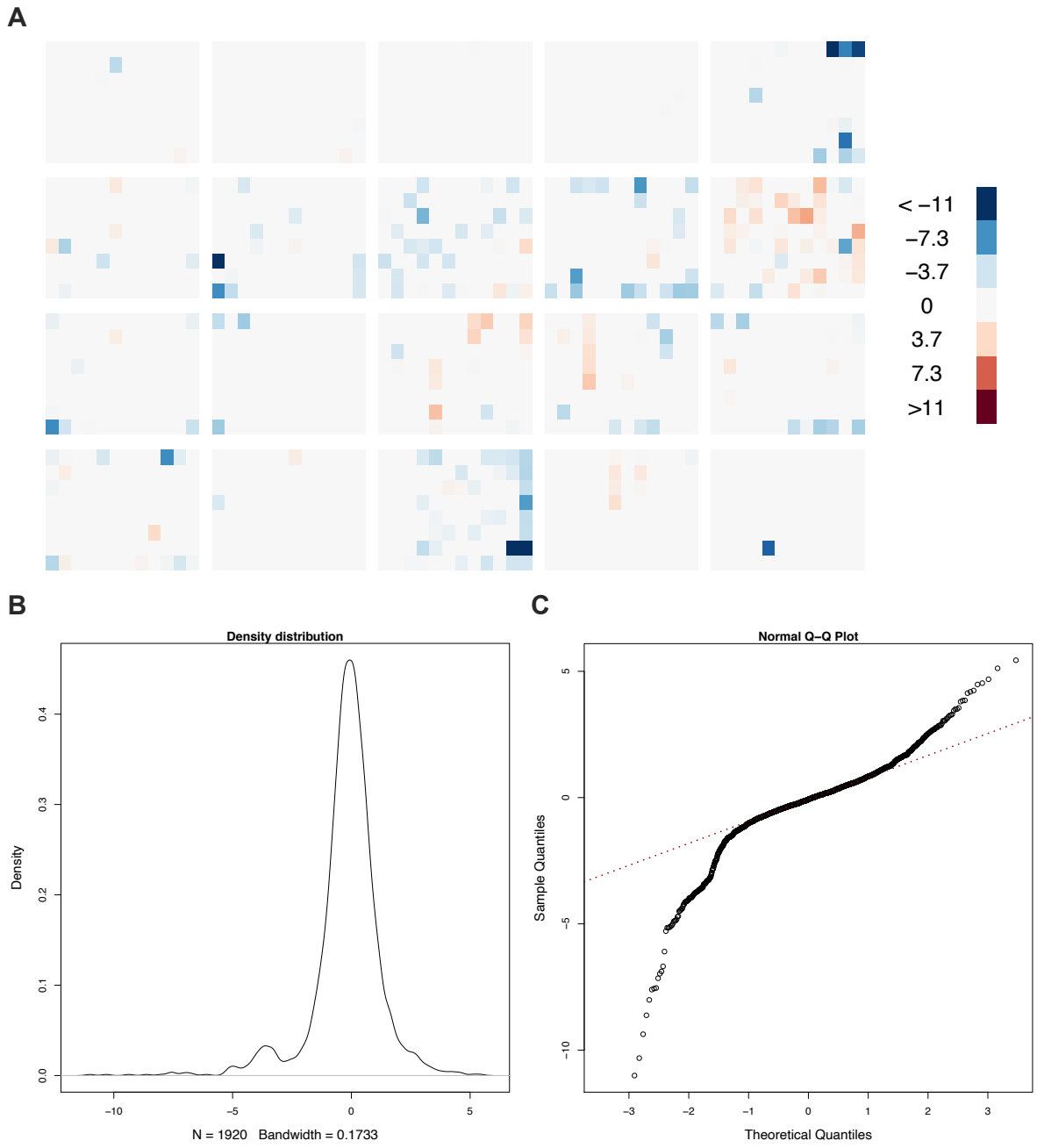

Figure 5.13 Summary representations of the mean scored values for total acidified bacteria number per well versus total macrophage number.

(**A**) Data presented in 20 plates in sequential arrangement from right to left, representing normalised data (z-scores). The extremes of the scale represented as blue (lowest values, lesser number of bacteria) and red (highest values, greater number of bacteria), with white representative of 50th percentile. (**B**) Density plot of the assay z-score distribution (D'Agostino & Pearson test: K2 713.3, P<0.0001; skewness -1.54, kurtosis 7.76). (**C**) Normal Q-Q plot of the assay z-scores, deviations from the line indicate non-normally distributed values.

5.5 Secondary NTML screen: confirmation of primary screen hits

Having defined and collated the primary hits, a custom secondary library containing 180 hits plus positive and negative controls divided across two 96-well plates was generated. The respective NTML mutant hits were obtained from the original NTML library stock and distributed across the 96-well plates as previously described in methods section 2.2.2.2.

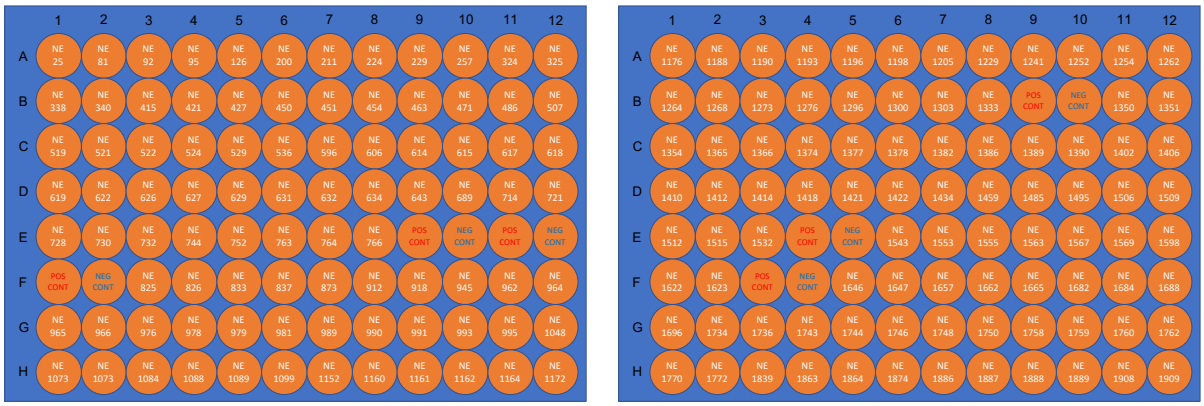

Figure 5.14 Schematic representation of secondary library assay layout.

Assay plates contained 180 candidates identified from the primary screen, with positive controls (heat-killed *S. aureus* USA300 strain JE2) and negative controls (*S. aureus* USA300 strain JE2).

The custom secondary library was subsequently subjected to nine rounds of rescreening using the methods employed in the primary screen. The resulting formatted raw data values, were subjected to the cellHTS2 R/Bioconductor analysis to generate normalised, summarised and scored outputs in respect to the three dual-channel and three single-channel assessments.

The primary objective of the secondary screen was to confirm an association between the *S. aureus* gene and the subversion of phagosomal acidification as identified in the primary screen. The secondary objective was to order the genes by value of acidification to proceed to validation.

5.5.1 Controls

Within each plate, 6 wells contained either live and heat-killed wild-type *S. aureus* USA300 strain JE2 which served as the negative and positive controls respectively (Fig 5.14). As previously demonstrated, it would be expected that the majority of heat-killed *S. aureus* are associated with an acidified phagosome. Hence within this screen, the resultant z-score would be expected to have a greater negative score compared to the live wild-type *S. aureus* control. The results are demonstrated within Figure 5.15. The heat-killed parental USA300 JE2 strain

obtained a mean Z-score of -1.798, with statistical significance obtained in paired comparison (Mann Whitney test) with the live USA300 JE2 strain. The live USA300 JE2 obtained a mean positive score (+0.3708), consistent with previous experimental data that only a minority of wild-type *S. aureus* progress to an acidified intracellular environment. These findings are also demonstrated within the secondary screen density plot and normal Q-Q plot (Figure 5.16) and secondary screen heatmap (Figure 5.17).

Of note, it is apparent when assessing the number of total bacteria number versus total macrophage number that the live wild-type bacteria were associated with a greater positive z-score compared to the general distribution. Assessment of the raw data identified that there were more bacteria within these wells compared to mutants under assessment.

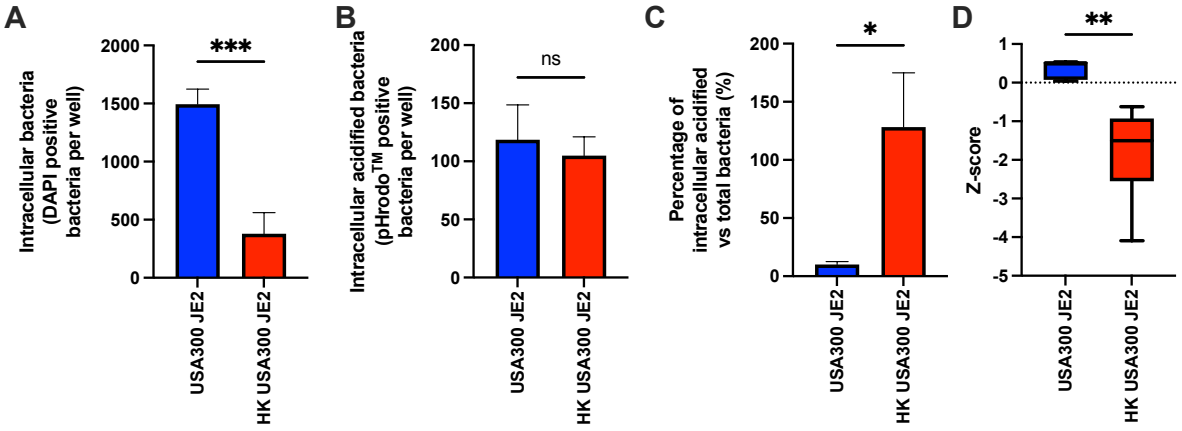

Figure 5.15 Secondary NTML screen summary of controls.

Differentiated monocyte-derived macrophages were challenged with either pHrodo^{TM}-labelled live or heat-killed *S. aureus* USA300 strain JE2 at a MOI of 5 bacteria per macrophage, for a period of 4 hours within 96-well format. Images acquired using ImageXpress^{MICRO} high-throughput microscope. (**A**) Plot of intracellular DAPI^{+} bacteria per well by condition. Data represent 7 experiments, performed in 6 replicates, line at mean with standard error of the mean (SEM), ***p<0.001, unpaired t test. (**B**) Plot of intracellular pHrodo^{+} bacteria per well by condition per well by condition. Data represent 7 experiments, performed in 6 replicates, line at mean with SEM, ns – not significant, unpaired t test (**C**) Plot of ratio of intracellular acidified bacteria versus total intracellular bacteria per well by percentage. Data represent 7 experiments, performed in 6 replicates, line at mean with SEM, *p<0.05, unpaired t test. (**D**) Box and whisker plot of Z-score by replicate, **p<0.01, Mann Whitney test.

5.5.2 Secondary NTML screen: Data Analyses

The outcomes of the secondary screen are summarised in the forms of a frequency distribution histogram and normal Q-Q plot (Figure 5.16) and heat map (Figure 5.17). The heat maps demonstrate the respective z-score based upon well position across each replicate and the mean score.

The P value acquired from the D'Agostino and Pearson normality test ($P<0.0001$) does not indicate if the population distribution is Gaussian or not, but that a randomly selected sample of data is highly probable to deviate from a Gaussian distribution. The distribution is skewed to the left (skewness -1.09) with more values present in the tails than a Gaussian distribution (kurtosis 2.01). The positive kurtosis reflects the number of outlying values beyond normal distribution. The difference between population mean (-0.07) and median scores (0.08) also reflects the skewed distribution to the left. Whereas in the primary screen most NTML mutant strains were not associated with phagosomal acidification (data skewed to the right), having selected for mutants associated with acidification it is desirable that on further screening, several mutants are exhibiting greater acidification. This is also demonstrated within the normal Q-Q plot, with positive controls and several mutants deviating from the reference line of expected normally distributed values.

As with the primary screen, technical screening problems can be recognised using these visual representations. For example, within plate A replicate 5, column 11, wells E-H have been scored with a positive z-score that is not typical compared to other replicates. On analysis of the raw values, within these wells minimal or no acidified bacteria have been detected. A further example of anomalous patterns is evident in both plates of replicate 9, where there are a greater number of wells with negative z-scores in plate A, row A and the bottom left corner of plate B. Assessment of these plates identified that few or no DAPI positive bacteria were identified within these wells. Utilising the summarised data visualised in the box and whisker plots (figures 5.18 and 5.19) representing normalised z-values and raw data respectively, it is evident that replicates 8 and 9 are suboptimal. In terms of raw values, there plates contain lower numbers of macrophages and lower total bacterial numbers. Consequently, the normalised data values demonstrate a greater interquartile range. Due to the inferior standard of these replicates, a subsequent analysis was undertaken with these replicates excluded.

The data displayed within figures 5.20, 5.21 and 5.22 presents data from the analysis of the seven replicates having excluded the plates that failed quality control assessment.

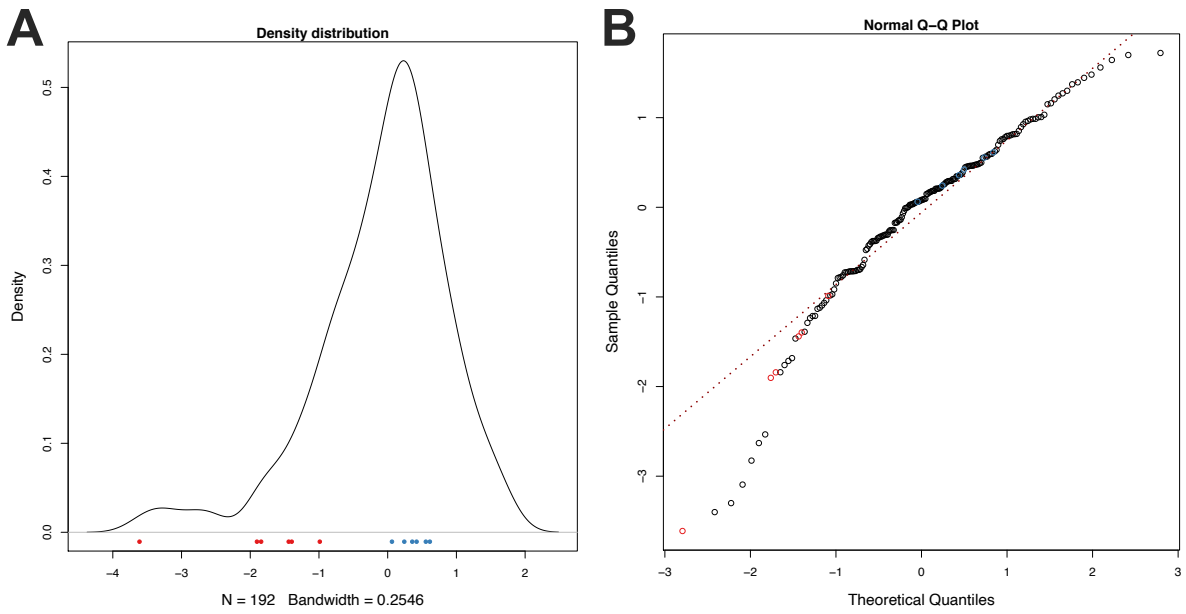

Figure 5.16 Secondary NTML screen summary.

Density plot of the assay z-score distribution (n=9). D'Agostino & Pearson test: K2 40.16, P<0.0001, skewness -1.09, kurtosis 2.01. (**B**) Normal Q-Q plot of the assay z-scores, deviations from the line indicate non-normally distributed values. The left-hand tail represents NTML mutants with greater intracellular acidification, and the right-hand tail represents NTML mutants with less intracellular acidification. Positive controls indicated by red circles. Negative controls indicated by blue circles.

A

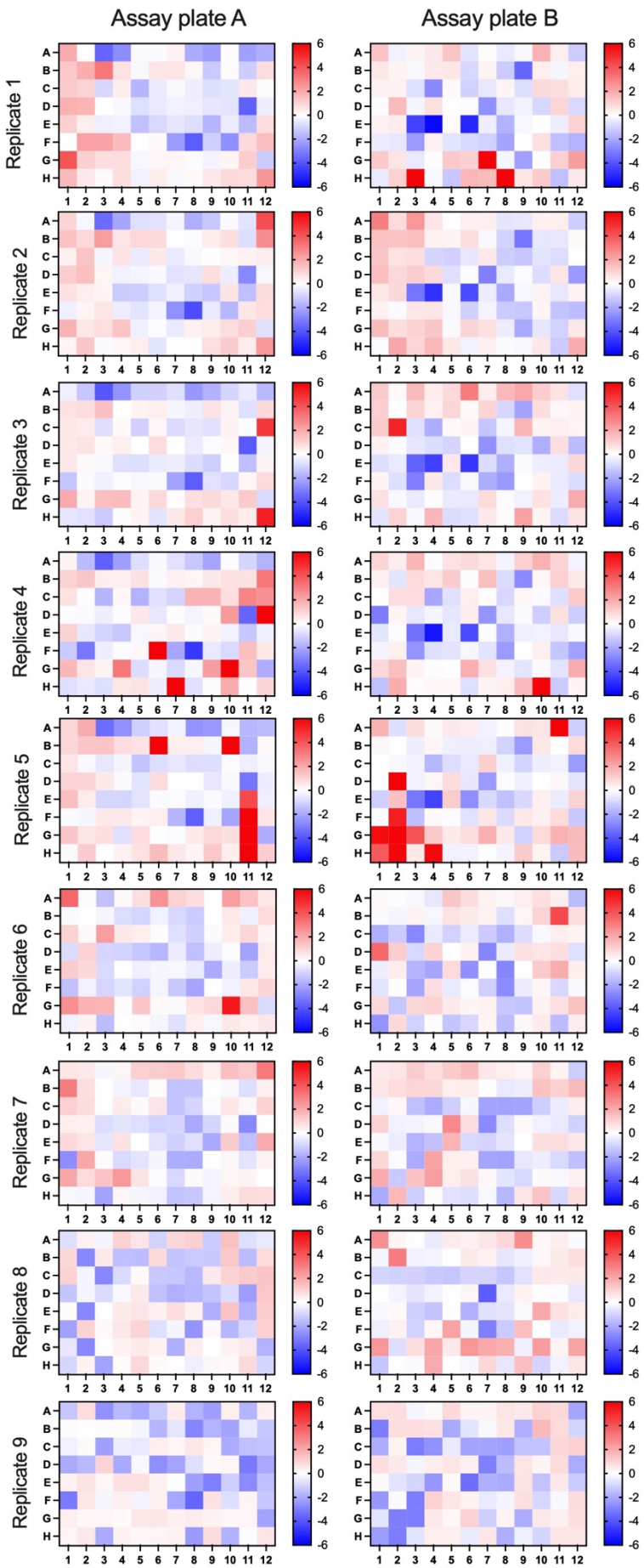
Assay plate A
Assay plate B
Replicate 1
Replicate 2
Replicate 3
Replicate 4
Replicate 5
Replicate 6
Replicate 7
Replicate 8
Replicate 9
A B C D E F G H
1 2 3 4 5 6 7 8 9 10 11 12
6 4 2 0 -2 -4 -6

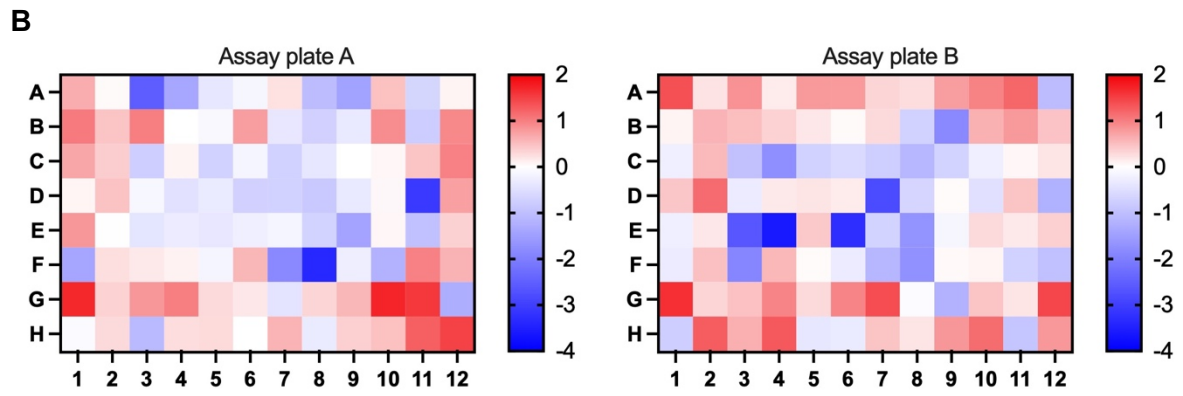

Figure 5.17 Secondary NTML screen heat map representation.

Assessment of acidified bacteria versus total bacteria. Data presented from the two confirmation plates representing normalised data (z-scores) (n=9). **A**) Individual replicate scores (n = 9); **B**) Mean scores. The extremes of the scale represented as blue (lowest values, greater acidification) and red (highest values, less acidification), with white representative of 50th percentile. Positive controls (heat-killed *S. aureus* USA300 strain JE2) located in plate A E9, E11 & F1 and plate B B9, E4 & F3. Negative controls (wild-type *S. aureus* USA300 strain JE2) located in plate A E10, E12 & F2 and plate B B10, E5 and F4.

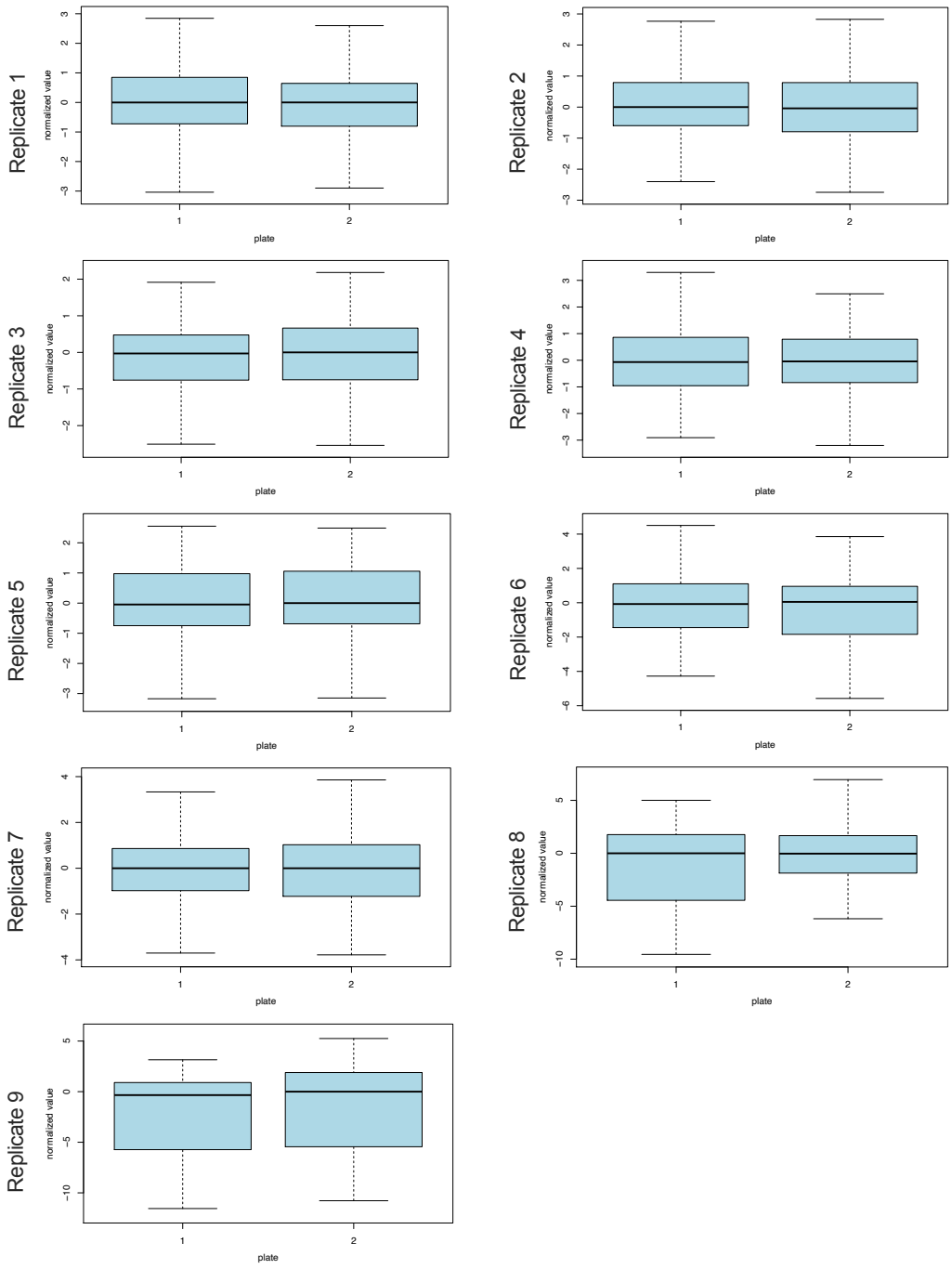

Figure 5.18 Secondary NTML screen box and whisker plots of normalised data values. Acidified bacteria versus total bacteria box-plot representation of data normalised across secondary library. Each plate summarised as box plot, where the box extends from the 25th and 75th percentiles, with the central line plotted at the plate median. The whiskers demarcate the 5th and 95th percentiles.

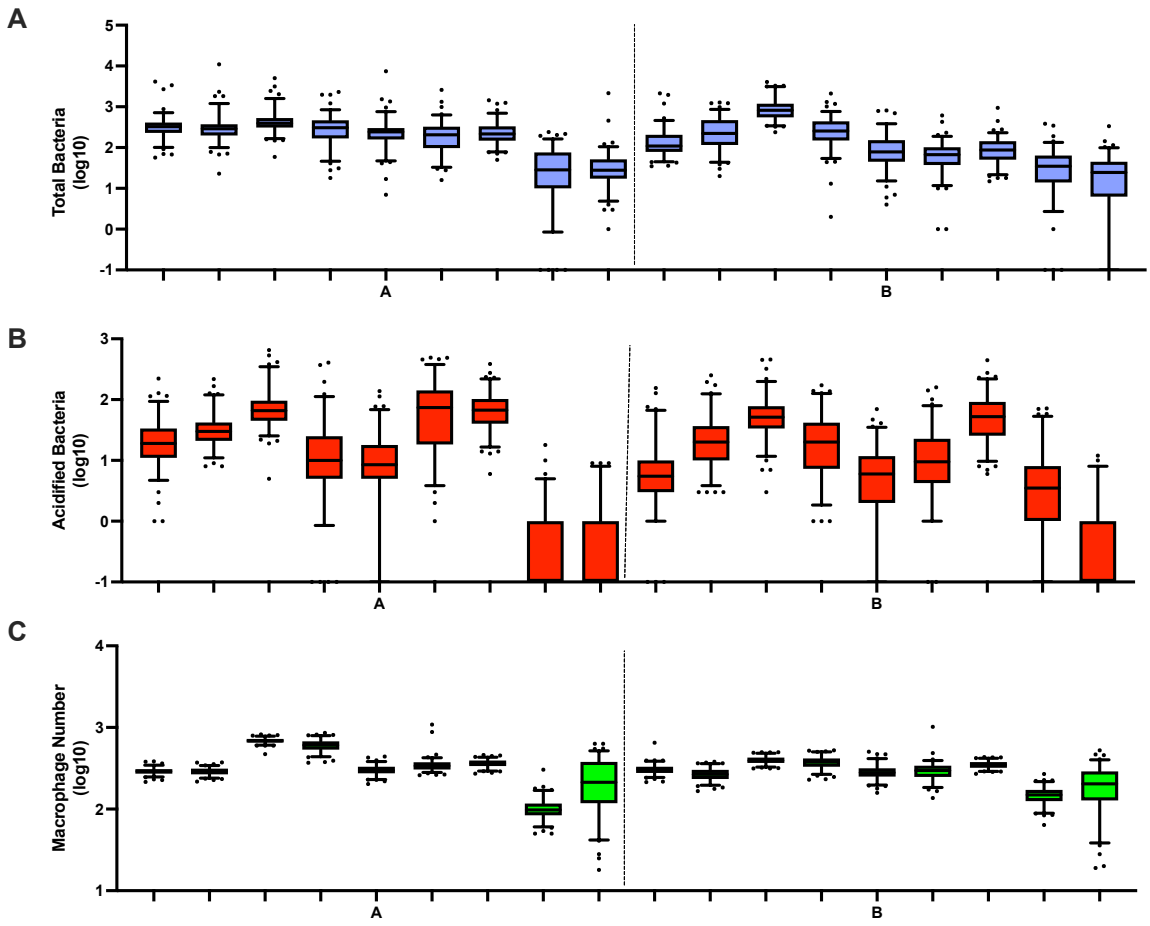

Figure 5.19 Secondary NTML screen box and whisker plots of summarised raw data. (**A**) Raw values of total bacteria number. (**B**) Raw values of total acidified bacteria number. (**C**) Raw values of total macrophage cell number. Each NTML plate replicate (1-3) summarised as box plot, where the box extends from the 25th and 75th percentiles, with the central line plotted at the plate median. The whiskers demarcate the 5th and 95th percentiles

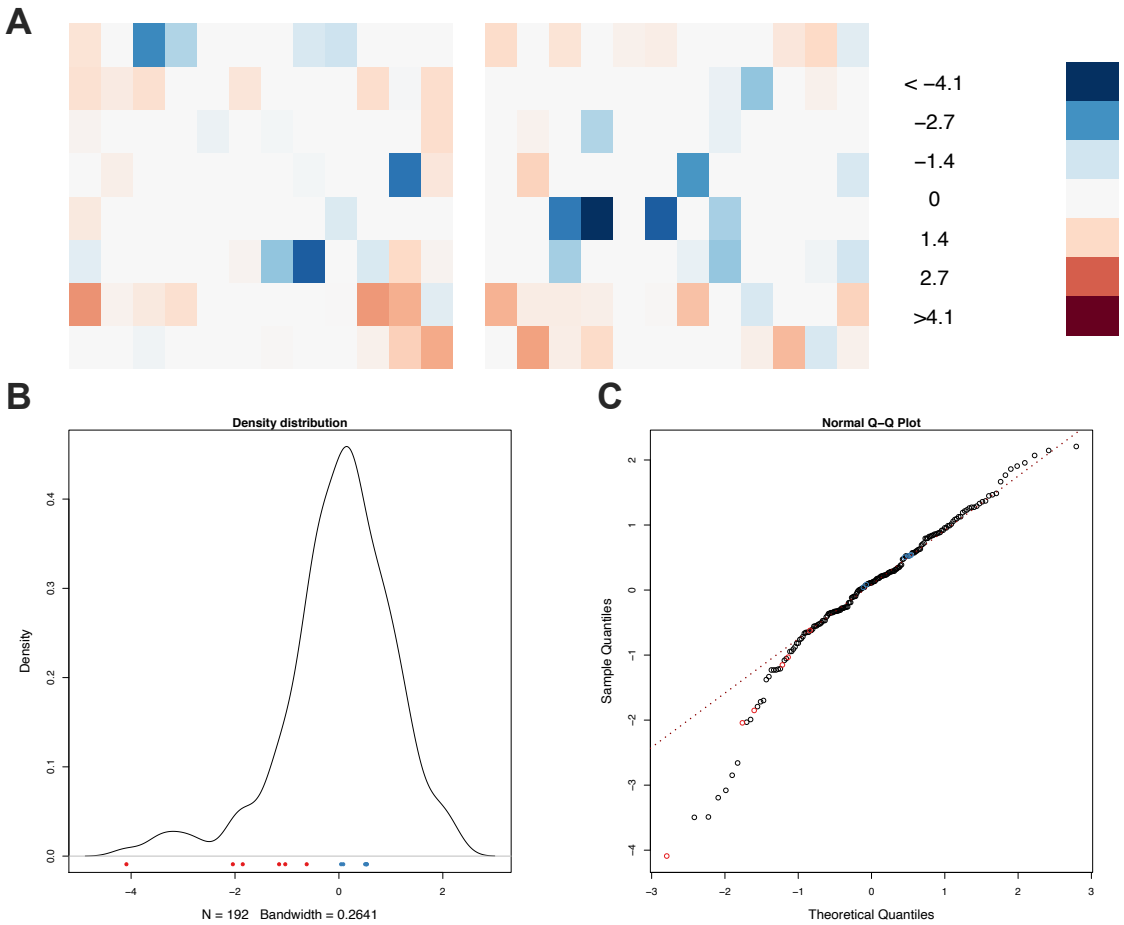

Fig 5.20 Secondary NTML screen summary representations of the mean scored values for total acidified bacteria versus total bacterial number per well.

Data presented in the two secondary assay plates in sequential arrangement from right to left, representing normalised data (z-scores) (n=7). The extremes of the scale represented as blue (representative of maximal bacterial acidification) and red (representative of minimal bacterial acidification), with white representative of 50th percentile. (**B**) Density plot of the assay z-score distribution. Range -4.09 to +2.24 (25% percentile -0.49, 75% percentile 0.68); Mean 0.004; Median 0.11; SD 1.06; Skewness -0.98; Kurtosis 2.09. D'Agostino & Pearson test: 36.40, P<0.0001. (**C**) Normal Q-Q plot of the assay z-scores, deviations from the line indicate non-normally distributed values.

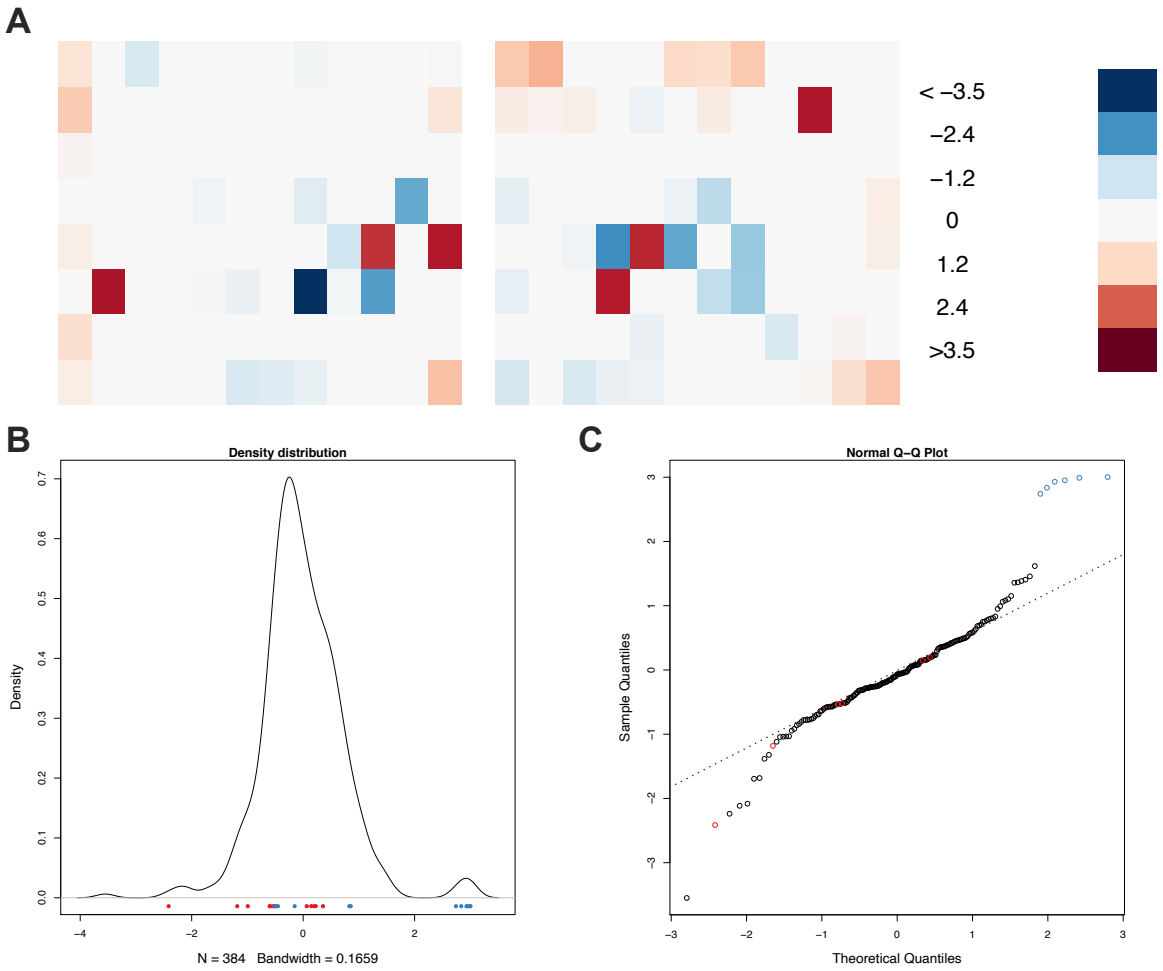

Fig 5.21 Secondary NTML screen summary representations of the mean scored values for total bacteria versus total macrophage number per well.

Data presented in the two secondary assay plates in sequential arrangement from right to left, representing normalised data (z-scores) (n=7). The extremes of the scale represented as blue (negative z-score) and red (positive z-score), with white representative of 50th percentile. (**B**) Normal Q-Q plot of the assay z-scores, deviations from the line indicate non-normally distributed values. (**C**) Density plot of the assay z-score distribution. Range -3.55 to +3.00 (25% percentile -0.50, 75% percentile 0.39); Mean -0.01; Median -0.07; SD 0.88; Skewness 0.49; Kurtosis 3.73. D'Agostino & Pearson test: 29.65, P<0.0001. (**C**) Normal Q-Q plot of the assay z-scores, deviations from the line indicate non-normally distributed values.

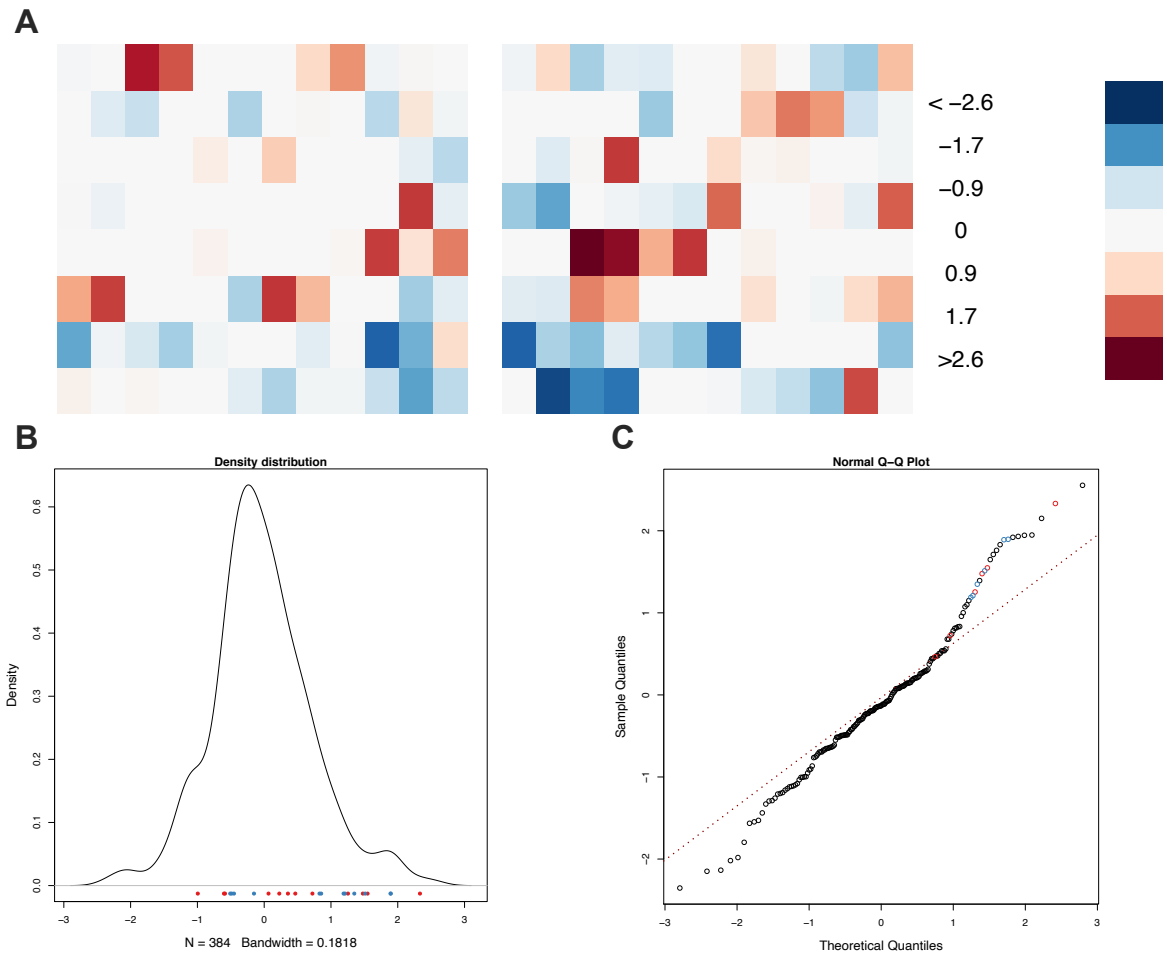

Fig 5.22 Secondary NTML screen summary representations of the mean scored values for total acidified bacteria versus total macrophage number per well.

Data presented in the two secondary assay plates in sequential arrangement from right to left, representing normalised data (z-scores) (n=7). The extremes of the scale represented as blue (negative z-score) and red (positive z-score), with white representative of 50th percentile. (**B**) Normal Q-Q plot of the assay z-scores, deviations from the line indicate non-normally distributed values. (**C**) Density plot of the assay z-score distribution. Range -2.35 to +2.55 (25% percentile -0.63, 75% percentile 0.40); Mean -0.05; Median -0.13; SD 0.91; Skewness 0.37; Kurtosis 0.42. D'Agostino & Pearson test: 5.92, P 0.05. (**C**) Normal Q-Q plot of the assay z-scores, deviations from the line indicate non-normally distributed values.

5.5.3 Defining true hits from the secondary NTML screen

The aim of the secondary screen was to identify a smaller number of NTML mutant strains maximally associated with intracellular bacterial acidification for validation. As previously described during the primary screen, these NTML mutants will have a negative Z-score (Figure 5.23). The Z-score is a measure of the probability that the ratio of bacterial acidification versus total bacterial number occurred by chance. Z-scores of -1, -2 and -3 correspond to the probabilities of 32%, 5% and 0.3% respectively. From the secondary screen, 7 NTML mutants had a mean Z-score less than -2; 20 NTML mutants had a mean Z-score less than -1. As a precedent for defining "hits", a Z-score of ±2 (equivalent to a p-value of <0.05) has been accepted as being of statistical significance (Fisher et al. 2012).

5.6 Defining "interesting" addition screen hits

The STRING (search tool for the retrieval of interacting genes/proteins) database has compiled data from known and predicted protein interactions, both direct and indirectly (Jensen et al. 2009). The known protein products from the 180 NTML mutants that were selected to secondary screening were submitted to the STRING v11.0 search tool, with the organism specified as *Staphylococcus aureus*. The genes and proteins that were recognised within the STRING search tool were mapped into specific pathways or processes (Figure 5.24).

The map provides an indication of networks and complexes potentially involved in the resistance of *S. aureus* to phagosomal maturation. It is to be expected that the two-component regulatory systems of *S. aureus* would be prominently recognised. Within the lower left side of the map, the regulatory complexes *agr, sae, arl* and *gra* are present, with prominent interaction pathways. Extending from this complex, multiple genes associated with oxidative stress responses are evident, for example catalase, superoxide dismutases and Clp protease subunits. The role of the superoxide dismutase complexes has been previously discussed following demonstration that a *S. aureus* mutant deficient of both *sodA* and *sodM* was associated with failure to subvert phagosomal acidification. The ClpP protease has previously been demonstrated to be important for *S. Aureus* virulence and oxidative stress response (Michel et al. 2006).

Further interrogation of the STRING pathways, informed by the respective scores obtained from the secondary screen, multiple genes associated with electron transport and respiratory metabolism are prominent. The quinol oxidase complex, qoxABCD, forms part of the terminal oxidase cytochrome aa_3 which catalyses the reduction of oxygen to water (Hammer et al. 2016). This enzyme has been demonstrated to contribute to the fitness and virulence of *S.*

aureus during colonisation (Götz & Mayer 2013). The STRING analysis associated the quinol oxidase complex with succinate dehydrogenase (*sdhA*) and protoheme IX farnesyltransferase (*cyoE*, also known as *ctaB*), due to putative homologs interacting in other organisms. These genes have been associated with the tricarboxylic acid cycle and associated with virulence and biofilm formation (Gaupp et al. 2010; Stevens et al. 2017).

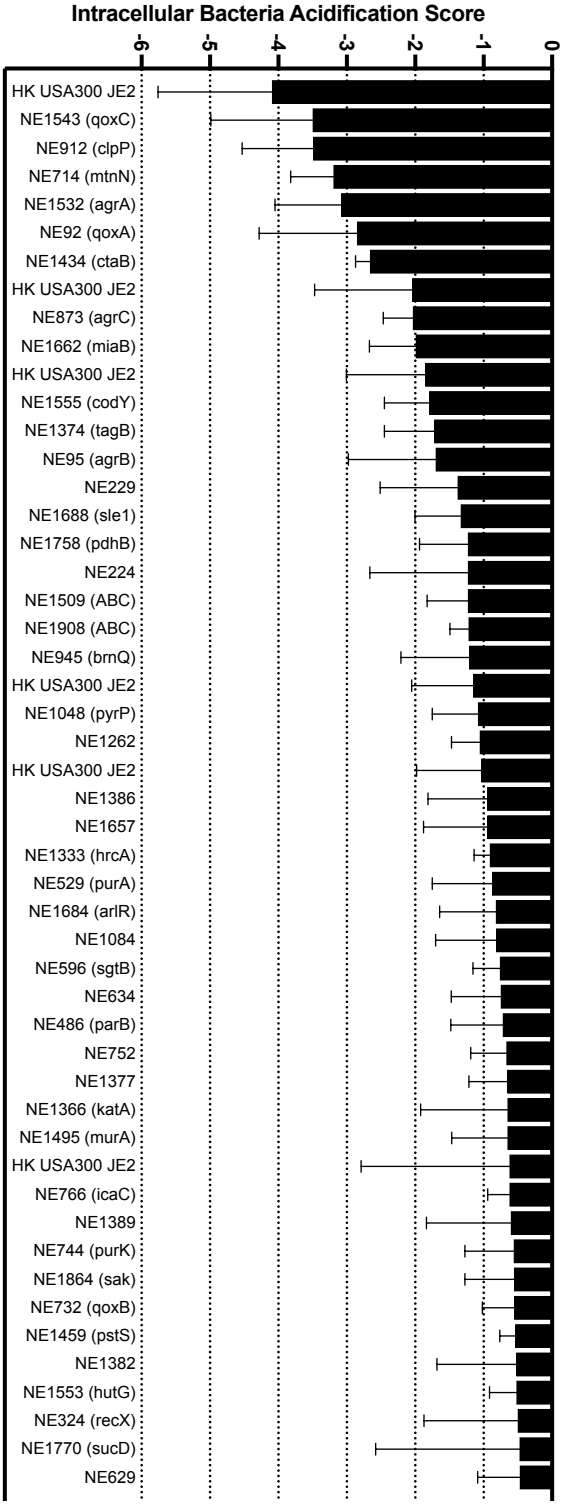

Figure 5.23 *S. aureus* NTML mutant secondary screen z-scores

Summary z-scores obtained for respective NTML mutants post analysis of raw data using cellHTS2 R/Bioconductor package. Mean score with standard deviation, n=7.

Table 5.1 Secondary NTML screen ranked by mean Z-score

Summary z-scores obtained for NTML mutant strain using cellHTS2 R/Bioconductor package. Mean score (n = 7). Primary screen rank and mean z-score (n = 3) also detailed.

Rank	Accession number	Strain name	Gene description	Secondary screen score	Primary screen Rank	Primary screen score
1	SAUSA300_0752	NE912	ATP-dependent Clp protease proteolytic subunit (clpP)	-3.400757979	69	-1.62276562
2	SAUSA300_0961	NE1543	quinol oxidase, subunit III (qoxC)	-3.300407148	14	-3.095018774
3	SAUSA300_1558	NE714	5'-methylthioadenosine/S-adenosylhomocysteine nucleosidase (mntN)	-3.093641083	56	-1.739109369
4	SAUSA300_1016	NE1434	protoheme IX farnesyltransferase (cyoE)	-2.826026331	138	-1.137161338
5	SAUSA300_1992	NE1532	accessory gene regulator protein A (agrA)	-2.630321847	110	-1.285420623
6	SAUSA300_0963	NE92	quinol oxidase, subunit II (qoxA)	-2.533897126	108	-1.305050119
7	SAUSA300_1991	NE873	accessory gene regulator protein C (agrC)	-1.840300575	116	-1.265899455
8	SAUSA300_0626	NE1374	teichoic acid biosynthesis protein B	-1.76018394	177	-1.040557573
9	SAUSA300_1185	NE1662	(dimethylallyl)adenosine tRNA methylthiotransferase (miaB)	-1.713878415	34	-2.092119061
10	SAUSA300_1148	NE1555	transcriptional repressor CodY	-1.682800336	43	-1.945467693
11	SAUSA300_1119	NE229	conserved hypothetical protein	-1.464116361	179	-1.036098513
12	SAUSA300_1989	NE95	accessory gene regulator protein B (agrB)	-1.388548779	156	-1.089651469
13	SAUSA300_1092	NE1048	uracil permease (pyrP)	-1.289223613	168	-1.06546601
14	SAUSA300_0630	NE1509	ABC transporter ATP-binding protein	-1.235862669	55	-1.74793727
15	SAUSA300_0188	NE945	branched-chain amino acid transport system II carrier protein (brnQ)	-1.21324191	44	-1.935356797
16	SAUSA300_0994	NE1758	pyruvate dehydrogenase E1 component, beta subunit (pdhB)	-1.212031066	6	-4.517636999
17	SAUSA300_1974	NE1386	Leukocidin/Hemolysin toxin family protein	-1.132966543	76	-1.568169817
18	SAUSA300_0476	NE1657	hypothetical protein	-1.120861575	95	-1.399164288
19	SAUSA300_1017	NE1084	hypothetical protein	-1.095219577	172	-1.051598669
20	SAUSA300_1984	NE1262	hypothetical protein	-1.066439816	31	-2.143249172
21	SAUSA300_0192	NE224	conserved hypothetical protein	-1.037059692	166	-1.071271818
22	SAUSA300_0438	NE1688	CHAP domain-contain protein	-0.982775056	167	-1.069496616
23	SAUSA300_1232	NE1366	catalase	-0.970742002	25	-2.268126571
24	SAUSA300_1911	NE1908	ABC transporter ATP-binding protein	-0.916692949	77	-1.550037838
25	SAUSA300_1809	NE634	putative membrane protein	-0.849371995	93	-1.419411641
26	SAUSA300_2643	NE486	putative chromosome partioning protein, ParB family	-0.7893017	67	-1.63197938
27	SAUSA300_1889	NE522	adenylosuccinate lyase (purB)	-0.781056303	20	-2.591478527
28	SAUSA300_1139	NE1770	succinyl-CoA synthetase subunit alpha (sucD)	-0.776065617	4	-4.635602375
29	SAUSA300_0594	NE1382	alcohol dehydrogenase	-0.758872604	17	-2.733232478
30	SAUSA300_1962	NE631	phiPVL ORF39-like protein	-0.72661006	28	-2.182743974
31	SAUSA300_2566	NE454	transcriptional regulator, Crp/Fnr family (arcR)	-0.725052923	57	-1.730208422
32	SAUSA300_0017	NE529	adenylosuccinate synthetase (purA)	-0.721170511	39	-1.996555301
33	SAUSA300_1308	NE1684	DNA-binding response regulator (arlR)	-0.714843571	136	-1.143180614
34	SAUSA300_1855	NE596	monofunctional glycosyltransferase (sgtB)	-0.714621557	71	-1.607136107
35	SAUSA300_0390	NE632	conserved hypothetical protein	-0.714118491	144	-1.119149894
36	SAUSA300_2511	NE1377	conserved hypothetical protein	-0.712159865	109	-1.291915149
37	SAUSA300_1542	NE1333	heat-inducible transcription repressor HrcA	-0.710054005	66	-1.64095922
38	SAUSA300_2602	NE766	intercellular adhesion protein C (icaC)	-0.698654817	79	-1.543003461
39	SAUSA300_1225	NE1389	aspartate kinase	-0.698358286	73	-1.601156775
40	SAUSA300_2281	NE1553	formimidoylglutamase (hutG)	-0.691259085	50	-1.80920489
41	SAUSA300_1854	NE324	regulatory protein RecX	-0.665036918	140	-1.129282587
42	SAUSA300_1283	NE1459	phosphate ABC transporter, phosphate-binding protein PstS	-0.643402502	104	-1.324896395

43	SAUSA300_0892	NE1378	oligopeptide ABC transporter, oligopeptide-binding protein	-0.5857576	63	-1.665665237
44	SAUSA300_2055	NE1495	UDP-N-acetylglucosamine 1-carboxyvinyltransferase (murA)	-0.476812492	65	-1.648794961
45	SAUSA300_2211	NE627	putative membrane protein	-0.462722705	120	-1.24545282
46	SAUSA300_0084	NE989	hypothetical protein	-0.426904234	87	-1.448175849
47	SAUSA300_0962	NE732	quinol oxidase, subunit I (qoxB)	-0.412177619	23	-2.32665548
48	SAUSA300_1922	NE1864	staphylokinase (sak)	-0.388915884	149	-1.11184014
49	SAUSA300_0199	NE606	conserved hypothetical protein	-0.376763278	135	-1.154168675
50	SAUSA300_2396	NE126	para-nitrobenzyl esterase	-0.376481551	173	-1.05152177
51	SAUSA300_2287	NE752	putative membrane protein	-0.375677562	178	-1.038412459
52	SAUSA300_2316	NE451	acetyltransferase, GNAT family	-0.371289374	70	-1.609934477
53	SAUSA300_0102	NE643	staphylococcal tandem lipoprotein	-0.344499834	148	-1.112473215
54	SAUSA300_1871	NE463	conserved hypothetical protein	-0.336603932	82	-1.484254091
55	SAUSA300_0417	NE1160	tandem lipoprotein	-0.327462314	7	-4.358251888
56	SAUSA300_0726	NE629	glycerate kinase family protein	-0.326720112	91	-1.427632665
57	SAUSA300_1569	NE1874	U32 family peptidase	-0.316166132	89	-1.430869312
58	SAUSA300_0691	NE1622	DNA-binding response regulator SaeR	-0.31337371	133	-1.180542114
59	SAUSA300_1365	NE1647	30S ribosomal protein S1 (rpsA)	-0.305278388	61	-1.692564787
60	SAUSA300_1568	NE1414	uridine kinase (udk)	-0.304982976	152	-1.101414956
61	SAUSA300_0967	NE744	phosphoribosylaminoimidazole carboxylase, ATPase subunit (purK)	-0.304720141	64	-1.651232745
62	SAUSA300_1938	NE918	phi77 ORF006-like protein capsid protein	-0.271137269	111	-1.284856271
63	SAUSA300_2341	NE1512	respiratory nitrate reductase, subunit delta (narJ)	-0.256274914	154	-1.098493173
64	SAUSA300_1058	NE1354	alpha-hemolysin precursor	-0.255490072	60	-1.696927313
65	SAUSA300_0339	NE763	conserved hypothetical protein	-0.253946356	153	-1.099367995
66	SAUSA300_0709	NE1390	5'(3')-deoxyribonucleotidase	-0.253420316	15	-3.094926773
67	SAUSA300_0780	NE536	conserved hypothetical protein	-0.173812775	137	-1.139677388
68	SAUSA300_1432	NE764	phiSLT ORF78-like protein	-0.170759756	150	-1.111187722
69	SAUSA300_1671	NE833	hypothetical protein	-0.168394068	121	-1.244849065
70	SAUSA300_2134	NE200	iron compound ABC transporter, permease protein	-0.149507658	139	-1.133513365
71	SAUSA300_0395	NE1563	superantigen-like protein	-0.141577781	122	-1.227467298
72	SAUSA300_1047	NE626	succinate dehydrogenase, flavoprotein subunit (sdhA)	-0.137617294	86	-1.458363933
73	SAUSA300_1801	NE427	fumarate hydratase, class II (fumC)	-0.110340605	105	-1.313719497
74	SAUSA300_0673	NE1072	cobalamin synthesis protein/P47K family protein	-0.069303223	131	-1.197434982
75	SAUSA300_2043	NE1750	hypothetical protein	-0.04065186	38	-1.999030914
76	SAUSA300_0711	NE421	conserved hypothetical protein	-0.010152645	162	-1.07478736
77	SAUSA300_2282	NE1099	hypothetical protein	-0.006649948	12	-3.373883635
78	SAUSA300_2439	NE614	UTP-glucose-1-phosphate uridylyltransferase (galU)	-0.001704584	143	-1.121378264
79	SAUSA300_0943	NE730	acetyltransferase, GNAT family	0.007487959	114	-1.275225858
80	SAUSA300_2083	NE1485	acetyltransferase	0.027133441	117	-1.265157037
81	SAUSA300_0145	NE1646	phosphonate ABC transporter phosphonate-binding protein	0.02862132	124	-1.217738147
82	SAUSA300_2285	NE81	aldose 1-epimerase (galM)	0.034124263	141	-1.129218754
83	SAUSA300_1975	NE1300	Aerolysin/leukocidin family protein	0.03542851	10	-3.854660543
84	SAUSA300_0859	NE1665	NADH-dependent flavin oxidoreductase	0.045846187	169	-1.058903864
85	SAUSA300_0655	NE689	conserved hypothetical protein	0.051031003	113	-1.277837478
86	SAUSA300_0040	NE615	conserved hypothetical protein	0.059464771	90	-1.42903524
87	SAUSA300_0590	NE1402	hypothetical protein	0.062844519	48	-1.842497315
88	SAUSA300_0307	NE619	5'-nucleotidase, lipoprotein e(P4) family	0.074158641	132	-1.194641583
89	SAUSA300_2367	NE1682	gamma-hemolysin component B (hlgB)	0.075957316	129	-1.203695351
90	SAUSA300_0371	NE524	conserved hypothetical protein	0.085291309	160	-1.077891361
91	SAUSA300_0457	NE325	5S ribosomal RNA (rrfA)	0.086051519	53	-1.776424358

92	SAUSA300_2400	NE1264	glutamyl-aminopeptidase	0.092136684	45	-1.915420692
93	SAUSA300_0159	NE826	capsular polysaccharide biosynthesis protein Cap5H	0.094882218	123	-1.217976042
94	SAUSA300_0783	NE1422	phosphoglycerate mutase family protein	0.14858816	180	-1.034367071
95	SAUSA300_0605	NE1193	accessory regulator A (SarA)	0.149808865	13	-3.22351457
96	SAUSA300_0402	NE1569	superantigen-like protein	0.163416768	159	-1.079968862
97	SAUSA300_2436	NE825	putative cell wall surface anchor family protein	0.167626093	78	-1.549178738
98	SAUSA300_2627	NE1418	2-oxoglutarate/malate translocator	0.174920651	119	-1.253910867
99	SAUSA300_2497	NE981	aminotransferase, class I	0.181753758	102	-1.335087037
100	SAUSA300_0690	NE1296	sensor histidine kinase SaeS	0.183129942	158	-1.087161914
101	SAUSA300_1427	NE1515	phiSLT ORF86-like protein	0.184170999	54	-1.76027027
102	SAUSA300_0409	NE1406	conserved hypothetical protein	0.206080776	18	-2.704902573
103	SAUSA300_0239	NE1421	PTS system, fructose-specific enzyme II, BC component	0.207619129	145	-1.118529178
104	SAUSA300_1599	NE1760	hypothetical protein	0.208122552	30	-2.162138444
105	SAUSA300_1473	NE1887	transcription antitermination protein NusB	0.208803454	94	-1.403124543
106	SAUSA300_1912	NE1188	putative membrane protein	0.213237174	35	-2.057013471
107	SAUSA300_1329	NE211	amino acid permease	0.225015578	112	-1.284430214
108	SAUSA300_1515	NE1229	ABC transporter permease	0.252120787	1	-5.719815013
109	SAUSA300_2167	NE1088	conserved hypothetical protein	0.259669566	74	-1.586612445
110	SAUSA300_1289	NE1567	dihydrodipicolinate reductase (dapB)	0.276516273	51	-1.805456513
111	SAUSA300_2308	NE1089	response regulator protein	0.284491986	26	-2.244360406
112	SAUSA300_1921	NE1303	truncated amidase	0.291426819	127	-1.207727674
113	SAUSA300_0234	NE1744	putative flavohemoprotein	0.293266583	128	-1.204241676
114	SAUSA300_0659	NE979	sugar efflux transporter	0.294702232	68	-1.628977212
115	SAUSA300_0810	NE1073	hypothetical protein	0.295000378	165	-1.072572814
116	SAUSA300_2550	NE1205	anaerobic ribonucleotide reductase, small subunit (nrdG)	0.315017308	22	-2.502620434
117	SAUSA300_0342	NE1734	hypothetical protein	0.316143552	16	-2.740184376
118	SAUSA300_0126	NE990	hypothetical protein	0.316830289	72	-1.606710871
119	SAUSA300_0848	NE966	hypothetical protein	0.34540938	80	-1.541183076
120	SAUSA300_1683	NE1276	bifunctional 3-deoxy-7-phosphoheptulonate synthase/chorismate mutase	0.347702665	21	-2.506729632
121	SAUSA300_2040	NE1598	hypothetical protein	0.362363417	157	-1.089129916
122	SAUSA300_0714	NE1161	integral membrane protein	0.369978999	2	-5.383650577
123	SAUSA300_2307	NE521	ABC transporter, permease protein	0.389176333	142	-1.129020715
124	SAUSA300_2065	NE1410	UDP-N-acetylglucosamine 2-epimerase	0.446124405	24	-2.278038178
125	SAUSA300_1097	NE1759	orotidine 5'-phosphate decarboxylase (pyrF)	0.452483374	155	-1.097181199
126	SAUSA300_2014	NE340	threonine dehydratase (ilvA)	0.455500404	97	-1.364062421
127	SAUSA300_0992	NE1886	hypothetical protein	0.460103097	96	-1.365803138
128	SAUSA300_1760	NE617	lantibiotic epidermin immunity protein F (epiG)	0.462858086	147	-1.115183696
129	SAUSA300_0951	NE1506	V8 protease (sspA)	0.462967006	103	-1.334719536
130	SAUSA300_1846	NE1351	conserved hypothetical protein	0.464728875	84	-1.466383723
131	SAUSA300_0313	NE622	putative nucleoside permease NupC	0.470839127	101	-1.342767503
132	SAUSA300_1623	NE257	conserved hypothetical protein	0.475677985	146	-1.1181259
133	SAUSA300_1506	NE1162	hypothetical protein	0.478876932	75	-1.579912281
134	SAUSA300_1724	NE1736	hypothetical protein	0.482144642	33	-2.117062524
135	SAUSA300_0832	NE1623	hypothetical protein	0.492113925	126	-1.207863033
136	SAUSA300_1260	NE1273	prephenate dehydrogenase	0.499317698	106	-1.312579627
137	SAUSA300_0825	NE1365	oxidoreductase, 2-nitropropane dioxygenase family	0.551636757	100	-1.34928135
138	SAUSA300_2106	NE837	putative transcriptional regulator	0.565558731	47	-1.872112954
139	SAUSA300_2344	NE991	uroporphyrin-III C-methyl transferase	0.566415209	46	-1.886236599
140	SAUSA300_2342	NE1152	respiratory nitrate reductase, beta subunit (narH)	0.586048701	81	-1.494544041
141	SAUSA300_0666	NE1268	hypothetical protein	0.593773362	99	-1.352216472

142	SAUSA300_0182	NE964	4'-phosphopantetheinyl transferase superfamily protein	0.596077123	37	-2.03347308
143	SAUSA300_0068	NE1839	cadmium-exporting ATPase, truncation	0.624372296	49	-1.828845796
144	SAUSA300_1905	NE25	PIN domain protein	0.642038519	151	-1.104194251
145	SAUSA300_1460	NE519	peptidase, M20/M25/M40 family	0.697306796	174	-1.04566072
146	SAUSA300_2100	NE721	lytic regulatory protein	0.739675303	125	-1.211827033
147	SAUSA300_0236	NE450	PTS system, IIBC components	0.758141584	115	-1.266381793
148	SAUSA300_1222	NE1241	thermonuclease (nuc)	0.761634888	58	-1.705118444
149	SAUSA300_0118	NE1198	pyridoxal-phosphate dependent enzyme superfamily protein	0.781705369	161	-1.076320132
150	SAUSA300_2546	NE1196	glycine betaine aldehyde dehydrogenase (betB)	0.795832704	36	-2.05660324
151	SAUSA300_2314	NE1350	conserved hypothetical protein	0.797804836	52	-1.782663301
152	SAUSA300_1720	NE1909	hypothetical protein	0.803937207	85	-1.465256724
153	SAUSA300_2440	NE728	fibronectin binding protein B (fnbB)	0.814360145	171	-1.054517009
154	SAUSA300_0877	NE976	Chaperone clpB	0.81585822	98	-1.358532112
155	SAUSA300_0183	NE1888	hypothetical protein	0.818835638	175	-1.044957003
156	SAUSA300_2256	NE1190	putative N-acetylmuramoyl-L-alanine amidase	0.852164994	88	-1.43710499
157	SAUSA300_1326	NE471	putative cell wall enzyme EbsB	0.894353512	163	-1.073352488
158	SAUSA300_1036	NE507	RNA methyltransferase, TrmH family	0.926125386	107	-1.309031158
159	SAUSA300_2088	NE1746	S-ribosylhomocysteinase (luxS)	0.953832916	9	-3.98800717
160	SAUSA300_0769	NE1743	hypothetical protein	0.96366578	29	-2.164078435
161	SAUSA300_0144	NE1252	phosphonate ABC transporter ATP-binding protein (phnC)	0.979717026	42	-1.958249425
162	SAUSA300_0730	NE962	GGDEF domain-containing protein	0.986550929	62	-1.675912984
163	SAUSA300_1638	NE618	sensory box histidine kinase PhoR	0.98727524	134	-1.175157383
164	SAUSA300_2526	NE978	dihydroorotate dehydrogenase (pyrD)	1.004106121	40	-1.983963598
165	SAUSA300_2259	NE415	putative transcriptional regulator	1.00698195	164	-1.072616491
166	SAUSA300_2603	NE338	triacylglycerol lipase precursor (lip)	1.032494759	92	-1.425976914
167	SAUSA300_2061	NE1889	F0F1 ATP synthase subunit delta (atpH)	1.149349519	27	-2.209514333
168	SAUSA300_0683	NE1412	transcriptional regulator, DeoR family	1.160503648	59	-1.699437951
169	SAUSA300_0310	NE1254	perfringolysin O regulator protein (pfoR)	1.204322071	130	-1.202328628
170	SAUSA300_2637	NE1164	hypothetical protein	1.246002228	3	-5.105313012
171	SAUSA300_2368	NE1772	hypothetical protein	1.271523562	32	-2.131497583
172	SAUSA300_0221	NE1863	pyruvate formate-lyase activating enzyme (pflA)	1.300120208	176	-1.04262899
173	SAUSA300_0511	NE1176	DNA repair protein RadA	1.372573614	8	-4.090874684
174	SAUSA300_2517	NE1748	amidohydrolase family protein	1.394371785	11	-3.582892927
175	SAUSA300_0540	NE1762	HAD family hydrolase	1.444303564	19	-2.648539953
176	SAUSA300_1033	NE1172	iron/heme permease	1.480416185	5	-4.536251557
177	SAUSA300_1594	NE995	preprotein translocase subunit YajC	1.559864557	170	-1.058746693
178	SAUSA300_1680	NE1696	acetoin utilisation protein AcuA	1.643498758	83	-1.477125752
179	SAUSA300_1363	NE965	NAD(P)H-dependent glycerol-3-phosphate dehydrogenase (gpsA)	1.698970332	41	-1.979198271
180	SAUSA300_2129	NE993	putative hemolysin III	1.72158756	118	-1.263559013

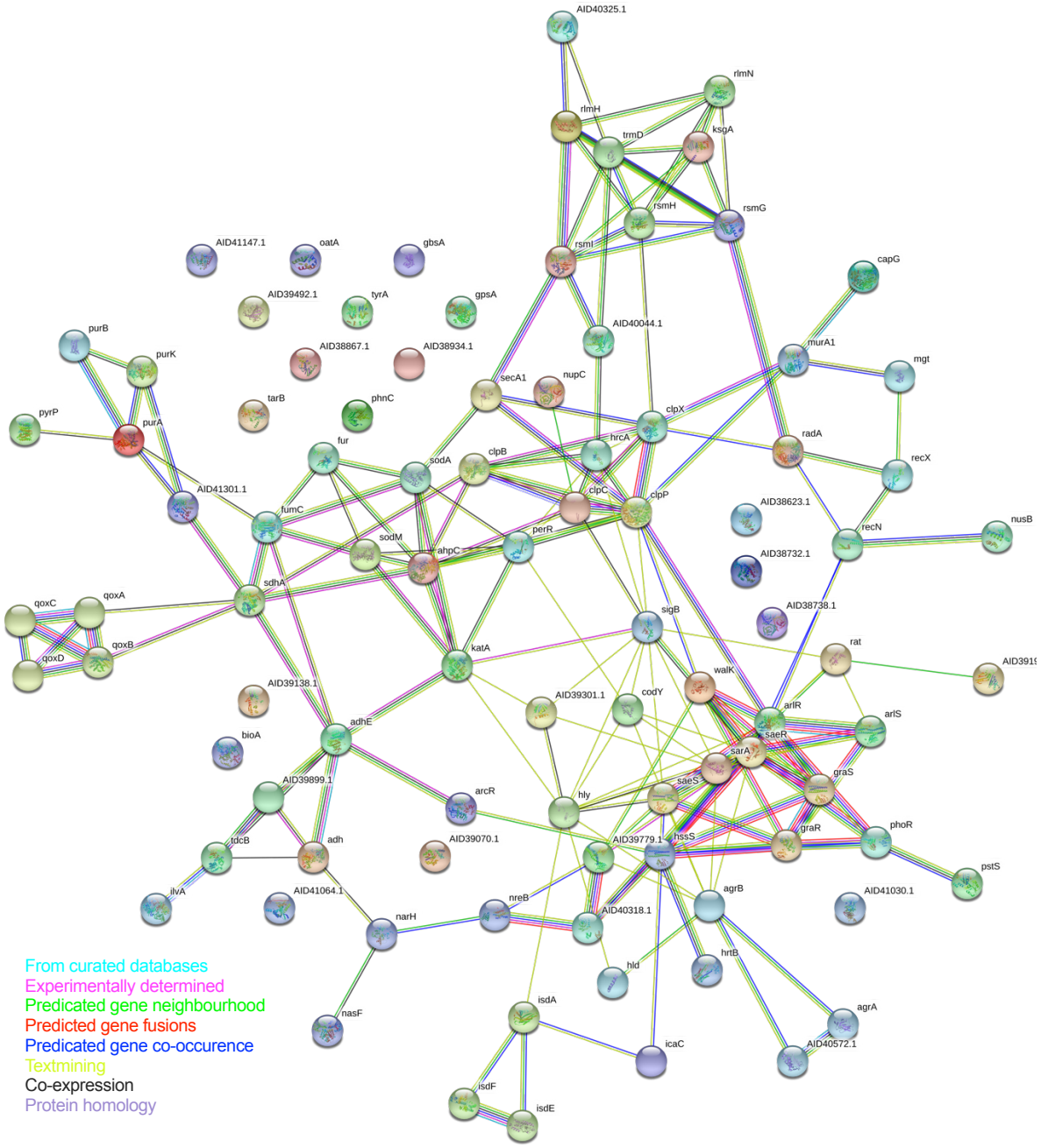

Figure 5.24 Analysis of *S. aureus* protein interaction pathways using STRING.

The 180 genes identified as hits from the primary screen were assessed using STRING to identify evidence for protein interaction. The associated proteins are connected by coloured lines, with the source of the data represented by the respective colour. Protein interaction maps made using STRING v11.0.

5.7 Transduction of selected mutations into wild-type *S. aureus* background

The final stage of assessing the NTML required the creation of a final "hit list" of genes maximally associated with the subversion of phagosomal acidification. The pathways visualised following STRING analysis supported the hypothesis that genes associated with oxidative stress were important to this process, but also indicated a role for the terminal oxidase groups and electron transport.

To validate that the phenotype of the NTML mutant was attributable to the transposon insertion and not a consequence of an unrelated secondary mutation, gene transduction was performed. The methods used for transduction are described in section 2.2.4. The aim was to transduce the strains with the greatest association with intracellular acidification into the existing genomic background, the USA300 JE2 wild-type strain, and the laboratory strain SH1000 that had been used in the development of the screen.

Within the Foster group bacteria library, several of these genes had already undergone successful gene transduction that had been confirmed by PCR. Of the twenty mutants with the greatest z-score from secondary assessment, 10 had previously been transduced into the required backgrounds. Given time limitations, transduction was attempted in the remaining 10 NTML top ranked mutants. Additionally, selected mutants based upon pathways identified from STRING analysis, specifically genes associated with two-component regulatory systems, oxidative stress response and terminal oxidase pathways. Thus, a total of 15 gene transductions were performed into the USA300 and SH1000 backgrounds. Despite repeated attempts, transduction of two transposon inserts failed into either background (USA300_0994 (pdhB) and USA300_1308 (arlR)).

5.8 Confirmation of successful transduction

Based upon the *S. aureus* USA300 FPR3757 whole genomic DNA sequence, PCR primer sequences were selected approximately 400 base pairs (bp) upstream and downstream of the desired transposon insertion sites. For each NTML mutant, these precise transposon insertion sites are detailed within the NTML database. The primer sequences used are detailed in table 2.4.

Transductant colonies were subjected to PCR amplification, the methods of which are detailed in section 2.3.2. If the transposon has been inserted correctly, the PCR amplification products would generate comprising the full transposon of approximately 4,000 bp. If the transduction had failed, the PCR amplification product would generate a smaller fragment of approximately 800 bp. The PCR amplification products were examined by gel electrophoresis, the methods

for which are detailed in section 2.3.3. Three transductant colonies from each background were assessed by PCR in duplicate (data not shown) to confirm successful transduction before proceeding to representative imaging detail below.

Figure 5.25 displays representative images of successful transduction of the USA300_0961 (quinol oxidase, subunit III (NE1542, qoxC)) and USA300_1232 (catalase, NE1366, katA) into the USA300 and SH1000 backgrounds. Appendix figure 7.1 displays representative images of all transductant strains generated during this study. The results showed that 10 of the 15 NTML mutant strains were successfully transduced the into both the USA300 and SH1000 backgrounds. The USA300_0188 (branched-chain amino acid chain transport system II carrier protein, brnQ) and USA300_1974 (leucocidin/haemolysin toxin family protein) transposon inserts were only successful into the USA300 background. The PCR verified mutant colonies were stored as bead stocks at -80°C for future study.

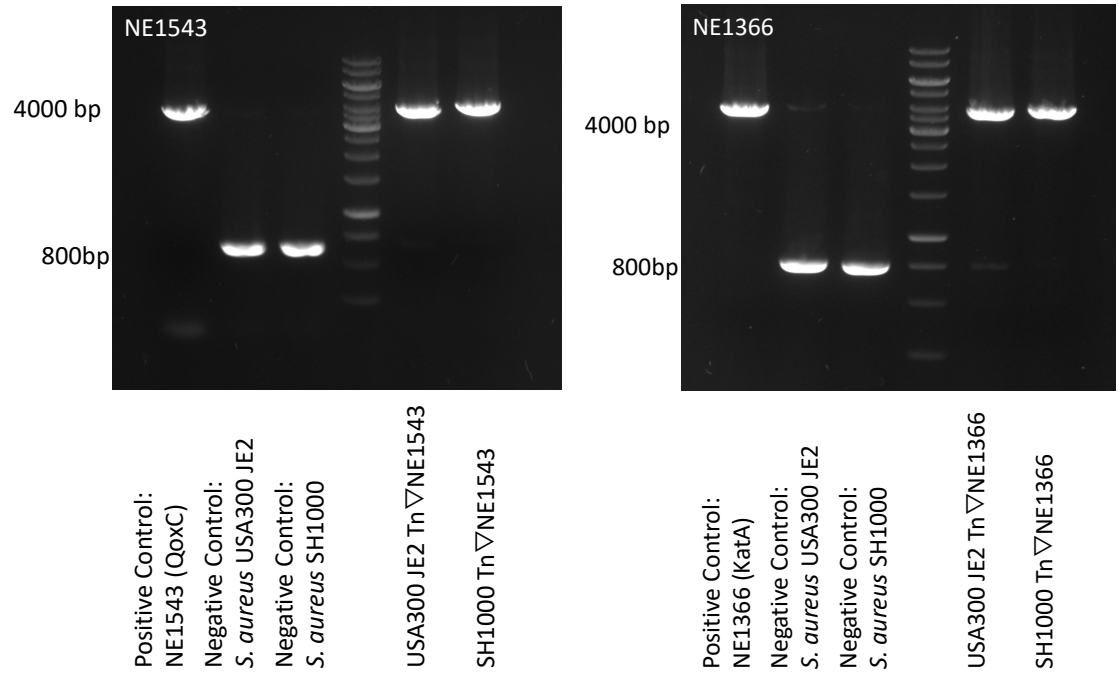

Figure 5.25 Confirmation of genetic transduction.

Representative images of successful transduction of the USA300_0961 (quinol oxidase, subunit III (NE1542, qoxC)) and USA300_1232 (catalase, NE1366, katA) into the USA300 and SH1000 backgrounds. PCR products of 400 bp upstream and 400 bp downstream of the NTML transposon insertion site of each gene were assessed by 1% (w/v) agarose gel electrophoresis. Correctly transduced strains would generate a full transposon product at approximately 4,000 bp, demonstrated by the original NTML mutant (positive control). Strains without the inserted transposon would generate a product at approximately 800 bp, demonstrated by wild-type strains (negative controls). Additional representative images for all successful transduction experiments presented in appendix figure 7.1

5.9 Assessment of intracellular acidification of validated transductant *S. aureus* mutants

The assessment of intracellular acidification of the PCR-validated transductants was conducted using the high-throughput screening method detailed previously. Two original 96-well libraries were created, detailed in Figure 5.26, containing the original NTML mutant strain in addition to the transduced mutants strains in the USA300 JE2 and SH1000 backgrounds.

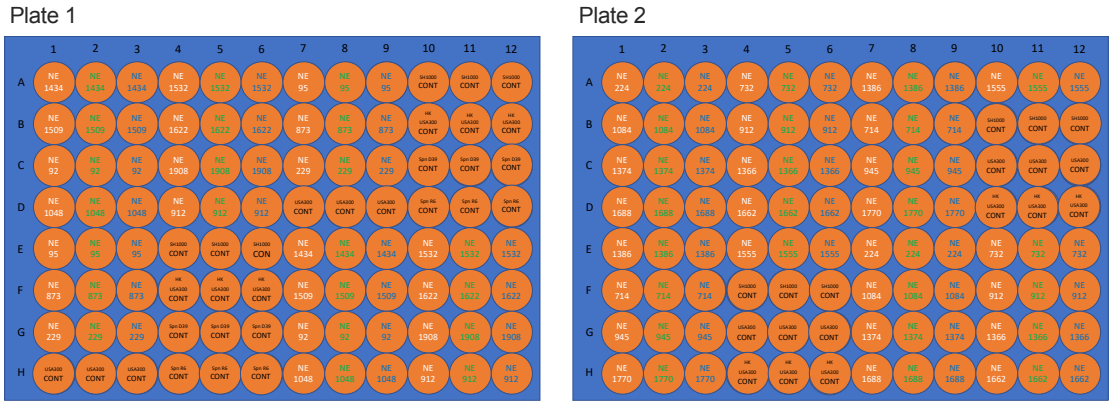

Figure 5.26 Validation assay plate layout.

Assay plates contained total of 24 NTML mutant strains (white) with respective transductants in USA300 JE2 background (green) and SH1000 background (blue). Wild-type USA300 JE2 strain and wild-type SH1000 strain acted as negative controls. Heat-killed USA300 JE2 strain and encapsulated serotype 2 *S. pneumoniae* strain D39 and unencapsulated *S. pneumoniae* strain R6 acted as positive controls

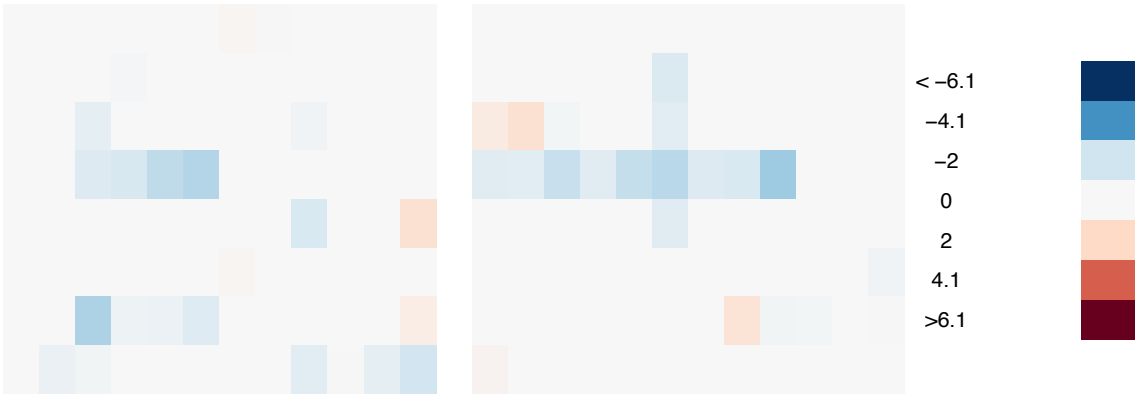

Figure 5.27 Validation assay representative heat map.

High-throughput microscopy performed using ImageXpress Micro high-content fluorescent microscopy and raw data extracted from images using MetaXpress 3.1 software. Raw data processed using cellHTS2 R/Bioconductor analysis package to generate z-score. Mean z-scores represented by coloured heat map, n=7.

5.9.1 Controls

The parental USA300 JE2 and SH1000 strains were included as negative controls to allow comparison with the transductant mutants derived from these strains. As previously demonstrated, and evident within this assay (Figures 5.28), a minority of these bacteria progress to an acidified environment. Post assessment analysis identified that the heat-killed USA300 JE2 strain had not been completely inactivated, as colonies were present on overnight growth plates. Consequently, the heat-killed bacteria were excluded from further analysis.

Unencapsulated laboratory *Streptococcus pneumonia* strain R6 and an unencapsulated serotype 2 strain D39 were also included as positive controls in this assay. The aim was to demonstrate that this assay could identify that the majority of intracellular *S. pneumoniae* bacteria, as had been previously demonstrated using low-throughput methods (Jubrail et al. 2016). Given difficulties experienced in labelling the encapsulated strain D39 within the format of a 96-well plate, I elected to use the mutant unencapsulated strain alongside the strain R6. Both strains demonstrated that the majority of intracellular bacteria progressed to an acidified intracellular environment, and thus act as a positive control for this assay.

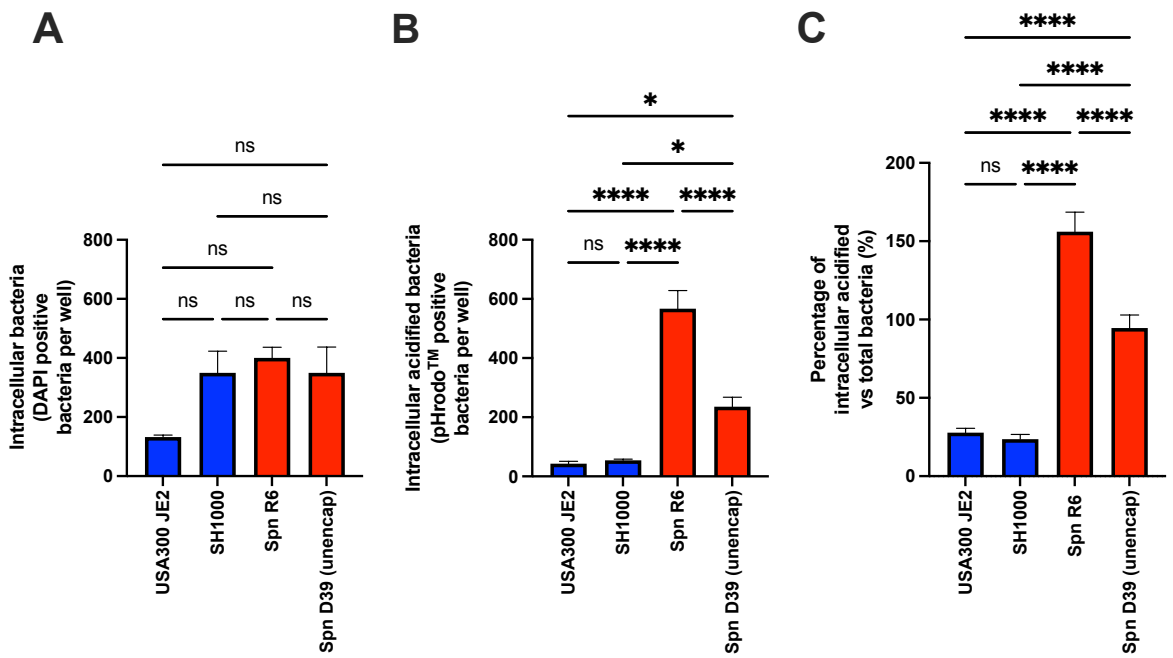

Figure 5.28 Validation assay summary of controls.

Differentiated monocyte-derived macrophages were challenged with either pHrodo^{TM}-labelled *S. aureus* strains USA300 JE2 or SH1000 at a MOI of 5 bacteria per macrophage, or *S. pneumoniae* strains R6 or unencapsulated D39 at a MOI of 10 bacteria per macrophage, for a period of 4 hours within 96-well format. Images acquired using ImageXpress^{MICRO} high-throughput microscope. (**A**) Plot of intracellular DAPI^{+} bacteria per well by condition. Data represent 7 experiments, performed in 6 replicates, line at mean with standard error of the mean (SEM). (**B**) Plot of intracellular pHrodo^{+} bacteria per well by condition per well by condition. Data represent 7 experiments, performed in 6 replicates, line at mean with SEM. (**C**) Scatter plot of percentage of intracellular acidified bacteria versus total intracellular bacteria per well. Data represent 7 experiments, performed in 6 replicates, line at mean with SEM. Statistical significance between groups determined using ordinary one-way ANOVA with Tukey's multiple comparisons test, ns (not significant), *p<0.05, ****p<0.0001.

5.9.2 NTML mutants

The priority of the validation screen was to confirm phenotypic behaviour of the genes obtained from the secondary screen “hit” list. The validation screen also generated opportunity for further scoring of the respective NTML mutants under this assessment. The raw data obtained following high-throughput microscopy and the MetaXpress 3.1 software were analysed using the cellHTS2 R/Bioconductor analysis package to generate a z-score pertaining to intracellular bacterial acidification. The results from this analysis are demonstrated in Figure 5.29.

In comparison with the secondary NTML screen scores (Figure 5.23), there is consistency in scores with several NTML mutant strains. For example, the top two hits from the secondary screen both appear in the top 10 hits of the validation screen. The *saeR* disrupted NTML mutant strain, which failed to obtain a score deemed significant in the secondary screen, was found to have a score of -1.90 during the validation assay. There were several NTML mutants however that failed to demonstrate a similar pattern of acidification that had been observed previously, for example *tagB and* NE1509.

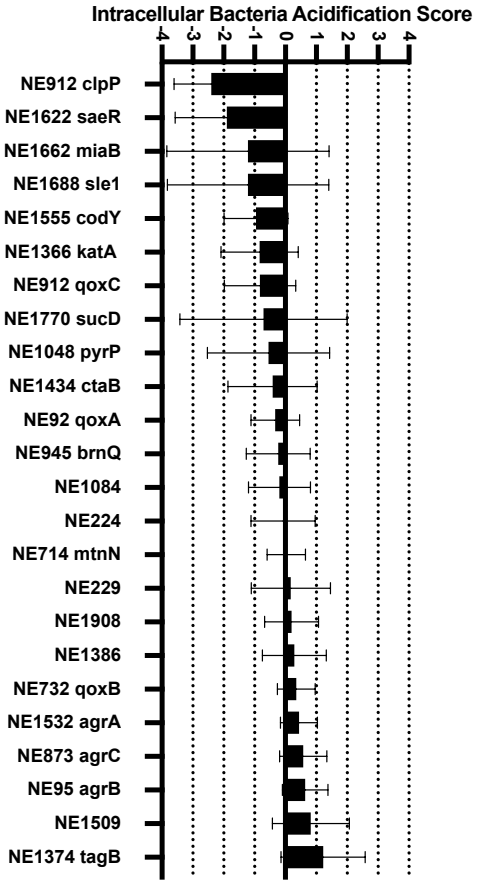

Figure 5.29 *S. aureus* NTML mutant validation screen z-scores

Summary z-scores obtained for respective NTML mutants post analysis of raw data using cellHTS2 R/Bioconductor package. Mean score with standard deviation, n=7.

5.9.3 Validation of NTML mutant phenotype.

As previously detailed, validating that the phenotype of the respective NTML mutant strain was attributable to the transposon-disrupted gene required creation of transductant mutant strains of the *S. aureus* USA300 JE2 and SH1000 background. Having either successfully created these transductants, or utilised those previously created, their phenotypic behaviour was assessed.

The percentage of intracellular acidified bacteria to total intracellular bacteria was calculated using raw data values obtained from high-throughput microscopy. The results are demonstrated within Figure 5.30. These figures directly compare the original NTML mutant with the transductant mutants, and the wild-type *S. aureus* background negative control.

The first observation is that the secondary screen "hits" with a score < -3 (NE1543 (*qoxC*), NE912 (*clpP*), NE714 (*mtnN*) and NE1532 (*agrA*)) all demonstrated an equivalent phenotype of intracellular acidification. Additionally, specific genes which have previously been associated within subversion of intracellular acidification within the candidate approach (e.g., *katA*, *agrB* and *saeR*) also demonstrated an equivalent phenotype in the transductant strains. Nine NTML mutant strains failed to obtain a statistically significant difference between the parental USA300 strain JE2 negative control during assessment: NE224, NE732 (*qoxB*), NE1374 (*tagB*), NE1386, NE1555 (*codY*), NE1509, NE1662 (*miaB*), NE1688 (*sle1*) and NE1770 (*sucD*). Although a number of these mutants (e.g., NE1662 (*miaB*) and NE1688 (*sle1*)) obtained a mean score of < -1 during the validation assay, the large standard deviation of scores accounts for failure to attain statistical significance.

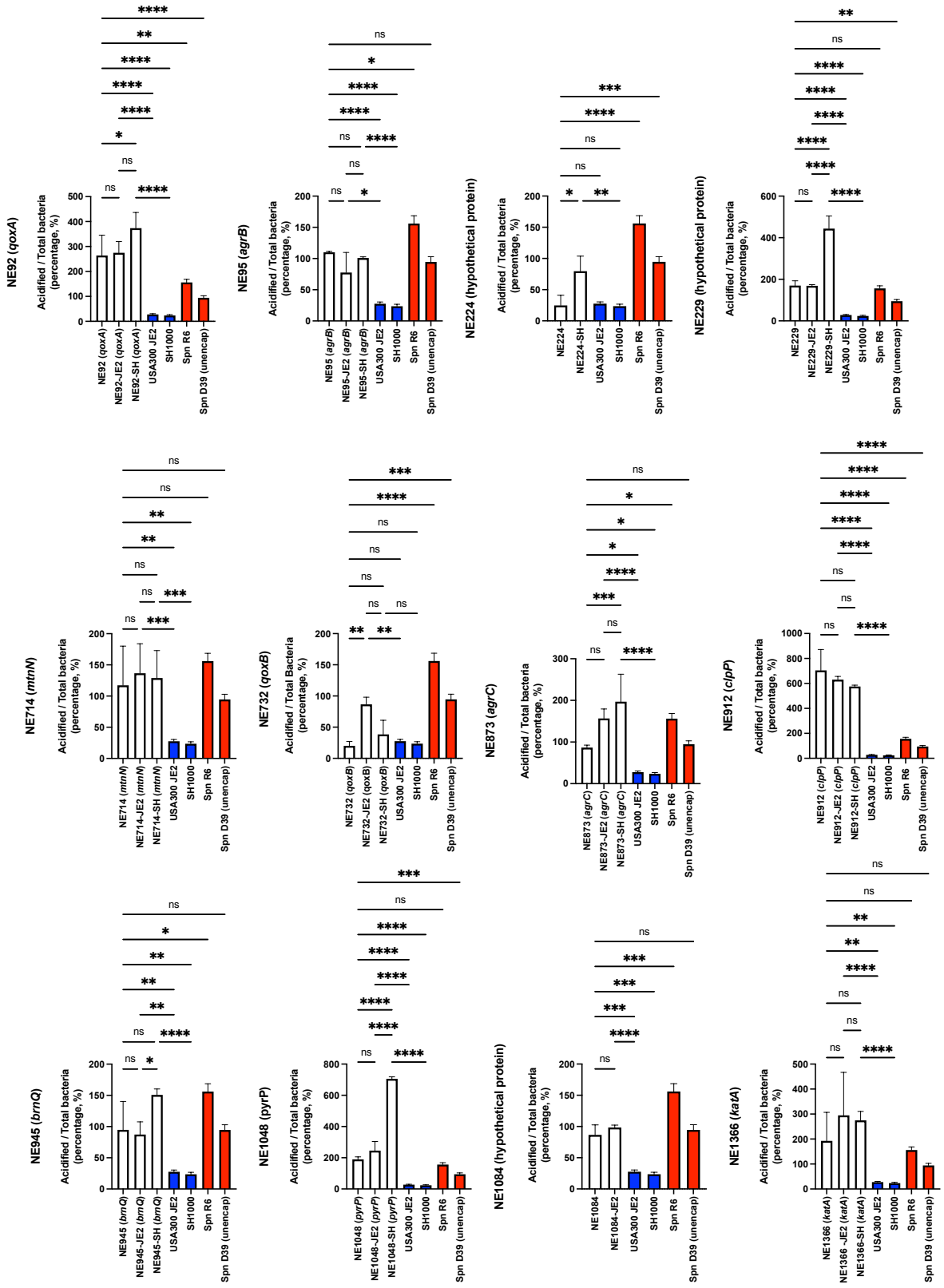
NE92 (qoxA)
Acidified / Total bacteria (percentage, %)
NE92 (qoxA)
NE92-JE2 (qoxA)
NE92-SH (qoxA)
USA300 JE2
SH1000
Spn R6
Spn D39 (unencap)
NE95 (agrB)
Acidified / Total bacteria (percentage, %)
NE95 (agrB)
NE95-JE2 (agrB)
NE95-SH (agrB)
USA300 JE2
SH1000
Spn R6
Spn D39 (unencap)
NE224 (hypothetical protein)
Acidified / Total bacteria (percentage, %)
NE224
NE224-SH
USA300 JE2
SH1000
Spn R6
Spn D39 (unencap)
NE229 (hypothetical protein)
Acidified / Total bacteria (percentage, %)
NE229
NE229-JE2
NE229-SH
USA300 JE2
SH1000
Spn R6
Spn D39 (unencap)
NE714 (mtnN)
Acidified / Total bacteria (percentage, %)
NE714 (mtnN)
NE714-JE2 (mtnN)
NE714-SH (mtnN)
USA300 JE2
SH1000
Spn R6
Spn D39 (unencap)
NE732 (qoxB)
Acidified / Total Bacteria (percentage, %)
NE732 (qoxB)
NE732-JE2 (qoxB)
NE732-SH (qoxB)
USA300 JE2
SH1000
Spn R6
Spn D39 (unencap)
NE873 (agrC)
Acidified / Total bacteria (percentage, %)
NE873 (agrC)
NE873-JE2 (agrC)
NE873-SH (agrC)
USA300 JE2
SH1000
Spn R6
Spn D39 (unencap)
NE912 (clpP)
Acidified / Total bacteria (percentage, %)
NE912 (clpP)
NE912-JE2 (clpP)
NE912-SH (clpP)
USA300 JE2
SH1000
Spn R6
Spn D39 (unencap)
NE945 (brnQ)
Acidified / Total bacteria (percentage, %)
NE945 (brnQ)
NE945-JE2 (brnQ)
NE945-SH (brnQ)
USA300 JE2
SH1000
Spn R6
Spn D39 (unencap)
NE1048 (pyrP)
Acidified / Total bacteria (percentage, %)
NE1048 (pyrP)
NE1048-JE2 (pyrP)
NE1048-SH (pyrP)
USA300 JE2
SH1000
Spn R6
Spn D39 (unencap)
NE1084 (hypothetical protein)
Acidified / Total bacteria (percentage, %)
NE1084
NE1084-JE2
USA300 JE2
SH1000
Spn R6
Spn D39 (unencap)
NE1366 (katA)
Acidified / Total bacteria (percentage, %)
NE1366 (katA)
NE1366-JE2 (katA)
NE1366-SH (katA)
USA300 JE2
SH1000
Spn R6
Spn D39 (unencap)

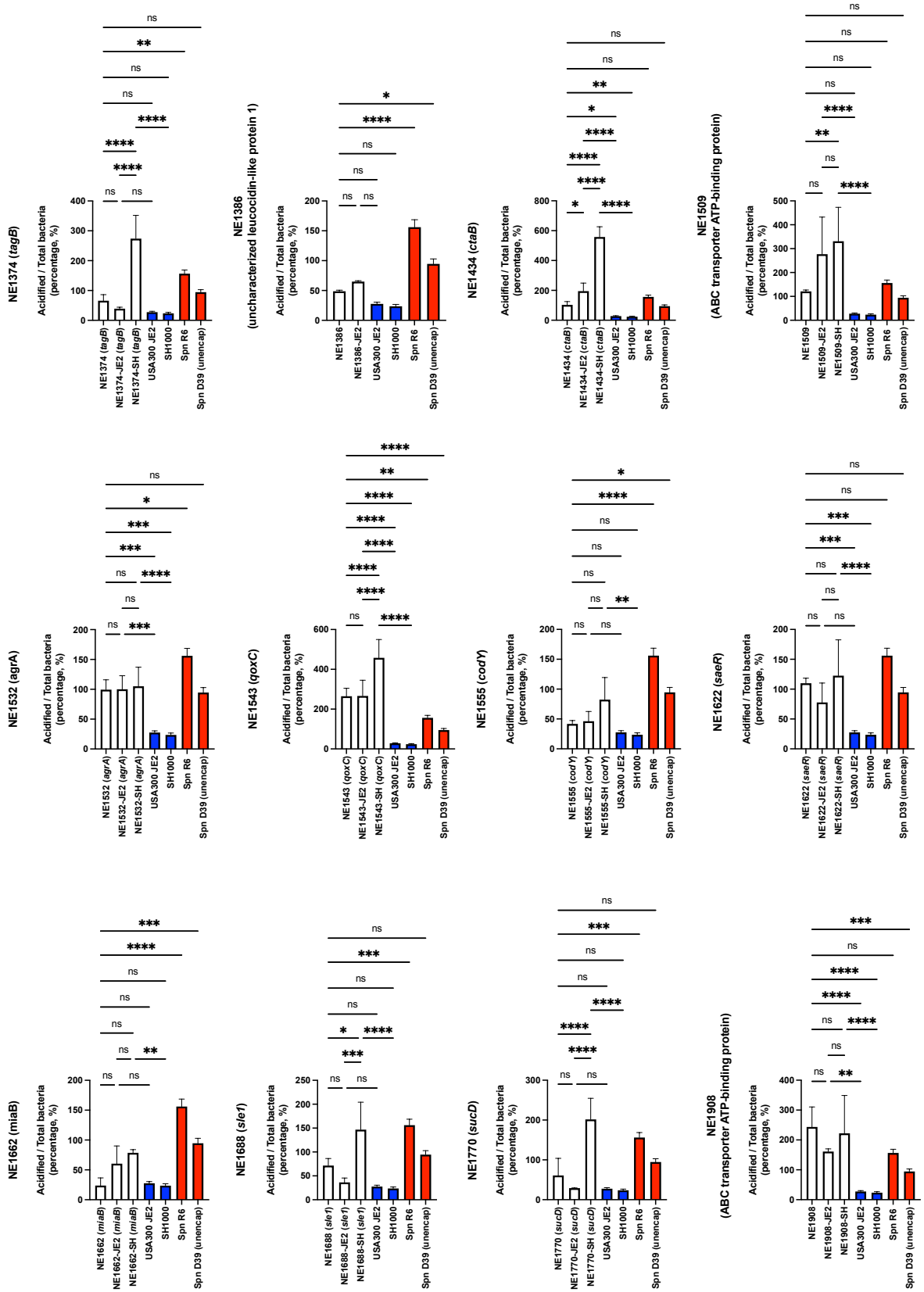
NE1374 (tagB)
Acidified / Total bacteria (percentage, %)
NE1374 (tagB)
NE1374-JE2 (tagB)
NE1374-SH (tagB)
USA300 JE2
SH1000
Spn R6
Spn D39 (unencap)
NE1386 (uncharacterized leucocidin-like protein 1)
NE1386
NE1386-JE2
NE1434 (ctaB)
NE1434 (ctaB)
NE1434-JE2 (ctaB)
NE1434-SH (ctaB)
NE1509 (ABC transporter ATP-binding protein)
NE1509
NE1509-JE2
NE1509-SH
NE1532 (agrA)
NE1532 (agrA)
NE1532-JE2 (agrA)
NE1532-SH (agrA)
NE1543 (qoxC)
NE1543 (qoxC)
NE1543-JE2 (qoxC)
NE1543-SH (qoxC)
NE1555 (codY)
NE1555 (codY)
NE1555-JE2 (codY)
NE1555-SH (codY)
NE1622 (saeR)
NE1622 (saeR)
NE1622-JE2 (saeR)
NE1622-SH (saeR)
NE1662 (miaB)
NE1662 (miaB)
NE1662-JE2 (miaB)
NE1662-SH (miaB)
NE1688 (sle1)
NE1688 (sle1)
NE1688-JE2 (sle1)
NE1688-SH (sle1)
NE1770 (sucD)
NE1770 (sucD)
NE1770-JE2 (sucD)
NE1770-SH (sucD)
NE1908 (ABC transporter ATP-binding protein)
NE1908
NE1908-JE2
NE1908-SH
USA300 JE2
SH1000
Spn R6
Spn D39 (unencap)

Figure 5.30 Comparison of intracellular acidification of NTML mutant strain against transductant wild-type *S. aureus* mutants.

Differentiated MDMs were challenged with the respective pHrodo™-labelled NTML mutant strain, or corresponding Tn-disrupted USA300 JE2 mutant or Tn-disrupted SH1000 mutant, MOI = 5, for 4 hours, with subsequent lysostaphin application, fixation and counterstaining with CellMask and DAPI. High-throughput microscopy performed using ImageXpress Micro high-content fluorescent microscopy and raw data extracted from images using MetaXpress 3.1 software. Wild-type *S. aureus* strains USA300 JE2 and SH1000 represent negative controls. Unencapsulated *S. pneumoniae* strains R6 and D39 used as positive controls. The data represent the mean with standard error of the mean (SEM); n=7, statistics by ordinary one-way ANOVA with Tukey's multiple comparisons test of mean percentage of intracellular / total bacteria ratio; ns not significant, *p<0.05, **p<0.01, ***p<0.001, ****p<0.0001.

5.10 Conclusions

The screening of a genome-wide *S. aureus* library of 1,920 transposon-mutant strains identified several genes associated with the subversion of intracellular bacterial acidification. Starting with 1,920 genes, the primary screen identified 180 mutant strains that underwent confirmatory screening. 24 single gene mutants were progressed to the final screening. A final 15 single gene mutants were validated by demonstrating failure to subvert intracellular acidification within the NTML stain and their respective transductant strains. At this juncture, it cannot be assumed that failure to subvert acidification corresponds to bacterial killing, this will require further investigation.

Regarding technical considerations, high-throughput microscopy has facilitated the screening of a complete bacterial genome within a relative short period. Although a few candidate genes were identified ahead of the screen using low throughput methods, the screen has identified less well characterised genes and pathways. This specific approach could be applied to the investigation of other bacteria associated with intracellular persistence to identify homologous pathways and genes to inform future work.

The screen utilised monocyte-derived macrophages rather than the monocytic THP-1 cell-line. Whereas THP-1 cells had been used successful in earlier experimental work, later attempts to differentiate this cell-line to a differentiated macrophage phenotype consistently failed. The screen subsequently utilised MDMs sourced from multiple different donors. Screen outcomes must be considered in the context of potential variable antimicrobial activity between donors. Person-person variation in MDM phagosome acidification in response to non-immunogenic and pathogenic stimuli is recognised (Tram et al. 2020). This does not mean that the observations and conclusions from the screen are invalid but may account for greater variation in phenotypic outcomes.

Over the course of the primary, secondary, and final validation screens multiple NTML mutants were consistently associated with intracellular acidification. Potential variation in MDM antimicrobial activity and phagosomal acidification may have contributed to a lower screen score, particularly during the primary screen where each NTML mutant was subjected to three different sourced donors. As demonstrated in the figures 5.3-5.5, there are variable numbers of $DAPI^{+}$ and $pHrodo^{+}$ bacteria between plates and between replicates. This could be attributable to variation in MDM antimicrobial activity, but could also be attributable to technical variation during assay set-up. The effect of donor variation in the secondary and validation screening processes would have been diminished due to increased replicate donor number. Due to limitations in time, donor numbers and hardware faults within the Sheffield RNAi

Screening Facility, the use of 3 replicate donors per NTML plate was deemed an acceptable compromise for the purpose of creating the initial “hit list”.

As within the limited candidate screen of chapter 4, virulence gene regulators feature in the list of genes associated with the intracellular acidification phenotype. Three genes of the Agr complex were identified within the primary “hit list” and secondary confirmation screen (NE1532 *agrA*, NE 873 *agrC* and NE95 *agrB*). The phenotypic pattern was subsequently validated in transductant mutants. The Agr global regulatory complex has been previously demonstrated to be essential to intracellular persistence within a macrophage model (Kubica et al. 2008) and other cell lines (Wesson et al. 1998; Qazi et al. 2001). Understanding how the Agr complex subverts the host response however is challenging given that there are at least 100 genes differentially regulated (Dunman et al. 2001).

As discussed previously, toxins are linked with escape of *S. aureus* from the phagolysosome into the intracellular environment (Grosz et al. 2013; Surewaard et al. 2013). The Agr complex is known to regulate expression of PSMs and leucotoxins (Queck et al. 2008; Wang et al. 2007; Dunman et al. 2001). Therefore, it has been frequently proposed that intracellular survival of *S. aureus* is attributed to toxin production. However, both this study and associated work (Jubrail et al. 2016) and work of other groups demonstrate the persistence of *S. aureus* within a phagosomal environment for sustained periods of time (Kubica et al. 2008). Kubica *et al*. proposed that α-toxin (*hla*) expression is subject to differential regulation in an intracellular macrophage environment. Within the NTML screen there was little indication that leukotoxins contribute to subverting phagosomal acidification within the 4-hour infection period observed. Following the primary screen, the NTML mutants NE1386 (leucocidin/haemolysin toxin family protein, Z-score -1.57), NE993 (putative haemolysin III, Z-score -1.26) and NE1682 (γ-haemolysin component B, *hlgB*, Z-score -1.21) were identified. Progressing to the secondary screen, only NE1386 (Z-score -1.13) progressed to the validation assay, where both NE1386 and the transductant strains failed to demonstrate greater intracellular acidification compared to the parental strain negative controls. Given the assay utilised a 4-hour bacterial challenge, upregulation and expression of leucocidins and other toxins may have not been significant or not with any phenotypic effect. This may explain the persistence of bacteria within a phagosomal location for sustained periods of time before escape into the cytoplasm at time point beyond 16h, as demonstrated in chapter 3.

Beyond leucotoxins, the Agr complex has been associated with differential expression of multiple pathways, such as nucleic acid metabolism, transcriptional regulation, amino acid

metabolism and ABC-type transport systems (Dunman et al. 2001). Such pathways have also been identified within this screen, for example NE1048 (uracil permease, pyrP, secondary screen Z-score -1.29), NE714 (5'-methylthioadenosine/S-adenosylhomocysteine nucleosidase, mtnN, secondary screen Z-score -3.09), NE945 (branched chain amino acid transport system II carrier protein, brnQ, secondary screen Z-score -1.21) and NE1509 (ABC transporter ATP-binding protein, secondary screen Z-score -1.24). A potential explanation for the significance of these genes can be hypothesised by the finding that the common skin commensal bacteria *Staphylococcus lugdunensis* resists macrophage killing for an extended period within an intraphagolysosomal environment (Flannagan et al. 2018). Although pathogenic, this bacteria is not known to have multiple virulence factors (Heilbronner et al. 2011). *S. lugdunensis* did not replicate within the phagolysosome environment, potentially under restriction by the host macrophage, but remained viable with the potential to act as a bacterial reservoir. Flannagan *et al*. speculate that persistence may be attributable to nutrient acquisition.

The NE912 strain (ATP-dependent Clp protease proteolytic subunit, clpP) obtained the top rank within the secondary screen (score -3.40; primary screen -1.62). The caseinolytic protease proteolytic subunit (ClpP) forms a proteolytic complex with Clp ATPases that facilitates removal of altered proteins when under environmental stress (Frees et al. 2003; Frees et al. 2004).

The caseinolytic protease (Clp) ATPases, and associated heat-shock protein 100 family, are necessary for stress tolerance and intracellular replication (Frees et al. 2004). Members of this family of proteins are capable of associating with the unrelated Clp proteolytic subunit (ClpP) to form a Clp proteolytic complex, with similarities to the eukaryotic 26S proteasome, that facilitates removal of altered proteins when under environmental stress (Kessel et al. 1995; Frees et al. 2003; Frees et al. 2004). The ClpP protease has also been associated with the formation of a *S. aureus* "persister" phenotype (Conlon et al. 2013). A persister phenotype describes a non-growing, antimicrobial tolerant subset of a regular population, which can revert back to the regular phenotype (Bigger 1944; Conlon 2014). The persister state is induced in response to environmental stress or altered nutrient resources, with reduction in protein synthesis, cell division and DNA replication (Amato et al. 2013; Bigger 1944). Conlon *et al.* demonstrated that a *clpP* mutant fails to attain a persister state resulting in increased sensitivity to antimicrobial agents (Conlon et al. 2013).

Interrogation of a *clpP* mutant identified that expression of genes within the PerR, Fur and MntR regulons were affected (Michel et al. 2006). Within the same study, deletion of *clpP* was

associated with the repression of the Agr regulatory complex and ArlRS, for which the decreased expression of multiple virulence factors, including Hla, was attributed. Within the Foster group, a screen of the NTML assessing *in vitro* neutrophil lysis identified that *clpP* mutants were associated with attenuated lysis, and reduced virulence was demonstrated within a zebrafish model of infection (D. Yang et al. 2019). This observation is indicative of resistance to killing by professional phagocytes. Similarities can be also drawn from other intracellular pathogens. Within macrophage challenge models with *Listeria* monocytogenes, ClpP is involved in the adaptive response to the intraphagosomal environment and essential for virulence when assessed in a murine model of infection (Gaillot et al. 2000). This has also been demonstrated with *Salmonella typhimurium* (Hensel et al. 1995). The internalisation of *Salmonella* by macrophages, with exposure to a nutritionally deplete acidified phagosome, induces a persister state (Helaine et al. 2014). Given this precedent, the results of the screen strongly indicate a role of *clpP* in responding to environmental stress of pH.

When compared to the low throughput candidate screen, described in chapter 4, the *saeR* gene, which encodes the response regulator component of the SaeRS two-component regulator, failed to obtain a significant score within the secondary screen. Nonetheless, the *saeR* NTML mutant strain was included in the validation screen based upon identified pathway in STRING analysis and preceding candidate gene assessment. This was justified by the subsequent performance of the NE1622 mutant strain and transductants in the validation assay. The importance of the SaeRS two-component system regarding virulence has been established repeatedly. Within the DeLeo group, a microarray analysis of *S. aureus* genes identified that in response to neutrophil phagocytosis, expression of *sae* genes were upregulated (Voyich et al. 2005). Subsequent work has demonstrated that the SaeRS complex is associated with the suppression of the pro-inflammatory cytokine TNF-α from infected monocytes (Sward et al. 2017).

It should also be noted that although the *sarA* NTML mutant obtained a primary screen Z-score of -3.22, and therefore the probability that the ratio of bacterial acidification versus total bacterial number occurred by chance is less than 0.3%, this mutant obtained a secondary screen Z-score of +0.15. Within the candidate screen the SH1000 *sarA* mutant strain was not found to progress to an acidified environment. There is also precedent that within a macrophage model SarA is not required for intracellular persistence (Kubica et al. 2008).

Finally, the NTML screen has indicated that the terminal oxidases of *S. aureus* participate in the subversion of phagosomal maturation and merit extended investigation. Terminal oxidases constitute the final complexes of the respiratory chain (also referred to as the electron transport

chain). Electrons, obtained from the separation of hydrogen atoms into protons and electrons, are transferred between membrane-bound electron donor and electron acceptor complexes via enzymatic action, with the concurrent efflux of protons. Ultimately, the electrons are accepted by oxygen molecules and form water ($2H_2 + O_2 \rightarrow 2H_2O$). The resultant proton gradient facilitates the generation of adenosine triphosphate (ATP) via ATPase (Mitchell 1961). In the absence of oxygen, electrons are transferred to alternative electron acceptors. Bacterial respiratory chains are composed of a combination of flavoproteins, iron-sulfur proteins, quinones and cytochromes, and are typically branched conferring adaptability to varying environmental conditions (Thöny-Meyer 1997). The oxidative branches encompass cytochrome-rich redox systems that oxidase quinol, cytochrome *c* and the terminal oxidoreductases that reduce O_2.

S. aureus is only known to feature one isoprenoid quinone, menaquinone (vitamin K_2), that facilitates the transfer of electrons between donor and acceptor complexes (White & Frerman 1967). One terminal oxidase of *S. aureus*, termed cytochrome aa_3, has been identified as the Qox system, encompassing a menaquinol oxidase (quinol oxidase, *qoxABCD*) and cytochrome *a* (Götz et al. 2006). A complementary second terminal oxidase is encoded by the *cydAB* locus and featuring a cytochrome *bd*-type menaquinol oxidase (Hammer et al. 2013).

Within this study, the qoxABCD complex featured prominently within both the primary and secondary screen rankings. NE1543 (quinol oxidase subunit III, *qoxC*) ranked 14 in the primary screen (Z-score -3.10) and ranked 2 in the secondary screen (Z-score -3.30). Other subunits from the complex, NE92 (quinol oxidase subunit II, *qoxA*) obtained a secondary screen rank of 6 (Z-score -2.53) and NE732 (quinol oxidase subunit I, *qoxB*) obtained a secondary screen rank of 47 (Z-score -0.41) having also obtained a primary screen rank of 23 (Z-score -2.33). Both the *qoxA* and *qoxC* NTML mutants were validated phenotypically with the transductant strains. Neither of the *cydAB* NTML mutants obtained a significant score in the primary screen, NE117 (*cydA*) scored -0.17 (rank 782) and NE1725 (*cydB*) scored +2.24 (rank 1801).

Both terminal oxidases contribute to growth and virulence during infection (Lan et al. 2010; Hammer et al. 2013). Curiously, within a murine model a differential pattern of infection was recognised within disruption of the respective loci; a *qoxB* mutant failed to cause significant infection in the liver and a *cydB* mutant was associated with reduced bacterial burden within the heart (Hammer et al. 2013). The Kubes laboratory has demonstrated *S. aureus* persistence within liver resident Kupffer cells (Surewaard et al. 2016); within a murine model, intravenous inoculation of *S. aureus* resulted in rapid sequestration within Kupffer cells. But

within this intracellular location, a population of *S. aureus* was demonstrated to resist microbicidal killing, and ultimately proliferate before causing host cell lysis and dissemination via the host circulation. Hypothetically, the *qox* mutant pattern of reduced hepatic infection could be related to the failure to subvert macrophage killing.

Cytochrome *bd* confers oxidative stress resistance via catalase-like activity in *E. coli* (Borisov et al. 2021). The role of cytochrome aa_3 in response to reactive oxygen species is less explored. Within *Rhodobacter sphaeroides* and *Paracoccus denitrificans*, cytochrome aa_3 can perform peroxidase and catalase activity (Bolshakov et al. 2010; Hilbers et al. 2013). The rate at which H_2O_2 is cleaved is tenfold greater than the equivalent mitochondrial cytochrome c oxidase. Bolashakov *et al*. proposed that the significant difference in catalase activity may be attributable to presence of manganese ions rather than magnesium ions within the bacterial enzyme, and not associated with the oxygen-reducing centre of the oxidase.

The cytochrome aa_3 menaquinol oxidase is a member of the heme-copper-oxygen reductase superfamily (Sousa et al. 2012), containing two heme molecules (Hammer et al. 2016). Heme is widely utilised within cells as a prosthetic group in various proteins with diverse functions, including respiration, biosynthesis, and environmental sensing (Wachenfeldt & Hederstedt 2002). Acquisition of heme, either by biosynthesis or obtained from host, is essential to bacterial pathogenesis (Choby & Skaar 2016). In the context of *S. aureus*, inhibiting the heme biosynthesis pathway by creation of a *hemA* mutant generated SCVs incapable of causing systemic infection in a murine model (Hammer et al. 2013). The SCVs associated with disrupted heme biosynthesis were slow growing, with decreased pigment and haemolysis activity, but were associated with intracellular persistence (Eiff et al. 1997). Beyond incorporation in cytochromes which will be discussed below, heme is integral to the oxidative stress response group of proteins, catalase, myeloperoxidase and flavohaemoglobin (Gaupp et al. 2012).

Although expected to feature two heme A molecules, disruption of the heme A biosynthesis pathway did not adversely affect QoxABCD oxidase function but was dependent upon the synthesis of heme O (Hammer et al. 2013; Hammer et al. 2016). The heme A molecule is synthesised from heme B via the enzymatic activity of CtaB (cytochrome assembly B), which converts heme A to O, and CtaA, which converts heme O to A (Svensson et al. 1993). Hammer *et al*. have also identified *ctaM*, a gene adjacent to *ctaB*, corresponding to the NTML hypothetical protein mutant NE1084 (Hammer et al. 2016). A functional QoxABCD complex is dependent upon the expression of the *ctaM* gene (Hammer et al. 2016).

Within this study, NE769 (cytochrome oxidase assembly protein, *ctaA*) ranked 955 in the primary screen (Z-score 0.00). It should however be noted that this mutant was located in well A01, plate 9, and had a wide range of scores of the three replicates (+3.23 – -2.24). Analysis of the raw values indicates that below average bacteria and above average macrophage numbers were identified. The NE1434 mutant (protoheme IX farnesyltransferase, *cyoE* or *ctaB*) obtained a secondary screen rank of 4 (Z-score -2.83) and NE1084 (*ctaM*) obtained a secondary screen rank of 19 (Z-score -1.10). Both of these mutant strains were subsequently validated with phenotypically matched transductants.

The cytochrome assembly (cta) complexes have been implicated as a virulence determinant. As within *qoxB* mutants, *ctaA* mutants demonstrated decreased survival *in vivo* despite enhanced carotenoid expression (Lan et al. 2010). Within a murine infection model, the bacterial load within the liver at 5 days was significant lower in the *qoxB* and *ctaA* mutants compared to the wild-type strain. These mutants have reduced haemolytic activity, but without significant change in *sarA* or *sigB* expression (Lan et al. 2010). A similar observation has been made with a *ctaB* mutant, which resulted in attenuated growth and virulence, but with enhanced pigment production and cells tolerant of intracellular stressors (T. Xu et al. 2016).

The role that cytochrome assembly genes and the cytochrome aa_3 genes *qoxABC* play in subverting phagosomal acidification merit further investigation. It is not apparent that this observed phenotype has an association with enhanced intracellular microbial killing. Prior investigation of respiratory chain mutants recognised that these genes are associated with development of SCVs. Additionally, disruption of *S. aureus* ATP levels has been demonstrated to generate a persister phenotype (Conlon et al. 2016). As discussed above, prior investigation of the *qoxB*, *ctaA* and *ctaB* mutants indicated that these genes are required for virulence, but also demonstrate tolerance of intracellular microbicidal environments. Hence future work would be directed towards identifying if the NTML mutant strains of interest demonstrate either a SCV or persister phenotype that is tolerant of low pH. *S. aureus* is generally considered to intolerant of low pH environments (pH 2), but adaptive tolerance has been demonstrated (P. F. Chan et al. 1998). As demonstrated within the Foster group, acid stress resistance developed following pre-exposure to an intermediate pH (pH 4), which was dependent upon alternative sigma factor B expression (P. F. Chan et al. 1998). It is not apparent if tolerance to acidic environments consequently facilitates intracellular persistence within professional phagocytes.

Having completed a genome-side *S. aureus* screen, a list of candidate genes has been derived that are associated with intracellular acidification within a differentiated macrophage.

It is not yet apparent how these genes are able to subvert acidification or potentially phagosomal maturation. It is possible that some of these single gene mutants are tolerant of an acidified environment. Nevertheless, the undertaking of a low-throughput screen of candidate mutants in assessment of macrophage killing will be informed by the results of this screen.

Chapter 6
Discussion

6.1 Summary of findings.

I have demonstrated that within human macrophages differentiated *in vitro* to a tissue macrophage phenotype, the *S. aureus* USA300 strain JE2 subverts phagosomal maturation in keeping with other *S. aureus* strains (Jubrail et al. 2016). The reduced phagosomal acidification in the context of *S. aureus* infection is specific to the proinflammatory macrophage phenotype that respond to bacterial infection within host tissues.

A high-throughput genome-wide assessment of the 1,920 single gene *S. aureus* mutant strains contained within the Nebraska transposon mutant library (NTML) demonstrated several genes are associated with subverting phagosomal acidification. The findings support prior published evidence for the role of virulence gene regulators associated with intracellular survival (Voyich et al. 2005; Kubica et al. 2008). In both a candidate screen approach and the comprehensive screen of the NTML, in the absence of regulatory genes *agrABC* and *saeR* phagosomal acidification was evident. Further validation of the screen was obtained in the demonstration that the regulator *sarA* was not associated with phagosomal acidification subversion in this model, supported by prior evidence that *sarA* is not essential to *S. aureus* survival within differentiated macrophages (Kubica et al. 2008).

The findings in this study are analogous to resistance to oxidative stress where multiple pathways are utilised, broadly categorised as enzymatic detoxification, scavenger molecules, iron sequestration, repair mechanisms and regulator stress responses (Fang 2004). In further validation of this study design, the positive identification of the catalase gene *katA* indicates the essential role of detoxification mechanisms. Although neither of the single superoxide dismutase (*sod*) genes were identified in the NTML screen, the double *sodAM* mutant was demonstrated in the candidate screen to be important to subversion of phagosomal acidification.

The screen of the NTML identified several *S. aureus* genes not previously associated with phagosomal maturation subversion. The *S. aureus* mutant strains deficient in *qoxA, qoxC, clpP, ctaB* and *ctaM* were associated with phagosomal acidification and subsequently confirmed in transductant mutants. Within the Foster group, the *clpP* mutant strain has been previously demonstrated to be important to virulence within a zebrafish infection model, for which Clp ATPase regulated post-phagocytosed stress tolerance was hypothesised as a mechanistic explanation (D. Yang et al. 2019). Mutants lacking a functional terminal oxidase

encoded by the *qoxABCD* complex have attenuated virulence within murine infection models (Lan et al. 2010; Hammer et al. 2013). The genes *ctaB* and recently identified *ctaM* are intrinsically associated with the terminal oxidase QoxABCD (Hammer et al. 2016). Mutations within the *cta* genes have also been associated with attenuated virulence (Lan et al. 2010; T. Xu et al. 2016). A mechanistic explanation however has not been obtained. A catalase-like function of the QoxABCD complex is conceivable given precedence in other bacteria (Bolshakov et al. 2010; Hilbers et al. 2013). However, given the role of terminal oxidases in aerobic respiration, mutations within the *qoxABCD* complex are proposed to create respiratory-deficient persister phenotype capable of resisting antimicrobial effector functions (Hammer et al. 2013; Proctor et al. 2006).

6.2 Implications for novel therapeutic design.

It has been hypothesised that the intracellular latent population of *S. aureus* may act as a mechanism for tissue persistence, metastatic infection, and relapsing disease (Gresham et al. 2000; Thwaites & Gant 2011; Prajsnar et al. 2012). However, standard antimicrobial agents used in the treatment of severe *S. aureus* infection, namely beta-lactam and glycopeptide antibiotics fail to attain microbicidal levels within eukaryotic cells (Carryn et al. 2003). Within an *in vitro* macrophage model, application of beta-lactam and glycopeptide antibiotics was associated with less effective killing of intracellular *S. aureus* when compared to extracellular populations (Barcia-Macay et al. 2006). Within the intracellular location, antibiotic effect is subject to the ability of the agent to attain sufficient concentrations and activity within specific intracellular compartments (Van Bambeke et al. 2006). These observations indicate that alternative treatment strategies should be investigated.

The susceptibility of *S. aureus* to antibiotics is related to phase of growth. Within the stationary phase, *S. aureus* is not susceptible to bactericidal antibiotics (Conlon et al. 2016). As described previously, *S. aureus* can attain a persister state in response to stress, reverting from exponential growth to a stationary phase (Keren et al. 2004). The ClpP protease is associated with persister formation within the inhospitable intracellular environment of the macrophage, and disruption of ClpP function with a novel antibiotic enables eradication (Conlon et al. 2013). The acyldepsipeptide ADEP4 kills *S. aureus* bacteria when in the typically antimicrobial resistant persister state by dissociating the ClpP protease from the Clp ATPase, causing unregulated proteolysis (Conlon et al. 2013).

Additional outcomes from this study indicate that the terminal oxidase QoxABCD of the respiratory chain contributes to the subversion of phagosomal acidification. The respiratory chain has proved to be a therapeutic target in the treatment of another intracellular pathogen

M. tuberculosis, with the ATP synthase inhibitor bedaquiline approved for clinical use (Koul et al. 2007; Bajeli et al. 2020). The discovery of bedaquiline has validated investigation of respiratory chain antagonism, particularly targeting enzymes distinct from those within mitochondria (Schurig-Briccio et al. 2014). However, in the context of *S. aureus*, disruption of the respiratory chain has been associated with the development of small colony variants (SCVs) and a persister phenotype, and limited antagonism by the redundancy of two terminal oxidases (Hammer et al. 2013; Hammer et al. 2016; T. Xu et al. 2016; Conlon et al. 2016). Nonetheless, recent publications have demonstrated that targeting the respiratory chain pathway sensitises *S. aureus* to both host antimicrobial effector molecules and antibiotics (Vestergaard et al. 2017; L. Liu et al. 2020; Schurig-Briccio et al. 2014). The effect of bedaquiline upon *S. aureus* has also been investigated. Curiously, despite having no extracellular effect upon extracellular populations, within a *S. aureus* challenge of macrophages, application of bedaquiline enhanced intracellular killing of *S. aureus* with no mechanistic explanation (Giraud-Gatineau et al. 2020).

The result of this study provides validation for investigation of these pathways. Understanding how *S. aureus* subverts the host immune response offers insight into how we might re-engage host immune responses to our advantage. This has been demonstrated in the case of the virulence factors *saeRS* and *agr.* Inhibition of these regulator systems, resulting in altered *S. aureus* virulence, was achieved through repurposing existing drugs (Yeo et al. 2018; Hendrix et al. 2016).

6.3 Limitations of methods used within study.

The primary high-throughput screen of the NTML was designed to capture “hits” in an efficient but robust manner. It is plausible that at this stage of the screen false negatives will have occurred and thus failed to be recognised as a “hit”. Having elected to utilise differentiated human monocyte-derived macrophages (MDMs), the screen will have been subject to donor variability (Tram et al. 2020). For the screen, equivalent rates of bacterial growth within the NTML were assumed but may also account for variable bacterial numbers when challenged against macrophages. As portrayed within the visual representations, rare plate edge effects attributable to fluid handling during assay setup were also detectable. Variation due to the above factors were minimised by subsequent data normalisation within the adapted-for-purpose cellHTS2 R/Bioconductor analysis package. The primary screen however was validated by the identification of virulence factors, namely *saeR*, *agrA, agrB,* and *agrC,* that were recognised within the candidate screen and prior assessment of *S. aureus* persistence within MDMs (Kubica et al. 2008). The subsequent round of screening and later validation then eliminated false positive mutant strains.

Within a *S. aureus* challenge of MDMs, the maximal rate of intracellular killing occurs within the first thirty minutes of internalisation (Jubrail et al. 2016). Greater resolution of timings, for example assessment within the first ten minutes of internalisation is not possible using the methods employed within this study. Alternative imaging methods, such as intravitreal microscopy may offer such an opportunity (Surewaard & Kubes 2017).

Having validated 15 single gene mutant strains that demonstrate a failure to subvert intracellular acidification, it would have been desirable to further characterise the intracellular fate of these strains. Although phagosomal acidification is associated with phagosomal maturation, ultimately progressing to the microbicidal environment of the phagolysosome, this study cannot conclude any association between intracellular acidification and bacterial death.

6.4 Future work.

Having completed a screen of the NTML and identified 15 genes of interest, complementation studies are necessary to confirm the roles of these genes. Unfortunately, this was not possible within the period of this project. Any genes confirmed by complementation would then progress to the assessment of intracellular persistence. The disruption of the terminal oxidase complex encoded by *qoxABCD* and the cytochrome assembly genes *ctaB* and *ctaM* has been associated with the development of a persister phenotype (Hammer et al. 2013; T. Xu et al. 2016). It is pertinent to investigate if these mutants are tolerant of acidification or are being killed within the macrophage. The observation that a *qoxB* mutant murine infection challenge is associated with a reduced bacterial burden within the liver may indicate killing within the Kupffer cells (Hammer et al. 2013).

For each mutant strain identified within the screen, macrophage killing assays will need to be performed to assess intracellular survival. Assessment of phagosomal maturation will also be required, specifically assessing for an association between the *S. aureus*-containing phagosome and lysosome fusion and subsequent cathepsin D activation. If any mutants were to be associated with phagosomal maturation, a comparison of these mutants and the wild-type strain regarding generation of proinflammatory cytokines in addition to generation of reactive oxygen and reactive nitrogen species would be undertaken.

As a member of the SHIELD AMR research consortium, the results of this study have been made available to collaborators within this group. The purpose of this consortium is to utilise data and understanding of host-pathogen interactions to identify known chemical agents that has the potential to enhance bacterial killing (Watson, 2020).

During this study, the Clinical Microbiology department of Sheffield Teaching Hospitals NHS Trust has been collecting *S. aureus* isolates associated with positive intravertebral disc biopsy culture. Hypothetically, these isolates have subverted the host immune defence mechanisms and established a metastatic infection. Within future work, I aim assess if these clinical strains demonstrate enhanced subversion of phagosomal maturation in comparison to laboratory strains. If significant differences are evident, the clinical strains would be genome sequenced to assess for mutations with the genes identified within this screen.

6.5 Conclusion.

Within clinical practice, *S. aureus* is a frequent cause of serious disease, associated with significant morbidity and mortality. In an era of growing antimicrobial resistance, identification of novel therapeutic strategies is paramount. This study demonstrated that the *S. aureus* USA300 strain JE2 actively subverts the macrophage phagosomal maturation pathway following internalisation, facilitating intracellular bacterial persistence. The *S. aureus*-containing phagosome fails to progress to the mature acidified microbicidal phagolysosomal state. A genome-wide library of *S. aureus* mutants underwent a high-throughput microscopy screen to identify bacterial genetic factors associated with the subversion of intracellular acidification within a macrophage infection model. Fifteen genes were identified as novel genes for subversion of macrophage phagosomal acidification, including the virulence regulators *agrA, agrB, agrC,* and *saeR*; the protease *clpP*; catalase *katA*; the terminal oxidase complex *qoxA* and *qoxC*; cytochrome assembly genes *ctaB* and *ctaM.* These findings have provided an insight into potential pathways utilised by *S. aureus* to subvert a key host immune response and offer potential targets for future antimicrobial development.

References

Abraham, E.P. & Chain, E., 1940. An enzyme from bacteria able to destroy penicillin. *Nature*, 146, p.837.

Abraham, E.P. et al., 1941. Further observations on penicillin. *The Lancet*, 358(1), pp.177–189.

Adams, D.H. & Shaw, S., 1994. Leucocyte-endothelial interactions and regulation of leucocyte migration. *The Lancet*, 343(8901), pp.831–836.

Aderem, A. & Underhill, D.M., 1999. Mechanisms of phagocytosis in macrophages. *Annual review of immunology*, 17(1), pp.593–623.

Aderem, A.A. et al., 1985. Ligated complement receptors do not activate the arachidonic acid cascade in resident peritoneal macrophages. *The Journal of experimental medicine*, 161(3), pp.617–622.

Akira, S., 2000. The role of IL-18 in innate immunity. *Current Opinion in Immunology*, 12(1), pp.59–63.

Akira, S., Uematsu, S. & Takeuchi, O., 2006. Pathogen Recognition and Innate Immunity. *Cell*, 124(4), pp.783–801.

Allen, L.A. & Aderem, A., 1996a. Mechanisms of phagocytosis. *Current Opinion in Immunology*, 8(1), pp.36–40.

Allen, L.A. & Aderem, A., 1996b. Molecular definition of distinct cytoskeletal structures involved in complement- and Fc receptor-mediated phagocytosis in macrophages. *The Journal of experimental medicine*, 184(2), pp.627–637.

Amato, S.M., Orman, M.A. & Brynildsen, M.P., 2013. Metabolic Control of Persister Formation in Escherichia coli. *Molecular cell*, 50(4), pp.475–487.

Arellano-Reynoso, B. et al., 2005. Cyclic β-1,2-glucan is a brucella virulence factor required for intracellular survival. *Nature Immunology*, 6(6), pp.618–625.

Athens, J.W. et al., 1961. Leukokinetic studies. IV. The total blood, circulating and marginal granulocyte pools and the granulocyte turnover rate in normal subjects. *Journal of Clinical Investigation*, 40(6), pp.989–995.

Auffray, C., Sieweke, M.H. & Geissmann, F., 2009. Blood Monocytes: Development, Heterogeneity, and Relationship with Dendritic Cells. *Annual review of immunology*, 27(1), pp.669–692.

Babior, B.M., 2004. NADPH oxidase. *Current Opinion in Immunology*, 16(1), pp.42–47.

Bainton, D.F., Ullyot, J.L. & Farquhar, M.G., 1971. The development of neutrophilic polymorphonuclear leukocytes in human bone marrow. *The Journal of experimental medicine*, 134(4), pp.907–934.

Bajeli, S. et al., 2020. Terminal Respiratory Oxidases: A Targetables Vulnerability of Mycobacterial Bioenergetics? *Frontiers in cellular and infection microbiology*, 10, p.589318.

Baker, J. et al., 2010. Copper stress induces a global stress response in Staphylococcus aureus and represses sae and agr expression and biofilm formation. *Applied and Environmental Microbiology*, 76(1), pp.150–160.

Barcia-Macay, M. et al., 2006. Pharmacodynamic evaluation of the intracellular activities of antibiotics against Staphylococcus aureus in a model of THP-1 macrophages. *Antimicrobial agents and chemotherapy*, 50(3), pp.841–851.

Baughn, R. & Bonventre, P.F., 1975. Phagocytosis and intracellular killing of Staphylococcus aureus by normal mouse peritoneal macrophages. *Infection and Immunity*, 12(2), pp.346–352.

Bayles, K.W. et al., 1998. Intracellular Staphylococcus aureus escapes the endosome and induces apoptosis in epithelial cells. *Infection and Immunity*, 66(1), pp.336–342.

Beauregard, K.E. et al., 1997. pH-dependent perforation of macrophage phagosomes by listeriolysin O from Listeria monocytogenes. *The Journal of experimental medicine*, 186(7), pp.1159–1163.

Bellingan, G.J. et al., 1996. In vivo fate of the inflammatory macrophage during the resolution of inflammation: inflammatory macrophages do not die locally, but emigrate to the draining lymph nodes. *Journal of immunology (Baltimore, Md. : 1950)*, 157(6), pp.2577–2585.

Bennett, W.E. & Cohn, Z.A., 1966. The isolation and selected properties of blood monocytes. *The Journal of experimental medicine*, 123(1), pp.145–160.

Benoit, M., Desnues, B. & Mege, J.L., 2008. Macrophage Polarization in Bacterial Infections. *Journal of immunology (Baltimore, Md. : 1950)*, 181(6), pp.3733–3739.

Bera, A. et al., 2004. Why are pathogenic staphylococci so lysozyme resistant? The peptidoglycan O-acetyltransferase OatA is the major determinant for lysozyme resistance of Staphylococcus aureus. *Molecular Microbiology*, 55(3), pp.778–787.

Beutler, B., Milsark, I.W. & Cerami, A.C., 1985. Passive immunization against cachectin/tumor necrosis factor protects mice from lethal effect of endotoxin. *Science*, 229(4716), pp.869–871.

Beutler, B.A., 2009. TLRs and innate immunity. *Blood*, 113(7), pp.1399–1407.

Bewley, M.A. et al., 2011. A Cardinal Role for Cathepsin D in Co-Ordinating the Host-Mediated Apoptosis of Macrophages and Killing of Pneumococci V. Deretic, ed. *PLoS Pathogens*, 7(1), pp.e1001262–17.

Bewley, M.A. et al., 2014. Pneumolysin activates macrophage lysosomal membrane permeabilization and executes apoptosis by distinct mechanisms without membrane pore formation., 5(5), pp.e01710–14.

Bigger, J.W., 1944. Treatment of Staphylococcal infections with penicillin. *The Lancet*, 2(6320), pp.497–500.

Binker, M.G. et al., 2007. Arrested maturation of Neisseria-containing phagosomes in the absence of the lysosome-associated membrane proteins, LAMP-1 and LAMP-2. *Cellular microbiology*, 9(9), pp.2153–2166.

Bischoff, M. et al., 2004. Microarray-based analysis of the Staphylococcus aureus sigmaB regulon. *Journal of Bacteriology*, 186(13), pp.4085–4099.

Blander, J.M. & Medzhitov, R., 2004. Regulation of phagosome maturation by signals from toll-like receptors. *Science*, 304(5673), pp.1014–1018.

Bogdan, C., Röllinghoff, M. & Diefenbach, A., 2000. Reactive oxygen and reactive nitrogen intermediates in innate and specific immunity. *Current Opinion in Immunology*, 12(1), pp.64–76.

Boldock, E. et al., 2018. Human skin commensals augment Staphylococcus aureus pathogenesis. *Nature Microbiology*, 3(8), pp.881–890.

Bolshakov, I.A. et al., 2010. Catalase activity of cytochrome C oxidase assayed with hydrogen peroxide-sensitive electrode microsensor. *Biochemistry. Biokhimiia*, 75(11), pp.1352–1360.

Bonamore, A. & Boffi, A., 2007. Flavohemoglobin: Structure and reactivity. *IUBMB Life*, 60(1), pp.19–28.

Borisov, V.B. et al., 2021. ROS Defense Systems and Terminal Oxidases in Bacteria. *Antioxidants (Basel, Switzerland)*, 10(6), p.839.

Borregaard, N. & Cowland, J.B., 1997. Granules of the human neutrophilic polymorphonuclear leukocyte. *Blood*, 89(10), pp.3503–3521.

BoseDasgupta, S. & Pieters, J., 2014. Inflammatory Stimuli Reprogram Macrophage Phagocytosis to Macropinocytosis for the Rapid Elimination of Pathogens S. Ehrt, ed. *PLoS Pathogens*, 10(1), pp.e1003879–18.

Botelho, R.J. & Grinstein, S., 2011. Phagocytosis. *CURBIO*, 21(14), pp.R533–R538.

Botella, E. et al., 2014. PhoR autokinase activity is controlled by an intermediate in wall teichoic acid metabolism that is sensed by the intracellular PASdomain during the PhoPR-mediated phosphate limitation response of Bacillus subtilis. *Molecular Microbiology*, 94(6), pp.1242–1259.

Boutros, M. et al., 2019. End-to-end analysis of cell-based screens: from raw intensity readings to the annotated hit list. pp.1–48.

Boutros, M., Brás, L.P. & Huber, W., 2006. Analysis of cell-based RNAi screens. *Genome biology*, 7(7), pp.R66–11.

Bowers, J.R. et al., 2018. Improved Subtyping of *Staphylococcus aureus* Clonal Complex 8 Strains Based on Whole-Genome Phylogenetic Analysis P. D. Fey, ed. *mSphere*, 3(3), pp.95–15.

Boyce, J.M. et al., 2005. Meticillin-resistant Staphylococcus aureus. *The Lancet Infectious Diseases*, 5(10), pp.653–663.

Brown, S., 2010. Institutional Profile: The Sheffield RNAi screening facility: a service for high-throughput, genome-wide DrosophilaRNAi screens. 2(12), pp.1805–1812.

Brunskill, E.W. & Bayles, K.W., 1996. Identification and molecular characterization of a putative regulatory locus that affects autolysis in Staphylococcus aureus. *Journal of Bacteriology*, 178(3), pp.611–618.

Bucci, C. et al., 1992. The small GTPase rab5 functions as a regulatory factor in the early endocytic pathway. *Cell*, 70(5), pp.715–728.

Canton, J. et al., 2014. Contrasting phagosome pH regulation and maturation in human M1 and M2 macrophages. *Molecular Biology of the Cell*, 25(21), pp.3330–3341.

Carryn, S. et al., 2003. Intracellular pharmacodynamics of antibiotics. *Infectious Disease Clinics of North America*, 17(3), pp.615–634.

Celli, J., 2006. Surviving inside a macrophage: The many ways of Brucella. *Research in Microbiology*, 157(2), pp.93–98.

Celli, J. et al., 2003. Brucella Evades Macrophage Killing via VirB-dependent Sustained Interactions with the Endoplasmic Reticulum. *The Journal of experimental medicine*, 198(4), pp.545–556.

Cellier, M.F., Courville, P. & Campion, C., 2007. Nramp1 phagocyte intracellular metal withdrawal defense. *Microbes and infection*, 9(14-15), pp.1662–1670.

Chan, P.F. & Foster, S.J., 1998a. Role of SarA in virulence determinant production and environmental signal transduction in Staphylococcus aureus. *Journal of Bacteriology*, 180(23), pp.6232–6241.

Chan, P.F. & Foster, S.J., 1998b. The role of environmental factors in the regulation of virulence-determinant expression in Staphylococcus aureus 8325-4. *Microbiology*, 144 (Pt 9)(9), pp.2469–2479.

Chan, P.F. et al., 1998. The Staphylococcus aureus alternative sigma factor sigmaB controls the environmental stress response but not starvation survival or pathogenicity in a mouse abscess model. *Journal of Bacteriology*, 180(23), pp.6082–6089.

Chan, Y.G.Y. et al., 2016. SagB Glucosaminidase Is a Determinant of Staphylococcus aureus Glycan Chain Length, Antibiotic Susceptibility, and Protein Secretion. *Journal of Bacteriology*, 198(7), pp.1123–1136.

Chavakis, T. et al., 2002. Staphylococcus aureus extracellular adherence protein serves as anti-inflammatory factor by inhibiting the recruitment of host leukocytes. *Nature Medicine*, 8(7), pp.687–693.

Cheung, A.L. et al., 1992. Regulation of exoprotein expression in Staphylococcus aureus by a locus (sar) distinct from agr. *Proceedings of the National Academy of Sciences*, 89(14), pp.6462–6466.

Cheung, A.L. et al., 2004. Regulation of virulence determinants in vitro and in vivo in Staphylococcus aureus. *FEMS Immunology & Medical Microbiology*, 40(1), pp.1–9.

Cheung, A.L., Bayer, M.G. & Heinrichs, J.H., 1997. sar Genetic determinants necessary for transcription of RNAII and RNAIII in the agr locus of Staphylococcus aureus. *Journal of Bacteriology*, 179(12), pp.3963–3971.

Choby, J.E. & Skaar, E.P., 2016. Heme Synthesis and Acquisition in Bacterial Pathogens. *Journal of molecular biology*, 428(17), pp.3408–3428.

Christoforidis, S. et al., 1999. The Rab5 effector EEA1 is a core component of endosome docking. *Nature*, 397(6720), pp.621–625.

Clemens, D.L. & Horwitz, M.A., 2007. Uptake and Intracellular Fate of Francisella tularensis in Human Macrophages. *Annals of the New York Academy of Sciences*, 1105(1), pp.160–186.

Clemens, D.L., Lee, B.Y. & Horwitz, M.A., 2000. Deviant expression of Rab5 on phagosomes containing the intracellular pathogens Mycobacterium tuberculosis and Legionella pneumophila is associated with altered phagosomal fate. *Infection and Immunity*, 68(5), pp.2671–2684.

Clemens, D.L., Lee, B.Y. & Horwitz, M.A., 2004. Virulent and Avirulent Strains of Francisella tularensis Prevent Acidification and Maturation of Their Phagosomes and Escape into the Cytoplasm in Human Macrophages. *Infection and Immunity*, 72(6), pp.3204–3217.

Clements, M.O., Watson, S.P. & Foster, S.J., 1999. Characterization of the major superoxide dismutase of Staphylococcus aureus and its role in starvation survival, stress resistance, and pathogenicity. *Journal of Bacteriology*, 181(13), pp.3898–3903.

Conlon, B.P., 2014. Staphylococcus aureuschronic and relapsing infections: Evidence of a role for persister cells. *BioEssays : news and reviews in molecular, cellular and developmental biology*, 36(10), pp.991–996.

Conlon, B.P. et al., 2013. Activated ClpP kills persisters and eradicates a chronic biofilm infection. *Nature*, 503(7476), pp.365–370.

Conlon, B.P. et al., 2016. Persister formation in Staphylococcus aureus is associated with ATP depletion. *Nature Microbiology*, 1, p.16051.

Cosgrove, K. et al., 2007. Catalase (KatA) and Alkyl Hydroperoxide Reductase (AhpC) Have Compensatory Roles in Peroxide Stress Resistance and Are Required for Survival, Persistence, and Nasal Colonization in Staphylococcus aureus. *Journal of Bacteriology*, 189(3), pp.1025–1035.

Cowell, B.A. et al., 2000. ExoT of cytotoxic Pseudomonas aeruginosa prevents uptake by corneal epithelial cells. *Infection and Immunity*, 68(1), pp.403–406.

Cox, D. et al., 1996. Syk tyrosine kinase is required for immunoreceptor tyrosine activation motif-dependent actin assembly. *Journal of Biological Chemistry*, 271(28), pp.16597–16602.

Daigneault, M. et al., 2010. The Identification of Markers of Macrophage Differentiation in PMA-Stimulated THP-1 Cells and Monocyte-Derived Macrophages T. M. Doherty, ed. *PLoS ONE*, 5(1), pp.e8668–10.

Das, D. & Bishayi, B., 2010. Contribution of Catalase and Superoxide Dismutase to the Intracellular Survival of Clinical Isolates of Staphylococcus aureus in Murine Macrophages. *Indian journal of microbiology*, 50(4), pp.375–384.

David, M.Z. et al., 2013. Comparing pulsed-field gel electrophoresis with multilocus sequence typing, spa typing, staphylococcal cassette chromosome mec (SCCmec)

typing, and PCR for panton-valentine leukocidin, arcA, and opp3 in methicillin-resistant Staphylococcus aureus isolates at a U.S. Medical Center. *Journal of Clinical Microbiology*, 51(3), pp.814–819.

Davies, J. & Davies, D., 2010. Origins and Evolution of Antibiotic Resistance. *Microbiology and Molecular Biology Reviews*, 74(3), pp.417–433.

Davies, L.C. et al., 2013. Tissue-resident macrophages. *Nature Immunology*, 14(10), pp.986–995.

Day, N.P. et al., 2001. A link between virulence and ecological abundance in natural populations of Staphylococcus aureus. *Science*, 292(5514), pp.114–116.

de Haas, C.J.C. et al., 2004. Chemotaxis Inhibitory Protein of Staphylococcus aureus, a Bacterial Antiinflammatory Agent. *The Journal of experimental medicine*, 199(5), pp.687–695.

de Kraker, M.E.A. et al., 2011. Mortality and hospital stay associated with resistant Staphylococcus aureus and Escherichia coli bacteremia: estimating the burden of antibiotic resistance in Europe. S. M. Opal, ed. *PLoS medicine*, 8(10), p.e1001104.

Delauné, A. et al., 2012. The WalKR system controls major staphylococcal virulence genes and is involved in triggering the host inflammatory response. A. Camilli, ed. *Infection and Immunity*, 80(10), pp.3438–3453.

Desjardins, M. et al., 1994. Biogenesis of phagolysosomes proceeds through a sequential series of interactions with the endocytic apparatus. *The Journal of cell biology*, 124(5), pp.677–688.

Diep, B.A. et al., 2006. Complete genome sequence of USA300, an epidemic clone of community-acquired meticillin-resistant Staphylococcus aureus. *The Lancet*, 367(9512), pp.731–739.

Dockrell, D.H. et al., 2001. Immune-mediated phagocytosis and killing of Streptococcus pneumoniae are associated with direct and bystander macrophage apoptosis. *The Journal of infectious diseases*, 184(6), pp.713–722.

Dong, N., Liu, L. & Shao, F., 2010. A bacterial effector targets host DH-PH domain RhoGEFs and antagonizes macrophage phagocytosis. *The EMBO journal*, 29(8), pp.1363–1376.

Dowling, J.K. & Mansell, A., 2016. Toll-like receptors: the swiss army knife of immunity and vaccine development. *Clinical & Translational Immunology*, 5(5), pp.e85–10.

Doyle, A.G. et al., 1994. Interleukin-13 alters the activation state of murine macrophages in vitro: comparison with interleukin-4 and interferon-gamma. *European Journal of Immunology*, 24(6), pp.1441–1445.

Dubrac, S. et al., 2007. New Insights into the WalK/WalR (YycG/YycF) Essential Signal Transduction Pathway Reveal a Major Role in Controlling Cell Wall Metabolism and Biofilm Formation in Staphylococcus aureus. *Journal of Bacteriology*, 189(22), pp.8257–8269.

DuMont, A.L. et al., 2013. Staphylococcus aureus Elaborates Leukocidin AB To Mediate Escape from within Human Neutrophils. *Infection and Immunity*, 81(5), pp.1830–1841.

Dunman, P.M. et al., 2001. Transcription Profiling-Based Identification of Staphylococcus aureus Genes Regulated by the agr and/or sarA Loci. *Journal of Bacteriology*, 183(24), pp.7341–7353.

Duthie, E.S. & Lorenz, L.L., 1952. Staphylococcal coagulase; mode of action and antigenicity. *Journal of general microbiology*, 6(1-2), pp.95–107.

Easmon, C.S., Lanyon, H. & Cole, P.J., 1978. Use of lysostaphin to remove cell-adherent staphylococci during in vitro assays of phagocyte function. *British journal of experimental pathology*, 59(4), pp.381–385.

Ebert, R.H. & Florey, H.W., 1939. The Extravascular Development of the Monocyte Observed *in vivo*. *British journal of experimental pathology*, 20(4), pp.342–356.

Edwards, J.P. et al., 2006. Biochemical and functional characterization of three activated macrophage populations. *Journal of Leukocyte Biology*, 80(6), pp.1298–1307.

Eiff, von, C. et al., 1997. A site-directed Staphylococcus aureus hemB mutant is a small-colony variant which persists intracellularly. *Journal of Bacteriology*, 179(15), pp.4706–4712.

Eiff, von, C. et al., 2001. Intracellular persistence of Staphylococcus aureus small-colony variants within keratinocytes: a cause for antibiotic treatment failure in a patient with darier's disease. *Clinical Infectious Diseases*, 32(11), pp.1643–1647.

Elasri, M.O. et al., 2002. Staphylococcus aureus collagen adhesin contributes to the pathogenesis of osteomyelitis. *Bone*, 30(1), pp.275–280.

Ellington, J.K. et al., 2005. Intracellular *Staphylococcus aureus* and antibiotic resistance: Implications for treatment of staphylococcal osteomyelitis. *Journal of Orthopaedic Research*, 24(1), pp.87–93.

Epelman, S., Lavine, K.J. & Randolph, G.J., 2014. Origin and Functions of Tissue Macrophages. *Immunity*, 41(1), pp.21–35.

Epelman, S., Lavine, K.J., Beaudin, A.E., et al., 2014. Embryonic and Adult-Derived Resident Cardiac Macrophages Are Maintained through Distinct Mechanisms at Steady State and during Inflammation. *Immunity*, 40(1), pp.91–104.

Epstein, J. et al., 1996. The collectins in innate immunity. *Current Opinion in Immunology*, 8(1), pp.29–35.

Ernst, J.D., 1998. Macrophage receptors for Mycobacterium tuberculosis. *Infection and Immunity*, 66(4), pp.1277–1281.

Falord, M. et al., 2011. Investigation of the *Staphylococcus aureus* GraSR Regulon Reveals Novel Links to Virulence, Stress Response and Cell Wall Signal Transduction Pathways M. James, ed. *PLoS ONE*, 6(7), pp.e21323–17.

Fang, F.C., 2011. Antimicrobial Actions of Reactive Oxygen Species. *mBio*, 2(5), pp.89–6.

Fang, F.C., 2004. Antimicrobial reactive oxygen and nitrogen species: concepts and controversies. *Nature Reviews Microbiology*, 2(10), pp.820–832.

Fedtke, I. et al., 2002. The Nitrate Reductase and Nitrite Reductase Operons and the narT Gene of Staphylococcus carnosus Are Positively Controlled by the Novel Two-Component System NreBC. *Journal of Bacteriology*, 184(23), pp.6624–6634.

Fey, P.D. et al., 2012. A Genetic Resource for Rapid and Comprehensive Phenotype Screening of Nonessential Staphylococcus aureus Genes. 4(1), pp.e00537–12–e00537–12.

Fillat, M.F., 2014. The FUR (ferric uptake regulator) superfamily: Diversity and versatility of key transcriptional regulators. *Archives of Biochemistry and Biophysics*, 546(C), pp.41–52.

Fisher, K.H. et al., 2012. Advances in genome-wide RNAi cellular screens: a case study using the Drosophila JAK/STAT pathway. *BMC Genomics*, 13(1), pp.1–1.

Flannagan, R.S. et al., 2011. Burkholderia cenocepacia disrupts host cell actin cytoskeleton by inactivating Rac and Cdc42. *Cellular microbiology*, 14(2), pp.239–254.

Flannagan, R.S. et al., 2018. The surreptitious survival of the emerging pathogen *Staphylococcus lugdunensis* within macrophages as an immune evasion strategy. *Cellular microbiology*, 20(11), pp.e12869–16.

Flannagan, R.S., Cosío, G. & Grinstein, S., 2009. Antimicrobial mechanisms of phagocytes and bacterial evasion strategies. *Nature Reviews Microbiology*, 7(5), pp.355–366.

Flannagan, R.S., Heit, B. & Heinrichs, D.E., 2015. Antimicrobial Mechanisms of Macrophages and the Immune Evasion Strategies of Staphylococcus aureus. *Pathogens*, 4(4), pp.826–868.

Flannagan, R.S., Heit, B. & Heinrichs, D.E., 2016. Intracellular replication of Staphylococcus aureus in mature phagolysosomes in macrophages precedes host cell death, and bacterial escape and dissemination. *Cellular microbiology*, 18(4), pp.514–535.

Flannagan, R.S., Jaumouillé, V. & Grinstein, S., 2012. The Cell Biology of Phagocytosis. *Annual Review of Pathology: Mechanisms of Disease*, 7(1), pp.61–98.

Fleming, A., 1929. On the antibacterial action of cultures of a penicillium, with special reference to their use in the isolation of B. influenzae. 1929. *The British Journal of Experimental Pathology*, 10, pp.226–236.

Foster, T.J., 2005. Immune evasion by staphylococci. *Nature Reviews Microbiology*, 3(12), pp.948–958.

Foster, T.J., 2019. The MSCRAMM Family of Cell-Wall-Anchored Surface Proteins of Gram-Positive Cocci. *Trends in Microbiology*, 27(11), pp.927-941.

Foster, T.J. & Hook, M., 1998. Surface protein adhesins of *Staphylococcus aureus. Trends in Microbiology*, 6(12), pp.484–488.

Fournier, B. & Hooper, D.C., 2000. A new two-component regulatory system involved in adhesion, autolysis, and extracellular proteolytic activity of Staphylococcus aureus. *Journal of Bacteriology*, 182(14), pp.3955–3964.

Fournier, B., Klier, A. & Rapoport, G., 2001. The two-component system ArlS-ArlR is a regulator of virulence gene expression in *Staphylococcus aureus*. *Molecular Microbiology*, 41(1), pp.247–261.

Fowler, V.G. et al., 2003. Clinical identifiers of complicated Staphylococcus aureus bacteremia. *Archives of internal medicine*, 163(17), pp.2066–2072.

Fowler, V.G., Jr & Proctor, R.A., 2014. Where does a Staphylococcus aureus vaccine stand? *Clinical Microbiology and Infection*, 20, pp.66–75.

Francis, J.S. et al., 2005. Severe community-onset pneumonia in healthy adults caused by methicillin-resistant Staphylococcus aureus carrying the Panton-Valentine leukocidin genes. *Clinical Infectious Diseases*, 40(1), pp.100–107.

Fraser, J.D. & Proft, T., 2008. The bacterial superantigen and superantigen-like proteins. *Immunological reviews*, 225(1), pp.226–243.

Fratti, R.A. et al., 2001. Role of phosphatidylinositol 3-kinase and Rab5 effectors in phagosomal biogenesis and mycobacterial phagosome maturation arrest. *The Journal of cell biology*, 154(3), pp.631–644.

Freeman, Z.N., Dorus, S. & Waterfield, N.R., 2013. The KdpD/KdpE Two-Component System: Integrating K+ Homeostasis and Virulence C. E. Chitnis, ed. *PLoS Pathogens*, 9(3), pp.e1003201–9.

Frees, D. et al., 2003. Alternative roles of ClpX and ClpP in Staphylococcus aureus stress tolerance and virulence. *Molecular Microbiology*, 48(6), pp.1565–1578.

Frees, D. et al., 2004. Clp ATPases are required for stress tolerance, intracellular replication and biofilm formation in Staphylococcus aureus. *Molecular Microbiology*, 54(5), pp.1445–1462.

Frimodt-Møller, N. et al., 1999. Epidemiology of Staphylococcus aureus bacteremia in Denmark from 1957 to 1990. *Clinical Microbiology and Infection*, 3(3), pp.297–305.

Fujita, T., Matsushita, M. & Endo, Y., 2004. The lectin-complement pathway--its role in innate immunity and evolution. *Immunological reviews*, 198, pp.185–202.

Gaillot, O. et al., 2000. The ClpP serine protease is essential for the intracellular parasitism and virulence of Listeria monocytogenes. *Molecular Microbiology*, 35(6), pp.1286–1294.

Galli, S.J., Borregaard, N. & Wynn, T.A., 2011. Phenotypic and functional plasticity of cells of innate immunity: macrophages, mast cells and neutrophils. *Nature Immunology*, 12(11), pp.1035–1044.

Gancz, H., Censini, S. & Merrell, D.S., 2006. Iron and pH homeostasis intersect at the level of Fur regulation in the gastric pathogen Helicobacter pylori. *Infection and Immunity*, 74(1), pp.602–614.

Garzoni, C. & Kelley, W.L., 2009. Staphylococcus aureus: new evidence for intracellular persistence. *Trends in Microbiology*, 17(2), pp.59–65.

Gaupp, R. et al., 2010. Advantage of upregulation of succinate dehydrogenase in Staphylococcus aureus biofilms. *Journal of Bacteriology*, 192(9), pp.2385–2394.

Gaupp, R., Ledala, N. & Somerville, G.A., 2012. Staphylococcal response to oxidative stress. *Frontiers in cellular and infection microbiology*, 2, p.33.

Gautier, E.L. et al., 2012. Gene-expression profiles and transcriptional regulatory pathways that underlie the identity and diversity of mouse tissue macrophages. *Nature Immunology*, 13(11), pp.1118–1128.

Geiger, T. et al., 2008. The Virulence Regulator Sae of Staphylococcus aureus: Promoter Activities and Response to Phagocytosis-Related Signals. *Journal of Bacteriology*, 190(10), pp.3419–3428.

Geissmann, F. et al., 2010. Development of Monocytes, Macrophages, and Dendritic Cells. *Science*, 327(5966), pp.656–661.

Geissmann, F., Jung, S. & Littman, D.R., 2003. Blood Monocytes Consist of Two Principal Subsets with Distinct Migratory Properties. *Immunity*, 19(1), pp.71–82.

George, S.E. et al., 2019. Oxidative stress drives the selection of quorum sensing mutants in the *Staphylococcus aureus* population. *Proceedings of the National Academy of Sciences of the United States of America*, 116(38), pp.19145–19154.

Gillaspy, A.F. et al., 1995. Role of the accessory gene regulator (agr) in pathogenesis of staphylococcal osteomyelitis. *Infection and Immunity*, 63(9), pp.3373–3380.

Ginhoux, F. & Jung, S., 2014. Monocytes and macrophages: developmental pathways and tissue homeostasis. *Nature Publishing Group*, 14(6), pp.392–404.

Giraud-Gatineau, A. et al., 2020. The antibiotic bedaquiline activates host macrophage innate immune resistance to bacterial infection. *eLife*, 9.

Giraudo, A.T. et al., 1994. Characterization of a Tn551-mutant of Staphylococcus aureus defective in the production of several exoproteins. *Canadian journal of microbiology*, 40(8), pp.677–681.

Giraudo, A.T., Cheung, A.L. & Nagel, R., 1997. The sae locus of Staphylococcus aureus controls exoprotein synthesis at the transcriptional level. *Archives of microbiology*, 168(1), pp.53–58.

Gladstone, G.P. & van Heyningen, W.E., 1957. Staphylococcal leucocidins. *British journal of experimental pathology*, 38(2), pp.123–137.

Gold, H.S., 2001. Vancomycin-resistant enterococci: mechanisms and clinical observations. *Clinical Infectious Diseases*, 33(2), pp.210–219.

Gordon, A.H., Hart, P.D. & Young, M.R., 1980. Ammonia inhibits phagosome-lysosome fusion in macrophages. *Nature*, 286(5768), pp.79–80.

Gordon, S. & Taylor, P.R., 2005. Monocyte and macrophage heterogeneity. *Nature Reviews Immunology*, 5(12), pp.953–964.

Götz, F., 2002. Staphylococcus and biofilms. *Molecular Microbiology*, 43(6), pp.1367–1378.

Götz, F. & Mayer, S., 2013. Both Terminal Oxidases Contribute to Fitness and Virulence during Organ-Specific Staphylococcus aureus Colonization. *mBio*, 4(6), pp.316–3.

Götz, F., Bannerman, T. & Schleifer, K.-H., 2006. The Genera *Staphylococcus* and *Macrococcus*. In *The Prokaryotes*. New York, NY: Springer US, pp. 5–75.

Green, D.R. & Reed, J.C., 1998. Mitochondria and apoptosis. *Science*, 281(5381), pp.1309–1312.

Gresham, H.D. et al., 2000. Survival of Staphylococcus aureus inside neutrophils contributes to infection. *The Journal of Immunology*, 164(7), pp.3713–3722.

Grosz, M. et al., 2013. Cytoplasmic replication of *Staphylococcus aureus* upon phagosomal escape triggered by phenol-soluble modulin α. 16(4), pp.451–465.

Gruenberg, J. & van der Goot, F.G., 2006. Mechanisms of pathogen entry through the endosomal compartments. *Nature Reviews Molecular Cell Biology*, 7(7), pp.495–504.

Guilliams, M. & Scott, C.L., 2017. Does niche competition determine the origin of tissue-resident macrophages? *Nature Reviews Immunology*, 128(7), pp.1–10.

Guilliams, M. et al., 2013. Alveolar macrophages develop from fetal monocytes that differentiate into long-lived cells in the first week of life via GM-CSF. *The Journal of experimental medicine*, 210(10), pp.1977–1992.

Haag, A.F. & Bagnoli, F., 2017. The Role of Two-Component Signal Transduction Systems in Staphylococcus aureus Virulence Regulation. *Current topics in microbiology and immunology*, 409(Pt 3), pp.145–198.

Hall, H.K. & Foster, J.W., 1996. The role of fur in the acid tolerance response of Salmonella typhimurium is physiologically and genetically separable from its role in iron acquisition. *Journal of Bacteriology*, 178(19), pp.5683–5691.

Hall, J.W. et al., 2017. The *Staphylococcus aureus* AirSR Two-Component System Mediates Reactive Oxygen Species Resistance via Transcriptional Regulation of Staphyloxanthin Production. F. C. Fang, ed. *Infection and Immunity*, 85(2), pp.603–12.

Hammer, N.D. et al., 2016. CtaM Is Required for Menaquinol Oxidase aa3Function in Staphylococcus aureus. *mBio*, 7(4), pp.1763–9.

Hammer, N.D. et al., 2013. Two Heme-Dependent Terminal Oxidases Power Staphylococcus aureus Organ-Specific Colonization of the Vertebrate Host M. S. Gilmore, ed. *mBio*, 4(4), pp.172–9.

Harraghy, N., 2005. sae is essential for expression of the staphylococcal adhesins Eap and Emp. *Microbiology*, 151(6), pp.1789–1800.

Harrison, J.E. & Schultz, J., 1976. Studies on the chlorinating activity of myeloperoxidase. *The Journal of biological chemistry*, 251(5), pp.1371–1374.

Harrison, R.E. et al., 2003. Phagosomes Fuse with Late Endosomes and/or Lysosomes by Extension of Membrane Protrusions along Microtubules: Role of Rab7 and RILP. *Molecular and Cellular Biology*, 23(18), pp.6494–6506.

Hashimoto, D. et al., 2013. Tissue-Resident Macrophages Self-Maintain Locally throughout Adult Life with Minimal Contribution from Circulating Monocytes. *Immunity*, 38(4), pp.792–804.

Hawkins, C. et al., 2007. Persistent Staphylococcus aureus bacteremia: an analysis of risk factors and outcomes. *Archives of internal medicine*, 167(17), pp.1861–1867.

Heilbronner, S. et al., 2011. Genome sequence of Staphylococcus lugdunensis N920143 allows identification of putative colonization and virulence factors. *FEMS Microbiology Letters*, 322(1), pp.60–67.

Heinzen, R.A. et al., 1996. Differential interaction with endocytic and exocytic pathways distinguish parasitophorous vacuoles of Coxiella burnetii and Chlamydia trachomatis. *Infection and Immunity*, 64(3), pp.796–809.

Helaine, S. et al., 2014. Internalization of Salmonella by macrophages induces formation of nonreplicating persisters. *Science*, 343(6167), pp.204–208.

Hendrix, A.S. et al., 2016. Repurposing the Nonsteroidal Anti-inflammatory Drug Diflunisal as an Osteoprotective, Antivirulence Therapy for Staphylococcus aureus Osteomyelitis. *Antimicrobial agents and chemotherapy*, 60(9), pp.5322–5330.

Henry, R. et al., 2006. Cytolysin-dependent delay of vacuole maturation in macrophages infected with Listeria monocytogenes. *Cellular microbiology*, 8(1), pp.107–119.

Hensel, M. et al., 1995. Simultaneous identification of bacterial virulence genes by negative selection. *Science*, 269(5222), pp.400–403.

Hilbers, F. et al., 2013. True wild type and recombinant wild type cytochrome c oxidase from Paracoccus denitrificans show a 20-fold difference in their catalase activity. *Biochimica et biophysica acta*, 1827(3), pp.319–327.

Hoepelman, I.M. et al., 1990. Bacterial iron enhances oxygen radical-mediated killing of Staphylococcus aureus by phagocytes. *Infection and Immunity*, 58(1), pp.26–31.

Hoffmann, J. & Akira, S., 2013. Innate immunity. *Current Opinion in Immunology*, 25(1), pp.1–3.

Holden, M.T.G. et al., 2013. A genomic portrait of the emergence, evolution, and global spread of a methicillin-resistant Staphylococcus aureus pandemic. *Genome Research*, 23(4), pp.653–664.

Holers, V.M., 2014. Complement and Its Receptors: New Insights into Human Disease. *Annual review of immunology*, 32(1), pp.433–459.

Holowka, D. et al., 2007. Insights into immunoglobulin E receptor signaling from structurally defined ligands. *Immunological reviews*, 217(1), pp.269–279.

Horsburgh, M.J., Aish, J.L., et al., 2002. Alternative factor sigma-B Modulates Virulence Determinant Expression and Stress Resistance: Characterization of a Functional rsbU Strain Derived from *Staphylococcus aureus* 8325-4. *Journal of Bacteriology*, 184(19), pp.5457–5467.

Horsburgh, M.J., Clements, M.O., et al., 2001. PerR Controls Oxidative Stress Resistance and Iron Storage Proteins and Is Required for Virulence in Staphylococcus aureus. *Infection and Immunity*, 69(6), pp.3744–3754.

Horsburgh, M.J., Ingham, E. & Foster, S.J., 2001. In Staphylococcus aureus, Fur Is an Interactive Regulator with PerR, Contributes to Virulence, and Is Necessary for

Oxidative Stress Resistance through Positive Regulation of Catalase and Iron Homeostasis. *Journal of Bacteriology*, 183(2), pp.468–475.

Horsburgh, M.J., Wharton, S.J., et al., 2002. MntR modulates expression of the PerR regulon and superoxide resistance in Staphylococcus aureus through control of manganese uptake. *Molecular Microbiology*, 44(5), pp.1269–1286.

Howden, B.P. et al., 2008. Genomic Analysis Reveals a Point Mutation in the Two-Component Sensor Gene graS That Leads to Intermediate Vancomycin Resistance in Clinical Staphylococcus aureus. *Antimicrobial agents and chemotherapy*, 52(10), pp.3755–3762.

Howe, R.A. et al., 1998. Vancomycin-resistant Staphylococcus aureus. *The Lancet*, 351(9102), pp.602–1.

Hsieh, M.M. et al., 2007. Prevalence of neutropenia in the U.S. population: age, sex, smoking status, and ethnic differences. *Annals of internal medicine*, 146(7), pp.486–492.

Huynh, K.K. & Grinstein, S., 2007. Regulation of Vacuolar pH and Its Modulation by Some Microbial Species. *Microbiology and Molecular Biology Reviews*, 71(3), pp.452–462.

Huynh, K.K. et al., 2010. Inactivation of Macrophage Rab7 by *Burkholderia cenocepacia*. *Journal of Innate Immunity*, 2(6), pp.522–533.

Huynh, K.K. et al., 2007. LAMP proteins are required for fusion of lysosomes with phagosomes. *The EMBO Journal*, 26(2), pp.313–324.

Hybiske, K. & Stephens, R.S., 2008. Exit strategies of intracellular pathogens. *Nature Reviews Microbiology*, 6(2), pp.99–110.

Hyslop, P.A. et al., 1995. Hydrogen peroxide as a potent bacteriostatic antibiotic: implications for host defense. *Free Radical Biology and Medicine*, 19(1), pp.31–37.

Imlay, J.A., 2003. Pathways of Oxidative Damage. *Annual Review of Microbiology*, 57(1), pp.395–418.

Imlay, J.A., Chin, S.M. & Linn, S., 1988. Toxic DNA damage by hydrogen peroxide through the Fenton reaction in vivo and in vitro. *Science*, 240(4852), pp.640–642.

Ingmundson, A. et al., 2007. Legionella pneumophila proteins that regulate Rab1 membrane cycling. *Nature*, 450(7168), pp.365–369.

Isberg, R.R., O'Connor, T.J. & Heidtman, M., 2009. The Legionella pneumophila replication vacuole: making a cosy niche inside host cells. *Nature Reviews Microbiology*, 7(1), pp.13–24.

Iwasaki, A. & Medzhitov, R., 2015. Control of adaptive immunity by the innate immune system. *Nature Immunology*, 16(4), pp.343–353.

Jabado, N. et al., 2000. Natural resistance to intracellular infections: natural resistance-associated macrophage protein 1 (Nramp1) functions as a pH-dependent manganese transporter at the phagosomal membrane. *The Journal of experimental medicine*, 192(9), pp.1237–1248.

James, K.L. et al., 2019. Interplay of Nitric Oxide Synthase (NOS) and SrrAB in Modulation of *Staphylococcus aureus* Metabolism and Virulence N. E. Freitag, ed. *Infection and Immunity*, 87(2), pp.222–20.

Janeway, C.A., 1989. Approaching the asymptote? Evolution and revolution in immunology. *Cold Spring Harbor symposia on quantitative biology*, 54 Pt 1, pp.1–13.

Jarry, T.M., Memmi, G. & Cheung, A.L., 2008. The expression of alpha-haemolysin is required for Staphylococcus aureus phagosomal escape after internalization in CFT-1 cells. *Cellular microbiology*, 10(9), pp.1801–1814.

Jenkins, M.K. et al., 2001. In vivo activation of antigen-specific CD4 T cells. *Annual review of immunology*, 19(1), pp.23–45.

Jensen, L.J. et al., 2009. STRING 8--a global view on proteins and their functional interactions in 630 organisms. *Nucleic acids research*, 37(Database issue), pp.D412–6.

Johnson, M. et al., 2011. Fur is required for the activation of virulence gene expression through the induction of the *sae* regulatory system in *Staphylococcus aureus*. *International journal of medical microbiology : IJMM*, 301(1), pp.44–52.

Jonsson, S. et al., 1985. Phagocytosis and killing of common bacterial pathogens of the lung by human alveolar macrophages. *The Journal of infectious diseases*, 152(1), pp.4–13.

Jorgensen, I. & Miao, E.A., 2015. Pyroptotic cell death defends against intracellular pathogens. *Immunological reviews*, 265(1), pp.130–142.

Jorgensen, I., Rayamajhi, M. & Miao, E.A., 2017. Programmed cell death as a defence against infection. *Nature Publishing Group*, 17(3), pp.1–14.

Josefsson, E. et al., 2001. Protection against experimental Staphylococcus aureus arthritis by vaccination with clumping factor A, a novel virulence determinant. *The Journal of infectious diseases*, 184(12), pp.1572–1580.

Jubrail, J. et al., 2016. Inability to sustain intraphagolysosomal killing of *Staphylococcus aureus* predisposes to bacterial persistence in macrophages. *Cellular microbiology*, 18(1), pp.80–96.

Jung, Y. & Rothenberg, M.E., 2014. Roles and Regulation of Gastrointestinal Eosinophils in Immunity and Disease. *Journal of immunology (Baltimore, Md. : 1950)*, 193(3), pp.999–1005.

Kahl, B.C., Becker, K. & Löffler, B., 2016. Clinical Significance and Pathogenesis of Staphylococcal Small Colony Variants in Persistent Infections. *Clinical microbiology reviews*, 29(2), pp.401–427.

Kapral, F.A. & Shayegani, M.G., 1959. Intracellular survival of staphylococci. *The Journal of experimental medicine*, 110(1), pp.123–138.

Karakawa, W.W. et al., 1988. Capsular antibodies induce type-specific phagocytosis of capsulated Staphylococcus aureus by human polymorphonuclear leukocytes. *Infection and Immunity*, 56(5), pp.1090–1095.

Karavolos, M.H., 2003. Role and regulation of the superoxide dismutases of *Staphylococcus aureus*. *Microbiology*, 149(10), pp.2749–2758.

Kawada-Matsuo, M. et al., 2014. Role of two-component systems in the resistance of *Staphylococcus aureus* to antibacterial agents. *Virulence*, 2(5), pp.427–430.

Keren, I. et al., 2004. Persister cells and tolerance to antimicrobials. *FEMS Microbiology Letters*, 230(1), pp.13–18.

Kessel, M. et al., 1995. Homology in structural organization between E. coli ClpAP protease and the eukaryotic 26 S proteasome. *Journal of molecular biology*, 250(5), pp.587–594.

Keyer, K. & Imlay, J.A., 1996. Superoxide accelerates DNA damage by elevating free-iron levels. *Proceedings of the National Academy of Sciences*, 93(24), pp.13635–13640.

Khatib, R. et al., 2006. Persistence in Staphylococcus aureus bacteremia: incidence, characteristics of patients and outcome. *Scandinavian journal of infectious diseases*, 38(1), pp.7–14.

Kinchen, J.M. et al., 2008. A pathway for phagosome maturation during engulfment of apoptotic cells. *Nature Cell Biology*, 10(5), pp.556–566.

Kinkel, T.L. et al., 2013. The *Staphylococcus aureus* SrrAB Two-Component System Promotes Resistance to Nitrosative Stress and Hypoxia M. S. Gilmore, ed. *mBio*, 4(6), pp.505–9.

Klevens, R.M. et al., 2007. Invasive methicillin-resistant Staphylococcus aureus infections in the United States. *JAMA*, 298(15), pp.1763–1771.

Klimek, J.W., Cavallito, C.J. & Bailey, J.H., 1948. Induced Resistance of Staphylococcus aureus to Various Antibiotics. *Journal of Bacteriology*, 55(2), pp.139–145.

Kloos, W.E., 1980. Natural populations of the genus Staphylococcus. *Annual Review of Microbiology*, 34(1), pp.559–592.

Klose, C.S.N. & Artis, D., 2016. Innate lymphoid cells as regulators of immunity, inflammation and tissue homeostasis. *Nature Immunology*, 17(7), pp.765–774.

Kluytmans, J., van Belkum, A. & Verbrugh, H., 1997. Nasal carriage of Staphylococcus aureus: epidemiology, underlying mechanisms, and associated risks. *Clinical microbiology reviews*, 10(3), pp.505–520.

Kondo, M., 2010. Lymphoid and myeloid lineage commitment in multipotent hematopoietic progenitors. *Immunological reviews*, 238(1), pp.37–46.

Koul, A. et al., 2007. Diarylquinolines target subunit c of mycobacterial ATP synthase. *Nature chemical biology*, 3(6), pp.323–324.

Koziel, J. et al., 2009. Phagocytosis of Staphylococcus aureus by Macrophages Exerts Cytoprotective Effects Manifested by the Upregulation of Antiapoptotic Factors A. J. Ratner, ed. *PLoS ONE*, 4(4), pp.e5210–14.

Koziel, J. et al., 2015. The Janus Face of a-Toxin: A Potent Mediator of Cytoprotection in Staphylococci-Infected Macrophages. *Journal of Innate Immunity*, 7(2), pp.187–198.

Kubica, M. et al., 2008. A Potential New Pathway for Staphylococcus aureus Dissemination: The Silent Survival of S. aureus Phagocytosed by Human Monocyte-Derived Macrophages R. May, ed. *PLoS ONE*, 3(1), pp.e1409–16.

Kuroda, M. et al., 2004. Two-component system VraSR positively modulates the regulation of cell-wall biosynthesis pathway in Staphylococcus aureus. *Molecular Microbiology*, 49(3), pp.807–821.

Kuroda, M. et al., 2001. Whole genome sequencing of meticillin-resistant Staphylococcus aureus. *The Lancet*, 357(9264), pp.1225–1240.

Kurtz, J., 2005. Specific memory within innate immune systems. *Trends in Immunology*, 26(4), pp.186–192.

Laarman, A.J. et al., 2012. Staphylococcus aureus Staphopain A inhibits CXCR2-dependent neutrophil activation and chemotaxis. *The EMBO journal*, 31(17), pp.3607–3619.

Lan, L. et al., 2010. Golden pigment production and virulence gene expression are affected by metabolisms in Staphylococcus aureus. *Journal of Bacteriology*, 192(12), pp.3068–3077.

Lanza, F., 1998. Clinical manifestation of myeloperoxidase deficiency. *Journal of Molecular Medicine*, 76(10), pp.676–681.

Lawrence, T. & Natoli, G., 2011. Transcriptional regulation of macrophage polarization: enabling diversity with identity. *Nature Publishing Group*, 11(11), pp.750–761.

Lee, L.Y.L. et al., 2004. Identification and Characterization of the C3 Binding Domain of the Staphylococcus aureus Extracellular Fibrinogen-binding Protein (Efb). *Journal of Biological Chemistry*, 279(49), pp.50710–50716.

Lehrer, R.I., Lichtenstein, A.K. & Ganz, T., 1993. Defensins: antimicrobial and cytotoxic peptides of mammalian cells. *Annual review of immunology*, 11(1), pp.105–128.

Li, M. et al., 2009. Evolution of virulence in epidemic community-associated methicillin-resistant Staphylococcus aureus. *Proceedings of the National Academy of Sciences of the United States of America*, 106(14), pp.5883–5888.

Liang, C. et al., 2016. A Staphylococcus aureus Proteome Overview: Shared and Specific Proteins and Protein Complexes from Representative Strains of All Three Clades. *Proteomes*, 4(1), pp.8–18.

Lieberman, L.A. & Hunter, C.A., 2002. Regulatory pathways involved in the infection-induced production of IFN-gamma by NK cells. *Microbes and infection*, 4(15), pp.1531–1538.

Lindsay, J.A., 2010a. Genomic variation and evolution of Staphylococcus aureus. *International Jl of Medical Microbiology*, 300(2-3), pp.98–103.

Lindsay, J.A., 2010b. Genomic variation and evolution of Staphylococcus aureus. *International Jl of Medical Microbiology*, 300(2-3), pp.98–103.

Lindsay, J.A. & Foster, S.J., 2001. zur: a Zn(2+)-responsive regulatory element of Staphylococcus aureus. *Microbiology*, 147(Pt 5), pp.1259–1266.

Lindsay, J.A. & Holden, M.T.G., 2004. Staphylococcus aureus : superbug, super genome? *Trends in Microbiology*, 12(8), pp.378–385.

Lindsay, J.A. et al., 1998. The gene for toxic shock toxin is carried by a family of mobile pathogenicity islands in Staphylococcus aureus. *Molecular Microbiology*, 29(2), pp.527–543.

Liu, G.Y. et al., 2005. *Staphylococcus aureus* golden pigment impairs neutrophil killing and promotes virulence through its antioxidant activity. *The Journal of experimental medicine*, 202(2), pp.209–215.

Liu, L. et al., 2020. Inhibition of the ATP synthase sensitizes Staphylococcus aureus towards human antimicrobial peptides. *Scientific Reports*, 10(1), pp.11391–9.

Lollike, K. et al., 1995. Lysozyme in human neutrophils and plasma. A parameter of myelopoietic activity. *Leukemia*, 9(1), pp.159–164.

Lowy, F.D., 2003. Antimicrobial resistance: the example of Staphylococcus aureus. *Journal of Clinical Investigation*, 111(9), pp.1265–1273.

Lowy, F.D., 1998. Staphylococcus aureus infections. *The New England journal of medicine*, 339(8), pp.520–532.

Machner, M.P. & Isberg, R.R., 2006. Targeting of Host Rab GTPase Function by the Intravacuolar Pathogen Legionella pneumophila. *Developmental Cell*, 11(1), pp.47–56.

Mackaness, G.B., 1962. Cellular resistance to infection. *The Journal of experimental medicine*, 116, pp.381–406.

MacMicking, J., Xie, Q.W. & Nathan, C., 1997. Nitric oxide and macrophage function. *Annual review of immunology*, 15(1), pp.323–350.

Malachowa, N. & DeLeo, F.R., 2010. Mobile genetic elements of *Staphylococcus aureus*. *Cellular and Molecular Life Sciences*, 67(18), pp.3057–3071.

Mandell, G.L., 1975. Catalase, superoxide dismutase, and virulence of Staphylococcus aureus. In vitro and in vivo studies with emphasis on staphylococcal--leukocyte interaction. *Journal of Clinical Investigation*, 55(3), pp.561–566.

Mantovani, A. et al., 2004. The chemokine system in diverse forms of macrophage activation and polarization. *Trends in Immunology*, 25(12), pp.677–686.

Mantovani, A., Sica, A. & Locati, M., 2005. Macrophage Polarization Comes of Age. *Immunity*, 23(4), pp.344–346.

Marriott, H.M. et al., 2005. Dynamic changes in Mcl-1 expression regulate macrophage viability or commitment to apoptosis during bacterial clearance. *Journal of Clinical Investigation*, 115(2), pp.359–368.

Masson, P.L., Heremans, J.F. & Schonne, E., 1969. Lactoferrin, an iron-binding protein in neutrophilic leukocytes. *The Journal of experimental medicine*, 130(3), pp.643–658.

Mazmanian, S.K. et al., 1999. Staphylococcus aureus sortase, an enzyme that anchors surface proteins to the cell wall. *Science*, 285(5428), pp.760–763.

Medzhitov, R. & Janeway, C., 2000a. Innate immune recognition: mechanisms and pathways. *Immunological reviews*, 173, pp.89–97.

Medzhitov, R. & Janeway, C., 2000b. Innate immunity. I. R. Mackay & F. S. Rosen, eds. *The New England journal of medicine*, 343(5), pp.338–344.

Mehta, S. et al., 2011. VraSR Two-Component Regulatory System Contributes to mprF-Mediated Decreased Susceptibility to Daptomycin in In Vivo-Selected Clinical Strains of

Methicillin-Resistant Staphylococcus aureus. *Antimicrobial agents and chemotherapy*, 56(1), pp.92–102.

Melly, M.A., Thomison, J.B. & Rogers, D.E., 1960. Fate of staphylococci within human leukocytes. *The Journal of experimental medicine*, 112, pp.1121–1130.

Melvin, J.A. et al., 2011. Staphylococcus aureus sortase A contributes to the Trojan horse mechanism of immune defense evasion with its intrinsic resistance to Cys184 oxidation. *Biochemistry*, 50(35), pp.7591–7599.

Michel, A. et al., 2006. Global Regulatory Impact of ClpP Protease of Staphylococcus aureus on Regulons Involved in Virulence, Oxidative Stress Response, Autolysis, and DNA Repair. *Journal of Bacteriology*, 188(16), pp.5783–5796.

Miller, L.G. et al., 2005. Necrotizing fasciitis caused by community-associated methicillin-resistant Staphylococcus aureus in Los Angeles. *The New England journal of medicine*, 352(14), pp.1445–1453.

Mills, C.D. et al., 2000. M-1/M-2 Macrophages and the Th1/Th2 Paradigm. *Journal of immunology (Baltimore, Md. : 1950)*, 164(12), pp.6166–6173.

Mitchell, P., 1961. Coupling of phosphorylation to electron and hydrogen transfer by a chemi-osmotic type of mechanism. *Nature*, 191(4784), pp.144–148.

Mokoena, T. & Gordon, S., 1985. Human macrophage activation. Modulation of mannosyl, fucosyl receptor activity in vitro by lymphokines, gamma and alpha interferons, and dexamethasone. *Journal of Clinical Investigation*, 75(2), pp.624–631.

Monecke, S. et al., 2011. A Field Guide to Pandemic, Epidemic and Sporadic Clones of Methicillin-Resistant Staphylococcus aureus P. J. Planet, ed. *PLoS ONE*, 6(4), pp.e17936–24.

Mosmann, T.R. et al., 1986. Two types of murine helper T cell clone. I. Definition according to profiles of lymphokine activities and secreted proteins. *Journal of immunology (Baltimore, Md. : 1950)*, 136(7), pp.2348–2357.

Mosser, D. & Edwards, J., 2008. Exploring the Full Spectrum of Macrophage Activation. *Nature Reviews Immunology*, 8(12), pp.958–969.

Mrak, L.N. et al., 2012. saeRS and sarA Act Synergistically to Repress Protease Production and Promote Biofilm Formation in Staphylococcus aureus N. E. Freitag, ed. *PLoS ONE*, 7(6), pp.e38453–10.

Nathan, C. & Shiloh, M.U., 2000. Reactive oxygen and nitrogen intermediates in the relationship between mammalian hosts and microbial pathogens. *Proceedings of the National Academy of Sciences*, 97(16), pp.8841–8848.

Nathan, C.F. et al., 1983. Identification of interferon-gamma as the lymphokine that activates human macrophage oxidative metabolism and antimicrobial activity. *The Journal of experimental medicine*, 158(3), pp.670–689.

Netea, M.G. et al., 2015. Innate immune memory: a paradigm shift in understanding host defense. *Nature Publishing Group*, 16(7), pp.675–679.

Netea, M.G. et al., 2016. Trained immunity: A program of innate immune memory in health and disease. *Science*, 352(6284), pp.aaf1098–aaf1098.

Nielsen, E. et al., 1999. Rab5 regulates motility of early endosomes on microtubules. *Nature Cell Biology*, 1(6), pp.376–382.

Nilsson, I.M. et al., 1997. The role of staphylococcal polysaccharide microcapsule expression in septicemia and septic arthritis. *Infection and Immunity*, 65(10), pp.4216–4221.

Nordmann, M. et al., 2010. The Mon1-Ccz1 Complex Is the GEF of the Late Endosomal Rab7 Homolog Ypt7. *CURBIO*, 20(18), pp.1654–1659.

Novick, R.P., 2003. Autoinduction and signal transduction in the regulation of staphylococcal virulence. *Molecular Microbiology*, 48(6), pp.1429–1449.

Novick, R.P., 1991. Genetic systems in staphylococci. *Methods in enzymology*, 204, pp.587–636.

Nygaard, T.K. et al., 2012. Alpha-Toxin Induces Programmed Cell Death of Human T cells, B cells, and Monocytes during USA300 Infection M. Otto, ed. *PLoS ONE*, 7(5), pp.e36532–11.

Ogston, A., 1882. Micrococcus Poisoning. *Journal of anatomy and physiology*, 17(Pt 1), pp.24–58.

Olson, M.E. et al., 2013. Staphylococcus aureus Nuclease Is an SaeRS-Dependent Virulence Factor F. C. Fang, ed. *Infection and Immunity*, 81(4), pp.1316–1324.

Ozanic, M. et al., 2015. The Divergent Intracellular Lifestyle of Francisella tularensis in Evolutionarily Distinct Host Cells V. L. Miller, ed. *PLoS Pathogens*, 11(12), pp.e1005208–8.

Palecanda, A. et al., 1999. Role of the scavenger receptor MARCO in alveolar macrophage binding of unopsonized environmental particles. *The Journal of experimental medicine*, 189(9), pp.1497–1506.

Pan, E.S. et al., 2003. Increasing prevalence of methicillin-resistant Staphylococcus aureus infection in California jails. *Clinical Infectious Diseases*, 37(10), pp.1384–1388.

Pandey, S., Sahukhal, G.S. & Elasri, M.O., 2019. The msaABCR Operon Regulates the Response to Oxidative Stress in *Staphylococcus aureus* M. J. Federle, ed. *Journal of Bacteriology*, 201(21), pp.520–20.

Panton, P.N. & Valentine, F.C.O., 1932. Staphylococcal Toxin. *The Lancet*, pp.506–508.

Patel, A.H. et al., 1987. Virulence of protein A-deficient and alpha-toxin-deficient mutants of Staphylococcus aureus isolated by allele replacement. *Infection and Immunity*, 55(12), pp.3103–3110.

Patel, R., 2005. Biofilms and Antimicrobial Resistance. *Clinical Orthopaedics and Related Research*, &NA;(437), pp.41–47.

Pelz, O., Gilsdorf, M. & Boutros, M., 2010. web cellHTS2: A web-application for the analysis of high-throughput screening data. *BMC Bioinformatics*, 11(1), pp.185–6.

Perichon, B. & Courvalin, P., 2009. VanA-Type Vancomycin-Resistant Staphylococcus aureus. *Antimicrobial agents and chemotherapy*, 53(11), pp.4580–4587.

Peschel, A., 2002. How do bacteria resist human antimicrobial peptides? *Trends in Microbiology*, 10(4), pp.179–186.

Peschel, A. & Otto, M., 2013. Phenol-soluble modulins and staphylococcal infection. *Nature Reviews Microbiology*, 11(10), pp.667–673.

Peschel, A. et al., 2001. Staphylococcus aureus resistance to human defensins and evasion of neutrophil killing via the novel virulence factor MprF is based on modification of membrane lipids with l-lysine. *The Journal of experimental medicine*, 193(9), pp.1067–1076.

Pillay, C.S., Elliott, E. & Dennison, C., 2002. Endolysosomal proteolysis and its regulation. *The Biochemical journal*, 363(Pt 3), pp.417–429.

Pizzolla, A. et al., 2012. Reactive Oxygen Species Produced by the NADPH Oxidase 2 Complex in Monocytes Protect Mice from Bacterial Infections. *The Journal of Immunology*, 188(10), pp.5003–5011.

Pollard, J.W., 2009. Trophic macrophages in development and disease. *Nature Reviews Immunology*, 9(4), pp.259–270.

Poltorak, A. et al., 1998. Defective LPS signaling in C3H/HeJ and C57BL/10ScCr mice: mutations in Tlr4 gene. *Science*, 282(5396), pp.2085–2088.

Poole, L.B., 2005. Bacterial defenses against oxidants: mechanistic features of cysteine-based peroxidases and their flavoprotein reductases. *Archives of Biochemistry and Biophysics*, 433(1), pp.240–254.

Porte, F. et al., 2003. Role of the Brucella suis Lipopolysaccharide O Antigen in Phagosomal Genesis and in Inhibition of Phagosome-Lysosome Fusion in Murine Macrophages. *Infection and Immunity*, 71(3), pp.1481–1490.

Porte, F., Liautard, J.P. & Köhler, S., 1999. Early acidification of phagosomes containing Brucella suis is essential for intracellular survival in murine macrophages. *Infection and Immunity*, 67(8), pp.4041–4047.

Powers, M.E. & Wardenburg, J.B., 2014. Igniting the Fire: Staphylococcus aureus Virulence Factors in the Pathogenesis of Sepsis J. Heitman, ed. *PLoS Pathogens*, 10(2), pp.e1003871–4.

Prajsnar, T.K. et al., 2012. A privileged intraphagocyte niche is responsible for disseminated infection of *Staphylococcus aureus* in a zebrafish model. 14(10), pp.1600–1619.

Prajsnar, T.K. et al., 2021. The autophagic response to Staphylococcus aureus provides an intracellular niche in neutrophils. *Autophagy*, 17(4), pp.888–902.

Prat, C. et al., 2006. A New Staphylococcal Anti-Inflammatory Protein That Antagonizes the Formyl Peptide Receptor-Like 1. *Journal of immunology (Baltimore, Md. : 1950)*, 177(11), pp.8017–8026.

Prévost, G. et al., 1995. Panton-Valentine leucocidin and gamma-hemolysin from Staphylococcus aureus ATCC 49775 are encoded by distinct genetic loci and have different biological activities. *Infection and Immunity*, 63(10), pp.4121–4129.

Proctor, R.A., 2012. Is there a future for a Staphylococcus aureus vaccine? *Vaccine*, 30(19), pp.2921–2927.

Proctor, R.A. et al., 2006. Small colony variants: a pathogenic form of bacteria that facilitates persistent and recurrent infections. *Nature Reviews Microbiology*, 4(4), pp.295–305.

Public Health England, 2020. UK Standards for Microbiology Investigations: Identification of *Staphylococcus* species, *Micrococcus* species and *Rothia* species. ID 07. Issue 4, May 2020, pp. 1-26.

Public Health England, 2021. Annual epidemiological commentary: Gram-negative bacteraemia, MRSA bacteraemia, MSSA bacteraemia and *C. difficile* infections, up to and including financial year April 2020 to March 2021. Sept 2021, pp. 1-96

Qazi, S.N. et al., 2001. agr expression precedes escape of internalized Staphylococcus aureus from the host endosome. *Infection and Immunity*, 69(11), pp.7074–7082.

Que, Y.-A. & Moreillon, P., 2010. *Staphylococcus aureus* (Including Staphylococcal Toxic Shock). In G. L. Mandell, J. E. Bennett, & R. Dolin, eds. *Mandell, Douglas, and Bennett's Principles and Practice of Infectious Diseases*. pp. 2543–2578.

Que, Y.-A. et al., 2005. Fibrinogen and fibronectin binding cooperate for valve infection and invasion in Staphylococcus aureusexperimental endocarditis. *The Journal of experimental medicine*, 201(10), pp.1627–1635.

Queck, S.Y. et al., 2008. RNAIII-Independent Target Gene Control by the agr Quorum-Sensing System: Insight into the Evolution of Virulence Regulation in Staphylococcus aureus. *Molecular cell*, 32(1), pp.150–158.

Rammelkamp, C.H. & Maxon, T., 1942. Resistance of *Staphylococcus aureus* to the action of penicillin. *Proc. Royal Soc. Exper. Biol. Med.*, 51, pp.386–389.

Ravetch, J.V., 1997. Fc receptors. *Current Opinion in Immunology*, 9(1), pp.121–125.

Reeves, E.P. et al., 2002. Killing activity of neutrophils is mediated through activation of proteases by K+ flux. *Nature*, 416(6878), pp.291–297.

Rehm, S.R., Gross, G.N. & Pierce, A.K., 1980. Early bacterial clearance from murine lungs. Species-dependent phagocyte response., 66(2), pp.194–199.

Renesto, P. et al., 2003. Identification and characterization of a phospholipase D-superfamily gene in rickettsiae. *The Journal of infectious diseases*, 188(9), pp.1276–1283.

Richardson, A.R., Dunman, P.M. & Fang, F.C., 2006. The nitrosative stress response of Staphylococcus aureus is required for resistance to innate immunity. *Molecular Microbiology*, 61(4), pp.927–939.

Rink, J. et al., 2005. Rab Conversion as a Mechanism of Progression from Early to Late Endosomes. *Cell*, 122(5), pp.735–749.

Robinson, C.G. & Roy, C.R., 2006. Attachment and fusion of endoplasmic reticulum with vacuoles containing Legionella pneumophila. *Cellular microbiology*, 8(5), pp.793–805.

Rogers, D.E. & Tompsett, R., 1952. The survival of staphylococci within human leukocytes. *The Journal of experimental medicine*, 95(2), pp.209–230.

Rooijakkers, S.H.M. et al., 2006. Early expression of SCIN and CHIPS drives instant immune evasion by *Staphylococcus aureus*. *Cellular microbiology*, 8(8), pp.1282–1293.

Rooijakkers, S.H.M. et al., 2005. Immune evasion by a staphylococcal complement inhibitor that acts on C3 convertases. *Nature Immunology*, 6(9), pp.920–927.

Santic, M. et al., 2008. Acquisition of the vacuolar ATPase proton pump and phagosome acidification are essential for escape of Francisella tularensis into the macrophage cytosol. *Infection and Immunity*, 76(6), pp.2671–2677.

Sato, T.K. et al., 2000. Class C Vps protein complex regulates vacuolar SNARE pairing and is required for vesicle docking/fusion. *Molecular cell*, 6(3), pp.661–671.

Schindelin, J. et al., 2012. Fiji: an open-source platform for biological-image analysis. *Nature Methods*, 9(7), pp.676–682.

Schneider, C.A., Rasband, W.S. & Eliceiri, K.W., 2012. NIH Image to ImageJ: 25 years of image analysis. *Nature Methods*, 9(7), pp.671–675.

Schroder, K., 2003. Interferon-γ : an overview of signals, mechanisms and functions. *Journal of Leukocyte Biology*, 75(2), pp.163–189.

Schurig-Briccio, L.A. et al., 2014. Characterization of the type 2 NADH:menaquinone oxidoreductases from Staphylococcus aureus and the bactericidal action of phenothiazines. *BBA - Bioenergetics*, 1837(7), pp.954–963.

Scott, C.C., Botelho, R.J. & Grinstein, S., 2003. Phagosome Maturation: A Few Bugs in the System. *Journal of Membrane Biology*, 193(3), pp.137–152.

Serbina, N.V. et al., 2008. Monocyte-Mediated Defense Against Microbial Pathogens. *Annual review of immunology*, 26(1), pp.421–452.

Seybold, U. et al., 2006. Emergence of community-associated methicillin-resistant Staphylococcus aureus USA300 genotype as a major cause of health care-associated blood stream infections. *Clinical Infectious Diseases*, 42(5), pp.647–656.

Sharma-Kuinkel, B.K. et al., 2009. The Staphylococcus aureus LytSR Two-Component Regulatory System Affects Biofilm Formation. *Journal of Bacteriology*, 191(15), pp.4767–4775.

Shaughnessy, L.M. et al., 2006. Membrane perforations inhibit lysosome fusion by altering pH and calcium in Listeria monocytogenes vacuoles. *Cellular microbiology*, 8(5), pp.781–792.

Shaw, L.N. et al., 2006. Investigations into sigmaB-modulated regulatory pathways governing extracellular virulence determinant production in Staphylococcus aureus. *Journal of Bacteriology*, 188(17), pp.6070–6080.

Silhavy, T.J., Kahne, D. & Walker, S., 2010. The Bacterial Cell Envelope. *Cold Spring Harbor Perspectives in Biology*, 2(5), pp.a000414–a000414.

Skinner, D. & Keefer, C.S., 1941. Significance of Bacteremia Cause by *Staphylococcus aureus*. *Archives of internal medicine*, 68(5), pp.851–875.

Slifka, M.K. & Ahmed, R., 1998. Long-lived plasma cells: a mechanism for maintaining persistent antibody production. *Current Opinion in Immunology*, 10(3), pp.252–258.

Sokolovska, A. et al., 2013. Activation of caspase-1 by the NLRP3 inflammasome regulates the NADPH oxidase NOX2 to control phagosome function. *Nature Immunology*, 14(6), pp.543–553.

Sousa, F.L. et al., 2012. The superfamily of heme-copper oxygen reductases: types and evolutionary considerations. *Biochimica et biophysica acta*, 1817(4), pp.629–637.

Spaan, A.N. et al., 2013. Neutrophils Versus Staphylococcus aureus: A Biological Tug of War. *Annual Review of Microbiology*, 67(1), pp.629–650.

Spaan, A.S.N. et al., 2013. The Staphylococcal Toxin Panton-Valentine Leukocidin Targets Human C5a Receptors. *Cell Host and Microbe*, 13(5), pp.584–594.

Spaulding, A.R. et al., 2012. Comparison of Staphylococcus aureus strains for ability to cause infective endocarditis and lethal sepsis in rabbits. *Frontiers in cellular and infection microbiology*, 2, p.18.

Sperandio, B., Fischer, N. & Sansonetti, P.J., 2015. Mucosal physical and chemical innate barriers: Lessons from microbial evasion strategies. *Seminars in Immunology*, 27(2), pp.111–118.

Spits, H., Bernink, J.H. & Lanier, L., 2016. NK cells and type 1 innate lymphoid cells: partners in host defense. *Nature Immunology*, 17(7), pp.758–764.

Stein, M. et al., 1992. Interleukin 4 potently enhances murine macrophage mannose receptor activity: a marker of alternative immunologic macrophage activation. *The Journal of experimental medicine*, 176(1), pp.287–292.

Steinman, R.M., Lustig, D.S. & Cohn, Z.A., 1974. Identification of a novel cell type in peripheral lymphoid organs of mice. 3. Functional properties in vivo. *The Journal of experimental medicine*, 139(6), pp.1431–1445.

Stevens, E. et al., 2017. Cytolytic toxin production by Staphylococcus aureus is dependent upon the activity of the protoheme IX farnesyltransferase. *Scientific Reports*, pp.1–9.

Stone, K.D., MD, C.P. & MD, D.D.M., 2010. IgE, mast cells, basophils, and eosinophils. *Journal of Allergy and Clinical Immunology*, 125(S2), pp.S73–S80.

Stout, R.D. & Bottomly, K., 1989. Antigen-specific activation of effector macrophages by IFN-gamma producing (TH1) T cell clones. Failure of IL-4-producing (TH2) T cell clones to activate effector function in macrophages. *Journal of immunology (Baltimore, Md. : 1950)*, 142(3), pp.760–765.

Strauss-Ayali, D., Conrad, S.M. & Mosser, D.M., 2007. Monocyte subpopulations and their differentiation patterns during infection. *Journal of Leukocyte Biology*, 82(2), pp.244–252.

Summers, C. et al., 2010. Neutrophil kinetics in health and disease. *Trends in Immunology*, 31(8), pp.318–324.

Sun, F. et al., 2011. AirSR, a [2Fe-2S] Cluster-Containing Two-Component System, Mediates Global Oxygen Sensing and Redox Signaling in Staphylococcus aureus. *Journal of the American Chemical Society*, 134(1), pp.305–314.

Surewaard, B.G.J. & Kubes, P., 2017. Measurement of bacterial capture and phagosome maturation of Kupffer cells by intravital microscopy. *Methods*, pp.1–8.

Surewaard, B.G.J. et al., 2016. Identification and treatment of the Staphylococcus aureus reservoir in vivo. *The Journal of experimental medicine*, 213(7), pp.1141–1151.

Surewaard, B.G.J. et al., 2013. Staphylococcal alpha-phenol soluble modulins contribute to neutrophil lysis after phagocytosis. 15(8), pp.1427–1437.

Svensson, B., Lübben, M. & Hederstedt, L., 1993. Bacillus subtilis CtaA and CtaB function in haem A biosynthesis. *Molecular Microbiology*, 10(1), pp.193–201.

Swanson, J.A. & Watts, C., 1995. Macropinocytosis. *Trends in Cell Biology*, 5(11), pp.424–428.

Sward, E.W. et al., 2017. *Staphylococcus aureus* SaeR/S-regulated Factors Decrease Monocyte-derived TNF-α to Reduce Neutrophil Bactericidal Activity. *The Journal of infectious diseases*, 217(6), pp.943–952.

Swirski, F.K. et al., 2009. Identification of Splenic Reservoir Monocytes and Their Deployment to Inflammatory Sites. *Science*, 325(5940), pp.612–616.

Takeuchi, O. & Akira, S., 2010. Pattern Recognition Receptors and Inflammation. *Cell*, 140(6), pp.805–820.

Tauber, A.I., 2003. *Metchnikoff and the phagocytosis theory*,

Taylor, P.R. & Gordon, S., 2003. Monocyte Heterogeneity and Innate Immunity. *Immunity*, 19(1), pp.2–4.

Taylor, R.C., Cullen, S.P. & Martin, S.J., 2008. Apoptosis: controlled demolition at the cellular level. *Nature Reviews Molecular Cell Biology*, 9(3), pp.231–241.

Thöny-Meyer, L., 1997. Biogenesis of respiratory cytochromes in bacteria. *Microbiology and Molecular Biology Reviews*, 61(3), pp.337–376.

Thwaites, G.E. & Gant, V., 2011. Are bloodstream leukocytes Trojan Horses for the metastasis of Staphylococcus aureus? *Nature Publishing Group*, 9(3), pp.215–222.

Thwaites, G.E. et al., 2011. Clinical management of Staphylococcus aureus bacteraemia. *The Lancet Infectious Diseases*, 11(3), pp.208–222.

Thwaites, G. E. et al., 2018. Adjunctive rifampicin for *Staphylococcus aureus* bacteraemia (ARREST): a multicentre, randomised, double-blind, placebo-controlled trial. *Lancet*, 391(10121), pp.668-678.

Tilney, L.G. et al., 2001. How the parasitic bacterium Legionella pneumophila modifies its phagosome and transforms it into rough ER: implications for conversion of plasma membrane to the ER membrane. *Journal of Cell Science*, 114(Pt 24), pp.4637–4650.

Tram, T.T.B. et al., 2020. Variations in Antimicrobial Activities of Human Monocyte-Derived Macrophage and Their Associations With Tuberculosis Clinical Manifestations. *Frontiers in cellular and infection microbiology*, 10, p.586101.

Tranchemontagne, Z.R. et al., 2015. Staphylococcus aureus Strain USA300 Perturbs Acquisition of Lysosomal Enzymes and Requires Phagosomal Acidification for Survival inside Macrophages C. R. Roy, ed. *Infection and Immunity*, 84(1), pp.241–253.

Tsuchiya, S. et al., 1980. Establishment and characterization of a human acute monocytic leukemia cell line (THP-1). *International journal of cancer*, 26(2), pp.171–176.

Van Bambeke, F. et al., 2006. Cellular pharmacodynamics and pharmacokinetics of antibiotics: current views and perspectives. *Current opinion in drug discovery & development*, 9(2), pp.218–230.

Van de Velde, H., 1894. Etude sur le mécanisme de la virulence du staphylocoque pyogène. *La Cellule*.

van der Meer, J.W.M. et al., 2015. Trained immunity: A smart way to enhance innate immune defence. *Molecular Immunology*, 68(1), pp.40–44.

van der Wel, N. et al., 2007. *M. tuberculosis* and *M. leprae* Translocate from the Phagolysosome to the Cytosol in Myeloid Cells. *Cell*, 129(7), pp.1287–1298.

Van Furth, R. & Cohn, Z.A., 1968. The origin and kinetics of mononuclear phagocytes. *The Journal of experimental medicine*, 128(3), pp.415–435.

Van Furth, R. & Sluiter, W., 1986. Distribution of blood monocytes between a marginating and a circulating pool. *The Journal of experimental medicine*, 163(2), pp.474–479.

Velayudhan, J. et al., 2007. The role of ferritins in the physiology of Salmonella enterica sv. Typhimurium: a unique role for ferritin B in iron-sulphur cluster repair and virulence. *Molecular Microbiology*, 63(5), pp.1495–1507.

Vergne, I. et al., 2005. Mechanism of phagolysosome biogenesis block by viable Mycobacterium tuberculosis. *Proceedings of the National Academy of Sciences*, 102(11), pp.4033–4038.

Verreck, F.A.W. et al., 2004. Human IL-23-producing type 1 macrophages promote but IL-10-producing type 2 macrophages subvert immunity to (myco)bacteria. *Proceedings of the National Academy of Sciences*, 101(13), pp.4560–4565.

Vestergaard, M. et al., 2017. Inhibition of the ATP Synthase Eliminates the Intrinsic Resistance of Staphylococcus aureustowards Polymyxins F. Baquero & G. B. Pier, eds. *mBio*, 8(5), pp.1206–10.

Voth, D.E. & Heinzen, R.A., 2007. Lounging in a lysosome: the intracellular lifestyle of Coxiella burnetii. *Cellular microbiology*, 9(4), pp.829–840.

Voyich, J.M. et al., 2005. Insights into Mechanisms Used by Staphylococcus aureus to Avoid Destruction by Human Neutrophils. *The Journal of Immunology*, 175(6), pp.3907–3919.

Voyich, J.M. et al., 2006. Is Panton-Valentine leukocidin the major virulence determinant in community-associated methicillin-resistant Staphylococcus aureus disease? *The Journal of infectious diseases*, 194(12), pp.1761–1770.

Voyich, J.M. et al., 2009. The SaeR/S gene regulatory system is essential for innate immune evasion by Staphylococcus aureus. *The Journal of infectious diseases*, 199(11), pp.1698–1706.

Voyich, J.M., Sturdevant, D.E. & DeLeo, F.R., 2008. Analysis of Staphylococcus aureus gene expression during PMN phagocytosis. *Methods in molecular biology (Clifton, N.J.)*, 431, pp.109–122.

Wachenfeldt, von, C. & Hederstedt, L., 2002. Respiratory Cytochromes, Other Heme Proteins, and Heme Biosynthesis. In *Bacillus subtilis and its Closest Relatives from Genes to Cells*. pp. 163–179.

Wade, N. et al., 2001. Syntaxin 7 Complexes with Mouse Vps10p Tail Interactor 1b, Syntaxin 6, Vesicle-associated Membrane Protein (VAMP)8, and VAMP7 in B16 Melanoma Cells. *Journal of Biological Chemistry*, 276(23), pp.19820–19827.

Wakeman, C.A. et al., 2014. Differential Activation of Staphylococcus aureus Heme Detoxification Machinery by Heme Analogues. *Journal of Bacteriology*, 196(7), pp.1335–1342.

Walker, J.A., Barlow, J.L. & McKenzie, A.N.J., 2013. Innate lymphoid cells — how did we miss them? *Nature Reviews Immunology*, 13(2), pp.75–87.

Wang, R. et al., 2007. Identification of novel cytolytic peptides as key virulence determinants for community-associated MRSA. *Nature Medicine*, 13(12), pp.1510–1514.

Watson, K. et al., 2020. Developing Novel Host-Based Therapies Targeting Microbicidal Responses in Macrophages and Neutrophils to Combat Bacterial Antimicrobial Resistance. *Frontiers in Immunology*, 11, pp.786-798.

Wertheim, H.F. et al., 2005. The role of nasal carriage in Staphylococcus aureus infections. *The Lancet Infectious Diseases*, 5(12), pp.751–762.

Wesson, C.A. et al., 1998. Staphylococcus aureus Agr and Sar global regulators influence internalization and induction of apoptosis. *Infection and Immunity*, 66(11), pp.5238–5243.

Wheeler, R. et al., 2015. Bacterial Cell Enlargement Requires Control of Cell Wall Stiffness Mediated by Peptidoglycan Hydrolases. *mBio*, 6(4), p.e00660.

White, D.C. & Frerman, F.E., 1967. Extraction, characterization, and cellular localization of the lipids of Staphylococcus aureus. *Journal of Bacteriology*, 94(6), pp.1854–1867.

Wilde, A.D. et al., 2015. Bacterial Hypoxic Responses Revealed as Critical Determinants of the Host-Pathogen Outcome by TnSeq Analysis of Staphylococcus aureus Invasive Infection M. Otto, ed. *PLoS Pathogens*, 11(12), pp.e1005341–24.

Witko-Sarsat, V. et al., 2000. Neutrophils: molecules, functions and pathophysiological aspects. *Laboratory investigation; a journal of technical methods and pathology*, 80(5), pp.617–653.

Wolf, A.J. et al., 2011. Phagosomal Degradation Increases TLR Access to Bacterial Ligands and Enhances Macrophage Sensitivity to Bacteria. *Journal of immunology (Baltimore, Md. : 1950)*, 187(11), pp.6002–6010.

Wong, D. et al., 2011. Mycobacterium tuberculosis protein tyrosine phosphatase (PtpA) excludes host vacuolar-H+-ATPase to inhibit phagosome acidification. *Proceedings of the National Academy of Sciences of the United States of America*, 108(48), pp.19371–19376.

Wong, P. & Pamer, E.G., 2003. CD8 T Cell Responses to Infectious Pathogens. *Annual review of immunology*, 21(1), pp.29–70.

Wright, S.D. & Silverstein, S.C., 1983. Receptors for C3b and C3bi promote phagocytosis but not the release of toxic oxygen from human phagocytes. *The Journal of experimental medicine*, 158(6), pp.2016–2023.

Wyllie, D.H., Crook, D.W. & Peto, T.E.A., 2006. Mortality after Staphylococcus aureus bacteraemia in two hospitals in Oxfordshire, 1997-2003: cohort study. *BMJ (Clinical research ed.)*, 333(7562), pp.281–0.

Wynn, T.A., Chawla, A. & Pollard, J.W., 2013. Macrophage biology in development, homeostasis and disease. *Nature*, 496(7446), pp.445–455.

Xu, L. et al., 2010. Inhibition of host vacuolar H+-ATPase activity by a Legionella pneumophila effector. *PLoS Pathogens*, 6(3), p.e1000822.

Xu, T. et al., 2016. Absence of Protoheme IX Farnesyltransferase CtaB Causes Virulence Attenuation but Enhances Pigment Production and Persister Survival in MRSA. *Frontiers in microbiology*, 7, p.1625.

Yang, D., 2018. *Identifying novel immune modulating factors in a genome-wide Staphylococcus aureus screen in human neutrophils*.

Yang, D. et al., 2019. A Genome-Wide Screen Identifies Factors Involved in *S. aureus*-Induced Human Neutrophil Cell Death and Pathogenesis. *Frontiers in immunology*, 10, pp.318–11.

Yang, S.-J. et al., 2012. The *Staphylococcus aureus* Two-Component Regulatory System, GraRS, Senses and Confers Resistance to Selected Cationic Antimicrobial Peptides J. N. Weiser, ed. *Infection and Immunity*, 80(1), pp.74–81.

Yang, T. et al., 1996. MCL-1, a member of the BLC-2 family, is induced rapidly in response to signals for cell differentiation or death, but not to signals for cell proliferation. *Journal of Cellular Physiology*, 166(3), pp.523–536.

Yeo, W.-S. et al., 2018. The FDA-approved anti-cancer drugs, streptozotocin and floxuridine, reduce the virulence of Staphylococcus aureus. *Scientific Reports*, pp.1–10.

Yona, S. et al., 2013. Fate Mapping Reveals Origins and Dynamics of Monocytes and Tissue Macrophages under Homeostasis. *Immunity*, 38(1), pp.79–91.

Yoong, P. & Torres, V.J., 2013. The effects of Staphylococcus aureus leukotoxins on the host: cell lysis and beyond. *Current Opinion in Microbiology*, 16(1), pp.63–69.

Zanetti, M., 2005. The role of cathelicidins in the innate host defenses of mammals. *Current issues in molecular biology*, 7(2), pp.179–196.

Zasloff, M., 2002. Antimicrobial peptides of multicellular organisms. *Nature*, 415(6870), pp.389–395.

Zerial, M. & McBride, H., 2001. Rab proteins as membrane organizers. *Nature Reviews Molecular Cell Biology*, 2(2), pp.107–117.

Zetola, N. et al., 2005. Community-acquired meticillin-resistant Staphylococcus aureus: an emerging threat. *The Lancet Infectious Diseases*, 5(5), pp.275–286.

Zheng, M. et al., 1999. OxyR and SoxRS regulation of fur. *Journal of Bacteriology*, 181(15), pp.4639–4643.

Zhu, J. & Paul, W.E., 2008. CD4 T cells: fates, functions, and faults. *Blood*, 112(5), pp.1557–1569.

Appendix

Table 7.1 Nebraska transposon mutant library strains used in this study

All NE strains contain Tn *bursa aurealis*

Strain name	Accession number	Plate	Well	Gene name	Gene description
NE1	SAUSA300_1327	1A	A1		cell surface protein
NE2	SAUSA300_1509	1A	A2		peptidase, rhomboid family
NE3	SAUSA300_1733	1A	A3		conserved hypothetical protein
NE4	SAUSA300_0309	1A	A4		ABC transporter ATP-binding protein
NE5	SAUSA300_2539	1A	A5		aminotransferase
NE6	SAUSA300_2258	1A	A6		formate dehydrogenase, alpha subunit
NE7	SAUSA300_1425	1A	A7		conserved hypothetical phage protein
NE8	SAUSA300_1481	1A	A8		putative membrane protein
NE9	SAUSA300_1294	1A	A9		conserved hypothetical protein
NE10	SAUSA300_2129	1A	A10		putative hemolysin III
NE11	SAUSA300_1592	1A	A11	recJ	single-stranded-DNA-specific exonuclease RecJ
NE12	SAUSA300_2126	1A	A12		drug resistance transporter, EmrB/QacA subfamily
NE13	SAUSA300_0264	1A	B1		ribose transporter RbsU
NE14	SAUSA300_2406	1A	B2		putative transporter
NE15	SAUSA300_2509	1A	B3		transcriptional regulator, TetR family
NE16	SAUSA300_2221	1A	B4	moaD	molybdopterin converting factor, subunit 1
NE17	SAUSA300_1705	1A	B5		putative drug transporter
NE18	SAUSA300_1851	1A	B6		putative membrane protein
NE19	SAUSA300_0369	1A	B7		conserved hypothetical protein
NE20	SAUSA300_0238	1A	B8		transcriptional antiterminator, BglG family
NE21	SAUSA300_2066	1A	B9	upp	uracil phosphoribosyltransferase
NE22	SAUSA300_1636	1A	B10	polA	DNA polymerase I superfamily
NE23	SAUSA300_0740	1A	B11		conserved hypothetical protein
NE24	SAUSA300_2503	1A	B12		secretory antigen precursor SsaA
NE25	SAUSA300_1905	1A	C1		conserved hypothetical protein
NE26	SAUSA300_0224	1A	C2	coa	staphylocoagulase precursor
NE27	SAUSA300_1895	1A	C3		nitric oxide synthase oxygenase
NE28	SAUSA300_0947	1A	C4		hydrolase, alpha/beta hydrolase fold family
NE29	SAUSA300_0512	1A	C5		PIN domain protein
NE30	SAUSA300_0600	1A	C6		hydrolase, haloacid dehalogenase-like family
NE31	SAUSA300_2093	1A	C7		conserved hypothetical protein
NE32	SAUSA300_0095	1A	C8		transcriptional regulator, LysR family domain protein
NE33	SAUSA300_2589	1A	C9		LPXTG-motif cell wall surface anchor family protein
NE34	SAUSA300_2313	1A	C10		L-lactate permease
NE35	SAUSA300_1264	1A	C11	trpD	anthranilate phosphoribosyltransferase
NE36	SAUSA300_2528	1A	C12		conserved hypothetical protein
NE37	SAUSA300_2600	1A	D1	icaA	intercellular adhesion protein A
NE38	SAUSA300_2254	1A	D2		similar to glycerate dehydrogenase
NE39	SAUSA300_2476	1A	D3	ptsG	phosphotransferase system, glucose-specific IIABC component
NE40	SAUSA300_1174	1A	D4		conserved hypothetical protein
NE41	SAUSA300_1979	1A	D5		cation transport family protein
NE42	SAUSA300_2212	1A	D6		conserved hypothetical protein
NE43	SAUSA300_2242	1A	D7	ureF	urease accessory protein UreF
NE44	SAUSA300_1300	1A	D8	brnQ	branched-chain amino acid transport system II carrier protein

NE45	SAUSA300_2587	1A	D9		accessory secretory protein Asp1
NE46	SAUSA300_1930	1A	D10		phi77 ORF001-like protein, phage tail tape measure protein
NE47	SAUSA300_1393	1A	D11		phiSLT ORF2067-like protein, phage tail tape measure protein
NE48	SAUSA300_0210	1A	D12		maltose ABC transporter, permease protein
NE49	SAUSA300_0217	1A	E1		DNA-binding response regulator, AraC family
NE50	SAUSA300_0935	1A	E2		conserved hypothetical protein
NE51	SAUSA300_1707	1A	E3		conserved hypothetical protein
NE52	SAUSA300_2394	1A	E4		conserved hypothetical protein
NE53	SAUSA300_2421	1A	E5		conserved hypothetical protein
NE54	SAUSA300_2375	1A	E6		ABC transporter, ATP-binding/permease protein
NE55	SAUSA300_0319	1A	E7		putative membrane protein
NE56	SAUSA300_1702	1A	E8		cell wall surface anchor family protein
NE57	SAUSA300_0771	1A	E9		acetyltransferase, GNAT family
NE58	SAUSA300_2551	1A	E10	nrdD	anaerobic ribonucleotide reductase, large subunit
NE59	SAUSA300_0404	1A	E11		exotoxin
NE60	SAUSA300_0434	1A	E12	metB	cystathionine gamma-synthase
NE61	SAUSA300_2150	1A	F1	lacE	PTS system, lactose-specific IIBC componen
NE62	SAUSA300_0794	1A	F2		Toprim domain protein
NE63	SAUSA300_1456	1A	F3		alpha glucosidase
NE64	SAUSA300_1781	1A	F4	hemG	protoporphyrinogen oxidase
NE65	SAUSA300_0233	1A	F5		conserved hypothetical protein
NE66	SAUSA300_2584	1A	F6		preprotein translocase, secA protein
NE67	SAUSA300_2573	1A	F7	isaB	immunodominant antigen B
NE68	SAUSA300_0620	1A	F8		ABC transporter ATP-binding protein
NE69	SAUSA300_1771	1A	F9		conserved hypothetical protein
NE70	SAUSA300_0648	1A	F10		ABC transporter, permease protein
NE71	SAUSA300_0640	1A	F11		putative membrane protein
NE72	SAUSA300_2504	1A	F12		acyltransferase
NE73	SAUSA300_2354	1A	G1		putative lipoprotein
NE74	SAUSA300_0828	1A	G2		5-nucleotidase family protein
NE75	SAUSA300_2597	1A	G3	cap1B	capsular polysaccharide biosynthesis protein Cap1B
NE76	SAUSA300_2011	1A	G4	leuB	3-isopropylmalate dehydrogenase
NE77	SAUSA300_0465	1A	G5	1	conserved hypothetical protein
NE78	SAUSA300_0104	1A	G6		transcriptional regulator, AraC family
NE79	SAUSA300_2148	1A	G7		conserved hypothetical protein
NE80	SAUSA300_1189	1A	G8	mutL	DNA mismatch repair protein mutL
NE81	SAUSA300_2285	1A	G9	galM	aldose 1-epimerase
NE82	SAUSA300_2472	1A	G10		putative membrane protein
NE83	SAUSA300_1980	1A	G11		acetyltransferase, GNAT family
NE84	SAUSA300_0741	1A	G12	uvrB	excinuclease ABC, B subunit
NE85	SAUSA300_2149	1A	H1	lacG	6-phospho-beta-galactosidase
NE86	SAUSA300_2085	1A	H2		conserved hypothetical protein
NE87	SAUSA300_1523	1A	H3		conserved hypothetical protein
NE88	SAUSA300_0045	1A	H4		HNH endonuclease family protein
NE89	SAUSA300_0128	1A	H5		conserved hypothetical protein
NE90	SAUSA300_1317	1A	H6	msrA	methionine-S-sulfoxide reductase
NE91	SAUSA300_2034	1A	H7	kdpA	K+-transporting ATPase, A subunit
NE92	SAUSA300_0963	1A	H8	qoxA	quinol oxidase, subunit II
NE93	SAUSA300_2001	1A	H9		similar to DNA mismatch repair protein
NE94	SAUSA300_1802	1A	H10		conserved hypothetical protein
NE95	SAUSA300_1989	1A	H11	agrB	accessory gene regulator protein B

NE96	SAUSA300_2438	1A	H12	sarU	staphylococcal accessory regulator U
NE97	SAUSA300_2130	1B	A1		UTP-glucose-1-phosphate uridylyltransferase family protein
NE98	SAUSA300_0548	1B	A2		sdrE protein
NE99	SAUSA300_1448	1B	A3		transcriptional regulator, Fur family
NE100	SAUSA300_1482	1B	A4		FtsK/SpoIIIE family protein
NE101	SAUSA300_0245	1B	A5		2-C-methyl-D-erythritol 4-phosphate cytidylyltransferase
NE102	SAUSA300_2568	1B	A6		arginine/ornithine antiporter
NE103	SAUSA300_2612	1B	A7		ATP phosphoribosyltransferase hisG
NE104	SAUSA300_0641	1B	A8		putative lipase/esterase
NE105	SAUSA300_0550	1B	A9		glycosyl transferase, group 1 family protein
NE106	SAUSA300_0863	1B	A10		argininosuccinate lyase
NE107	SAUSA300_1785	1B	A11		putative ABC transporter protein EcsB
NE108	SAUSA300_0700	1B	A12		conserved hypothetical protein
NE109	SAUSA300_1668	1B	B1		OsmC/Ohr family protein
NE110	SAUSA300_0110	1B	B2		transcriptional regulator, GntRfamily/aminotransferase, class I
NE111	SAUSA300_0883	1B	B3		putative surface protein
NE112	SAUSA300_0194	1B	B4		sucrose-specific PTS transporter protein
NE113	SAUSA300_1041	1B	B5		conserved hypothetical protein
NE114	SAUSA300_0151	1B	B6	adhE	alcohol dehydrogenase, iron-containing
NE115	SAUSA300_0105	1B	B7		peptidase, M20/M25/M40 family
NE116	SAUSA300_1219	1B	B8		putative sensor histidine kinase
NE117	SAUSA300_0986	1B	B9		cytochrome D ubiquinol oxidase, subunit I
NE118	SAUSA300_1986	1B	B10		nitroreductase family protein
NE119	SAUSA300_0181	1B	B11		non-ribosomal peptide synthetase
NE120	SAUSA300_0341	1B	B12		putative membrane protein
NE121	SAUSA300_0207	1B	C1		conserved hypothetical protein
NE122	SAUSA300_0055	1B	C2		alcohol dehydrogenase, zinc-containing
NE123	SAUSA300_0977	1B	C3		cobalt transport family protein
NE124	SAUSA300_0044	1B	C4		metallo-beta-lactamase family protein
NE125	SAUSA300_0246	1B	C5		2-C-methyl-D-erythritol 4-phosphate cytidylyltransferase
NE126	SAUSA300_2396	1B	C6		para-nitrobenzyl esterase
NE127	SAUSA300_0656	1B	C7		conserved hypothetical protein
NE128	SAUSA300_2458	1B	C8		glyoxylase family protein
NE129	SAUSA300_1547	1B	C9		DNA internalization-related competence protein ComEC/Rec2
NE130	SAUSA300_1560	1B	C10		conserved hypothetical protein
NE131	SAUSA300_1415	1B	C11		phiSLT ORF 77-like protein
NE132	SAUSA300_2640	1B	C12		putative transcriptional regulator
NE133	SAUSA300_0464	1B	D1		Methyltransferase
NE134	SAUSA300_2114	1B	D2		arginase
NE135	SAUSA300_0153	1B	D3	cap5B	capsular polysaccharide biosynthesis protein Cap5B
NE136	SAUSA300_1805	1B	D4		RNA methyltransferase
NE137	SAUSA300_0168	1B	D5		conserved hypothetical protein
NE138	SAUSA300_0275	1B	D6		putative membrane protein
NE139	SAUSA300_2374	1B	D7		ABC transporter, ATP-binding/permease protein
NE140	SAUSA300_1440	1B	D8		conserved hypothetical protein
NE141	SAUSA300_2645	1B	D9	gidB	glucose-inhibited division protein B
NE142	SAUSA300_1252	1B	D10		amino acid carrier protein
NE143	SAUSA300_1301	1B	D11		conserved hypothetical protein
NE144	SAUSA300_0139	1B	D12		putative tetracycline resistance protein
NE145	SAUSA300_0742	1B	E1	uvrA	excinuclease ABC, A subunit
NE146	SAUSA300_0718	1B	E2		iron compound ABC transporter, permease

NE147	SAUSA300_0254	1B	E3		sensor histidine kinase
NE148	SAUSA300_0283	1B	E4		essC protein
NE149	SAUSA300_2075	1B	E5	rho	transcription termination factor Rho
NE150	SAUSA300_0097	1B	E6		conserved hypothetical protein
NE151	SAUSA300_1928	1B	E7		phi77 ORF109-like protein
NE152	SAUSA300_2208	1B	E8	topB	DNA topoisomerase III
NE153	SAUSA300_1807	1B	E9		amino acid ABC transporter, ATP-binding protein
NE154	SAUSA300_2385	1B	E10		putative membrane protein
NE155	SAUSA300_0779	1B	E11		conserved hypothetical protein
NE156	SAUSA300_0351	1B	E12		putative membrane protein
NE157	SAUSA300_0678	1B	F1		putative membrane protein
NE158	SAUSA300_2138	1B	F2		conserved hypothetical protein
NE159	SAUSA300_0935	1B	F3		Conserved hypothetical protein
NE160	SAUSA300_2371	1B	F4	bioB	biotin synthase
NE161	SAUSA300_0812	1B	F5		conserved hypothetical protein
NE162	SAUSA300_0559	1B	F6		putative substrate--CoA ligase
NE163	SAUSA300_2572	1B	F7	aur	zinc metalloproteinase aureolysin
NE164	SAUSA300_1800	1B	F8		ribosomal large subunit pseudouridine synthase, RluD subfamily
NE165	SAUSA300_0114	1B	F9		staphylococcal accessory regulator
NE166	SAUSA300_0230	1B	F10		putative membrane protein
NE167	SAUSA300_1939	1B	F11		phi77 ORF015-like protein, putative protease / phage portal protein
NE168	SAUSA300_1276	1B	F12	opp-2B	peptide ABC transporter, permease protein / oligopeptide permease, channel-forming protein
NE169	SAUSA300_0167	1B	G1	cap5P	capsular polysaccharide biosynthesis protein Cap5P
NE170	SAUSA300_0745	1B	G2		putative acetyltransferase
NE171	SAUSA300_1927	1B	G3		phi77 ORF109-like protein / phi77 ORF002-like protein, phage minor structural protein
NE172	SAUSA300_0191	1B	G4	ptsG	PTS system, glucose-specific IIBC component domain protein
NE173	SAUSA300_0734	1B	G5		putative comf operon protein 1
NE174	SAUSA300_1265	1B	G6	trpC	N-(5'phosphoribosyl)anthranilate isomerase
NE175	SAUSA300_0132	1B	G7		glycosyl transferase, group 1 family protein
NE176	SAUSA300_0676	1B	G8		anion transporter family protein
NE177	SAUSA300_2448	1B	G9		putative membrane protein
NE178	SAUSA300_0879	1B	G10		isopropylmalate synthase-related protein
NE179	SAUSA300_2360	1B	G11		multidrug resistance protein
NE180	SAUSA300_2403	1B	G12		putative lipoprotein
NE181	SAUSA300_1936	1B	H1		conserved hypothetical phage protein
NE182	SAUSA300_1802	1B	H2		Conserved hypothetical protein
NE183	SAUSA300_2254	1B	H3		glycerate dehydrogenase-like protein
NE184	SAUSA300_1533	1B	H4		conserved hypothetical protein
NE185	SAUSA300_0122	1B	H5		siderophore biosynthesis protein, IucA/IucC family
NE186	SAUSA300_2441	1B	H6	fnbA	fibronectin binding protein A
NE187	SAUSA300_0650	1B	H7		phosphate transporter family protein
NE188	SAUSA300_0481	1B	H8	mfd	transcription-repair coupling factor
NE189	SAUSA300_1571	1B	H9		O-methyltransferase family protein
NE190	SAUSA300_2428	1B	H10		staphylococcal tandem lipoprotein
NE191	SAUSA300_0965	1B	H11		methylenetetrahydrofolate dehydrogenase/methenyltetrahydrofolate cyclohydrolase
NE192	SAUSA300_2520	1B	H12		transporter gate domain protein
NE193	SAUSA300_1059	1C	A1		putative exotoxin 1
NE194	SAUSA300_0206	1C	A2		flavodoxin family protein
NE195	SAUSA300_1278	1C	A3	pepF	oligoendopeptidase F

NE196	SAUSA300_0466	1C	A4		conserved hypothetical protein
NE197	SAUSA300_2383	1C	A5		amino acid permease
NE198	SAUSA300_1655	1C	A6	ald	alanine dehydrogenase
NE199	SAUSA300_2099	1C	A7		cation efflux family protein
NE200	SAUSA300_2134	1C	A8		iron compound ABC transporter, permease protein
NE201	SAUSA300_1438	1C	A9		phiSLT ORF401-like protein, integrase
NE202	SAUSA300_1902	1C	A10		conserved hypothetical protein
NE203	SAUSA300_0661	1C	A11		conserved hypothetical protein
NE204	SAUSA300_1194	1C	A12		hydrolase, alpha/beta hydrolase fold family
NE205	SAUSA300_0732	1C	B1		conserved hypothetical protein
NE206	SAUSA300_2538	1C	B2		amino acid permease family protein
NE207	SAUSA300_1864	1C	B3		putative membrane protein
NE208	SAUSA300_0880	1C	B4		conserved hypothetical protein
NE209	SAUSA300_1961	1C	B5		phiPVL ORF41-like protein
NE210	SAUSA300_2247	1C	B6		staphylococcal accessory regulator
NE211	SAUSA300_1329	1C	B7		amino acid permease
NE212	SAUSA300_1710	1C	B8		putative lysophospholipase
NE213	SAUSA300_2067	1C	B9	glyA	serine hydroxymethyltransferase
NE214	SAUSA300_0123	1C	B10		siderophore biosynthesis protein, IucC family"
NE215	SAUSA300_0203	1C	B11		putative lipoprotein
NE216	SAUSA300_0636	1C	B12		dihydroxyacetone kinase, DhaK subunit
NE217	SAUSA300_1113	1C	C1	pknB	protein kinase
NE218	SAUSA300_0218	1C	C2		sensor histidine kinase family protein
NE219	SAUSA300_0579	1C	C3		conserved hypothetical protein
NE220	SAUSA300_0595	1C	C4		conserved hypothetical protein
NE221	SAUSA300_0046	1C	C5		conserved hypothetical protein
NE222	SAUSA300_1662	1C	C6		aminotransferase, class V
NE223	SAUSA300_2173	1C	C7		tRNA pseudouridine synthase A
NE224	SAUSA300_0192	1C	C8		conserved hypothetical protein
NE225	SAUSA300_0340	1C	C9		NADH-dependent FMN reductase
NE226	SAUSA300_1996	1C	C10	amt	ammonium transporter
NE227	SAUSA300_0073	1C	C11		peptide ABC transporter, peptide-binding protein
NE228	SAUSA300_2357	1C	C12		ABC transporter, permease protein
NE229	SAUSA300_1119	1C	D1		conserved hypothetical protein
NE230	SAUSA300_1071	1C	D2		conserved hypothetical protein
NE231	SAUSA300_0432	1C	D3		sodium dependent transporter
NE232	SAUSA300_0125	1C	D4		pyridoxal-dependent decarboxylase
NE233	SAUSA300_1193	1C	D5	glpD	glycerol-3-phosphate dehydrogenase
NE234	SAUSA300_0160	1C	D6	cap5I	capsular polysaccharide biosynthesis proteinCap5I
NE235	SAUSA300_0847	1C	D7		conserved hypothetical protein
NE236	SAUSA300_0428	1C	D8		conserved hypothetical protein
NE237	SAUSA300_1054	1C	D9		conserved hypothetical protein
NE238	SAUSA300_2554	1C	D10		sulfite reductase flavoprotein
NE239	SAUSA300_1711	1C	D11	putA	proline dehydrogenase
NE240	SAUSA300_2301	1C	D12	tcaB	teicoplanin resistance associated membrane protein TcaB protein
NE241	SAUSA300_0674	1C	E1		oxidoreductase, aldo/keto reductase family
NE242	SAUSA300_1142	1C	E2	dprA	DNA protecting protein DprA
NE243	SAUSA300_1423	1C	E3	polA	phage related DNA polymerase, family A
NE244	SAUSA300_1932	1C	E4		conserved hypothetical phage protein
NE245	SAUSA300_1761	1C	E5	epiE	lantibiotic epidermin immunity protein F
NE246	SAUSA300_1970	1C	E6		putative exonuclease

NE247	SAUSA300_1844	1C	E7		bacterioferritin comigratory protein
NE248	SAUSA300_2626	1C	E8		conserved hypothetical protein
NE249	SAUSA300_2644	1C	E9		glucose-inhibited division protein B
NE250	SAUSA300_1503	1C	E10		putative competence protein ComGB
NE251	SAUSA300_0482	1C	E11		polysaccharide biosynthesis protein
NE252	SAUSA300_0171	1C	E12		cation efflux family protein
NE253	SAUSA300_2045	1C	F1		HD domain protein
NE254	SAUSA300_0204	1C	F2	ggt	gamma-glutamyltranspeptidase
NE255	SAUSA300_0876	1C	F3		putative membrane protein
NE256	SAUSA300_0535	1C	F4		putative pyridoxal phosphate-dependent acyltransferase
NE257	SAUSA300_1623	1C	F5		conserved hypothetical protein
NE258	SAUSA300_2044	1C	F6	cls	cardiolipin synthetase
NE259	SAUSA300_1167	1C	F7	pnpA	polyribopolyribonucleotide nucleotidyltransferase
NE260	SAUSA300_0227	1C	F8	fadD	acyl-CoA dehydrogenase FadD
NE261	SAUSA300_1898	1C	F9		conserved hypothetical protein
NE262	SAUSA300_1220	1C	F10		DNA-binding response regulator, LuxR family
NE263	SAUSA300_0229	1C	F11		putative acyl-CoA transferase FadX
NE264	SAUSA300_0829	1C	F12	lipA	lipoic acid synthetase
NE265	SAUSA300_1651	1C	G1		CBS domain protein
NE266	SAUSA300_0328	1C	G2		lipoate-protein ligase A family protein
NE267	SAUSA300_1676	1C	G3	sgtA	probable transglycosylase
NE268	SAUSA300_2418	1C	G4		conserved hypothetical protein
NE269	SAUSA300_0720	1C	G5		putative iron compound ABC transporter, ATP-binding protein
NE270	SAUSA300_1681	1C	G6	acuC	acetoin utilization protein AcuC
NE271	SAUSA300_2390	1C	G7	opuCd	glycine betaine/carnitine/choline transport system permease
NE272	SAUSA300_2311	1C	G8		conserved hypothetical protein
NE273	SAUSA300_2449	1C	G9		putative transporter
NE274	SAUSA300_1867	1C	G10		conserved hypothetical protein
NE275	SAUSA300_0721	1C	G11		transferrin receptor
NE276	SAUSA300_0293	1C	G12		conserved hypothetical protein
NE277	SAUSA300_2073	1C	H1	tdk	thymidine kinase
NE278	SAUSA300_0424	1C	H2		putative cobalamin synthesis protein
NE279	SAUSA300_0677	1C	H3		putative deoxyribodipyrimidine photolyase
NE280	SAUSA300_0387	1C	H4	pbuX	xanthine permease
NE281	SAUSA300_2452	1C	H5		transcriptional regulator, MarR family
NE282	SAUSA300_0925	1C	H6		5' nucleotidase family protein
NE283	SAUSA300_2207	1C	H7		xanthine/uracil permease family protein
NE284	SAUSA300_2362	1C	H8	gpmA	2,3-bisphosphoglycerate-dependent phosphoglycerate mutase
NE285	SAUSA300_2302	1C	H9	tcaA	teicoplanin resistance associated membrane protein TcaA protein
NE286	SAUSA300_0113	1C	H10		immunoglobulin G binding protein A precursor
NE287	SAUSA300_1744	1C	H11		conserved hypothetical protein
NE288	SAUSA300_2540	1C	H12		fructose-bisphosphate aldolase class-I
NE289	SAUSA300_0215	1D	A1		conserved hypothetical protein
NE290	SAUSA300_0721	1D	A2		Transferrin receptor
NE291	SAUSA300_2328	1D	A3		conserved hypothetical protein
NE292	SAUSA300_0539	1D	A4	ilvE	branched-chain amino acid aminotransferase
NE293	SAUSA300_1285	1D	A5		ABC transporter, ATP-binding protein
NE294	SAUSA300_1784	1D	A6		signal transduction protein TRAP
NE295	SAUSA300_0025	1D	A7		5'-nucleotidase family protein
NE296	SAUSA300_0654	1D	A8		staphylococcal accessory protein X
NE297	SAUSA300_0063	1D	A9		cyclic nucleotide-binding domain protein

NE298	SAUSA300_2398	1D	A10		putative membrane protein
NE299	SAUSA300_2304	1D	A11		putative membrane protein
NE300	SAUSA300_0701	1D	A12		conserved hypothetical protein TIGR00370
NE301	SAUSA300_0643	1D	B1		acetyltransferase, GNAT family
NE302	SAUSA300_0152	1D	B2	Cap5A	capsular polysaccharide biosynthesis protein Cap5A
NE303	SAUSA300_1614	1D	B3	hemL	glutamate-1-semialdehyde-2,1-aminomutase
NE304	SAUSA300_1268	1D	B4	trpA	tryptophan synthase, alpha subunit
NE305	SAUSA300_0814	1D	B5		conserved hypothetical protein
NE306	SAUSA300_1491	1D	B6		proline dipeptidase
NE307	SAUSA300_1190	1D	B7	glpP	glycerol uptake operon anti-terminator regulatory protein
NE308	SAUSA300_0911	1D	B8		transporter, monovalent cation:proton antiporter-2 (CPA2) family protein
NE309	SAUSA300_1559	1D	B9		putative enterotoxin type A
NE310	SAUSA300_1267	1D	B10		tryptophan synthase, beta subunit
NE311	SAUSA300_2097	1D	B11		conserved hypothetical protein"
NE312	SAUSA300_0212	1D	B12		oxidoreductase, Gfo/Idh/MocA family
NE313	SAUSA300_2450	1D	C1		DedA family protein
NE314	SAUSA300_0140	1D	C2		deoxyribose-phosphate aldolase
NE315	SAUSA300_0133	1D	C3		putative membrane protein
NE316	SAUSA300_1858	1D	C4		conserved hypothetical protein
NE317	SAUSA300_0881	1D	C5		putative membrane protein
NE318	SAUSA300_1236	1D	C6		conserved hypothetical protein
NE319	SAUSA300_1701	1D	C7		conserved hypothetical protein
NE320	SAUSA300_0748	1D	C8		conserved hypothetical protein
NE321	SAUSA300_0170	1D	C9		aldehyde dehydrogenase
NE322	SAUSA300_1500	1D	C10		putative competence protein ComYC
NE323	SAUSA300_0362	1D	C11		conserved hypothetical protein
NE324	SAUSA300_1854	1D	C12		regulatory protein RecX
NE325	SAUSA300_0457	1D	D1	rrfA	5S ribosomal RNA
NE326	SAUSA300_2343	1D	D2		respiratory nitrate reductase, alpha subunit
NE327	SAUSA300_1972	1D	D3	int	integrase
NE328	SAUSA300_1543	1D	D4		oxygen-independent coproporphyrinogen III oxidase
NE329	SAUSA300_2220	1D	D5	mobA	molybdopterin-guanine dinucleotide biosynthesis protein A
NE330	SAUSA300_0039	1D	D6		conserved hypothetical protein"
NE331	SAUSA300_0870	1D	D7	rexA	exonuclease RexA
NE332	SAUSA300_1029	1D	D8		iron transport associated domain protein
NE333	SAUSA300_0209	1D	D9		putative maltose ABC transporter, maltose-binding protein
NE334	SAUSA300_2161	1D	D10		Hyaluronate lyase precursor
NE335	SAUSA300_0039	1D	D11		Conserved hypothetical protein
NE336	SAUSA300_2157	1D	D12		NAD-dependent deacetylase
NE337	SAUSA300_0109	1D	E1		integral membrane domain protein
NE338	SAUSA300_2603	1D	E2	lip	triacylglycerol lipase precursor
NE339	SAUSA300_0784	1D	E3		LysE/YggA family protein
NE340	SAUSA300_2014	1D	E4	ilvA	threonine dehydratase
NE341	SAUSA300_1584	1D	E5		ATPase, AAA family
NE342	SAUSA300_1196	1D	E6	hfq	RNA chaperone, host factor-1 protein
NE343	SAUSA300_2613	1D	E7		conserved hypothetical protein
NE344	SAUSA300_2103	1D	E8		ABC transporter, ATP-binding protein
NE345	SAUSA300_0934	1D	E9		membrane protein"
NE346	SAUSA300_1346	1D	E10		putative DnaQ family exonuclease/DinG family helicase
NE347	SAUSA300_0662	1D	E11		acetyltransferase, GNAT family

NE348	SAUSA300_1169	1D	E12	ftsK	DNA translocase FtsK
NE349	SAUSA300_0081	1D	F1		conserved hypothetical protein
NE350	SAUSA300_0364	1D	F2	ychF	GTP-binding protein YchF
NE351	SAUSA300_2463	1D	F3	ddh	D-lactate dehydrogenase
NE352	SAUSA300_1114	1D	F4	rsgA	ribosome small subunit-dependent GTPase A
NE353	SAUSA300_0975	1D	F5		bifunctional purine biosynthesis protein
NE354	SAUSA300_0503	1D	F6		transcriptional regulator, gntR family protein
NE355	SAUSA300_2515	1D	F7		transcriptional regulator, TetR family
NE356	SAUSA300_1098	1D	F8	pyrE	orotate phosphoribosyltransferase
NE357	SAUSA300_0107	1D	F9		Na/Pi cotransporter family protein
NE358	SAUSA300_0294	1D	F10		conserved hypothetical protein
NE359	SAUSA300_2388	1D	F11	panE	2-dehydropantoate 2-reductase
NE360	SAUSA300_1929	1D	F12		phi77 ORF004-like protein, putative phage tail component
NE361	SAUSA300_2068	1D	G1		conserved hypothetical protein
NE362	SAUSA300_0247	1D	G2		putative teichoic acid biosynthesis protein B
NE363	SAUSA300_0103	1D	G3		staphylococcal tandem lipoprotein
NE364	SAUSA300_0671	1D	G4		ABC transporter, ATP-binding protein, MsbA family
NE365	SAUSA300_1738	1D	G5		putative lipoprotein
NE366	SAUSA300_2384	1D	G6		putative Na+/H+ antiporter
NE367	SAUSA300_2571	1D	G7		arginine repressor
NE368	SAUSA300_2545	1D	G8		choline dehydrogenase
NE369	SAUSA300_1235	1D	G9	guaC	guanosine monophosphate reductase
NE370	SAUSA300_1847	1D	G10		conserved hypothetical protein
NE371	SAUSA300_0222	1D	G11		putative membrane protein
NE372	SAUSA300_2101	1D	G12		SAP domain protein
NE373	SAUSA300_2642	1D	H1		conserved hypothetical protein
NE374	SAUSA300_2487	1D	H2	feoB	ferrous iron transport protein B
NE375	SAUSA300_0815	1D	H3	ear	Ear protein
NE376	SAUSA300_1334	1D	H4		putative membrane protein
NE377	SAUSA300_1505	1D	H5		conserved hypothetical protein
NE378	SAUSA300_0010	1D	H6		putative membrane protein
NE379	SAUSA300_2137	1D	H7		conserved hypothetical protein
NE380	SAUSA300_2531	1D	H8		hydrolase, CocE/NonD family
NE381	SAUSA300_0549	1D	H9		glycosyl transferase, group 1 family protein
NE382	SAUSA300_2498	1D	H10	crtN	squalene synthase
NE383	SAUSA300_0279	1D	H11		putative membrane protein
NE384	SAUSA300_0281	1D	H12		conserved hypothetical protein
NE385	SAUSA300_1679	2A	A1	acsA	acetyl-coenzyme A synthetase
NE386	SAUSA300_1708	2A	A2	rot	staphylococcal accessory regulator Rot
NE387	SAUSA300_2493	2A	A3		conserved hypothetical protein
NE388	SAUSA300_1897	2A	A4		sodium-dependent transporter
NE389	SAUSA300_1906	2A	A5		conserved hypothetical protein
NE390	SAUSA300_0445	2A	A6	gltB	glutamate synthase, large subunit
NE391	SAUSA300_2565	2A	A7	clfB	clumping factor B
NE392	SAUSA300_0200	2A	A8		peptide ABC transporter, ATP-binding protein
NE393	SAUSA300_1458	2A	A9		glyoxalase family protein
NE394	SAUSA300_0893	2A	A10	oppF	oligopeptide ABC transporter, ATP-binding protein
NE395	SAUSA300_0686	2A	A11	nagA	N-acetylglucosamine-6-phosphate deacetylase
NE396	SAUSA300_0462	2A	A12		conserved hypothetical protein
NE397	SAUSA300_1062	2A	B1	argF	ornithine carbamoyltransferase
NE398	SAUSA300_0096	2A	B2		conserved hypothetical protein

NE399	SAUSA300_2588	2A	B3		preprotein translocase, SecY protein
NE400	SAUSA300_2136	2A	B4		iron compound ABC transporter, iron compound-binding protein
NE401	SAUSA300_1417	2A	B5		phiSLT ORF 175-like protein
NE402	SAUSA300_1140	2A	B6	lytN	cell wall hydrolase
NE403	SAUSA300_1318	2A	B7		DegV family protein
NE404	SAUSA300_0474	2A	B8		putative endoribonuclease L-PSP
NE405	SAUSA300_0335	2A	B9		MATE efflux family protein
NE406	SAUSA300_0633	2A	B10	fhuA	ferrichrome transport ATP-binding protein fhuA
NE407	SAUSA300_2405	2A	B11		putative membrane protein
NE408	SAUSA300_2424	2A	B12		putative staphylococcal tandem lipoprotein
NE409	SAUSA300_2267	2A	C1		hydrolase, haloacid dehalogenase-like family
NE410	SAUSA300_2240	2A	C2	ureC	urease, alpha subunit
NE411	SAUSA300_2578	2A	C3		putative phage infection protein
NE412	SAUSA300_1374	2A	C4		conserved hypothetical protein
NE413	SAUSA300_1412	2A	C5		phiSLT ORF 50-like protein
NE414	SAUSA300_0272	2A	C6		conserved hypothetical protein
NE415	SAUSA300_2259	2A	C7		putative transcriptional regulator
NE416	SAUSA300_2519	2A	C8		putative cobalamin synthesis protein
NE417	SAUSA300_0799	2A	C9	int	integrase
NE418	SAUSA300_2363	2A	C10		cation efflux family protein
NE419	SAUSA300_2297	2A	C11		conserved hypothetical protein
NE420	SAUSA300_1512	2A	C12	pbp3	penicillin-binding protein 3
NE421	SAUSA300_0711	2A	D1		conserved hypothetical protein
NE422	SAUSA300_0324	2A	D2		conserved hypothetical protein
NE423	SAUSA300_2035	2A	D3	kdpD	sensor histidine kinase, KdpD
NE424	SAUSA300_2089	2A	D4	pdp	pyrimidine nucleoside phosphorylase
NE425	SAUSA300_0265	2A	D5		putative ribose operon repressor
NE426	SAUSA300_0347	2A	D6	tatC	Sec-independent protein translocase TatC
NE427	SAUSA300_1801	2A	D7	fumC	fumarate hydratase, class II
NE428	SAUSA300_2222	2A	D8	moaE	molybdopterin converting factor, subunit 2
NE429	SAUSA300_0154	2A	D9	cap5C	capsular polysaccharide biosynthesis protein cap5C
NE430	SAUSA300_2417	2A	D10		putative transporter
NE431	SAUSA300_0621	2A	D11		iron-dependent repressor
NE432	SAUSA300_0546	2A	D12	sdrC	sdrC protein
NE433	SAUSA300_1282	2A	E1	pstC	phosphate ABC transporter, permease protein PstC
NE434	SAUSA300_2271	2A	E2		phosphosugar-binding transcriptional regulator
NE435	SAUSA300_2278	2A	E3	hutU	urocanate hydratase
NE436	SAUSA300_2156	2A	E4		lactose phosphotransferase system repressor
NE437	SAUSA300_0291	2A	E5		putative membrane protein
NE438	SAUSA300_0161	2A	E6	Cap5J	capsular polysaccharide biosynthesis protein Cap5J
NE439	SAUSA300_0269	2A	E7		choloylglycine hydrolase family protein
NE440	SAUSA300_0891	2A	E8	oppA	oligopeptide ABC transporter, substrate-binding protein
NE441	SAUSA300_2462	2A	E9	frp	NAD(P)H-flavin oxidoreductase
NE442	SAUSA300_1421	2A	E10		phiSLT ORF122-like protein, DNA polymerase
NE443	SAUSA300_2621	2A	E11		conserved hypothetical protein
NE444	SAUSA300_1860	2A	E12	pepS	aminopeptidase PepS
NE445	SAUSA300_1259	2A	F1		ImpB/MucB/SamB family protein
NE446	SAUSA300_0921	2A	F2	prfC	peptide chain release factor 3
NE447	SAUSA300_1806	2A	F3		putative iron-sulfur cluster-binding protein
NE448	SAUSA300_1324	2A	F4		putative membrane protein
NE449	SAUSA300_1389	2A	F5		phiSLT ORF636-like protein

NE450	SAUSA300_0236	2A	F6		PTS system, IIBC components
NE451	SAUSA300_2316	2A	F7		acetyltransferase, GNAT family
NE452	SAUSA300_2523	2A	F8		conserved hypothetical protein
NE453	SAUSA300_2364	2A	F9	sbi	IgG-binding protein SBI
NE454	SAUSA300_2566	2A	F10	arcR	transcriptional regulator, Crp/Fnr family
NE455	SAUSA300_1580	2A	F11		bacterial luciferase family protein
NE456	SAUSA300_1019	2A	F12		conserved hypothetical protein
NE457	SAUSA300_0202	2A	G1		peptide ABC transporter, permease protein
NE458	SAUSA300_1472	2A	G2	xseA	exodeoxyribonuclease VII, large subunit
NE459	SAUSA300_2356	2A	G3	fmhA	fmhA protein
NE460	SAUSA300_0955	2A	G4	atl	autolysin
NE461	SAUSA300_0134	2A	G5		polysaccharide extrusion protein
NE462	SAUSA300_0917	2A	G6		putative membrane protein
NE463	SAUSA300_1871	2A	G7		conserved hypothetical protein
NE464	SAUSA300_2623	2A	G8	pcp	pyrrolidone-carboxylate peptidase
NE465	SAUSA300_2377	2A	G9		glycerate kinase
NE466	SAUSA300_0809	2A	G10		putative DNA primase
NE467	SAUSA300_0644	2A	G11		conserved hypothetical protein
NE468	SAUSA300_2501	2A	G12		phytoene dehydrogenase
NE469	SAUSA300_1994	2A	H1	scrB	sucrose-6-phosphate hydrolase
NE470	SAUSA300_0346	2A	H2		putative membrane protein
NE471	SAUSA300_1326	2A	H3		putative cell wall enzyme EbsB
NE472	SAUSA300_2109	2A	H4	fmtB	truncated FmtB protein
NE473	SAUSA300_0013	2A	H5		putative membrane protein
NE474	SAUSA300_2446	2A	H6		conserved hypothetical protein
NE475	SAUSA300_1060	2A	H7		putative exotoxin 4
NE476	SAUSA300_2079	2A	H8	fba	fructose bisphosphate aldolase
NE477	SAUSA300_0138	2A	H9	deoD	purine nucleoside phosphorylase
NE478	SAUSA300_0142	2A	H10	phnE	phosphonate ABC transporter, permease protein
NE479	SAUSA300_1504	2A	H11		putative competence protein ComGA
NE480	SAUSA300_0669	2A	H12		undecaprenol kinase
NE481	SAUSA300_0645	2B	A1		DNA-binding response regulator
NE482	SAUSA300_0890	2B	A2	oppF	oligopeptide ABC transporter, ATP-binding protein
NE483	SAUSA300_0727	2B	A3	pepT	peptidase T
NE484	SAUSA300_1808	2B	A4		amino acid ABC transporter, permease/substrate-binding protein
NE485	SAUSA300_1496	2B	A5		glycine dehydrogenase, subunit 2
NE486	SAUSA300_2643	2B	A6		putative chromosome partioning protein, ParB family
NE487	SAUSA300_0042	2B	A7		conserved hypothetical protein
NE488	SAUSA300_0953	2B	A8		putative membrane protein
NE489	SAUSA300_0403	2B	A9		exotoxin
NE490	SAUSA300_0746	2B	A10		TPR domain protein
NE491	SAUSA300_1640	2B	A11	icd	isocitrate dehydrogenase, NADP-dependent
NE492	SAUSA300_1793	2B	A12		conserved hypothetical protein
NE493	SAUSA300_2158	2B	B1		conserved hypothetical protein
NE494	SAUSA300_0970	2B	B2	purQ	phosphoribosylformylglycinamidine synthase I
NE495	SAUSA300_0037	2B	B3	ccrB	cassette chromosome recombinase B
NE496	SAUSA300_1064	2B	B4		transporter, TRAP family
NE497	SAUSA300_0179	2B	B5		putative D-isomer specific 2-hydroxyacid dehydrogenase
NE498	SAUSA300_0286	2B	B6		conserved hypothetical protein
NE499	SAUSA300_0817	2B	B7		putative membrane protein
NE500	SAUSA300_0226	2B	B8		3-hydroxyacyl-CoA dehydrogenase

NE501	SAUSA300_0764	2B	B9	rnr	ribonuclease R
NE502	SAUSA300_1977	2B	B10		conserved hypothetical protein
NE503	SAUSA300_2564	2B	B11	estA	tributyrin esterase
NE504	SAUSA300_1392	2B	B12		phiSLT ORF191-like protein
NE505	SAUSA300_0093	2B	C1		transcriptional regulator, LysR family domain protein
NE506	SAUSA300_2215	2B	C2		conserved hypothetical protein
NE507	SAUSA300_1036	2B	C3		RNA methyltransferase, TrmH family
NE508	SAUSA300_0864	2B	C4	argG	argininosuccinate synthase
NE509	SAUSA300_0205	2B	C5		staphylococcal tandem lipoprotein
NE510	SAUSA300_2110	2B	C6	fmtB	truncated FmtB protein
NE511	SAUSA300_0061	2B	C7	arcC	carbamate kinase
NE512	SAUSA300_2228	2B	C8	modC	molybdenum ABC transporter, ATP-binding protein ModC
NE513	SAUSA300_2431	2B	C9		putative helicase
NE514	SAUSA300_2437	2B	C10	sarT	staphylococcal accessory regulator T
NE515	SAUSA300_1330	2B	C11	ilvA	threonine dehydratase
NE516	SAUSA300_1508	2B	C12		conserved hypothetical protein
NE517	SAUSA300_0034	2B	D1		IS1272, transposase
NE518	SAUSA300_2500	2B	D2		glycosyl transferase
NE519	SAUSA300_1460	2B	D3		peptidase, M20/M25/M40 family
NE520	SAUSA300_1452	2B	D4	proC	pyrroline-5-carboxylate reductase
NE521	SAUSA300_2307	2B	D5		ABC transporter, permease protein
NE522	SAUSA300_1889	2B	D6	purB	adenylosuccinate lyase
NE523	SAUSA300_1969	2B	D7		phi77 ORF011-like protein, phage transcriptional repressor
NE524	SAUSA300_0371	2B	D8		conserved hypothetical protein
NE525	SAUSA300_1648	2B	D9		putative NADP-dependent malic enzyme
NE526	SAUSA300_0694	2B	D10		putative membrane protein
NE527	SAUSA300_1766	2B	D11	epiB	lantibiotic epidermin biosynthesis protein EpiB
NE528	SAUSA300_0091	2B	D12		putative permease
NE529	SAUSA300_0017	2B	E1	purA	adenylosuccinate synthetase
NE530	SAUSA300_2248	2B	E2		transcriptional regulator, AraC family
NE531	SAUSA300_2128	2B	E3		putative drug transporter
NE532	SAUSA300_2473	2B	E4		conserved hypothetical protein
NE533	SAUSA300_0436	2B	E5		ABC transporter, permease protein
NE534	SAUSA300_1537	2B	E6		conserved hypothetical protein
NE535	SAUSA300_0867	2B	E7	spsA	signal peptidase IA
NE536	SAUSA300_0780	2B	E8		conserved hypothetical protein
NE537	SAUSA300_0378	2B	E9		conserved hypothetical protein
NE538	SAUSA300_1661	2B	E10	thiI	thiamine biosynthesis protein ThiI
NE539	SAUSA300_0228	2B	E11	fadE	acyl-CoA synthetase FadE
NE540	SAUSA300_2615	2B	E12		conserved hypothetical protein
NE541	SAUSA300_0201	2B	F1		peptide ABC transporter, permease protein
NE542	SAUSA300_2455	2B	F2		putative fructose-1,6-bisphosphatase
NE543	SAUSA300_0772	2B	F3	clfA	clumping factor A
NE544	SAUSA300_0506	2B	F4	nupC	pyrimidine nucleoside transport protein
NE545	SAUSA300_0298	2B	F5		conserved hypothetical protein
NE546	SAUSA300_0564	2B	F6		conserved hypothetical protein
NE547	SAUSA300_1306	2B	F7	sucA	2-oxoglutarate dehydrogenase, E1 component
NE548	SAUSA300_2139	2B	F8		putative transporter
NE549	SAUSA300_1226	2B	F9		homoserine dehydrogenase
NE550	SAUSA300_2269	2B	F10		conserved hypothetical protein
NE551	SAUSA300_1101	2B	F11		putative fibronectin/fibrinogen binding protein

NE552	SAUSA300_2408	2B	F12		oligopeptide ABC transporter, ATP-binding protein
NE553	SAUSA300_0261	2B	G1		conserved hypothetical protein
NE554	SAUSA300_1865	2B	G2	vraR	DNA-binding response regulator
NE555	SAUSA300_0004	2B	G3	recF	DNA replication and repair protein recF
NE556	SAUSA300_2510	2B	G4		conserved hypothetical protein
NE557	SAUSA300_1030	2B	G5		iron transport associated domain protein
NE558	SAUSA300_1769	2B	G6	lukE	leukotoxin LukE
NE559	SAUSA300_1426	2B	G7		conserved hypothetical phage protein
NE560	SAUSA300_2291	2B	G8	gltS	sodium/glutamate symporter
NE561	SAUSA300_2494	2B	G9		copper-translocating P-type ATPase
NE562	SAUSA300_0316	2B	G10		ROK family protein
NE563	SAUSA300_2555	2B	G11		glutathione peroxidase
NE564	SAUSA300_2477	2B	G12	cidC	pyruvate oxidase
NE565	SAUSA300_2037	2B	H1		ATP-dependent RNA helicase
NE566	SAUSA300_2329	2B	H2	gltT	proton/sodium-glutamate symport protein
NE567	SAUSA300_2331	2B	H3		transcriptional regulator, MarR family
NE568	SAUSA300_2351	2B	H4		Zn-binding lipoprotein adcA-like protein
NE569	SAUSA300_1138	2B	H5	sucC	succinyl-CoA synthetase, beta subunit
NE570	SAUSA300_0008	2B	H6	hutH	histidine ammonia-lyase
NE571	SAUSA300_2263	2B	H7		putative transposase
NE572	SAUSA300_0834	2B	H8		D-isomer specific 2-hydroxyacid dehydrogenase
NE573	SAUSA300_1713	2B	H9	ribBA	riboflavin biosynthesis protein
NE574	SAUSA300_0072	2B	H10		hypothetical protein
NE575	SAUSA300_1450	2B	H11		oxidoreductase, aldo/keto reductase family
NE576	SAUSA300_0242	2B	H12	gutB	sorbitol dehydrogenase
NE577	SAUSA300_1310	2C	A1		PAP2 family protein
NE578	SAUSA300_0599	2C	A2		iron compound ABC transporter, permease protein
NE579	SAUSA300_1286	2C	A3		aspartate kinase
NE580	SAUSA300_0158	2C	A4	cap5G	capsular polysaccharide biosynthesis protein cap5G
NE581	SAUSA300_0972	2C	A5	purF	amidophosphoribosyltransferase
NE582	SAUSA300_1333	2C	A6		conserved hypothetical protein
NE583	SAUSA300_1716	2C	A7		conserved hypothetical protein
NE584	SAUSA300_2333	2C	A8	narK	nitrite extrusion protein
NE585	SAUSA300_0130	2C	A9		NAD-dependent epimerase/dehydratase family protein
NE586	SAUSA300_2277	2C	A10	hutI	imidazolonepropionase
NE587	SAUSA300_1896	2C	A11	pheA	prephenate dehydratase
NE588	SAUSA300_1441	2C	A12	srrB	staphylococcal respiratory response protein, srrB
NE589	SAUSA300_2268	2C	B1		sodium/bile acid symporter family protein
NE590	SAUSA300_0078	2C	B2	copA	ATPase copper transport
NE591	SAUSA300_0359	2C	B3		trans-sulfuration enzyme family protein
NE592	SAUSA300_2060	2C	B4	atpA	ATP synthase F1, alpha subunit
NE593	SAUSA300_1262	2C	B5	trpE	anthranilate synthase component I
NE594	SAUSA300_1641	2C	B6	gltA	citrate synthase II
NE595	SAUSA300_0185	2C	B7	argJ	arginine biosynthesis bifunctional protein ArgJ
NE596	SAUSA300_1855	2C	B8	sgtB	monofunctional glycosyltransferase
NE597	SAUSA300_0472	2C	B9	ispE	4-diphosphocytidyl-2C-methyl-D-erythritol kinase
NE598	SAUSA300_2631	2C	B10		putative N-acetyltransferase
NE599	SAUSA300_0146	2C	B11		conserved hypothetical protein
NE600	SAUSA300_2087	2C	B12		putative peptidase
NE601	SAUSA300_0660	2C	C1		conserved hypothetical protein
NE602	SAUSA300_2376	2C	C2		conserved hypothetical protein

NE603	SAUSA300_2224	2C	C3	moeA	molybdopterin biosynthesis protein A
NE604	SAUSA300_0284	2C	C4		conserved hypothetical protein
NE605	SAUSA300_0306	2C	C5	brnQ	branched-chain amino acid transport system II carrier protein
NE606	SAUSA300_0199	2C	C6		conserved hypothetical protein
NE607	SAUSA300_0143	2C	C7	phnE	phosphonate ABC transporter, permease protein
NE608	SAUSA300_1210	2C	C8		conserved hypothetical protein
NE609	SAUSA300_0086	2C	C9		conserved hypothetical protein
NE610	SAUSA300_1628	2C	C10	lysP	lysine-specific permease
NE611	SAUSA300_0939	2C	C11		glycosyl transferase, group 1 family protein
NE612	SAUSA300_0220	2C	C12	pflB	formate acetyltransferase
NE613	SAUSA300_0509	2C	D1		ATP guanido phosphotransferase
NE614	SAUSA300_2439	2C	D2	galU	UTP-glucose-1-phosphate uridylyltransferase
NE615	SAUSA300_0040	2C	D3		conserved hypothetical protein
NE616	SAUSA300_0754	2C	D4		conserved hypothetical protein
NE617	SAUSA300_1760	2C	D5	epiG	lantibiotic epidermin immunity protein F
NE618	SAUSA300_1638	2C	D6	phoR	sensory box histidine kinase PhoR
NE619	SAUSA300_0307	2C	D7		5'-nucleotidase, lipoprotein e(P4) family
NE620	SAUSA300_0429	2C	D8		PAP2 family protein
NE621	SAUSA300_0581	2C	D9		conserved hypothetical protein
NE622	SAUSA300_0313	2C	D10		putative nucleoside permease NupC
NE623	SAUSA300_2570	2C	D11	arcA	arginine deiminase
NE624	SAUSA300_0679	2C	D12		conserved hypothetical protein
NE625	SAUSA300_0382	2C	E1		sodium:dicarboxylate symporter family protein
NE626	SAUSA300_1047	2C	E2	sdhA	succinate dehydrogenase, flavoprotein subunit
NE627	SAUSA300_2211	2C	E3		putative membrane protein
NE628	SAUSA300_2349	2C	E4		formate/nitrite transporter family protein
NE629	SAUSA300_0726	2C	E5		glycerate kinase family protein
NE630	SAUSA300_0665	2C	E6		acetyltransferase, GNAT family
NE631	SAUSA300_1962	2C	E7		phiPVL ORF39-like protein
NE632	SAUSA300_0390	2C	E8		conserved hypothetical protein
NE633	SAUSA300_2415	2C	E9		conserved hypothetical protein
NE634	SAUSA300_1809	2C	E10		putative membrane protein
NE635	SAUSA300_1714	2C	E11	ribE	riboflavin synthase, alpha subunit
NE636	SAUSA300_1065	2C	E12		exfoliative toxin A
NE637	SAUSA300_1791	2C	F1	cbf1	cmp-binding-factor 1
NE638	SAUSA300_0353	2C	F2		conserved hypothetical protein
NE639	SAUSA300_0030	2C	F3		putative glycerophosphoryl diester phosphodiesterase
NE640	SAUSA300_1413	2C	F4		conserved hypothetical phage protein
NE641	SAUSA300_0270	2C	F5	lytM	peptidoglycan hydrolase
NE642	SAUSA300_2536	2C	F6	budA	alpha-acetolactate decarboxylase
NE643	SAUSA300_0102	2C	F7		staphylococcal tandem lipoprotein
NE644	SAUSA300_2595	2C	F8		acetyltransferase, GNAT family
NE645	SAUSA300_0647	2C	F9		ABC transporter, ATP-binding protein
NE646	SAUSA300_2082	2C	F10	rpoE	DNA-directed RNA polymerase, delta subunit
NE647	SAUSA300_1485	2C	F11		conserved hypothetical protein
NE648	SAUSA300_2270	2C	F12	glvC	PTS system, arbutin-like IIBC component
NE649	SAUSA300_0101	2C	G1		staphylococcal tandem lipoprotein
NE650	SAUSA300_2091	2C	G2	deoD	purine nucleoside phosphorylase
NE651	SAUSA300_0400	2C	G3		exotoxin
NE652	SAUSA300_0845	2C	G4	ampA	cytosol aminopeptidase
NE653	SAUSA300_0297	2C	G5		putative lipoprotein

NE654	SAUSA300_0604	2C	G6		hydrolase, alpha/beta hydrolase fold family
NE655	SAUSA300_1316	2C	G7	msrB	methionine-R-sulfoxide reductase
NE656	SAUSA300_1787	2C	G8		HIT family protein
NE657	SAUSA300_2532	2C	G9	panD	aspartate 1-decarboxylase
NE658	SAUSA300_1002	2C	G10	potD	spermidine/putrescine ABC transporter, spermidine/putrescine-binding protein
NE659	SAUSA300_2414	2C	G11		conserved hypothetical protein
NE660	SAUSA300_1498	2C	G12	gcvT	aminomethyltransferase (glycine cleavage system T protein)
NE661	SAUSA300_0616	2C	H1		putative Na+/H+ antiporter, MnhG component
NE662	SAUSA300_0381	2C	H2		putative NAD(P)H-flavin oxidoreductase
NE663	SAUSA300_0211	2C	H3		maltose ABC transporter, permease protein
NE664	SAUSA300_0516	2C	H4		conserved hypothetical protein
NE665	SAUSA300_1842	2C	H5		transcriptional regulator, Fur family
NE666	SAUSA300_2219	2C	H6	moaA	molybdenum cofactor biosynthesis protein A
NE667	SAUSA300_0196	2C	H7	hsdR	type I restriction-modification enzyme, R subunit
NE668	SAUSA300_2274	2C	H8		putative membrane protein
NE669	SAUSA300_0166	2C	H9	Cap5O	capsular polysaccharide biosynthesis protein Cap5O
NE670	SAUSA300_0874	2C	H10		conserved hypothetical protein
NE671	SAUSA300_2310	2C	H11		conserved hypothetical protein
NE672	SAUSA300_1228	2C	H12		homoserine kinase
NE673	SAUSA300_0872	2D	A1		conserved hypothetical protein
NE674	SAUSA300_1056	2D	A2		conserved hypothetical protein
NE675	SAUSA300_0116	2D	A3	sirB	iron compound ABC transporter, permease protein SirB
NE676	SAUSA300_2468	2D	A4		acetyltransferase, GNAT family
NE677	SAUSA300_2549	2D	A5	bccT	choline/carnitine/betaine transporter, BCCT family
NE678	SAUSA300_0099	2D	A6	plc	1-phosphatidylinositol phosphodiesterase
NE679	SAUSA300_0629	2D	A7	pbp4	penicillin-binding protein 4
NE680	SAUSA300_0915	2D	A8		conserved hypothetical protein
NE681	SAUSA300_2033	2D	A9	kdpB	K+-transporting ATPase, B subunit
NE682	SAUSA300_0668	2D	A10		conserved hypothetical protein
NE683	SAUSA300_0895	2D	A11	oppB	oligopeptide ABC transporter, permease protein
NE684	SAUSA300_1081	2D	A12		conserved hypothetical protein
NE685	SAUSA300_0047	2D	B1		conserved hypothetical protein
NE686	SAUSA300_1998	2D	B2		putative membrane protein
NE687	SAUSA300_1981	2D	B3		phage terminase family protein
NE688	SAUSA300_2086	2D	B4		conserved hypothetical protein
NE689	SAUSA300_0655	2D	B5		conserved hypothetical protein
NE690	SAUSA300_2445	2D	B6		transcriptional regulator, MerR family
NE691	SAUSA300_2255	2D	B7		monooxygenase family protein
NE692	SAUSA300_1903	2D	B8		conserved hypothetical protein
NE693	SAUSA300_2223	2D	B9	mobB	molybdopterin-guanine dinucleotide biosynthesis protein B
NE694	SAUSA300_1173	2D	B10		putative acetoacetyl-CoA reductase
NE695	SAUSA300_0333	2D	B11		transcriptional antiterminator, BglG family
NE696	SAUSA300_0375	2D	B12		putative phosphoglycerate mutase family protein
NE697	SAUSA300_0433	2D	C1	cysM	cysteine synthase/cystathionine beta-synthase
NE698	SAUSA300_1483	2D	C2		conserved hypothetical protein
NE699	SAUSA300_0510	2D	C3	clpC	endopeptidase
NE700	SAUSA300_0664	2D	C4		conserved hypothetical protein
NE701	SAUSA300_1609	2D	C5		type III leader peptidase family protein
NE702	SAUSA300_2609	2D	C6	hisB	imidazole glycerol phosphate dehydratase hisB
NE703	SAUSA300_1750	2D	C7		conserved hypothetical protein

NE704	SAUSA300_0537	2D	C8		L-ribulokinase
NE705	SAUSA300_1940	2D	C9		phage portal protein
NE706	SAUSA300_1678	2D	C10	fhs	formate-tetrahydrofolate ligase
NE707	SAUSA300_1379	2D	C11		putative lipoprotein
NE708	SAUSA300_1941	2D	C12		phi77 ORF003-like protein, phage terminase,large subunit
NE709	SAUSA300_1810	2D	D1		IS1181, transposase
NE710	SAUSA300_0776	2D	D2		thermonuclease precursor
NE711	SAUSA300_1652	2D	D3		conserved hypothetical protein
NE712	SAUSA300_1551	2D	D4		conserved hypothetical protein
NE713	SAUSA300_0577	2D	D5		putative transcriptional regulator
NE714	SAUSA300_1558	2D	D6	mtnN	5'-methylthioadenosine/S-adenosylhomocysteine nucleosidase
NE715	SAUSA300_2348	2D	D7		conserved hypothetical protein
NE716	SAUSA300_1637	2D	D8		putative membrane protein
NE717	SAUSA300_1376	2D	D9		putative lipoprotein
NE718	SAUSA300_2006	2D	D10	ilvD	dihydroxy-acid dehydratase
NE719	SAUSA300_2293	2D	D11	corA	magnesium and cobalt transport protein
NE720	SAUSA300_1663	2D	D12		conserved hypothetical protein
NE721	SAUSA300_2100	2D	E1		lytic regulatory protein
NE722	SAUSA300_1388	2D	E2		phiSLT ORF488-like protein
NE723	SAUSA300_1514	2D	E3	fur	ferric uptake regulation protein
NE724	SAUSA300_0719	2D	E4		iron compound ABC transporter, permease protein
NE725	SAUSA300_0377	2D	E5		putative lipoprotein
NE726	SAUSA300_1719	2D	E6	arsC	arsenate reductase
NE727	SAUSA300_2464	2D	E7		hydrolase, haloacid dehalogenase-like family
NE728	SAUSA300_2440	2D	E8	fnbB	fibronectin binding protein B
NE729	SAUSA300_1699	2D	E9		pseudouridine synthase, family 1
NE730	SAUSA300_0943	2D	E10		acetyltransferase, GNAT family family
NE731	SAUSA300_0622	2D	E11		putative membrane protein
NE732	SAUSA300_0962	2D	E12	qoxB	quinol oxidase, subunit I
NE733	SAUSA300_0274	2D	F1		conserved hypothetical protein
NE734	SAUSA300_1978	2D	F2		ferric hydroxamate receptor
NE735	SAUSA300_1006	2D	F3		conserved hypothetical protein
NE736	SAUSA300_0910	2D	F4	mgtE	magnesium transporter
NE737	SAUSA300_0797	2D	F5		ABC transporter permease protein
NE738	SAUSA300_2209	2D	F6		conserved hypothetical protein
NE739	SAUSA300_0165	2D	F7	Cap5N	capsular polysaccharide biosynthesis protein Cap5N
NE740	SAUSA300_1164	2D	F8	truB	tRNA pseudouridine synthase B
NE741	SAUSA300_0894	2D	F9		oligopeptide ABC transporter, ATP-binding protein
NE742	SAUSA300_1995	2D	F10	scrR	sucrose operon repressor
NE743	SAUSA300_0180	2D	F11		integral membrane protein LmrP
NE744	SAUSA300_0967	2D	F12	purK	phosphoribosylaminoimidazole carboxylase, ATPase subunit
NE745	SAUSA300_2140	2D	G1		conserved hypothetical protein
NE746	SAUSA300_1734	2D	G2		conserved hypothetical protein
NE747	SAUSA300_0177	2D	G3		conserved hypothetical protein
NE748	SAUSA300_1406	2D	G4		phiSLT ORF 104b-like protein
NE749	SAUSA300_0121	2D	G5		putative drug transporter
NE750	SAUSA300_0976	2D	G6	purD	phosphoribosylamine--glycine ligase
NE751	SAUSA300_1693	2D	G7		conserved hypothetical protein
NE752	SAUSA300_2287	2D	G8		putative membrane protein
NE753	SAUSA300_0100	2D	G9		staphylococcal tandem lipoprotein
NE754	SAUSA300_1014	2D	G10	pyc	pyruvate carboxylase

NE755	SAUSA300_1170	2D	G11		transcriptional regulator, GntR family
NE756	SAUSA300_0352	2D	G12		ABC transporter, ATP-binding protein
NE757	SAUSA300_0108	2D	H1		antigen, 67 kDa
NE758	SAUSA300_0330	2D	H2		putative transport protein SgaT
NE759	SAUSA300_1507	2D	H3	glk	glucokinase
NE760	SAUSA300_0900	2D	H4		putative competence protein
NE761	SAUSA300_1343	2D	H5	nth	endonuclease III
NE762	SAUSA300_2262	2D	H6		putative membrane protein
NE763	SAUSA300_0339	2D	H7		conserved hypothetical protein
NE764	SAUSA300_1432	2D	H8		phiSLT ORF78-like protein
NE765	SAUSA300_2320	2D	H9		conserved hypothetical protein
NE766	SAUSA300_2602	2D	H10	icaC	intercellular adhesion protein C
NE767	SAUSA300_2324	2D	H11		PTS system, sucrose-specific IIBC component
NE768	SAUSA300_0685	2D	H12	fruA	fructose specific permease
NE769	SAUSA300_1015	3A	A1	ctaA	cytochrome oxidase assembly protein
NE770	SAUSA300_0704	3A	A2	-	ABC transporter ATP-binding protein
NE771	SAUSA300_2379	3A	A3	-	putative transporter protein
NE772	SAUSA300_0361	3A	A4	-	ParB-like partition protein
NE773	SAUSA300_2451	3A	A5	-	drug transporter
NE774	SAUSA300_2596	3A	A6	cap1C	capsular polysaccharide biosynthesis protein Cap1C
NE775	SAUSA300_2634	3A	A7	-	ABC transporter permease
NE776	SAUSA300_1565	3A	A8	-	hypothetical protein
NE777	SAUSA300_2373	3A	A9	bioD	dethiobiotin synthase
NE778	SAUSA300_0862	3A	A10	glpQ	glycerophosphoryl diester phosphodiesterase
NE779	SAUSA300_1254	3A	A11	-	hypothetical protein
NE780	SAUSA300_0901	3A	A12	-	putative competence protein
NE781	SAUSA300_2298	3A	B1	-	multidrug resistance protein B, drug resistance transporter
NE782	SAUSA300_2392	3A	B2	opuCb	glycine betaine/carnitine/choline ABC transporter
NE783	SAUSA300_1410	3A	B3	-	virulence-associated protein E
NE784	SAUSA300_2535	3A	B4	panE	2-dehydropantoate 2-reductase
NE785	SAUSA300_0576	3A	B5	-	putative pyridine nucleotide-disulfide oxidoreductase
NE786	SAUSA300_2160	3A	B6	-	MerR family transcriptional regulator
NE787	SAUSA300_0198	3A	B7	-	hypothetical protein
NE788	SAUSA300_0988	3A	B8	trkA	potassium uptake protein
NE789	SAUSA300_1332	3A	B9	-	putative 5'-3' exonuclease
NE790	SAUSA300_2000	3A	B10	vga	ABC transporter ATP-binding protein
NE791	SAUSA300_0098	3A	B11	-	hypothetical protein
NE792	SAUSA300_2583	3A	B12	-	putative glycosyl transferase
NE793	SAUSA300_1090	3A	C1	-	hypothetical protein
NE794	SAUSA300_0556	3A	C2		SIS domain protein
NE795	SAUSA300_0049	3A	C3	-	hypothetical protein
NE796	SAUSA300_1545	3A	C4	rpsT	30S ribosomal protein S20
NE797	SAUSA300_2381	3A	C5		conserved hypothetical protein
NE798	SAUSA300_0796	3A	C6	-	ABC transporter ATP-binding protein
NE799	SAUSA300_1292	3A	C7	alr2	alanine racemase
NE800	SAUSA300_2581	3A	C8	-	putative surface anchored protein
NE801	SAUSA300_0592	3A	C9	-	hypothetical protein
NE802	SAUSA300_0543	3A	C10	-	putative deaminase
NE803	SAUSA300_0164	3A	C11	cap5M	capsular polysaccharide biosynthesis protein Cap5M
NE804	SAUSA300_0260	3A	C12	bglA	6-phospho-beta-glucosidase
NE805	SAUSA300_1178	3A	D1	recA	recombinase A

NE806	SAUSA300_0060	3A	D2	-	putative transposase
NE807	SAUSA300_1658	3A	D3	-	hypothetical protein
NE808	SAUSA300_1048	3A	D4	sdhB	succinate dehydrogenase iron-sulfur subunit
NE809	SAUSA300_1214	3A	D5	-	hypothetical protein
NE810	SAUSA300_1642	3A	D6	-	D-serine/D-alanine/glycine transporter
NE811	SAUSA300_1206	3A	D7	-	hypothetical protein
NE812	SAUSA300_0299	3A	D8	-	hypothetical protein
NE813	SAUSA300_2630	3A	D9	nixA	high-affinity nickel-transporter
NE814	SAUSA300_0394	3A	D10	-	FAD/NAD(P)-binding Rossmann fold superfamily protein
NE815	SAUSA300_0162	3A	D11	cap5K	capsular polysaccharide biosynthesis protein Cap5K
NE816	SAUSA300_2155	3A	D12	lacA	galactose-6-phosphate isomerase subunit LacA
NE817	SAUSA300_2624	3A	E1	-	hypothetical protein
NE818	SAUSA300_0176	3A	E2	-	ABC transporter permease
NE819	SAUSA300_1607	3A	E3	-	hypothetical protein
NE820	SAUSA300_2309	3A	E4	-	sensor histidine kinase
NE821	SAUSA300_0698	3A	E5	pabA	para-aminobenzoate synthase, glutamine amidotransferase, component II
NE822	SAUSA300_0909	3A	E6	-	RluA family pseudouridine synthase
NE823	SAUSA300_1866	3A	E7	vraS	two-component sensor histidine kinase
NE824	SAUSA300_1958	3A	E8	-	single-strand binding protein
NE825	SAUSA300_2436	3A	E9	-	putative cell wall surface anchor family protein
NE826	SAUSA300_0159	3A	E10	cap5H	capsular polysaccharide biosynthesis protein Cap5H
NE827	SAUSA300_2605	3A	E11	hisIE	bifunctional phosphoribosyl-AMP cyclohydrolase/phosphoribosyl-ATP pyrophosphatase protein
NE828	SAUSA300_1916	3A	E12	-	hypothetical protein
NE829	SAUSA300_2174	3A	F1	-	cobalt transport family protein
NE830	SAUSA300_0127	3A	F2	-	hypothetical protein
NE831	SAUSA300_2159	3A	F3	-	aldo/keto reductase family protein
NE832	SAUSA300_1549	3A	F4	-	ComE operon protein 1
NE833	SAUSA300_1671	3A	F5	-	hypothetical protein
NE834	SAUSA300_2175	3A	F6	cbiO	cobalt transporter ATP-binding subunit
NE835	SAUSA300_0684	3A	F7	fruB	fructose 1-phosphate kinase
NE836	SAUSA300_0437	3A	F8	-	NLPA lipoprotein
NE837	SAUSA300_2106	3A	F9	-	putative transcriptional regulator
NE838	SAUSA300_0736	3A	F10	yfiA	ribosomal subunit interface protein
NE839	SAUSA300_0033	3A	F11	-	methicillin-resistance MecR1 regulatory protein
NE840	SAUSA300_1353	3A	F12	-	hypothetical protein
NE841	SAUSA300_0932	3A	G1	-	hypothetical protein
NE842	SAUSA300_1354	3A	G2	-	hypothetical protein
NE843	SAUSA300_1670	3A	G3	serA	D-3-phosphoglycerate dehydrogenase
NE844	SAUSA300_0670	3A	G4	-	ABC transporter ATP-binding protein
NE845	SAUSA300_0052	3A	G5	-	hypothetical protein
NE846	SAUSA300_0615	3A	G6	-	putative monovalent cation/H+ antiporter subunit F
NE847	SAUSA300_1313	3A	G7	ctpA	carboxyl-terminal protease
NE848	SAUSA300_1660	3A	G8	-	hypothetical protein
NE849	SAUSA300_0232	3A	G9	-	hypothetical protein
NE850	SAUSA300_0575	3A	G10	-	hypothetical protein
NE851	SAUSA300_0833	3A	G11	-	hypothetical protein
NE852	SAUSA300_1258	3A	G12	-	4-oxalocrotonate tautomerase
NE853	SAUSA300_0578	3A	H1	-	hypothetical protein
NE854	SAUSA300_2454	3A	H2	-	membrane spanning protein

NE855	SAUSA300_1706	3A	H3	-	hypothetical protein
NE856	SAUSA300_0449	3A	H4	treC	alpha,alpha-phosphotrehalase
NE857	SAUSA300_2346	3A	H5	nirB	nitrite reductase [NAD(P)H], large subunit
NE858	SAUSA300_1604	3A	H6	mreD	rod shape-determining protein MreD
NE859	SAUSA300_2629	3A	H7		conserved hypothetical protein
NE860	SAUSA300_1408	3A	H8	-	phage helicase
NE861	SAUSA300_1246	3A	H9	acnA	aconitate hydratase
NE862	SAUSA300_2420	3A	H10		conserved hypothetical protein
NE863	SAUSA300_1234	3A	H11	rpsN	30S ribosomal protein S14
NE864	SAUSA300_0208	3A	H12	-	putative maltose ABC transporter ATP-binding protein
NE865	SAUSA300_1544	3B	A1	lepA	GTP-binding protein LepA
NE866	SAUSA300_2213	3B	A2		AcrB/AcrD/AcrF family protein
NE867	SAUSA300_0483	3B	A3	-	tetrapyrrole methylase family protein
NE868	SAUSA300_2382	3B	A4	-	hypothetical protein
NE869	SAUSA300_2135	3B	A5	-	iron compound ABC transporter permease
NE870	SAUSA300_0075	3B	A6	opp-3C	oligopeptide permease, channel-forming protein
NE871	SAUSA300_2636	3B	A7	-	integrase/recombinase
NE872	SAUSA300_0653	3B	A8	-	AraC family transcriptional regulator
NE873	SAUSA300_1991	3B	A9	agrC	accessory gene regulator protein C
NE874	SAUSA300_1085	3B	A10	-	hypothetical protein
NE875	SAUSA300_2012	3B	A11	leuC	isopropylmalate isomerase large subunit
NE876	SAUSA300_0057	3B	A12	-	hypothetical protein
NE877	SAUSA300_0584	3B	B1	-	hypothetical protein
NE878	SAUSA300_0282	3B	B2		conserved hypothetical protein
NE879	SAUSA300_1497	3B	B3	-	glycine dehydrogenase subunit 1
NE880	SAUSA300_2232	3B	B4	-	acetyltransferase
NE881	SAUSA300_0923	3B	B5	htrA	serine protease
NE882	SAUSA300_0197	3B	B6	-	hypothetical protein
NE883	SAUSA300_1145	3B	B7	xerC	tyrosine recombinase xerC
NE884	SAUSA300_2409	3B	B8	-	oligopeptide ABC transporter permease
NE885	SAUSA300_1182	3B	B9	-	pyruvate ferredoxin oxidoreductase, alpha subunit
NE886	SAUSA300_1227	3B	B10	thrC	threonine synthase
NE887	SAUSA300_1366	3B	B11	-	hypothetical protein
NE888	SAUSA300_0563	3B	B12	ung	uracil-DNA glycosylase
NE889	SAUSA300_1883	3B	C1	putP	high affinity proline permease
NE890	SAUSA300_2560	3B	C2	-	hypothetical protein
NE891	SAUSA300_0924	3B	C3	-	sodium transport family protein
NE892	SAUSA300_2013	3B	C4	leuD	isopropylmalate isomerase small subunit
NE893	SAUSA300_0041	3B	C5	-	hypothetical protein
NE894	SAUSA300_2153	3B	C6	lacC	tagatose-6-phosphate kinase
NE895	SAUSA300_0458	3B	C7	-	Orn/Lys/Arg decarboxylase
NE896	SAUSA300_0903	3B	C8	-	hypothetical protein
NE897	SAUSA300_1195	3B	C9	miaA	tRNA delta(2)-isopentenylpyrophosphate transferase
NE898	SAUSA300_1401	3B	C10	-	phiSLT ORF387-like protein
NE899	SAUSA300_2321	3B	C11	-	hypothetical protein
NE900	SAUSA300_2031	3B	C12	-	hypothetical protein
NE901	SAUSA300_0268	3B	D1	-	putative drug transporter
NE902	SAUSA300_1957	3B	D2	-	phiPVL ORF046-like protein
NE903	SAUSA300_1451	3B	D3	-	short chain dehydrogenase/reductase family oxidoreductase
NE904	SAUSA300_0290	3B	D4	-	putative lipoprotein
NE905	SAUSA300_0469	3B	D5	-	hypothetical protein

NE906	SAUSA300_1732	3B	D6	-	putative transposase
NE907	SAUSA300_1868	3B	D7	-	hypothetical protein
NE908	SAUSA300_1892	3B	D8	-	hypothetical protein
NE909	SAUSA300_0787	3B	D9	aroD	3-dehydroquinate dehydratase
NE910	SAUSA300_1309	3B	D10	-	IS200 family transposase
NE911	SAUSA300_0380	3B	D11	ahpC	alkyl hydroperoxide reductase subunit C
NE912	SAUSA300_0752	3B	D12	clpP	ATP-dependent Clp protease proteolytic subunit
NE913	SAUSA300_2090	3B	E1	deoC	deoxyribose-phosphate aldolase
NE914	SAUSA300_1622	3B	E2	tig	trigger factor
NE915	SAUSA300_2575	3B	E3	-	BglG family transcriptional antiterminator
NE916	SAUSA300_2433	3B	E4	-	phosphoglucomutase/phosphomannomutase family protein
NE917	SAUSA300_1437	3B	E5	-	phiSLT ORF204-like protein
NE918	SAUSA300_1938	3B	E6	-	phi77 ORF006-like protein capsid protein
NE919	SAUSA300_0451	3B	E7	-	acetyltransferase
NE920	SAUSA300_0856	3B	E8	-	hypothetical protein
NE921	SAUSA300_1691	3B	E9	-	glutamyl-aminopeptidase
NE922	SAUSA300_0124	3B	E10	-	HPCH/HPAI aldolase family protein
NE923	SAUSA300_2286	3B	E11	-	hypothetical protein
NE924	SAUSA300_1110	3B	E12	sun	ribosomal RNA small subunit methyltransferase B
NE925	SAUSA300_0401	3B	F1	-	superantigen-like protein 7
NE926	SAUSA300_1106	3B	F2	-	putative lipoprotein
NE927	SAUSA300_0326	3B	F3	-	hypothetical protein
NE928	SAUSA300_0598	3B	F4	-	putative iron compound ABC transporter iron compound-binding protein
NE929	SAUSA300_2105	3B	F5	mtlF	PTS system, mannitol specific IIBC component
NE930	SAUSA300_0860	3B	F6	rocD	ornithine--oxo-acid transaminase
NE931	SAUSA300_0308	3B	F7	-	ABC transporter permease
NE932	SAUSA300_0147	3B	F8		5' nucleotidase family protein
NE933	SAUSA300_2235	3B	F9	-	iron compound ABC transporter iron compound-binding protein
NE934	SAUSA300_0950	3B	F10		cysteine protease precursor
NE935	SAUSA300_2478	3B	F11	cidB	hypothetical protein
NE936	SAUSA300_0517	3B	F12	-	RNA methyltransferase
NE937	SAUSA300_1993	3B	G1	-	PfkB family kinase
NE938	SAUSA300_0413	3B	G2	-	tandem lipoprotein
NE939	SAUSA300_2078	3B	G3	murA	UDP-N-acetylglucosamine 1-carboxyvinyltransferase
NE940	SAUSA300_1403	3B	G4	-	phiSLT ORF412-like protein, portal protein
NE941	SAUSA300_2492	3B	G5	-	acetyltransferase family protein
NE942	SAUSA300_0252	3B	G6	-	glycosyl transferase, group 2 family protein
NE943	SAUSA300_0178	3B	G7	-	hypothetical protein
NE944	SAUSA300_0357	3B	G8	metE	5-methyltetrahydropteroyltriglutamate-- homocysteine S-methyltransferase
NE945	SAUSA300_0188	3B	G9	brnQ	branched-chain amino acid transport system II carrier protein
NE946	SAUSA300_0816	3B	G10	-	CsbD-like superfamily protein
NE947	SAUSA300_1042	3B	G11	-	hypothetical protein
NE948	SAUSA300_0349	3B	G12	-	hypothetical protein
NE949	SAUSA300_1752	3B	H1	hsdM	type I restriction-modification system, M subunit
NE950	SAUSA300_0968	3B	H2		phosphoribosylaminoimidazole-succinocarboxamide synthase
NE951	SAUSA300_1613	3B	H3	-	putative abrB protein
NE952	SAUSA300_2442	3B	H4	gntP	gluconate permease
NE953	SAUSA300_0770	3B	H5	-	hypothetical protein
NE954	SAUSA300_2327	3B	H6	-	hypothetical protein

NE955	SAUSA300_2340	3B	H7	narI	respiratory nitrate reductase, gamma subunit
NE956	SAUSA300_1524	3B	H8	-	CBS domain-containing protein
NE957	SAUSA300_0340	3B	H9		NADH-dependent FMN reductase
NE958	SAUSA300_0255	3B	H10	-	two-component response regulator
NE959	SAUSA300_1242	3B	H11		exonuclease SbcD
NE960	SAUSA300_0601	3B	H12	-	alpha/beta fold family hydrolase
NE961	SAUSA300_2391	3C	A1	opuCc	glycine betaine/carnitine/choline ABC transporter
NE962	SAUSA300_0730	3C	A2	-	GGDEF domain-containing protein
NE963	SAUSA300_1859	3C	A3	-	hypothetical protein
NE964	SAUSA300_0182	3C	A4	-	4'-phosphopantetheinyl transferase superfamily protein
NE965	SAUSA300_1363	3C	A5	gpsA	NAD(P)H-dependent glycerol-3-phosphate dehydrogenase
NE966	SAUSA300_0848	3C	A6	-	hypothetical protein
NE967	SAUSA300_0846	3C	A7	-	Na+/H+ antiporter family protein
NE968	SAUSA300_0327	3C	A8	-	hypothetical protein
NE969	SAUSA300_0314	3C	A9		sodium:solute symporter family protein
NE970	SAUSA300_2162	3C	A10		M23/M37 peptidase domain protein
NE971	SAUSA300_0712	3C	A11		amino acid/peptide transporter (Peptide:H+ symporter)
NE972	SAUSA300_0705	3C	A12	recQ	ATP-dependent DNA helicase RecQ
NE973	SAUSA300_0277	3C	B1		putative staphyloxanthin biosynthesis protein
NE974	SAUSA300_1188	3C	B2	mutS	DNA mismatch repair protein mutS
NE975	SAUSA300_2586	3C	B3		accessory secretory protein Asp2
NE976	SAUSA300_0877	3C	B4	clpB	Chaperone clpB
NE977	SAUSA300_1852	3C	B5		putative ABC transporter, ATP-binding protein
NE978	SAUSA300_2526	3C	B6	pyrD	dihydroorotate dehydrogenase
NE979	SAUSA300_0659	3C	B7		sugar efflux transporter
NE980	SAUSA300_2317	3C	B8	-	putative zinc-binding dehydrogenase
NE981	SAUSA300_2497	3C	B9	-	aminotransferase, class I
NE982	SAUSA300_1751	3C	B10	hsdS	type I restriction-modification enzyme, S subunit
NE983	SAUSA300_2416	3C	B11	-	glucose 1-dehydrogenase-like protein
NE984	SAUSA300_0667	3C	B12	-	hypothetical protein
NE985	SAUSA300_0408	3C	C1	-	hypothetical protein
NE986	SAUSA300_2412	3C	C2	-	hypothetical protein
NE987	SAUSA300_2249	3C	C3	ssaA	secretory antigen precursor SsaA
NE988	SAUSA300_0383	3C	C4	-	hypothetical protein
NE989	SAUSA300_0084	3C	C5	-	hypothetical protein
NE990	SAUSA300_0126	3C	C6	-	hypothetical protein
NE991	SAUSA300_2344	3C	C7	-	uroporphyrin-III C-methyl transferase
NE992	SAUSA300_0241	3C	C8	-	PTS system, sorbitol-specific IIC component
NE993	SAUSA300_2129	3C	C9	-	putative hemolysin III
NE994	SAUSA300_2622	3C	C10	-	hypothetical protein
NE995	SAUSA300_1594	3C	C11	yajC	preprotein translocase subunit YajC
NE996	SAUSA300_2397	3C	C12	-	putative transport protein
NE997	SAUSA300_2071	3C	D1	-	HemK family modification methylase
NE998	SAUSA300_1229	3C	D2	-	HAD superfamily hydrolase
NE999	SAUSA300_2369	3C	D3	-	6-carboxyhexanoate--CoA ligase
NE1000	SAUSA300_0612	3C	D4	-	putative monovalent cation/H+ antiporter subunit C
NE1001	SAUSA300_0258	3C	D5	-	GntR family transcriptional regulator
NE1002	SAUSA300_0396	3C	D6	set7	superantigen-like protein
NE1003	SAUSA300_2312	3C	D7	mqo	malate:quinone oxidoreductase
NE1004	SAUSA300_0027	3C	D8	-	hypothetical protein
NE1005	SAUSA300_2543	3C	D9	-	hypothetical protein

NE1006	SAUSA300_0702	3C	D10	-	hypothetical protein
NE1007	SAUSA300_0558	3C	D11	-	putative proline/betaine transporter
NE1008	SAUSA300_2470	3C	D12	sdaAB	L-serine dehydratase, iron-sulfur-dependent, beta subunit
NE1009	SAUSA300_0567	3C	E1	-	hypothetical protein
NE1010	SAUSA300_2378	3C	E2	-	hypothetical protein
NE1011	SAUSA300_0173	3C	E3	-	hypothetical protein
NE1012	SAUSA300_0869	3C	E4	rexB	exonuclease RexB
NE1013	SAUSA300_0826	3C	E5	-	hypothetical protein
NE1014	SAUSA300_0175	3C	E6	-	putative lipoprotein
NE1015	SAUSA300_0305	3C	E7	-	formate/nitrite transporter family protein
NE1016	SAUSA300_0785	3C	E8	-	acetyltransferase
NE1017	SAUSA300_1352	3C	E9	-	hypothetical protein
NE1018	SAUSA300_1479	3C	E10	-	hypothetical protein
NE1019	SAUSA300_1763	3C	E11	epiP	lantibiotic epidermin leader peptide processing serine protease EpiP
NE1020	SAUSA300_1031	3C	E12		conserved hypothetical protein
NE1021	SAUSA300_0157	3C	F1	cap5F	capsular polysaccharide biosynthesis protein Cap5F
NE1022	SAUSA300_0959	3C	F2	fmt	fmt protein
NE1023	SAUSA300_0984	3C	F3	ptsI	phosphoenolpyruvate-protein phosphotransferase
NE1024	SAUSA300_1404	3C	F4	-	phiSLT ORF 563-like protein, terminase, large subunit
NE1025	SAUSA300_0729	3C	F5		integral membrane protein
NE1026	SAUSA300_1298	3C	F6	-	hypothetical protein
NE1027	SAUSA300_1435	3C	F7	-	phiSLT ORF153-like protein
NE1028	SAUSA300_1517	3C	F8	-	endonuclease IV
NE1029	SAUSA300_1780	3C	F9		conserved hypothetical protein
NE1030	SAUSA300_2628	3C	F10	rarD	RarD protein
NE1031	SAUSA300_0120	3C	F11	sbnC	IucC family siderophore biosynthesis protein
NE1032	SAUSA300_0136	3C	F12	-	cell wall surface anchor family protein
NE1033	SAUSA300_2466	3C	G1		putative membrane protein
NE1034	SAUSA300_0680	3C	G2	norA	multi drug resistance protein
NE1035	SAUSA300_2253	3C	G3	ssaA	secretory antigen precursor SsaA
NE1036	SAUSA300_2542	3C	G4	-	putative AMP-binding enzyme
NE1037	SAUSA300_0318	3C	G5	-	N-acetylmannosamine-6-phosphate 2-epimerase
NE1038	SAUSA300_2610	3C	G6	hisC	histidinol-phosphate aminotransferase hisC
NE1039	SAUSA300_0312	3C	G7	-	hypothetical protein
NE1040	SAUSA300_1849	3C	G8	mutY	A/G-specific adenine glycosylase
NE1041	SAUSA300_2217	3C	G9	-	putative drug transporter
NE1042	SAUSA300_2529	3C	G10	-	hypothetical protein
NE1043	SAUSA300_2585	3C	G11	-	hypothetical protein
NE1044	SAUSA300_0980	3C	G12	-	hypothetical protein
NE1045	SAUSA300_1550	3C	H1	-	hypothetical protein
NE1046	SAUSA300_2231	3C	H2	fdhD	formate dehydrogenase accessory protein
NE1047	SAUSA300_0062	3C	H3	arcB	ornithine carbamoyltransferase
NE1048	SAUSA300_1092	3C	H4	pyrP	uracil permease
NE1049	SAUSA300_2058	3C	H5	atpD	F0F1 ATP synthase subunit beta
NE1050	SAUSA300_0129	3C	H6	-	acetoin reductase
NE1051	SAUSA300_0778	3C	H7	-	hypothetical protein
NE1052	SAUSA300_1275	3C	H8	-	peptide ABC transporter permease
NE1053	SAUSA300_1799	3C	H9	-	putative sensor histidine kinase
NE1054	SAUSA300_2419	3C	H10	-	hypothetical protein
NE1055	SAUSA300_0627	3C	H11	tagX	teichoic acid biosynthesis protein X
NE1056	SAUSA300_2169	3C	H12	-	hypothetical protein

NE1057	SAUSA300_2521	3D	A1	-	hypothetical protein
NE1058	SAUSA300_0591	3D	A2	-	acetyltransferase
NE1059	SAUSA300_1486	3D	A3	-	hypothetical protein
NE1060	SAUSA300_1570	3D	A4	-	U32 family peptidase
NE1061	SAUSA300_2260	3D	A5	-	inositol monophosphatase family protein
NE1062	SAUSA300_0410	3D	A6	-	tandem lipoprotein
NE1063	SAUSA300_0699	3D	A7	-	chorismate-binding domain-containing protein
NE1064	SAUSA300_2322	3D	A8	-	TetR family transcriptional regulator
NE1065	SAUSA300_0707	3D	A9	-	osmoprotectant ABC transporter permease
NE1066	SAUSA300_0954	3D	A10	-	MarR family transcriptional regulator
NE1067	SAUSA300_2266	3D	A11	-	hypothetical protein
NE1068	SAUSA300_2552	3D	A12	-	citrate transporter, permease
NE1069	SAUSA300_0187	3D	B1	rocD	ornithine aminotransferase
NE1070	SAUSA300_0329	3D	B2	-	putative oxidoreductase
NE1071	SAUSA300_0538	3D	B3	-	NAD-dependent epimerase/dehydratase family protein
NE1072	SAUSA300_0673	3D	B4	-	cobalamin synthesis protein/P47K family protein
NE1073	SAUSA300_0810	3D	B5	-	hypothetical protein
NE1074	SAUSA300_0887	3D	B6	oppB	oligopeptide ABC transporter permease
NE1075	SAUSA300_1677	3D	B7		cell wall surface anchor family protein
NE1076	SAUSA300_2289	3D	B8	-	hypothetical protein
NE1077	SAUSA300_0262	3D	B9	rbsK	ribokinase
NE1078	SAUSA300_1698	3D	B10	-	hypothetical protein
NE1079	SAUSA300_2021	3D	B11	-	S1 RNA-binding domain-containing protein
NE1080	SAUSA300_1762	3D	B12	epiF	lantibiotic epidermin immunity protein F
NE1081	SAUSA300_2561	3D	C1	phoB	alkaline phosphatase
NE1082	SAUSA300_2635	3D	C2	-	hypothetical protein
NE1083	SAUSA300_1001	3D	C3	potC	spermidine/putrescine ABC transporter permease
NE1084	SAUSA300_1017	3D	C4	-	hypothetical protein
NE1085	SAUSA300_1444	3D	C5	scpB	segregation and condensation protein B
NE1086	SAUSA300_1845	3D	C6	hemL	glutamate-1-semialdehyde aminotransferase
NE1087	SAUSA300_1884	3D	C7	-	CamS sex pheromone cAM373
NE1088	SAUSA300_2167	3D	C8		conserved hypothetical protein
NE1089	SAUSA300_2308	3D	C9	-	response regulator protein
NE1090	SAUSA300_2372	3D	C10	bioA	adenosylmethionine-8-amino-7-oxononanoate transaminase
NE1091	SAUSA300_2402	3D	C11	-	hypothetical protein
NE1092	SAUSA300_0225	3D	C12	-	putative acyl-CoA acetyltransferase FadA
NE1093	SAUSA300_0586	3D	D1	-	hypothetical protein
NE1094	SAUSA300_1385	3D	D2	-	phiSLT ORF 99-like protein
NE1095	SAUSA300_1901	3D	D3	aldA2	aldehyde dehydrogenase
NE1096	SAUSA300_2404	3D	D4		conserved hypothetical protein"
NE1097	SAUSA300_1005	3D	D5	-	manganese transport protein MntH
NE1098	SAUSA300_1756	3D	D6	splC	serine protease SplC
NE1099	SAUSA300_2282	3D	D7	-	hypothetical protein
NE1100	SAUSA300_0446	3D	D8	gltD	glutamate synthase subunit beta
NE1101	SAUSA300_0973	3D	D9	purM	phosphoribosylaminoimidazole synthetase
NE1102	SAUSA300_1028	3D	D10	-	iron transport associated domain-containing protein
NE1103	SAUSA300_2010	3D	D11	leuA	2-isopropylmalate synthase
NE1104	SAUSA300_2102	3D	D12	-	haloacid dehalogenase-like hydrolase
NE1105	SAUSA300_2556	3D	E1	-	ABC transporter protein
NE1106	SAUSA300_0420	3D	E2	-	hypothetical protein
NE1107	SAUSA300_1177	3D	E3	cinA	competence/damage-inducible protein cinA

NE1108	SAUSA300_1223	3D	E4	-	hypothetical protein
NE1109	SAUSA300_2022	3D	E5	rpoF	RNA polymerase sigma factor SigB
NE1110	SAUSA300_2315	3D	E6	-	hypothetical protein
NE1111	SAUSA300_0031	3D	E7	-	hypothetical protein
NE1112	SAUSA300_0276	3D	E8	-	hypothetical protein
NE1113	SAUSA300_2243	3D	E9	ureG	urease accessory protein UreG
NE1114	SAUSA300_2471	3D	E10	-	perfringolysin O regulator protein
NE1115	SAUSA300_2434	3D	E11	-	transporter protein
NE1116	SAUSA300_2558	3D	E12	nsaS	nisin susceptibility-associated sensor histidine kinase
NE1117	SAUSA300_0518	3D	F1	-	hypothetical protein
NE1118	SAUSA300_1290	3D	F2	dapD	tetrahydrodipicolinate acetyltransferase
NE1119	SAUSA300_1322	3D	F3	-	hypothetical protein
NE1120	SAUSA300_1387	3D	F4	-	phiSLT ORF129-like protein
NE1121	SAUSA300_1247	3D	F5		conserved hypothetical protein
NE1122	SAUSA300_0763	3D	F6	est	carboxylesterase
NE1123	SAUSA300_1402	3D	F7		phiSLT ORF257-like protein, putative prophage protease
NE1124	SAUSA300_2443	3D	F8	gntK	gluconate kinase
NE1125	SAUSA300_0064	3D	F9	arcD	arginine/oirnithine antiporter
NE1126	SAUSA300_0266	3D	F10	-	hypothetical protein
NE1127	SAUSA300_0414	3D	F11	-	tandem lipoprotein
NE1128	SAUSA300_0490	3D	F12	hslO	Hsp33-like chaperonin
NE1129	SAUSA300_0724	3D	G1	-	hypothetical protein
NE1130	SAUSA300_1561	3D	G2	-	hypothetical protein
NE1131	SAUSA300_2395	3D	G3	-	amino acid permease
NE1132	SAUSA300_2599	3D	G4	tetR	intercellular adhesion operon transcription regulator
NE1133	SAUSA300_0941	3D	G5	-	putative ferrichrome ABC transporter
NE1134	SAUSA300_0969	3D	G6	purS	phosphoribosylformylglycinamidine synthase
NE1135	SAUSA300_1245	3D	G7	opuD	glycine betaine transporter opuD
NE1136	SAUSA300_1331	3D	G8	ald	alanine dehydrogenase
NE1137	SAUSA300_2145	3D	G9	-	glycine betaine transporter
NE1138	SAUSA300_2387	3D	G10	-	NAD dependent epimerase/dehydratase family protein
NE1139	SAUSA300_0613	3D	G11	-	putative monovalent cation/H+ antiporter subunit D
NE1140	SAUSA300_1293	3D	G12	lysA	diaminopimelate decarboxylase
NE1141	SAUSA300_1674	3D	H1	-	putative serine protease HtrA
NE1142	SAUSA300_2264	3D	H2	-	RpiR family phosphosugar-binding transcriptional regulator
NE1143	SAUSA300_0831	3D	H3	-	hypothetical protein
NE1144	SAUSA300_1287	3D	H4	asd	aspartate semialdehyde dehydrogenase
NE1145	SAUSA300_1536	3D	H5	-	hypothetical protein
NE1146	SAUSA300_2131	3D	H6	-	hypothetical protein
NE1147	SAUSA300_2146	3D	H7	-	alcohol dehydrogenase, zinc-containing
NE1148	SAUSA300_2176	3D	H8	cbiO	cobalt transporter ATP-binding subunit
NE1149	SAUSA300_0190	3D	H9	ipdC	indole-3-pyruvate decarboxylase
NE1150	SAUSA300_0866	3D	H10	-	hypothetical protein
NE1151	SAUSA300_2251	3D	H11	-	dehydrogenase family protein
NE1152	SAUSA300_2342	3D	H12	narH	respiratory nitrate reductase, beta subunit
NE1153	SAUSA300_2614	4A	A1	-	hypothetical protein
NE1154	SAUSA300_0216	4A	A2	uhpT	sugar phosphate antiporter
NE1155	SAUSA300_0336	4A	A3	-	hypothetical protein
NE1156	SAUSA300_0405	4A	A4	hsdM	type I restriction-modification system, M subunit
NE1157	SAUSA300_2338	4A	A5		sensor histidine kinase
NE1158	SAUSA300_1999	4A	A6	rex	redox-sensing transcriptional repressor Rex

NE1159	SAUSA300_0999	4A	A7	potA	spermidine/putrescine ABC transporter ATP-binding protein
NE1160	SAUSA300_0417	4A	A8	-	tandem lipoprotein
NE1161	SAUSA300_0714	4A	A9	-	integral membrane protein
NE1162	SAUSA300_1506	4A	A10	-	hypothetical protein
NE1163	SAUSA300_2319	4A	A11	-	pyridine nucleotide-disulfide oxidoreductase
NE1164	SAUSA300_2637	4A	A12	-	hypothetical protein
NE1165	SAUSA300_0553	4A	B1	-	hypothetical protein
NE1166	SAUSA300_2007	4A	B2	ilvB	acetolactate synthase large subunit
NE1167	SAUSA300_2601	4A	B3	icaB	intercellular adhesion protein B
NE1168	SAUSA300_0271	4A	B4	-	ABC transporter ATP-binding protein
NE1169	SAUSA300_0902	4A	B5	pepF	oligoendopeptidase F
NE1170	SAUSA300_1725	4A	B6	-	putative translaldolase
NE1171	SAUSA300_0632	4A	B7	-	hypothetical protein
NE1172	SAUSA300_1033	4A	B8	-	iron/heme permease
NE1173	SAUSA300_1792	4A	B9	-	hypothetical protein
NE1174	SAUSA300_2411	4A	B10	opp-1A	oligopeptide permease, peptide-binding protein
NE1175	SAUSA300_2423	4A	B11	-	hypothetical protein
NE1176	SAUSA300_0511	4A	B12	radA	DNA repair protein RadA
NE1177	SAUSA300_2009	4A	C1	ilvC	ketol-acid reductoisomerase
NE1178	SAUSA300_2577	4A	C2	manA	mannose-6-phosphate isomerase
NE1179	SAUSA300_2594	4A	C3	msrA	methionine sulfoxide reductase A
NE1180	SAUSA300_0753	4A	C4	-	hypothetical protein
NE1181	SAUSA300_0773	4A	C5	-	putative staphylocoagulase
NE1182	SAUSA300_1284	4A	C6	-	hypothetical protein
NE1183	SAUSA300_1307	4A	C7	arlS	sensor histidine kinase protein
NE1184	SAUSA300_1328	4A	C8	-	putative drug transporter
NE1185	SAUSA300_2336	4A	C9	-	MerR family transcriptional regulator
NE1186	SAUSA300_2617	4A	C10	-	putative cobalt ABC transporter ATP-binding protein
NE1187	SAUSA300_0321	4A	C11	-	hypothetical protein
NE1188	SAUSA300_1912	4A	C12		putative membrane protein
NE1189	SAUSA300_2216	4A	D1	-	MarR family transcriptional regulator
NE1190	SAUSA300_2256	4A	D2	-	putative N-acetylmuramoyl-L-alanine amidase
NE1191	SAUSA300_2332	4A	D3	-	heat shock protein
NE1192	SAUSA300_0311	4A	D4	-	PfkB family carbohydrate kinase
NE1193	SAUSA300_0605	4A	D5	sarA	accessory regulator A
NE1194	SAUSA300_1061	4A	D6	-	superantigen-like protein
NE1195	SAUSA300_1399	4A	D7	-	phiSLT ORF110-like protein
NE1196	SAUSA300_2546	4A	D8	betB	glycine betaine aldehyde dehydrogenase
NE1197	SAUSA300_2616	4A	D9	-	cobalt transport family protein
NE1198	SAUSA300_0118	4A	D10	-	pyridoxal-phosphate dependent enzyme superfamily protein
NE1199	SAUSA300_0322	4A	D11	-	Oye family NADH-dependent flavin oxidoreductase
NE1200	SAUSA300_0358	4A	D12	-	bifunctional homocysteine S-methyltransferase/5,10-methylenetetrahydrofolate reductase protein
NE1201	SAUSA300_2547	4A	E1	-	hypothetical protein
NE1202	SAUSA300_1850	4A	E2	-	hypothetical protein
NE1203	SAUSA300_1495	4A	E3	-	hypothetical protein
NE1204	SAUSA300_2489	4A	E4	-	antibiotic transport-associated protein-like protein
NE1205	SAUSA300_2550	4A	E5	nrdG	anaerobic ribonucleotide reductase, small subunit
NE1206	SAUSA300_2056	4A	E6	-	hypothetical protein
NE1207	SAUSA300_1757	4A	E7	splB	serine protease SplB
NE1208	SAUSA300_1650	4A	E8	-	hypothetical protein

NE1209	SAUSA300_2410	4A	E9		oligopeptide ABC transporter, permease protein
NE1210	SAUSA300_1534	4A	E10	-	hypothetical protein
NE1211	SAUSA300_0411	4A	E11	-	tandem lipoprotein
NE1212	SAUSA300_1045	4A	E12	uvrC	excinuclease ABC subunit C
NE1213	SAUSA300_2355	4A	F1	-	putative lipoprotein
NE1214	SAUSA300_2273	4A	F2	-	Na+/H+ antiporter family protein
NE1215	SAUSA300_1266	4A	F3	trpF	N-(5'-phosphoribosyl)anthranilate isomerase
NE1216	SAUSA300_2530	4A	F4	-	TetR family transcriptional regulator
NE1217	SAUSA300_2165	4A	F5	budA	alpha-acetolactate decarboxylase
NE1218	SAUSA300_2050	4A	F6	-	TENA/THI-4 family protein
NE1219	SAUSA300_2486	4A	F7	-	putative ATP-dependent Clp proteinase
NE1220	SAUSA300_2168	4A	F8	-	hypothetical protein
NE1221	SAUSA300_0536	4A	F9	-	chaperone protein HchA
NE1222	SAUSA300_1976	4A	F10	-	succinyl-diaminopimelate desuccinylase
NE1223	SAUSA300_2513	4A	F11	-	hypothetical protein
NE1224	SAUSA300_0135	4A	F12	-	Fe/Mn family superoxide dismutase
NE1225	SAUSA300_0421	4A	G1	-	hypothetical protein
NE1226	SAUSA300_0373	4A	G2	-	hypothetical protein
NE1227	SAUSA300_0560	4A	G3	vraB	acetyl-CoA c-acetyltransferase
NE1228	SAUSA300_0811	4A	G4	-	hypothetical protein
NE1229	SAUSA300_1515	4A	G5	-	ABC transporter permease
NE1230	SAUSA300_0048	4A	G6	-	hypothetical protein
NE1231	SAUSA300_0430	4A	G7	-	hypothetical protein
NE1232	SAUSA300_2606	4A	G8	hisF	imidazole glycerol phosphate synthase subunit HisF
NE1233	SAUSA300_0066	4A	G9	argR	arginine repressor
NE1234	SAUSA300_0112	4A	G10	lctP	L-lactate permease
NE1235	SAUSA300_0156	4A	G11	cap5E	capsular polysaccharide biosynthesis protein Cap5E
NE1236	SAUSA300_0338	4A	G12	-	glyoxalase family protein
NE1237	SAUSA300_0473	4A	H1	purR	pur operon repressor
NE1238	SAUSA300_0214	4A	H2		conserved hypothetical protein
NE1239	SAUSA300_1040	4A	H3	-	hypothetical protein
NE1240	SAUSA300_1768	4A	H4	lukD	leukotoxin LukD
NE1241	SAUSA300_1222	4A	H5	nuc	thermonuclease
NE1242	SAUSA300_1391	4A	H6	-	phiSLT ORF527-like protein
NE1243	SAUSA300_1398	4A	H7	-	phiSLT ORF123-like protein
NE1244	SAUSA300_1443	4A	H8	rluB	ribosomal large subunit pseudouridine synthase B
NE1245	SAUSA300_1484	4A	H9	-	hypothetical protein
NE1246	SAUSA300_1722	4A	H10	-	hypothetical protein
NE1247	SAUSA300_1796	4A	H11	-	hypothetical protein
NE1248	SAUSA300_1971	4A	H12	-	phi77 ORF017-like protein
NE1249	SAUSA300_2036	4B	A1	kdpE	DNA-binding response regulator, KdpE
NE1250	SAUSA300_2076	4B	A2	-	aldehyde dehydrogenase family protein
NE1251	SAUSA300_2534	4B	A3	panB	3-methyl-2-oxobutanoate hydroxymethyltransferase
NE1252	SAUSA300_0144	4B	A4	phnC	phosphonate ABC transporter ATP-binding protein
NE1253	SAUSA300_0193	4B	A5	murQ	N-acetylmuramic acid-6-phosphate etherase
NE1254	SAUSA300_0310	4B	A6	pfoR	perfringolysin O regulator protein
NE1255	SAUSA300_0800	4B	A7	sek	enterotoxin K
NE1256	SAUSA300_0882	4B	A8	-	hypothetical protein
NE1257	SAUSA300_0930	4B	A9	-	lipoate-protein ligase A family protein
NE1258	SAUSA300_0406	4B	A10	-	putative restriction/modification system specificity protein
NE1259	SAUSA300_1489	4B	A11	-	hypothetical protein

NE1260	SAUSA300_1731	4B	A12	pckA	phosphoenolpyruvate carboxykinase
NE1261	SAUSA300_1973	4B	B1	-	truncated beta-hemolysin
NE1262	SAUSA300_1984	4B	B2	-	hypothetical protein
NE1263	SAUSA300_2108	4B	B3	mtlD	mannitol-1-phosphate 5-dehydrogenase
NE1264	SAUSA300_2400	4B	B4	-	glutamyl-aminopeptidase
NE1265	SAUSA300_2461	4B	B5	-	glyoxalase family protein
NE1266	SAUSA300_2611	4B	B6	hisD	histidinol dehydrogenase
NE1267	SAUSA300_0391	4B	B7	-	hypothetical protein
NE1268	SAUSA300_0666	4B	B8	-	hypothetical protein
NE1269	SAUSA300_0786	4B	B9	-	OsmC/Ohr family protein
NE1270	SAUSA300_0913	4B	B10	-	hypothetical protein
NE1271	SAUSA300_0942	4B	B11	-	hypothetical protein
NE1272	SAUSA300_1207	4B	B12	-	hypothetical protein
NE1273	SAUSA300_1260	4B	C1	-	prephenate dehydrogenase
NE1274	SAUSA300_1281	4B	C2	pstA	phosphate ABC transporter permease PstA
NE1275	SAUSA300_1304	4B	C3	-	hypothetical protein
NE1276	SAUSA300_1683	4B	C4	-	bifunctional 3-deoxy-7-phosphoheptulonate synthase/chorismate mutase
NE1277	SAUSA300_1759	4B	C5	-	hypothetical protein
NE1278	SAUSA300_1890	4B	C6	-	staphopain A
NE1279	SAUSA300_2345	4B	C7	nirD	nitrite reductase [NAD(P)H], small subunit
NE1280	SAUSA300_0231	4B	C8		ABC transporter, substrate-binding protein
NE1281	SAUSA300_0725	4B	C9	-	hypothetical protein
NE1282	SAUSA300_0332	4B	C10	-	PTS system, IIA component
NE1283	SAUSA300_0028	4B	C11		putative transposase
NE1284	SAUSA300_1378	4B	C12	-	hypothetical protein
NE1285	SAUSA300_0775	4B	D1	-	hypothetical protein
NE1286	SAUSA300_2598	4B	D2		capsular polysaccharide biosynthesis protein Cap1A
NE1287	SAUSA300_1216	4B	D3		cardiolipin synthetase
NE1288	SAUSA300_0426	4B	D4		hypothetical protein
NE1289	SAUSA300_0547	4B	D5	sdrD	sdrD protein
NE1290	SAUSA300_2576	4B	D6		phosphotransferase system, fructose-specific IIABC component
NE1291	SAUSA300_1955	4B	D7		putative endodeoxyribonuclease RusA
NE1292	SAUSA300_0614	4B	D8		putative Na+/H+ antiporter, MnhE component
NE1293	SAUSA300_1583	4B	D9	-	hypothetical protein
NE1294	SAUSA300_1199	4B	D10		hypothetical protein
NE1295	SAUSA300_0456	4B	D11	rrlA	23S ribosomal RNA
NE1296	SAUSA300_0690	4B	D12	saeS	sensor histidine kinase SaeS
NE1297	SAUSA300_1987	4B	E1	-	carbon-nitrogen family hydrolase
NE1298	SAUSA300_1964	4B	E2	-	hypothetical protein
NE1299	SAUSA300_0905	4B	E3	-	hypothetical protein
NE1300	SAUSA300_1975	4B	E4	-	Aerolysin/leukocidin family protein
NE1301	SAUSA300_1093	4B	E5	pyrB	aspartate carbamoyltransferase catalytic subunit
NE1302	SAUSA300_0083	4B	E6	-	hypothetical protein
NE1303	SAUSA300_1921	4B	E7	-	truncated amidase
NE1304	SAUSA300_2326	4B	E8	-	transcription regulatory protein
NE1305	SAUSA300_1696	4B	E9	dat	D-alanine aminotransferase
NE1306	SAUSA300_1261	4B	E10	-	putative glutamyl aminopeptidase
NE1307	SAUSA300_2386	4B	E11	-	beta-lactamase
NE1308	SAUSA300_2244	4B	E12	ureD	urease accessory protein UreD
NE1309	SAUSA300_1442	4B	F1	srrA	respiratory response protein, SrrA

NE1310	SAUSA300_1942	4B	F2	-	hypothetical protein
NE1311	SAUSA300_0174	4B	F3	-	hypothetical protein
NE1312	SAUSA300_0422	4B	F4	-	hypothetical protein
NE1313	SAUSA300_0489	4B	F5	-	putative cell division protein FtsH
NE1314	SAUSA300_0896	4B	F6	oppC	oligopeptide ABC transporter permease
NE1315	SAUSA300_0899	4B	F7	-	adaptor protein
NE1316	SAUSA300_1279	4B	F8	phoU	phosphate transport system regulatory protein PhoU
NE1317	SAUSA300_1488	4B	F9	-	hypothetical protein
NE1318	SAUSA300_1712	4B	F10	ribH	6,7-dimethyl-8-ribityllumazine synthase
NE1319	SAUSA300_1740	4B	F11	-	hypothetical protein
NE1320	SAUSA300_1875	4B	F12	-	exonuclease
NE1321	SAUSA300_2003	4B	G1	rimI	ribosomal-protein-alanine acetyltransferase
NE1322	SAUSA300_2042	4B	G2	-	hypothetical protein
NE1323	SAUSA300_2098	4B	G3	arsR	ArsR family transcriptional regulator
NE1324	SAUSA300_2305	4B	G4	-	transposase, truncation
NE1325	SAUSA300_1198	4B	G5	-	putative GTP-binding protein
NE1326	SAUSA300_0034	4B	G6		IS1272, transposase
NE1327	SAUSA300_0393	4B	G7	-	hypothetical protein
NE1328	SAUSA300_0442	4B	G8	-	hypothetical protein
NE1329	SAUSA300_0793	4B	G9	-	hypothetical protein
NE1330	SAUSA300_1238	4B	G10	-	hypothetical protein
NE1331	SAUSA300_1358	4B	G11	ndk	nucleoside diphosphate kinase
NE1332	SAUSA300_1659	4B	G12	tpx	thiol peroxidase
NE1333	SAUSA300_1542	4B	H1	hrcA	heat-inducible transcription repressor HrcA
NE1334	SAUSA300_1494	4B	H2	-	hypothetical protein
NE1335	SAUSA300_2505	4B	H3	-	acetyltransferase
NE1336	SAUSA300_1935	4B	H4	-	phi77 ORF029-like protein
NE1337	SAUSA300_1023	4B	H5	-	hypothetical protein
NE1338	SAUSA300_1952	4B	H6	-	phiPV083 ORF027-like protein
NE1339	SAUSA300_0468	4B	H7	-	TatD family hydrolase
NE1340	SAUSA300_1692	4B	H8	-	hypothetical protein
NE1341	SAUSA300_0300	4B	H9	-	hypothetical protein
NE1342	SAUSA300_1127	4B	H10	smc	chromosome segregation protein SMC
NE1343	SAUSA300_1633	4B	H11	gap	glyceraldehyde 3-phosphate dehydrogenase 2
NE1344	SAUSA300_1120	4B	H12	recG	ATP-dependent DNA helicase RecG
NE1345	SAUSA300_0946	4C	A1	menD	2-succinyl-6-hydroxy-2, 4-cyclohexadiene-1-carboxylic acid synthase/2-oxoglutarate decarboxylase
NE1346	SAUSA300_1461	4C	A2	-	hypothetical protein
NE1347	SAUSA300_1862	4C	A3	-	hypothetical protein
NE1348	SAUSA300_1948	4C	A4	-	phi77 ORF069-like protein
NE1349	SAUSA300_1372	4C	A5		conserved hypothetical protein
NE1350	SAUSA300_2314	4C	A6		conserved hypothetical protein
NE1351	SAUSA300_1846	4C	A7		conserved hypothetical protein
NE1352	SAUSA300_2347	4C	A8		nitrite reductase transcriptional regulator NirR
NE1353	SAUSA300_2579	4C	A9		N-acetylmuramoyl-L-alanine amidase domainprotein
NE1354	SAUSA300_1058	4C	A10		alpha-hemolysin precursor
NE1355	SAUSA300_2230	4C	A11		molybdenum ABC transporter, molybdenum-binding protein ModA
NE1356	SAUSA300_2237	4C	A12		putative urea transporter
NE1357	SAUSA300_1337	4C	B1	-	hypothetical protein
NE1358	SAUSA300_0603	4C	B2		conserved hypothetical protein
NE1359	SAUSA300_1665	4C	B3		conserved hypothetical protein

NE1360	SAUSA300_1255	4C	B4	fmtC	oxacillin resistance-related FmtC protein
NE1361	SAUSA300_1224	4C	B5		conserved hypothetical protein
NE1362	SAUSA300_0998	4C	B6		conserved hypothetical protein
NE1363	SAUSA300_1034	4C	B7	srtB	sortase B
NE1364	SAUSA300_2095	4C	B8		conserved hypothetical protein
NE1365	SAUSA300_0825	4C	B9		oxidoreductase, 2-nitropropane dioxygenase family
NE1366	SAUSA300_1232	4C	B10		catalase
NE1367	SAUSA300_0137	4C	B11		transcriptional regulator, GntR family
NE1368	SAUSA300_1538	4C	B12		ribosomal protein L11 methyltransferase
NE1369	SAUSA300_1588	4C	C1		N-acetylmuramoyl-L-alanine amidase
NE1370	SAUSA300_0728	4C	C2		conserved hypothetical protein
NE1371	SAUSA300_1967	4C	C3		conserved hypothetical phage protein
NE1372	SAUSA300_0384	4C	C4	-	hypothetical protein
NE1373	SAUSA300_0012	4C	C5		putative homoserine O-acetyltransferase
NE1374	SAUSA300_0626	4C	C6		teichoic acid biosynthesis protein B
NE1375	SAUSA300_1012	4C	C7		conserved hypothetical protein
NE1376	SAUSA300_2323	4C	C8	cobI	transporter, CorA family
NE1377	SAUSA300_2511	4C	C9		conserved hypothetical protein
NE1378	SAUSA300_0892	4C	C10		oligopeptide ABC transporter, oligopeptide-binding protein
NE1379	SAUSA300_1596	4C	C11		S-adenosylmethionine:tRNA ribosyltransferase-isomerase
NE1380	SAUSA300_0978	4C	C12		ABC transporter, ATP-binding protein
NE1381	SAUSA300_2541	4C	D1	mqo	malate:quinone-oxidoreductase
NE1382	SAUSA300_0594	4C	D2		alcohol dehydrogenase
NE1383	SAUSA300_0713	4C	D3		GTP cyclohydrolase I
NE1384	SAUSA300_0957	4C	D4	-	hypothetical protein
NE1385	SAUSA300_0287	4C	D5		conserved hypothetical protein
NE1386	SAUSA300_1974	4C	D6		Leukocidin/Hemolysin toxin family protein
NE1387	SAUSA300_2276	4C	D7		peptidase, M20/M25/M40 family
NE1388	SAUSA300_0337	4C	D8		glycerol-3-phosphate transporter
NE1389	SAUSA300_1225	4C	D9		aspartate kinase
NE1390	SAUSA300_0709	4C	D10		5'(3')-deoxyribonucleotidase
NE1391	SAUSA300_1305	4C	D11		2-oxoglutarate dehydrogenase, E2 component, dihydrolipoamide succinyltransferase
NE1392	SAUSA300_1531	4C	D12		phosphate starvation-induced protein, PhoH family
NE1393	SAUSA300_2490	4C	E1	-	TetR family regulatory protein
NE1394	SAUSA300_0213	4C	E2	-	Gfo/Idh/MocA family oxidoreductase
NE1395	SAUSA300_1946	4C	E3		phiPVL ORF057-like protein, transcriptionalactivator RinB
NE1396	SAUSA300_0038	4C	E4	ccrA	cassette chromosome recombinase A
NE1397	SAUSA300_2166	4C	E5	alsS	alpha-acetolactate synthase
NE1398	SAUSA300_1084	4C	E6		conserved hypothetical protein
NE1399	SAUSA300_2365	4C	E7	hlgA	gamma-hemolysin component A
NE1400	SAUSA300_2389	4C	E8		putative drug transporter
NE1401	SAUSA300_1853	4C	E9		conserved hypothetical protein
NE1402	SAUSA300_0590	4C	E10	-	hypothetical protein
NE1403	SAUSA300_1585	4C	E11		conserved hypothetical protein
NE1404	SAUSA300_1605	4C	E12	mreC	rod shape-determining protein MreC
NE1405	SAUSA300_2210	4C	F1	glcU	probable glucose uptake protein"
NE1406	SAUSA300_0409	4C	F2		conserved hypothetical protein
NE1407	SAUSA300_1644	4C	F3	pyk	pyruvate kinase
NE1408	SAUSA300_1430	4C	F4		phiSLT ORF 87-like protein, putative DNA-binding protein
NE1409	SAUSA300_0407	4C	F5		exotoxin

NE1410	SAUSA300_2065	4C	F6		UDP-N-acetylglucosamine 2-epimerase
NE1411	SAUSA300_1244	4C	F7	mscL	large conductance mechanosensitive channel protein
NE1412	SAUSA300_0683	4C	F8		transcriptional regulator, DeoR family
NE1413	SAUSA300_1180	4C	F9		conserved hypothetical protein
NE1414	SAUSA300_1568	4C	F10	udk	uridine kinase
NE1415	SAUSA300_1253	4C	F11	glcT	transcription antiterminator
NE1416	SAUSA300_2147	4C	F12		alcohol dehydrogenase, zinc-containing
NE1417	SAUSA300_0940	4C	G1	-	hypothetical protein
NE1418	SAUSA300_2627	4C	G2		2-oxoglutarate/malate translocator
NE1419	SAUSA300_0631	4C	G3		putative nucleoside transporter
NE1420	SAUSA300_1003	4C	G4		conserved hypothetical protein
NE1421	SAUSA300_0239	4C	G5		PTS system, fructose-specific enzyme II, BC component
NE1422	SAUSA300_0783	4C	G6		phosphoglycerate mutase family protein
NE1423	SAUSA300_1764	4C	G7	epiD	lantibiotic epidermin biosynthesis protein EpiD
NE1424	SAUSA300_2069	4C	G8		conserved hypothetical protein
NE1425	SAUSA300_0169	4C	G9		conserved hypothetical protein
NE1426	SAUSA300_0354	4C	G10	ltrA	low temperature requirement protein LtrA
NE1427	SAUSA300_1576	4C	G11		helicase, RecD/TraA family
NE1428	SAUSA300_2049	4C	G12	thiD	phosphomethylpyrimidine kinase
NE1429	SAUSA300_2475	4C	H1		conserved hypothetical protein
NE1430	SAUSA300_0356	4C	H2		conserved hypothetical protein
NE1431	SAUSA300_0580	4C	H3		conserved hypothetical protein
NE1432	SAUSA300_0267	4C	H4		transposase
NE1433	SAUSA300_0317	4C	H5		conserved hypothetical protein
NE1434	SAUSA300_1016	4C	H6	cyoE	protoheme IX farnesyltransferase
NE1435	SAUSA300_2265	4C	H7		putative amino acid permease
NE1436	SAUSA300_0888	4C	H8	oppC	oligopeptide ABC transporter, permease protein
NE1437	SAUSA300_2353	4C	H9		conserved hypothetical protein
NE1438	SAUSA300_0256	4C	H10		holin-like protein lrgA
NE1439	SAUSA300_1457	4C	H11	malR	maltose operon transcriptional repressor
NE1440	SAUSA300_1487	4C	H12		replication initiation factor family protein
NE1441	SAUSA300_1728	4D	A1		oxidoreductase, aldo/keto reductase family
NE1442	SAUSA300_1878	4D	A2	rumA	RNA methyltransferase, TrmA family
NE1443	SAUSA300_1747	4D	A3		conserved hypothetical protein
NE1444	SAUSA300_2499	4D	A4	crtM	squalene desaturase
NE1445	SAUSA300_1797	4D	A5		conserved hypothetical protein
NE1446	SAUSA300_1141	4D	A6		endopeptidase resistance gene
NE1447	SAUSA300_1470	4D	A7		geranyltranstransferase
NE1448	SAUSA300_1947	4D	A8		phi77 ORF031-like protein
NE1449	SAUSA300_2366	4D	A9	hlgC	gamma-hemolysin component C
NE1450	SAUSA300_1907	4D	A10	-	hypothetical protein
NE1451	SAUSA300_1243	4D	A11	sbcC	exonuclease SbcC
NE1452	SAUSA300_1945	4D	A12		phi77 ORF071-like protein
NE1453	SAUSA300_1501	4D	B1		putative competence protein ComG
NE1454	SAUSA300_1096	4D	B2	carB	carbamoyl phosphate synthase large subunit
NE1455	SAUSA300_0534	4D	B3		amidohydrolase
NE1456	SAUSA300_0873	4D	B4	cdr	coenzyme A disulfide reductase
NE1457	SAUSA300_1672	4D	B5	nagE	phosphotransferase system, N-acetylglucosamine-specific IIBC component
NE1458	SAUSA300_2094	4D	B6		conserved hypothetical protein
NE1459	SAUSA300_1283	4D	B7		phosphate ABC transporter, phosphate-binding protein PstS

NE1460	SAUSA300_1843	4D	B8		D-isomer specific 2-hydroxyacid dehydrogenase family protein
NE1461	SAUSA300_0385	4D	B9		conserved hypothetical protein
NE1462	SAUSA300_1043	4D	B10	mutS2	DNA mismatch repair MutS2 protein
NE1463	SAUSA300_0914	4D	B11		sodium:alanine symporter family protein
NE1464	SAUSA300_0971	4D	B12	purL	phosphoribosylformylglycinamidine synthase II
NE1465	SAUSA300_1008	4D	C1		conserved hypothetical protein
NE1466	SAUSA300_2480	4D	C2		transcriptional regulator, LysR family
NE1467	SAUSA300_2569	4D	C3	arcB	ornithine carbamoyltransferase
NE1468	SAUSA300_0635	4D	C4	fhuG	ferrichrome transport permease protein fhuG
NE1469	SAUSA300_0059	4D	C5		conserved hypothetical protein
NE1470	SAUSA300_2250	4D	C6	nhaC	Na+/H+ antiporter NhaC
NE1471	SAUSA300_2300	4D	C7		transcriptional regulator, TetR family
NE1472	SAUSA300_2023	4D	C8	rsbW	anti-sigma-B factor, serine-protein kinase
NE1473	SAUSA300_2048	4D	C9	thiM	hydroxyethylthiazole kinase
NE1474	SAUSA300_1518	4D	C10		ATP-dependent RNA helicase, DEAD/DEAH box family
NE1475	SAUSA300_0131	4D	C11		putative Bacterial sugar transferase
NE1476	SAUSA300_0813	4D	C12	-	hypothetical protein
NE1477	SAUSA300_0189	4D	D1	entB	isochorismatase
NE1478	SAUSA300_2133	4D	D2	-	transporter gate domain-containing protein
NE1479	SAUSA300_2280	4D	D3	fosB	fosfomycin resistance protein FosB
NE1480	SAUSA300_2275	4D	D4	-	short chain dehydrogenase/reductase family oxidoreductase
NE1481	SAUSA300_1687	4D	D5	-	FtsK/SpoIIIE family protein
NE1482	SAUSA300_1654	4D	D6	-	proline dipeptidase
NE1483	SAUSA300_1934	4D	D7	-	phi77 ORF020-like protein, phage major tail protein
NE1484	SAUSA300_1718	4D	D8	arsB	aresenical pump membrane protein
NE1485	SAUSA300_2083	4D	D9	-	acetyltransferase
NE1486	SAUSA300_1639	4D	D10	phoP	alkaline phosphatase synthesis transcriptional regulatory protein
NE1487	SAUSA300_2288	4D	D11	-	ABC transporter ATP-binding protein
NE1488	SAUSA300_0323	4D	D12	-	hypothetical protein
NE1489	SAUSA300_2306	4D	E1	-	ABC transporter ATP-binding protein
NE1490	SAUSA300_0448	4D	E2	treP	PTS system, trehalose-specific IIBC component
NE1491	SAUSA300_1021	4D	E3	-	hypothetical protein
NE1492	SAUSA300_2522	4D	E4	-	hypothetical protein
NE1493	SAUSA300_0871	4D	E5	-	hypothetical protein
NE1494	SAUSA300_1126	4D	E6	rnc	ribonuclease III
NE1495	SAUSA300_2055	4D	E7	murA	UDP-N-acetylglucosamine 1-carboxyvinyltransferase
NE1496	SAUSA300_0372	4D	E8	-	hypothetical protein
NE1497	SAUSA300_0675	4D	E9	-	hypothetical protein
NE1498	SAUSA300_1183	4D	E10	-	2-oxoglutarate ferredoxin oxidoreductase subunit beta
NE1499	SAUSA300_0074	4D	E11	opp-3B	oligopeptide permease, channel-forming protein
NE1500	SAUSA300_0043	4D	E12	-	hypothetical protein
NE1501	SAUSA300_1618	4D	F1	hemX	hemA concentration negative effector hemX
NE1502	SAUSA300_1345	4D	F2	asnC	asparaginyl-tRNA synthetase
NE1503	SAUSA300_0561	4D	F3	-	hypothetical protein
NE1504	SAUSA300_0617	4D	F4	-	Na+/H+ antiporter
NE1505	SAUSA300_0840	4D	F5	-	hypothetical protein
NE1506	SAUSA300_0951	4D	F6	sspA	V8 protease
NE1507	SAUSA300_1519	4D	F7	-	hypothetical protein
NE1508	SAUSA300_2496	4D	F8	-	D-lactate dehydrogenase
NE1509	SAUSA300_0630	4D	F9	-	ABC transporter ATP-binding protein
NE1510	SAUSA300_0723	4D	F10	-	hypothetical protein

NE1511	SAUSA300_2279	4D	F11	-	LysR family regulatory protein
NE1512	SAUSA300_2341	4D	F12	narJ	respiratory nitrate reductase, subunit delta
NE1513	SAUSA300_1297	4D	G1	-	acylphosphatase
NE1514	SAUSA300_1231	4D	G2	-	gamma-aminobutyrate permease
NE1515	SAUSA300_1427	4D	G3	-	phiSLT ORF86-like protein
NE1516	SAUSA300_0606	4D	G4	-	hypothetical protein
NE1517	SAUSA300_1172	4D	G5	-	M16 family peptidase
NE1518	SAUSA300_0861	4D	G6	gudB	NAD-specific glutamate dehydrogenase
NE1519	SAUSA300_1563	4D	G7	accC	acetyl-CoA carboxylase, biotin carboxylase
NE1520	SAUSA300_2030	4D	G8	-	hypothetical protein
NE1521	SAUSA300_2620	4D	G9	-	hypothetical protein
NE1522	SAUSA300_0219	4D	G10	-	putative iron compound A C transporter, iron compound-binding protein
NE1523	SAUSA300_0470	4D	G11	ksgA	dimethyladenosine transferase
NE1524	SAUSA300_0415	4D	G12	lpl3	tandem lipoprotein
NE1525	SAUSA300_1745	4D	H1	-	hypothetical protein
NE1526	SAUSA300_1095	4D	H2	carA	carbamoyl phosphate synthase small subunit
NE1527	SAUSA300_2516	4D	H3	-	short chain dehydrogenase/reductase family oxidoreductase
NE1528	SAUSA300_1371	4D	H4	recQ	ATP-dependent DNA helicase RecQ
NE1529	SAUSA300_2125	4D	H5	-	ATP-binding Mrp/Nbp35 family protein
NE1530	SAUSA300_1368	4D	H6	ansA	L-asparaginase
NE1531	SAUSA300_0505	4D	H7	-	glutamine amidotransferase subunit PdxT
NE1532	SAUSA300_1992	4D	H8	agrA	accessory gene regulator protein A
NE1533	SAUSA300_0007	4D	H9	-	hypothetical protein
NE1534	SAUSA300_0070	4D	H10	-	putative lysophospholipase
NE1535	SAUSA300_2154	4D	H11	lacB	galactose-6-phosphate isomerase subunit LacB
NE1536	SAUSA300_0791	4D	H12	gcvH	glycine cleavage system protein H
NE1537	SAUSA300_0545	5A	A1	-	hypothetical protein
NE1538	SAUSA300_2502	5A	A2	-	hypothetical protein
NE1539	SAUSA300_0301	5A	A3	-	hypothetical protein
NE1540	SAUSA300_0733	5A	A4	-	degV family protein
NE1541	SAUSA300_2233	5A	A5	-	BioY family protein
NE1542	SAUSA300_2632	5A	A6	-	hypothetical protein
NE1543	SAUSA300_0961	5A	A7	qoxC	quinol oxidase, subunit III
NE1544	SAUSA300_1020	5A	A8	-	glycerophosphoryl diester phosphodiesterase family protein
NE1545	SAUSA300_2227	5A	A9	moeB	molybdopterin biosynthesis protein B
NE1546	SAUSA300_0981	5A	A10	-	hypothetical protein
NE1547	SAUSA300_2508	5A	A11	-	hypothetical protein
NE1548	SAUSA300_2064	5A	A12	atpB	F0F1 ATP synthase subunit A
NE1549	SAUSA300_0692	5A	B1	-	hypothetical protein
NE1550	SAUSA300_0788	5A	B2	-	nitroreductase family protein
NE1551	SAUSA300_2236	5A	B3	-	hypothetical protein
NE1552	SAUSA300_0706	5A	B4	-	putative osmoprotectant ABC transporter ATP-binding protein
NE1553	SAUSA300_2281	5A	B5	hutG	formimidoylglutamase
NE1554	SAUSA300_0376	5A	B6	-	hypothetical protein
NE1555	SAUSA300_1148	5A	B7	codY	transcriptional repressor CodY
NE1556	SAUSA300_0938	5A	B8	-	hypothetical protein
NE1557	SAUSA300_2252	5A	B9	-	hypothetical protein
NE1558	SAUSA300_0774	5A	B10	empbp	secretory extracellular matrix and plasma binding protein
NE1559	SAUSA300_0344	5A	B11	-	putative lipoprotein
NE1560	SAUSA300_0658	5A	B12	-	LysR family transcriptional regulator

NE1561	SAUSA300_1370	5A	C1	ebpS	cell surface elastin binding protein
NE1562	SAUSA300_1717	5A	C2	arsR	arsenical resistance operon repressor
NE1563	SAUSA300_0395	5A	C3	-	superantigen-like protein
NE1564	SAUSA300_1384	5A	C4	-	phiSLT ORF100b-like protein, holin
NE1565	SAUSA300_0288	5A	C5	-	hypothetical protein
NE1566	SAUSA300_0115	5A	C6	sirC	iron compound ABC transporter permease SirC
NE1567	SAUSA300_1289	5A	C7	dapB	dihydrodipicolinate reductase
NE1568	SAUSA300_2008	5A	C8	ilvN	acetolactate synthase 1 regulatory subunit
NE1569	SAUSA300_0402	5A	C9	-	superantigen-like protein
NE1570	SAUSA300_0431	5A	C10	-	hypothetical protein
NE1571	SAUSA300_0379	5A	C11	ahpF	alkyl hydroperoxide reductase subunit F
NE1572	SAUSA300_2163	5A	C12	-	hypothetical protein
NE1573	SAUSA300_0141	5A	D1	deoB	phosphopentomutase
NE1574	SAUSA300_0767	5A	D2	-	hypothetical protein
NE1575	SAUSA300_2646	5A	D3	trmE	tRNA modification GTPase TrmE
NE1576	SAUSA300_1342	5A	D4	-	hypothetical protein
NE1577	SAUSA300_1755	5A	D5	splD	serine protease SplD
NE1578	SAUSA300_0945	5A	D6	-	isochorismate synthase family protein
NE1579	SAUSA300_0952	5A	D7	-	aminotransferase, class I
NE1580	SAUSA300_1191	5A	D8	glpF	glycerol uptake facilitator
NE1581	SAUSA300_2350	5A	D9	-	hypothetical protein
NE1582	SAUSA300_0423	5A	D10	-	hypothetical protein
NE1583	SAUSA300_2234	5A	D11	-	inosine-uridine preferring nucleoside hydrolase
NE1584	SAUSA300_0259	5A	D12	-	PTS system, IIA component
NE1585	SAUSA300_0807	5A	E1	-	hypothetical protein
NE1586	SAUSA300_0263	5A	E2	rbsD	D-ribose pyranase
NE1587	SAUSA300_1192	5A	E3	glpK	glycerol kinase
NE1588	SAUSA300_1783	5A	E4	hemE	uroporphyrinogen decarboxylase
NE1589	SAUSA300_0798	5A	E5	-	ABC transporter substrate-binding protein
NE1590	SAUSA300_1409	5A	E6	-	hypothetical protein
NE1591	SAUSA300_1577	5A	E7	-	TPR domain-containing protein
NE1592	SAUSA300_2359	5A	E8	-	amino acid ABC transporter amino acid-binding protein
NE1593	SAUSA300_2482	5A	E9	-	hypothetical protein
NE1594	SAUSA300_0065	5A	E10	arcA	arginine deiminase
NE1595	SAUSA300_0588	5A	E11	-	hypothetical protein
NE1596	SAUSA300_0552	5A	E12	-	hypothetical protein
NE1597	SAUSA300_1135	5A	F1	-	hypothetical protein
NE1598	SAUSA300_2040	5A	F2	-	hypothetical protein
NE1599	SAUSA300_1743	5A	F3	-	hypothetical protein
NE1600	SAUSA300_0808	5A	F4	-	hypothetical protein
NE1601	SAUSA300_2303	5A	F5	tcaR	transcriptional regulator TcaR
NE1602	SAUSA300_1419	5A	F6	-	phiSLT ORF80-like protein
NE1603	SAUSA300_0077	5A	F7	-	ABC transporter ATP-binding protein
NE1604	SAUSA300_2407	5A	F8	-	oligopeptide ABC transporter ATP-binding protein
NE1605	SAUSA300_0801	5A	F9	seq	enterotoxin Q
NE1606	SAUSA300_0544	5A	F10	-	HAD superfamily hydrolase
NE1607	SAUSA300_2025	5A	F11	rsbU	sigma-B regulation protein
NE1608	SAUSA300_2047	5A	F12	thiE	thiamine-phosphate pyrophosphorylase
NE1609	SAUSA300_1273	5A	G1	opp-2F	oligopeptide permease, ATP-binding protein
NE1610	SAUSA300_0996	5A	G2	lpdA	dihydrolipoamide dehydrogenase
NE1611	SAUSA300_1271	5A	G3	-	hydrolase-like protein

NE1612	SAUSA300_1397	5A	G4	-	phiSLT ORF213-like protein, major tail protein
NE1613	SAUSA300_2290	5A	G5	-	putative 3-methyladenine DNA glycosylase
NE1614	SAUSA300_2325	5A	G6	-	hypothetical protein
NE1615	SAUSA300_0618	5A	G7	-	ABC transporter substrate-binding protein
NE1616	SAUSA300_2127	5A	G8	-	hypothetical protein
NE1617	SAUSA300_2272	5A	G9	-	hypothetical protein
NE1618	SAUSA300_2593	5A	G10	-	hypothetical protein
NE1619	SAUSA300_0163	5A	G11	cap5L	capsular polysaccharide biosynthesis protein Cap5L
NE1620	SAUSA300_0240	5A	G12	-	PTS system, galactitol-specific enzyme II, B component
NE1621	SAUSA300_0557	5A	H1	-	HAD family hydrolase
NE1622	SAUSA300_0691	5A	H2	saeR	DNA-binding response regulator SaeR
NE1623	SAUSA300_0832	5A	H3	-	hypothetical protein
NE1624	SAUSA300_1339	5A	H4	-	hypothetical protein
NE1625	SAUSA300_2413	5A	H5	-	hypothetical protein
NE1626	SAUSA300_0119	5A	H6	-	ornithine cyclodeaminase
NE1627	SAUSA300_1394	5A	H7	-	hypothetical protein
NE1628	SAUSA300_1424	5A	H8	-	hypothetical protein
NE1629	SAUSA300_2618	5A	H9	-	hypothetical protein
NE1630	SAUSA300_0076	5A	H10	-	ABC transporter ATP-binding protein
NE1631	SAUSA300_1204	5A	H11	-	hypothetical protein
NE1632	SAUSA300_2294	5A	H12	-	hypothetical protein
NE1633	SAUSA300_0889	5B	a1	oppD	oligopeptide ABC transporter ATP-binding protein
NE1634	SAUSA300_1312	5B	a2	-	acetyltransferase
NE1635	SAUSA300_1478	5B	a3	-	putative lipoprotein
NE1636	SAUSA300_1925	5B	a4	-	phiPVL ORF17-like protein
NE1637	SAUSA300_0237	5B	a5	-	inosine-uridine preferring nucleoside hydrolase
NE1638	SAUSA300_1111	5B	a6	-	ribosomal RNA large subunit methyltransferase N
NE1639	SAUSA300_1749	5B	a7	-	hypothetical protein
NE1640	SAUSA300_0739	5B	a8	-	LysM domain-containing protein
NE1641	SAUSA300_1463	5B	a9	-	hypothetical protein
NE1642	SAUSA300_2239	5B	a10	ureB	urease subunit beta
NE1643	SAUSA300_2559	5B	a11	-	DNA-binding response regulator
NE1644	SAUSA300_1788	5B	a12	-	hypothetical protein
NE1645	SAUSA300_2096	5B	b1	manA	mannose-6-phosphate isomerase
NE1646	SAUSA300_0145	5B	b2	-	phosphonate ABC transporter phosphonate-binding protein
NE1647	SAUSA300_1365	5B	b3	rpsA	30S ribosomal protein S1
NE1648	SAUSA300_0056	5B	b4	-	hypothetical protein
NE1649	SAUSA300_0651	5B	b5	-	CHAP domain-contain protein
NE1650	SAUSA300_0348	5B	b6	-	twin arginine-targeting protein translocase
NE1651	SAUSA300_0184	5B	b7	argB	acetylglutamate kinase
NE1652	SAUSA300_1669	5B	b8	-	aminotransferase, class V
NE1653	SAUSA300_2432	5B	b9	-	MutT/NUDIX family hydrolase
NE1654	SAUSA300_0657	5B	b10	-	hypothetical protein
NE1655	SAUSA300_1383	5B	b11	-	phiSLT ORF484-like protein, lysin
NE1656	SAUSA300_1715	5B	b12	ribD	riboflavin biosynthesis protein
NE1657	SAUSA300_0476	5B	c1	-	hypothetical protein
NE1658	SAUSA300_1861	5B	c2	-	hypothetical protein
NE1659	SAUSA300_0195	5B	c3	-	transcriptional regulator
NE1660	SAUSA300_2495	5B	c4	-	copper chaperone copZ
NE1661	SAUSA300_1667	5B	c5	-	putative glycerophosphoryl diester phosphodiesterase
NE1662	SAUSA300_1185	5B	c6	miaB	(dimethylallyl)adenosine tRNA methylthiotransferase

NE1663	SAUSA300_0918	5B	c7	-	diacylglycerol glucosyltransferase
NE1664	SAUSA300_2567	5B	c8	arcC	carbamate kinase
NE1665	SAUSA300_0859	5B	c9	-	NADH-dependent flavin oxidoreductase
NE1666	SAUSA300_0642	5B	c10	-	hypothetical protein
NE1667	SAUSA300_1937	5B	c11	-	phi77 ORF045-like protein
NE1668	SAUSA300_1291	5B	c12	-	hippurate hydrolase
NE1669	SAUSA300_2337	5B	d1	-	DegU family transcriptional regulator
NE1670	SAUSA300_1682	5B	d2	ccpA	catabolite control protein A
NE1671	SAUSA300_0526	5B	d3	-	methyltransferase small subunit
NE1672	SAUSA300_1694	5B	d4	trmB	tRNA (guanine-N(7)-)-methyltransferase
NE1673	SAUSA300_2132	5B	d5	-	hypothetical protein
NE1674	SAUSA300_0562	5B	d6	thiD	phosphomethylpyrimidine kinase
NE1675	SAUSA300_1653	5B	d7	-	metal-dependent hydrolase
NE1676	SAUSA300_2607	5B	D8	hisA	1-(5-phosphoribosyl)-5-[(5-phosphoribosylamino)methylideneamino] imidazole-4-carboxamide isomerase
NE1677	SAUSA300_1144	5B	D9	gid	tRNA (uracil-5-)-methyltransferase Gid
NE1678	SAUSA300_1721	5B	D10	-	hypothetical protein
NE1679	SAUSA300_2052	5B	D11	-	single-stranded DNA- binding protein family
NE1680	SAUSA300_1433	5B	D12	-	putative phage regulatory protein
NE1681	SAUSA300_0693	5B	E1	-	hypothetical protein
NE1682	SAUSA300_2367	5B	E2	hlgB	gamma-hemolysin component B
NE1683	SAUSA300_0186	5B	E3	argC	N-acetyl-gamma-glutamyl-phosphate reductase
NE1684	SAUSA300_1308	5B	E4	arlR	DNA-binding response regulator
NE1685	SAUSA300_1070	5B	E5	-	hypothetical protein
NE1686	SAUSA300_0750	5B	E6	-	hypothetical protein
NE1687	SAUSA300_0450	5B	E7	treR	trehalose operon repressor
NE1688	SAUSA300_0438	5B	E8	-	CHAP domain-contain protein
NE1689	SAUSA300_1887	5B	E9	pcrB	geranylgeranylglyceryl phosphate synthase-like protein
NE1690	SAUSA300_2548	5B	E10	-	hypothetical protein
NE1691	SAUSA300_1336	5B	E11	-	hypothetical protein
NE1692	SAUSA300_2479	5B	E12	cidA	holin-like protein cidA
NE1693	SAUSA300_0022	5B	F1	-	hypothetical protein
NE1694	SAUSA300_1009	5B	F2	typA	GTP-binding protein
NE1695	SAUSA300_0995	5B	F3	-	branched-chain alpha-keto acid dehydrogenase subunit E2
NE1696	SAUSA300_1680	5B	F4	acuA	acetoin utilization protein AcuA
NE1697	SAUSA300_1338	5B	F5	-	hypothetical protein
NE1698	SAUSA300_1449	5B	F6	-	MutT/nudix family protein
NE1699	SAUSA300_2334	5B	F7	-	hypothetical protein
NE1700	SAUSA300_0223	5B	F8	-	hypothetical protein
NE1701	SAUSA300_1288	5B	F9	dapA	dihydrodipicolinate synthase
NE1702	SAUSA300_0244	5B	F10	-	zinc-binding dehydrogenase family oxidoreductase
NE1703	SAUSA300_0471	5B	F11	-	hypothetical protein
NE1704	SAUSA300_2330	5B	F12	-	hypothetical protein
NE1705	SAUSA300_2582	5B	G1	-	hypothetical protein
NE1706	SAUSA300_1870	5B	G2	-	hypothetical protein
NE1707	SAUSA300_1184	5B	G3	-	hypothetical protein
NE1708	SAUSA300_1147	5B	G4	hslU	ATP-dependent protease ATP-binding subunit HslU
NE1709	SAUSA300_0566	5B	G5	-	amino acid permease
NE1710	SAUSA300_0638	5B	G6	-	phosphotransferase mannnose-specific family component IIA
NE1711	SAUSA300_1051	5B	G7	-	hypothetical protein
NE1712	SAUSA300_1548	5B	G8	-	ComE operon protein 2

NE1713	SAUSA300_2027	5B	G9	alr	alanine racemase
NE1714	SAUSA300_1590	5B	G10	-	GTP pyrophosphokinase
NE1715	SAUSA300_1069	5B	G11	-	hypothetical protein
NE1716	SAUSA300_1920	5B	G12	chs	chemotaxis-inhibiting protein CHIPS
NE1717	SAUSA300_1357	5B	H1	aroC	chorismate synthase
NE1718	SAUSA300_2459	5B	H2	-	MarR family transcriptional regulator
NE1719	SAUSA300_1063	5B	H3	arcC	carbamate kinase
NE1720	SAUSA300_0583	5B	H4	-	hypothetical protein
NE1721	SAUSA300_1203	5B	H5	-	hypothetical protein
NE1722	SAUSA300_1213	5B	H6	-	hypothetical protein
NE1723	SAUSA300_0094	5B	H7	-	hypothetical protein
NE1724	SAUSA300_0993	5B	H8	pdhA	pyruvate dehydrogenase E1 component, alpha subunit
NE1725	SAUSA300_0987	5B	H9	-	cytochrome D ubiquinol oxidase, subunit II
NE1726	SAUSA300_0257	5B	H10		antiholin-like protein LrgB
NE1727	SAUSA300_1695	5B	H11	-	hypothetical protein
NE1728	SAUSA300_1349	5B	H12	-	glycosyl transferase, group 1 family protein
NE1729	SAUSA300_0399	5C	a1	-	superantigen-like protein 5
NE1730	SAUSA300_1197	5C	a2	-	glutathione peroxidase
NE1731	SAUSA300_2456	5C	a3	-	hypothetical protein
NE1732	SAUSA300_1274	5C	a4	-	peptide ABC transporter ATP-binding protein
NE1733	SAUSA300_0827	5C	a5	-	hypothetical protein
NE1734	SAUSA300_0342	5C	a6	-	hypothetical protein
NE1735	SAUSA300_1118	5C	a7	-	hypothetical protein
NE1736	SAUSA300_1724	5C	a8	-	hypothetical protein
NE1737	SAUSA300_2107	5C	a9	mtlA	PTS system, mannitol specific IIA component
NE1738	SAUSA300_1899	5C	a10	-	hypothetical protein
NE1739	SAUSA300_1321	5C	a11	-	hypothetical protein
NE1740	SAUSA300_1445	5C	a12	scpA	hypothetical protein
NE1741	SAUSA300_1356	5C	B1	aroB	3-dehydroquinate synthase
NE1742	SAUSA300_1619	5C	b2	hemA	glutamyl-tRNA reductase
NE1743	SAUSA300_0769	5C	b3	-	hypothetical protein
NE1744	SAUSA300_0234	5C	b4	-	putative flavohemoprotein
NE1745	SAUSA300_1926	5C	b5	-	phi77 ORF044-like protein
NE1746	SAUSA300_2088	5C	b6	luxS	S-ribosylhomocysteinase
NE1747	SAUSA300_0085	5C	b7	-	hypothetical protein
NE1748	SAUSA300_2517	5C	b8	-	amidohydrolase family protein
NE1749	SAUSA300_1909	5C	b9	-	hypothetical protein
NE1750	SAUSA300_2043	5C	b10	-	hypothetical protein
NE1751	SAUSA300_0979	5C	b11	-	hypothetical protein
NE1752	SAUSA300_1163	5C	b12	rbfA	ribosome-binding factor A
NE1753	SAUSA300_0936	5C	c1	-	ABC transporter ATP-binding protein
NE1754	SAUSA300_2525	5C	c2	-	hypothetical protein
NE1755	SAUSA300_2641	5C	c3	-	hypothetical protein
NE1756	SAUSA300_0646	5C	c4	-	sensor histidine kinase
NE1757	SAUSA300_1089	5C	c5	lspA	lipoprotein signal peptidase
NE1758	SAUSA300_0994	5C	c6	pdhB	pyruvate dehydrogenase E1 component, beta subunit
NE1759	SAUSA300_1097	5C	c7	pyrF	orotidine 5'-phosphate decarboxylase
NE1760	SAUSA300_1599	5C	c8	-	hypothetical protein
NE1761	SAUSA300_1302	5C	c9	-	ATPase family protein
NE1762	SAUSA300_0540	5C	c10	-	HAD family hydrolase
NE1763	SAUSA300_1480	5C	c11	-	putative traG membrane protein

NE1764	SAUSA300_1753	5C	C12	splF	serine protease SplF
NE1765	SAUSA300_1187	5C	d1	-	hypothetical protein
NE1766	SAUSA300_2557	5C	d2	-	ABC transporter protein
NE1767	SAUSA300_0117	5C	d3	sirA	iron compound ABC transporter iron compound-binding protein SirA
NE1768	SAUSA300_2633	5C	d4	-	ABC transporter ATP-binding protein
NE1769	SAUSA300_0857	5C	d5	-	hypothetical protein
NE1770	SAUSA300_1139	5C	d6	sucD	succinyl-CoA synthetase subunit alpha
NE1771	SAUSA300_0602	5C	d7	-	hypothetical protein
NE1772	SAUSA300_2368	5C	D8	-	hypothetical protein
NE1773	SAUSA300_2457	5C	D9	-	phospholipase/carboxylesterase family protein
NE1774	SAUSA300_2358	5C	D10	-	ABC transporter permease
NE1775	SAUSA300_0320	5C	D11	-	triacylglycerol lipase
NE1776	SAUSA300_1011	5C	D12	-	hypothetical protein
NE1777	SAUSA300_0937	5C	E1	-	hypothetical protein
NE1778	SAUSA300_0958	5C	E2	-	hypothetical protein
NE1779	SAUSA300_2518	5C	E3	-	hydrolase family protein
NE1780	SAUSA300_0568	5C	E4	-	hypothetical protein
NE1781	SAUSA300_0334	5C	E5	-	MarR family transcriptional regulator
NE1782	SAUSA300_2246	5C	E6	-	hypothetical protein
NE1783	SAUSA300_1684	5C	E7	-	hypothetical protein
NE1784	SAUSA300_0619	5C	E8	-	ABC transporter permease
NE1785	SAUSA300_0974	5C	E9	purN	phosphoribosylglycinamide formyltransferase
NE1786	SAUSA300_1966	5C	E10	-	phi77 ORF014-like protein, phage anti-repressor protein
NE1787	SAUSA300_2467	5C	E11	srtA	sortase
NE1788	SAUSA300_0982	5C	E12	-	hypothetical protein
NE1789	SAUSA300_2544	5C	F1	-	hypothetical protein
NE1790	SAUSA300_1217	5C	F2	-	ABC transporter ATP-binding protein
NE1791	SAUSA300_2152	5C	F3	lacD	tagatose 1,6-diphosphate aldolase
NE1792	SAUSA300_1943	5C	F4	-	phi77 ORF040-like protein
NE1793	SAUSA300_1296	5C	F5	-	hypothetical protein
NE1794	SAUSA300_1573	5C	F6	-	Holliday junction resolvase-like protein
NE1795	SAUSA300_0839	5C	F7	-	hypothetical protein
NE1796	SAUSA300_0708	5C	F8	hisC	histidinol-phosphate aminotransferase
NE1797	SAUSA300_0652	5C	F9	-	hypothetical protein
NE1798	SAUSA300_1949	5C	F10	dut	dUTP diphosphatase
NE1799	SAUSA300_0519	5C	F11	-	hypothetical protein
NE1800	SAUSA300_0904	5C	F12	-	hypothetical protein
NE1801	SAUSA300_0841	5C	G1	-	hypothetical protein
NE1802	SAUSA300_0688	5C	G2	-	aldo/keto reductase family oxidoreductase
NE1803	SAUSA300_0789	5C	G3	-	putative thioredoxin
NE1804	SAUSA300_0106	5C	G4	-	putative drug transporter
NE1805	SAUSA300_1919	5C	G5	-	hypothetical protein
NE1806	SAUSA300_1857	5C	G6	-	hypothetical protein
NE1807	SAUSA300_0067	5C	G7	-	universal stress protein
NE1808	SAUSA300_1032	5C	G8	-	putative iron compound ABC transporter iron compound-binding protein
NE1809	SAUSA300_0370	5C	G9	-	putative enterotoxin
NE1810	SAUSA300_2299	5C	G10	-	hypothetical protein
NE1811	SAUSA300_1739	5C	G11	-	hypothetical protein
NE1812	SAUSA300_1741	5C	G12	-	putative lipoprotein
NE1813	SAUSA300_1256	5C	H1	msrA	methionine sulfoxide reductase A

NE1814	SAUSA300_1395	5C	H2	-	phiSLT ORF116b-like protein
NE1815	SAUSA300_2226	5C	H3	moaB	molybdenum cofactor biosynthesis protein B
NE1816	SAUSA300_2537	5C	H4	-	L-lactate dehydrogenase
NE1817	SAUSA300_1000	5C	H5	potB	spermidine/putrescine ABC transporter permease
NE1818	SAUSA300_1428	5C	H6	-	hypothetical protein
NE1819	SAUSA300_2206	5C	H7	-	hypothetical protein
NE1820	SAUSA300_2604	5C	H8	-	hypothetical protein
NE1821	SAUSA300_1968	5C	H9	-	putative phage transcriptional regulator
NE1822	SAUSA300_1218	5C	H10	-	ABC transporter permease
NE1823	SAUSA300_0345	5C	H11	-	Tat-translocated protein
NE1824	SAUSA300_0035	5C	H12	-	hypothetical protein
NE1825	SAUSA300_1612	5D	a1		DNA-3-methyladenine glycosidase
NE1826	SAUSA300_1953	5D	a2	-	phiPVL ORF051-like protein
NE1827	SAUSA300_0011	5D	a3	-	hypothetical protein
NE1828	SAUSA300_0504	5D	a4	-	pyridoxal biosynthesis lyase PdxS
NE1829	SAUSA300_1465	5D	a5		2-oxoisovalerate dehydrogenase, E1 component, beta subunit
NE1830	SAUSA300_1960	5D	a6		putative phage-related DNA recombination protein
NE1831	SAUSA300_0443	5D	a7		YibE/F-like protein
NE1832	SAUSA300_1088	5D	a8		glyoxalase family protein
NE1833	SAUSA300_2026	5D	a9	-	PemK family protein
NE1834	SAUSA300_2507	5D	a10	-	hypothetical protein
NE1835	SAUSA300_0315	5D	a11		N-acetylneuraminate lyase
NE1836	SAUSA300_1904	5D	a12	-	hypothetical protein
NE1837	SAUSA300_2608	5D	b1	hisH	imidazole glycerol phosphate synthase subunit HisH
NE1838	SAUSA300_0565	5D	b2		conserved hypothetical protein
NE1839	SAUSA300_0068	5D	b3	-	cadmium-exporting ATPase, truncation
NE1840	SAUSA300_1985	5D	b4		serine-aspartate repeat-containing protein SdrH
NE1841	SAUSA300_1474	5D	b5	-	hypothetical protein
NE1842	SAUSA300_0397	5D	b6	-	superantigen-like protein
NE1843	SAUSA300_0582	5D	b7	-	hypothetical protein
NE1844	SAUSA300_1754	5D	b8	splE	serine protease SplE
NE1845	SAUSA300_1615	5D	b9	hemB	delta-aminolevulinic acid dehydratase
NE1846	SAUSA300_0053	5D	b10	speG	spermidine N(1)-acetyltransferase
NE1847	SAUSA300_0687	5D	b11	-	putative hemolysin
NE1848	SAUSA300_1382	5D	b12	lukS-PV	Panton-Valentine leukocidin, LukS-PV
NE1849	SAUSA300_0735	5D	c1	-	hypothetical protein
NE1850	SAUSA300_2059	5D	c2	atpG	F0F1 ATP synthase subunit gamma
NE1851	SAUSA300_0029	5D	c3	-	hypothetical protein
NE1852	SAUSA300_1208	5D	c4	-	hypothetical protein
NE1853	SAUSA300_2352	5D	c5	-	addiction module antitoxin
NE1854	SAUSA300_1502	5D	c6	-	putative competence protein ComGC
NE1855	SAUSA300_0689	5D	c7	-	glycosyl transferase, group 2 family protein
NE1856	SAUSA300_1765	5D	c8	epiC	lantibiotic epidermin biosynthesis protein EpiC
NE1857	SAUSA300_0253	5D	c9	scdA	cell wall biosynthesis protein ScdA
NE1858	SAUSA300_2453	5D	c10	-	ABC transporter ATP-binding protein
NE1859	SAUSA300_1566	5D	c11	-	hypothetical protein
NE1860	SAUSA300_2491	5D	c12	-	1-pyrroline-5-carboxylate dehydrogenase
NE1861	SAUSA300_0090	5D	d1	-	hypothetical protein
NE1862	SAUSA300_0398	5D	d2	-	superantigen-like protein
NE1863	SAUSA300_0221	5D	d3	pflA	pyruvate formate-lyase activating enzyme
NE1864	SAUSA300_1922	5D	d4	sak	staphylokinase

NE1865	SAUSA300_0023	5D	d5	-	hypothetical protein
NE1866	SAUSA300_1876	5D	d6	-	DNA polymerase IV
NE1867	SAUSA300_1386	5D	d7	-	phiETA ORF59-like protein
NE1868	SAUSA300_0032	5D	D8	mecA	penicillin-binding protein 2'
NE1869	SAUSA300_0243	5D	D9	-	hypothetical protein
NE1870	SAUSA300_2080	5D	D10		conserved hypothetical protein
NE1871	SAUSA300_2284	5D	D11	-	hypothetical protein
NE1872	SAUSA300_2024	5D	D12	rsbV	anti-sigma-B factor, antagonist
NE1873	SAUSA300_1742	5D	E1	-	hypothetical protein
NE1874	SAUSA300_1569	5D	E2	-	U32 family peptidase
NE1875	SAUSA300_1918	5D	E3	-	truncated beta-hemolysin
NE1876	SAUSA300_2533	5D	E4	panC	pantoate--beta-alanine ligase
NE1877	SAUSA300_0824	5D	E5	-	hypothetical protein
NE1878	SAUSA300_0597	5D	E6	-	putative endonuclease III
NE1879	SAUSA300_2115	5D	E7	tnp	IS1181, transposase
NE1880	SAUSA300_0416	5D	E8	-	tandem lipoprotein
NE1881	SAUSA300_0634	5D	E9	fhuB	ferrichrome transport permease fhuB
NE1882	SAUSA300_2393	5D	E10	opuCa	glycine betaine/carnitine/choline ABC transporter ATP-binding protein
NE1883	SAUSA300_0444	5D	E11	gltC	LysR family regulatory protein
NE1884	SAUSA300_0844	5D	E12	-	hypothetical protein
NE1885	SAUSA300_1595	5D	F1	tgt	queuine tRNA-ribosyltransferase
NE1886	SAUSA300_0992	5D	F2	-	hypothetical protein
NE1887	SAUSA300_1473	5D	F3	nusB	transcription antitermination protein NusB
NE1888	SAUSA300_0183	5D	F4	-	hypothetical protein
NE1889	SAUSA300_2061	5D	F5	atpH	F0F1 ATP synthase subunit delta
NE1890	SAUSA300_1422	5D	F6	-	phiSLT ORF65-like protein
NE1891	SAUSA300_0759	5D	F7	gpmI	phosphoglyceromutase
NE1892	SAUSA300_1171	5D	F8	-	hypothetical protein
NE1893	SAUSA300_0916	5D	F9	-	hypothetical protein
NE1894	SAUSA300_1908	5D	F10	-	hypothetical protein
NE1895	SAUSA300_1469	5D	F11	argR	arginine repressor
NE1896	SAUSA300_1467	5D	F12	lpdA	dihydrolipoamide dehydrogenase
NE1897	SAUSA300_1789	5D	G1	-	hypothetical protein
NE1898	SAUSA300_1697	5D	G2	-	dipeptidase PepV
NE1899	SAUSA300_0419	5D	G3	-	tandem lipoprotein
NE1900	SAUSA300_0365	5D	G4	-	hypothetical protein
NE1901	SAUSA300_0355	5D	G5	-	acetyl-CoA acetyltransferase
NE1902	SAUSA300_2225	5D	G6	moaC	molybdenum cofactor biosynthesis protein MoaC
NE1903	SAUSA300_1455	5D	G7	-	AraC family transcriptional regulator
NE1904	SAUSA300_1233	5D	G8	rpmG	50S ribosomal protein L33
NE1905	SAUSA300_0744	5D	G9	lgt	prolipoprotein diacylglyceryl transferase
NE1906	SAUSA300_0587	5D	G10	-	hypothetical protein
NE1907	SAUSA300_2485	5D	G11	-	methylated DNA-protein cysteine methyltransferase
NE1908	SAUSA300_1911	5D	G12	-	ABC transporter ATP-binding protein
NE1909	SAUSA300_1720	5D	H1	-	hypothetical protein
NE1910	SAUSA300_1248	5D	H2	-	hypothetical protein
NE1911	SAUSA300_0585	5D	H3	-	hypothetical protein
NE1912	SAUSA300_0071	5D	H4	-	ISSep1-like transposase
NE1913	SAUSA300_0079	5D	H5		putative lipoprotein
NE1914	SAUSA300_0997	5D	H6	-	hypothetical protein
NE1915	SAUSA300_0649	5D	H7		hypothetical protein

NE1916	SAUSA300_0795	5D	H8		hypothetical protein
NE1917	SAUSA300_1950	5D	H9		hypothetical protein
NE1918	SAUSA300_1429	5D	H10		phiSLT ORF53-like protein
NE1919	SAUSA300_1112	5D	H11		protein phosphatase 2C domain-containing protein
NE1920	SAUSA300_1359	5D	H12	-	polyprenyl synthetase

Table 7.2 Primary screen NTML strains Z-scores

Order by strain name. Mean score in bold (n = 3), with individual replicate scores.

Strain Name	GeneID	**Mean Z-score**	Replicate 1	Replicate 2	Replicate 3
NE1	cell surface protein	**0.6294**	0.5544	0.5978	0.7360
NE2	peptidase, rhomboid family	**-0.0239**	0.1534	-0.1293	-0.0959
NE3	conserved hypothetical protein	**0.5018**	0.9726	0.3186	0.2143
NE4	ABC transporter ATP-binding protein	**0.4147**	0.9866	-0.0908	0.3483
NE5	aminotransferase	**0.0200**	-0.0352	0.0991	-0.0040
NE6	formate dehydrogenase, alpha subunit	**0.3528**	0.1233	0.6243	0.3107
NE7	conserved hypothetical phage protein	**-0.1530**	0.0894	-0.3525	-0.1960
NE8	putative membrane protein	**0.1247**	-0.1419	0.1192	0.3969
NE9	conserved hypothetical protein	**0.2650**	0.1162	0.2249	0.4539
NE10	putative hemolysin III	**0.4379**	0.0068	-0.0586	1.3654
NE11	single-stranded-DNA-specific exonuclease (RecJ)	**0.6599**	0.6680	0.4692	0.8424
NE12	drug resistance transporter, EmrB/QacA subfamily	**0.3743**	0.2908	0.3945	0.4377
NE13	ribose transporter (RbsU)	**-0.4522**	-0.5818	-0.7404	-0.0345
NE14	putative transporter	**0.2914**	0.9866	-0.1939	0.0814
NE15	transcriptional regulator, TetR family	**0.0004**	-0.1943	-0.0510	0.2465
NE16	molybdopterin converting factor, subunit 1 (moaD)	**-0.5520**	-0.5000	-0.6932	-0.4628
NE17	putative drug transporter	**-0.7572**	-0.7593	-0.8528	-0.6595
NE18	putative membrane protein	**2.0558**	5.6439	0.1344	0.3890
NE19	conserved hypothetical protein	**-0.4552**	-0.6944	-0.9213	0.2503
NE20	transcriptional antiterminator, BglG family	**-0.3204**	-0.0935	-0.4671	-0.4005
NE21	uracil phosphoribosyltransferase (upp)	**-0.2210**	-0.3770	0.1408	-0.4267
NE22	DNA polymerase I superfamily (polA)	**-0.1130**	0.0809	-0.5648	0.1451
NE23	conserved hypothetical protein	**-0.0737**	0.0760	0.0906	-0.3876
NE24	secretory antigen precursor SsaA	**0.2266**	0.4670	-0.0535	0.2663
NE25	conserved hypothetical protein	**-0.2274**	-0.1623	-0.3225	-0.1974
NE26	staphylocoagulase precursor (coa)	**0.1397**	0.4284	-0.0133	0.0040
NE27	nitric oxide synthase oxygenase	**-0.5605**	-0.8322	-0.4776	-0.3716
NE28	hydrolase, alpha/beta hydrolase fold family	**-0.3992**	-0.0727	-0.4580	-0.6668
NE29	PIN domain protein	**-1.1042**	-0.8381	-1.7246	-0.7499
NE30	hydrolase, haloacid dehalogenase-like family	**-0.2934**	-0.3387	-0.3454	-0.1961
NE31	conserved hypothetical protein	**-0.5363**	-0.3199	-0.7674	-0.5215
NE32	transcriptional regulator, LysR family domain protein	**-0.6136**	-0.9530	-0.0972	-0.7907
NE33	LPXTG-motif cell wall surface anchor family protein	**-0.3007**	-0.3787	-0.4826	-0.0407
NE34	L-lactate permease	**0.0911**	0.5460	-0.4450	0.1723
NE35	anthranilate phosphoribosyltransferase (trpD)	**0.0413**	0.4004	0.0782	-0.3546
NE36	conserved hypothetical protein	**0.8791**	1.6798	0.5981	0.3594
NE37	intercellular adhesion protein A (icaA)	**-0.5834**	-0.3309	-0.6227	-0.7965
NE38	similar to glycerate dehydrogenase	**-0.0550**	0.5811	-0.0006	-0.7455
NE39	phosphotransferase system, glucose-specific IIABC component (ptsG)	**0.1854**	0.1373	0.1257	0.2931
NE40	conserved hypothetical protein	**-0.3895**	-0.5769	-0.1332	-0.4585
NE41	cation transport family protein	**-0.9426**	-1.1241	-1.0856	-0.6183
NE42	conserved hypothetical protein	**-0.5010**	-0.4247	-0.3074	-0.7710
NE43	urease accessory protein (UreF)	**-0.1919**	-0.5007	-0.2460	0.1710
NE44	branched-chain amino acid transport system II carrier protein (brnQ)	**0.6743**	0.8279	0.5718	0.6232
NE45	accessory secretory protein (Asp1)	**-0.1821**	-0.0307	-0.5591	0.0435

NE46	phi77 ORF001-like protein, phage tail tape measure protein	**-0.0121**	-0.5013	0.5007	-0.0358
NE47	phiSLT ORF2067-like protein, phage tail tape measure protein	**-0.2135**	-0.4274	0.1161	-0.3293
NE48	maltose ABC transporter, permease protein	**1.0655**	0.5848	1.0955	1.5161
NE49	DNA-binding response regulator, AraC family	**-0.1982**	0.1867	0.1147	-0.8962
NE50	conserved hypothetical protein	**0.8461**	1.5129	0.5276	0.4977
NE51	conserved hypothetical protein	**0.7282**	0.7209	0.8146	0.6492
NE52	conserved hypothetical protein	**-0.4888**	-0.2494	-0.6634	-0.5536
NE53	conserved hypothetical protein	**-0.0368**	-0.2735	0.3040	-0.1408
NE54	ABC transporter, ATP-binding/permease protein	**-0.1210**	-0.0068	0.1689	-0.5252
NE55	putative membrane protein	**-0.2863**	-0.5494	0.0006	-0.3102
NE56	cell wall surface anchor family protein	**0.6316**	0.1990	1.1416	0.5543
NE57	acetyltransferase, GNAT family	**0.6441**	0.8455	0.7775	0.3094
NE58	anaerobic ribonucleotide reductase, large subunit (nrdD)	**0.0431**	-0.3754	0.1696	0.3351
NE59	exotoxin	**0.4939**	0.2918	0.8753	0.3147
NE60	cystathionine gamma-synthase (metB)	**0.5932**	0.4989	0.9707	0.3101
NE61	PTS system, lactose-specific IIBC component (lacE)	**0.1864**	0.7683	-0.0015	-0.2075
NE62	Toprim domain protein	**0.7834**	1.1103	0.5722	0.6676
NE63	alpha glucosidase	**0.6299**	0.0538	1.1788	0.6571
NE64	protoporphyrinogen oxidase (hemG)	**-0.0630**	0.1236	-0.1748	-0.1377
NE65	conserved hypothetical protein	**-0.1483**	-0.0076	-0.1876	-0.2498
NE66	preprotein translocase, secA protein	**-0.5762**	-0.9372	-0.0913	-0.7001
NE67	immunodominant antigen B (isaB)	**-0.5269**	-0.7974	-0.3769	-0.4064
NE68	ABC transporter ATP-binding protein	**-0.6677**	-0.8437	-0.8593	-0.3002
NE69	conserved hypothetical protein	**0.5361**	0.9526	0.4809	0.1749
NE70	ABC transporter, permease protein	**1.0681**	0.6498	1.3981	1.1564
NE71	putative membrane protein	**0.3685**	0.1016	0.5135	0.4903
NE72	acyltransferase	**0.4282**	0.1634	0.1743	0.9470
NE73	putative lipoprotein	**-0.3259**	-0.6862	0.1975	-0.4891
NE74	5-nucleotidase family protein	**-0.0886**	-0.4382	0.3522	-0.1797
NE75	capsular polysaccharide biosynthesis protein (Cap1B)	**-0.3155**	-0.5505	-0.4846	0.0884
NE76	3-isopropylmalate dehydrogenase (leuB)	**-0.6570**	-0.7270	-0.7003	-0.5436
NE77	conserved hypothetical protein	**-0.7705**	-1.0709	-0.5666	-0.6738
NE78	transcriptional regulator, AraC family	**-0.2308**	-0.2998	-0.1146	-0.2780
NE79	conserved hypothetical protein	**-0.5321**	-1.0178	-0.0594	-0.5192
NE80	DNA mismatch repair protein (mutL)	**1.1571**	1.2376	0.8352	1.3984
NE81	aldose 1-epimerase (galM)	**-1.1292**	-1.3987	-0.9501	-1.0389
NE82	putative membrane protein	**0.0254**	0.1752	-0.0677	-0.0312
NE83	acetyltransferase, GNAT family	**0.2013**	-0.4999	1.1838	-0.0802
NE84	excinuclease ABC, B subunit (uvrB)	**0.9360**	0.5634	1.6407	0.6039
NE85	6-phospho-beta-galactosidase (lacG)	**0.9357**	1.4565	0.5986	0.7521
NE86	conserved hypothetical protein	**1.0711**	1.2039	1.1761	0.8334
NE87	conserved hypothetical protein	**1.2676**	0.5823	1.3607	1.8598
NE88	HNH endonuclease family protein	**-0.3582**	-0.3770	-0.5409	-0.1568
NE89	conserved hypothetical protein	**-0.0233**	0.1150	-0.4073	0.2223
NE90	methionine-S-sulfoxide reductase (msrA)	**0.2589**	-0.0400	0.6565	0.1604
NE91	K+-transporting ATPase, A subunit (kdpA)	**0.6758**	0.5355	0.9301	0.5618
NE92	quinol oxidase, subunit II (qoxA)	**-1.3051**	-1.3630	-1.4439	-1.1083
NE93	similar to DNA mismatch repair protein	**0.2982**	0.1291	0.4503	0.3153
NE94	conserved hypothetical protein	**0.1389**	-0.3622	0.5725	0.2064
NE95	accessory gene regulator protein B (agrB)	**-1.0897**	-1.3461	-1.0383	-0.8846

NE96	staphylococcal accessory regulator U (sarU)	**0.5134**	0.4925	0.4366	0.6110
NE97	UTP-glucose-1-phosphate uridylyltransferase family protein	**0.6498**	1.0715	1.2626	-0.3848
NE98	sdrE protein	**0.0570**	-0.5315	0.5939	0.1085
NE99	transcriptional regulator, Fur family	**1.3771**	0.5225	2.1888	1.4199
NE100	FtsK/SpoIIIE family protein	**0.4580**	-0.0777	1.7533	-0.3017
NE101	2-C-methyl-D-erythritol 4-phosphate cytidylyltransferase	**-0.6243**	-0.1203	-0.8057	-0.9470
NE102	arginine/ornithine antiporter	**-0.2669**	-0.6286	-0.4418	0.2698
NE103	ATP phosphoribosyltransferase hisG	**0.0918**	-0.3649	0.2715	0.3687
NE104	putative lipase/esterase	**0.6783**	-0.2036	1.0260	1.2125
NE105	glycosyl transferase, group 1 family protein	**0.3720**	0.1241	0.7934	0.1984
NE106	argininosuccinate lyase	**0.4514**	0.2609	0.8037	0.2895
NE107	putative ABC transporter protein EcsB	**0.1747**	0.0996	0.6968	-0.2722
NE108	conserved hypothetical protein	**1.7323**	0.9946	2.4563	1.7461
NE109	OsmC/Ohr family protein	**-0.6878**	-0.0943	-0.7272	-1.2418
NE110	transcriptional regulator, GntRfamily/aminotransferase, class I	**-0.0354**	0.0329	-0.0872	-0.0520
NE111	putative surface protein	**-0.4322**	-0.5767	-0.2917	-0.4283
NE112	sucrose-specific PTS tranporter protein	**-0.3709**	-0.6886	0.0450	-0.4692
NE113	conserved hypothetical protein	**-0.7115**	-0.5586	-0.3469	-1.2289
NE114	alcohol dehydrogenase, iron-containing (adhE)	**-0.2669**	0.5794	-0.5013	-0.8787
NE115	peptidase, M20/M25/M40 family	**-0.9127**	-1.4033	-0.4816	-0.8534
NE116	putative sensor histidine kinase	**-0.5251**	-1.1377	-0.4201	-0.0176
NE117	cytochrome D ubiquinol oxidase, subunit I	**-0.1711**	-0.5357	-0.1775	0.1999
NE118	nitroreductase family protein	**0.1487**	0.3663	-0.2195	0.2992
NE119	non-ribosomal peptide synthetase	**-0.6400**	-0.3810	-0.8699	-0.6693
NE120	putative membrane protein	**0.8321**	0.9147	1.6117	-0.0302
NE121	conserved hypothetical protein	**-0.2065**	-0.0729	-0.2874	-0.2591
NE122	alcohol dehydrogenase, zinc-containing	**-0.0573**	-0.2162	-0.1437	0.1880
NE123	cobalt transport family protein	**-0.6722**	0.0031	-0.7061	-1.3137
NE124	metallo-beta-lactamase family protein	**-0.5607**	-0.3697	-0.6148	-0.6977
NE125	2-C-methyl-D-erythritol 4-phosphate cytidylyltransferase	**-0.9337**	-1.1277	-0.9254	-0.7479
NE126	para-nitrobenzyl esterase	**-1.0515**	-0.8052	-1.2337	-1.1157
NE127	conserved hypothetical protein	**-0.4337**	-0.6717	-0.0450	-0.5843
NE128	glyoxylase family protein	**-0.6031**	-0.7794	-0.2304	-0.7995
NE129	DNA internalization-related competence proteinComEC/Rec2	**-0.0894**	-0.0983	-0.1577	-0.0122
NE130	conserved hypothetical protein	**0.1230**	-0.2552	0.3536	0.2706
NE131	phiSLT ORF 77-like protein	**0.7781**	0.7583	0.1469	1.4291
NE132	putative transcriptional regulator	**0.8810**	0.4403	1.8058	0.3969
NE133	Methyltransferase	**0.0935**	0.1256	0.6143	-0.4595
NE134	arginase	**-0.0399**	-0.2231	-0.0743	0.1779
NE135	capsular polysaccharide biosynthesis protein (Cap5B)	**0.1717**	-0.1434	0.1199	0.5386
NE136	RNA methyltransferase	**-0.2672**	-0.2991	-0.2698	-0.2327
NE137	conserved hypothetical protein	**-0.7520**	-0.7476	-0.7813	-0.7270
NE138	putative membrane protein	**-0.6399**	-0.3918	-0.7336	-0.7943
NE139	ABC transporter, ATP-binding/permease protein	**-0.4372**	-0.1460	-1.1441	-0.0213
NE140	conserved hypothetical protein	**0.3795**	0.3229	0.5566	0.2589
NE141	glucose-inhibited division protein B (gidB)	**-0.0417**	-0.0065	-0.6602	0.5417
NE142	amino acid carrier protein	**-0.1357**	-0.0837	-0.3207	-0.0027
NE143	conserved hypothetical protein	**0.0118**	-0.3053	0.3362	0.0044
NE144	putative tetracycline resistance protein	**1.2177**	1.3439	1.4913	0.8178

NE145	excinuclease ABC, A subunit (uvrA)	**-0.1586**	0.0886	-0.1768	-0.3877
NE146	iron compound ABC transporter, permease	**0.1245**	0.1856	0.1026	0.0852
NE147	sensor histidine kinase	**0.2025**	0.3197	0.2276	0.0603
NE148	essC protein	**-0.0414**	0.1764	-0.3203	0.0196
NE149	transcription termination factor (Rho)	**-0.6960**	-0.7251	-0.5320	-0.8311
NE150	conserved hypothetical protein	**-0.1398**	-0.1955	0.1430	-0.3668
NE151	phi77 ORF109-like protein	**-0.5665**	-0.2461	-0.6058	-0.8476
NE152	DNA topoisomerase III (topB)	**0.0723**	0.0764	0.1518	-0.0112
NE153	amino acid ABC transporter, ATP-binding protein	**-0.0286**	0.0472	0.1077	-0.2409
NE154	putative membrane protein	**0.4642**	0.5190	0.4430	0.4306
NE155	conserved hypothetical protein	**-0.2324**	-0.1367	-0.5631	0.0027
NE156	putative membrane protein	**1.0467**	0.6908	1.6149	0.8344
NE157	putative membrane protein	**0.1824**	0.3971	0.1153	0.0348
NE158	conserved hypothetical protein	**-0.3978**	-0.0031	-0.8195	-0.3708
NE159	Conserved hypothetical protein	**0.1951**	0.6345	0.3147	-0.3640
NE160	biotin synthase (bioB)	**0.0661**	0.1230	-0.1668	0.2421
NE161	conserved hypothetical protein	**-0.2484**	-0.2030	-0.2024	-0.3398
NE162	putative substrate--CoA ligase	**-0.9108**	-0.7508	-1.1209	-0.8608
NE163	zinc metalloproteinase aureolysin (aur)	**-0.6510**	-0.3093	-1.2306	-0.4130
NE164	ribosomal large subunit pseudouridine synthase, RluD subfamily	**0.6286**	1.2327	0.2739	0.3793
NE165	staphylococcal accessory regulator	**-0.2020**	-0.0304	-0.1316	-0.4439
NE166	putative membrane protein	**0.6399**	0.6481	0.2208	1.0507
NE167	phi77 ORF015-like protein, putative protease / phage portal protein	**0.8512**	1.0066	0.2448	1.3022
NE168	peptide ABC transporter, permease protein / oligopeptide permease, channel-forming protein (opp-2B)	**1.9430**	0.8898	3.3540	1.5853
NE169	capsular polysaccharide biosynthesis protein (Cap5P)	**-0.1542**	-0.1810	0.1172	-0.3988
NE170	putative acetyltransferase	**-0.5760**	0.2310	-0.6469	-1.3122
NE171	phi77 ORF109-like protein / phi77 ORF002-like protein, phage minor structural protein	**0.0441**	-0.0562	0.1721	0.0165
NE172	PTS system, glucose-specific IIBC component domain protein (ptsG)	**-0.4597**	0.2348	-0.5985	-1.0154
NE173	putative comf operon protein 1	**-0.5384**	-0.1877	-0.5896	-0.8377
NE174	N-(5'phosphoribosyl)anthranilate isomerase (trpC)	**0.3619**	0.5002	-0.5481	1.1336
NE175	glycosyl transferase, group 1 family protein	**0.0162**	-0.1075	-0.6387	0.7949
NE176	anion transporter family protein	**0.4765**	0.3059	0.6650	0.4587
NE177	putative membrane protein	**0.0388**	0.2799	-0.2961	0.1326
NE178	isopropylmalate synthase-related protein	**0.7159**	0.3182	1.1925	0.6370
NE179	multidrug resistance protein	**0.6511**	0.2948	0.8368	0.8218
NE180	putative lipoprotein	**1.1281**	0.6274	2.0616	0.6952
NE181	conserved hypothetical phage protein	**0.4808**	0.0376	1.1370	0.2678
NE182	Conserved hypothetical protein	**0.5397**	0.6525	0.7904	0.1762
NE183	glycerate dehydrogenase-like protein	**0.2546**	0.4868	0.0810	0.1960
NE184	conserved hypothetical protein	**0.4374**	0.8340	0.4251	0.0533
NE185	siderophore biosynthesis protein, IucA/IucC family	**0.3430**	0.3480	0.5334	0.1476
NE186	fibronectin binding protein A (fnbA)	**-0.3965**	-0.1736	-0.6763	-0.3397
NE187	phosphate transporter family protein	**-0.2418**	-0.1542	-0.1482	-0.4229
NE188	transcription-repair coupling factor (mfd)	**0.2828**	0.3193	0.3173	0.2119
NE189	O-methyltransferase family protein	**0.0674**	0.0675	0.4504	-0.3158
NE190	staphylococcal tandem lipoprotein	**1.1855**	1.1804	1.5652	0.8108

NE191	methylenetetrahydrofolate dehydrogenase/methenyltetrahydrofolate cyclohydrolase	**-1.0246**	-0.2828	-1.3535	-1.4374
NE192	transporter gate domain protein	**1.1040**	1.0261	2.1410	0.1450
NE193	putative exotoxin 1	**0.7220**	0.4738	0.7018	0.9905
NE194	flavodoxin family protein	**0.4729**	-0.0403	0.7990	0.6601
NE195	oligoendopeptidase F (pepF)	**0.9573**	0.8346	0.8221	1.2152
NE196	conserved hypothetical protein	**0.3129**	-0.0972	0.4533	0.5828
NE197	amino acid permease	**-0.0446**	-0.3799	-0.0909	0.3369
NE198	alanine dehydrogenase (ald)	**1.3196**	-0.2091	2.9445	1.2234
NE199	cation efflux family protein	**-0.4543**	-1.1522	-0.1266	-0.0840
NE200	iron compound ABC transporter, permease protein	**-1.1335**	-0.9255	-1.4514	-1.0236
NE201	phiSLT ORF401-like protein, integrase	**0.4178**	0.4408	0.7999	0.0126
NE202	conserved hypothetical protein	**0.2587**	0.4719	0.2532	0.0511
NE203	conserved hypothetical protein	**0.2630**	0.2421	0.0207	0.5262
NE204	hydrolase, alpha/beta hydrolase fold family	**0.3439**	0.4065	0.3553	0.2698
NE205	conserved hypothetical protein	**-0.0067**	-0.5400	0.3985	0.1215
NE206	amino acid permease family protein	**-0.3476**	-0.6531	-0.0386	-0.3512
NE207	putative membrane protein	**-0.0133**	-0.1711	-0.0392	0.1703
NE208	conserved hypothetical protein	**-0.1091**	-0.1024	0.1436	-0.3685
NE209	phiPVL ORF41-like protein	**0.0304**	-0.4623	0.3912	0.1624
NE210	staphylococcal accessory regulator	**0.0608**	0.1837	0.3478	-0.3491
NE211	amino acid permease	**-1.2844**	-1.5228	-1.1626	-1.1678
NE212	putative lysophospholipase	**-0.5894**	-0.6419	-0.7969	-0.3294
NE213	serine hydroxymethyltransferase (glyA)	**0.0167**	-0.1931	0.1870	0.0562
NE214	siderophore biosynthesis protein, IucC family"	**0.0485**	0.0207	-0.0266	0.1515
NE215	putative lipoprotein	**0.3203**	0.3812	0.1970	0.3827
NE216	dihydroxyacetone kinase, DhaK subunit	**0.6543**	0.2984	0.7499	0.9145
NE217	protein kinase (pknB)	**0.1221**	0.0888	0.4220	-0.1446
NE218	sensor histidine kinase family protein	**-0.4361**	-0.7562	-0.2757	-0.2764
NE219	conserved hypothetical protein	**-0.8363**	-0.8867	-0.7047	-0.9175
NE220	conserved hypothetical protein	**-0.5705**	-0.6826	-0.2478	-0.7809
NE221	conserved hypothetical protein	**-0.2473**	0.2250	-0.5275	-0.4395
NE222	aminotransferase, class V	**-0.7872**	-0.7923	-1.0758	-0.4935
NE223	tRNA pseudouridine synthase A	**-0.3003**	-0.2069	-0.3983	-0.2958
NE224	conserved hypothetical protein	**-1.0713**	-0.7633	-1.4914	-0.9591
NE225	NADH-dependent FMN reductase	**-0.0082**	-0.2916	0.2007	0.0664
NE226	ammonium transporter (amt)	**-0.2838**	0.0699	-0.7695	-0.1519
NE227	peptide ABC transporter, peptide-bindingprotein	**0.1473**	0.0486	0.6031	-0.2099
NE228	ABC transporter, permease protein	**0.7482**	0.6482	0.9855	0.6110
NE229	conserved hypothetical protein	**-1.0361**	-1.1517	-1.0762	-0.8804
NE230	conserved hypothetical protein	**-0.8763**	-0.9680	-0.9838	-0.6772
NE231	sodium dependent transporter	**-0.7819**	-0.2748	-0.7079	-1.3631
NE232	pyridoxal-dependent decarboxylase	**-0.9289**	-0.2979	-1.2926	-1.1961
NE233	glycerol-3-phosphate dehydrogenase (glpD)	**-0.9998**	-0.5705	-1.1179	-1.3109
NE234	capsular polysaccharide biosynthesis protein (Cap5I)	**0.0820**	0.5173	-0.5272	0.2558
NE235	conserved hypothetical protein	**-0.4700**	-0.1864	-0.8014	-0.4224
NE236	conserved hypothetical protein	**-0.1431**	0.1216	-0.7038	0.1528
NE237	conserved hypothetical protein	**0.5712**	0.5915	0.1949	0.9271
NE238	sulfite reductase flavoprotein	**0.0157**	1.2995	-0.6058	-0.6467
NE239	proline dehydrogenase (putA)	**0.6733**	0.9308	0.4853	0.6039
NE240	teicoplanin resistance associated membrane protein (TcaB)	**0.4503**	0.4846	0.6049	0.2615

NE241	oxidoreductase, aldo/keto reductase family	**-0.2543**	-0.5549	0.1189	-0.3268
NE242	DNA protecting protein (DprA)	**-0.9622**	-0.9415	-0.8367	-1.1084
NE243	phage related DNA polymerase, family A (polA)	**-0.1205**	-0.0686	0.1677	-0.4604
NE244	conserved hypothetical phage protein	**-0.1841**	-0.5899	-0.5542	0.5918
NE245	lantibiotic epidermin immunity protein F (epiE)	**-0.6125**	-0.3510	-0.8241	-0.6623
NE246	putative exonuclease	**0.0694**	-0.6615	-0.9459	1.8157
NE247	bacterioferritin comigratory protein	**-0.5929**	-0.7785	-0.3930	-0.6071
NE248	conserved hypothetical protein	**-0.4212**	-0.1993	-0.7514	-0.3128
NE249	glucose-inhibited division protein B	**0.4277**	0.5666	0.1190	0.5973
NE250	putative competence protein ComGB	**-0.2637**	-0.0714	-0.1655	-0.5540
NE251	polysaccharide biosynthesis protein	**0.0888**	0.0479	0.2480	-0.0294
NE252	cation efflux family protein	**0.8175**	1.6562	0.1482	0.6480
NE253	HD domain protein	**0.4360**	0.4547	0.5972	0.2561
NE254	gamma-glutamyltranspeptidase (ggt)	**0.8220**	1.1241	0.8091	0.5328
NE255	putative membrane protein	**0.2924**	0.3083	0.3709	0.1980
NE256	putative pyridoxal phosphate-dependent acyltransferase	**-0.0057**	0.0739	-0.1851	0.0941
NE257	conserved hypothetical protein	**-1.1181**	-0.7304	-1.3776	-1.2463
NE258	cardiolipin synthetase (cls)	**-0.6015**	-0.5398	-0.8145	-0.4502
NE259	polyribopolyribonucleotide nucleotidyltransferase (pnpA)	**-0.6107**	-0.4542	-0.6720	-0.7059
NE260	acyl-CoA dehydrogenase (FadD)	**-0.6881**	-0.7670	-0.7034	-0.5937
NE261	conserved hypothetical protein	**-0.1237**	-0.0171	0.0932	-0.4471
NE262	DNA-binding response regulator, LuxR family	**0.0010**	-0.1923	0.2033	-0.0080
NE263	putative acyl-CoA transferase (FadX)	**0.2424**	0.1711	0.4487	0.1074
NE264	lipoic acid synthetase (lipA)	**0.8355**	1.2087	0.9682	0.3296
NE265	CBS domain protein	**0.3476**	-0.0188	0.7891	0.2724
NE266	lipoate-protein ligase A family protein	**-0.0878**	-0.0751	0.0819	-0.2702
NE267	probable transglycosylase (sgtA)	**-0.5028**	-0.3489	-0.5273	-0.6321
NE268	conserved hypothetical protein	**0.3730**	0.4373	0.6738	0.0080
NE269	putative iron compound ABC transporter, ATP-binding protein	**-0.0466**	0.5236	-0.1210	-0.5425
NE270	acetoin utilization protein (AcuC)	**0.3241**	0.2455	0.1871	0.5396
NE271	glycine betaine/carnitine/choline transport system permease (opuCd)	**-0.1627**	0.0469	-0.3632	-0.1719
NE272	conserved hypothetical protein	**0.2058**	0.5797	-0.1781	0.2156
NE273	putative transporter	**0.1165**	0.0171	0.2968	0.0355
NE274	conserved hypothetical protein	**-0.3036**	-0.2729	-0.3501	-0.2878
NE275	transferrin receptor	**0.4535**	0.5268	0.9199	-0.0862
NE276	conserved hypothetical protein	**0.0516**	0.3513	-0.0207	-0.1757
NE277	thymidine kinase (tdk)	**0.1580**	0.4176	0.1448	-0.0885
NE278	putative cobalamin synthesis protein	**-0.5725**	-0.4902	-0.5679	-0.6593
NE279	putative deoxyribodipyrimidine photolyase	**0.2223**	0.4170	-0.0443	0.2943
NE280	xanthine permease (pbuX)	**-0.6282**	-0.5249	-0.8397	-0.5201
NE281	transcriptional regulator, MarR family	**0.6485**	0.7682	0.2914	0.8859
NE282	5' nucleotidase family protein	**0.5513**	0.6330	0.1855	0.8354
NE283	xanthine/uracil permease family protein	**0.4263**	1.5119	-0.5732	0.3402
NE284	2,3-bisphosphoglycerate-dependent phosphoglycerate mutase (gpmA)	**0.2730**	0.5023	-0.1717	0.4885
NE285	teicoplanin resistance associated membrane protein TcaA protein (tcaA)	**1.2835**	1.2045	1.0949	1.5511
NE286	immunoglobulin G binding protein A precursor	**0.3451**	0.4912	0.2721	0.2718
NE287	conserved hypothetical protein	**1.8835**	0.4859	4.9810	0.1835
NE288	fructose-bisphosphate aldolase class-I	**0.7535**	1.1447	0.6837	0.4322

NE289	conserved hypothetical protein	**1.0506**	0.6786	1.4095	1.0636
NE290	Transfferin receptor	**0.7980**	0.2289	1.2549	0.9101
NE291	conserved hypothetical protein	**1.0523**	0.7206	1.1133	1.3229
NE292	branched-chain amino acid aminotransferase (ilvE)	**0.7654**	0.6162	0.8449	0.8351
NE293	ABC transporter, ATP-binding protein	**0.9797**	1.3303	0.7980	0.8108
NE294	signal transduction protein TRAP	**-0.8215**	-0.6461	-0.6274	-1.1911
NE295	5'-nucleotidase family protein	**0.8039**	0.9410	0.6498	0.8209
NE296	staphylococcal accessory protein X	**0.9423**	0.6997	1.1735	0.9536
NE297	cyclic nucleotide-binding domain protein	**0.7550**	1.1236	0.6048	0.5365
NE298	putative membrane protein	**0.9954**	0.9237	1.3546	0.7078
NE299	putative membrane protein	**1.0794**	1.0427	1.1495	1.0461
NE300	conserved hypothetical protein TIGR00370	**1.2385**	0.9451	2.0911	0.6792
NE301	acetyltransferase, GNAT family	**-0.0710**	-0.6759	0.3721	0.0908
NE302	capsular polysaccharide biosynthesis protein (Cap5A)	**-0.9983**	-1.0884	-0.8788	-1.0278
NE303	glutamate-1-semialdehyde-2,1-aminomutase (hemL)	**-0.8025**	-1.2329	-0.5713	-0.6032
NE304	tryptophan synthase, alpha subunit (trpA)	**-0.3767**	-0.5542	-0.5244	-0.0516
NE305	conserved hypothetical protein	**-0.1491**	0.0385	-0.3846	-0.1013
NE306	proline dipeptidase	**-0.2404**	0.0656	-0.0750	-0.7120
NE307	glycerol uptake operon antiterminator regulatory protein (glpP)	**-0.0859**	0.0165	-0.3039	0.0296
NE308	transporter, monovalent cation:proton antiporter-2 (CPA2) family protein	**0.6753**	0.6520	0.8981	0.4757
NE309	putative enterotoxin type A	**0.5368**	0.3793	1.1197	0.1114
NE310	tryptophan synthase, beta subunit	**0.2232**	-0.0096	0.4669	0.2123
NE311	conserved hypothetical protein"	**1.6966**	0.8792	3.5645	0.6462
NE312	oxidoreductase, Gfo/Idh/MocA family	**-0.1861**	0.4928	-0.3520	-0.6991
NE313	DedA family protein	**-0.3324**	-0.7498	-0.3925	0.1450
NE314	deoxyribose-phosphate aldolase	**-0.7963**	-1.1981	0.0450	-1.2358
NE315	putative membrane protein	**0.5685**	-0.7151	2.9510	-0.5302
NE316	conserved hypothetical protein	**-0.6624**	-0.5948	-0.5026	-0.8896
NE317	putative membrane protein	**-0.4995**	-0.3721	-0.3761	-0.7504
NE318	conserved hypothetical protein	**-0.8440**	-0.2551	-1.0049	-1.2719
NE319	conserved hypothetical protein	**-0.0976**	0.3326	-0.1423	-0.4831
NE320	conserved hypothetical protein	**-0.3343**	-0.2050	-0.2189	-0.5791
NE321	aldehyde dehydrogenase	**0.0782**	0.9709	-0.2947	-0.4416
NE322	putative competence protein ComYC	**-0.1673**	-0.3212	0.2047	-0.3853
NE323	conserved hypothetical protein	**0.3957**	0.8775	0.2269	0.0826
NE324	regulatory protein RecX	**-1.1293**	0.0829	-1.6478	-1.8229
NE325	5S ribosomal RNA (rrfA)	**-1.7764**	-2.0341	-2.0073	-1.2878
NE326	respiratory nitrate reductase, alpha subunit	**-0.9318**	-1.0679	-0.7943	-0.9331
NE327	integrase (int)	**-0.6523**	-0.8664	-0.5943	-0.4962
NE328	oxygen-independent coproporphyrinogen III oxidase	**-0.3355**	0.2485	-0.5032	-0.7517
NE329	molybdopterin-guanine dinucleotide biosynthesis protein A (mobA)	**-0.6465**	-0.0756	-0.8806	-0.9833
NE330	conserved hypothetical protein	**-0.3407**	-0.1159	-0.4515	-0.4548
NE331	exonuclease (RexA)	**0.0611**	0.0225	0.2247	-0.0638
NE332	iron transport associated domain protein	**-0.0830**	-0.1256	0.0872	-0.2105
NE333	putative maltose ABC transporter,maltose-binding protein	**0.1517**	0.0490	0.3383	0.0679
NE334	Hyaluronate lyase precursor	**0.3086**	0.7964	-0.2120	0.3413
NE335	Conserved hypothetical protein	**1.7609**	3.1702	0.9467	1.1658
NE336	NAD-dependent deacetylase	**1.0227**	0.8441	1.3717	0.8521
NE337	integral membrane domain protein	**-0.1487**	-0.7073	0.6899	-0.4288

NE338	triacylglycerol lipase precursor (lip)	**-1.4260**	-1.7275	-1.0950	-1.4555
NE339	LysE/YggA family protein	**-0.7607**	-0.8492	-0.4406	-0.9922
NE340	threonine dehydratase (ilvA)	**-1.3641**	-1.4848	-1.0926	-1.5148
NE341	ATPase, AAA family	**0.0611**	0.2836	-0.0683	-0.0319
NE342	RNA chaperone, host factor-1 protein (hfq)	**-0.7139**	-0.1421	-1.1706	-0.8289
NE343	conserved hypothetical protein	**-0.1203**	-0.1136	-0.1538	-0.0936
NE344	ABC transporter, ATP-binding protein	**0.0236**	-0.6825	0.3616	0.3918
NE345	membrane protein	**0.5843**	0.1656	0.8548	0.7325
NE346	putative DnaQ family exonuclease/DinG family helicase	**0.3838**	0.6354	-0.1958	0.7116
NE347	acetyltransferase, GNAT family	**0.5228**	0.5107	0.6086	0.4490
NE348	DNA translocase (FtsK)	**0.8887**	0.7019	0.8114	1.1529
NE349	conserved hypothetical protein	**0.5963**	0.1693	1.0106	0.6091
NE350	GTP-binding protein (YchF)	**-0.4132**	-0.6990	-0.0302	-0.5105
NE351	D-lactate dehydrogenase (ddh)	**0.1771**	0.7192	-0.2246	0.0368
NE352	ribosome small subunit-dependent GTPase A (rsgA)	**-0.6527**	-0.7308	-0.7948	-0.4325
NE353	bifunctional purine biosynthesis protein	**-0.4707**	-0.3874	-0.1345	-0.8903
NE354	transcriptional regulator, gntR family protein	**-0.8593**	0.1492	-1.4744	-1.2527
NE355	transcriptional regulator, TetR family	**-0.3148**	-0.0887	-0.1611	-0.6947
NE356	orotate phosphoribosyltransferase (pyrE)	**-0.5024**	-0.6456	-0.6316	-0.2300
NE357	Na/Pi cotransporter family protein	**0.0360**	0.0096	0.2040	-0.1056
NE358	conserved hypothetical protein	**0.0531**	0.4760	-0.2254	-0.0914
NE359	2-dehydropantoate 2-reductase (panE)	**0.2483**	1.1864	0.1515	-0.5930
NE360	phi77 ORF004-like protein, putative phage tail component	**0.5578**	0.7212	0.3790	0.5730
NE361	conserved hypothetical protein	**0.6738**	0.4427	1.1107	0.4679
NE362	putative teichoic acid biosynthesis protein B	**-0.6358**	-0.8386	-0.4647	-0.6041
NE363	staphylococcal tandem lipoprotein	**-0.2615**	-0.4796	-0.0928	-0.2121
NE364	ABC transporter, ATP-binding protein, MsbA family	**-0.5674**	-0.5613	-0.8224	-0.3184
NE365	putative lipoprotein	**0.1233**	-0.0894	0.3519	0.1075
NE366	putative Na+/H+ antiporter	**0.5579**	0.0100	1.0389	0.6249
NE367	arginine repressor	**-0.3527**	-0.9500	0.0302	-0.1384
NE368	choline dehydrogenase	**-0.1158**	-0.5742	0.1770	0.0497
NE369	guanosine monophosphate reductase (guaC)	**0.2757**	-0.2400	0.1911	0.8759
NE370	conserved hypothetical protein	**0.1750**	0.4555	-0.2100	0.2794
NE371	putative membrane protein	**0.6673**	-0.0353	0.9398	1.0972
NE372	SAP domain protein	**1.2839**	0.2306	2.1215	1.4996
NE373	conserved hypothetical protein	**0.7718**	0.4117	1.1897	0.7140
NE374	ferrous iron transport protein B (feoB)	**-0.1700**	-0.2409	-0.2365	-0.0325
NE375	Ear protein	**0.0942**	-0.4269	-0.1191	0.8286
NE376	putative membrane protein	**-0.5397**	-0.9419	-0.5165	-0.1608
NE377	conserved hypothetical protein	**-0.0999**	-0.3484	-0.1115	0.1601
NE378	putative membrane protein	**0.0141**	-0.4832	0.3252	0.2001
NE379	conserved hypothetical protein	**-0.2536**	-0.4613	-0.2701	-0.0296
NE380	hydrolase, CocE/NonD family	**-0.2135**	-0.5105	-0.3790	0.2490
NE381	glycosyl transferase, group 1 family protein	**0.8439**	1.5461	0.4898	0.4959
NE382	squalene synthase (crtN)	**0.1884**	-0.4054	0.5051	0.4655
NE383	putative membrane protein	**0.9898**	0.4445	1.4818	1.0431
NE384	conserved hypothetical protein	**1.2319**	0.5980	1.8334	1.2643
NE385	acetyl-coenzyme A synthetase (acsA)	**-0.1162**	0.0016	-0.3325	-0.0176
NE386	staphylococcal accessory regulator (Rot)	**0.3346**	-0.2476	1.9726	-0.7213
NE387	conserved hypothetical protein	**0.1344**	-0.1877	-0.3407	0.9317
NE388	sodium-dependent transporter	**1.0710**	0.5201	1.2115	1.4815

NE389	conserved hypothetical protein	**0.2265**	0.1624	0.2282	0.2889
NE390	glutamate synthase, large subunit (gltB)	**1.5457**	1.3652	1.3751	1.8967
NE391	clumping factor B (clfB)	**0.8833**	0.4730	1.3535	0.8233
NE392	peptide ABC transporter, ATP-binding protein	**0.5426**	-0.3131	2.0446	-0.1037
NE393	glyoxalase family protein	**-0.6855**	-0.7094	-0.2976	-1.0496
NE394	oligopeptide ABC transporter, ATP-binding protein (oppF)	**7.2339**	6.9238	6.9846	7.7933
NE395	N-acetylglucosamine-6-phosphate deacetylase (nagA)	**4.9589**	0.9360	6.5718	7.3690
NE396	conserved hypothetical protein	**4.8870**	2.6986	5.7234	6.2390
NE397	ornithine carbamoyltransferase (argF)	**-0.1701**	0.0205	-0.4178	-0.1131
NE398	conserved hypothetical protein	**0.1621**	0.4215	0.5553	-0.4905
NE399	preprotein translocase, SecY protein	**0.2917**	-0.0335	0.4438	0.4649
NE400	iron compound ABC transporter, iron compound-binding protein	**1.3797**	0.8412	1.4960	1.8018
NE401	phiSLT ORF 175-like protein	**1.0841**	-0.3615	2.2007	1.4131
NE402	cell wall hydrolase (lytN)	**0.6469**	0.2537	1.3315	0.3554
NE403	DegV family protein	**-0.3025**	-0.7625	0.2985	-0.4434
NE404	putative endoribonuclease L-PSP	**1.0672**	0.6157	0.6764	1.9094
NE405	MATE efflux family protein	**-0.9515**	-0.4861	-1.4646	-0.9040
NE406	ferrichrome transport ATP-binding protein fhuA	**0.4553**	-0.0469	0.9610	0.4517
NE407	putative membrane protein	**1.7173**	0.8343	2.7311	1.5865
NE408	putative staphylococcal tandem lipoprotein	**0.2183**	0.1107	0.0880	0.4562
NE409	hydrolase, haloacid dehalogenase-like family	**0.1485**	0.7001	-0.1918	-0.0627
NE410	urease, alpha subunit (ureC)	**-0.2901**	-1.0354	0.2619	-0.0969
NE411	putative phage infection protein	**0.9961**	0.5421	1.2516	1.1946
NE412	conserved hypothetical protein	**1.1916**	1.3361	1.5610	0.6777
NE413	phiSLT ORF 50-like protein	**-0.3165**	-0.6362	-0.7316	0.4184
NE414	conserved hypothetical protein	**1.0525**	1.1329	1.2207	0.8040
NE415	putative transcriptional regulator	**-1.0726**	-1.4215	-1.0663	-0.7300
NE416	putative cobalamin synthesis protein	**0.6287**	2.1227	0.4131	-0.6497
NE417	integrase (int)	**0.0805**	0.1744	-0.3630	0.4302
NE418	cation efflux family protein	**0.9488**	-0.1018	1.2818	1.6664
NE419	conserved hypothetical protein	**1.2190**	0.9434	1.6247	1.0888
NE420	penicillin-binding protein 3 (pbp3)	**0.7625**	-0.0640	1.0596	1.2919
NE421	conserved hypothetical protein	**-1.0748**	-1.0570	-1.0781	-1.0892
NE422	conserved hypothetical protein	**-0.7021**	-0.7990	-0.1499	-1.1574
NE423	sensor histidine kinase, KdpD	**-0.6993**	-0.8197	-0.7277	-0.5503
NE424	pyrimidine nucleoside phosphorylase (pdp)	**2.8287**	0.6663	6.7774	1.0424
NE425	putative ribose operon repressor	**0.4926**	0.5800	0.6289	0.2690
NE426	Sec-independent protein translocase TatC	**-0.0811**	0.0735	-0.0427	-0.2740
NE427	fumarate hydratase, class II (fumC)	**-1.3137**	-0.6656	-1.6527	-1.6228
NE428	molybdopterin converting factor, subunit 2 (moaE)	**-0.1542**	-0.3805	0.0143	-0.0965
NE429	capsular polysaccharide biosynthesis protein cap5C	**-0.4047**	-0.3534	0.3857	-1.2464
NE430	putative transporter	**-0.4308**	0.1125	-1.2955	-0.1094
NE431	iron-dependent repressor	**1.5388**	1.4948	1.3697	1.7518
NE432	sdrC protein	**-0.1323**	0.4175	-0.7400	-0.0744
NE433	phosphate ABC transporter, permease protein PstC	**-0.5543**	-0.4328	-0.1193	-1.1107
NE434	phosphosugar-binding transcriptional regulator	**-0.7398**	-0.4240	-0.8003	-0.9951
NE435	urocanate hydratase (hutU)	**0.4053**	-0.3936	1.6300	-0.0206
NE436	lactose phosphotransferase system repressor	**0.3230**	0.5600	-0.5125	0.9213
NE437	putative membrane protein	**-0.2786**	-0.4293	0.0582	-0.4647
NE438	capsular polysaccharide biosynthesis protein Cap5J	**-0.5827**	-0.5670	-1.1397	-0.0414

NE439	choloylglycine hydrolase family protein	**-1.0237**	-0.8082	-1.4574	-0.8055
NE440	oligopeptide ABC transporter, substrate-binding protein (oppA)	**-0.1677**	-0.5457	-0.3799	0.4224
NE441	NAD(P)H-flavin oxidoreductase (frp)	**0.1545**	0.5402	-0.2352	0.1585
NE442	phiSLT ORF122-like protein, DNA polymerase	**-0.1784**	0.2357	-0.8250	0.0542
NE443	conserved hypothetical protein	**1.0855**	0.4407	1.2049	1.6108
NE444	aminopeptidase PepS	**0.7018**	-0.0518	1.5393	0.6179
NE445	ImpB/MucB/SamB family protein	**-0.2220**	0.1582	-0.2596	-0.5646
NE446	peptide chain release factor 3 (prfC)	**-0.2338**	-0.8475	0.1284	0.0176
NE447	putative iron-sulfur cluster-binding protein	**-0.3378**	-0.0016	-1.1637	0.1520
NE448	putative membrane protein	**-0.1299**	0.2029	-0.5149	-0.0777
NE449	phiSLT ORF636-like protein	**-0.2166**	0.8343	-0.5849	-0.8993
NE450	PTS system, IIBC components	**-1.2664**	-0.7247	-1.1679	-1.9066
NE451	acetyltransferase, GNAT family	**-1.6099**	-1.2516	-2.0213	-1.5569
NE452	conserved hypothetical protein	**-0.7875**	-0.2341	-1.1373	-0.9912
NE453	IgG-binding protein SBI	**-0.3627**	0.0898	-0.4480	-0.7298
NE454	transcriptional regulator, Crp/Fnr family (arcR)	**-1.7302**	-1.4826	-2.0972	-1.6108
NE455	bacterial luciferase family protein	**1.6369**	2.2837	0.4113	2.2156
NE456	conserved hypothetical protein	**-0.1263**	0.2890	-0.5647	-0.1030
NE457	peptide ABC transporter, permease protein	**-0.5051**	-0.0627	-0.0681	-1.3846
NE458	exodeoxyribonuclease VII, large subunit (xseA)	**-0.8568**	-0.8955	-1.5507	-0.1241
NE459	fmhA protein	**-0.8934**	-1.0775	-1.2436	-0.3591
NE460	autolysin (atl)	**-0.3997**	-0.1297	-1.6151	0.5455
NE461	polysaccharide extrusion protein	**-0.9980**	-0.9938	-1.8182	-0.1820
NE462	putative membrane protein	**-0.0144**	0.1287	0.3831	-0.5551
NE463	conserved hypothetical protein	**-1.4843**	-1.1341	-1.9471	-1.3715
NE464	pyrrolidone-carboxylate peptidase (pcp)	**-0.3363**	-1.1944	-0.4886	0.6740
NE465	glycerate kinase	**0.5380**	0.4493	0.8165	0.3482
NE466	putative DNA primase	**-0.8826**	-0.8034	-1.1872	-0.6570
NE467	conserved hypothetical protein	**6.8734**	3.8158	7.7352	9.0692
NE468	phytoene dehydrogenase	**0.3653**	0.2688	0.6786	0.1486
NE469	sucrose-6-phosphate hydrolase (scrB)	**0.0025**	-0.5943	0.3864	0.2155
NE470	putative membrane protein	**1.3992**	0.6908	3.0830	0.4237
NE471	putative cell wall enzyme EbsB	**-1.0734**	-1.3235	-0.4394	-1.4572
NE472	truncated FmtB protein	**-0.1952**	0.0244	-0.7950	0.1851
NE473	putative membrane protein	**-0.5783**	-1.1060	0.2492	-0.8780
NE474	conserved hypothetical protein	**-0.5758**	-0.4786	-0.3645	-0.8844
NE475	putative exotoxin 4	**-0.7410**	-0.8340	-0.4490	-0.9401
NE476	fructose bisphosphate aldolase (fba)	**-0.9244**	-1.0204	-0.0143	-1.7384
NE477	purine nucleoside phosphorylase (deoD)	**4.3539**	1.4379	9.2629	2.3610
NE478	phosphonate ABC transporter, permease protein (phnE)	**0.3535**	0.7872	-0.0649	0.3383
NE479	putative competence protein ComGA	**4.1755**	0.6903	8.3811	3.4552
NE480	undecaprenol kinase	**2.2682**	0.1528	5.9077	0.7443
NE481	DNA-binding response regulator (graR)	**0.5305**	0.1380	0.8831	0.5704
NE482	oligopeptide ABC transporter, ATP-binding protein (oppF)	**0.5149**	0.6336	0.2565	0.6546
NE483	peptidase T (pepT)	**0.9077**	1.2578	1.1958	0.2695
NE484	amino acid ABC transporter, permease/substrate-binding protein	**0.1531**	0.2788	0.3981	-0.2175
NE485	glycine dehydrogenase, subunit 2	**0.4343**	0.7115	0.7414	-0.1500
NE486	putative chromosome partioning protein, ParB family	**-1.6320**	-0.9597	-2.4571	-1.4792
NE487	conserved hypothetical protein	**0.9318**	0.9857	1.2456	0.5642

NE488	putative membrane protein	**0.6123**	0.6687	1.1738	-0.0057
NE489	exotoxin	**0.7393**	0.7907	1.0979	0.3294
NE490	TPR domain protein	**0.4023**	0.6850	-0.0283	0.5503
NE491	isocitrate dehydrogenase, NADP-dependent (icd)	**0.7035**	0.2417	0.9812	0.8877
NE492	conserved hypothetical protein	**1.9582**	1.0853	2.4998	2.2896
NE493	conserved hypothetical protein	**0.3532**	0.0099	0.6251	0.4247
NE494	phosphoribosylformylglycinamidine synthase I (purQ)	**-0.9891**	-0.7372	-1.0130	-1.2170
NE495	cassette chromosome recombinase B (ccrB)	**-0.5333**	-0.5777	-0.1359	-0.8863
NE496	transporter, TRAP family	**-0.3940**	-0.9481	-0.5477	0.3139
NE497	putative D-isomer specific 2-hydroxyacid dehydrogenase	**-0.1049**	-0.6083	0.7106	-0.4172
NE498	conserved hypothetical protein	**-0.3573**	-0.7146	0.2187	-0.5760
NE499	putative membrane protein	**0.8466**	0.5292	1.0004	1.0100
NE500	3-hydroxyacyl-CoA dehydrogenase	**-0.0081**	-0.3377	0.3678	-0.0544
NE501	ribonuclease R (rnr)	**-0.8144**	-1.0850	-1.0855	-0.2727
NE502	conserved hypothetical protein	**0.2573**	0.0609	0.3066	0.4044
NE503	tributyrin esterase (estA)	**0.2287**	0.6102	-0.3357	0.4117
NE504	phiSLT ORF191-like protein	**0.3583**	0.1513	0.9598	-0.0361
NE505	transcriptional regulator, LysR family domain protein	**-0.4589**	-0.4081	-0.5146	-0.4542
NE506	conserved hypothetical protein	**-0.4948**	-0.6529	0.0263	-0.8577
NE507	RNA methyltransferase, TrmH family	**-1.3090**	-1.3163	-1.4371	-1.1736
NE508	argininosuccinate synthase (argG)	**-0.3078**	-0.1239	-0.2010	-0.5985
NE509	staphylococcal tandem lipoprotein	**-0.6560**	-1.5247	0.2675	-0.7108
NE510	truncated FmtB protein	**-0.4362**	-0.8972	0.2592	-0.6707
NE511	carbamate kinase (arcC)	**-0.3564**	-0.4044	0.0304	-0.6953
NE512	molybdenum ABC transporter, ATP-binding protein ModC	**-0.2823**	-0.6823	-0.0910	-0.0735
NE513	putative helicase	**0.5541**	0.9449	-0.0653	0.7827
NE514	staphylococcal accessory regulator T (sarT)	**-0.0491**	-0.0530	-0.1323	0.0381
NE515	threonine dehydratase (ilvA)	**0.2609**	0.4173	-0.0083	0.3736
NE516	conserved hypothetical protein	**0.4728**	-0.0737	0.7213	0.7708
NE517	IS1272, transposase	**0.0329**	-0.0050	0.0083	0.0955
NE518	glycosyl transferase	**-0.4168**	-0.3798	-0.8545	-0.0160
NE519	peptidase, M20/M25/M40 family	**-1.0457**	-1.5798	-1.3871	-0.1700
NE520	pyrroline-5-carboxylate reductase (proC)	**-0.4745**	-0.9406	-0.8453	0.3624
NE521	ABC transporter, permease protein	**-1.1290**	-1.1649	-0.7952	-1.4270
NE522	adenylosuccinate lyase (purB)	**-2.5915**	-2.4988	-2.7794	-2.4962
NE523	phi77 ORF011-like protein, phage transcriptional repressor	**-1.0121**	-1.3889	-1.4348	-0.2125
NE524	conserved hypothetical protein	**-1.0779**	-1.2708	-1.2183	-0.7445
NE525	putative NADP-dependent malic enzyme	**-0.9269**	-1.4426	-0.6838	-0.6542
NE526	putative membrane protein	**0.1797**	0.1537	-0.2338	0.6192
NE527	lantibiotic epidermin biosynthesis protein EpiB	**-0.1952**	-0.2690	-0.3587	0.0421
NE528	putative permease	**0.8602**	1.0665	1.4808	0.0332
NE529	adenylosuccinate synthetase (purA)	**-1.9966**	-1.3170	-2.2552	-2.4174
NE530	transcriptional regulator, AraC family	**3.2002**	7.2411	2.2008	0.1587
NE531	putative drug transporter	**-0.6255**	-0.9146	-0.8204	-0.1416
NE532	conserved hypothetical protein	**-0.8465**	-0.7614	-1.1575	-0.6205
NE533	ABC transporter, permease protein	**-0.9315**	-0.5491	-1.8049	-0.4406
NE534	conserved hypothetical protein	**-0.6584**	-1.3475	0.0816	-0.7093
NE535	signal peptidase IA (spsA)	**-0.3621**	-0.2538	-1.2210	0.3884
NE536	conserved hypothetical protein	**-1.1397**	-1.2639	-1.5016	-0.6535
NE537	conserved hypothetical protein	**-0.3515**	-0.0157	-0.7625	-0.2763
NE538	thiamine biosynthesis protein ThiI	**-0.3613**	-0.6991	-0.2076	-0.1772

NE539	acyl-CoA synthetase FadE	**0.3937**	0.2277	0.4610	0.4923
NE540	conserved hypothetical protein	**1.6240**	1.2458	1.9838	1.6423
NE541	peptide ABC transporter, permease protein	**0.5102**	0.1380	0.9727	0.4199
NE542	putative fructose-1,6-bisphosphatase	**-0.1732**	-0.1808	-0.1113	-0.2275
NE543	clumping factor A (clfA)	**0.2941**	0.3286	-0.1565	0.7102
NE544	pyrimidine nucleoside transport protein (nupC)	**0.5808**	1.0739	-0.3049	0.9735
NE545	conserved hypothetical protein	**2.1169**	6.2700	-0.0713	0.1519
NE546	conserved hypothetical protein	**0.1430**	0.3630	-0.4471	0.5130
NE547	2-oxoglutarate dehydrogenase, E1 component (sucA)	**-0.4042**	0.3222	-0.8223	-0.7126
NE548	putative transporter	**-0.1981**	0.1952	-0.7403	-0.0493
NE549	homoserine dehydrogenase	**0.0727**	0.3115	-0.5740	0.4807
NE550	conserved hypothetical protein	**0.0593**	-0.1476	0.2823	0.0433
NE551	putative fibronectin/fibrinogen binding protein	**0.1416**	0.5112	-0.0430	-0.0435
NE552	oligopeptide ABC transporter, ATP-binding protein	**2.4518**	2.5752	2.1067	2.6734
NE553	conserved hypothetical protein	**0.6897**	1.6319	-0.3521	0.7893
NE554	DNA-binding response regulator (vraR)	**0.2304**	-0.0229	0.5687	0.1455
NE555	DNA replication and repair protein recF	**0.6126**	1.2315	0.1280	0.4784
NE556	conserved hypothetical protein	**-0.3759**	-0.8687	-0.0841	-0.1748
NE557	iron transport associated domain protein	**-0.0847**	-0.4074	0.3102	-0.1571
NE558	leukotoxin LukE	**-0.0871**	-0.4160	0.4277	-0.2732
NE559	conserved hypothetical phage protein	**-0.3340**	-0.7110	-0.1234	-0.1675
NE560	sodium/glutamate symporter (gltS)	**-0.1732**	0.3460	-0.9266	0.0612
NE561	copper-translocating P-type ATPase	**-0.2040**	-0.4977	-0.0775	-0.0368
NE562	ROK family protein	**0.4228**	0.4015	0.9558	-0.0889
NE563	glutathione peroxidase	**0.3709**	0.4810	0.5450	0.0869
NE564	pyruvate oxidase (cidC)	**2.0220**	0.9875	3.0438	2.0348
NE565	ATP-dependent RNA helicase	**1.1352**	1.4839	1.8553	0.0664
NE566	proton/sodium-glutamate symport protein (gltT)	**1.6181**	2.0162	1.4914	1.3468
NE567	transcriptional regulator, MarR family	**0.3713**	-0.0905	0.9269	0.2775
NE568	Zn-binding lipoprotein adcA-like protein	**0.3621**	0.0050	1.2167	-0.1355
NE569	succinyl-CoA synthetase, beta subunit (sucC)	**-0.0306**	0.1173	-0.1292	-0.0800
NE570	histidine ammonia-lyase (hutH)	**0.6404**	1.6298	0.2027	0.0888
NE571	putative transposase	**0.4920**	0.5108	0.3446	0.6206
NE572	D-isomer specific 2-hydroxyacid dehydrogenase	**0.3391**	0.5194	0.9817	-0.4839
NE573	riboflavin biosynthesis protein (ribBA)	**-0.1730**	-0.0948	-0.4300	0.0057
NE574	hypothetical protein	**-0.2770**	-0.6412	0.2384	-0.4284
NE575	oxidoreductase, aldo/keto reductase family	**0.5733**	0.6082	0.1655	0.9461
NE576	sorbitol dehydrogenase (gutB)	**1.4686**	1.3191	2.0349	1.0518
NE577	PAP2 family protein	**-0.1129**	-0.5422	1.0569	-0.8533
NE578	iron compound ABC transporter, permease protein	**1.2011**	2.0069	0.9685	0.6280
NE579	aspartate kinase	**3.2530**	1.8314	8.2642	-0.3367
NE580	capsular polysaccharide biosynthesis protein cap5G	**0.7707**	1.1659	-0.4786	1.6246
NE581	amidophosphoribosyltransferase (purF)	**0.1391**	0.8998	0.5672	-1.0498
NE582	conserved hypothetical protein	**0.4781**	0.1538	0.4950	0.7854
NE583	conserved hypothetical protein	**0.2891**	0.3361	0.4103	0.1208
NE584	nitrite extrusion protein (narK)	**0.6255**	0.0532	1.5623	0.2610
NE585	NAD-dependent epimerase/dehydratase family protein	**0.8582**	1.0672	0.8611	0.6464
NE586	imidazolonepropionase (hutI)	**-0.2475**	0.0444	-0.8768	0.0900
NE587	prephenate dehydratase (pheA)	**0.6935**	0.8700	0.0953	1.1151
NE588	staphylococcal respiratory response protein, srrB	**0.9410**	0.5397	1.3951	0.8884
NE589	sodium/bile acid symporter family protein	**0.4569**	0.9365	0.3078	0.1263

NE590	ATPase copper transport (copA)	**-0.0450**	-0.2209	-0.2161	0.3019
NE591	trans-sulfuration enzyme family protein	**-0.0277**	-0.0076	0.0175	-0.0930
NE592	ATP synthase F1, alpha subunit (atpA)	**-0.9193**	-1.1138	-1.5841	-0.0600
NE593	anthranilate synthase component I (trpE)	**0.1500**	0.1051	0.0550	0.2900
NE594	citrate synthase II (gltA)	**-0.5322**	-0.8825	-1.6299	0.9159
NE595	arginine biosynthesis bifunctional protein ArgJ	**-0.4871**	-0.7947	-1.1175	0.4510
NE596	monofunctional glycosyltransferase (sgtB)	**-1.6071**	-1.5956	-1.5962	-1.6295
NE597	4-diphosphocytidyl-2C-methyl-D-erythritol kinase (ispE)	**0.5343**	0.0076	0.7559	0.8394
NE598	putative N-acetyltransferase	**0.0680**	0.6404	0.1375	-0.5739
NE599	conserved hypothetical protein	**1.1283**	1.0640	1.6184	0.7025
NE600	putative peptidase	**2.0482**	1.3238	1.9120	2.9087
NE601	conserved hypothetical protein	**1.4092**	2.0357	1.7150	0.4769
NE602	conserved hypothetical protein	**-0.2701**	-0.4331	-0.6355	0.2583
NE603	molybdopterin biosynthesis protein A (moeA)	**-0.0854**	-0.5743	-0.0447	0.3626
NE604	conserved hypothetical protein	**0.4230**	-0.5262	-0.1479	1.9429
NE605	branched-chain amino acid transport system II carrier protein (brnQ)	**0.6564**	0.2412	-0.5479	2.2760
NE606	conserved hypothetical protein	**-1.1542**	-1.0464	-1.8033	-0.6128
NE607	phosphonate ABC transporter, permease protein (phnE)	**2.3121**	-0.1376	6.7308	0.3430
NE608	conserved hypothetical protein	**-0.3847**	-0.5267	-1.4407	0.8133
NE609	conserved hypothetical protein	**-0.2081**	0.5758	-1.1500	-0.0499
NE610	lysine-specific permease (lysP)	**-0.7582**	-0.9154	-1.3113	-0.0479
NE611	glycosyl transferase, group 1 family protein	**1.0089**	1.3863	0.8022	0.8382
NE612	formate acetyltransferase (pflB)	**0.9077**	0.5445	0.6423	1.5364
NE613	ATP guanido phosphotransferase	**-0.2242**	-0.3372	-0.8065	0.4710
NE614	UTP-glucose-1-phosphate uridylyltransferase (galU)	**-1.1214**	-1.5011	-0.7666	-1.0965
NE615	conserved hypothetical protein	**-1.4290**	-1.4868	-1.9650	-0.8354
NE616	conserved hypothetical protein	**1.8798**	-0.7373	6.9251	-0.5484
NE617	lantibiotic epidermin immunity protein F (epiG)	**-1.1152**	-0.8950	-2.0028	-0.4477
NE618	sensory box histidine kinase PhoR	**-1.1752**	-1.0877	-1.3770	-1.0607
NE619	5'-nucleotidase, lipoprotein e(P4) family	**-1.1946**	-1.6095	-1.4553	-0.5192
NE620	PAP2 family protein	**-0.6816**	-0.4793	-1.3718	-0.1936
NE621	conserved hypothetical protein	**-0.2924**	-0.0566	-1.1402	0.3196
NE622	putative nucleoside permease NupC	**-1.3428**	-1.2448	-1.9529	-0.8306
NE623	arginine deiminase (arcA)	**0.4747**	0.9239	0.4973	0.0027
NE624	conserved hypothetical protein	**0.3112**	0.4208	0.3378	0.1750
NE625	sodium:dicarboxylate symporter family protein	**-0.5366**	-0.2975	-1.2952	-0.0172
NE626	succinate dehydrogenase, flavoprotein subunit (sdhA)	**-1.4584**	-1.6493	-1.5533	-1.1726
NE627	putative membrane protein	**-1.2455**	-0.8657	-1.7554	-1.1153
NE628	formate/nitrite transporter family protein	**0.6338**	5.4148	-1.5000	-2.0135
NE629	glycerate kinase family protein	**-1.4276**	-1.5985	-1.7783	-0.9061
NE630	acetyltransferase, GNAT family	**-0.7561**	0.8365	-1.8025	-1.3023
NE631	phiPVL ORF39-like protein	**-2.1827**	-1.9219	-2.9281	-1.6983
NE632	conserved hypothetical protein	**-1.1191**	-1.2602	-0.5089	-1.5884
NE633	conserved hypothetical protein	**-0.7598**	-0.5880	-0.8921	-0.7994
NE634	putative membrane protein	**-1.4194**	-1.5259	-1.7621	-0.9702
NE635	riboflavin synthase, alpha subunit (ribE)	**0.2064**	-0.7746	1.3706	0.0234
NE636	exfoliative toxin A	**0.1438**	0.3636	0.0707	-0.0027
NE637	cmp-binding-factor 1 (cbf1)	**0.4341**	0.0436	0.8247	Inf
NE638	conserved hypothetical protein	**0.7886**	-0.2632	1.3421	1.2868
NE639	putative glycerophosphoryl diester phosphodiesterase	**-0.5661**	-0.8334	0.0780	-0.9430

NE640	conserved hypothetical phage protein	**-0.1155**	-0.5928	-0.1603	0.4065
NE641	peptidoglycan hydrolase (lytM)	**-0.5252**	-0.3867	-0.9737	-0.2151
NE642	alpha-acetolactate decarboxylase (budA)	**-0.8241**	-1.0123	-0.9704	-0.4896
NE643	staphylococcal tandem lipoprotein	**-1.1125**	-1.0869	-1.1292	-1.1213
NE644	acetyltransferase, GNAT family	**-0.1726**	0.5235	-0.5566	-0.4846
NE645	ABC transporter, ATP-binding protein	**0.1016**	0.8867	0.0644	-0.6462
NE646	DNA-directed RNA polymerase, delta subunit (rpoE)	**-0.7644**	-0.3831	-1.1373	-0.7729
NE647	conserved hypothetical protein	**-0.3194**	-0.0391	-0.8950	-0.0241
NE648	PTS system, arbutin-like IIBC component (glvC)	**3.0195**	2.0622	6.9141	0.0822
NE649	staphylococcal tandem lipoprotein	**0.9617**	0.1517	0.9551	1.7784
NE650	purine nucleoside phosphorylase (deoD)	**1.4660**	1.1854	2.4075	0.8053
NE651	exotoxin	**-0.5421**	-1.5075	1.4805	-1.5994
NE652	cytosol aminopeptidase (ampA)	**0.6915**	1.9958	0.4301	-0.3512
NE653	putative lipoprotein	**0.3333**	-0.2364	1.6249	-0.3887
NE654	hydrolase, alpha/beta hydrolase fold family	**-0.9489**	-0.9402	-1.0002	-0.9064
NE655	methionine-R-sulfoxide reductase (msrB)	**0.8346**	0.9963	1.9559	-0.4484
NE656	HIT family protein	**0.0644**	1.1311	-0.0175	-0.9203
NE657	aspartate 1-decarboxylase (panD)	**-0.3026**	-0.2118	-0.0766	-0.6193
NE658	spermidine/putrescine ABC transporter, spermidine/putrescine-binding protein (potD)	**-0.7821**	-0.6293	-0.5678	-1.1492
NE659	conserved hypothetical protein	**0.2924**	0.1975	0.7999	-0.1201
NE660	aminomethyltransferase (glycine cleavage system T protein) (gcvT)	**3.3127**	0.9342	7.8620	1.1418
NE661	putative Na+/H+ antiporter, MnhG component	**6.5654**	1.9056	8.4096	9.3810
NE662	putative NAD(P)H-flavin oxidoreductase	**3.4166**	0.8756	0.1457	9.2286
NE663	maltose ABC transporter, permease protein	**1.1029**	1.1875	0.4425	1.6787
NE664	conserved hypothetical protein	**1.1514**	0.7398	0.8888	1.8256
NE665	transcriptional regulator, Fur family	**-0.1877**	-0.1253	-0.6712	0.2335
NE666	molybdenum cofactor biosynthesis protein A (moaA)	**0.3220**	0.0952	-0.3883	1.2591
NE667	type I restriction-modification enzyme, R subunit (hsdR)	**0.2961**	0.4358	0.2671	0.1853
NE668	putative membrane protein	**-0.0604**	0.8747	-0.1803	-0.8756
NE669	capsular polysaccharide biosynthesis protein Cap5O	**0.8752**	0.8620	0.8993	0.8642
NE670	conserved hypothetical protein	**1.1053**	0.4915	2.2050	0.6195
NE671	conserved hypothetical protein	**-0.0013**	-0.1346	0.3767	-0.2460
NE672	homoserine kinase	**3.4916**	0.9560	7.9165	1.6022
NE673	conserved hypothetical protein	**-0.1884**	-0.2277	0.2909	-0.6283
NE674	conserved hypothetical protein	**-0.8851**	0.5040	-1.3267	-1.8326
NE675	iron compound ABC transporter, permease protein SirB	**0.2388**	-0.4485	1.1128	0.0522
NE676	acetyltransferase, GNAT family	**3.1889**	2.0301	7.3567	0.1798
NE677	choline/carnitine/betaine transporter, BCCT family (bccT)	**0.1070**	0.3856	0.3552	-0.4200
NE678	1-phosphatidylinositol phosphodiesterase (plc)	**0.4085**	-0.0070	0.9496	0.2831
NE679	penicillin-binding protein 4 (pbp4)	**0.9595**	0.7274	1.3571	0.7940
NE680	conserved hypothetical protein	**-0.4280**	0.1129	-0.9009	-0.4960
NE681	K+-transporting ATPase, B subunit (kdpB)	**2.4850**	0.0344	7.6884	-0.2677
NE682	conserved hypothetical protein	**-0.8209**	-0.9642	-0.2468	-1.2517
NE683	oligopeptide ABC transporter, permease protein (oppB)	**3.5998**	1.3160	0.5287	8.9546
NE684	conserved hypothetical protein	**1.2378**	0.9253	1.1555	1.6327
NE685	conserved hypothetical protein	**-0.1137**	0.4256	-0.4742	-0.2924
NE686	putative membrane protein	**-0.8385**	-1.0612	-1.2022	-0.2521
NE687	phage terminase family protein	**3.2046**	1.0515	7.9109	0.6513
NE688	conserved hypothetical protein	**0.0282**	0.0548	-0.8597	0.8895

NE689	conserved hypothetical protein	**-1.2778**	-0.5709	-1.9613	-1.3014
NE690	transcriptional regulator, MerR family	**-0.5209**	1.3102	-0.9526	-1.9201
NE691	monooxygenase family protein	**0.6701**	0.7565	1.3701	-0.1162
NE692	conserved hypothetical protein	**-0.1954**	-0.4353	0.1293	-0.2802
NE693	molybdopterin-guanine dinucleotide biosynthesis protein B (mobB)	**0.0246**	-0.7701	0.1296	0.7142
NE694	putative acetoacetyl-CoA reductase	**-0.5189**	-0.6232	-0.0383	-0.8950
NE695	transcriptional antiterminator, BglG family	**1.4158**	0.8087	1.3205	2.1181
NE696	putative phosphoglycerate mutase family protein	**1.6727**	1.1590	2.6712	1.1878
NE697	cysteine synthase/cystathionine beta-synthase (cysM)	**1.2676**	1.2562	1.0829	1.4636
NE698	conserved hypothetical protein	**-0.0268**	-0.0847	1.0109	-1.0065
NE699	endopeptidase (clpC)	**0.1978**	-0.1709	0.0122	0.7521
NE700	conserved hypothetical protein	**4.8049**	6.6166	7.3454	0.4526
NE701	type III leader peptidase family protein	**-0.1409**	0.5524	-0.4176	-0.5576
NE702	imidazole glycerol phosphate dehydratase hisB	**0.0370**	0.5709	-0.5486	0.0889
NE703	conserved hypothetical protein	**0.8000**	1.1604	0.2941	0.9455
NE704	L-ribulokinase	**0.3190**	-0.5508	0.8976	0.6102
NE705	phage portal protein	**0.3445**	-0.0238	-0.3041	1.3612
NE706	formate-tetrahydrofolate ligase (fhs)	**3.4877**	1.9017	7.1042	1.4571
NE707	putative lipoprotein	**1.3837**	0.9559	1.9004	1.2949
NE708	phi77 ORF003-like protein, phage terminase,large subunit	**3.7043**	0.6105	8.4581	2.0442
NE709	IS1181, transposase	**0.7569**	1.6784	0.8842	-0.2918
NE710	thermonuclease precursor	**0.5095**	0.0426	3.1726	-1.6868
NE711	conserved hypothetical protein	**-0.1696**	0.1352	-0.5159	-0.1283
NE712	conserved hypothetical protein	**-0.9489**	0.3374	-1.6378	-1.5463
NE713	putative transcriptional regulator	**-0.2693**	0.0070	-1.3098	0.4950
NE714	5'-methylthioadenosine/S-adenosylhomocysteine nucleosidase (mntN)	**-1.7391**	-2.0029	-1.6422	-1.5723
NE715	conserved hypothetical protein	**2.4998**	-0.4861	-0.1576	8.1432
NE716	putative membrane protein	**-0.6307**	0.1140	-1.3356	-0.6705
NE717	putative lipoprotein	**2.4179**	-0.4843	7.1668	0.5712
NE718	dihydroxy-acid dehydratase (ilvD)	**-0.1266**	-0.9470	1.5704	-1.0030
NE719	magnesium and cobalt transport protein (corA)	**0.2497**	-0.0422	1.2082	-0.4168
NE720	conserved hypothetical protein	**-0.0767**	-0.9225	0.4896	0.2028
NE721	lytic regulatory protein	**-1.2118**	-1.1244	-0.8732	-1.6379
NE722	phiSLT ORF488-like protein	**-0.3827**	0.4881	-0.3410	-1.2953
NE723	ferric uptake regulation protein (fur)	**2.3510**	6.6687	-0.0122	0.3963
NE724	iron compound ABC transporter, permease protein	**2.1777**	0.3488	7.0199	-0.8357
NE725	putative lipoprotein	**2.7940**	-0.1291	-0.0797	8.5909
NE726	arsenate reductase (arsC)	**-0.0964**	-0.8366	-0.6762	1.2237
NE727	hydrolase, haloacid dehalogenase-like family	**-0.2020**	0.6118	-0.1554	-1.0625
NE728	fibronectin binding protein B (fnbB)	**-1.0545**	-0.9540	-1.4377	-0.7719
NE729	pseudouridine synthase, family 1	**0.4193**	-0.6583	0.6196	1.2967
NE730	acetyltransferase, GNAT family family	**-1.2752**	-1.6475	-0.5486	-1.6296
NE731	putative membrane protein	**-0.0128**	-0.7731	-0.2350	0.9695
NE732	quinol oxidase, subunit I (qoxB)	**-2.3267**	-2.7093	-1.8789	-2.3918
NE733	conserved hypothetical protein	**3.6377**	1.1812	8.5421	1.1897
NE734	ferric hydroxamate receptor	**1.0257**	0.5394	0.3643	2.1734
NE735	conserved hypothetical protein	**0.0583**	0.6849	-0.4378	-0.0723
NE736	magnesium transporter (mgtE)	**2.7954**	0.2340	7.3291	0.8231
NE737	ABC transporter permease protein	**1.0918**	1.3110	0.4311	1.5333

NE738	conserved hypothetical protein	**2.4765**	6.8003	-0.3977	1.0269
NE739	capsular polysaccharide biosynthesis protein Cap5N	**-0.4062**	0.2659	-1.0074	-0.4771
NE740	tRNA pseudouridine synthase B (truB)	**-0.5747**	-0.6725	-0.7252	-0.3263
NE741	oligopeptide ABC transporter, ATP-binding protein	**-0.5706**	-0.9973	0.3116	-1.0260
NE742	sucrose operon repressor (scrR)	**-0.6033**	-0.4811	-1.3477	0.0188
NE743	integral membrane protein LmrP	**0.2903**	-0.7024	1.4613	0.1120
NE744	phosphoribosylaminoimidazole carboxylase, ATPase subunit (purK)	**-1.6512**	-1.9925	-0.6674	-2.2938
NE745	conserved hypothetical protein	**0.6771**	0.9074	0.5381	0.5857
NE746	conserved hypothetical protein	**2.4169**	0.6954	6.5740	-0.0188
NE747	conserved hypothetical protein	**0.6122**	2.2813	-1.4986	1.0539
NE748	phiSLT ORF 104b-like protein	**0.1524**	-0.2649	-1.6289	2.3512
NE749	putative drug transporter	**-0.6188**	0.1513	-0.9612	-1.0464
NE750	phosphoribosylamine--glycine ligase (purD)	**-0.8125**	-0.3587	-2.1089	0.0302
NE751	conserved hypothetical protein	**0.1000**	-0.6852	-1.1739	2.1591
NE752	putative membrane protein	**-1.0384**	-1.3347	-1.6359	-0.1447
NE753	staphylococcal tandem lipoprotein	**-0.7145**	-0.9315	-0.8581	-0.3540
NE754	pyruvate carboxylase (pyc)	**-0.8071**	-0.2810	-0.5481	-1.5921
NE755	transcriptional regulator, GntR family	**-0.0842**	-1.0900	-0.3772	1.2147
NE756	ABC transporter, ATP-binding protein	**-0.3872**	-1.6300	0.2957	0.1727
NE757	antigen, 67 kDa	**0.1710**	-0.3635	0.9796	-0.1029
NE758	putative transport protein SgaT	**3.3595**	0.1840	8.1811	1.7136
NE759	glucokinase (glk)	**1.3419**	0.8940	1.7912	1.3404
NE760	putative competence protein	**1.7300**	0.8827	1.8222	2.4851
NE761	endonuclease III (nth)	**0.1462**	-0.9028	1.7005	-0.3589
NE762	putative membrane protein	**2.4974**	0.0431	7.7279	-0.2789
NE763	conserved hypothetical protein	**-1.0994**	-1.3617	-0.9384	-0.9980
NE764	phiSLT ORF78-like protein	**-1.1112**	-1.8075	-0.0974	-1.4287
NE765	conserved hypothetical protein	**-0.7938**	-1.8961	-0.4444	-0.0407
NE766	intercellular adhesion protein C (icaC)	**-1.5430**	-1.3435	-1.4939	-1.7916
NE767	PTS system, sucrose-specific IIBC component	**3.0909**	-0.0980	8.9053	0.4654
NE768	fructose specific permease (fruA)	**-0.7754**	-1.7648	-0.0149	-0.5466
NE769	cytochrome oxidase assembly protein (ctaA)	**0.0053**	3.2313	-0.9716	-2.2437
NE770	ABC transporter ATP-binding protein	**-0.9507**	-0.4322	-0.6089	-1.8109
NE771	putative transporter protein	**3.4219**	1.7761	9.3895	-0.8999
NE772	ParB-like partition protein	**1.7693**	1.0624	-2.4581	6.7037
NE773	drug transporter	**1.4725**	-0.2862	6.4586	-1.7550
NE774	capsular polysaccharide biosynthesis protein Cap1C	**-0.2401**	0.4760	-0.8521	-0.3443
NE775	ABC transporter permease	**-0.7195**	0.2243	0.9633	-3.3463
NE776	hypothetical protein	**6.1029**	1.2032	9.1463	7.9591
NE777	dethiobiotin synthase (bioD)	**-1.0380**	0.2807	0.3157	-3.7103
NE778	glycerophosphoryl diester phosphodiesterase (glpQ)	**-2.5542**	-6.4983	-0.6089	-0.5555
NE779	hypothetical protein	**0.0427**	2.1401	0.4428	-2.4549
NE780	putative competence protein	**2.2639**	-0.6983	1.7359	5.7540
NE781	multidrug resistance protein B, drug resistance transporter	**-0.1450**	1.0815	-0.4928	-1.0238
NE782	glycine betaine/carnitine/choline ABC transporter (opuCb)	**0.5618**	0.6390	-0.5566	1.6031
NE783	virulence-associated protein E	**-0.2108**	-0.4196	-0.1184	-0.0945
NE784	2-dehydropantoate 2-reductase (panE)	**-0.1129**	-0.3248	-0.2252	0.2112
NE785	putative pyridine nucleotide-disulfide oxidoreductase	**0.6827**	0.7112	0.9426	0.3942
NE786	MerR family transcriptional regulator	**-0.8448**	-0.2940	-0.9065	-1.3337
NE787	hypothetical protein	**-0.2354**	-0.5007	0.6994	-0.9048

NE788	potassium uptake protein (trkA)	**4.3922**	1.8934	2.9647	8.3185
NE789	putative 5'-3' exonuclease	**0.0758**	-0.5202	-0.4133	1.1609
NE790	ABC transporter ATP-binding protein (vga)	**-0.0007**	0.4821	-0.0680	-0.4161
NE791	hypothetical protein	**-0.1626**	-0.4196	-0.0680	0.0000
NE792	putative glycosyl transferase	**0.0369**	-0.8525	0.9633	0.0000
NE793	hypothetical protein	**-1.1918**	-1.0632	-1.2358	-1.2763
NE794	SIS domain protein	**-3.7801**	-7.3627	-2.0540	-1.9236
NE795	hypothetical protein	**0.8176**	1.1612	-0.3581	1.6496
NE796	30S ribosomal protein S20 (rpsT)	**-0.5741**	-0.6303	0.5747	-1.6666
NE797	conserved hypothetical protein	**4.4875**	1.2292	3.2831	8.9503
NE798	ABC transporter ATP-binding protein	**0.5095**	0.5977	0.8566	0.0741
NE799	alanine racemase (alr2)	**-0.6535**	-6.4762	1.7811	2.7346
NE800	putative surface anchored protein	**1.1746**	-0.4810	1.0998	2.9050
NE801	hypothetical protein	**-0.6994**	0.3604	-0.6089	-1.8495
NE802	putative deaminase	**-0.4284**	0.3099	-1.0394	-0.5555
NE803	capsular polysaccharide biosynthesis protein Cap5M	**2.1705**	-1.1103	0.3625	7.2592
NE804	6-phospho-beta-glucosidase (bglA)	**1.8980**	5.6372	0.0567	0.0000
NE805	recombinase A (recA)	**0.4144**	0.1823	0.9971	0.0637
NE806	putative transposase	**-2.7692**	-7.7602	-1.7718	1.2246
NE807	hypothetical protein	**0.3968**	0.1823	0.4225	0.5856
NE808	succinate dehydrogenase iron-sulfur subunit (sdhB)	**-0.3629**	-0.0681	0.0387	-1.0593
NE809	hypothetical protein	**1.8836**	1.2032	3.5442	0.9032
NE810	D-serine/D-alanine/glycine transporter	**-0.5189**	-0.8034	-0.6089	-0.1444
NE811	hypothetical protein	**-1.3912**	-6.4309	1.3860	0.8714
NE812	hypothetical protein	**-0.4401**	-0.7625	0.3919	-0.9497
NE813	high-affinity nickel-transporter (nixA)	**0.4977**	1.6575	-0.4033	0.2389
NE814	FAD/NAD(P)-binding Rossmann fold superfamily protein	**-0.5708**	-0.6872	-0.8637	-0.1614
NE815	capsular polysaccharide biosynthesis protein Cap5K	**2.7302**	0.1589	0.0725	7.9591
NE816	galactose-6-phosphate isomerase subunit LacA	**-0.3403**	-0.3324	-0.1331	-0.5555
NE817	hypothetical protein	**-0.3069**	-0.0076	1.3974	-2.3105
NE818	ABC transporter permease	**-0.6877**	-0.3877	-1.1198	-0.5555
NE819	hypothetical protein	**0.5734**	1.1150	-0.2252	0.8305
NE820	sensor histidine kinase	**-0.5254**	-0.9971	-0.1987	-0.3804
NE821	para-aminobenzoate synthase, glutamine amidotransferase, component II (pabA)	**-0.5058**	0.6656	-0.9065	-1.2763
NE822	RluA family pseudouridine synthase	**-0.8326**	-0.6732	-1.0577	-0.7667
NE823	two-component sensor histidine kinase (vraS)	**0.9402**	0.1136	2.3127	0.3942
NE824	single-strand binding protein	**-0.1388**	-0.5007	1.0858	-1.0014
NE825	putative cell wall surface anchor family protein	**-1.5492**	-0.2684	-1.3279	-3.0513
NE826	capsular polysaccharide biosynthesis protein Cap5H	**-1.2180**	-0.6390	-2.4096	-0.6054
NE827	bifunctional phosphoribosyl-AMP cyclohydrolase/phosphoribosyl-ATP pyrophosphatase protein (hisIE)	**-0.3599**	0.0198	-1.4937	0.3942
NE828	hypothetical protein	**-0.0856**	0.3842	-0.8521	0.2112
NE829	cobalt transport family protein	**-0.1100**	0.4460	2.2345	-3.0104
NE830	hypothetical protein	**0.1944**	-0.6783	-0.0387	1.3003
NE831	aldo/keto reductase family protein	**-0.7811**	0.3142	-2.1018	-0.5555
NE832	ComE operon protein 1	**0.5083**	-0.2624	0.1376	1.6496
NE833	hypothetical protein	**-1.2448**	-0.7933	-0.3112	-2.6300
NE834	cobalt transporter ATP-binding subunit (cbiO)	**-0.1556**	0.5385	-1.0054	0.0000
NE835	fructose 1-phosphate kinase (fruB)	**-0.1353**	0.5006	-0.9065	0.0000
NE836	NLPA lipoprotein	**-0.6300**	-0.8951	1.1542	-2.1492

NE837	putative transcriptional regulator	**-1.8721**	-0.7216	-2.2569	-2.6378
NE838	ribosomal subunit interface protein (yfiA)	**-0.1088**	-0.8811	-1.2431	1.7978
NE839	methicillin-resistance MecR1 regulatory protein	**0.3907**	-0.3841	-0.1601	1.7164
NE840	hypothetical protein	**-1.0578**	-6.2017	1.8672	1.1609
NE841	hypothetical protein	**-0.5850**	0.5506	-0.3861	-1.9194
NE842	hypothetical protein	**0.3779**	0.9234	0.0387	0.1715
NE843	D-3-phosphoglycerate dehydrogenase (serA)	**5.2247**	-1.3016	9.7164	7.2592
NE844	ABC transporter ATP-binding protein	**0.5168**	3.2809	-0.2252	-1.5052
NE845	hypothetical protein	**0.9342**	-0.0225	1.9217	0.9032
NE846	putative monovalent cation/H+ antiporter subunit F	**-0.2691**	0.8549	-0.4875	-1.1748
NE847	carboxyl-terminal protease (ctpA)	**0.0801**	0.2061	1.0622	-1.0280
NE848	hypothetical protein	**-0.8146**	-0.8811	-0.2404	-1.3223
NE849	hypothetical protein	**0.3917**	-1.3956	0.0417	2.5290
NE850	hypothetical protein	**-0.4930**	-0.2257	-0.6979	-0.5555
NE851	hypothetical protein	**1.3721**	3.2908	0.9868	-0.1614
NE852	4-oxalocrotonate tautomerase	**5.5731**	1.7042	1.3368	13.6784
NE853	hypothetical protein	**3.2174**	0.9234	1.4695	7.2592
NE854	membrane spanning protein	**-0.2263**	0.4110	-0.1402	-0.9497
NE855	hypothetical protein	**3.1331**	1.4754	7.9240	0.0000
NE856	alpha,alpha-phosphotrehalase (treC)	**0.3244**	0.0076	-0.1952	1.1609
NE857	nitrite reductase [NAD(P)H], large subunit (nirB)	**0.2177**	0.1705	-1.0226	1.5052
NE858	rod shape-determining protein MreD (mreD)	**-0.5154**	-1.4485	0.1522	-0.2498
NE859	conserved hypothetical protein	**2.8295**	-0.3548	3.0895	5.7540
NE860	phage helicase	**2.4642**	-0.8233	1.2065	7.0094
NE861	aconitate hydratase (acnA)	**0.7138**	0.5628	0.6290	0.9497
NE862	conserved hypothetical protein	**1.5570**	-1.2205	0.1376	5.7540
NE863	30S ribosomal protein S14 (rpsN)	**3.5609**	1.0561	9.2324	0.3942
NE864	putative maltose ABC transporter ATP-binding protein	**4.3470**	1.6717	10.0256	1.3438
NE865	GTP-binding protein LepA	**-0.4110**	1.3075	-0.8842	-1.6563
NE866	AcrB/AcrD/AcrF family protein	**0.9328**	2.9091	0.0404	-0.1511
NE867	tetrapyrrole methylase family protein	**-1.8046**	-2.6221	-2.8905	0.0987
NE868	hypothetical protein	**-4.3805**	-2.9545	-10.3417	0.1546
NE869	iron compound ABC transporter permease	**1.2951**	-2.1536	-3.2742	9.3132
NE870	oligopeptide permease, channel-forming protein (opp-3C)	**0.7180**	3.2415	-1.4250	0.3376
NE871	integrase/recombinase	**0.3147**	1.8977	0.1472	-1.1008
NE872	AraC family transcriptional regulator	**1.8852**	2.8086	2.3542	0.4929
NE873	accessory gene regulator protein C (agrC)	**-1.2659**	-4.4115	-0.0404	0.6542
NE874	hypothetical protein	**3.7979**	3.7571	1.5059	6.1308
NE875	isopropylmalate isomerase large subunit (leuC)	**4.8789**	4.6253	7.3135	2.6980
NE876	hypothetical protein	**1.6409**	3.0016	0.3558	1.5653
NE877	hypothetical protein	**2.3990**	3.8024	1.6464	1.7483
NE878	conserved hypothetical protein	**0.5384**	1.8977	0.4242	-0.7066
NE879	glycine dehydrogenase subunit 1	**-2.5252**	-3.5446	-1.4250	-2.6060
NE880	acetyltransferase	**-2.3648**	-4.0131	-1.4250	-1.6563
NE881	serine protease (htrA)	**-0.4036**	-1.6598	-0.7436	1.1927
NE882	hypothetical protein	**-4.4321**	-3.0342	-0.1377	-10.1245
NE883	tyrosine recombinase xerC	**0.4539**	-1.9430	2.2310	1.0735
NE884	oligopeptide ABC transporter permease	**2.1093**	3.0872	3.3916	-0.1511
NE885	pyruvate ferredoxin oxidoreductase, alpha subunit	**0.0032**	-2.9700	1.8134	1.1661
NE886	threonine synthase (thrC)	**3.4487**	3.3116	2.3144	4.7201
NE887	hypothetical protein	**2.7336**	3.2415	4.9273	0.0319

NE888	uracil-DNA glycosylase (ung)	**1.9824**	-0.2341	2.6040	3.5774
NE889	high affinity proline permease (putP)	**0.0356**	2.2864	-1.7227	-0.4568
NE890	hypothetical protein	**-3.0537**	-4.1784	-3.8151	-1.1676
NE891	sodium transport family protein	**0.8455**	-2.7438	5.6425	-0.3623
NE892	isopropylmalate isomerase small subunit (leuD)	**-3.3032**	-4.6358	-4.3559	-0.9178
NE893	hypothetical protein	**-3.6256**	-2.2333	-8.4925	-0.1511
NE894	tagatose-6-phosphate kinase (lacC)	**1.0706**	3.6094	-1.4250	1.0275
NE895	Orn/Lys/Arg decarboxylase	**-5.7073**	-5.1606	-2.4901	-9.4710
NE896	hypothetical protein	**-3.7916**	-5.7508	-3.4313	-2.1927
NE897	tRNA delta(2)-isopentenylpyrophosphate transferase (miaA)	**-1.5013**	-5.2824	2.2734	-1.4949
NE898	phiSLT ORF387-like protein	**0.5026**	-2.4114	1.5059	2.4135
NE899	hypothetical protein	**2.0873**	2.4407	2.4670	1.3541
NE900	hypothetical protein	**2.3559**	4.0423	2.5710	0.4543
NE901	putative drug transporter	**-0.7116**	2.2864	-1.9659	-2.4553
NE902	phiPVL ORF046-like protein	**-2.1706**	-2.2333	-3.5719	-0.7066
NE903	short chain dehydrogenase/reductase family oxidoreductase	**-4.3363**	-3.8350	-9.4171	0.2431
NE904	putative lipoprotein	**-3.6776**	-2.3643	-7.5679	-1.1008
NE905	hypothetical protein	**-0.7373**	-1.6106	-2.3496	1.7483
NE906	putative transposase	**-1.0342**	-1.3149	0.4242	-2.2118
NE907	hypothetical protein	**-1.8702**	-5.7508	-1.4250	1.5653
NE908	hypothetical protein	**0.6371**	3.3776	-1.4250	-0.0414
NE909	3-dehydroquinate dehydratase (aroD)	**-0.7883**	-3.1198	-0.7436	1.4985
NE910	IS200 family transposase	**1.8236**	3.4993	0.4242	1.5474
NE911	alkyl hydroperoxide reductase subunit C (ahpC)	**1.2745**	-3.4229	6.5670	0.6794
NE912	ATP-dependent Clp protease proteolytic subunit (clpP)	**-1.6228**	-5.3448	-0.5688	1.0454
NE913	deoxyribose-phosphate aldolase (deoC)	**-0.5601**	1.8977	-2.1715	-1.4065
NE914	trigger factor (tig)	**-1.8558**	-4.1492	-0.5004	-0.9178
NE915	BglG family transcriptional antiterminator	**-4.1834**	3.4993	-9.0333	-7.0161
NE916	phosphoglucomutase/phosphomannomutase family protein	**-0.6602**	2.8086	0.7218	-5.5109
NE917	phiSLT ORF204-like protein	**1.9849**	3.2415	0.9650	1.7483
NE918	phi77 ORF006-like protein capsid protein	**-1.2849**	-2.5657	-0.7436	-0.5452
NE919	acetyltransferase	**-1.5823**	4.0779	-1.8088	-7.0161
NE920	hypothetical protein	**-0.8585**	-1.2427	-1.1818	-0.1511
NE921	glutamyl-aminopeptidase	**3.5690**	3.7571	-0.4196	7.3693
NE922	HPCH/HPAI aldolase family protein	**-0.0291**	-1.3149	0.2461	0.9815
NE923	hypothetical protein	**7.6473**	4.1124	7.1079	11.7216
NE924	ribosomal RNA small subunit methyltransferase B (sun)	**0.0786**	-1.7649	0.8079	1.1927
NE925	superantigen-like protein 7	**-3.1204**	-5.2824	-1.7227	-2.3562
NE926	putative lipoprotein	**-4.1470**	4.0423	-7.5679	-8.9155
NE927	hypothetical protein	**-0.9443**	4.8611	-8.4925	0.7986
NE928	putative iron compound ABC transporter iron compound-binding protein	**-1.7510**	-1.1747	4.7179	-8.7963
NE929	PTS system, mannitol specific IIBC component (mtlF)	**0.5715**	4.7093	-1.1274	-1.8675
NE930	ornithine--oxo-acid transaminase (rocD)	**4.0302**	4.5580	9.2985	-1.7660
NE931	ABC transporter permease	**-0.8384**	-2.7874	8.2381	-7.9658
NE932	5' nucleotidase family protein	**2.4387**	5.4152	-0.2414	2.1424
NE933	iron compound ABC transporter iron compound-binding protein	**1.9962**	4.4362	-0.0516	1.6039
NE934	cysteine protease precursor	**2.0590**	0.0835	2.0952	3.9983
NE935	hypothetical protein (cidB)	**0.0267**	-3.4229	1.8896	1.6134
NE936	RNA methyltransferase	**-0.2916**	-1.3149	0.7218	-0.2817

NE937	PfkB family kinase	**-0.7413**	1.3075	-1.4250	-2.1064
NE938	tandem lipoprotein	**-2.9245**	2.8086	-9.7147	-1.8675
NE939	UDP-N-acetylglucosamine 1-carboxyvinyltransferase (murA)	**-0.3336**	3.7571	-2.8905	-1.8675
NE940	phiSLT ORF412-like protein, portal protein	**1.5736**	4.8065	-0.8842	0.7986
NE941	acetyltransferase family protein	**-1.5084**	-1.6349	-0.6785	-2.2118
NE942	glycosyl transferase, group 2 family protein	**1.8032**	4.2709	1.1707	-0.0319
NE943	hypothetical protein	**1.3996**	5.0864	0.4242	-1.3120
NE944	5-methyltetrahydropteroyltriglutamate-- homocysteine S-methyltransferase (metE)	**-0.0898**	-1.9113	2.1873	-0.5452
NE945	branched-chain amino acid transport system II carrier protein (brnQ)	**-1.9354**	-3.8350	-0.5993	-1.3718
NE946	CsbD-like superfamily protein	**1.3215**	-0.0835	2.4305	1.6177
NE947	hypothetical protein	**0.3161**	-1.4325	2.4305	-0.0495
NE948	hypothetical protein	**-0.1706**	-2.8099	1.3898	0.9083
NE949	type I restriction-modification system, M subunit (hsdM)	**-0.1433**	1.3075	-1.4250	-0.3125
NE950	phosphoribosylaminoimidazole-succinocarboxamide synthase	**-0.3272**	2.5768	-1.4250	-2.1335
NE951	putative abrB protein	**-0.8776**	-5.2824	0.4242	2.2255
NE952	gluconate permease (gntP)	**4.9178**	3.4993	7.7893	3.4647
NE953	hypothetical protein	**-3.1735**	2.1083	-9.4171	-2.2118
NE954	hypothetical protein	**2.4345**	-3.0342	8.1393	2.1984
NE955	respiratory nitrate reductase, gamma subunit (narI)	**-0.2006**	-1.5181	1.4032	-0.4869
NE956	CBS domain-containing protein	**1.9436**	3.8024	1.9964	0.0319
NE957	NADH-dependent FMN reductase	**2.0292**	-1.4745	3.3364	4.2258
NE958	two-component response regulator	**3.1395**	4.5580	2.0397	2.8207
NE959	exonuclease SbcD	**3.4538**	4.3287	3.2788	2.7539
NE960	alpha/beta fold family hydrolase	**3.1188**	3.7100	2.3929	3.2535
NE961	glycine betaine/carnitine/choline ABC transporter (opuCc)	**1.6697**	1.4096	2.1304	1.4689
NE962	GGDEF domain-containing protein	**-1.6759**	-1.6231	-1.6991	-1.7056
NE963	hypothetical protein	**-0.6194**	-0.5880	-1.5120	0.2418
NE964	4'-phosphopantetheinyl transferase superfamily protein	**-2.0335**	-3.3785	-2.3664	-0.3556
NE965	NAD(P)H-dependent glycerol-3-phosphate dehydrogenase (gpsA)	**-1.9792**	-3.2411	-1.5753	-1.1213
NE966	hypothetical protein	**-1.5412**	-2.3468	-1.1893	-1.0874
NE967	Na+/H+ antiporter family protein	**-0.9664**	-1.3888	-0.3502	-1.1602
NE968	hypothetical protein	**-0.5069**	-1.0674	-0.7274	0.2741
NE969	sodium:solute symporter family protein	**-0.5822**	-1.1471	-0.2018	-0.3977
NE970	M23/M37 peptidase domain protein	**1.3118**	1.3494	2.2426	0.3434
NE971	amino acid/peptide transporter (Peptide:H+ symporter)	**-0.3227**	0.4750	-0.3766	-1.0664
NE972	ATP-dependent DNA helicase RecQ	**0.9566**	1.8599	0.0023	1.0074
NE973	putative staphyloxanthin biosynthesis protein	**0.0086**	0.0887	-0.1207	0.0577
NE974	DNA mismatch repair protein mutS	**-0.1913**	0.4125	-0.7166	-0.2697
NE975	accessory secretory protein Asp2	**-0.4400**	-0.0859	-0.6443	-0.5898
NE976	Chaperone clpB	**-1.3585**	-2.3367	-0.7427	-0.9962
NE977	putative ABC transporter, ATP-binding protein	**-0.8121**	-0.9615	-1.6236	0.1487
NE978	dihydroorotate dehydrogenase (pyrD)	**-1.9840**	-2.2413	-2.6182	-1.0924
NE979	sugar efflux transporter	**-1.6290**	-2.1866	-1.3696	-1.3307
NE980	putative zinc-binding dehydrogenase	**-0.4175**	-1.5448	0.3950	-0.1027
NE981	aminotransferase, class I	**-1.3351**	-2.9269	-0.2055	-0.8728
NE982	type I restriction-modification enzyme, S subunit (hsdS)	**0.5207**	0.0658	0.2080	1.2883
NE983	glucose 1-dehydrogenase-like protein	**-0.6219**	-0.1565	-0.9843	-0.7250

NE984	hypothetical protein	**-0.0511**	-0.6249	0.1058	0.3657
NE985	hypothetical protein	**0.5891**	0.4750	0.8380	0.4544
NE986	hypothetical protein	**-0.1305**	0.2451	-0.4276	-0.2089
NE987	secretory antigen precursor SsaA	**-0.0913**	0.3923	-0.8750	0.2089
NE988	hypothetical protein	**-0.3830**	-0.5332	-0.2107	-0.4052
NE989	hypothetical protein	**-1.4482**	-3.7656	-0.8056	0.2266
NE990	hypothetical protein	**-1.6067**	-1.6246	-2.5528	-0.6428
NE991	uroporphyrin-III C-methyl transferase	**-1.8862**	-2.4835	-2.0840	-1.0912
NE992	PTS system, sorbitol-specific IIC component	**-0.7589**	-1.7236	-0.2452	-0.3078
NE993	putative hemolysin III	**-1.2636**	-2.3468	-0.7471	-0.6968
NE994	hypothetical protein	**-0.9742**	-2.1961	-0.4659	-0.2606
NE995	preprotein translocase subunit YajC	**-1.0587**	-3.6421	0.1068	0.3590
NE996	putative transport protein	**-0.0658**	-0.4772	0.2005	0.0792
NE997	HemK family modification methylase	**0.9941**	1.0652	1.0436	0.8735
NE998	HAD superfamily hydrolase	**0.7208**	0.6789	0.3312	1.1524
NE999	6-carboxyhexanoate--CoA ligase	**1.3999**	3.3255	-0.3934	1.2677
NE1000	putative monovalent cation/H+ antiporter subunit C	**-0.7399**	-1.8454	0.9400	-1.3143
NE1001	GntR family transcriptional regulator	**-0.3137**	-1.5495	0.3981	0.2103
NE1002	superantigen-like protein (set7)	**-0.8609**	-0.7724	-0.2606	-1.5498
NE1003	malate:quinone oxidoreductase (mqo)	**-0.7495**	-2.0636	0.1474	-0.3324
NE1004	hypothetical protein	**0.5889**	1.4452	0.4570	-0.1356
NE1005	hypothetical protein	**-0.2909**	-0.0775	-0.3045	-0.4906
NE1006	hypothetical protein	**0.2805**	-1.4685	2.3719	-0.0620
NE1007	putative proline/betaine transporter	**0.3614**	-0.7207	1.5424	0.2625
NE1008	L-serine dehydratase, iron-sulfur-dependent, beta subunit (sdaAB)	**-0.7451**	-1.6805	0.2358	-0.7907
NE1009	hypothetical protein	**-0.1109**	-0.1152	-0.4905	0.2729
NE1010	hypothetical protein	**0.6071**	1.1473	-0.1334	0.8073
NE1011	hypothetical protein	**-0.0388**	0.0476	-0.6605	0.4966
NE1012	exonuclease RexB	**-0.5205**	0.3615	-0.5071	-1.4159
NE1013	hypothetical protein	**-0.2461**	-0.8162	0.4440	-0.3660
NE1014	putative lipoprotein	**0.0540**	0.8284	-0.4834	-0.1831
NE1015	formate/nitrite transporter family protein	**-0.6105**	-0.5397	-0.4329	-0.8588
NE1016	acetyltransferase	**0.5743**	0.4337	0.3888	0.9005
NE1017	hypothetical protein	**-0.5868**	-0.9098	-0.2523	-0.5984
NE1018	hypothetical protein	**0.8873**	0.5342	1.4642	0.6636
NE1019	lantibiotic epidermin leader peptide processing serine protease EpiP	**0.3056**	-1.0674	2.1099	-0.1258
NE1020	conserved hypothetical protein	**0.1112**	-1.3252	0.9395	0.7194
NE1021	capsular polysaccharide biosynthesis protein Cap5F	**0.5254**	1.6818	0.0433	-0.1488
NE1022	fmt protein	**-0.9699**	1.2758	-4.1818	-0.0038
NE1023	phosphoenolpyruvate-protein phosphotransferase (ptsI)	**0.3071**	1.4839	-0.5664	0.0038
NE1024	phiSLT ORF 563-like protein, terminase, large subunit	**0.1302**	0.6957	0.0237	-0.3288
NE1025	integral membrane protein	**0.1915**	-0.1601	-0.0708	0.8054
NE1026	hypothetical protein	**0.0255**	-0.1620	0.9107	-0.6721
NE1027	phiSLT ORF153-like protein	**-0.8326**	-0.9033	0.0071	-1.6017
NE1028	endonuclease IV	**0.1376**	0.1467	0.3175	-0.0513
NE1029	conserved hypothetical protein	**-0.1535**	-0.0476	0.3915	-0.8043
NE1030	RarD protein	**0.1615**	0.1864	0.2473	0.0507
NE1031	IucC family siderophore biosynthesis protein (sbnC(	**-0.0206**	-0.9839	0.3940	0.5281
NE1032	cell wall surface anchor family protein	**-0.1510**	-1.0853	0.5039	0.1284

NE1033	putative membrane protein	**0.7152**	1.5929	0.9797	-0.4269
NE1034	multi drug resistance protein (norA)	**0.6384**	0.5109	1.2753	0.1289
NE1035	secretory antigen precursor SsaA	**0.6173**	0.6111	0.7322	0.5087
NE1036	putative AMP-binding enzyme	**0.2961**	0.0740	1.3421	-0.5277
NE1037	N-acetylmannosamine-6-phosphate 2-epimerase	**1.4367**	0.7287	3.2880	0.2935
NE1038	histidinol-phosphate aminotransferase hisC	**1.6595**	0.1553	1.4891	3.3342
NE1039	hypothetical protein	**-0.1679**	0.6444	-0.0023	-1.1457
NE1040	A/G-specific adenine glycosylase (mutY)	**1.6789**	3.0664	1.2669	0.7034
NE1041	putative drug transporter	**0.2955**	0.6518	0.4380	-0.2033
NE1042	hypothetical protein	**0.2370**	0.1583	1.1351	-0.5822
NE1043	hypothetical protein	**0.7003**	0.3909	1.4508	0.2592
NE1044	hypothetical protein	**0.8644**	-0.5686	2.7407	0.4211
NE1045	hypothetical protein	**5.4041**	7.5797	6.7559	1.8767
NE1046	formate dehydrogenase accessory protein (fdhD)	**3.0090**	7.4565	-0.0473	1.6178
NE1047	ornithine carbamoyltransferase (arcB)	**0.1035**	0.4494	-0.7092	0.5704
NE1048	uracil permease (pyrP)	**-1.0655**	-0.3463	-2.7754	-0.0747
NE1049	F0F1 ATP synthase subunit beta (atpD)	**0.2514**	0.3866	-0.1627	0.5304
NE1050	acetoin reductase	**0.6578**	1.0352	0.2607	0.6775
NE1051	hypothetical protein	**0.7074**	1.9136	-0.2474	0.4560
NE1052	peptide ABC transporter permease	**0.8193**	1.7644	-0.3483	1.0419
NE1053	putative sensor histidine kinase	**1.4318**	3.4477	-1.0432	1.8909
NE1054	hypothetical protein	**0.9250**	2.4052	0.3102	0.0597
NE1055	teichoic acid biosynthesis protein X (tagX)	**0.9858**	2.1287	0.6222	0.2066
NE1056	hypothetical protein	**3.4002**	8.0351	1.4809	0.6847
NE1057	hypothetical protein	**2.3732**	8.1311	-0.6871	-0.3245
NE1058	acetyltransferase	**1.7647**	3.9793	0.3191	0.9959
NE1059	hypothetical protein	**5.2096**	3.9489	11.6462	0.0338
NE1060	U32 family peptidase	**0.3515**	0.6011	-0.3427	0.7962
NE1061	inositol monophosphatase family protein	**0.4234**	1.2089	-0.3758	0.4372
NE1062	tandem lipoprotein	**-0.5401**	-2.2230	0.1590	0.4436
NE1063	chorismate-binding domain-containing protein	**-0.5471**	-1.1035	-0.7914	0.2536
NE1064	TetR family transcriptional regulator	**-0.3215**	-0.4399	0.1638	-0.6884
NE1065	osmoprotectant ABC transporter permease	**-0.2168**	-1.1035	-0.2775	0.7306
NE1066	MarR family transcriptional regulator	**-0.4220**	-0.9973	0.5721	-0.8408
NE1067	hypothetical protein	**1.0890**	1.6337	-0.0819	1.7152
NE1068	citrate transporter, permease	**0.1734**	2.2675	-1.6582	-0.0892
NE1069	ornithine aminotransferase (rocD)	**0.8250**	2.6563	-0.3178	0.1366
NE1070	putative oxidoreductase	**0.8235**	1.7656	0.5416	0.1631
NE1071	NAD-dependent epimerase/dehydratase family protein	**-0.4599**	0.1274	-0.9848	-0.5223
NE1072	cobalamin synthesis protein/P47K family protein	**-1.1974**	-2.4725	-0.8765	-0.2433
NE1073	hypothetical protein	**-1.0726**	-2.1120	-0.5645	-0.5412
NE1074	oligopeptide ABC transporter permease (oppB)	**-0.5522**	-1.6859	-0.3052	0.3345
NE1075	cell wall surface anchor family protein	**-1.0024**	-1.9762	-0.6606	-0.3704
NE1076	hypothetical protein	**-0.4666**	-1.2771	-0.5147	0.3920
NE1077	ribokinase (rbsK)	**-0.7619**	-2.2131	-0.3199	0.2472
NE1078	hypothetical protein	**0.4558**	-0.1903	0.2658	1.2920
NE1079	S1 RNA-binding domain-containing protein	**-0.0830**	-1.0393	0.8449	-0.0546
NE1080	lantibiotic epidermin immunity protein F (epiF)	**-0.2091**	-0.4784	-1.0243	0.8755
NE1081	alkaline phosphatase (phoB)	**0.2200**	0.7404	-0.0813	0.0009
NE1082	hypothetical protein	**0.5211**	2.7780	-0.7181	-0.4967
NE1083	spermidine/putrescine ABC transporter permease (potC)	**0.3864**	1.8768	-0.0019	-0.7158

NE1084	hypothetical protein	**-1.0516**	-0.8612	-1.4420	-0.8515
NE1085	segregation and condensation protein B (scpB)	**-0.6600**	-0.3486	-1.2436	-0.3877
NE1086	glutamate-1-semialdehyde aminotransferase (hemL)	**-1.0020**	-0.3071	-1.3861	-1.3128
NE1087	CamS sex pheromone cAM373	**-0.7233**	-1.1610	-0.7709	-0.2378
NE1088	conserved hypothetical protein	**-1.5866**	-1.1035	-1.3147	-2.3416
NE1089	response regulator protein	**-2.2444**	-2.0473	-2.0589	-2.6269
NE1090	adenosylmethionine-8-amino-7-oxononanoate transaminase (bioA)	**-0.4688**	-0.3071	-0.0125	-1.0866
NE1091	hypothetical protein	**-0.6248**	-1.2771	0.2603	-0.8575
NE1092	putative acyl-CoA acetyltransferase FadA	**-0.7397**	-0.7196	-1.4097	-0.0897
NE1093	hypothetical protein	**1.3313**	3.1429	1.1945	-0.3437
NE1094	phiSLT ORF 99-like protein	**0.9988**	2.4782	0.6197	-0.1015
NE1095	aldehyde dehydrogenase (aldA2)	**0.1281**	0.8596	-0.2861	-0.1892
NE1096	conserved hypothetical protein	**-0.0165**	0.2300	-0.2785	-0.0009
NE1097	manganese transport protein MntH	**0.2431**	-0.1821	0.5374	0.3740
NE1098	serine protease SplC	**-0.4266**	0.2403	-1.3928	-0.1275
NE1099	hypothetical protein	**-3.3739**	-7.8306	-2.1218	-0.1692
NE1100	glutamate synthase subunit beta (gltD)	**-0.5137**	-0.5288	-0.6804	-0.3317
NE1101	phosphoribosylaminoimidazole synthetase (purM)	**0.5968**	0.7404	0.8599	0.1901
NE1102	iron transport associated domain-containing protein	**-0.1314**	-0.5288	0.0019	0.1327
NE1103	2-isopropylmalate synthase (leuA)	**-0.8299**	-1.9199	-0.0571	-0.5128
NE1104	haloacid dehalogenase-like hydrolase	**-0.4534**	-0.3507	-0.7753	-0.2342
NE1105	ABC transporter protein	**1.5210**	3.1785	1.2773	0.1073
NE1106	hypothetical protein	**1.4726**	2.3239	1.9455	0.1484
NE1107	competence/damage-inducible protein cinA	**0.1870**	0.9511	0.2691	-0.6592
NE1108	hypothetical protein	**0.1544**	0.0981	0.3077	0.0572
NE1109	RNA polymerase sigma factor SigB	**-0.1937**	0.0401	-0.4853	-0.1361
NE1110	hypothetical protein	**-0.2367**	-0.3436	-0.9501	0.5836
NE1111	hypothetical protein	**-0.4985**	-0.5980	-0.9316	0.0342
NE1112	hypothetical protein	**-0.3213**	-0.6506	-0.5134	0.2000
NE1113	urease accessory protein UreG	**0.6103**	0.4081	0.6756	0.7473
NE1114	perfringolysin O regulator protein	**0.0938**	-0.2177	0.8179	-0.3189
NE1115	transporter protein	**-0.3358**	-1.9944	0.7947	0.1922
NE1116	nisin susceptibility-associated sensor histidine kinase (nsaS)	**-0.1250**	0.8947	-1.0426	-0.2272
NE1117	hypothetical protein	**0.9762**	2.6563	0.4583	-0.1859
NE1118	tetrahydrodipicolinate acetyltransferase (dapD)	**0.1885**	0.9982	0.0062	-0.4388
NE1119	hypothetical protein	**-0.1136**	0.9257	-0.3420	-0.9244
NE1120	phiSLT ORF129-like protein	**0.3421**	0.8273	0.6828	-0.4839
NE1121	conserved hypothetical protein	**-0.0732**	0.3912	0.0624	-0.6733
NE1122	carboxylesterase (est)	**-0.3555**	-0.5171	0.2398	-0.7893
NE1123	phiSLT ORF257-like protein, putative prophage protease	**-0.3615**	-0.0248	-0.1739	-0.8858
NE1124	gluconate kinase (gntK)	**-0.3206**	0.2652	-0.6004	-0.6265
NE1125	arginine/oirnithine antiporter (arcD)	**0.1807**	-0.1350	0.8496	-0.1726
NE1126	hypothetical protein	**-0.1583**	-0.8749	0.5456	-0.1457
NE1127	tandem lipoprotein	**-0.3175**	-0.8957	0.6608	-0.7175
NE1128	Hsp33-like chaperonin (hslO)	**0.4507**	0.2300	0.4202	0.7018
NE1129	hypothetical protein	**1.8315**	3.3415	1.7296	0.4234
NE1130	hypothetical protein	**0.9188**	1.4332	1.0756	0.2477
NE1131	amino acid permease	**0.7010**	-0.0604	1.8097	0.3537
NE1132	intercellular adhesion operon transcription regulator (tetR)	**0.4272**	0.6780	0.3605	0.2431
NE1133	putative ferrichrome ABC transporter	**0.6112**	-0.0604	1.8139	0.0802

NE1134	phosphoribosylformylglycinamidine synthase (purS)	**0.0729**	-0.3507	0.6795	-0.1102
NE1135	glycine betaine transporter opuD	**0.4147**	-0.0142	0.8588	0.3996
NE1136	alanine dehydrogenase (ald)	**0.1570**	0.0142	0.9866	-0.5298
NE1137	glycine betaine transporter	**1.7953**	0.4741	3.2234	1.6886
NE1138	NAD dependent epimerase/dehydratase family protein	**1.2387**	-0.1304	2.0225	1.8240
NE1139	putative monovalent cation/H+ antiporter subunit D	**0.4073**	-0.0949	1.4083	-0.0914
NE1140	diaminopimelate decarboxylase (lysA)	**1.0561**	1.0308	1.2953	0.8423
NE1141	putative serine protease HtrA	**5.0706**	12.7557	3.1740	-0.7179
NE1142	RpiR family phosphosugar-binding transcriptional regulator	**1.1705**	3.5368	-0.0548	0.0295
NE1143	hypothetical protein	**0.3026**	0.3156	0.1885	0.4036
NE1144	aspartate semialdehyde dehydrogenase (asd)	**0.4172**	0.6659	0.1961	0.3895
NE1145	hypothetical protein	**-0.0020**	-0.3267	-0.3722	0.6930
NE1146	hypothetical protein	**0.0868**	-0.1529	-0.2561	0.6693
NE1147	alcohol dehydrogenase, zinc-containing	**1.3977**	3.5622	-0.2834	0.9144
NE1148	cobalt transporter ATP-binding subunit (cbiO)	**0.5377**	1.0827	0.0888	0.4414
NE1149	indole-3-pyruvate decarboxylase (ipdC)	**0.7795**	0.6659	0.5970	1.0756
NE1150	hypothetical protein	**1.1586**	1.4667	-0.0612	2.0703
NE1151	dehydrogenase family protein	**1.5432**	3.1429	0.0526	1.4340
NE1152	respiratory nitrate reductase, beta subunit (narH)	**-1.4945**	-4.9125	-0.9537	1.3826
NE1153	hypothetical protein	**1.2245**	0.9278	1.3511	1.3947
NE1154	sugar phosphate antiporter (uhpT)	**-0.1401**	0.0000	-0.2503	-0.1700
NE1155	hypothetical protein	**-0.4571**	-0.1926	-0.5790	-0.5996
NE1156	type I restriction-modification system, M subunit (hsdM)	**0.4254**	0.5044	0.8138	-0.0422
NE1157	sensor histidine kinase	**-0.7805**	-0.3083	-0.0381	-1.9951
NE1158	redox-sensing transcriptional repressor Rex	**-0.2503**	0.0902	-0.8082	-0.0328
NE1159	spermidine/putrescine ABC transporter ATP-binding protein (potA)	**0.4411**	2.3692	-0.1341	-0.9117
NE1160	tandem lipoprotein	**-4.3583**	-3.3171	-4.0139	-5.7438
NE1161	integral membrane protein	**-5.3837**	-4.4185	-4.7367	-6.9957
NE1162	hypothetical protein	**-1.5799**	-1.2092	-0.7195	-2.8110
NE1163	pyridine nucleotide-disulfide oxidoreductase	**0.0306**	0.3110	0.1091	-0.3281
NE1164	hypothetical protein	**-5.1053**	-3.8148	-4.6310	-6.8702
NE1165	hypothetical protein	**0.1006**	0.6454	-0.4900	0.1464
NE1166	acetolactate synthase large subunit (ilvB)	**-0.0472**	-0.4375	-0.4099	0.7056
NE1167	intercellular adhesion protein B (icaB)	**-0.5246**	-0.7354	-0.7288	-0.1095
NE1168	ABC transporter ATP-binding protein	**0.6734**	0.6737	1.0681	0.2785
NE1169	oligoendopeptidase F (pepF)	**-0.7233**	-0.0383	-1.2304	-0.9011
NE1170	putative translaldolase	**-0.3341**	-0.0827	-0.6474	-0.2723
NE1171	hypothetical protein	**0.0373**	0.2044	0.3345	-0.4270
NE1172	iron/heme permease	**-4.5363**	-3.6096	-4.0826	-5.9166
NE1173	hypothetical protein	**-1.6505**	-2.6507	0.6095	-2.9101
NE1174	oligopeptide permease, peptide-binding protein (opp-1A)	**-0.1521**	-0.4864	-0.2813	0.3115
NE1175	hypothetical protein	**-0.0781**	0.0000	-0.3905	0.1562
NE1176	DNA repair protein RadA	**-4.0909**	-2.7027	-4.2539	-5.3161
NE1177	ketol-acid reductoisomerase (ilvC)	**0.6455**	0.7229	1.0659	0.1479
NE1178	mannose-6-phosphate isomerase (manA)	**3.4435**	0.9012	0.3535	9.0759
NE1179	methionine sulfoxide reductase A (msrA)	**-0.1777**	0.7009	-0.6252	-0.6088
NE1180	hypothetical protein	**0.9967**	0.3433	0.5027	2.1440
NE1181	putative staphylocoagulase	**-0.9633**	-0.4735	-0.8828	-1.5337
NE1182	hypothetical protein	**-0.2797**	-0.6476	-0.7281	0.5366
NE1183	sensor histidine kinase protein (arlS)	**-1.0227**	-0.9306	-1.3331	-0.8045

NE1184	putative drug transporter	**-0.6446**	-0.4264	0.1354	-1.6428
NE1185	MerR family transcriptional regulator	**-0.7445**	-0.6431	0.3456	-1.9362
NE1186	putative cobalt ABC transporter ATP-binding protein	**0.0587**	0.0109	0.3456	-0.1803
NE1187	hypothetical protein	**-0.1248**	0.2900	0.2946	-0.9590
NE1188	putative membrane protein	**-2.0570**	-1.4770	-1.8936	-2.8004
NE1189	MarR family transcriptional regulator	**1.1021**	-0.0678	1.2766	2.0976
NE1190	putative N-acetylmuramoyl-L-alanine amidase	**-1.4371**	-1.4344	-1.3149	-1.5620
NE1191	heat shock protein	**-0.4136**	0.1280	-1.5311	0.1623
NE1192	PfkB family carbohydrate kinase	**-0.6678**	-0.2717	-1.7187	-0.0130
NE1193	accessory regulator A (sarA)	**-3.2235**	-2.1502	-2.9804	-4.5400
NE1194	superantigen-like protein	**-0.2351**	-0.3889	-0.5088	0.1923
NE1195	phiSLT ORF110-like protein	**0.0905**	0.4388	0.0381	-0.2054
NE1196	glycine betaine aldehyde dehydrogenase (betB)	**-2.0566**	-1.4180	-2.2566	-2.4952
NE1197	cobalt transport family protein	**-0.2128**	-0.4909	-0.1606	0.0130
NE1198	pyridoxal-phosphate dependent enzyme superfamily protein	**-1.0763**	-1.0086	-0.5657	-1.6547
NE1199	Oye family NADH-dependent flavin oxidoreductase	**0.8834**	-0.0976	0.7294	2.0186
NE1200	bifunctional homocysteine S-methyltransferase/5,10-methylenetetrahydrofolate reductase protein	**0.1810**	0.4388	0.1334	-0.0293
NE1201	hypothetical protein	**0.4187**	0.1114	1.1056	0.0391
NE1202	hypothetical protein	**0.6167**	0.0241	0.9374	0.8886
NE1203	hypothetical protein	**0.2431**	-0.4655	0.7294	0.4656
NE1204	antibiotic transport-associated protein-like protein	**0.9015**	0.1293	0.7442	1.8311
NE1205	anaerobic ribonucleotide reductase, small subunit (nrdG)	**-2.5026**	-1.8262	-2.4820	-3.1996
NE1206	hypothetical protein	**1.0117**	0.8662	-0.3478	2.5166
NE1207	serine protease SplB	**0.7417**	0.9199	-0.2129	1.5182
NE1208	hypothetical protein	**-0.2657**	-0.4079	0.1675	-0.5568
NE1209	oligopeptide ABC transporter, permease protein	**-0.3398**	-0.3667	0.4597	-1.1123
NE1210	hypothetical protein	**-0.0006**	-0.8984	-0.0885	0.9850
NE1211	tandem lipoprotein	**-0.1555**	-0.1072	0.3456	-0.7050
NE1212	excinuclease ABC subunit C (uvrC)	**1.0709**	0.3208	2.3143	0.5775
NE1213	putative lipoprotein	**0.6929**	0.7637	0.8641	0.4509
NE1214	Na+/H+ antiporter family protein	**-0.5295**	-0.7593	-0.1753	-0.6538
NE1215	N-(5'-phosphoribosyl)anthranilate isomerase (trpF)	**-0.3312**	-0.5259	-0.4384	-0.0293
NE1216	TetR family transcriptional regulator	**0.6696**	0.0339	0.1801	1.7948
NE1217	alpha-acetolactate decarboxylase (budA)	**-0.3821**	-0.6345	0.2143	-0.7263
NE1218	TENA/THI-4 family protein	**-0.0920**	-0.9719	-0.7625	1.4583
NE1219	putative ATP-dependent Clp proteinase	**-0.8404**	-0.5273	-0.8886	-1.1053
NE1220	hypothetical protein	**0.1170**	0.2235	-0.3810	0.5086
NE1221	chaperone protein HchA	**-0.7403**	0.4209	-1.7745	-0.8674
NE1222	succinyl-diaminopimelate desuccinylase	**0.2546**	1.3303	-0.6540	0.0876
NE1223	hypothetical protein	**1.1171**	1.7963	0.6241	0.9308
NE1224	Fe/Mn family superoxide dismutase	**0.9304**	0.4622	1.1347	1.1943
NE1225	hypothetical protein	**0.3548**	0.2717	-0.1222	0.9151
NE1226	hypothetical protein	**-0.4609**	-0.4823	-0.8222	-0.0783
NE1227	acetyl-CoA c-acetyltransferase (vraB)	**0.0861**	0.1346	-0.3966	0.5202
NE1228	hypothetical protein	**-0.0749**	-0.4864	0.4575	-0.1960
NE1229	ABC transporter permease	**-5.7198**	-3.4466	-6.7136	-6.9992
NE1230	hypothetical protein	**0.4119**	0.2116	0.5586	0.4656
NE1231	hypothetical protein	**-0.1087**	-0.1054	0.0539	-0.2745
NE1232	imidazole glycerol phosphate synthase subunit HisF	**0.2638**	-0.6476	0.2971	1.1420
NE1233	arginine repressor (argR)	**2.2204**	2.2186	2.1525	2.2901

NE1234	L-lactate permease (lctP)	**1.2775**	1.1413	1.5826	1.1085
NE1235	capsular polysaccharide biosynthesis protein Cap5E	**0.8777**	0.5737	1.4379	0.6216
NE1236	glyoxalase family protein	**0.9633**	0.8094	0.8725	1.2080
NE1237	pur operon repressor (purR)	**1.0815**	0.3308	2.0503	0.8634
NE1238	conserved hypothetical protein	**0.4867**	0.4660	0.3640	0.6302
NE1239	hypothetical protein	**0.5455**	-0.6147	0.3383	1.9127
NE1240	leukotoxin LukD	**2.0141**	1.0124	3.3747	1.6553
NE1241	thermonuclease (nuc)	**-1.7051**	-0.6762	-2.2912	-2.1479
NE1242	phiSLT ORF527-like protein	**2.1535**	2.2551	1.8308	2.3746
NE1243	phiSLT ORF123-like protein	**0.9690**	0.4316	1.4679	1.0075
NE1244	ribosomal large subunit pseudouridine synthase B (rluB)	**-0.2757**	0.0314	-0.1275	-0.7310
NE1245	hypothetical protein	**1.3389**	1.3807	0.9726	1.6635
NE1246	hypothetical protein	**1.8112**	1.1488	1.9896	2.2952
NE1247	hypothetical protein	**2.2761**	2.0677	2.5416	2.2190
NE1248	phi77 ORF017-like protein	**2.1334**	1.7619	2.0030	2.6353
NE1249	DNA-binding response regulator, KdpE	**-0.9883**	-1.5651	-1.1363	-0.2636
NE1250	aldehyde dehydrogenase family protein	**0.3192**	0.1909	-0.5159	1.2825
NE1251	3-methyl-2-oxobutanoate hydroxymethyltransferase (panB)	**0.3695**	0.3508	1.1518	-0.3942
NE1252	phosphonate ABC transporter ATP-binding protein (phnC)	**-1.9582**	-1.4646	-1.2996	-3.1106
NE1253	N-acetylmuramic acid-6-phosphate etherase (murQ)	**0.4047**	-0.6486	-0.0021	1.8647
NE1254	perfringolysin O regulator protein (pfoR)	**-1.2023**	-1.0712	-0.7978	-1.7380
NE1255	enterotoxin K (sek)	**-0.5870**	0.0026	-0.6407	-1.1229
NE1256	hypothetical protein	**-0.9954**	-0.4584	-0.6772	-1.8504
NE1257	lipoate-protein ligase A family protein	**2.9573**	0.6553	0.4721	7.7445
NE1258	putative restriction/modification system specificity protein	**0.3178**	1.6854	0.6677	-1.3998
NE1259	hypothetical protein	**1.8133**	1.0027	2.0171	2.4202
NE1260	phosphoenolpyruvate carboxykinase (pckA)	**3.6048**	1.8414	1.9163	7.0565
NE1261	truncated beta-hemolysin	**-0.5754**	-1.6752	-0.3220	0.2710
NE1262	hypothetical protein	**-2.1432**	-2.4065	-1.1989	-2.8243
NE1263	mannitol-1-phosphate 5-dehydrogenase (mtlD)	**-0.9066**	-1.0784	-0.5473	-1.0940
NE1264	glutamyl-aminopeptidase	**-1.9154**	-1.5519	-1.5006	-2.6938
NE1265	glyoxalase family protein	**0.6896**	0.0066	0.3071	1.7550
NE1266	histidinol dehydrogenase (hisD)	**0.2424**	1.3848	0.3624	-1.0200
NE1267	hypothetical protein	**-0.0765**	-0.6100	0.4509	-0.0703
NE1268	hypothetical protein	**-1.3522**	-0.7237	-1.3871	-1.9458
NE1269	OsmC/Ohr family protein	**1.1270**	0.4253	0.9653	1.9905
NE1270	hypothetical protein	**6.2021**	6.9260	2.4308	9.2497
NE1271	hypothetical protein	**1.6654**	0.5503	1.5547	2.8912
NE1272	hypothetical protein	**0.1300**	-1.3332	0.7398	0.9835
NE1273	prephenate dehydrogenase	**-1.3126**	-2.0010	-0.9168	-1.0200
NE1274	phosphate ABC transporter permease PstA	**0.6886**	-0.3187	0.9495	1.4349
NE1275	hypothetical protein	**-0.7084**	-0.3083	-0.0788	-1.7380
NE1276	bifunctional 3-deoxy-7-phosphoheptulonate synthase/chorismate mutase	**-2.5067**	-1.2865	-3.1349	-3.0988
NE1277	hypothetical protein	**-0.1756**	-0.4543	-0.0021	-0.0703
NE1278	staphopain A	**-0.1080**	0.0366	-0.4274	0.0668
NE1279	nitrite reductase [NAD(P)H], small subunit (nirD)	**-0.8075**	0.2874	-0.8376	-1.8722
NE1280	ABC transporter, substrate-binding protein	**0.1011**	-0.2633	0.7439	-0.1774
NE1281	hypothetical protein	**0.9613**	0.6958	0.1504	2.0377
NE1282	PTS system, IIA component	**3.4884**	1.9463	0.5735	7.9453
NE1283	putative transposase	**-0.1684**	0.1727	0.2719	-0.9497

NE1284	hypothetical protein	**0.7461**	0.3975	-0.2046	2.0454
NE1285	hypothetical protein	**-0.7058**	-1.4750	-0.9549	0.3126
NE1286	capsular polysaccharide biosynthesis protein Cap1A	**2.7466**	-0.8440	-0.5546	9.6382
NE1287	cardiolipin synthetase	**2.0756**	0.5730	0.7948	4.8589
NE1288	hypothetical protein	**-0.7066**	3.2665	-1.8958	-3.4906
NE1289	sdrD protein	**-0.0354**	-0.0026	0.0407	-0.1444
NE1290	phosphotransferase system, fructose-specific IIABC component	**-0.1702**	-0.1807	0.3031	-0.6330
NE1291	putative endodeoxyribonuclease RusA	**-0.4663**	0.1371	-0.1708	-1.3651
NE1292	putative Na+/H+ antiporter, MnhE component	**1.0924**	0.8730	1.2706	1.1337
NE1293	hypothetical protein	**-0.5521**	-0.2958	0.2189	-1.5793
NE1294	hypothetical protein	**0.0618**	1.0773	0.1463	-1.0381
NE1295	23S ribosomal RNA (rrlA)	**0.2270**	0.1244	0.5914	-0.0347
NE1296	sensor histidine kinase SaeS	**-1.0872**	-2.7338	-0.6706	0.1430
NE1297	carbon-nitrogen family hydrolase	**0.2598**	-1.2327	-0.6041	2.6163
NE1298	hypothetical protein	**0.4948**	-1.2799	0.1788	2.5855
NE1299	hypothetical protein	**0.0604**	-0.5370	0.1356	0.5827
NE1300	Aerolysin/leukocidin family protein	**-3.8547**	-2.1341	-4.1071	-5.3228
NE1301	aspartate carbamoyltransferase catalytic subunit (pyrB)	**-0.8573**	-1.2049	-0.4691	-0.8980
NE1302	hypothetical protein	**0.1607**	1.0027	-0.2569	-0.2636
NE1303	truncated amidase	**-1.2077**	-0.6969	-1.3350	-1.5912
NE1304	transcription regulatory protein	**-0.5122**	-0.3618	-0.9225	-0.2523
NE1305	D-alanine aminotransferase (dat)	**0.6009**	-1.0674	1.4352	1.4349
NE1306	putative glutamyl aminopeptidase	**1.2668**	1.1206	1.6391	1.0408
NE1307	beta-lactamase	**0.4808**	0.2060	0.7511	0.4852
NE1308	urease accessory protein UreD	**1.2439**	0.0366	0.3700	3.3252
NE1309	respiratory response protein, SrrA	**-0.4224**	-1.1935	-0.4265	0.3529
NE1310	hypothetical protein	**-0.4555**	-0.7643	-0.7327	0.1306
NE1311	hypothetical protein	**0.6114**	-0.4739	-0.1807	2.4887
NE1312	hypothetical protein	**-1.0078**	-1.5871	-1.1973	-0.2389
NE1313	putative cell division protein FtsH	**-0.2660**	0.4350	-0.4140	-0.8191
NE1314	oligopeptide ABC transporter permease (oppC)	**0.2215**	0.0366	0.6279	0.0000
NE1315	adaptor protein	**-0.9922**	-1.4434	-1.0687	-0.4644
NE1316	phosphate transport system regulatory protein PhoU	**-0.2007**	0.0958	0.0021	-0.6999
NE1317	hypothetical protein	**0.8127**	-0.5928	2.1159	0.9150
NE1318	6,7-dimethyl-8-ribityllumazine synthase (ribH)	**0.1232**	-0.0995	0.7328	-0.2636
NE1319	hypothetical protein	**0.5208**	1.3059	0.8733	-0.6168
NE1320	exonuclease	**0.1614**	0.7837	-0.4239	0.1243
NE1321	ribosomal-protein-alanine acetyltransferase (riml)	**-0.1540**	-0.5175	-1.0916	1.1471
NE1322	hypothetical protein	**3.1183**	1.4276	-0.0788	8.0062
NE1323	ArsR family transcriptional regulator	**-0.5037**	-1.4990	-0.0788	0.0668
NE1324	transposase, truncation	**-0.0361**	0.1075	-0.2159	0.0000
NE1325	putative GTP-binding protein	**0.6786**	0.7837	-0.0303	1.2825
NE1326	IS1272, transposase	**0.1092**	0.3689	-0.4525	0.4112
NE1327	hypothetical protein	**-0.2025**	0.6888	-0.0061	-1.2901
NE1328	hypothetical protein	**1.8578**	1.6546	2.5579	1.3609
NE1329	hypothetical protein	**-0.7305**	-0.4319	-0.9045	-0.8552
NE1330	hypothetical protein	**0.4883**	-0.1907	0.7145	0.9411
NE1331	nucleoside diphosphate kinase (ndk)	**0.7965**	0.1583	0.2510	1.9801
NE1332	thiol peroxidase (tpx)	**-0.1187**	0.9943	-0.0950	-1.2554
NE1333	heat-inducible transcription repressor HrcA	**-1.6410**	-0.1415	-3.8985	-0.8828

NE1334	hypothetical protein	**-0.2225**	-0.1328	-0.5001	-0.0347
NE1335	acetyltransferase	**0.1505**	-0.2704	0.4721	0.2498
NE1336	phi77 ORF029-like protein	**-0.0297**	0.9975	0.7244	-1.8109
NE1337	hypothetical protein	**0.1495**	0.1503	0.5007	-0.2027
NE1338	phiPV083 ORF027-like protein	**3.1133**	0.7982	0.7270	7.8147
NE1339	TatD family hydrolase	**-0.5803**	-0.4019	0.9546	-2.2935
NE1340	hypothetical protein	**2.7560**	0.2019	0.9512	7.1149
NE1341	hypothetical protein	**3.3293**	0.1727	1.9337	7.8816
NE1342	chromosome segregation protein SMC	**0.1171**	-0.1349	1.1861	-0.6999
NE1343	glyceraldehyde 3-phosphate dehydrogenase 2 (gap)	**0.9646**	0.2516	1.1369	1.5052
NE1344	ATP-dependent DNA helicase RecG	**1.3238**	0.5358	1.7390	1.6967
NE1345	2-succinyl-6-hydroxy-2, 4-cyclohexadiene-1-carboxylic acid synthase/2-oxoglutarate decarboxylase (menD)	**0.4046**	1.1332	1.3161	-1.2355
NE1346	hypothetical protein	**0.3553**	0.1878	0.9527	-0.0747
NE1347	hypothetical protein	**4.1601**	1.6941	1.8305	8.9558
NE1348	phi77 ORF069-like protein	**1.0720**	1.1649	1.4889	0.5623
NE1349	conserved hypothetical protein	**0.9134**	0.9789	0.6790	1.0822
NE1350	conserved hypothetical protein	**-1.7827**	-1.9634	-0.9882	-2.3964
NE1351	conserved hypothetical protein	**-1.4664**	-2.2830	-0.8806	-1.2355
NE1352	nitrite reductase transcriptional regulator NirR	**0.3417**	1.0216	0.7781	-0.7745
NE1353	N-acetylmuramoyl-L-alanine amidase domainprotein	**-0.8284**	-0.1870	-1.3202	-0.9779
NE1354	alpha-hemolysin precursor	**-1.6969**	-3.3151	-1.2610	-0.5148
NE1355	molybdenum ABC transporter, molybdenum-binding protein ModA	**1.3348**	-0.7517	2.7483	2.0076
NE1356	putative urea transporter	**2.7864**	2.4589	2.4991	3.4014
NE1357	hypothetical protein	**0.7533**	1.0645	1.0203	0.1751
NE1358	conserved hypothetical protein	**0.0007**	0.0971	0.5352	-0.6302
NE1359	conserved hypothetical protein	**-0.5647**	-1.4474	-0.3202	0.0736
NE1360	oxacillin resistance-related FmtC protein	**1.4142**	0.6647	2.4601	1.1178
NE1361	conserved hypothetical protein	**0.1227**	-0.2041	0.5251	0.0470
NE1362	conserved hypothetical protein	**-0.3457**	-0.4977	0.6258	-1.1653
NE1363	sortase B (srtB)	**1.1642**	0.6466	1.1336	1.7126
NE1364	conserved hypothetical protein	**1.3176**	1.6860	1.1358	1.1309
NE1365	oxidoreductase, 2-nitropropane dioxygenase family	**-1.3493**	-1.6580	-0.6295	-1.7603
NE1366	catalase	**-2.2681**	-3.0070	-0.7123	-3.0851
NE1367	transcriptional regulator, GntR family	**1.8214**	2.1326	1.6842	1.6473
NE1368	ribosomal protein L11 methyltransferase	**2.0056**	2.2482	2.1550	1.6135
NE1369	N-acetylmuramoyl-L-alanine amidase	**0.1035**	-0.8444	-0.3236	1.4786
NE1370	conserved hypothetical protein	**-0.1168**	0.1670	-0.0137	-0.5038
NE1371	conserved hypothetical phage protein	**0.0700**	-0.2578	-0.1258	0.5935
NE1372	hypothetical protein	**1.0757**	1.3113	0.7910	1.1248
NE1373	putative homoserine O-acetyltransferase	**0.9504**	1.6017	0.7688	0.4809
NE1374	teichoic acid biosynthesis protein B	**-1.0406**	-1.3129	-0.5283	-1.2805
NE1375	conserved hypothetical protein	**1.1554**	0.8864	0.4492	2.1304
NE1376	transporter, CorA family (cobI)	**0.8792**	0.7617	1.0132	0.8627
NE1377	conserved hypothetical protein	**-1.2919**	-1.6619	-0.8477	-1.3661
NE1378	oligopeptide ABC transporter, oligopeptide-binding protein	**-1.6657**	-1.4474	-0.3588	-3.1908
NE1379	S-adenosylmethionine:tRNA ribosyltransferase-isomerase	**1.5771**	1.4656	2.0928	1.1729
NE1380	ABC transporter, ATP-binding protein	**1.1732**	0.6110	1.8223	1.0862
NE1381	malate:quinone-oxidoreductase (mqo)	**0.2897**	-0.4685	0.9938	0.3437
NE1382	alcohol dehydrogenase	**-2.7332**	-2.8619	-1.5837	-3.7542

NE1383	GTP cyclohydrolase I	**-0.9712**	-1.4121	-0.4273	-1.0742
NE1384	hypothetical protein	**1.1010**	1.1804	0.5674	1.5552
NE1385	conserved hypothetical protein	**-0.4306**	-0.8213	-0.0166	-0.4538
NE1386	Leukocidin/Hemolysin toxin family protein	**-1.5682**	-2.3407	-0.3615	-2.0023
NE1387	peptidase, M20/M25/M40 family	**0.1839**	-0.5482	0.3881	0.7119
NE1388	glycerol-3-phosphate transporter	**-0.4769**	-0.8805	0.5241	-1.0742
NE1389	aspartate kinase	**-1.6012**	-1.2693	-1.3490	-2.1852
NE1390	5'(3')-deoxyribonucleotidase	**-3.0949**	-3.2238	-2.3706	-3.6904
NE1391	2-oxoglutarate dehydrogenase, E2 component, dihydrolipoamide succinyltransferase	**-0.0900**	0.1425	0.4555	-0.8680
NE1392	phosphate starvation-induced protein, PhoH family	**1.2445**	1.3195	2.1443	0.2697
NE1393	TetR family regulatory protein	**-0.2884**	-0.3208	-0.2586	-0.2859
NE1394	Gfo/Idh/MocA family oxidoreductase	**-0.4621**	-0.8177	-0.5884	0.0199
NE1395	phiPVL ORF057-like protein, transcriptionalactivator RinB	**0.4222**	0.4826	0.5144	0.2697
NE1396	cassette chromosome recombinase A (ccrA)	**0.2348**	0.1394	-0.5350	1.1001
NE1397	alpha-acetolactate synthase (alsS)	**-0.1450**	-0.4685	0.0137	0.0199
NE1398	conserved hypothetical protein	**0.4152**	3.3023	-0.3603	-1.6965
NE1399	gamma-hemolysin component A (hlgA)	**0.0953**	0.0132	0.9225	-0.6499
NE1400	putative drug transporter	**-0.4560**	-0.2970	0.2109	-1.2820
NE1401	conserved hypothetical protein	**-0.3155**	0.0472	0.5313	-1.5251
NE1402	hypothetical protein	**-1.8425**	-2.1447	-1.1031	-2.2798
NE1403	conserved hypothetical protein	**0.8800**	0.8669	1.3591	0.4140
NE1404	rod shape-determining protein MreC	**2.0034**	0.9511	2.0910	2.9680
NE1405	probable glucose uptake protein (glcU)	**-0.3273**	0.1994	-1.0397	-0.1415
NE1406	conserved hypothetical protein	**-2.7049**	-2.2545	-2.9082	-2.9520
NE1407	pyruvate kinase (pyk)	**-0.5131**	0.1217	-1.0309	-0.6302
NE1408	phiSLT ORF 87-like protein, putative DNA-binding protein	**-0.6299**	-0.3423	-1.4058	-0.1415
NE1409	exotoxin	**-0.6937**	-0.1361	-0.2845	-1.6605
NE1410	UDP-N-acetylglucosamine 2-epimerase	**-2.2780**	-1.6276	-3.0213	-2.1852
NE1411	large conductance mechanosensitive channel protein (mscL)	**-0.2292**	0.3324	-1.6837	0.6638
NE1412	transcriptional regulator, DeoR family	**-1.6994**	-0.6791	-2.5059	-1.9133
NE1413	conserved hypothetical protein	**0.1930**	-0.3795	-0.2144	1.1729
NE1414	uridine kinase (udk)	**-1.1014**	-0.9962	-1.4909	-0.8171
NE1415	transcription antiterminator (glcT)	**-0.9848**	-0.8008	-1.0196	-1.1340
NE1416	alcohol dehydrogenase, zinc-containing	**0.4208**	0.5001	-0.6111	1.3734
NE1417	hypothetical protein	**-0.4169**	0.3729	-0.2575	-1.3661
NE1418	2-oxoglutarate/malate translocator	**-1.2539**	-1.3681	-1.6619	-0.7317
NE1419	putative nucleoside transporter	**-0.5363**	-0.2286	-0.9751	-0.4051
NE1420	conserved hypothetical protein	**-0.4653**	-0.0564	-1.2826	-0.0570
NE1421	PTS system, fructose-specific enzyme II, BC component	**-1.1185**	-0.6299	-0.5404	-2.1852
NE1422	phosphoglycerate mutase family protein	**-1.0344**	-1.0586	-1.2699	-0.7745
NE1423	lantibiotic epidermin biosynthesis protein EpiD	**-0.2897**	-0.1781	-1.2579	0.5671
NE1424	conserved hypothetical protein	**-0.0395**	-0.0889	-0.5743	0.5446
NE1425	conserved hypothetical protein	**0.5708**	1.0586	0.3842	0.2697
NE1426	low temperature requirement protein LtrA	**0.7368**	1.1592	0.3043	0.7469
NE1427	helicase, RecD/TraA family	**0.2974**	0.5902	-0.8390	1.1410
NE1428	phosphomethylpyrimidine kinase (thiD)	**0.0755**	0.3659	-1.4147	1.2753
NE1429	conserved hypothetical protein	**0.5398**	0.0000	0.3259	1.2934
NE1430	conserved hypothetical protein	**0.5267**	0.0000	0.1494	1.4305
NE1431	conserved hypothetical protein	**0.2216**	0.2786	-0.4389	0.8252

NE1432	transposase	**-0.1716**	-0.3282	0.0993	-0.2859
NE1433	conserved hypothetical protein	**-0.1368**	-0.0700	0.2300	-0.5704
NE1434	protoheme IX farnesyltransferase (cyoE)	**-1.1372**	-1.0586	-1.2057	-1.1471
NE1435	putative amino acid permease	**2.6118**	0.5105	7.3449	-0.0199
NE1436	oligopeptide ABC transporter, permease protein (oppC)	**1.4633**	0.1878	2.8731	1.3290
NE1437	conserved hypothetical protein	**3.0642**	0.1781	8.0913	0.9231
NE1438	holin-like protein lrgA	**3.2184**	0.4159	9.0159	0.2232
NE1439	maltose operon transcriptional repressor (malR)	**1.3034**	0.8633	3.0088	0.0380
NE1440	replication initiation factor family protein	**2.8770**	1.0164	7.3449	0.2697
NE1441	oxidoreductase, aldo/keto reductase family	**2.3415**	2.2166	0.4684	4.3396
NE1442	RNA methyltransferase, TrmA family (rumA)	**2.6696**	2.3046	4.3292	1.3751
NE1443	conserved hypothetical protein	**0.8392**	1.8009	0.7268	-0.0100
NE1444	squalene desaturase (crtM)	**1.1481**	0.2032	-0.4146	3.6558
NE1445	conserved hypothetical protein	**3.1285**	6.5073	-0.1886	3.0668
NE1446	endopeptidase resistance gene	**0.4472**	1.2395	0.5818	-0.4798
NE1447	geranyltranstransferase	**-0.8052**	-1.0981	0.7128	-2.0302
NE1448	phi77 ORF031-like protein	**0.3792**	0.9136	1.4891	-1.2649
NE1449	gamma-hemolysin component C (hlgC)	**0.4301**	0.3654	0.4964	0.4284
NE1450	hypothetical protein	**6.0728**	7.5034	1.7248	8.9903
NE1451	exonuclease SbcC	**1.9144**	1.5341	1.7279	2.4811
NE1452	phi77 ORF071-like protein	**-0.3411**	0.0330	-0.6292	-0.4271
NE1453	putative competence protein ComG	**0.6275**	2.1123	-0.6091	0.3795
NE1454	carbamoyl phosphate synthase large subunit (carB)	**-0.5803**	-0.2677	-0.5063	-0.9670
NE1455	amidohydrolase	**-0.2195**	1.8128	-0.3958	-2.0754
NE1456	coenzyme A disulfide reductase (cdr)	**0.4681**	0.2945	-0.6690	1.7788
NE1457	phosphotransferase system, N-acetylglucosamine-specific IIBC component (nagE)	**1.9112**	2.6584	0.1512	2.9240
NE1458	conserved hypothetical protein	**-0.6666**	-0.7436	-0.5229	-0.7334
NE1459	phosphate ABC transporter, phosphate-binding protein PstS	**-1.3249**	-0.5511	-1.2495	-2.1741
NE1460	D-isomer specific 2-hydroxyacid dehydrogenase family protein	**-0.4405**	0.0602	0.0546	-1.4362
NE1461	conserved hypothetical protein	**-0.8752**	0.2541	-0.4410	-2.4387
NE1462	DNA mismatch repair MutS2 protein	**0.1609**	1.0582	0.6844	-1.2600
NE1463	sodium:alanine symporter family protein	**0.5267**	1.8361	0.8002	-1.0563
NE1464	phosphoribosylformylglycinamidine synthase II (purL)	**0.3025**	0.5668	1.2301	-0.8893
NE1465	conserved hypothetical protein	**2.5757**	5.0035	0.6455	2.0780
NE1466	transcriptional regulator, LysR family	**0.3406**	-0.7988	0.0665	1.7541
NE1467	ornithine carbamoyltransferase (arcB)	**0.8053**	-0.0625	0.5327	1.9456
NE1468	ferrichrome transport permease protein fhuG	**-0.0961**	-1.4144	0.3217	0.8044
NE1469	conserved hypothetical protein	**-0.0587**	-0.8748	-0.7321	1.4307
NE1470	Na+/H+ antiporter NhaC	**0.3238**	-0.8098	0.5487	1.2324
NE1471	transcriptional regulator, TetR family	**-0.9395**	-0.9824	0.0028	-1.8390
NE1472	anti-sigma-B factor, serine-protein kinase (rsbW)	**-0.2764**	0.5659	0.7645	-2.1595
NE1473	hydroxyethylthiazole kinase (thiM)	**-0.5754**	-0.2069	-0.2839	-1.2354
NE1474	ATP-dependent RNA helicase, DEAD/DEAH box family	**0.4193**	-0.4296	0.7318	0.9556
NE1475	putative Bacterial sugar transferase	**2.1366**	5.5770	1.2427	-0.4101
NE1476	hypothetical protein	**-0.1878**	-0.0467	0.2270	-0.7436
NE1477	isochorismatase (entB)	**-0.0127**	-0.0330	-0.6752	0.6702
NE1478	transporter gate domain-containing protein	**-0.0409**	-0.0826	-1.5580	1.5180
NE1479	fosfomycin resistance protein FosB	**-0.5132**	0.7182	-0.4710	-1.7868
NE1480	short chain dehydrogenase/reductase family oxidoreductase	**1.9531**	-0.2111	4.3073	1.7632

NE1481	FtsK/SpoIIIE family protein	**-0.3774**	-0.6135	-1.1600	0.6413
NE1482	proline dipeptidase	**-0.4358**	-0.6581	-0.8751	0.2259
NE1483	phi77 ORF020-like protein, phage major tail protein	**-0.8667**	-0.4006	-0.3103	-1.8893
NE1484	aresenical pump membrane protein (arsB)	**-0.6738**	-0.1612	0.1175	-1.9777
NE1485	acetyltransferase	**-1.2652**	-0.9815	-1.6246	-1.1894
NE1486	alkaline phosphatase synthesis transcriptional regulatory protein (phoP)	**0.0619**	-0.2994	0.0328	0.4523
NE1487	ABC transporter ATP-binding protein	**0.8104**	0.8876	1.2677	0.2761
NE1488	hypothetical protein	**-0.1151**	1.1170	-1.4418	-0.0206
NE1489	ABC transporter ATP-binding protein	**-0.4565**	-1.2481	-1.1127	0.9912
NE1490	PTS system, trehalose-specific IIBC component (treP)	**-0.2864**	-0.2902	-0.5789	0.0100
NE1491	hypothetical protein	**-1.0240**	-0.5084	-0.6383	-1.9254
NE1492	hypothetical protein	**-0.1148**	-0.1909	-0.4907	0.3373
NE1493	hypothetical protein	**-0.5439**	-0.5410	-0.6805	-0.4101
NE1494	ribonuclease III (rnc)	**-0.3434**	-0.1824	-0.0028	-0.8451
NE1495	UDP-N-acetylglucosamine 1-carboxyvinyltransferase (murA)	**-1.6488**	-1.6642	-0.9783	-2.3039
NE1496	hypothetical protein	**-0.3717**	-0.6414	0.9852	-1.4589
NE1497	hypothetical protein	**-0.1338**	0.3072	-0.8434	0.1347
NE1498	2-oxoglutarate ferredoxin oxidoreductase subunit beta	**-0.5630**	-0.4473	0.1820	-1.4237
NE1499	oligopeptide permease, channel-forming protein (opp-3B)	**1.5510**	1.0353	3.2803	0.3373
NE1500	hypothetical protein	**-0.2182**	-0.3366	-0.2839	-0.0342
NE1501	hemA concentration negative effector hemX	**-0.5330**	-0.1612	-1.3424	-0.0954
NE1502	asparaginyl-tRNA synthetase (asnC)	**-0.5445**	-1.3108	-0.3490	0.0263
NE1503	hypothetical protein	**-0.2369**	-1.2441	0.0348	0.4987
NE1504	Na+/H+ antiporter	**0.0417**	0.5197	-1.1473	0.7527
NE1505	hypothetical protein	**-0.2566**	2.0076	-0.5795	-2.1979
NE1506	V8 protease (sspA)	**-1.3347**	-1.2783	-1.0936	-1.6323
NE1507	hypothetical protein	**-0.9647**	-0.9080	-0.4410	-1.5450
NE1508	D-lactate dehydrogenase	**0.0280**	0.3654	-0.3342	0.0529
NE1509	ABC transporter ATP-binding protein	**-1.7479**	-0.4993	-2.2155	-2.5289
NE1510	hypothetical protein	**-0.2318**	0.6095	0.4959	-1.8009
NE1511	LysR family regulatory protein	**2.0622**	2.3992	2.4793	1.3083
NE1512	respiratory nitrate reductase, subunit delta (narJ)	**-1.0985**	-0.0559	-1.6475	-1.5921
NE1513	acylphosphatase	**-0.0258**	2.3499	-0.9074	-1.5199
NE1514	gamma-aminobutyrate permease	**-0.7089**	-0.8670	-0.4044	-0.8553
NE1515	phiSLT ORF86-like protein	**-1.7603**	-1.4070	-1.6308	-2.2430
NE1516	hypothetical protein	**0.1278**	0.0824	-0.5571	0.8582
NE1517	M16 family peptidase	**0.3180**	0.1993	-0.9047	1.6596
NE1518	NAD-specific glutamate dehydrogenase (gudB)	**-0.7221**	-1.0952	-0.1875	-0.8837
NE1519	acetyl-CoA carboxylase, biotin carboxylase (accC)	**0.0132**	0.2945	0.0623	-0.3172
NE1520	hypothetical protein	**0.0194**	1.1703	-0.7941	-0.3181
NE1521	hypothetical protein	**-0.3457**	-0.7001	-0.7654	0.4284
NE1522	putative iron compound A C transporter, iron compound-binding protein	**0.3291**	0.2945	0.2404	0.4523
NE1523	dimethyladenosine transferase (ksgA)	**0.1058**	-0.2173	0.1973	0.3373
NE1524	tandem lipoprotein (lpl3)	**0.6275**	1.7769	1.2789	-1.1732
NE1525	hypothetical protein	**3.4740**	7.2456	0.5670	2.6093
NE1526	carbamoyl phosphate synthase small subunit (carA)	**-0.9988**	-1.1839	-1.1786	-0.6339
NE1527	short chain dehydrogenase/reductase family oxidoreductase	**0.4255**	0.5340	0.4268	0.3158
NE1528	ATP-dependent DNA helicase RecQ	**1.4247**	0.6298	1.2181	2.4263
NE1529	ATP-binding Mrp/Nbp35 family protein	**0.5450**	-0.1100	1.0350	0.7099

NE1530	L-asparaginase (ansA)	**0.1617**	-0.5063	0.4185	0.5728
NE1531	glutamine amidotransferase subunit PdxT	**1.2389**	3.4846	0.6958	-0.4637
NE1532	accessory gene regulator protein A (agrA)	**-1.2854**	-0.4807	-1.5565	-1.8190
NE1533	hypothetical protein	**2.2496**	3.3891	0.4351	2.9248
NE1534	putative lysophospholipase	**1.4244**	0.4191	1.7058	2.1483
NE1535	galactose-6-phosphate isomerase subunit LacB	**3.4102**	6.5856	2.6215	1.0235
NE1536	glycine cleavage system protein H (gcvH)	**1.7682**	0.7182	1.7836	2.8029
NE1537	hypothetical protein	**-0.0740**	1.0562	-1.1745	-0.1038
NE1538	hypothetical protein	**-0.0953**	1.0195	-0.2456	-1.0599
NE1539	hypothetical protein	**-0.1172**	1.0615	-1.0671	-0.3461
NE1540	degV family protein	**-0.3496**	-0.6642	-0.1629	-0.2216
NE1541	BioY family protein	**-0.2898**	-0.5311	0.0988	-0.4372
NE1542	hypothetical protein	**-0.9282**	-2.1471	0.1791	-0.8167
NE1543	quinol oxidase, subunit III (qoxC)	**-3.0950**	-3.5046	-2.3695	-3.4109
NE1544	glycerophosphoryl diester phosphodiesterase family protein	**-0.0957**	-0.8910	0.5929	0.0111
NE1545	molybdopterin biosynthesis protein B (moeB)	**-0.5435**	-1.4661	0.1885	-0.3529
NE1546	hypothetical protein	**0.5692**	-0.4419	1.2110	0.9385
NE1547	hypothetical protein	**0.9244**	0.9781	1.0890	0.7061
NE1548	F0F1 ATP synthase subunit A (atpB)	**2.1613**	2.9958	1.7171	1.7710
NE1549	hypothetical protein	**-0.6803**	0.1120	-1.7351	-0.4178
NE1550	nitroreductase family protein	**0.4230**	-0.8319	-0.7582	2.8592
NE1551	hypothetical protein	**-0.3856**	0.3589	-0.3418	-1.1740
NE1552	putative osmoprotectant ABC transporter ATP-binding protein	**-0.1693**	0.7268	-0.1836	-1.0512
NE1553	formimidoylglutamase (hutG)	**-1.8092**	-1.6194	-0.6197	-3.1885
NE1554	hypothetical protein	**0.4148**	0.0175	1.6990	-0.4723
NE1555	transcriptional repressor CodY	**-1.9455**	-2.7350	-0.7538	-2.3477
NE1556	hypothetical protein	**0.0133**	-1.1220	1.1958	-0.0338
NE1557	hypothetical protein	**-0.3581**	-1.1888	0.5257	-0.4113
NE1558	secretory extracellular matrix and plasma binding protein (empbp)	**0.7402**	-0.2498	0.7429	1.7275
NE1559	putative lipoprotein	**0.2659**	0.0725	0.4605	0.2645
NE1560	LysR family transcriptional regulator	**2.4963**	2.7459	2.2609	2.4822
NE1561	cell surface elastin binding protein (ebpS)	**-0.4536**	0.3434	-0.5245	-1.1795
NE1562	arsenical resistance operon repressor (arsR)	**-0.6893**	-0.4165	-0.8772	-0.7741
NE1563	superantigen-like protein	**-1.2275**	-0.8025	-1.5442	-1.3356
NE1564	phiSLT ORF100b-like protein, holin	**-0.0435**	0.1011	0.4321	-0.6636
NE1565	hypothetical protein	**-0.4592**	-0.6420	-0.7244	-0.0111
NE1566	iron compound ABC transporter permease SirC	**-0.6123**	-0.9761	-0.4952	-0.3656
NE1567	dihydrodipicolinate reductase (dapB)	**-1.8055**	-2.2172	-0.9577	-2.2415
NE1568	acetolactate synthase 1 regulatory subunit (ilvN)	**0.0699**	-0.2089	0.9368	-0.5183
NE1569	superantigen-like protein	**-1.0800**	-1.3510	-0.9775	-0.9114
NE1570	hypothetical protein	**0.0651**	-0.0683	0.6026	-0.3390
NE1571	alkyl hydroperoxide reductase subunit F (ahpF)	**-0.4052**	-0.6642	0.1856	-0.7370
NE1572	hypothetical protein	**1.8016**	2.5639	0.8361	2.0050
NE1573	phosphopentomutase (deoB)	**2.3550**	-1.0870	9.3934	-1.2414
NE1574	hypothetical protein	**-0.3946**	0.0214	-1.2353	0.0303
NE1575	tRNA modification GTPase TrmE	**-0.4808**	-0.5756	0.1141	-0.9807
NE1576	hypothetical protein	**-0.6359**	-0.1968	-1.1082	-0.6027
NE1577	serine protease SplD	**0.5188**	0.2996	0.7270	0.5296
NE1578	isochorismate synthase family protein	**-0.4161**	-0.5241	-0.8105	0.0862

NE1579	aminotransferase, class I	**0.1599**	-0.7646	0.3135	0.9307
NE1580	glycerol uptake facilitator (glpF)	**0.8823**	0.4943	1.4283	0.7243
NE1581	hypothetical protein	**0.9488**	0.9019	1.4482	0.4964
NE1582	hypothetical protein	**0.5784**	-0.1262	1.4683	0.3930
NE1583	inosine-uridine preferring nucleoside hydrolase	**0.4351**	0.6679	0.3730	0.2642
NE1584	PTS system, IIA component	**1.6302**	2.0351	1.0453	1.8103
NE1585	hypothetical protein	**0.5181**	1.0281	-0.1976	0.7239
NE1586	D-ribose pyranase (rbsD)	**0.0131**	0.2615	0.1141	-0.3361
NE1587	glycerol kinase (glpK)	**-0.5971**	-0.3059	-0.8105	-0.6750
NE1588	uroporphyrinogen decarboxylase (hemE)	**1.0286**	0.3410	2.0008	0.7440
NE1589	ABC transporter substrate-binding protein	**0.7407**	1.2005	0.4768	0.5447
NE1590	hypothetical protein	**-0.8499**	-0.8915	-0.7806	-0.8776
NE1591	TPR domain-containing protein	**-0.0898**	-0.1848	0.0073	-0.0919
NE1592	amino acid ABC transporter amino acid-binding protein	**0.4611**	-0.1096	0.3279	1.1650
NE1593	hypothetical protein	**-0.8632**	-0.8778	-1.1593	-0.5524
NE1594	arginine deiminase (arcA)	**0.0251**	0.0214	-0.1061	0.1600
NE1595	hypothetical protein	**0.9102**	1.3140	0.4930	0.9236
NE1596	hypothetical protein	**1.3658**	1.6630	0.9182	1.5163
NE1597	hypothetical protein	**-0.1207**	0.3589	-1.3010	0.5800
NE1598	hypothetical protein	**-1.0891**	-0.7314	-1.6271	-0.9089
NE1599	hypothetical protein	**-0.7676**	-0.1796	-2.0328	-0.0904
NE1600	hypothetical protein	**-0.7298**	-0.9976	-1.0671	-0.1246
NE1601	transcriptional regulator TcaR	**-0.1399**	0.4503	-0.3026	-0.5674
NE1602	phiSLT ORF80-like protein	**0.3422**	-0.2313	0.2971	0.9608
NE1603	ABC transporter ATP-binding protein	**-0.6485**	-1.1506	-1.0288	0.2338
NE1604	oligopeptide ABC transporter ATP-binding protein	**0.1677**	0.1741	-0.0073	0.3363
NE1605	enterotoxin Q (seq)	**-0.0386**	0.3178	-0.1354	-0.2982
NE1606	HAD superfamily hydrolase	**0.9329**	0.7896	1.4283	0.5809
NE1607	sigma-B regulation protein (rsbU)	**0.9932**	1.7728	1.2217	-0.0150
NE1608	thiamine-phosphate pyrophosphorylase (thiE)	**1.4257**	2.3034	0.1007	1.8730
NE1609	oligopeptide permease, ATP-binding protein (opp-2F)	**0.6926**	1.1956	0.1791	0.7032
NE1610	dihydrolipoamide dehydrogenase (lpdA)	**-0.8245**	-0.0394	-1.1428	-1.2914
NE1611	hydrolase-like protein	**-0.4144**	0.6335	-1.4582	-0.4186
NE1612	phiSLT ORF213-like protein, major tail protein	**-0.1739**	0.2439	-0.8419	0.0764
NE1613	putative 3-methyladenine DNA glycosylase	**0.5330**	0.2874	0.6005	0.7110
NE1614	hypothetical protein	**-0.5132**	-0.8013	-0.3451	-0.3934
NE1615	ABC transporter substrate-binding protein	**-0.3909**	-0.5651	-0.8618	0.2542
NE1616	hypothetical protein	**0.6007**	-0.6556	2.2922	0.1657
NE1617	hypothetical protein	**1.2479**	2.1299	0.1644	1.4495
NE1618	hypothetical protein	**0.1821**	0.4606	-0.8431	0.9288
NE1619	capsular polysaccharide biosynthesis protein Cap5L	**1.1198**	1.3312	0.5014	1.5267
NE1620	PTS system, galactitol-specific enzyme II, B component	**1.2900**	3.0466	-1.1751	1.9985
NE1621	HAD family hydrolase	**0.9025**	1.5485	0.9368	0.2223
NE1622	DNA-binding response regulator SaeR	**-1.1805**	-0.4053	-3.2216	0.0852
NE1623	hypothetical protein	**-1.2079**	-0.8918	-1.4685	-1.2633
NE1624	hypothetical protein	**0.7913**	-0.0175	2.6407	-0.2492
NE1625	hypothetical protein	**-0.2264**	0.2203	-0.7414	-0.1582
NE1626	ornithine cyclodeaminase	**-0.3942**	-0.3374	-1.4037	0.5583
NE1627	hypothetical protein	**-0.4027**	-0.2448	-0.7316	-0.2317
NE1628	hypothetical protein	**-0.5403**	-0.6532	-1.0398	0.0720
NE1629	hypothetical protein	**0.9145**	1.3212	-0.7048	2.1271

NE1630	ABC transporter ATP-binding protein	**1.2683**	1.0753	1.3139	1.4157
NE1631	hypothetical protein	**1.4320**	2.3685	1.0890	0.8386
NE1632	hypothetical protein	**1.8570**	2.3189	1.5111	1.7411
NE1633	oligopeptide ABC transporter ATP-binding protein (oppD)	**0.1938**	-0.3133	2.2804	-1.3856
NE1634	acetyltransferase	**0.1544**	0.1048	-0.0205	0.3788
NE1635	putative lipoprotein	**0.5862**	0.7687	1.0974	-0.1076
NE1636	phiPVL ORF17-like protein	**3.5038**	0.3537	1.1124	9.0454
NE1637	inosine-uridine preferring nucleoside hydrolase	**3.4823**	2.4984	1.0831	6.8654
NE1638	ribosomal RNA large subunit methyltransferase N	**0.7560**	0.1138	0.0102	2.1439
NE1639	hypothetical protein	**0.6467**	0.4282	1.0415	0.4702
NE1640	LysM domain-containing protein	**0.9263**	1.4495	0.9041	0.4253
NE1641	hypothetical protein	**2.6935**	0.0021	0.7579	7.3205
NE1642	urease subunit beta (ureB)	**2.5464**	0.6849	0.6443	6.3099
NE1643	DNA-binding response regulator	**3.9060**	4.7954	0.0162	6.9063
NE1644	hypothetical protein	**3.3959**	9.2047	2.0291	-1.0461
NE1645	mannose-6-phosphate isomerase (manA)	**-0.8550**	0.2533	-0.4292	-2.3891
NE1646	phosphonate ABC transporter phosphonate-binding protein	**-1.2177**	-0.6969	-0.5627	-2.3936
NE1647	30S ribosomal protein S1 (rpsA)	**-1.6926**	-1.6859	-0.3319	-3.0599
NE1648	hypothetical protein	**0.1291**	-0.2333	1.0566	-0.4360
NE1649	CHAP domain-contain protein	**0.2038**	1.0444	1.2523	-1.6853
NE1650	twin arginine-targeting protein translocase	**-0.8625**	-0.8363	0.2782	-2.0296
NE1651	acetylglutamate kinase (argB)	**2.1582**	0.3467	-0.2428	6.3708
NE1652	aminotransferase, class V	**-0.0903**	0.8151	0.1245	-1.2105
NE1653	MutT/NUDIX family hydrolase	**0.8106**	1.5482	0.6543	0.2292
NE1654	hypothetical protein	**2.1733**	0.4502	0.1963	5.8736
NE1655	phiSLT ORF484-like protein, lysin	**2.1910**	-0.9752	0.0336	7.5145
NE1656	riboflavin biosynthesis protein (ribD)	**2.1992**	8.5932	-0.2158	-1.7798
NE1657	hypothetical protein	**-1.3992**	-0.0097	-0.6916	-3.4962
NE1658	hypothetical protein	**-0.6249**	-1.0937	-0.5804	-0.2005
NE1659	transcriptional regulator	**-0.7717**	-1.0028	-1.0753	-0.2370
NE1660	copper chaperone copZ	**-0.3144**	-0.5039	0.0549	-0.4943
NE1661	putative glycerophosphoryl diester phosphodiesterase	**0.1278**	-0.5119	0.0759	0.8194
NE1662	(dimethylallyl)adenosine tRNA methylthiotransferase (miaB)	**-2.0921**	-1.4500	-0.9118	-3.9146
NE1663	diacylglycerol glucosyltransferase	**-0.8577**	-1.2685	0.2640	-1.5686
NE1664	carbamate kinase (arcC)	**1.3670**	-1.2596	0.2754	5.0853
NE1665	NADH-dependent flavin oxidoreductase	**-1.0589**	-0.7105	-1.5658	-0.9004
NE1666	hypothetical protein	**-0.4154**	-0.4722	-0.5735	-0.2005
NE1667	phi77 ORF045-like protein	**-0.2319**	-1.1014	0.5590	-0.1533
NE1668	hippurate hydrolase	**2.8992**	8.9188	0.9603	-1.1814
NE1669	DegU family transcriptional regulator	**-0.1555**	0.8826	-0.4960	-0.8531
NE1670	catabolite control protein A (ccpA)	**0.3818**	0.1540	-0.2135	1.2050
NE1671	methyltransferase small subunit	**0.0901**	-0.0699	0.3715	-0.0311
NE1672	tRNA (guanine-N(7)-)-methyltransferase (trmB)	**2.4950**	0.8084	-0.0583	6.7348
NE1673	hypothetical protein	**-0.0157**	0.0525	0.1008	-0.2005
NE1674	phosphomethylpyrimidine kinase (thiD)	**0.4634**	0.5604	0.2330	0.5968
NE1675	metal-dependent hydrolase	**-0.7243**	-1.0081	0.0982	-1.2629
NE1676	1-(5-phosphoribosyl)-5-[(5-phosphoribosylamino)methylideneamino] imidazole-4-carboxamide isomerase (hisA)	**-0.8416**	-0.6044	-0.2502	-1.6701
NE1677	tRNA (uracil-5-)-methyltransferase Gid	**-0.9380**	0.2369	-1.4381	-1.6128
NE1678	hypothetical protein	**0.0449**	0.8967	-1.5111	0.7492

NE1679	single-stranded DNA- binding protein family	**0.5554**	0.1551	0.6578	0.8533
NE1680	putative phage regulatory protein	**4.7196**	9.1227	-0.3242	5.3602
NE1681	hypothetical protein	**-0.7162**	-0.5883	-0.9084	-0.6519
NE1682	gamma-hemolysin component B (hlgB)	**-1.2037**	-1.1585	-0.2924	-2.1602
NE1683	N-acetyl-gamma-glutamyl-phosphate reductase (argC)	**0.0097**	0.2836	-1.0394	0.7848
NE1684	DNA-binding response regulator (arlR)	**-1.1432**	-1.9417	-0.4748	-1.0131
NE1685	hypothetical protein	**1.5249**	-0.9993	-0.0152	5.5891
NE1686	hypothetical protein	**-0.9520**	-1.1250	-0.5067	-1.2243
NE1687	trehalose operon repressor (treR)	**-0.7138**	-1.5314	-0.6412	0.0311
NE1688	CHAP domain-contain protein	**-1.0695**	-1.5303	-0.5177	-1.1605
NE1689	geranylgeranylglyceryl phosphate synthase-like protein (pcrB)	**2.2551**	-0.8261	-0.1156	7.7071
NE1690	hypothetical protein	**1.5245**	-0.0021	-0.6540	5.2296
NE1691	hypothetical protein	**0.3362**	0.3832	0.4318	0.1936
NE1692	holin-like protein cidA	**4.5175**	9.1726	3.5604	0.8194
NE1693	hypothetical protein	**0.4153**	0.2281	0.2330	0.7848
NE1694	GTP-binding protein (typA)	**-0.8797**	-1.1625	-0.0911	-1.3856
NE1695	branched-chain alpha-keto acid dehydrogenase subunit E2	**0.4829**	-0.3938	0.2960	1.5465
NE1696	acetoin utilization protein AcuA	**-1.4771**	-1.5647	-0.9316	-1.9351
NE1697	hypothetical protein	**2.6132**	-0.5119	1.8126	6.5388
NE1698	MutT/nudix family protein	**1.6791**	-0.3400	-0.1022	5.4794
NE1699	hypothetical protein	**-0.6521**	-1.2871	-0.6220	-0.0472
NE1700	hypothetical protein	**1.7077**	-1.6464	-0.5510	7.3205
NE1701	dihydrodipicolinate synthase (dapA)	**-0.2854**	-0.5299	-0.3675	0.0413
NE1702	zinc-binding dehydrogenase family oxidoreductase	**-0.4587**	-0.6423	-0.2979	-0.4360
NE1703	hypothetical protein	**-0.3668**	-0.9804	0.2330	-0.3529
NE1704	hypothetical protein	**3.0505**	8.7203	0.3115	0.1196
NE1705	hypothetical protein	**2.8916**	5.3007	3.9930	-0.6189
NE1706	hypothetical protein	**-0.8318**	-1.0729	-0.4733	-0.9493
NE1707	hypothetical protein	**0.0425**	3.0673	-1.4427	-1.4971
NE1708	ATP-dependent protease ATP-binding subunit HslU	**2.5806**	2.0863	0.1762	5.4794
NE1709	amino acid permease	**2.3640**	1.1366	-0.4735	6.4291
NE1710	phosphotransferase mannnose-specific family component IIA	**-0.8966**	-0.6044	-0.2472	-1.8381
NE1711	hypothetical protein	**-0.9118**	-0.3212	-0.6550	-1.7592
NE1712	ComE operon protein 2	**-0.3026**	-0.4893	-0.8738	0.4554
NE1713	alanine racemase (alr)	**-0.5769**	-0.5820	-0.1616	-0.9872
NE1714	GTP pyrophosphokinase	**-0.9780**	-0.1923	-0.5371	-2.2047
NE1715	hypothetical protein	**1.1943**	2.0167	0.3719	Inf
NE1716	chemotaxis-inhibiting protein CHIPS (chs)	**4.6649**	8.5382	0.7915	Inf
NE1717	chorismate synthase (aroC)	**1.0746**	2.0559	1.2644	-0.0964
NE1718	MarR family transcriptional regulator	**0.6246**	1.1272	0.2330	0.5137
NE1719	carbamate kinase (arcC)	**1.3467**	2.4446	0.3398	1.2558
NE1720	hypothetical protein	**1.4803**	3.2992	-0.4046	1.5465
NE1721	hypothetical protein	**-0.7143**	-1.0962	-0.4760	-0.5708
NE1722	hypothetical protein	**-0.4109**	0.2710	-0.4239	-1.0799
NE1723	hypothetical protein	**1.6951**	-0.5951	-0.0102	5.6906
NE1724	pyruvate dehydrogenase E1 component, alpha subunit (pdhA)	**-0.2508**	-0.3671	0.3707	-0.7560
NE1725	cytochrome D ubiquinol oxidase, subunit II	**2.2398**	0.7069	0.1388	5.8736
NE1726	antiholin-like protein LrgB	**1.8875**	3.1891	1.8766	0.5968
NE1727	hypothetical protein	**3.3328**	6.6502	0.6168	2.7316

NE1728	glycosyl transferase, group 1 family protein	**3.1256**	8.4196	0.3014	0.6559
NE1729	superantigen-like protein 5	**0.7840**	1.5297	0.2364	0.5859
NE1730	glutathione peroxidase	**0.3634**	1.4946	-0.4846	0.0801
NE1731	hypothetical protein	**-0.5402**	-1.0893	-0.4821	-0.0491
NE1732	peptide ABC transporter ATP-binding protein	**-0.6199**	-1.2332	0.1309	-0.7574
NE1733	hypothetical protein	**-0.4113**	-0.4532	0.0024	-0.7832
NE1734	hypothetical protein	**-2.7402**	-2.7479	-2.6037	-2.8690
NE1735	hypothetical protein	**-0.7380**	-1.2332	-0.3929	-0.5879
NE1736	hypothetical protein	**-2.1171**	-2.1324	-1.6985	-2.5203
NE1737	PTS system, mannitol specific IIA component (mtlA)	**-0.2428**	-1.1190	0.4629	-0.0723
NE1738	hypothetical protein	**-0.2243**	0.3581	-0.3814	-0.6496
NE1739	hypothetical protein	**0.3642**	0.1158	0.7940	0.1829
NE1740	hypothetical protein (scpA)	**1.8814**	3.5378	1.5871	0.5194
NE1741	3-dehydroquinate synthase (aroB)	**0.0330**	0.3415	-0.2302	-0.0123
NE1742	glutamyl-tRNA reductase (hemA)	**-0.4928**	-0.8393	-0.9369	0.2977
NE1743	hypothetical protein	**-2.1641**	-2.4351	-2.4362	-1.6210
NE1744	putative flavohemoprotein	**-1.2042**	-2.0243	-0.5607	-1.0277
NE1745	phi77 ORF044-like protein	**0.3448**	0.3736	-0.3259	0.9868
NE1746	S-ribosylhomocysteinase (luxS)	**-3.9880**	-5.2163	-2.8327	-3.9151
NE1747	hypothetical protein	**0.1460**	0.1451	-0.3193	0.6124
NE1748	amidohydrolase family protein	**-3.5829**	-4.4448	-2.7360	-3.5678
NE1749	hypothetical protein	**0.0252**	0.4288	-0.5629	0.2097
NE1750	hypothetical protein	**-1.9990**	-3.5378	-1.0482	-1.4112
NE1751	hypothetical protein	**0.9689**	2.0090	0.4544	0.4432
NE1752	ribosome-binding factor A (rbfA)	**0.7873**	0.3477	1.2744	0.7397
NE1753	ABC transporter ATP-binding protein	**0.9255**	1.1199	0.8842	0.7725
NE1754	hypothetical protein	**-0.3980**	-0.7911	-0.7097	0.3066
NE1755	hypothetical protein	**-0.3729**	0.0203	-0.1654	-0.9734
NE1756	sensor histidine kinase	**0.7606**	1.4237	0.2327	0.6256
NE1757	lipoprotein signal peptidase (lspA)	**0.1809**	-0.3526	0.5956	0.2999
NE1758	pyruvate dehydrogenase E1 component, beta subunit (pdhB)	**-4.5176**	-4.9470	-4.5555	-4.0504
NE1759	orotidine 5'-phosphate decarboxylase (pyrF)	**-1.0972**	-1.2796	-1.2356	-0.7763
NE1760	hypothetical protein	**-2.1621**	-2.9469	-1.8109	-1.7286
NE1761	ATPase family protein	**0.0288**	-0.4040	0.9177	-0.4275
NE1762	HAD family hydrolase	**-2.6485**	-4.0716	-1.7179	-2.1561
NE1763	putative traG membrane protein	**1.2831**	0.5843	0.9125	2.3526
NE1764	serine protease SplF	**1.2060**	2.0132	0.1025	1.5024
NE1765	hypothetical protein	**1.2058**	1.7569	0.9765	0.8841
NE1766	ABC transporter protein	**-0.0324**	0.1033	0.1628	-0.3634
NE1767	iron compound ABC transporter iron compound-binding protein SirA	**-0.5581**	-1.1902	-0.7570	0.2730
NE1768	ABC transporter ATP-binding protein	**-0.2148**	-0.8067	-0.1444	0.3066
NE1769	hypothetical protein	**-0.4725**	-1.0588	0.0936	-0.4523
NE1770	succinyl-CoA synthetase subunit alpha (sucD)	**-4.6356**	-5.3921	-3.5445	-4.9702
NE1771	hypothetical protein	**-0.2634**	-1.0610	-0.0024	0.2730
NE1772	hypothetical protein	**-2.1315**	-1.5002	-2.4195	-2.4748
NE1773	phospholipase/carboxylesterase family protein	**-0.3823**	0.2754	-0.2765	-1.1458
NE1774	ABC transporter permease	**-0.7217**	-0.8822	-0.5689	-0.7141
NE1775	triacylglycerol lipase	**-0.3081**	-0.0203	-0.6100	-0.2941
NE1776	hypothetical protein	**0.4252**	1.6514	-0.7915	0.4157

NE1777	hypothetical protein	**0.3180**	0.6800	0.4216	-0.1477
NE1778	hypothetical protein	**0.3042**	-0.0495	0.3727	0.5894
NE1779	hydrolase family protein	**0.2655**	-0.3241	-0.2302	1.3509
NE1780	hypothetical protein	**0.5260**	1.0150	0.5198	0.0431
NE1781	MarR family transcriptional regulator	**0.2193**	-0.6358	1.2825	0.0114
NE1782	hypothetical protein	**-0.6186**	-1.2928	-0.4871	-0.0760
NE1783	hypothetical protein	**-0.3549**	-0.7256	-0.3276	-0.0114
NE1784	ABC transporter permease	**-0.3910**	-0.6170	-0.5301	-0.0257
NE1785	phosphoribosylglycinamide formyltransferase (purN)	**-0.5421**	-0.5879	-1.4723	0.4339
NE1786	phi77 ORF014-like protein, phage anti-repressor protein	**0.3376**	0.2539	-0.4464	1.2054
NE1787	sortase (srtA)	**1.7340**	1.4476	2.5552	1.1991
NE1788	hypothetical protein	**0.7751**	1.7799	1.2130	-0.6677
NE1789	hypothetical protein	**0.8985**	1.7175	0.8932	0.0848
NE1790	ABC transporter ATP-binding protein	**0.5361**	0.0942	1.0245	0.4896
NE1791	tagatose 1,6-diphosphate aldolase (lacD)	**0.1320**	0.4257	0.1409	-0.1707
NE1792	phi77 ORF040-like protein	**0.1755**	0.3172	0.0260	0.1834
NE1793	hypothetical protein	**-0.3248**	0.0214	-0.2425	-0.7534
NE1794	Holliday junction resolvase-like protein	**-0.2278**	-0.2110	-0.0929	-0.3795
NE1795	hypothetical protein	**0.1259**	0.6645	0.2687	-0.5554
NE1796	histidinol-phosphate aminotransferase (hisC)	**-0.1919**	-0.6430	0.5084	-0.4412
NE1797	hypothetical protein	**-0.2160**	-0.3526	0.1127	-0.4080
NE1798	dUTP diphosphatase (dut)	**0.3878**	-0.9491	1.5134	0.5990
NE1799	hypothetical protein	**0.9405**	0.6345	0.0500	2.1370
NE1800	hypothetical protein	**-0.0103**	0.0989	0.5170	-0.6467
NE1801	hypothetical protein	**0.7207**	1.7712	0.1950	0.1959
NE1802	aldo/keto reductase family oxidoreductase	**0.1583**	0.3736	-0.0575	0.1588
NE1803	putative thioredoxin	**-0.1724**	0.1158	-0.3725	-0.2606
NE1804	putative drug transporter	**0.2658**	0.4767	0.2456	0.0750
NE1805	hypothetical protein	**-0.1752**	-0.2649	-0.4269	0.1661
NE1806	hypothetical protein	**-0.0664**	-0.2764	-0.0168	0.0942
NE1807	universal stress protein	**-0.1601**	0.1603	-0.0741	-0.5665
NE1808	putative iron compound ABC transporter iron compound-binding protein	**-0.4524**	-1.3853	0.6493	-0.6213
NE1809	putative enterotoxin	**-0.5691**	-0.7832	-0.7511	-0.1730
NE1810	hypothetical protein	**-0.1262**	-0.2309	0.3370	-0.4848
NE1811	hypothetical protein	**-0.2008**	-0.5633	0.1094	-0.1485
NE1812	putative lipoprotein	**1.2467**	3.0492	0.4736	0.2173
NE1813	methionine sulfoxide reductase A (msrA)	**1.0794**	1.8642	0.1325	1.2416
NE1814	phiSLT ORF116b-like protein	**0.6104**	0.6263	0.2456	0.9594
NE1815	molybdenum cofactor biosynthesis protein B (moaB)	**-0.2011**	-0.7229	-0.0614	0.1808
NE1816	L-lactate dehydrogenase	**-0.5402**	-0.5307	-0.4514	-0.6386
NE1817	spermidine/putrescine ABC transporter permease (potB)	**-0.5144**	-0.9327	0.1050	-0.7155
NE1818	hypothetical protein	**-0.2195**	0.2852	-0.7071	-0.2366
NE1819	hypothetical protein	**0.3576**	0.4203	0.5141	0.1383
NE1820	hypothetical protein	**0.9347**	0.1838	1.6968	0.9237
NE1821	putative phage transcriptional regulator	**0.4926**	0.6467	0.4299	0.4012
NE1822	ABC transporter permease	**0.8120**	0.2163	0.8586	1.3610
NE1823	Tat-translocated protein	**1.1003**	1.1998	1.1390	0.9621
NE1824	hypothetical protein	**2.0283**	4.3485	1.3401	0.3963
NE1825	DNA-3-methyladenine glycosidase	**1.4968**	0.8046	2.1602	1.5256
NE1826	phiPVL ORF051-like protein	**0.3392**	0.5287	1.1388	-0.6500

NE1827	hypothetical protein	**-0.3637**	0.0191	1.2715	-2.3817
NE1828	pyridoxal biosynthesis lyase PdxS	**0.1081**	-0.4037	-0.0434	0.7712
NE1829	2-oxoisovalerate dehydrogenase, E1 component, beta subunit	**-0.0840**	0.9645	0.2889	-1.5053
NE1830	putative phage-related DNA recombination protein	**-0.2458**	-0.6549	0.1594	-0.2419
NE1831	YibE/F-like protein	**0.2580**	-1.0853	0.3066	1.5527
NE1832	glyoxalase family protein	**0.0801**	-0.4241	0.5696	0.0948
NE1833	PemK family protein	**-0.5565**	-1.0520	0.2846	-0.9022
NE1834	hypothetical protein	**0.2227**	-0.0675	-0.4207	1.1562
NE1835	N-acetylneuraminate lyase	**0.1645**	-0.6007	1.4804	-0.3860
NE1836	hypothetical protein	**1.3036**	1.7663	2.1381	0.0062
NE1837	imidazole glycerol phosphate synthase subunit HisH	**-0.5767**	-1.3851	-0.1368	-0.2082
NE1838	conserved hypothetical protein	**-0.8349**	-1.0077	-2.2848	0.7878
NE1839	cadmium-exporting ATPase, truncation	**-1.8288**	-1.9734	-1.6271	-1.8861
NE1840	serine-aspartate repeat-containing protein SdrH	**-0.6891**	-1.0281	-0.2601	-0.7790
NE1841	hypothetical protein	**-0.6506**	-1.3034	-0.9245	0.2759
NE1842	superantigen-like protein	**-0.2291**	0.8702	-0.7041	-0.8534
NE1843	hypothetical protein	**-0.1642**	-0.1360	-0.2827	-0.0739
NE1844	serine protease SplE	**-0.0026**	1.3016	-1.8666	0.5572
NE1845	delta-aminolevulinic acid dehydratase (hemB)	**-0.2877**	-0.0465	-0.6001	-0.2165
NE1846	spermidine N(1)-acetyltransferase (speG)	**0.0655**	-0.1948	-0.4161	0.8074
NE1847	putative hemolysin	**0.7216**	1.2295	-0.3544	1.2896
NE1848	Panton-Valentine leukocidin, LukS-PV	**0.7043**	1.7451	0.7678	-0.4001
NE1849	hypothetical protein	**2.3538**	1.9628	3.9189	1.1797
NE1850	F0F1 ATP synthase subunit gamma (atpG)	**-0.4590**	-0.0191	0.6663	-2.0241
NE1851	hypothetical protein	**-0.8795**	-0.8621	0.2429	-2.0193
NE1852	hypothetical protein	**0.8836**	1.8210	0.0434	0.7865
NE1853	addiction module antitoxin	**0.6639**	0.9386	1.5864	-0.5334
NE1854	putative competence protein ComGC	**-0.2444**	-0.6753	0.3230	-0.3809
NE1855	glycosyl transferase, group 2 family protein	**0.5245**	1.0589	0.5209	-0.0062
NE1856	lantibiotic epidermin biosynthesis protein EpiC	**-0.4449**	-0.4146	0.4055	-1.3257
NE1857	cell wall biosynthesis protein ScdA	**0.0932**	-0.0403	-0.1191	0.4391
NE1858	ABC transporter ATP-binding protein	**0.0787**	0.4041	-0.5635	0.3955
NE1859	hypothetical protein	**0.7447**	1.8508	-0.0434	0.4268
NE1860	1-pyrroline-5-carboxylate dehydrogenase	**0.7055**	0.4494	-1.1829	2.8500
NE1861	hypothetical protein	**-0.8717**	-1.3514	1.2764	-2.5400
NE1862	superantigen-like protein	**-1.0326**	-1.3710	-0.9825	-0.7444
NE1863	pyruvate formate-lyase activating enzyme (pflA)	**-1.0426**	-1.3297	-1.4020	-0.3962
NE1864	staphylokinase (sak)	**-1.1118**	-1.2202	-1.5591	-0.5562
NE1865	hypothetical protein	**-0.2761**	-0.7114	-0.1346	0.0177
NE1866	DNA polymerase IV	**0.0623**	0.4637	-0.2098	-0.0671
NE1867	phiETA ORF59-like protein	**0.4237**	0.2144	0.1724	0.8843
NE1868	penicillin-binding protein 2 (mecA)	**-0.1946**	0.1255	-0.2882	-0.4210
NE1869	hypothetical protein	**-0.2371**	0.4362	-0.0771	-1.0704
NE1870	conserved hypothetical protein	**1.0511**	1.3172	1.0749	0.7613
NE1871	hypothetical protein	**0.5869**	1.2731	0.6727	-0.1851
NE1872	anti-sigma-B factor, antagonist (rsbV)	**1.2216**	1.4160	1.1451	1.1038
NE1873	hypothetical protein	**3.3922**	1.5019	1.4107	7.2641
NE1874	U32 family peptidase	**-1.4309**	-1.6334	-1.0376	-1.6216
NE1875	truncated beta-hemolysin	**-0.0961**	0.6494	0.8912	-1.8288
NE1876	pantoate--beta-alanine ligase (panC)	**0.3134**	0.6975	0.4517	-0.2090

NE1877	hypothetical protein	**-0.8344**	-0.8606	0.2486	-1.8913
NE1878	putative endonuclease III	**0.9849**	-0.4923	-0.2666	3.7137
NE1879	IS1181, transposase (tnp)	**0.4419**	0.9176	0.1168	0.2912
NE1880	tandem lipoprotein	**-0.6904**	-0.1333	-0.9279	-1.0100
NE1881	ferrichrome transport permease fhuB	**-0.2746**	-1.1438	-0.2542	0.5742
NE1882	glycine betaine/carnitine/choline ABC transporter ATP-binding protein (opuCa)	**1.2593**	1.7797	1.1065	0.8917
NE1883	LysR family regulatory protein (gltC)	**0.5368**	-0.0269	-0.4538	2.0912
NE1884	hypothetical protein	**0.7615**	0.4253	0.6528	1.2063
NE1885	queuine tRNA-ribosyltransferase (tgt)	**-0.9150**	-2.6126	-2.1455	2.0131
NE1886	hypothetical protein	**-1.3658**	-0.9360	-1.8402	-1.3212
NE1887	transcription antitermination protein NusB	**-1.4031**	-1.1283	-2.4081	-0.6730
NE1888	hypothetical protein	**-1.0450**	-0.6128	-1.4314	-1.0907
NE1889	F0F1 ATP synthase subunit delta (atpH)	**-2.2095**	-0.9986	-3.9764	-1.6536
NE1890	phiSLT ORF65-like protein	**-0.7173**	-1.2439	-1.1829	0.2749
NE1891	phosphoglyceromutase (gpmI)	**-0.9771**	-1.1870	-1.8478	0.1034
NE1892	hypothetical protein	**-0.9990**	-0.9331	-2.0060	-0.0579
NE1893	hypothetical protein	**0.0632**	0.9582	-0.4310	-0.3376
NE1894	hypothetical protein	**-0.0921**	-0.5482	-1.2320	1.5041
NE1895	arginine repressor (argR)	**0.3569**	0.6991	-0.2583	0.6300
NE1896	dihydrolipoamide dehydrogenase (lpdA)	**-0.9393**	-1.4728	-2.2677	0.9225
NE1897	hypothetical protein	**0.1633**	1.3575	1.7012	-2.5687
NE1898	dipeptidase PepV	**0.7520**	0.9805	1.9629	-0.6875
NE1899	tandem lipoprotein	**0.5352**	-0.2573	1.0317	0.8313
NE1900	hypothetical protein	**2.1868**	2.6056	2.4535	1.5014
NE1901	acetyl-CoA acetyltransferase	**5.8084**	7.5162	9.1372	0.7718
NE1902	molybdenum cofactor biosynthesis protein MoaC	**0.4834**	1.1492	1.2665	-0.9655
NE1903	AraC family transcriptional regulator	**2.1591**	0.4019	0.2498	5.8254
NE1904	50S ribosomal protein L33 (rpmG)	**-0.4016**	0.3439	-0.6031	-0.9457
NE1905	prolipoprotein diacylglyceryl transferase (lgt)	**0.8244**	1.6171	1.1041	-0.2480
NE1906	hypothetical protein	**1.2021**	1.6177	1.7023	0.2864
NE1907	methylated DNA-protein cysteine methyltransferase	**0.6156**	0.8306	0.4771	0.5390
NE1908	ABC transporter ATP-binding protein	**-1.5500**	-1.5030	-1.6276	-1.5195
NE1909	hypothetical protein	**-1.4653**	-2.9097	-1.8310	0.3449
NE1910	hypothetical protein	**-0.9145**	-0.7306	-1.2320	-0.7808
NE1911	hypothetical protein	**0.2511**	0.1043	0.6627	-0.0137
NE1912	ISSep1-like transposase	**-0.0635**	-0.1063	-0.4384	0.3542
NE1913	putative lipoprotein	**-0.0912**	-0.4647	-0.8108	1.0021
NE1914	hypothetical protein	**0.2782**	0.0537	0.1795	0.6015
NE1915	hypothetical protein	**0.2152**	0.4121	-0.0655	0.2989
NE1916	hypothetical protein	**-0.0092**	0.5623	0.7356	-1.3255
NE1917	hypothetical protein	**0.7033**	-0.3429	0.5089	1.9439
NE1918	phiSLT ORF53-like protein	**2.0952**	2.8871	2.3165	1.0820
NE1919	protein phosphatase 2C domain-containing protein	**1.2250**	2.1795	0.2814	1.2141
NE1920	polyprenyl synthetase	**1.4974**	3.2001	2.3374	-1.0452

Table 7.3 Primary screen NTML "hit list" Z-scores

Ranked by mean z-score (n = 3).

Rank	Accession number	Strain name	Gene description	Mean Score
1	SAUSA300_1515	NE1229	ABC transporter permease	-5.719815013
2	SAUSA300_0714	NE1161	integral membrane protein	-5.383650577
3	SAUSA300_2637	NE1164	hypothetical protein	-5.105313012
4	SAUSA300_1139	NE1770	succinyl-CoA synthetase subunit alpha (sucD)	-4.635602375
5	SAUSA300_1033	NE1172	iron/heme permease	-4.536251557
6	SAUSA300_0994	NE1758	pyruvate dehydrogenase E1 component, beta subunit (pdhB)	-4.517636999
7	SAUSA300_0417	NE1160	tandem lipoprotein	-4.358251888
8	SAUSA300_0511	NE1176	DNA repair protein RadA	-4.090874684
9	SAUSA300_2088	NE1746	S-ribosylhomocysteinase (luxS)	-3.98800717
10	SAUSA300_1975	NE1300	Aerolysin/leukocidin family protein	-3.854660543
11	SAUSA300_2517	NE1748	amidohydrolase family protein	-3.582892927
12	SAUSA300_2282	NE1099	hypothetical protein	-3.373883635
13	SAUSA300_0605	NE1193	accessory regulator A (sarA)	-3.22351457
14	SAUSA300_0961	NE1543	quinol oxidase, subunit III (qoxC)	-3.095018774
15	SAUSA300_0709	NE1390	5'(3')-deoxyribonucleotidase	-3.094926773
16	SAUSA300_0342	NE1734	hypothetical protein	-2.740184376
17	SAUSA300_0594	NE1382	alcohol dehydrogenase	-2.733232478
18	SAUSA300_0409	NE1406	conserved hypothetical protein	-2.704902573
19	SAUSA300_0540	NE1762	HAD family hydrolase	-2.648539953
20	SAUSA300_1889	NE522	adenylosuccinate lyase (purB)	-2.591478527
21	SAUSA300_1683	NE1276	bifunctional 3-deoxy-7-phosphoheptulonate synthase/chorismate mutase	-2.506729632
22	SAUSA300_2550	NE1205	anaerobic ribonucleotide reductase, small subunit (nrdG)	-2.502620434
23	SAUSA300_0962	NE732	quinol oxidase, subunit I (qoxB)	-2.32665548
24	SAUSA300_2065	NE1410	UDP-N-acetylglucosamine 2-epimerase	-2.278038178
25	SAUSA300_1232	NE1366	catalase	-2.268126571
26	SAUSA300_2308	NE1089	response regulator protein	-2.244360406
27	SAUSA300_2061	NE1889	F0F1 ATP synthase subunit delta (atpH)	-2.209514333
28	SAUSA300_1962	NE631	phiPVL ORF39-like protein	-2.182743974
29	SAUSA300_0769	NE1743	hypothetical protein	-2.164078435
30	SAUSA300_1599	NE1760	hypothetical protein	-2.162138444
31	SAUSA300_1984	NE1262	hypothetical protein	-2.143249172
32	SAUSA300_2368	NE1772	hypothetical protein	-2.131497583
33	SAUSA300_1724	NE1736	hypothetical protein	-2.117062524
34	SAUSA300_1185	NE1662	(dimethylallyl)adenosine tRNA methylthiotransferase (miaB)	-2.092119061
35	SAUSA300_1912	NE1188	putative membrane protein	-2.057013471
36	SAUSA300_2546	NE1196	glycine betaine aldehyde dehydrogenase (betB)	-2.05660324
37	SAUSA300_0182	NE964	4'-phosphopantetheinyl transferase superfamily protein	-2.03347308
38	SAUSA300_2043	NE1750	hypothetical protein	-1.999030914
39	SAUSA300_0017	NE529	adenylosuccinate synthetase (purA)	-1.996555301
40	SAUSA300_2526	NE978	dihydroorotate dehydrogenase (pyrD)	-1.983963598
41	SAUSA300_1363	NE965	NAD(P)H-dependent glycerol-3-phosphate dehydrogenase (gpsA)	-1.979198271
42	SAUSA300_0144	NE1252	phosphonate ABC transporter ATP-binding protein (phnC)	-1.958249425

43	SAUSA300_1148	NE1555	transcriptional repressor CodY	-1.945467693
44	SAUSA300_0188	NE945	branched-chain amino acid transport system II carrier protein (brnQ)	-1.935356797
45	SAUSA300_2400	NE1264	glutamyl-aminopeptidase	-1.915420692
46	SAUSA300_2344	NE991	uroporphyrin-III C-methyl transferase	-1.886236599
47	SAUSA300_2106	NE837	putative transcriptional regulator	-1.872112954
48	SAUSA300_0590	NE1402	hypothetical protein	-1.842497315
49	SAUSA300_0068	NE1839	cadmium-exporting ATPase, truncation	-1.828845796
50	SAUSA300_2281	NE1553	formimidoylglutamase (hutG)	-1.80920489
51	SAUSA300_1289	NE1567	dihydrodipicolinate reductase (dapB)	-1.805456513
52	SAUSA300_2314	NE1350	conserved hypothetical protein	-1.782663301
53	SAUSA300_0457	NE325	5S ribosomal RNA (rrfA)	-1.776424358
54	SAUSA300_1427	NE1515	phiSLT ORF86-like protein	-1.76027027
55	SAUSA300_0630	NE1509	ABC transporter ATP-binding protein	-1.74793727
56	SAUSA300_1558	NE714	5'-methylthioadenosine/S-adenosylhomocysteine nucleosidase (mntN)	-1.739109369
57	SAUSA300_2566	NE454	transcriptional regulator, Crp/Fnr family (arcR)	-1.730208422
58	SAUSA300_1222	NE1241	thermonuclease (nuc)	-1.705118444
59	SAUSA300_0683	NE1412	transcriptional regulator, DeoR family	-1.699437951
60	SAUSA300_1058	NE1354	alpha-hemolysin precursor	-1.696927313
61	SAUSA300_1365	NE1647	30S ribosomal protein S1 (rpsA)	-1.692564787
62	SAUSA300_0730	NE962	GGDEF domain-containing protein	-1.675912984
63	SAUSA300_0892	NE1378	oligopeptide ABC transporter, oligopeptide-binding protein	-1.665665237
64	SAUSA300_0967	NE744	phosphoribosylaminoimidazole carboxylase, ATPase subunit (purK)	-1.651232745
65	SAUSA300_2055	NE1495	UDP-N-acetylglucosamine 1-carboxyvinyltransferase (murA)	-1.648794961
66	SAUSA300_1542	NE1333	heat-inducible transcription repressor HrcA	-1.64095922
67	SAUSA300_2643	NE486	putative chromosome partioning protein, ParB family	-1.63197938
68	SAUSA300_0659	NE979	sugar efflux transporter	-1.628977212
69	SAUSA300_0752	NE912	ATP-dependent Clp protease proteolytic subunit (clpP)	-1.62276562
70	SAUSA300_2316	NE451	acetyltransferase, GNAT family	-1.609934477
71	SAUSA300_1855	NE596	monofunctional glycosyltransferase (sgtB)	-1.607136107
72	SAUSA300_0126	NE990	hypothetical protein	-1.606710871
73	SAUSA300_1225	NE1389	aspartate kinase	-1.601156775
74	SAUSA300_2167	NE1088	conserved hypothetical protein	-1.586612445
75	SAUSA300_1506	NE1162	hypothetical protein	-1.579912281
76	SAUSA300_1974	NE1386	Leukocidin/Hemolysin toxin family protein	-1.568169817
77	SAUSA300_1911	NE1908	ABC transporter ATP-binding protein	-1.550037838
78	SAUSA300_2436	NE825	putative cell wall surface anchor family protein	-1.549178738
79	SAUSA300_2602	NE766	intercellular adhesion protein C (icaC)	-1.543003461
80	SAUSA300_0848	NE966	hypothetical protein	-1.541183076
81	SAUSA300_2342	NE1152	respiratory nitrate reductase, beta subunit (narH)	-1.494544041
82	SAUSA300_1871	NE463	conserved hypothetical protein	-1.484254091
83	SAUSA300_1680	NE1696	acetoin utilization protein AcuA	-1.477125752
84	SAUSA300_1846	NE1351	conserved hypothetical protein	-1.466383723
85	SAUSA300_1720	NE1909	hypothetical protein	-1.465256724
86	SAUSA300_1047	NE626	succinate dehydrogenase, flavoprotein subunit (sdhA)	-1.458363933
87	SAUSA300_0084	NE989	hypothetical protein	-1.448175849

88	SAUSA300_2256	NE1190	putative N-acetylmuramoyl-L-alanine amidase	-1.43710499
89	SAUSA300_1569	NE1874	U32 family peptidase	-1.430869312
90	SAUSA300_0040	NE615	conserved hypothetical protein	-1.42903524
91	SAUSA300_0726	NE629	glycerate kinase family protein	-1.427632665
92	SAUSA300_2603	NE338	triacylglycerol lipase precursor (lip)	-1.425976914
93	SAUSA300_1809	NE634	putative membrane protein	-1.419411641
94	SAUSA300_1473	NE1887	transcription antitermination protein NusB	-1.403124543
95	SAUSA300_0476	NE1657	hypothetical protein	-1.399164288
96	SAUSA300_0992	NE1886	hypothetical protein	-1.365803138
97	SAUSA300_2014	NE340	threonine dehydratase (ilvA)	-1.364062421
98	SAUSA300_0877	NE976	Chaperone clpB	-1.358532112
99	SAUSA300_0666	NE1268	hypothetical protein	-1.352216472
100	SAUSA300_0825	NE1365	oxidoreductase, 2-nitropropane dioxygenase family	-1.34928135
101	SAUSA300_0313	NE622	putative nucleoside permease NupC	-1.342767503
102	SAUSA300_2497	NE981	aminotransferase, class I	-1.335087037
103	SAUSA300_0951	NE1506	V8 protease (sspA)	-1.334719536
104	SAUSA300_1283	NE1459	phosphate ABC transporter, phosphate-binding protein PstS	-1.324896395
105	SAUSA300_1801	NE427	fumarate hydratase, class II (fumC)	-1.313719497
106	SAUSA300_1260	NE1273	prephenate dehydrogenase	-1.312579627
107	SAUSA300_1036	NE507	RNA methyltransferase, TrmH family	-1.309031158
108	SAUSA300_0963	NE92	quinol oxidase, subunit II (qoxA)	-1.305050119
109	SAUSA300_2511	NE1377	conserved hypothetical protein	-1.291915149
110	SAUSA300_1992	NE1532	accessory gene regulator protein A (agrA)	-1.285420623
111	SAUSA300_1938	NE918	phi77 ORF006-like protein capsid protein	-1.284856271
112	SAUSA300_1329	NE211	amino acid permease	-1.284430214
113	SAUSA300_0655	NE689	conserved hypothetical protein	-1.277837478
114	SAUSA300_0943	NE730	acetyltransferase, GNAT family family	-1.275225858
115	SAUSA300_0236	NE450	PTS system, IIBC components	-1.266381793
116	SAUSA300_1991	NE873	accessory gene regulator protein C (agrC)	-1.265899455
117	SAUSA300_2083	NE1485	acetyltransferase	-1.265157037
118	SAUSA300_2129	NE993	putative hemolysin III	-1.263559013
119	SAUSA300_2627	NE1418	2-oxoglutarate/malate translocator	-1.253910867
120	SAUSA300_2211	NE627	putative membrane protein	-1.24545282
121	SAUSA300_1671	NE833	hypothetical protein	-1.244849065
122	SAUSA300_0395	NE1563	superantigen-like protein	-1.227467298
123	SAUSA300_0159	NE826	capsular polysaccharide biosynthesis protein Cap5H	-1.217976042
124	SAUSA300_0145	NE1646	phosphonate ABC transporter phosphonate-binding protein	-1.217738147
125	SAUSA300_2100	NE721	lytic regulatory protein	-1.211827033
126	SAUSA300_0832	NE1623	hypothetical protein	-1.207863033
127	SAUSA300_1921	NE1303	truncated amidase	-1.207727674
128	SAUSA300_0234	NE1744	putative flavohemoprotein	-1.204241676
129	SAUSA300_2367	NE1682	gamma-hemolysin component B (hlgB)	-1.203695351
130	SAUSA300_0310	NE1254	perfringolysin O regulator protein (pfoR)	-1.202328628
131	SAUSA300_0673	NE1072	cobalamin synthesis protein/P47K family protein	-1.197434982
132	SAUSA300_0307	NE619	5'-nucleotidase, lipoprotein e(P4) family	-1.194641583
133	SAUSA300_0691	NE1622	DNA-binding response regulator SaeR	-1.180542114
134	SAUSA300_1638	NE618	sensory box histidine kinase PhoR	-1.175157383
135	SAUSA300_0199	NE606	conserved hypothetical protein	-1.154168675

136	SAUSA300_1308	NE1684	DNA-binding response regulator (arlR)	-1.143180614
137	SAUSA300_0780	NE536	conserved hypothetical protein	-1.139677388
138	SAUSA300_1016	NE1434	protoheme IX farnesyltransferase (cyoE)	-1.137161338
139	SAUSA300_2134	NE200	iron compound ABC transporter, permease protein	-1.133513365
140	SAUSA300_1854	NE324	regulatory protein RecX	-1.129282587
141	SAUSA300_2285	NE81	aldose 1-epimerase (galM)	-1.129218754
142	SAUSA300_2307	NE521	ABC transporter, permease protein	-1.129020715
143	SAUSA300_2439	NE614	UTP-glucose-1-phosphate uridylyltransferase (galU)	-1.121378264
144	SAUSA300_0390	NE632	conserved hypothetical protein	-1.119149894
145	SAUSA300_0239	NE1421	PTS system, fructose-specific enzyme II, BC component	-1.118529178
146	SAUSA300_1623	NE257	conserved hypothetical protein	-1.1181259
147	SAUSA300_1760	NE617	lantibiotic epidermin immunity protein F (epiG)	-1.115183696
148	SAUSA300_0102	NE643	staphylococcal tandem lipoprotein	-1.112473215
149	SAUSA300_1922	NE1864	staphylokinase (sak)	-1.11184014
150	SAUSA300_1432	NE764	phiSLT ORF78-like protein	-1.111187722
151	SAUSA300_1905	NE25	PIN domain protein	-1.104194251
152	SAUSA300_1568	NE1414	uridine kinase (udk)	-1.101414956
153	SAUSA300_0339	NE763	conserved hypothetical protein	-1.099367995
154	SAUSA300_2341	NE1512	respiratory nitrate reductase, subunit delta (narJ)	-1.098493173
155	SAUSA300_1097	NE1759	orotidine 5'-phosphate decarboxylase (pyrF)	-1.097181199
156	SAUSA300_1989	NE95	accessory gene regulator protein B (agrB)	-1.089651469
157	SAUSA300_2040	NE1598	hypothetical protein	-1.089129916
158	SAUSA300_0690	NE1296	sensor histidine kinase SaeS	-1.087161914
159	SAUSA300_0402	NE1569	superantigen-like protein	-1.079968862
160	SAUSA300_0371	NE524	conserved hypothetical protein	-1.077891361
161	SAUSA300_0118	NE1198	pyridoxal-phosphate dependent enzyme superfamily protein	-1.076320132
162	SAUSA300_0711	NE421	conserved hypothetical protein	-1.07478736
163	SAUSA300_1326	NE471	putative cell wall enzyme EbsB	-1.073352488
164	SAUSA300_2259	NE415	putative transcriptional regulator	-1.072616491
165	SAUSA300_0810	NE1073	hypothetical protein	-1.072572814
166	SAUSA300_0192	NE224	conserved hypothetical protein	-1.071271818
167	SAUSA300_0438	NE1688	CHAP domain-contain protein	-1.069496616
168	SAUSA300_1092	NE1048	uracil permease (pyrP)	-1.06546601
169	SAUSA300_0859	NE1665	NADH-dependent flavin oxidoreductase	-1.058903864
170	SAUSA300_1594	NE995	preprotein translocase subunit YajC	-1.058746693
171	SAUSA300_2440	NE728	fibronectin binding protein B (fnbB)	-1.054517009
172	SAUSA300_1017	NE1084	hypothetical protein	-1.051598669
173	SAUSA300_2396	NE126	para-nitrobenzyl esterase	-1.05152177
174	SAUSA300_1460	NE519	peptidase, M20/M25/M40 family	-1.04566072
175	SAUSA300_0183	NE1888	hypothetical protein	-1.044957003
176	SAUSA300_0221	NE1863	pyruvate formate-lyase activating enzyme (pflA)	-1.04262899
177	SAUSA300_0626	NE1374	teichoic acid biosynthesis protein B	-1.040557573
178	SAUSA300_2287	NE752	putative membrane protein	-1.038412459
179	SAUSA300_1119	NE229	conserved hypothetical protein	-1.036098513
180	SAUSA300_0783	NE1422	phosphoglycerate mutase family protein	-1.034367071

NE224
4000 bp
800bp
*USA300 JE2 Tn▽NE224 failed
Positive Control: NE0224
Negative Control: S. aureus USA300 JE2
Negative Control: S. aureus SH1000
USA300 JE2 Tn▽NE0224
SH1000 Tn▽NE0224
NE714
4000 bp
800bp
Positive Control: NE0714 (MntN)
Negative Control: S. aureus USA300 JE2
Negative Control: S. aureus SH1000
USA300 JE2 Tn▽NE0714
SH1000 Tn▽NE0714
NE732
4000 bp
800bp
Positive Control: NE0732
Negative Control: S. aureus USA300 JE2
Negative Control: S. aureus SH1000
USA300 JE2 Tn▽NE0732
SH1000 Tn▽NE0732
NE732
4000 bp
800bp
Positive Control: NE0732
Negative Control: S. aureus USA300 JE2
Negative Control: S. aureus SH1000
USA300 JE2 Tn▽NE0732
SH1000 Tn▽NE0732
NE945
4000 bp
800bp
Positive Control: NE0945
Negative Control: S. aureus USA300 JE2
Negative Control: S. aureus SH1000
USA300 JE2 Tn▽NE0945
SH1000 Tn▽NE0945
NE1084
4000 bp
800 bp
Positive Control: NE1084
Negative Control: S. aureus USA300 JE2
Negative Control: S. aureus SH1000
USA300 JE2 Tn▽NE1084
SH1000 Tn▽NE1084
NE1366
4000 bp
800bp
Positive Control: NE1366 (KatA)
Negative Control: S. aureus USA300 JE2
Negative Control: S. aureus SH1000
USA300 JE2 Tn▽NE1366
SH1000 Tn▽NE1366
NE1374
4000 bp
800bp
Positive Control: NE1374
Negative Control: S. aureus USA300 JE2
Negative Control: S. aureus SH1000
USA300 JE2 Tn▽NE1374
SH1000 Tn▽NE1374
NE1555
4000 bp
800bp
Positive Control: NE1555 (CodY)
Negative Control: S. aureus USA300 JE2
Negative Control: S. aureus SH1000
USA300 JE2 Tn▽NE1555
SH1000 Tn▽NE1555

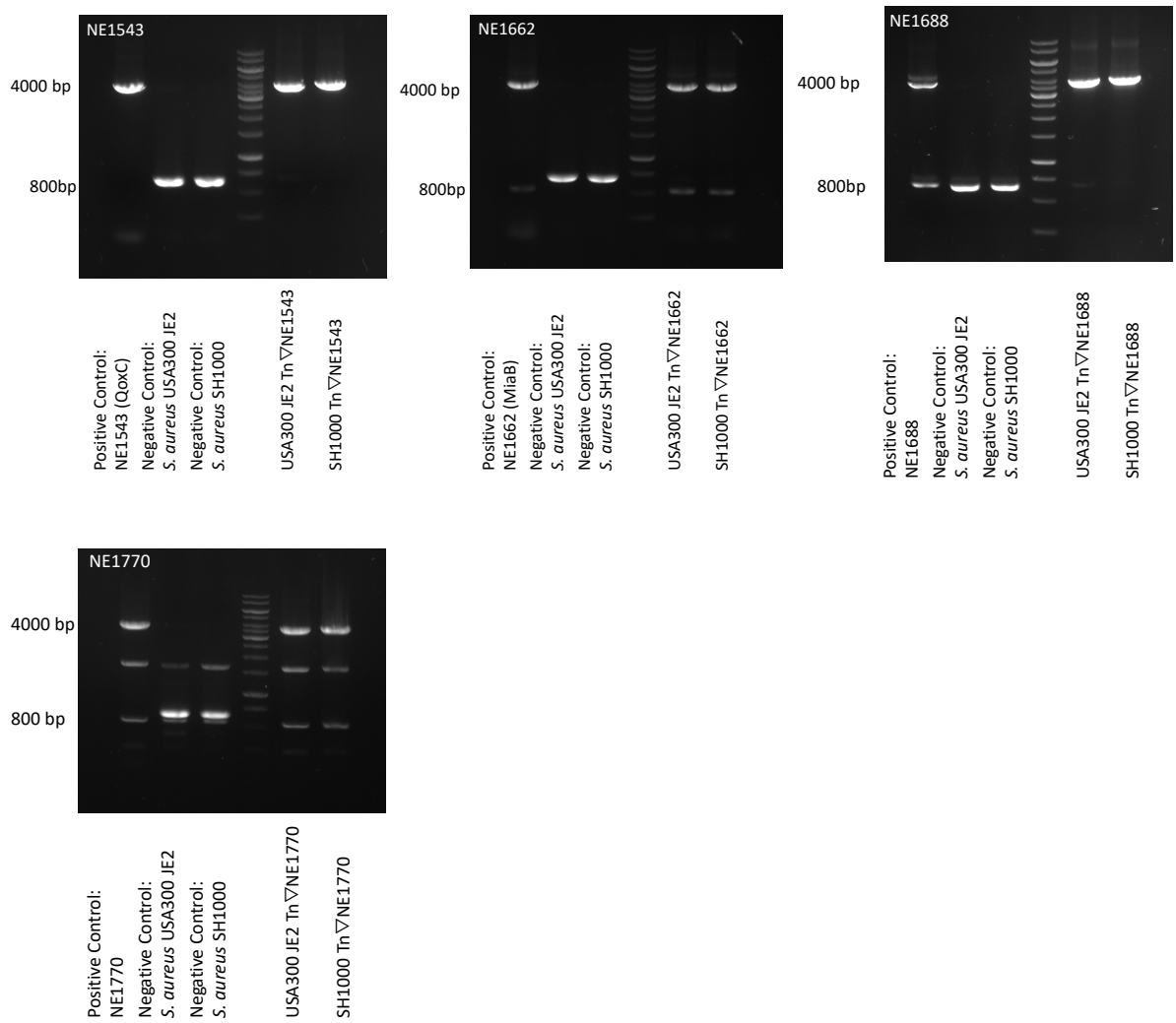

Figure 7.1 Confirmation of genetic transduction.

Representative images of successful transduction of the respective NTML mutant strains (indicated by strain name) into the USA300 strain JE2 and SH1000 backgrounds. PCR products of 400 bp upstream and 400 bp downstream of the NTML transposon insertion site of each gene were assessed by 1% (w/v) agarose gel electrophoresis. Correctly transduced strains generate a full transposon product at approximately 4,000 bp, demonstrated by the original NTML mutant (positive control). Strains without the inserted transposon would generate a product at approximately 800 bp, demonstrated by wild-type strains (negative controls).